INSIGHTS IN MOLECULAR INNATE IMMUNITY: 2021

EDITED BY: Francesca Granucci and Uday Kishore
PUBLISHED IN: Frontiers in Immunology

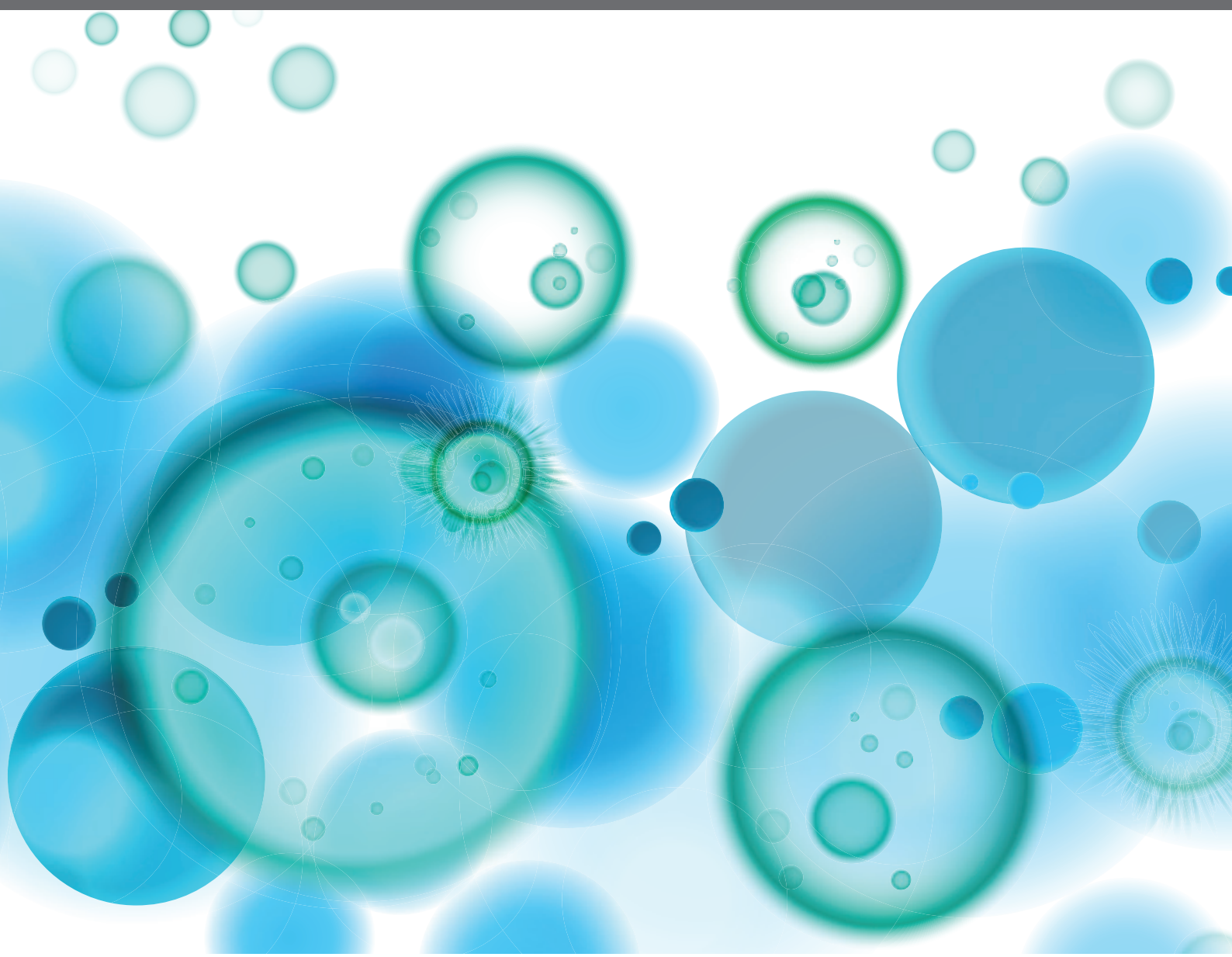

frontiers Research Topics

frontiers

ISSN 1664-8714
ISBN 978-2-83250-486-4
DOI 10.3389/978-2-83250-486-4

About Frontiers

Frontiers is more than just an open-access publisher of scholarly articles: it is a pioneering approach to the world of academia, radically improving the way scholarly research is managed. The grand vision of Frontiers is a world where all people have an equal opportunity to seek, share and generate knowledge. Frontiers provides immediate and permanent online open access to all its publications, but this alone is not enough to realize our grand goals.

Frontiers Journal Series

The Frontiers Journal Series is a multi-tier and interdisciplinary set of open-access, online journals, promising a paradigm shift from the current review, selection and dissemination processes in academic publishing. All Frontiers journals are driven by researchers for researchers; therefore, they constitute a service to the scholarly community. At the same time, the Frontiers Journal Series operates on a revolutionary invention, the tiered publishing system, initially addressing specific communities of scholars, and gradually climbing up to broader public understanding, thus serving the interests of the lay society, too.

Dedication to Quality

Each Frontiers article is a landmark of the highest quality, thanks to genuinely collaborative interactions between authors and review editors, who include some of the world's best academicians. Research must be certified by peers before entering a stream of knowledge that may eventually reach the public - and shape society; therefore, Frontiers only applies the most rigorous and unbiased reviews.
Frontiers revolutionizes research publishing by freely delivering the most outstanding research, evaluated with no bias from both the academic and social point of view. By applying the most advanced information technologies, Frontiers is catapulting scholarly publishing into a new generation.

What are Frontiers Research Topics?

Frontiers Research Topics are very popular trademarks of the Frontiers Journals Series: they are collections of at least ten articles, all centered on a particular subject. With their unique mix of varied contributions from Original Research to Review Articles, Frontiers Research Topics unify the most influential researchers, the latest key findings and historical advances in a hot research area! Find out more on how to host your own Frontiers Research Topic or contribute to one as an author by contacting the Frontiers Editorial Office: frontiersin.org/about/contact

INSIGHTS IN MOLECULAR INNATE IMMUNITY: 2021

Topic Editors:
Francesca Granucci, University of Milano-Bicocca, Italy
Uday Kishore, Brunel University London, United Kingdom

Citation: Granucci, F., Kishore, U., eds. (2022). Insights in Molecular Innate Immunity: 2021. Lausanne: Frontiers Media SA. doi: 10.3389/978-2-83250-486-4

Table of Contents

frontiers in Immunology

REVIEW
published: 17 November 2021
doi: 10.3389/fimmu.2021.775168

COVID-19, Pre-Eclampsia, and Complement System

Chiara Agostinis[1†], Alessandro Mangogna[1†], Andrea Balduit[2], Azin Aghamajidi[3], Giuseppe Ricci[1,4], Uday Kishore[5] and Roberta Bulla[2]*

[1] Institute for Maternal and Child Health, Istituto di Ricovero e Cura a Carattere Scientifico (IRCCS) Burlo Garofolo, Trieste, Italy, [2] Department of Life Sciences, University of Trieste, Trieste, Italy, [3] Department of Immunology, School of Medicine, Iran University of Medical Sciences, Tehran, Iran, [4] Department of Medical, Surgical and Health Science, University of Trieste, Trieste, Italy, [5] Biosciences, College of Health, Medicine and Life Sciences, Brunel University London, Uxbridge, United Kingdom

COVID-19 is characterized by virus-induced injury leading to multi-organ failure, together with inflammatory reaction, endothelial cell (EC) injury, and prothrombotic coagulopathy with thrombotic events. Complement system (C) *via* its cross-talk with the contact and coagulation systems contributes significantly to the severity and pathological consequences due to SARS-CoV-2 infection. These immunopathological mechanisms overlap in COVID-19 and pre-eclampsia (PE). Thus, mothers contracting SARS-CoV-2 infection during pregnancy are more vulnerable to developing PE. SARS-CoV-2 infection of ECs, *via* its receptor ACE2 and co-receptor TMPRSS2, can provoke endothelial dysfunction and disruption of vascular integrity, causing hyperinflammation and hypercoagulability. This is aggravated by bradykinin increase due to inhibition of ACE2 activity by the virus. C is important for the progression of normal pregnancy, and its dysregulation can impact in the form of PE-like syndrome as a consequence of SARS-CoV-2 infection. Thus, there is also an overlap between treatment regimens of COVID-19 and PE. C inhibitors, especially those targeting C3 or MASP-2, are exciting options for treating COVID-19 and consequent PE. In this review, we examine the role of C, contact and coagulation systems as well as endothelial hyperactivation with respect to SARS-CoV-2 infection during pregnancy and likely development of PE.

Keywords: COVID-19, complement system, SARS-CoV-2, pregnancy, pre-eclampsia

OPEN ACCESS

Edited by:
Taruna Madan, National Institute for Research in Reproductive Health (ICMR), India

Reviewed by:
Eleni Gavriilaki, G. Papanikolaou General Hospital, Greece
Christian Drouet, U1016 Institut Cochin (INSERM), France

****Correspondence:***
Andrea Balduit
abalduit@units.it
orcid.org/0000-0001-5902-3205

[†]These authors have contributed equally to this work and share first authorship

Specialty section:
This article was submitted to Molecular Innate Immunity, a section of the journal Frontiers in Immunology

Received: *13 September 2021*
Accepted: *25 October 2021*
Published: *17 November 2021*

Citation:
Agostinis C, Mangogna A, Balduit A, Aghamajidi A, Ricci G, Kishore U and Bulla R (2021) COVID-19, Pre-Eclampsia, and Complement System. Front. Immunol. 12:775168. doi: 10.3389/fimmu.2021.775168

INTRODUCTION

The first case of severe acute respiratory syndrome coronavirus 2 (SARS-CoV-2) infection, responsible for the coronavirus disease 2019 (COVID-19) outbreak, was reported in the Chinese town of Wuhan in the late 2019 (1). The emerging coronavirus spread worldwide over the following months has been officially recognized as a global pandemic since 11th March 2020 (2).

SARS-CoV-2 resembles several characteristics and pathways of infection with other two members of the *Coronaviridae* family: the SARS pandemic in 2002 and the Middle East respiratory syndrome (MERS) in 2012, with a fatality rate of 10% and 36%, respectively (3). CoVs encompass a group of enveloped and single-stranded RNA viruses identified in birds and mammals, and can cause gastrointestinal, central nervous system, and respiratory tract infections (4). The main structural proteins, encoded by specific genes in open reading frame (ORF)-1

downstream regions, include Spike (S), Envelope (E), Membrane (M), and Nucleocapsid (N), S protein being responsible for SARS-CoV-2 invasion of the host cells (5, 6). Among the different receptors identified as cellular entry mediators, the main target receptor of the SARS-CoV-2 virus is the angiotensin-converting enzyme 2 (ACE2) (7), which plays an important role in the renin-angiotensin-aldosterone system (RAAS) for the regulation of blood pressure and electrolyte homeostasis (8), and is widely expressed by most tissues, accounting for the high tropism of the virus. SARS-CoV-2 cell entry also depends on the cellular transmembrane serine protease 2 (TMPRSS2), responsible for S protein priming (7). Extracellular matrix metalloproteinase inducer (EMMPRIN, also known as basigin or CD147), a cell surface glycoprotein that belongs to the immunoglobulin superfamily and activates metalloproteases, has been regarded as a target for SARS-CoV-2 attachment and entry into the host cell (9, 10). In addition, the receptor for Semaphorin-3, named neuropilin-1, has also been demonstrated to facilitate SARS-CoV-2 infection (11).

The SARS-CoV-2 infection damages various organs *via* different pathogenic mechanisms, including direct viral damage to the host cells/tissues through pneumocyte syncytia formation (12) and Golgi apparatus rupture (13), RAAS disruption and endothelial cell (EC) damage resulting in inflammation, endotheliitis and thrombosis (14). Moreover, an unfavorable dysregulation of immune response characterized by lymphopenia and cytokine storm has been reported as a key pathogenic mechanism in COVID-19 (15, 16). In this context, the complement system (C) primary role as a first line of defense against infectious agents would suggest for a protective function in enhancing virus neutralization and phagocytosis. However, C activation has been proposed as a contributor in disease progression to a more severe and lethal stage, which shares important pathophysiological features, in particular endothelial damage, with a pregnancy disorder called pre-eclampsia (PE) (17, 18). This review aims to shed light on the role of the C in pregnant women with COVID-19 developing PE.

THE COMPLEMENT SYSTEM

The C, as a powerful arm of the innate immunity, has a pivotal role in the recognition of potential danger signals and in the clearance of pathogens, apoptotic and necrotic cells (19). The C acts as a functional bridge between innate and adaptive immunity, being a system that "complements" the function of antibodies in the modulation of an integrated host defense (20). The C is comprised of over 50 plasma and cell surface proteins, including activation effectors, regulators and cell surface receptors (21). These proteins are organized to take part in three independent but interactive activation pathways (**Figure 1**): classical, lectin and alternative, converging on the common activation of the major component C3 and in the production of proinflammatory mediators, opsonization, membrane attack complex (MAC) formation, and target cell lysis (22).

Classical Pathway

The classical pathway is mainly triggered by the interaction between the C1 and immune complexes, apoptotic and necrotic cells (23). C1 complex consists of three sub-components: the classical pathway recognition molecule C1q and the serine proteases C1r and C1s. The activation process is initiated by C1q recognition of the Fc domain of an array of IgM or IgG bound to an antigen. The consequent C1q conformational change is responsible for the activation of C1r serine-protease activity (24), which, in turn, acts as a trigger to the proteolytic activity of C1s, inducing C4 and C2 cleavage into two active components (C4b and C2a) and two small fragments released in the fluid phase (C4a and C2b) (25). C4b is able to covalently bind to membrane proteins and carbohydrates (26), and non-covalently to C2a inducing the C4b2a complex formation, also known as C3 convertase of the classical pathway (25). C3 convertase, attached to the target surface, is responsible for C3 cleavage into C3b and C3a anaphylatoxin (**Figure 1**).

Lectin Pathway

The lectin pathway is an antibody-independent route in which mannan-binding lectin (MBL), ficolins (ficolin-1, -2 and -3) or collectin-11 act as pattern-recognition molecules through their binding to mannose residues and other carbohydrate ligands in the form of pathogen-associated molecular patterns (PAMPs), or damage-associated molecular patterns (DAMPs) (27). This binding triggers MBL interaction with MBL-associated serine proteases (MASPs), a family of serine proteases including three enzymatic proteins (MASP-1, MASP-2 and MASP-3) and two non-enzymatic factors (Map19 and Map44). MASP-3 is mainly involved in the alternative pathway activation (28), whilst MASP-2 activation by MASP-1, forming a dimer, activate the lectin pathway *via* C4 and C2 cleavage and C3 convertase formation (29).

Alternative Pathway

The initiation of the alternative pathway is independent of immune complexes, being constitutively active at basal levels in the so-called "tick-over" mechanism and assuring a rapid and robust C activation in the presence of pathogens (30). Under normal physiological conditions, C3 undergoes constant low-grade activation by spontaneous hydrolysis, producing the C3(H_2O) molecule, which is rapidly inactivated in the circulation (31). After its binding to C3 (H_2O), the plasma protein factor B (FB) is cleaved by the serine protease factor D (FD), losing the small fragment Ba, whilst the residual fragment Bb remains bound to C3(H_2O) forming the fluid phase C3 convertase, C3(H_2O)Bb. C3(H_2O)Bb has the ability to cleave large amounts of C3 molecules into C3a and C3b. C3b is partly inactivated by hydrolysis; however, the interaction of C3b with surface components of microbial agents and damaged host cells can accelerate the alternative pathway and induce the association with FB, further cleaved by FD, and generation of the amplification loop convertase C3bBb. The rapid amplification loop is also boosted by the C3b molecules generated by either the classical or lectin pathway. The alternative pathway C3 convertases are highly labile, so they need to be stabilized by an up-regulator called factor P or properdin, increasing its half-life by 10-fold (32).

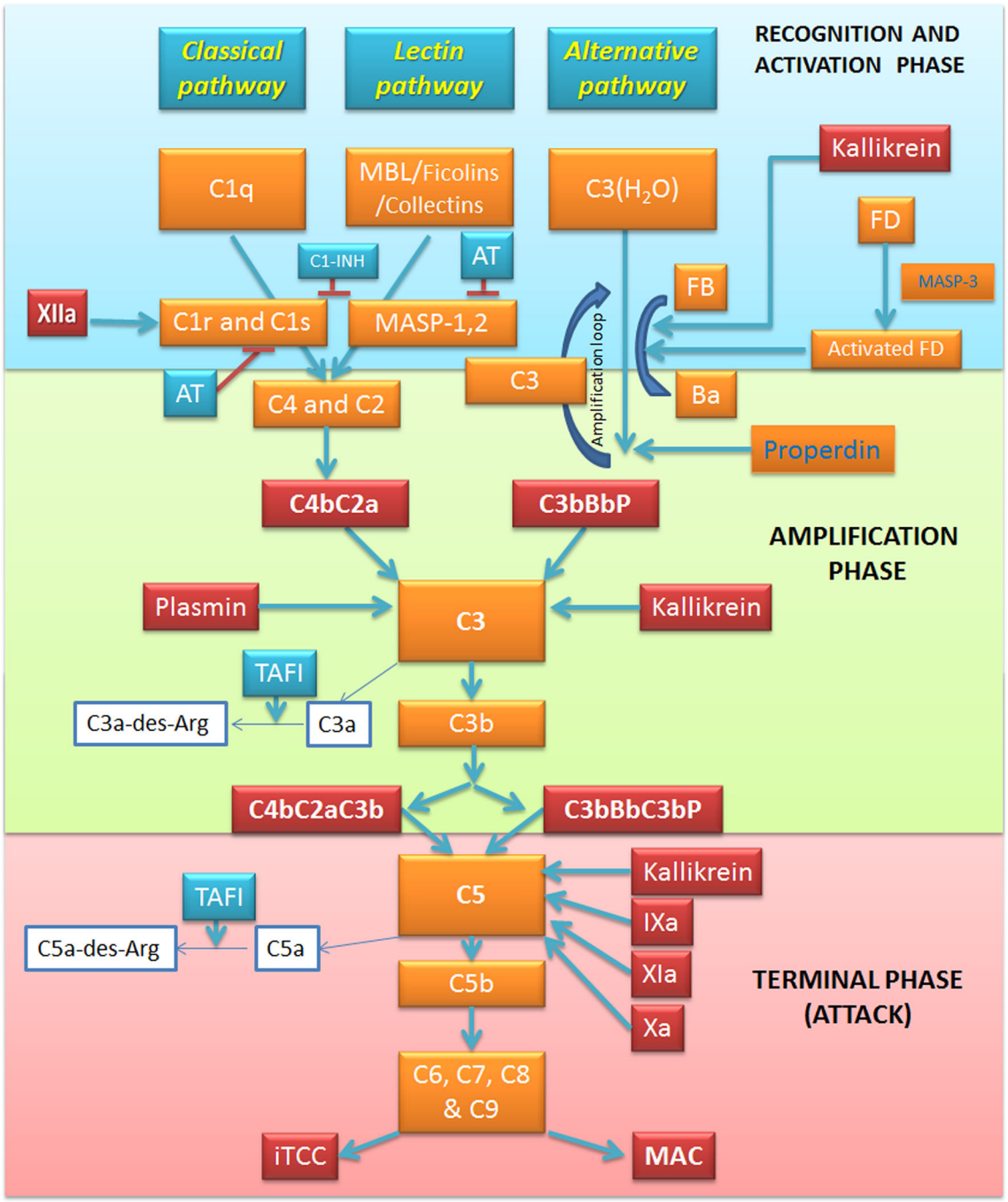

FIGURE 1 | Overview of the complement system (C) and its interplay with the coagulation and kallikrein-kinin pathways. The activation of C *via* three pathways: classical, alternative and lectin. The recognition and activation phases in each pathway converge on the formation of C3 convertase. The amplification phase is initiated when the C3 convertase cleaves C3, and C3b attachment to C3 convertases changes their substrate specificity, allowing them to become C5 convertase. The C5 convertase cleaves C5, starting the last phase (Terminal-Attack phase), in which C5b forms the membrane-attack complex with C6, C7, C8, and C9, resulting in cell perturbation. Kallikrein exerts its activity on C activation in all these three phases. Factor (F) XIIa activates the classical pathway, whereas plasmin enhances the amplification loop. Thrombin, FIXa, FXa, FXIa, and kallikrein directly activate C5. AT, Antithrombin; C1-INH, C1-inhibitor; F, Factor; MAC, Membrane attack complex; MASP, MBL associated serine protease; MBL, Mannose binding lectin; iTCC, Inactive terminal complement complex; TAFI, Thrombin activatable fibrinolysis inhibitor.

Membrane Attack Complex Formation

All the three C activation pathways converge on the common C3 convertase formation and C3 cleavage into the anaphylatoxin C3a and the opsonin C3b (19, 33). The incorporation of the C3b fragment in the C3 convertase gives rise to the production of C5 convertase, which in turn, cleaves C5 to yield C5b and the anaphylatoxin C5a. Then, C5b sequentially interacts with the terminal C components C6, C7, C8, and C9, resulting in the formation of the C5b-9 terminal C complex (TCC). If TCC is fully inserted into a cell plasma membrane, it is called the MAC. MAC-mediated cell death can release DAMPs, which can result in further C activation. In many clinical conditions associated with massive C activation, in plasma or other fluids, the formation of a cytolytically inactive TCC (iTCC)' also called soluble C5b-9 (sC5b-9) complex, is helpful in several pro-inflammatory responses acting directly on endothelium (34).

Main Regulators of Complement Activation

Abnormal C activation can be responsible for severe inflammatory conditions, as hereditary angioedema, paroxysmal nocturnal haemoglobinuria, and haemolytic uremic syndrome (25, 35). Several cell membrane-bound or soluble C regulators exist to control this system. C1-inhibitor (C1-INH) inhibits both classical and lectin pathway initiation through its action on C1r, C1s and MASP-2, disassembling C1 or ficolin/MBL-MASP complexes' respectively (36, 37). Moreover, C1-INH is also able to downregulate the alternative pathway convertase by interacting with C3b and inhibiting its binding to FB (38). At the C3 convertase level, the main regulator is FI (39)' a serine protease responsible for C3b and C4b cleavage. It needs several cofactors for enhancing its activity. C4b-binding protein (C4bp) represents the main cofactor of FI for C4b cleavage (40). Another cofactor of FI is FH that can bind to polyanionic molecules exposed on the membrane such as glycosaminoglycans, heparin and sialic acid. FH interacts with C3b promoting its hydrolysis by FI (39). In addition, the membrane-bound regulatory proteins, C Receptor 1 (CR1, CD35) (41) and Decay Accelerating Factor (DAF; CD55) (42), participate in C3b and C4b degradation. Membrane Cofactor Protein (MCP; also called CD46) (43) is involved in the acceleration of their decay of the C3- and C5-convertases. CD59 (also known as protectin), by binding to C5b-8, limits the incorporation of the C9 molecules, and consequently, formation of the MAC (44). If the cell is protected from lysis by CD59 (45), the sublytic attack can induce the release of inflammatory mediators (46, 47). When C5b-7, C5b-8 or C5b-9 assemble in plasma, the binding of the plasma proteins' vitronectin (alternative names S-protein) (48) and clusterin (49) (also known as SP40.40)' can lead to iTCC formation, preventing insertion into lipid bilayers and MAC formation.

ROLE OF COMPLEMENT SYSTEM IN VIRAL INFECTIONS INCLUDING SARS-CoV-2

Acting in concert, the three pathways of the C cascade are effective in targeting both cell-free viral particles and virus-infected cells, boosting the anti-viral innate and adaptive immune responses (50). The antiviral activity of the C system usually takes place through four different, but not exclusive, mechanisms of action: C deposition and opsonization, MAC formation and viral cell lysis, production of pro-inflammatory anaphylatoxins, as well as enhancement of adaptive immunity (**Figure 2**) (51). The 'eat me' signal by C1q, C3b, and C4b components on the non-self-agents prompts opsonization and enhanced phagocytosis; this process can progress to MAC assembly and viral envelope lysis. Moreover, C3a and C5a anaphylatoxins are able to recruit neutrophils, mast cells, monocytes, macrophages, basophils, eosinophils, T and B cells, giving an important contribution to chemotaxis, NETosis, degranulation, production of cytokines, inflammation' and reactive oxygen species (ROS) production (52–54).

The most striking evidence supporting the importance of C in viral infection outcome is provided by the evolution of specific evasion mechanisms employed by viruses for subverting C (55). First of all, viruses can recruit and exploit soluble and membrane-bound host C regulators, as well as encode their own C regulatory proteins (56). Moreover, they are also capable of using C regulators and receptors for cellular entry or even to modulate C protein expression through the upregulation of C regulators or the downregulation of C activators (57).

It is now widely accepted that, during the initial stages of the infection, SARS-CoV-2 proteins are able to directly activate all three pathways of C (58): N protein is able to induce the MASP-2-mediated activation of lectin pathway (59) and S protein is responsible for the alternative pathway activation (60), whilst classical pathway is usually activated at advanced stages *via* immune complexes and C-reactive protein involvement (61, 62). Evidence so far suggests that C may be beneficial in the early stages of SARS-CoV-2 infection due to its participation in virus elimination; however, C activation may be severely harmful in later phases.

In COVID-19, the initial viral invasion phase is usually followed by an immunopathological phase, which is characterized by an uncontrolled immunological response causing pulmonary, and sometimes, systemic inflammation, in which C is also involved. In particular, recent findings indicate that excessive or deregulated C activation may occur in COVID-19 patients (62, 63), triggering anaphylatoxin generation and binding to their receptors (64), with subsequent inflammatory cell recruitment in the lungs and other organs (65). This contributes to cytokine storm, EC injury, intravascular coagulation and thrombosis (66, 67).

ENDOTHELIITIS, COMPLEMENT SYSTEM, AND PATHOGENESIS OF COVID-19

COVID-19 pathogenesis is characterized by an initial virus-induced injury and consequent multi-organ failure, coupled with an intense inflammatory reaction, EC injury, and a prothrombotic coagulopathy with thrombotic events. The progression from mild to severe COVID-19 is characterized by the transition from an epithelial to an endothelial disease (14, 68).

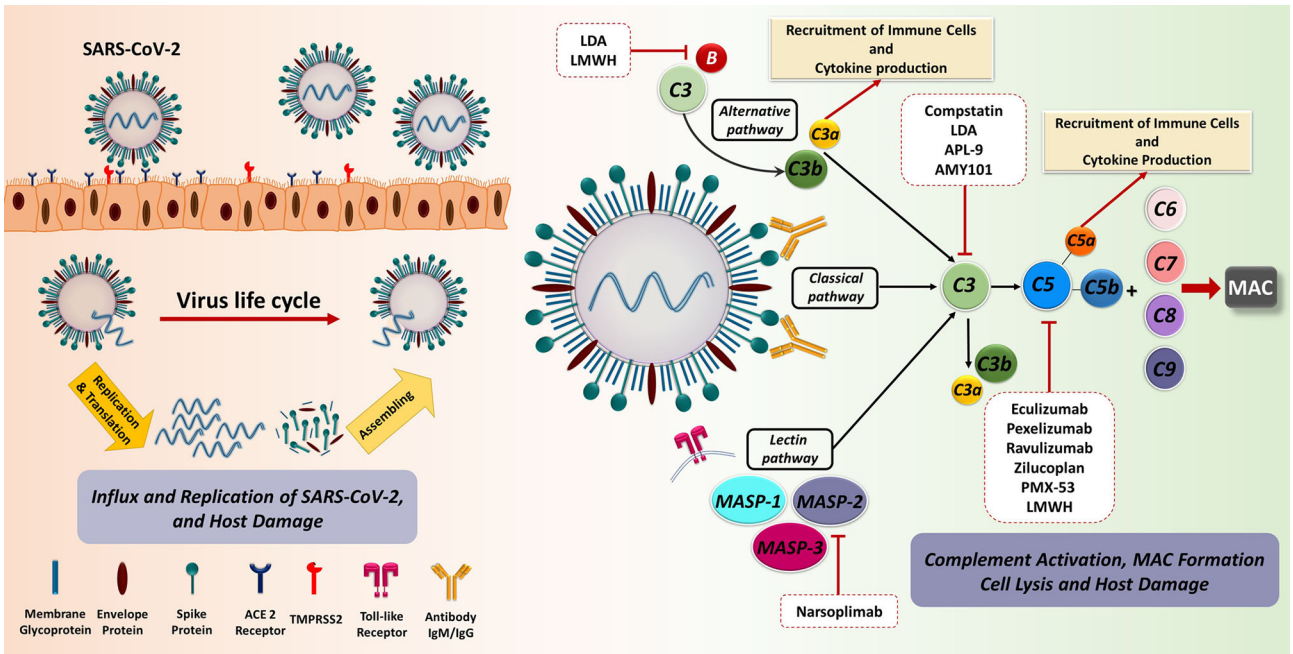

FIGURE 2 | The recognition and binding of S protein to the ACE2 receptor are fundamental key events in SARS-CoV-2 invasion of the host cells. The engagement of ACE2 receptor and S protein of SARS-CoV-2 induces the fusion of virus and target cell. This process is orchestrated by the cleavage of S protein into S1 and S2 subunits *via* transmembrane serine protease priming known as TMPRSS. Subsequently, prompt viral replication occurs inside the infected cell, contributing to the dissemination of infection. The C as a first line of innate immune defence could recognize the virus. SARS-CoV-2 is capable of directly activating the C through the classical, alternative, and especially lectin pathways. Dysregulated C activation during the SARS-CoV-2 infection can cause serious damage to different organs. The blockade of C effectors has a potential therapeutic effect through the prevention of the recruitment of immune cell as well as immune activation. ACE2, Angiotensin-converting enzyme 2; LDA, Low-dose aspirin; LMWH, Low-molecular weight heparin; MAC, Membrane attack complex; MASP, MBL (mannose binding lectin) associated serine protease; SARS-CoV-2, Severe acute respiratory syndrome coronavirus 2; TMPRSS2, Transmembrane serine protease 2.

Indeed, ECs, playing a pivotal role in the regulation of immune response, initiation, and maintenance of inflammatory process (69), coagulation, and platelet function, are key players in various pathological manifestations associated with COVID-19 (**Figure 3**) (70, 71).

Direct viral infection of ECs, *via* SARS-CoV-2 receptors, ACE2 and TMPRSS2, present on their surface (7), is able to provoke endothelial dysfunction and disruption of vascular integrity, leading to hyperinflammation and hypercoagulability (72). The binding of SARS-CoV-2 to ACE2 hampers its enzymatic activity, with consequent enhanced vascular permeability (72) associated with activation of kallikrein-kinin system and bradykinin (BK) accumulation (7, 73). Furthermore, reduced ACE2 expression by binding of SARS-CoV-2 on ECs limits the degradation of des-Arg^9-BK, the active metabolite of BK, into inactive peptides, increasing prothrombotic signaling *via* the activation of BK receptor 1, expressed during inflammatory conditions (72, 74). ACE2 downregulation determines angiotensin II accumulation, which enhances vascular permeability through AT1 receptor and promotes tissue damage, but also reduces Mas activation by angiotensin 1-7, supporting a local pro-inflammatory and pro-thrombotic EC phenotype (75, 76).

Not only a direct virus-dependent effect on ECs has been observed, but also host-specific factors seem to contribute to systemic endothelial dysfunction in COVID-19. The C seems primarily involved in this process, the activation of its three pathways and MAC formation as contributors to EC swelling and even disruption (77). Indeed, in severe disease conditions, elevated levels of serum MAC (62), as well as a strong immunohistochemical staining for deposited C5b-9 in the microvasculature, have been detected (61) in co-localization studies with SARS-CoV-2 N protein (62, 78). MBL, MASP-2, C4a and C3 deposits have also been observed (78).

Immune complexes comprising SARS-CoV-2 specific antibodies and viral antigens may lead to EC injury through the activation of C1 complex of the classical pathway and induction of antibody-dependent cytotoxicity. Increased levels of C3a and C5a, due to C hyperactivation, amplify the vicious cycle of vascular integrity disruption, promoting infiltration of neutrophils which potentiates ROS production, degranulation and NETosis, ultimately provoking further injury to ECs (79). Elevated serum levels of C5a, the most potent C anaphylatoxin, have also been reported in severe COVID-19 patients, whereas circulating C5a levels in patients with mild manifestations are similar to those of the healthy controls (62). Furthermore, a close association of C5a-C5aR axis with inflammation and endotheliitis has been observed in the pathogenesis of severe COVID-19 (64).

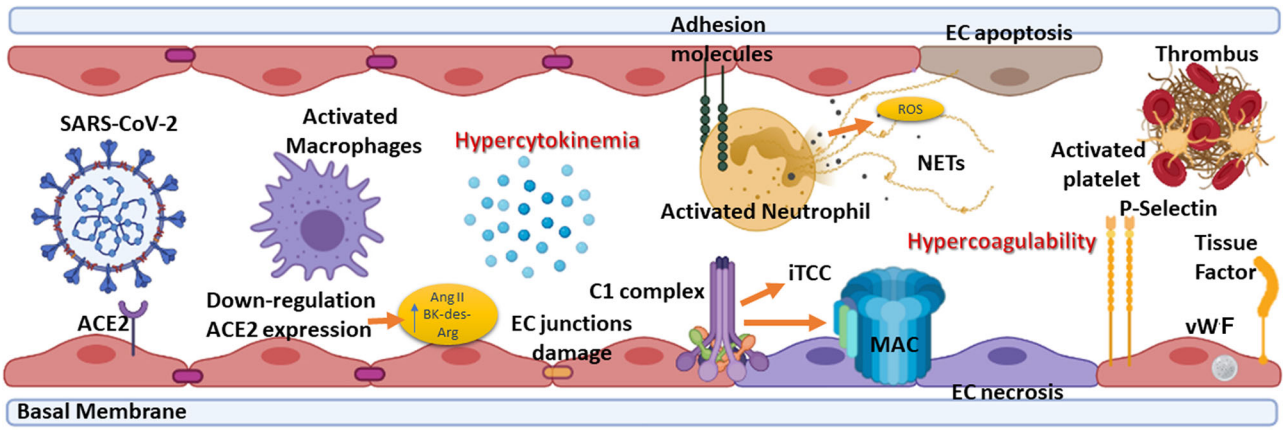

FIGURE 3 | Summary of the elements involved in endotheliitis. COVID-19 pathogenesis is characterized by an initial virus-induced injury leading to multi-organ failure, coupled with an intense inflammatory reaction, endothelial cell (EC) injury, and a prothrombotic coagulopathy with thrombotic events. The hypercytokinemia induced by severe acute respiratory syndrome coronavirus 2 (SARS-CoV-2) causes the expression by ECs of adhesion molecules such as intercellular adhesion molecule 1 (ICAM-1), vascular cell adhesion molecule 1 (VCAM-1) and P-selectin. Neutrophils are recruited and contribute to this process through the release of neutrophil extracellular traps (NETs), which directly activate factor XII and, thus, the contact-dependent pathway of coagulation. NETs also bind von Willebrand factor (vWF) and help to recruit platelets. The feed-forward loop is amplified by the effect of P-selectin, vWF, and fibrinogen expression by ECs in response to hypercytokinemia, causing platelets to directly bind to ECs leading to their activation and hypercontractility, which can lead to disruption of cell-cell junctions and vascular leakage. ACE2, Angiotensin-converting enzyme 2; Ang II, Angiotensin II; BK, Bradykinin; MAC, Membrane attack complex; iTCC, Inactive terminal complement complex; ROS, Reactive oxygen species.

EC damage, characterized by disruption of cell-cell junctions and vascular leakage, exposes basement membrane to circulatory platelets, initiating platelet aggregation, hypercoagulable state and thrombotic events (72) (**Figure 3**), which are frequently observed in severe COVID-19 patients (80).

COMPLEMENT SYSTEM AND ITS ROLE IN THE THROMBOTIC EVENTS IN COVID-19

The C activation has been associated with COVID-19-related coagulopathy and thromboembolia (81), suggesting an interplay between C and coagulation system (**Figure 1**). Interestingly, SARS-CoV-2 infection is able to induce the transcription of C (C1r, C1s, factor B and C3) and coagulation genes (fibrinogen) in pneumocytes and hepatocytes (81).

C and coagulation systems are evolutionarily linked in terms of functional similarities and shared structural motifs (82). The process of coagulation is activated through the contact (intrinsic) and the Tissue Factor (TF) (extrinsic) pathways, both converging on factor (F) X activation. The intrinsic pathway starts from FXII activation by negatively charged surfaces, such as phospholipids present on activated platelets and exposed subendothelial collagen (83) (**Figure 4**). The extrinsic pathway is responsible for a quick and efficient *in vivo* hemostasis, once activated by TF release by damaged cells or expression on the surface of activated monocytes, ECs, and other non-vascular cells. TF then converts FVII to FVIIa (82). The common factor X, upon activation, is then responsible for prothrombin (FII) activation in thrombin (FIIa), which in turn, triggers the formation of fibrin from the soluble fibrinogen (84) (**Figure 4**).

When generated, FXIIa is also responsible of the C activation *via* C1r and C1s (85), and that of the inflammatory kallikrein-kinin pathway by converting pre-kallikrein into active plasma kallikrein, which cleaves FXII into FXIIa and high molecular weight kininogen to BK and the fibrinolytic system by plasma kallikrein activation of pro-urokinase into urokinase, which in turn, cleaves plasminogen into plasmin, an enzyme that degrades fibrin clots (86, 87) (**Figure 5**).

The coagulation system is also involved in inflammation and tissue remodelling through the interaction of coagulation proteases with four distinct protease-activated receptors (PAR1, PAR2, PAR3 and PAR4) (83). The interplay between thrombosis and inflammation is ensured by PAR1 (previously known as the thrombin receptor) cleavage, upon thrombin-PAR1 interaction, resulting into an overall pro-inflammatory state characterized by the release of P-selectin, von Willebrand factor (vWF) and the disruption of the endothelial barrier function (88).

Complement and Tissue Factor Expression

TF (also known also thromboplastin), a transmembrane receptor for FVII/VIIa, acts as initiator of the extrinsic coagulation pathway (89). Several C activation factors induce TF expression on leukocytes and ECs (90–92). C5a increases TF activity in the circulation (93). C5a, by interacting with C5aR, mediates the expression of TF in neutrophils enhancing their procoagulant activity (93) The TF expression in monocytes can also be induced by the membrane insertion of the C5b-7 (94). In addition, the terminal components of the C cascade stimulate the synthesis and release of TF (90); in fact, sublytic MAC (92) and iTCC (91) have been shown to stimulate the expression of TF on ECs,

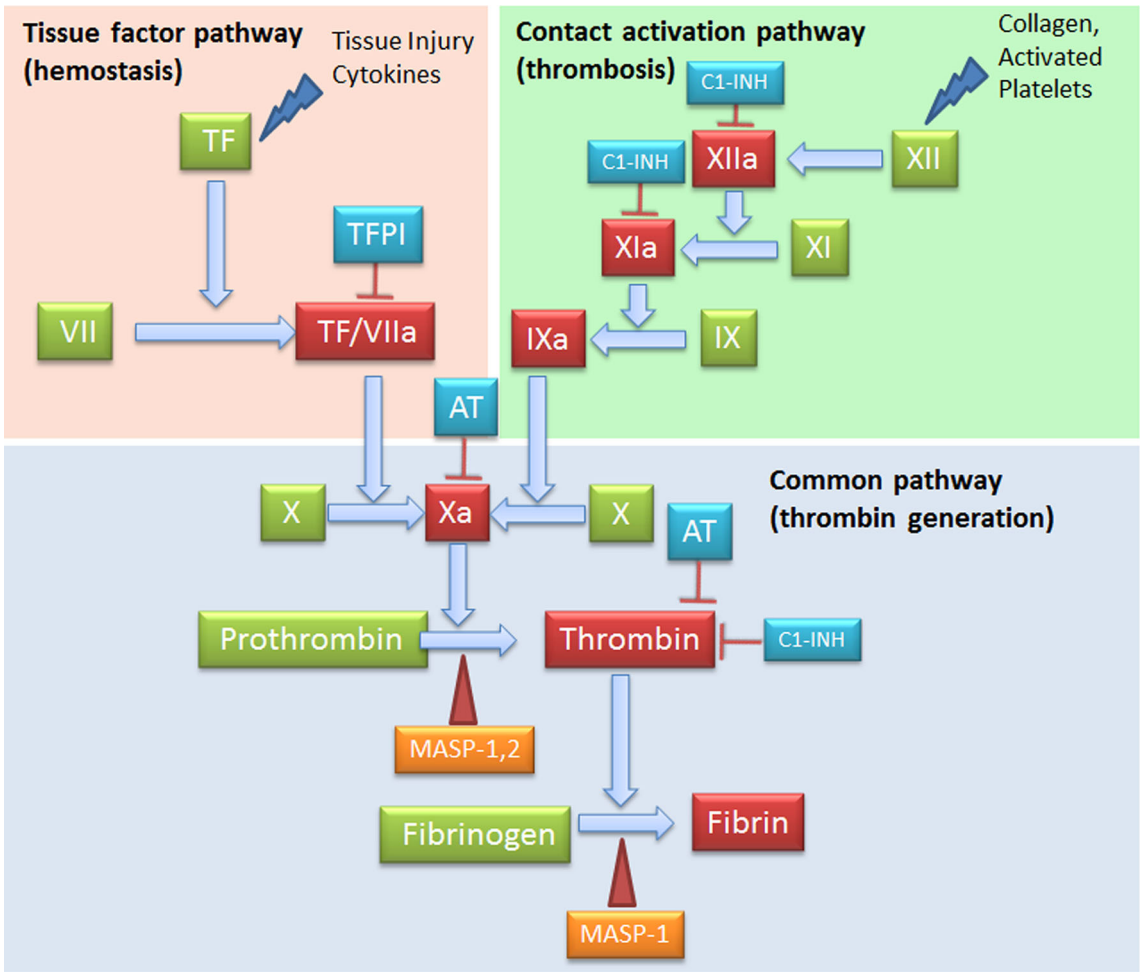

FIGURE 4 | Complement Components that act on the coagulation system. The intrinsic (FXII) and the extrinsic (TF/thromboplastin) pathways initiate the coagulation cascade, both converging at the common point of FX activation. FXa is causes prothrombin (FII) activation in thrombin (FIIa), which leads to the formation of fibrin from the soluble fibrinogen. MASP-1 and MASP-2 directly activate thrombin by cleaving prothrombin, and MASP-1 is able to cleave fibrinogen to generate fibrin monomers. C1-INH exerts its inhibitory activity on the coagulation system by acting on FXIIa, FXIa and thrombin. AT, Antithrombin; C1-INH, C1-inhibitor; MASP, MBL (mannose binding lectin) associated serine protease; TF, Tissue factor; TFPI, Tissue factor pathway inhibitor.

triggering a prothrombotic state through FVII-dependent activation of FX.

A C-linked release of TF has been observed in COVID-19, mainly due to a direct virus-dependent effect on ECs, in which viral infection of the endothelium provokes release of viral proteins able to activate C with consequent stimulation of TF production by neutrophils, monocytes and ECs, as well as causes endothelial injury that would expose subendothelial TF (66, 67, 95, 96).

Complement and von Willebrand Factor Interaction

vWF is a complex multimeric plasma glycoprotein critical for normal haemostatic function; under physiological conditions, it is synthesized by ECs and stored in the Weibel–Palade bodies, and by megakaryocytes, being primarily stored in α-granules of platelets, as ultra-large vWF (97, 98). vWF has two main roles in haemostasis: firstly, to recruit and tether platelets at sites of vascular injury, facilitating aggregation; secondly, vWF acts as a protective carrier molecule for procoagulant FVIII. The assembly of C5b-9 on human ECs results in the secretion of high molecular weight multimers of vWF and release of membrane particles from the EC surface, which express binding sites for FVa, supporting prothrombinase activity (99, 100). Moreover, ultra-large vWF offers an activating surface for the assembly of the alternative pathway convertase; FH is able to reduce ultra-large vWF to smaller forms (101).

Plasma vWF levels are significantly increased in patients with COVID-19 (102), due to EC activation, thereby facilitating recruitment and aggregation of platelets (103) and tethering of leucocytes to the vessel wall (104). A C-linked release of vWF has been observed in response to sublytic MAC addition to ECs (99, 105).

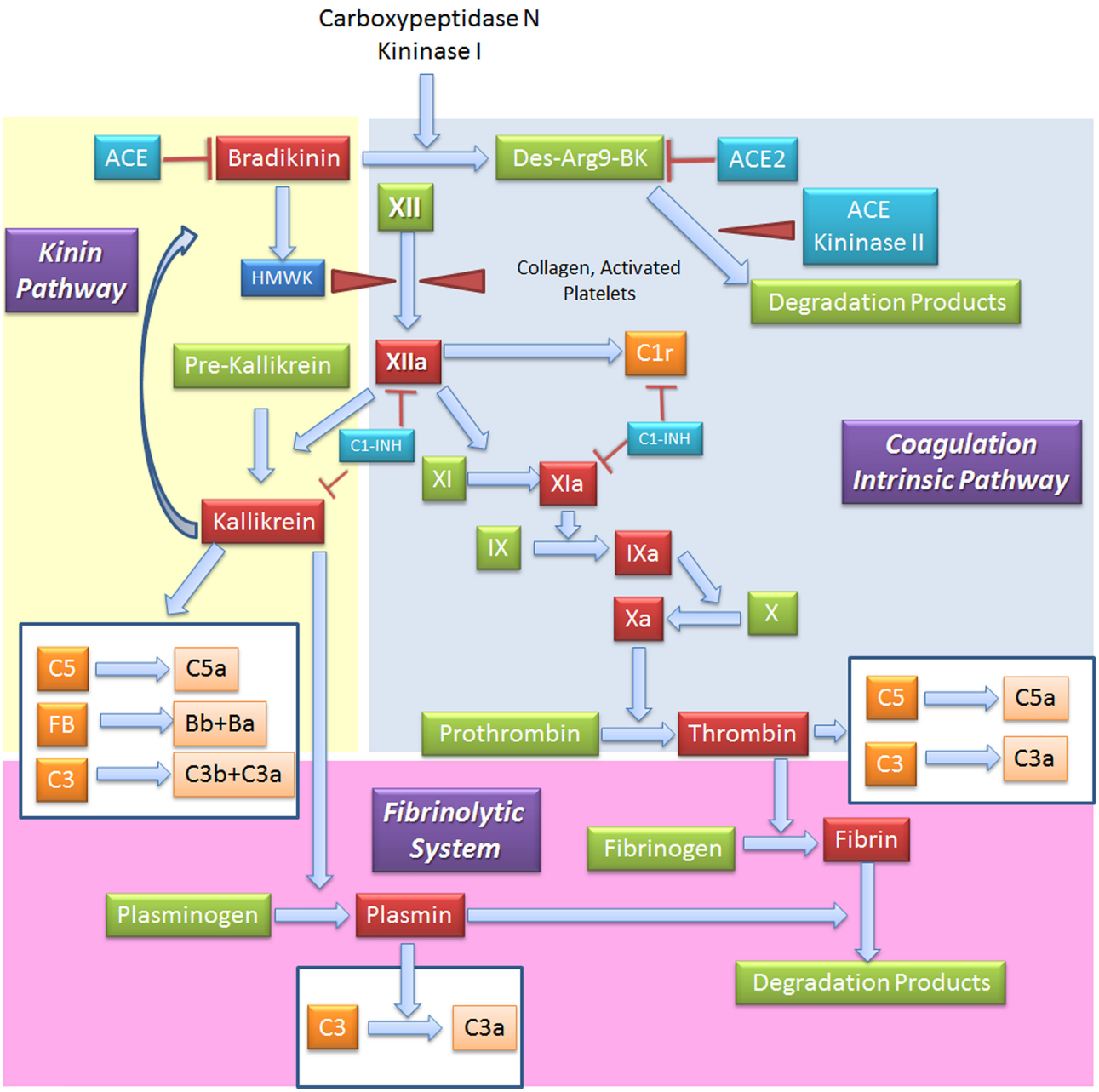

FIGURE 5 | Interplay between coagulation, fibrinolytic, contact and complement systems. The kinin system is comprised of proteins that participate in the coagulation and inflammation. In the kinin/contact system activation may occur *via* auto-activation of FXII in contact with negatively charged surfaces, or the plasma kallikrein-kinin system, as activation in plasma may be driven by pre-kallikrein activation. Kinins are vasoactive peptides produced by the action of a specific protease, called plasma kallikrein on kininogens. Plasma kallikrein, through the cleavage of the plasma glycoprotein precursor high-molecular-weight kininogen (HMWK), produces bradykinin. Bradykinin (BK) causes increase in vascular permeability, contraction of smooth muscle, dilation of blood vessels, and pain when injected into the skin, with similar effects to histamine. It exerts profibrinolytic properties by stimulating release of tissue plasminogen activator from endothelial cells. BK is quickly inactivated by redundant membrane and soluble kininase. The coagulation intrinsic pathway of the coagulation system is composed by plasma proteins activated by FXII, a protein synthesized by the liver that can be activated by collagens, basal membrane and activated platelets. The coagulation system culminates in the formation of thrombin (FIIa) from prothrombin (FII) and in the formation of fibrin from the soluble fibrinogen. When generated, FXIIa is also responsible of the activation of other three systems: (a) C, *via* activation of C1r and C1s; (b) inflammatory kallikrein-kinin pathway by converting pre-kallikrein into active plasma kallikrein, inducing the cleavage of both FXII into FXIIa and high molecular weight kininogen to BK; and (c) fibrinolytic system by plasma kallikrein activation, in turn cleaving plasminogen into plasmin, an enzyme that degrades fibrin clots. Several coagulation system enzymes, including thrombin, FIXa, FXa, FXIa, and kallikrein, directly activate C5. Kallikrein also activates C3 and factor. ACE, Angiotensin-converting enzyme; C1-INH, C1-inhibitor; FB, Factor B.

Complement and Thrombin Generation

MASPs associated with surface-bound MBL or ficolins exert their activity also in the coagulation process by cleaving coagulation factors, despite a slower kinetics as compared to coagulation proteases (27). MASP-1 and MASP-2 directly cleave prothrombin causing thrombin generation; MASP-1 is also able to cleave fibrinogen to generate fibrin monomers. Furthermore, MASP-1 is able to induce the formation of FXIIIa, a fibrin stabilizing factor, and that of thrombin-activatable fibrinolysis inhibitor (TAFI), an attenuator of the fibrinolytic rate. Among thrombin inhibitors, C1-INH and anti-thrombin III+heparin exert their inhibitory effect also on MASP-1 and MASP-2, whereas α2-macroglobulin does not abolish lectin pathway activation (37). The key TF Pathway Inhibitor (TFPI), expressed by microvascular ECs, can interfere with the lectin pathway by blocking MASP-2 (106). In addition to MASPs, sC5b-9 can also be involved in thrombin generation and in the flipping of EC and platelet phospholipid membranes, supporting prothrombinase assembly (FXa and FVa binding) (107).

It has been shown that thrombin can cleave C3 and C5, producing biologically active anaphylatoxins, C3a and C5a (108). Within the context of an overall increased thrombin generation, as observed in COVID-19, this mechanism accounts for the amplification of the feed-forward loop between C and coagulation, linking both cascades *via* multiple direct interactions.

Reciprocal Regulation of Complement and Coagulation Pathways

Several C factors are able to control different steps of the coagulation pathway and vice versa (**Figures 1**, **5**). C1-INH can exert a dual inhibitory function on C and coagulation, by respectively inhibiting C1 complex and FXIIa, which is also responsible for C activation through C1r and C1s; regulation of contact system is also C1-INH-dependent through inactivation of plasma kallikrein (109). Furthermore, C1-INH is able to inhibit FXIa (110) and thrombin (111). Interestingly, the interaction of SARS-CoV proteins with C1-INH during viral infection determines C1-INH blockage (112, 113). Low C1-INH serum levels were shown as a predictive factor of progression to respiratory distress in COVID-19 (114).

Among coagulation regulators, an important cross-talk is represented by thrombomodulin (TM), a cell-bound regulator with anticoagulant properties, which can interact with FH enhancing its regulatory activity and consequently accelerating the degradation of C3b into inactive iC3b (115). Several coagulation system enzymes, such as thrombin, factor IXa, factor Xa, factor XIa, and kallikrein, are responsible for direct C5 activation. Kallikrein also activates C3 and factor B. In animal models of arterial and venous thrombosis, plasmin also exerts C5 convertase activity (116) (**Figure 5**). TAFI, also known as plasma carboxypeptidase B2 or R, suppresses fibrinolysis in physiological conditions. Following activation by thrombin/TM and/or plasmin, it can inactivate C3a and C5a, potentiating the action of the constitutive carboxypeptidase N as a supplementary inhibitor (117). Interestingly, markedly elevated circulating TAFI levels are reported in COVID-19 patients, being implicated in microvascular fibrin deposition (118).

Complement-Platelet Crosstalk

Platelet activation is also responsible for the release of C components, including C1q, C3, C4, and C5b-9 (119, 120). C3a, C5a and, to a lesser extent, C4a, promote platelet aggregation and activation through their binding to cognate receptors C3aR or C5aR1 and C5aR2 (121, 122). Despite the absence of a specifically recognized receptor for C4a, it is able to bind to PAR1 and PAR4, participating in platelet activation. Activated platelets expose P-selectin, which is a receptor for C3b, providing a site for the assembly of the alternative pathway C3 convertase (123). Concurrently, C5a and the C5b-9 induce the expression of P-selectin and vWF by ECs (105), promoting platelet adhesion and aggregation, and release of TM from cell surface (124), triggering the coagulation cascade.

MAC is able to activate platelets and promote platelet aggregation (107, 125). The assembly of MAC on human platelets also results in a dose-dependent increase in the binding of FVa and FXa, which increases platelet prothrombinase activity.

PRE-ECLAMPSIA IN COVID-19 AND THE ROLE OF COMPLEMENT SYSTEM

PE is a frequent pregnancy-related disease (2-6% incidence in healthy nulliparous women), contributing to 20-25% of perinatal mortality, characterized by the onset of hypertension, proteinuria and multi-organ impairments. PE has been defined by the International Society for the Study of Hypertension in Pregnancy as the manifestation of arterial hypertension and proteinuria (300 mg/d) occurring after 20 weeks of gestation or as new-onset arterial hypertension combined with organ dysfunctions, such as renal failure, liver dysfunction, hematological or neurological abnormalities, intrauterine growth restriction, or uteroplacental insufficiency (126, 127). Approximately 10-20% of women with severe PE develop HELLP (hemolysis, elevated liver enzymes and low platelets) syndrome as a further complication (128).

From an etiological perspective, PE is commonly distinct in early onset PE (EOPE) and late onset PE (LOPE), occurring before or after 34 weeks of gestation, respectively. EOPE is associated with poor trophoblast invasion and inadequate arterial remodeling and its pathophysiology is considered to be related to the placental development (129, 130). In physiological placentation, the maternal spiral arteries are invaded by extravillous trophoblast cells, which through a process named endovascular migration, gradually replace decidual ECs, leading to spiral artery remodeling (131–133) (**Figure 6**). When this process is impaired, it causes placental hypo-perfusion, tissue ischemia, vascular endothelium dysfunction, microangiopathic thrombosis, oxidative stress, and inflammatory response (134–136). In general, the cause of PE can be ascribed to an excessive maternal systemic inflammation in response to pregnancy through both innate and adaptive immune activation (137). Excessive inflammation during PE has also been confirmed through the measurement of procalcitonin, as a marker of sepsis or severe inflammation (138). The cause of the LOPE is more debatable, but the basal inflammatory state of the mother

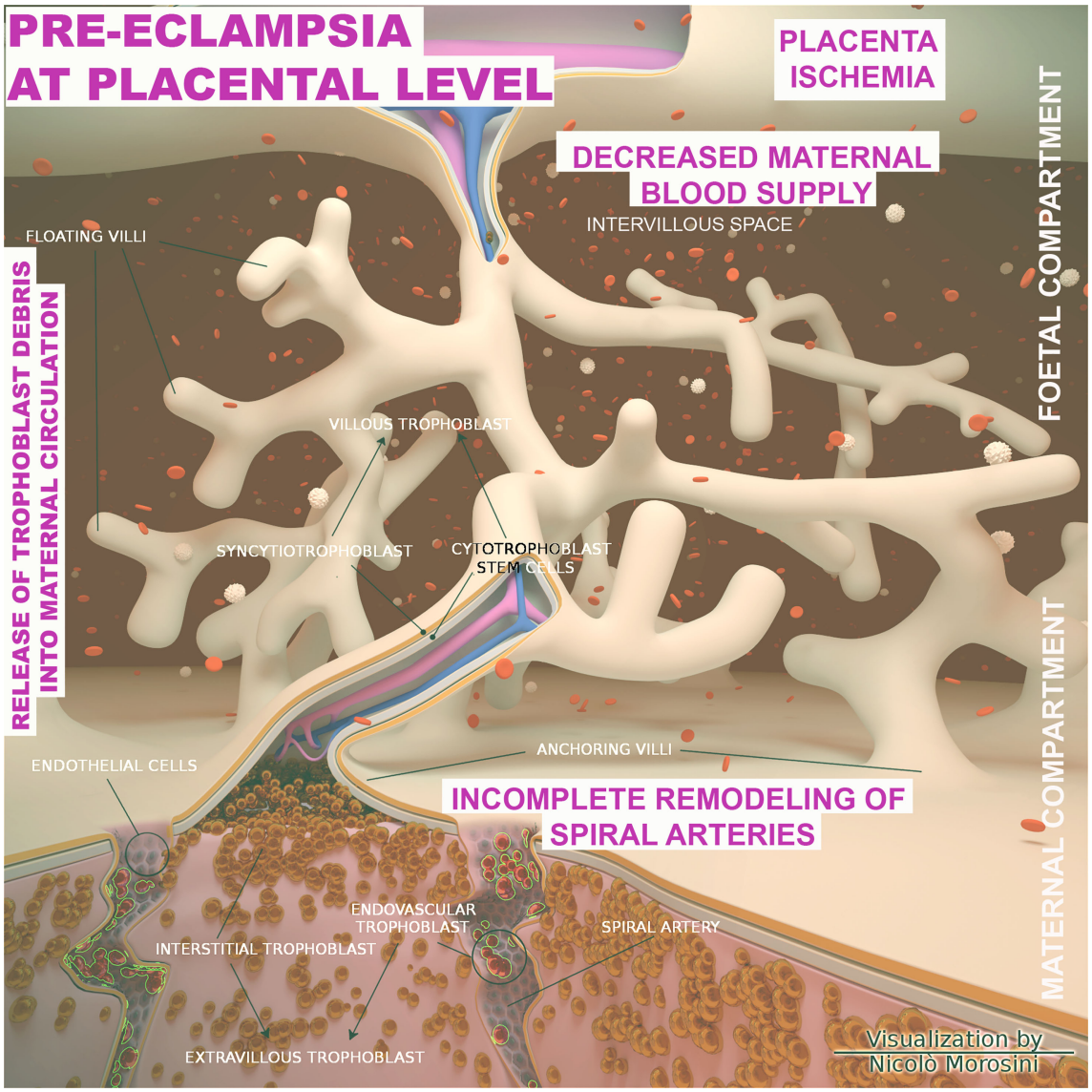

FIGURE 6 | Schematic representation of the placenta architecture in pre-eclampsia (PE). Overview of the structural organization of the placenta and feto/maternal interface during the abnormal placentation in PE. The diagram was designed using the Blender 3D (Blender Foundation, Stichting Blender Foundation, Buikslotermeerplein, Amsterdam, the Netherlands). Edited with permission from Balduit et al. (133).

and the incompatibility between maternal supply and metabolic needs of the developing fetus (130) are considered key precipitating factors.

Important Contribution of the Complement System in the Pathogenesis of Pre-Eclampsia

The C is an important component of the inflammatory process in PE (17, 18). Increased levels of C components and their activation products, including C1q, C3a, C5a and C5b-9 complex, in the circulation of PE patients as compared to normal pregnancy have been reported (17, 139–141), although the results in this field are quite discordant (141). C activation products have also been found in the urine of severe PE patients and are considered a marker of C-mediated renal damage (142). Elevated levels of the activation fragment Bb of the alternative pathway have been proposed as a predictive marker for the development of PE (143). Furthermore, increased C activation was demonstrated in several models of PE (144–146).

Pre-Eclampsia: Diagnostic Criteria

Despite not sharing common pathological pathways, EOPE and LOPE are diagnosed by mutual clinical criteria (147). Uteroplacental under-perfusion, measured by the uterine artery

pulsatility index (UtAPI), induces placental ischemia, which in turn, gives rise to oxidative-inflammation cascade activation, increased production of antiangiogenic factors, such as soluble fms-like tyrosine kinase 1 (sFlt-1) and soluble endoglin (sEng), and reduced production of angiogenic factors, such as placental growth factor (PlGF) (148, 149), both in the intrauterine environment and maternal endothelium. Interestingly, low maternal circulating levels of PlGF are measured prior to the clinical manifestation of PE and intrauterine growth restriction, as a marker of abnormal placentation (150). sFlt-1 is a soluble form of the vascular-endothelial growth factor (VEGF) and a receptor for PlGF. In the maternal circulation, sFlt-1 is able to bind to free VEGF and PlGF, reducing their bioavailability for membrane receptors (151). The use of a diagnostic test based on sFlt-1/PlGF ratio for the prediction of the short-term risk of PE may be a useful tool for patient management (152). In fact, with a sFlt-1/PlGF ratio of ≤ 38 PE occurrence in the next week can be excluded with a negative predictive value of 99.3% (97.9% for ruling out within 2 weeks), whereas a ratio of >38 is associated to an enhanced risk of developing PE in the next 4 weeks (152, 153).

Pre-Eclampsia in COVID-19 Pregnancy

Despite similar clinical manifestations between pregnant and non-pregnant women with COVID-19 (154), an increased rate of preterm delivery, PE, and cesarean section has been noticed in COVID-19 pregnant women (155–158). The INTERCOVID prospective longitudinal study showed an increased incidence of PE in pregnant women with COVID-19 (8.1%), as compared with non-diagnosed COVID-19 (4.4%), especially in nulliparous women; the association appeared to be independent of preexisting conditions and other risk factors, such as obesity, diabetes and hypertension (159). Mendoza et al. reported that a PE-like syndrome could be manifested in some pregnancies with critical COVID-19, according to the presence of severe pneumonia (160). The authors used the term PE-like syndrome to highlight some diverging aspects as compared to classical PE; in their cohort' the PE-like syndrome patients showed PE clinical signs and symptoms but normal parameters, such as sFlt-1/PlGF ratio, UtAPI and LDH <600 IU/l. This information could improve the management of these pregnancies since PE-like syndrome alone may not be considered as an obstetric indication for delivery (160).

Differential diagnosis in COVID-19 pregnant women developing hypertension, thrombocytopenia, proteinuria, as well as increased levels of liver enzymes, might be challenging, since misdiagnosis may occur due to COVID-19 and PE overlapping clinical features (147). In fact, a recent study suggested a two-fold increased risk of developing hypertensive disorders of pregnancy in patients who manifested COVID-19, especially early in their pregnancy (161); this is considered as a consequence of COVID-19-mediated modulation of placental ACE2 expression (162).

A common denominator in the pathophysiology of PE or PE-like syndrome and COVID-19 is the endothelial injury, due to disrupted placentation in PE (135, 163) and to directly or indirectly SARS-CoV-2-mediated damage to ECs in COVID-19 (71, 96, 164, 165). To clarify the extent of endothelial injury, the evaluation of two well-studied markers, such as the antiangiogenic factor sFlt-1 and the angiogenetic factor PlGF (166–168) can be useful. An imbalance between angiogenic and anti-angiogenic factors has been observed in COVID-19. Negro et al. indicated that an increase in sFlt-1 levels could be considered a good biomarker to predict survival and thrombotic events in COVID-19 patients (169). Smadja et al. considered PlGF increase as a relevant predictive factor for in-hospital mortality to discriminate COVID-19 severity (170), whereas Giardini et al. have used sFlt-1/PlGF ratio as a tool to stratify the severity of endothelial dysfunction (171). Interestingly, in PE-like syndrome, Mendoza et al. noted a normal sFlt-1/PlGF ratio and UtAPI assessment (160), suggesting normal values of sFlt-1/PlGF and UtAPI in COVID-19 patients with normal early phase of placental implantation, despite their symptomatic manifestations. Thus, an interplay between two different phenomena can be proposed in the clinical setting of SARS-CoV-2-infected obstetric patients at risk of developing COVID-19. At one hand, COVID-19 may mimic PE, particularly in early pregnancy; on the other hand, an already established PE may act as a risk factor for the development of severe or critical COVID-19. These two separate clinical conditions merit further investigation when clinical and epidemiological criteria indicate patients at risk of one or the other, or both conditions (172).

Common Pathophysiology of Pre-Eclampsia and Severe COVID-19

Endothelial damage can be responsible for multi-organ dysfunction in both PE and COVID-19 (165, 173), as well as for an augmented risk of non-cardiogenic pulmonary oedema and venous thromboembolism (165). An increased hypercoagulable state characterizes PE women as compared to normal pregnancies, showing a rise in factor VIII, vWF, thrombin-antithrombin complex, D-dimers, soluble fibrin and TM levels (174). At the same time, the fibrinolytic system also plays an important role in PE, considering the significant increase in plasma plasminogen activator inhibitor type-1 (PAI-1) (174, 175). COVID-19 is also linked to a thrombogenic coagulopathy with a wide range of manifestations. COVID-19 patients commonly manifest mild thrombocytopenia (176) and increased D dimer levels (177) in accordance with disease severity, whereas other coagulation measurements are more variable (178, 179). Another feature shared between PE and COVID-19 patients is represented by an overall inflammatory microenvironment, characterized by an increase in serum and placental levels of pro-inflammatory and decrease of anti-inflammatory cytokines (180, 181).

In the context of endothelial damage, three common players have been proposed in PE and severe COVID-19 pathophysiological mechanisms: NETosis, anti-phospholipid antibodies (aPLAs) and α-1-antitrypsin (182). However, only the first two aspects concern an engagement of C.

There is an overwhelming case for the involvement of neutrophil extracellular traps (NETs) in immunothrombosis through several mechanisms: (a) NETs bind to vWF and recruit platelets; (b) NETs are able to trigger platelet activation; (c) NETs binding to TF provokes extrinsic pathway activation

and thrombin generation; (d) Cleavage induced by neutrophil elastase and other neutrophil serine proteases inactivate anticoagulants, including TFPI and TM; and (e) NETs can directly support FXII activation mediated by platelet-derived polyphosphates (183). Interestingly, NETs have also been reported as contributors to PE pathogenesis, usually associated with maternal vasculitis, maternal-fetal interface hemorrhage and laminar decidual necrosis (184), and COVID-19-related endothelial damage and immunothrombosis through platelet-neutrophil interactions (185). NETs formation due to SARS-CoV-2 infection contains C3, factor B and properdin, triggering and stabilizing the alternative pathway convertase (67). An hyper-inflammatory immune state in response to abnormal neutrophil activation and NET formation, together with excessive or deregulated C activation, contributes to the well-documented clinical manifestations observed in severe COVID-19 (186). Moreover, NETs induce an excessive production of thrombin and the subsequent generation of C3a and C5a (108, 186). Hence, a feed-forward loop beginning with C activation may proceed with NETosis, consequently increased thrombin production, further stimulation of the C, and enhanced NET formation (67).

Another potential link between PE and COVID-19 is the presence of anti-phospholipid antibodies (aPLAs), since they have been indicated as an important risk factor for PE, especially EOPE (187). A recent study has reported elevated aPLA levels in nearly 52% of COVID-19 patients (188). In placenta, aPLAs promote platelet and EC activation, directly inducing procoagulant activity by interacting with factors of the coagulation pathway. This activity, however, was greatly reduced in C3 gene knock-out mice (189). Anti-β 2-glycoprotein-I, the primary pathogenic antibody in anti-phospholipid syndrome (190), is associated with an increased C activation (191), amplifying the production of other mediators of effector cell activation, including C3a, C5a, and MAC, with consequent thrombosis, tissue hypoxia, and inflammation within the placenta.

Interestingly, several findings suggest that genetic susceptibility may be involved in the dysregulation of C activation frequently observed in the progression to moderate/severe form of COVID-19 and in PE. Pathogenetic mutations or deletions in C factor and regulatory genes, which predispose to an increased C activation, have been identified both in pregnant women with PE/HELLP syndrome and in patient with COVID-19. C gene mutations were attributed to FH, MCP, FI and C3 (192–194). In COVID-19, gender differences were also observed in C-related variants, with women more genetically susceptible to C dysregulation (194).

THERAPEUTIC CONSIDERATIONS

Emerging evidence suggests that C is constantly activated in severe COVID-19 as well as PE; due to its ubiquity, potency and rapidity, it is reasonably considered as a potential drug target.

At present, the only effective treatment for PE remains parturition, since therapeutic approaches are mainly symptomatic. However, several preventative therapies are effective if administered early in the pregnancy (before 16 weeks of gestation): Low-dose Aspirin (LDA) and low-molecular weight heparin (LMWH) are the most common preventive treatments for PE. Both these drugs also modulate the C activity: LDA is able to down-regulate the levels of C3 and factor B expression in placenta (195, 196), whereas LMWH inhibits the activation of the alternative pathway and directly C5a (197–199). For its anti-thrombotic, anti-inflammatory, analgesic, and anti-pyretic effects, aspirin was also proposed in COVID-19 treatment, despite its clinical use for preventive or curative purposes has not been accepted yet (200–202). According to the beneficial anticoagulation effects of heparin observed in COVID-19 patients, with moderate or severe illness (203), pregnant women with severe COVID-19 should undergo thromboprophylaxis during hospitalization and at least until discharge (155). Moreover, in pregnant women with COVID-19, the use of steroids (dexamethasone followed by methylprednisolone) is recommended if clinically indicated (155). Several studies have reported the ability of methylprednisolone to inhibit C activation, particularly by acting on alternative pathway amplification (204, 205).

Other drugs are potentially used to prevent PE, especially targeting immunological conditions. For instance, it is well known that systemic lupus erythematosus (SLE) and anti-phospholipid Syndrome (APS) predispose to a higher risk of developing PE. Hydroxychloroquine (HCQ), an antimalarial drug, is often used in the treatment of SLE (206), resulting in a lower incidence of PE (196, 206). The mechanisms of action of HCQ on the C is debatable, so is its efficacy in the treatment of COVID-19. Most clinical trials have failed to demonstrate the efficacy of HCQ treatment in COVID-19 (207).

Recently, Lefkou et al. reported that the use of LDA+LMWH in addition to pravastatin (HMG-CoA reductase inhibitor) in APS-affected women at risk of developing PE reduced the onset of adverse outcomes, increasing placenta perfusion, reducing PE onset and improving neonatal outcomes (208). In murine studies, pravastatin inhibited C activation (C5a) by increasing the expression of C inhibitor, DAF (209).

The first C inhibitor to be approved for clinical trials was eculizumab, a monoclonal antibody able to block C5 and decrease C5a and C5b-9 formation (210). The use of eculizumab for C5 inhibition is a reasonable therapeutic option also in PE (196, 210), as suggested by a case report of a patient with severe PE/HELLP at 26 weeks of gestation, showing an improvement of woman and foetus clinical endpoints after eculizumab treatment (pregnancy was prolonged by 17 days, resulting in a reduction of neonatal morbidity).

There are currently 13 clinical studies investigating the effect of C inhibitors in the treatment of severe forms of COVID-19, but none of them include pregnant patients. These are mainly C3 and C5 inhibitors, including zilucoplan, AMY101, APL-9, eculizumab, and ravulizumab (211–214). In particular, eculizumab and ruxolitinib (JAK1/2 inhibitor) treatment resulted in clinical improvement within 3 days; this may be also due to their inhibitory effect on pathways responsible for local and hepatic C synthesis, such as NF-κB and STAT1/2 (215). Compstatin-based C3 inhibitor, AMY-101, showed a satisfactory

efficacy in the treatment of severe COVID-19 pneumonia (63, 212). The lectin pathway inhibitor, narsoplimab, which exerts its activity by blocking MASP-2, has been shown to prevent EC damage and thrombotic microangiopathy; recovery and survival was observed in all COVID-19 patients treated with narsoplimab (216).

Despite the promising results in clinical trials, the potential use of both C3- and C5-targeted therapies in COVID-19 patients is undermined by some limitations as comparted to selective inhibitors (217). First, the relevance of C3 inhibitors is dependent on the timing: blocking the activation of all three C pathways may undesirably reduce viral clearance during the early disease, whilst they may be useful in advanced phases preventing uncontrolled C activation (77). On the other hand, blocking C5 activation prevents the proinflammatory and prothrombotic actions of the terminal products of the C cascade (C5a and C5b-9) activated by SARS-CoV-2, whilst preserving the activity of early C components involved in viral clearance and activation of the adaptive immune response (218); although, this exposes patients to the risk of developing other infections, especially bacterial (219).

Thus, a selective blockage of C5a (vilobelimab) or C5aR (avdoralimab) could be more beneficial since it preserves the formation of C5b-9 complex as a crucial player in pathogen elimination (220, 221). The blockage of C5a-C5aR1 axis limits the infiltration of myeloid cells in damaged organs, hampers the production of pro-thrombotic factors by immune cells, platelets, and ECs, as well as prevents the excessive lung inflammation and endotheliitis associated with acute respiratory distress syndrome in patients with COVID-19 (58, 64, 222).

Another interesting therapeutic option under clinical investigation is the recombinant human C1–INH conestat alfa, which yielded encouraging results (223). Due to its multifaceted inhibitory action, C1–INH prevents all three C pathways' activation (36–38, 113) and inhibits components of the coagulation cascade, plasmin and kallikrein, reducing C-driven inflammation and coagulation (113).

CONCLUSIONS AND PERSPECTIVES

A link between PE and COVID-19 has clearly emerged due to overarching pathophysiological mechanisms involved, which are triggered by an interplay between C and coagulation. Mothers or women who have recovered from COVID-19 need to be monitored closely during subsequent pregnancies for immune deviations. A very important question that is not yet solved and described in the use of C inhibitors for COVID-19 patients is the definition of the right window of opportunity for treatment. In these high-risk patients, with a major genetic susceptibility associated to complement polymorphisms, genetic testing might be an important tool aiming at intensified monitoring and early initiation of specific treatment with C inhibitors. Furthermore, the exact role of the C in severe COVID-19 development is yet to be clarified, which includes C-driven cytokines and viral protein activation of C–coagulation crosstalk.

AUTHOR CONTRIBUTIONS

CA, AM, AB, AA, GR, UK, and RB reviewed the literature and wrote sections of the review article. CA and AA created figures. UK critically reviewed the entire manuscript. All authors contributed to the article and approved the submitted version.

FUNDING

This research was supported by Ferring COVID-19 Investigational Grant (GRAVISAR to RB) and by the Institute for Maternal and Child Health, IRCCS Burlo Garofolo, Trieste, Italy (RC24/19 to GR and 09/21 to CA). The funder Ferring Pharmaceuticals was not involved in the study design, collection, analysis, interpretation of data, the writing of this article or the decision to submit it for publication.

REFERENCES

1. Zhu N, Zhang D, Wang W, Li X, Yang B, Song J, et al. A Novel Coronavirus From Patients With Pneumonia in China, 2019. *N Engl J Med* (2020) 382 (8):727–33. doi: 10.1056/NEJMoa2001017
2. Lai CC, Shih TP, Ko WC, Tang HJ, Hsueh PR. Severe Acute Respiratory Syndrome Coronavirus 2 (SARS-CoV-2) and Coronavirus Disease-2019 (COVID-19): The Epidemic and the Challenges. *Int J Antimicrob Agents* (2020) 55(3):105924. doi: 10.1016/j.ijantimicag.2020.105924
3. Lu L, Zhong W, Bian Z, Li Z, Zhang K, Liang B, et al. A Comparison of Mortality-Related Risk Factors of COVID-19, SARS, and MERS: A Systematic Review and Meta-Analysis. *J Infect* (2020) 81(4):e18–25. doi: 10.1016/j.jinf.2020.07.002
4. Paules CI, Marston HD, Fauci AS. Coronavirus Infections-More Than Just the Common Cold. *JAMA* (2020) 323(8):707–8. doi: 10.1001/jama.2020.0757
5. Mousavizadeh L, Ghasemi S. Genotype and Phenotype of COVID-19: Their Roles in Pathogenesis. *J Microbiol Immunol Infect* (2021) 54(2):159–63. doi: 10.1016/j.jmii.2020.03.022
6. Hu B, Guo H, Zhou P, Shi ZL. Characteristics of SARS-CoV-2 and COVID-19. *Nat Rev Microbiol* (2021) 19(3):141–54. doi: 10.1038/s41579-020-00459-7
7. Hoffmann M, Kleine-Weber H, Schroeder S, Kruger N, Herrler T, Erichsen S, et al. SARS-CoV-2 Cell Entry Depends on ACE2 and TMPRSS2 and Is Blocked by a Clinically Proven Protease Inhibitor. *Cell* (2020) 181(2):271–80.e8. doi: 10.1016/j.cell.2020.02.052
8. Patel S, Rauf A, Khan H, Abu-Izneid T. Renin-Angiotensin-Aldosterone (RAAS): The Ubiquitous System for Homeostasis and Pathologies. *BioMed Pharmacother* (2017) 94:317–25. doi: 10.1016/j.biopha.2017.07.091
9. Yan R, Zhang Y, Li Y, Xia L, Guo Y, Zhou Q. Structural Basis for the Recognition of SARS-CoV-2 by Full-Length Human ACE2. *Science* (2020) 367(6485):1444–8. doi: 10.1126/science.abb2762
10. Varadarajan S, Balaji TM, Sarode SC, Sarode GS, Sharma NK, Gondivkar S, et al. EMMPRIN/BASIGIN as a Biological Modulator of Oral Cancer and COVID-19 Interaction: Novel Propositions. *Med Hypotheses* (2020) 143:110089. doi: 10.1016/j.mehy.2020.110089
11. Cantuti-Castelvetri L, Ojha R, Pedro LD, Djannatian M, Franz J, Kuivanen S, et al. Neuropilin-1 Facilitates SARS-CoV-2 Cell Entry and Infectivity. *Science* (2020) 370(6518):856–60. doi: 10.1126/science.abd2985
12. Bussani R, Schneider E, Zentilin L, Collesi C, Ali H, Braga L, et al. Persistence of Viral RNA, Pneumocyte Syncytia and Thrombosis Are Hallmarks of Advanced COVID-19 Pathology. *EBioMedicine* (2020) 61:103104. doi: 10.1016/j.ebiom.2020.103104

13. Saraste J, Prydz K. Assembly and Cellular Exit of Coronaviruses: Hijacking an Unconventional Secretory Pathway From the Pre-Golgi Intermediate Compartment via the Golgi Ribbon to the Extracellular Space. *Cells* (2021) 10(3):503. doi: 10.3390/cells10030503
14. Gupta A, Madhavan MV, Sehgal K, Nair N, Mahajan S, Sehrawat TS, et al. Extrapulmonary Manifestations of COVID-19. *Nat Med* (2020) 26(7):1017–32. doi: 10.1038/s41591-020-0968-3
15. Jamal M, Bangash HI, Habiba M, Lei Y, Xie T, Sun J, et al. Immune Dysregulation and System Pathology in COVID-19. *Virulence* (2021) 12 (1):918–36. doi: 10.1080/21505594.2021.1898790
16. Garcia LF. Immune Response, Inflammation, and the Clinical Spectrum of COVID-19. *Front Immunol* (2020) 11:1441. doi: 10.3389/fimmu.2020.01441
17. Derzsy Z, Prohaszka Z, Rigo J Jr, Fust G, Molvarec A. Activation of the Complement System in Normal Pregnancy and Preeclampsia. *Mol Immunol* (2010) 47(7-8):1500–6. doi: 10.1016/j.molimm.2010.01.021
18. Girardi G, Bulla R, Salmon JE, Tedesco F. The Complement System in the Pathophysiology of Pregnancy. *Mol Immunol* (2006) 43(1-2):68–77. doi: 10.1016/j.molimm.2005.06.017
19. Walport MJ. Complement. First of Two Parts. *N Engl J Med* (2001) 344 (14):1058–66. doi: 10.1056/NEJM200104053441406
20. Hajishengallis G, Reis ES, Mastellos DC, Ricklin D, Lambris JD. Novel Mechanisms and Functions of Complement. *Nat Immunol* (2017) 18 (12):1288–98. doi: 10.1038/ni.3858
21. Ghebrehiwet B. The Complement System: An Evolution in Progress. *F1000Res* (2016) 5:2840. doi: 10.12688/f1000research.10065.1
22. Merle NS, Church SE, Fremeaux-Bacchi V, Roumenina LT. Complement System Part I - Molecular Mechanisms of Activation and Regulation. *Front Immunol* (2015) 6:262. doi: 10.3389/fimmu.2015.00262
23. Mortensen SA, Sander B, Jensen RK, Pedersen JS, Golas MM, Jensenius JC, et al. Structure and Activation of C1, the Complex Initiating the Classical Pathway of the Complement Cascade. *Proc Natl Acad Sci USA* (2017) 114 (5):986–91. doi: 10.1073/pnas.1616998114
24. Lu J, Kishore U. C1 Complex: An Adaptable Proteolytic Module for Complement and Non-Complement Functions. *Front Immunol* (2017) 8:592. doi: 10.3389/fimmu.2017.00592
25. Noris M, Remuzzi G. Overview of Complement Activation and Regulation. *Semin Nephrol* (2013) 33(6):479–92. doi: 10.1016/j.semnephrol.2013.08.001
26. Ehrnthaller C, Ignatius A, Gebhard F, Huber-Lang M. New Insights of an Old Defense System: Structure, Function, and Clinical Relevance of the Complement System. *Mol Med* (2011) 17(3-4):317–29. doi: 10.2119/molmed.2010.00149
27. Garred P, Genster N, Pilely K, Bayarri-Olmos R, Rosbjerg A, Ma YJ, et al. A Journey Through the Lectin Pathway of Complement-MBL and Beyond. *Immunol Rev* (2016) 274(1):74–97. doi: 10.1111/imr.12468
28. Iwaki D, Kanno K, Takahashi M, Endo Y, Matsushita M, Fujita T. The Role of Mannose-Binding Lectin-Associated Serine Protease-3 in Activation of the Alternative Complement Pathway. *J Immunol* (2011) 187(7):3751–8. doi: 10.4049/jimmunol.1100280
29. Heja D, Kocsis A, Dobo J, Szilagyi K, Szasz R, Zavodszky P, et al. Revised Mechanism of Complement Lectin-Pathway Activation Revealing the Role of Serine Protease MASP-1 as the Exclusive Activator of MASP-2. *Proc Natl Acad Sci USA* (2012) 109(26):10498–503. doi: 10.1073/pnas.1202588109
30. Dunkelberger JR, Song WC. Complement and Its Role in Innate and Adaptive Immune Responses. *Cell Res* (2010) 20(1):34–50. doi: 10.1038/cr.2009.139
31. Fishelson Z, Pangburn MK, Muller-Eberhard HJ. Characterization of the Initial C3 Convertase of the Alternative Pathway of Human Complement. *J Immunol* (1984) 132(3):1430–4.
32. Lesher AM, Nilsson B, Song WC. Properdin in Complement Activation and Tissue Injury. *Mol Immunol* (2013) 56(3):191–8. doi: 10.1016/j.molimm.2013.06.002
33. Walport MJ. Complement. Second of Two Parts. *N Engl J Med* (2001) 344 (15):1140–4. doi: 10.1056/NEJM200104123441506
34. Dobrina A, Pausa M, Fischetti F, Bulla R, Vecile E, Ferrero E, et al. Cytolytically Inactive Terminal Complement Complex Causes Transendothelial Migration of Polymorphonuclear Leukocytes *In Vitro* and *In Vivo*. *Blood* (2002) 99(1):185–92. doi: 10.1182/blood.v99.1.185
35. Wong EKS, Kavanagh D. Diseases of Complement Dysregulation-An Overview. *Semin Immunopathol* (2018) 40(1):49–64. doi: 10.1007/s00281-017-0663-8
36. Kajdacsi E, Jandrasics Z, Veszeli N, Mako V, Koncz A, Gulyas D, et al. Patterns of C1-Inhibitor/Plasma Serine Protease Complexes in Healthy Humans and in Hereditary Angioedema Patients. *Front Immunol* (2020) 11:794. doi: 10.3389/fimmu.2020.00794
37. Parej K, Dobo J, Zavodszky P, Gal P. The Control of the Complement Lectin Pathway Activation Revisited: Both C1-Inhibitor and Antithrombin Are Likely Physiological Inhibitors, While Alpha2-Macroglobulin Is Not. *Mol Immunol* (2013) 54(3-4):415–22. doi: 10.1016/j.molimm.2013.01.009
38. Jiang H, Wagner E, Zhang H, Frank MM. Complement 1 Inhibitor Is a Regulator of the Alternative Complement Pathway. *J Exp Med* (2001) 194 (11):1609–16. doi: 10.1084/jem.194.11.1609
39. Parente R, Clark SJ, Inforzato A, Day AJ. Complement Factor H in Host Defense and Immune Evasion. *Cell Mol Life Sci* (2017) 74(9):1605–24. doi: 10.1007/s00018-016-2418-4
40. Fujita T, Gigli I, Nussenzweig V. Human C4-Binding Protein. II. Role in Proteolysis of C4b by C3b-Inactivator. *J Exp Med* (1978) 148(4):1044–51. doi: 10.1084/jem.148.4.1044
41. Iida K, Nussenzweig V. Complement Receptor Is an Inhibitor of the Complement Cascade. *J Exp Med* (1981) 153(5):1138–50. doi: 10.1084/jem.153.5.1138
42. Nicholson-Weller A, Wang CE. Structure and Function of Decay Accelerating Factor CD55. *J Lab Clin Med* (1994) 123(4):485–91.
43. Liszewski MK, Post TW, Atkinson JP. Membrane Cofactor Protein (MCP or CD46): Newest Member of the Regulators of Complement Activation Gene Cluster. *Annu Rev Immunol* (1991) 9:431–55. doi: 10.1146/annurev.iy.09.040191.002243
44. Tedesco F, Bulla R, Fischetti F. Terminal Complement Complex: Regulation of Formation and Pathophysiological Functions. In: J Szebeni, editor. *The Complement System: Novel Roles in Health and Disease*. Boston, MA: Springer US (2004). p. 97–127.
45. Morgan BP, Meri S. Membrane Proteins That Protect Against Complement Lysis. *Springer Semin Immunopathol* (1994) 15(4):369–96. doi: 10.1007/BF01837366
46. Morgan BP, Campbell AK. The Recovery of Human Polymorphonuclear Leucocytes From Sublytic Complement Attack Is Mediated by Changes in Intracellular Free Calcium. *Biochem J* (1985) 231(1):205–8. doi: 10.1042/bj2310205
47. Zhang J, Li Y, Shan K, Wang L, Qiu W, Lu Y, et al. Sublytic C5b-9 Induces IL-6 and TGF-Beta1 Production by Glomerular Mesangial Cells in Rat Thy-1 Nephritis Through P300-Mediated C/EBPbeta Acetylation. *FASEB J* (2014) 28(3):1511–25. doi: 10.1096/fj.13-242693
48. Podack ER, Kolb WP, Muller-Eberhard HJ. The C5b-6 Complex: Formation, Isolation, and Inhibition of Its Activity by Lipoprotein and the S-Protein of Human Serum. *J Immunol* (1978) 120(6):1841–8.
49. Murphy BF, Kirszbaum L, Walker ID, d'Apice AJ. SP-40,40, a Newly Identified Normal Human Serum Protein Found in the SC5b-9 Complex of Complement and in the Immune Deposits in Glomerulonephritis. *J Clin Invest* (1988) 81(6):1858–64. doi: 10.1172/JCI113531
50. Murugaiah V, Varghese PM, Beirag N, De Cordova S, Sim RB, Kishore U. Complement Proteins as Soluble Pattern Recognition Receptors for Pathogenic Viruses. *Viruses* (2021) 13(5):824. doi: 10.3390/v13050824
51. Mellors J, Tipton T, Longet S, Carroll M. Viral Evasion of the Complement System and Its Importance for Vaccines and Therapeutics. *Front Immunol* (2020) 11:1450. doi: 10.3389/fimmu.2020.01450
52. Markiewski MM, Lambris JD. The Role of Complement in Inflammatory Diseases From Behind the Scenes Into the Spotlight. *Am J Pathol* (2007) 171 (3):715–27. doi: 10.2353/ajpath.2007.070166
53. Köhl J. Self, Non-Self, and Danger: A Complementary View. *Adv Exp Med Biol* (2006) 586:71–94. doi: 10.1007/0-387-34134-X_6
54. Zhou W. The New Face of Anaphylatoxins in Immune Regulation. *Immunobiology* (2012) 217(2):225–34. doi: 10.1016/j.imbio.2011.07.016
55. Agrawal P, Nawadkar R, Ojha H, Kumar J, Sahu A. Complement Evasion Strategies of Viruses: An Overview. *Front Microbiol* (2017) 8:1117. doi: 10.3389/fmicb.2017.01117
56. Sinha A, Singh AK, Kadni TS, Mullick J, Sahu A. Virus-Encoded Complement Regulators: Current Status. *Viruses* (2021) 13(2):208. doi: 10.3390/v13020208
57. Agrawal P, Sharma S, Pal P, Ojha H, Mullick J, Sahu A. The Imitation Game: A Viral Strategy to Subvert the Complement System. *FEBS Lett* (2020) 594 (16):2518–42. doi: 10.1002/1873-3468.13856

58. Noris M, Benigni A, Remuzzi G. The Case of Complement Activation in COVID-19 Multiorgan Impact. *Kidney Int* (2020) 98(2):314–22. doi: 10.1016/j.kint.2020.05.013
59. Ali YM, Ferrari M, Lynch NJ, Yaseen S, Dudler T, Gragerov S, et al. Lectin Pathway Mediates Complement Activation by SARS-CoV-2 Proteins. *Front Immunol* (2021) 12:714511. doi: 10.3389/fimmu.2021.714511
60. Yu J, Yuan X, Chen H, Chaturvedi S, Braunstein EM, Brodsky RA. Direct Activation of the Alternative Complement Pathway by SARS-CoV-2 Spike Proteins Is Blocked by Factor D Inhibition. *Blood* (2020) 136(18):2080–9. doi: 10.1182/blood.2020008248
61. Macor P, Durigutto P, Mangogna A, Bussani R, De Maso L, D'Errico S, et al. Multiple-Organ Complement Deposition on Vascular Endothelium in COVID-19 Patients. *Biomedicines* (2021) 9(8):1003. doi: 10.3390/biomedicines9081003
62. Gao T, Hu M, Zhang X, Li H, Zhu L, Liu H, et al. Highly Pathogenic Coronavirus N Protein Aggravates Lung Injury by MASP-2-Mediated Complement Over-Activation. *medRxiv* (2020). doi: 10.1101/2020.03.29.20041962 2020.03.29.20041962.
63. Risitano AM, Mastellos DC, Huber-Lang M, Yancopoulou D, Garlanda C, Ciceri F, et al. Complement as a Target in COVID-19? *Nat Rev Immunol* (2020) 20(6):343–4. doi: 10.1038/s41577-020-0320-7
64. Carvelli J, Demaria O, Vely F, Batista L, Chouaki Benmansour N, Fares J, et al. Association of COVID-19 Inflammation With Activation of the C5a-C5aR1 Axis. *Nature* (2020) 588(7836):146–50. doi: 10.1038/s41586-020-2600-6
65. Fodil S, Annane D. Complement Inhibition and COVID-19: The Story So Far. *Immunotargets Ther* (2021) 10:273–84. doi: 10.2147/ITT.S284830
66. Lo MW, Kemper C, Woodruff TM. COVID-19: Complement, Coagulation, and Collateral Damage. *J Immunol* (2020) 205(6):1488–95. doi: 10.4049/jimmunol.2000644
67. Java A, Apicelli AJ, Liszewski MK, Coler-Reilly A, Atkinson JP, Kim AH, et al. The Complement System in COVID-19: Friend and Foe? *JCI Insight* (2020) 5(15):e140711. doi: 10.1172/jci.insight.140711
68. Chouaki Benmansour N, Carvelli J, Vivier E. Complement Cascade in Severe Forms of COVID-19: Recent Advances in Therapy. *Eur J Immunol* (2021) 51(7):1652–9. doi: 10.1002/eji.202048959
69. Goveia J, Rohlenova K, Taverna F, Treps L, Conradi LC, Pircher A, et al. An Integrated Gene Expression Landscape Profiling Approach to Identify Lung Tumor Endothelial Cell Heterogeneity and Angiogenic Candidates. *Cancer Cell* (2020) 37(1):21–36.e13. doi: 10.1016/j.ccell.2019.12.001
70. Siddiqi HK, Libby P, Ridker PM. COVID-19 - A Vascular Disease. *Trends Cardiovasc Med* (2021) 31(1):1–5. doi: 10.1016/j.tcm.2020.10.005
71. Libby P, Luscher T. COVID-19 Is, in the End, an Endothelial Disease. *Eur Heart J* (2020) 41(32):3038–44. doi: 10.1093/eurheartj/ehaa623
72. Teuwen LA, Geldhof V, Pasut A, Carmeliet P. COVID-19: The Vasculature Unleashed. *Nat Rev Immunol* (2020) 20(7):389–91. doi: 10.1038/s41577-020-0343-0
73. Abassi Z, Skorecki K, Hamo-Giladi DB, Kruzel-Davila E, Heyman SN. Kinins and Chymase: The Forgotten Components of the Renin-Angiotensin System and Their Implications in COVID-19 Disease. *Am J Physiol Lung Cell Mol Physiol* (2021) 320(3):L422–9. doi: 10.1152/ajplung.00548.2020
74. Dagnino APA, Campos MM, Silva RBM. Kinins and Their Receptors in Infectious Diseases. *Pharmaceut (Basel)* (2020) 13(9):215. doi: 10.3390/ph13090215
75. Simoes e Silva AC, Silveira KD, Ferreira AJ, Teixeira MM. ACE2, Angiotensin-(1-7) and Mas Receptor Axis in Inflammation and Fibrosis. *Br J Pharmacol* (2013) 169(3):477–92. doi: 10.1111/bph.12159
76. Perico L, Benigni A, Casiraghi F, Ng LFP, Renia L, Remuzzi G. Immunity, Endothelial Injury and Complement-Induced Coagulopathy in COVID-19. *Nat Rev Nephrol* (2021) 17(1):46–64. doi: 10.1038/s41581-020-00357-4
77. Song WC, FitzGerald GA. COVID-19, Microangiopathy, Hemostatic Activation, and Complement. *J Clin Invest* (2020) 130(8):3950–3. doi: 10.1172/JCI140183
78. Magro C, Mulvey JJ, Berlin D, Nuovo G, Salvatore S, Harp J, et al. Complement Associated Microvascular Injury and Thrombosis in the Pathogenesis of Severe COVID-19 Infection: A Report of Five Cases. *Transl Res* (2020) 220:1–13. doi: 10.1016/j.trsl.2020.04.007
79. Barrett CD, Hsu AT, Ellson CD, Miyazawa BY, Kong YW, Greenwood JD, et al. Blood Clotting and Traumatic Injury With Shock Mediates Complement-Dependent Neutrophil Priming for Extracellular ROS, ROS-Dependent Organ Injury and Coagulopathy. *Clin Exp Immunol* (2018) 194(1):103–17. doi: 10.1111/cei.13166
80. Panigada M, Bottino N, Tagliabue P, Grasselli G, Novembrino C, Chantarangkul V, et al. Hypercoagulability of COVID-19 Patients in Intensive Care Unit: A Report of Thromboelastography Findings and Other Parameters of Hemostasis. *J Thromb Haemost* (2020) 18(7):1738–42. doi: 10.1111/jth.14850
81. Bosmann M. Complement Control for COVID-19. *Sci Immunol* (2021) 6(59):eabj1014. doi: 10.1126/sciimmunol.abj1014
82. Markiewski MM, Nilsson B, Ekdahl KN, Mollnes TE, Lambris JD. Complement and Coagulation: Strangers or Partners in Crime? *Trends Immunol* (2007) 28(4):184–92. doi: 10.1016/j.it.2007.02.006
83. Madhusudhan T, Kerlin BA, Isermann B. The Emerging Role of Coagulation Proteases in Kidney Disease. *Nat Rev Nephrol* (2016) 12(2):94–109. doi: 10.1038/nrneph.2015.177
84. Weidmann H, Heikaus L, Long AT, Naudin C, Schluter H, Renne T. The Plasma Contact System, a Protease Cascade at the Nexus of Inflammation, Coagulation and Immunity. *Biochim Biophys Acta Mol Cell Res* (2017) 1864(11 Pt B):2118–27. doi: 10.1016/j.bbamcr.2017.07.009
85. Amara U, Rittirsch D, Flierl M, Bruckner U, Klos A, Gebhard F, et al. Interaction Between the Coagulation and Complement System. *Adv Exp Med Biol* (2008) 632:71–9. doi: 10.1007/978-0-387-78952-1_6
86. Schmaier AH, Stavrou EX. Factor XII - What's Important But Not Commonly Thought About. *Res Pract Thromb Haemost* (2019) 3(4):599–606. doi: 10.1002/rth2.12235
87. Maas C. Plasminflammation-An Emerging Pathway to Bradykinin Production. *Front Immunol* (2019) 10:2046. doi: 10.3389/fimmu.2019.02046
88. Rovai ES, Alves T, Holzhausen M. Protease-Activated Receptor 1 as a Potential Therapeutic Target for COVID-19. *Exp Biol Med (Maywood)* (2021) 246(6):688–94. doi: 10.1177/1535370220978372
89. Cimmino G, Cirillo P. Tissue Factor: Newer Concepts in Thrombosis and Its Role Beyond Thrombosis and Hemostasis. *Cardiovasc Diagn Ther* (2018) 8(5):581–93. doi: 10.21037/cdt.2018.10.14
90. Tedesco F, Fischetti F, Pausa M, Dobrina A, Sim RB, Daha MR. Complement-Endothelial Cell Interactions: Pathophysiological Implications. *Mol Immunol* (1999) 36(4-5):261–8. doi: 10.1016/s0161-5890(99)90054-8
91. Tedesco F, Pausa M, Nardon E, Introna M, Mantovani A, Dobrina A. The Cytolytically Inactive Terminal Complement Complex Activates Endothelial Cells to Express Adhesion Molecules and Tissue Factor Procoagulant Activity. *J Exp Med* (1997) 185(9):1619–27. doi: 10.1084/jem.185.9.1619
92. Saadi S, Holzknecht RA, Patte CP, Stern DM, Platt JL. Complement-Mediated Regulation of Tissue Factor Activity in Endothelium. *J Exp Med* (1995) 182(6):1807–14. doi: 10.1084/jem.182.6.1807
93. Ritis K, Doumas M, Mastellos D, Micheli A, Giaglis S, Magotti P, et al. A Novel C5a Receptor-Tissue Factor Cross-Talk in Neutrophils Links Innate Immunity to Coagulation Pathways. *J Immunol* (2006) 177(7):4794–802. doi: 10.4049/jimmunol.177.7.4794
94. Langer F, Spath B, Fischer C, Stolz M, Ayuk FA, Kroger N, et al. Rapid Activation of Monocyte Tissue Factor by Antithymocyte Globulin Is Dependent on Complement and Protein Disulfide Isomerase. *Blood* (2013) 121(12):2324–35. doi: 10.1182/blood-2012-10-460493
95. Escher R, Breakey N, Lammle B. Severe COVID-19 Infection Associated With Endothelial Activation. *Thromb Res* (2020) 190:62. doi: 10.1016/j.thromres.2020.04.014
96. Varga Z, Flammer AJ, Steiger P, Haberecker M, Andermatt R, Zinkernagel AS, et al. Endothelial Cell Infection and Endotheliitis in COVID-19. *Lancet* (2020) 395(10234):1417–8. doi: 10.1016/S0140-6736(20)30937-5
97. Sadler JE. Biochemistry and Genetics of Von Willebrand Factor. *Annu Rev Biochem* (1998) 67:395–424. doi: 10.1146/annurev.biochem.67.1.395
98. Patmore S, Dhami SPS, O'Sullivan JM. Von Willebrand Factor and Cancer; Metastasis and Coagulopathies. *J Thromb Haemost* (2020) 18(10):2444–56. doi: 10.1111/jth.14976
99. Hattori R, Hamilton KK, McEver RP, Sims PJ. Complement Proteins C5b-9 Induce Secretion of High Molecular Weight Multimers of Endothelial Von Willebrand Factor and Translocation of Granule Membrane Protein GMP-140 to the Cell Surface. *J Biol Chem* (1989) 264(15):9053–60. doi: 10.1016/S0021-9258(18)81901-9

100. Hamilton KK, Hattori R, Esmon CT, Sims PJ. Complement Proteins C5b-9 Induce Vesiculation of the Endothelial Plasma Membrane and Expose Catalytic Surface for Assembly of the Prothrombinase Enzyme Complex. *J Biol Chem* (1990) 265(7):3809–14. doi: 10.1016/S0021-9258(19)39666-8
101. Nolasco L, Nolasco J, Feng S, Afshar-Kharghan V, Moake J. Human Complement Factor H Is a Reductase for Large Soluble Von Willebrand Factor Multimers–Brief Report. *Arterioscler Thromb Vasc Biol* (2013) 33(11):2524–8. doi: 10.1161/ATVBAHA.113.302280
102. Goshua G, Pine AB, Meizlish ML, Chang CH, Zhang H, Bahel P, et al. Endotheliopathy in COVID-19-Associated Coagulopathy: Evidence From a Single-Centre, Cross-Sectional Study. *Lancet Haematol* (2020) 7(8):e575–82. doi: 10.1016/S2352-3026(20)30216-7
103. Ruggeri ZM, Mendolicchio GL. Adhesion Mechanisms in Platelet Function. *Circ Res* (2007) 100(12):1673–85. doi: 10.1161/01.RES.0000267878.97021.ab
104. Petri B, Broermann A, Li H, Khandoga AG, Zarbock A, Krombach F, et al. Von Willebrand Factor Promotes Leukocyte Extravasation. *Blood* (2010) 116(22):4712–9. doi: 10.1182/blood-2010-03-276311
105. Hattori R, Hamilton KK, Fugate RD, McEver RP, Sims PJ. Stimulated Secretion of Endothelial Von Willebrand Factor Is Accompanied by Rapid Redistribution to the Cell Surface of the Intracellular Granule Membrane Protein GMP-140. *J Biol Chem* (1989) 264(14):7768–71. doi: 10.1016/S0021-9258(18)83104-0
106. Keizer MP, Pouw RB, Kamp AM, Patiwael S, Marsman G, Hart MH, et al. TFPI Inhibits Lectin Pathway of Complement Activation by Direct Interaction With MASP-2. *Eur J Immunol* (2015) 45(2):544–50. doi: 10.1002/eji.201445070
107. Sims PJ, Faioni E, Wiedmer T, Shattil S. Complement Proteins C5b-9 Cause Release of Membrane Vesicles From the Platelet Surface That Are Enriched in the Membrane Receptor for Coagulation Factor Va and Express Prothrombinase Activity. *J Biol Chem* (1988) 263(34):18205–12. doi: 10.1016/S0021-9258(19)81346-7
108. Amara U, Flierl MA, Rittirsch D, Klos A, Chen H, Acker B, et al. Molecular Intercommunication Between the Complement and Coagulation Systems. *J Immunol* (2010) 185(9):5628–36. doi: 10.4049/jimmunol.0903678
109. Davis AE3rd. Biological Effects of C1 Inhibitor. *Drug News Perspect* (2004) 17(7):439–46. doi: 10.1358/dnp.2004.17.7.863703
110. Meijers JC, Vlooswijk RA, Bouma BN. Inhibition of Human Blood Coagulation Factor XIa by C-1 Inhibitor. *Biochemistry* (1988) 27(3):959–63. doi: 10.1021/bi00403a018
111. Cugno M, Bos I, Lubbers Y, Hack CE, Agostoni A. *In Vitro* Interaction of C1-Inhibitor With Thrombin. *Blood Coagul Fibrinolysis* (2001) 12(4):253–60. doi: 10.1097/00001721-200106000-00005
112. Thomson TM, Toscano-Guerra E, Casis E, Paciucci R. C1 Esterase Inhibitor and the Contact System in COVID-19. *Br J Haematol* (2020) 190(4):520–4. doi: 10.1111/bjh.16938
113. Adesanya TMA, Campbell CM, Cheng L, Ogbogu PU, Kahwash R. C1 Esterase Inhibition: Targeting Multiple Systems in COVID-19. *J Clin Immunol* (2021) 41(4):729–32. doi: 10.1007/s10875-021-00972-1
114. Shen B, Yi X, Sun Y, Bi X, Du J, Zhang C, et al. Proteomic and Metabolomic Characterization of COVID-19 Patient Sera. *Cell* (2020) 182(1):59–72 e15. doi: 10.1016/j.cell.2020.05.032
115. Heurich M, Preston RJ, O'Donnell VB, Morgan BP, Collins PW. Thrombomodulin Enhances Complement Regulation Through Strong Affinity Interactions With Factor H and C3b-Factor H Complex. *Thromb Res* (2016) 145:84–92. doi: 10.1016/j.thromres.2016.07.017
116. Foley JH, Walton BL, Aleman MM, O'Byrne AM, Lei V, Harrasser M, et al. Complement Activation in Arterial and Venous Thrombosis Is Mediated by Plasmin. *EBioMedicine* (2016) 5:175–82. doi: 10.1016/j.ebiom.2016.02.011
117. Campbell WD, Lazoura E, Okada N, Okada H. Inactivation of C3a and C5a Octapeptides by Carboxypeptidase R and Carboxypeptidase N. *Microbiol Immunol* (2002) 46(2):131–4. doi: 10.1111/j.1348-0421.2002.tb02669.x
118. Nougier C, Benoit R, Simon M, Desmurs-Clavel H, Marcotte G, Argaud L, et al. Hypofibrinolytic State and High Thrombin Generation may Play a Major Role in SARS-COV2 Associated Thrombosis. *J Thromb Haemost* (2020) 18(9):2215–9. doi: 10.1111/jth.15016
119. Speth C, Rambach G, Wurzner R, Lass-Florl C, Kozarcanin H, Hamad OA, et al. Complement and Platelets: Mutual Interference in the Immune Network. *Mol Immunol* (2015) 67(1):108–18. doi: 10.1016/j.molimm.2015.03.244
120. Kim H, Conway EM. Platelets and Complement Cross-Talk in Early Atherogenesis. *Front Cardiovasc Med* (2019) 6:131. doi: 10.3389/fcvm.2019.00131
121. Klos A, Tenner AJ, Johswich KO, Ager RR, Reis ES, Kohl J. The Role of the Anaphylatoxins in Health and Disease. *Mol Immunol* (2009) 46(14):2753–66. doi: 10.1016/j.molimm.2009.04.027
122. Polley MJ, Nachman RL. Human Platelet Activation by C3a and C3a Des-Arg. *J Exp Med* (1983) 158(2):603–15. doi: 10.1084/jem.158.2.603
123. Del Conde I, Cruz MA, Zhang H, Lopez JA, Afshar-Kharghan V. Platelet Activation Leads to Activation and Propagation of the Complement System. *J Exp Med* (2005) 201(6):871–9. doi: 10.1084/jem.20041497
124. Bettoni S, Galbusera M, Gastoldi S, Donadelli R, Tentori C, Sparta G, et al. Interaction Between Multimeric Von Willebrand Factor and Complement: A Fresh Look to the Pathophysiology of Microvascular Thrombosis. *J Immunol* (2017) 199(3):1021–40. doi: 10.4049/jimmunol.1601121
125. Wiedmer T, Esmon CT, Sims PJ. Complement Proteins C5b-9 Stimulate Procoagulant Activity Through Platelet Prothrombinase. *Blood* (1986) 68(4):875–80. doi: 10.1182/blood.V68.4.875.875
126. Mol BWJ, Roberts CT, Thangaratinam S, Magee LA, de Groot CJM, Hofmeyr GJ. Pre-Eclampsia. *Lancet* (2016) 387(10022):999–1011. doi: 10.1016/S0140-6736(15)00070-7
127. Sjaus A, McKeen DM, George RB. Hypertensive Disorders of Pregnancy. *Can J Anaesth* (2016) 63(9):1075–97. doi: 10.1007/s12630-016-0689-8
128. Haram K, Svendsen E, Abildgaard U. The HELLP Syndrome: Clinical Issues and Management. A Review. *BMC Pregnancy Childbirth* (2009) 9:8. doi: 10.1186/1471-2393-9-8
129. Redman CW, Sargent IL, Staff AC. IFPA Senior Award Lecture: Making Sense of Pre-Eclampsia - Two Placental Causes of Preeclampsia? *Placenta* (2014) 35 Suppl:S20–5. doi: 10.1016/j.placenta.2013.12.008
130. Burton GJ, Redman CW, Roberts JM, Moffett A. Pre-Eclampsia: Pathophysiology and Clinical Implications. *BMJ* (2019) 366:l2381. doi: 10.1136/bmj.l2381
131. Bulla R, Villa A, Bossi F, Cassetti A, Radillo O, Spessotto P, et al. VE-Cadherin Is a Critical Molecule for Trophoblast-Endothelial Cell Interaction in Decidual Spiral Arteries. *Exp Cell Res* (2005) 303(1):101–13. doi: 10.1016/j.yexcr.2004.09.015
132. Agostinis C, Bulla R, Tripodo C, Gismondi A, Stabile H, Bossi F, et al. An Alternative Role of C1q in Cell Migration and Tissue Remodeling: Contribution to Trophoblast Invasion and Placental Development. *J Immunol* (2010) 185(7):4420–9. doi: 10.4049/jimmunol.0903215
133. Balduit A, Mangogna A, Agostinis C, Zito G, Romano F, Ricci G, et al. Zinc Oxide Exerts Anti-Inflammatory Properties on Human Placental Cells. *Nutrients* (2020) 12(6):1822. doi: 10.3390/nu12061822
134. Bulla R, Fischetti F, Bossi F, Tedesco F. Feto-Maternal Immune Interaction at the Placental Level. *Lupus* (2004) 13(9):625–9. doi: 10.1191/0961203304lu2010oa
135. Roland CS, Hu J, Ren CE, Chen H, Li J, Varvoutis MS, et al. Morphological Changes of Placental Syncytium and Their Implications for the Pathogenesis of Preeclampsia. *Cell Mol Life Sci* (2016) 73(2):365–76. doi: 10.1007/s00018-015-2069-x
136. Bulla R, Bossi F, Radillo O, de Seta F, Tedesco F. Placental Trophoblast and Endothelial Cells as Target of Maternal Immune Response. *Autoimmunity* (2003) 36(1):11–8. doi: 10.1080/0891693031000067331
137. Saito S, Shiozaki A, Nakashima A, Sakai M, Sasaki Y. The Role of the Immune System in Preeclampsia. *Mol Aspects Med* (2007) 28(2):192–209. doi: 10.1016/j.mam.2007.02.006
138. Mangogna A, Agostinis C, Ricci G, Romano F, Bulla R. Overview of Procalcitonin in Pregnancy and in Pre-Eclampsia. *Clin Exp Immunol* (2019) 198(1):37–46. doi: 10.1111/cei.13311
139. Haeger M, Bengtson A, Karlsson K, Heideman M. Complement Activation and Anaphylatoxin (C3a and C5a) Formation in Preeclampsia and by Amniotic Fluid. *Obstet Gynecol* (1989) 73(4):551–6.
140. Denny KJ, Coulthard LG, Finnell RH, Callaway LK, Taylor SM, Woodruff TM. Elevated Complement Factor C5a in Maternal and Umbilical Cord Plasma in Preeclampsia. *J Reprod Immunol* (2013) 97(2):211–6. doi: 10.1016/j.jri.2012.11.006

141. Agostinis C, Stampalija T, Tannetta D, Loganes C, Vecchi Brumatti L, De Seta F, et al. Complement Component C1q as Potential Diagnostic But Not Predictive Marker of Preeclampsia. *Am J Reprod Immunol* (2016) 76(6):475–81. doi: 10.1111/aji.12586
142. Burwick RM, Fichorova RN, Dawood HY, Yamamoto HS, Feinberg BB. Urinary Excretion of C5b-9 in Severe Preeclampsia: Tipping the Balance of Complement Activation in Pregnancy. *Hypertension* (2013) 62(6):1040–5. doi: 10.1161/HYPERTENSIONAHA.113.01420
143. Lynch AM, Gibbs RS, Murphy JR, Byers T, Neville MC, Giclas PC, et al. Complement Activation Fragment Bb in Early Pregnancy and Spontaneous Preterm Birth. *Am J Obstet Gynecol* (2008) 199(4):354.e1–8. doi: 10.1016/j.ajog.2008.07.044
144. Petitbarat M, Durigutto P, Macor P, Bulla R, Palmioli A, Bernardi A, et al. Critical Role and Therapeutic Control of the Lectin Pathway of Complement Activation in an Abortion-Prone Mouse Mating. *J Immunol* (2015) 195 (12):5602–7. doi: 10.4049/jimmunol.1501361
145. Lokki AI, Heikkinen-Eloranta J, Jarva H, Saisto T, Lokki ML, Laivuori H, et al. Complement Activation and Regulation in Preeclamptic Placenta. *Front Immunol* (2014) 5:312. doi: 10.3389/fimmu.2014.00312
146. Chaouat G, Petitbarat M, Bulla R, Dubanchet S, Valdivia K, Ledee N, et al. Early Regulators in Abortion and Implications for a Preeclampsia Model. *J Reprod Immunol* (2009) 82(2):131–40. doi: 10.1016/j.jri.2009.08.004
147. Hypertension in pregnancy. Report of the American College of Obstetricians and Gynecologists' Task Force on Hypertension in Pregnancy. *Obstet Gynecol* (2013) 122(5):1122–31. doi: 10.1097/01.AOG.0000437382.03963.88
148. Powers RW, Jeyabalan A, Clifton RG, Van Dorsten P, Hauth JC, Klebanoff MA, et al. Soluble Fms-Like Tyrosine Kinase 1 (Sflt1), Endoglin and Placental Growth Factor (PlGF) in Preeclampsia Among High Risk Pregnancies. *PloS One* (2010) 5 (10):e13263. doi: 10.1371/journal.pone.0013263
149. Kleinrouweler CE, Wiegerinck MM, Ris-Stalpers C, Bossuyt PM, van der Post JA, von Dadelszen P, et al. Accuracy of Circulating Placental Growth Factor, Vascular Endothelial Growth Factor, Soluble Fms-Like Tyrosine Kinase 1 and Soluble Endoglin in the Prediction of Pre-Eclampsia: A Systematic Review and Meta-Analysis. *BJOG* (2012) 119(7):778–87. doi: 10.1111/j.1471-0528.2012.03311.x
150. Chau K, Hennessy A, Makris A. Placental Growth Factor and Pre-Eclampsia. *J Hum Hypertens* (2017) 31(12):782–6. doi: 10.1038/jhh.2017.61
151. Lecarpentier E, Tsatsaris V. Angiogenic Balance (Sflt-1/PlGF) and Preeclampsia. *Ann Endocrinol (Paris)* (2016) 77(2):97–100. doi: 10.1016/j.ando.2016.04.007
152. Zeisler H, Llurba E, Chantraine F, Vatish M, Staff AC, Sennstrom M, et al. Predictive Value of the Sflt-1:PlGF Ratio in Women With Suspected Preeclampsia. *N Engl J Med* (2016) 374(1):13–22. doi: 10.1056/NEJMoa1414838
153. Hund M, Allegranza D, Schoedl M, Dilba P, Verhagen-Kamerbeek W, Stepan H. Multicenter Prospective Clinical Study to Evaluate the Prediction of Short-Term Outcome in Pregnant Women With Suspected Preeclampsia (PROGNOSIS): Study Protocol. *BMC Pregnancy Childbirth* (2014) 14:324. doi: 10.1186/1471-2393-14-324
154. Zaigham M, Andersson O. Maternal and Perinatal Outcomes With COVID-19: A Systematic Review of 108 Pregnancies. *Acta Obstet Gynecol Scand* (2020) 99(7):823–9. doi: 10.1111/aogs.13867
155. Di Mascio D, Buca D, Berghella V, Khalil A, Rizzo G, Odibo A, et al. Counseling in Maternal-Fetal Medicine: SARS-CoV-2 Infection in Pregnancy. *Ultrasound Obstet Gynecol* (2021) 57(5):687–97. doi: 10.1002/uog.23628
156. Abedzadeh-Kalahroudi M, Sehat M, Vahedpour Z, Talebian P, Haghighi A. Clinical and Obstetric Characteristics of Pregnant Women With Covid-19: A Case Series Study on 26 Patients. *Taiwan J Obstet Gynecol* (2021) 60(3):458–62. doi: 10.1016/j.tjog.2021.03.012
157. Chen H, Guo J, Wang C, Luo F, Yu X, Zhang W, et al. Clinical Characteristics and Intrauterine Vertical Transmission Potential of COVID-19 Infection in Nine Pregnant Women: A Retrospective Review of Medical Records. *Lancet* (2020) 395(10226):809–15. doi: 10.1016/S0140-6736(20)30360-3
158. Narang K, Enninga EAL, Gunaratne M, Ibirogba ER, Trad ATA, Elrefaei A, et al. SARS-CoV-2 Infection and COVID-19 During Pregnancy: A Multidisciplinary Review. *Mayo Clin Proc* (2020) 95(8):1750–65. doi: 10.1016/j.mayocp.2020.05.011
159. Papageorghiou AT, Deruelle P, Gunier RB, Rauch S, Garcia-May PK, Mhatre M, et al. Preeclampsia and COVID-19: Results From the INTERCOVID Prospective Longitudinal Study. *Am J Obstet Gynecol* (2021) 225(3):289.e1–e17. doi: 10.1016/j.ajog.2021.05.014
160. Mendoza M, Garcia-Ruiz I, Maiz N, Rodo C, Garcia-Manau P, Serrano B, et al. Pre-Eclampsia-Like Syndrome Induced by Severe COVID-19: A Prospective Observational Study. *BJOG* (2020) 127(11):1374–80. doi: 10.1111/1471-0528.16339
161. Rosenbloom JI, Raghuraman N, Carter EB, Kelly JC. Coronavirus Disease 2019 Infection and Hypertensive Disorders of Pregnancy. *Am J Obstet Gynecol* (2021) 224(6):623–4. doi: 10.1016/j.ajog.2021.03.001
162. Jing Y, Run-Qian L, Hao-Ran W, Hao-Ran C, Ya-Bin L, Yang G, et al. Potential Influence of COVID-19/ACE2 on the Female Reproductive System. *Mol Hum Reprod* (2020) 26(6):367–73. doi: 10.1093/molehr/gaaa030
163. Kornacki J, Wirstlein P, Wender-Ozegowska E. Serum Levels of Soluble FMS-Like Tyrosine Kinase 1 and Endothelial Glycocalyx Components in Early- and Late-Onset Preeclampsia. *J Matern Fetal Neonatal Med* (2021) 1–5. doi: 10.1080/14767058.2021.1949704
164. Ackermann M, Verleden SE, Kuehnel M, Haverich A, Welte T, Laenger F, et al. Pulmonary Vascular Endothelialitis, Thrombosis, and Angiogenesis in Covid-19. *N Engl J Med* (2020) 383(2):120–8. doi: 10.1056/NEJMoa2015432
165. Smadja DM, Mentzer SJ, Fontenay M, Laffan MA, Ackermann M, Helms J, et al. COVID-19 Is a Systemic Vascular Hemopathy: Insight for Mechanistic and Clinical Aspects. *Angiogenesis* (2021) 24(4):755–88. doi: 10.1007/s10456-021-09805-6
166. Shapiro NI, Schuetz P, Yano K, Sorasaki M, Parikh SM, Jones AE, et al. The Association of Endothelial Cell Signaling, Severity of Illness, and Organ Dysfunction in Sepsis. *Crit Care* (2010) 14(5):R182. doi: 10.1186/cc9290
167. Palmer KR, Tong S, Kaitu'u-Lino TJ. Placental-Specific sFLT-1: Role in Pre-Eclamptic Pathophysiology and Its Translational Possibilities for Clinical Prediction and Diagnosis. *Mol Hum Reprod* (2017) 23(2):69–78. doi: 10.1093/molehr/gaw077
168. Smadja DM, Nunes H, Juvin K, Bertil S, Valeyre D, Gaussem P, et al. Increase in Both Angiogenic and Angiostatic Mediators in Patients With Idiopathic Pulmonary Fibrosis. *Pathol Biol (Paris)* (2014) 62(6):391–4. doi: 10.1016/j.patbio.2014.07.006
169. Negro A, Fama A, Penna D, Belloni L, Zerbini A, Giuri PG. SFLT-1 Levels in COVID-19 Patients: Association With Outcome and Thrombosis. *Am J Hematol* (2021) 96(2):E41–3. doi: 10.1002/ajh.26037
170. Smadja DM, Philippe A, Bory O, Gendron N, Beauvais A, Gruest M, et al. Placental Growth Factor Level in Plasma Predicts COVID-19 Severity and in-Hospital Mortality. *J Thromb Haemost* (2021) 19(7):1823–30. doi: 10.1111/jth.15339
171. Giardini V, Carrer A, Casati M, Contro E, Vergani P, Gambacorti-Passerini C. Increased sFLT-1/PlGF Ratio in COVID-19: A Novel Link to Angiotensin II-Mediated Endothelial Dysfunction. *Am J Hematol* (2020) 95(8):E188–91. doi: 10.1002/ajh.25882
172. Amorim MM, Takemoto MLS, Katz L. Re: Pre-Eclampsia-Like Syndrome Induced by Severe Coronavirus Disease 2019: A Prospective Observational Study. *BJOG* (2020) 127(12):1577. doi: 10.1111/1471-0528.16402
173. Young BC, Levine RJ, Karumanchi SA. Pathogenesis of Preeclampsia. *Annu Rev Pathol* (2010) 5:173–92. doi: 10.1146/annurev-pathol-121808-102149
174. Dusse LM, Rios DR, Pinheiro MB, Cooper AJ, Lwaleed BA. Pre-Eclampsia: Relationship Between Coagulation, Fibrinolysis and Inflammation. *Clin Chim Acta* (2011) 412(1-2):17–21. doi: 10.1016/j.cca.2010.09.030
175. Pinheiro MB, Gomes KB, Dusse LM. Fibrinolytic System in Preeclampsia. *Clin Chim Acta* (2013) 416:67–71. doi: 10.1016/j.cca.2012.10.060
176. Lippi G, Plebani M, Henry BM. Thrombocytopenia Is Associated With Severe Coronavirus Disease 2019 (COVID-19) Infections: A Meta-Analysis. *Clin Chim Acta* (2020) 506:145–8. doi: 10.1016/j.cca.2020.03.022
177. Lippi G, Favaloro EJ. D-Dimer Is Associated With Severity of Coronavirus Disease 2019: A Pooled Analysis. *Thromb Haemost* (2020) 120(5):876–8. doi: 10.1055/s-0040-1709650
178. Huang C, Wang Y, Li X, Ren L, Zhao J, Hu Y, et al. Clinical Features of Patients Infected With 2019 Novel Coronavirus in Wuhan, China. *Lancet* (2020) 395(10223):497–506. doi: 10.1016/S0140-6736(20)30183-5
179. Wang D, Hu B, Hu C, Zhu F, Liu X, Zhang J, et al. Clinical Characteristics of 138 Hospitalized Patients With 2019 Novel Coronavirus-Infected

Pneumonia in Wuhan, China. *JAMA* (2020) 323(11):1061–9. doi: 10.1001/jama.2020.1585
180. Medeiros LT, Peracoli JC, Bannwart-Castro CF, Romao M, Weel IC, Golim MA, et al. Monocytes From Pregnant Women With Pre-Eclampsia Are Polarized to a M1 Phenotype. *Am J Reprod Immunol* (2014) 72(1):5–13. doi: 10.1111/aji.12222
181. Costela-Ruiz VJ, Illescas-Montes R, Puerta-Puerta JM, Ruiz C, Melguizo-Rodriguez L. SARS-CoV-2 Infection: The Role of Cytokines in COVID-19 Disease. *Cytokine Growth Factor Rev* (2020) 54:62–75. doi: 10.1016/j.cytogfr.2020.06.001
182. Leavitt AO, Li Q, Chan ED. Re: Pre-Eclampsia-Like Syndrome Induced by Severe COVID-19: A Prospective Observational Study: Common Pathophysiology of Pre-Eclampsia and Severe COVID-19? *BJOG* (2021) 128(3):618–9. doi: 10.1111/1471-0528.16584
183. Jayarangaiah A, Kariyanna PT, Chen X, Jayarangaiah A, Kumar A. COVID-19-Associated Coagulopathy: An Exacerbated Immunothrombosis Response. *Clin Appl Thromb Hemost* (2020) 26:1076029620943293. doi: 10.1177/1076029620943293
184. Marder W, Knight JS, Kaplan MJ, Somers EC, Zhang X, O'Dell AA, et al. Placental Histology and Neutrophil Extracellular Traps in Lupus and Pre-Eclampsia Pregnancies. *Lupus Sci Med* (2016) 3(1):e000134. doi: 10.1136/lupus-2015-000134
185. Middleton EA, He XY, Denorme F, Campbell RA, Ng D, Salvatore SP, et al. Neutrophil Extracellular Traps Contribute to Immunothrombosis in COVID-19 Acute Respiratory Distress Syndrome. *Blood* (2020) 136 (10):1169–79. doi: 10.1182/blood.2020007008
186. de Bont CM, Boelens WC, Pruijn GJM. NETosis, Complement, and Coagulation: A Triangular Relationship. *Cell Mol Immunol* (2019) 16 (1):19–27. doi: 10.1038/s41423-018-0024-0
187. Zemet R, Dulitzki M, Baum M, Ofer Friedman H, Morag I, Simchen MJ. Early-Onset Preeclampsia - The Impact of Antiphospholipid Antibodies on Disease Severity. *Eur J Obstet Gynecol Reprod Biol* (2021) 263:79–84. doi: 10.1016/j.ejogrb.2021.06.006
188. Zuo Y, Estes SK, Ali RA, Gandhi AA, Yalavarthi S, Shi H, et al. Prothrombotic Autoantibodies in Serum From Patients Hospitalized With COVID-19. *Sci Transl Med* (2020) 12(570):eabd3876. doi: 10.1126/scitranslmed.abd3876
189. Holers VM, Girardi G, Mo L, Guthridge JM, Molina H, Pierangeli SS, et al. Complement C3 Activation Is Required for Antiphospholipid Antibody-Induced Fetal Loss. *J Exp Med* (2002) 195(2):211–20. doi: 10.1084/jem.200116116
190. Galli M, Borrelli G, Jacobsen EM, Marfisi RM, Finazzi G, Marchioli R, et al. Clinical Significance of Different Antiphospholipid Antibodies in the WAPS (Warfarin in the Antiphospholipid Syndrome) Study. *Blood* (2007) 110 (4):1178–83. doi: 10.1182/blood-2007-01-066043
191. Chaturvedi S, Brodsky RA, McCrae KR. Complement in the Pathophysiology of the Antiphospholipid Syndrome. *Front Immunol* (2019) 10:449. doi: 10.3389/fimmu.2019.00449
192. Burwick RM, Feinberg BB. Complement Activation and Regulation in Preeclampsia and Hemolysis, Elevated Liver Enzymes, and Low Platelet Count Syndrome. *Am J Obstet Gynecol* (2020). doi: 10.1016/j.ajog.2020.09.038
193. Vaught AJ, Braunstein EM, Jasem J, Yuan X, Makhlin I, Eloundou S, et al. Germline Mutations in the Alternative Pathway of Complement Predispose to HELLP Syndrome. *JCI Insight* (2018) 3(6):e99128. doi: 10.1172/jci.insight.99128
194. Gavriilaki E, Asteris PG, Touloumenidou T, Koravou EE, Koutra M, Papayanni PG, et al. Genetic Justification of Severe COVID-19 Using a Rigorous Algorithm. *Clin Immunol* (2021) 226:108726. doi: 10.1016/j.clim.2021.108726
195. Roberge S, Bujold E, Nicolaides KH. Aspirin for the Prevention of Preterm and Term Preeclampsia: Systematic Review and Metaanalysis. *Am J Obstet Gynecol* (2018) 218(3):287–93.e1. doi: 10.1016/j.ajog.2017.11.561
196. Pierik E, Prins JR, van Goor H, Dekker GA, Daha MR, Seelen MAJ, et al. Dysregulation of Complement Activation and Placental Dysfunction: A Potential Target to Treat Preeclampsia? *Front Immunol* (2019) 10:3098. doi: 10.3389/fimmu.2019.03098
197. Wang X, Gao H. Prevention of Preeclampsia in High-Risk Patients With Low-Molecular-Weight Heparin: A Meta-Analysis. *J Matern Fetal Neonatal Med* (2020) 33(13):2202–8. doi: 10.1080/14767058.2018.1543656
198. Roberge S, Demers S, Nicolaides KH, Bureau M, Cote S, Bujold E. Prevention of Pre-Eclampsia by Low-Molecular-Weight Heparin in Addition to Aspirin: A Meta-Analysis. *Ultrasound Obstet Gynecol* (2016) 47(5):548–53. doi: 10.1002/uog.15789
199. Kazatchkine MD, Fearon DT, Silbert JE, Austen KF. Surface-Associated Heparin Inhibits Zymosan-Induced Activation of the Human Alternative Complement Pathway by Augmenting the Regulatory Action of the Control Proteins on Particle-Bound C3b. *J Exp Med* (1979) 150(5):1202–15. doi: 10.1084/jem.150.5.1202
200. Bianconi V, Violi F, Fallarino F, Pignatelli P, Sahebkar A, Pirro M. Is Acetylsalicylic Acid a Safe and Potentially Useful Choice for Adult Patients With COVID-19? *Drugs* (2020) 80(14):1383–96. doi: 10.1007/s40265-020-01365-1
201. *Protective Effect of Aspirin on COVID-19 Patients* (2020). Available at: https://ClinicalTrials.gov/show/NCT04365309.
202. Gautret P, Lagier JC, Parola P, Hoang VT, Meddeb L, Mailhe M, et al. Hydroxychloroquine and Azithromycin as a Treatment of COVID-19: Results of an Open-Label Non-Randomized Clinical Trial. *Int J Antimicrob Agents* (2020) 56(1):105949. doi: 10.1016/j.ijantimicag.2020.105949
203. Billett HH, Reyes-Gil M, Szymanski J, Ikemura K, Stahl LR, Lo Y, et al. Anticoagulation in COVID-19: Effect of Enoxaparin, Heparin, and Apixaban on Mortality. *Thromb Haemost* (2020) 120(12):1691–9. doi: 10.1055/s-0040-1720978
204. Packard BD, Weiler JM. Steroids Inhibit Activation of the Alternative-Amplification Pathway of Complement. *Infect Immun* (1983) 40(3):1011–4. doi: 10.1128/iai.40.3.1011-1014.1983
205. Weiler JM, Packard BD. Methylprednisolone Inhibits the Alternative and Amplification Pathways of Complement. *Infect Immun* (1982) 38(1):122–6. doi: 10.1128/iai.38.1.122-126.1982
206. Seo MR, Chae J, Kim YM, Cha HS, Choi SJ, Oh S, et al. Hydroxychloroquine Treatment During Pregnancy in Lupus Patients Is Associated With Lower Risk of Preeclampsia. *Lupus* (2019) 28(6):722–30. doi: 10.1177/0961203319843343
207. Elavarasi A, Prasad M, Seth T, Sahoo RK, Madan K, Nischal N, et al. Chloroquine and Hydroxychloroquine for the Treatment of COVID-19: A Systematic Review and Meta-Analysis. *J Gen Intern Med* (2020) 35 (11):3308–14. doi: 10.1007/s11606-020-06146-w
208. Lefkou E, Mamopoulos A, Dagklis T, Vosnakis C, Rousso D, Girardi G. Pravastatin Improves Pregnancy Outcomes in Obstetric Antiphospholipid Syndrome Refractory to Antithrombotic Therapy. *J Clin Invest* (2016) 126 (8):2933–40. doi: 10.1172/JCI86957
209. Gonzalez JM, Pedroni SM, Girardi G. Statins Prevent Cervical Remodeling, Myometrial Contractions and Preterm Labor Through a Mechanism That Involves Hemoxygenase-1 and Complement Inhibition. *Mol Hum Reprod* (2014) 20(6):579–89. doi: 10.1093/molehr/gau019
210. Burwick RM, Feinberg BB. Eculizumab for the Treatment of Preeclampsia/HELLP Syndrome. *Placenta* (2013) 34(2):201–3. doi: 10.1016/j.placenta.2012.11.014
211. Declercq J, Bosteels C, Van Damme K, De Leeuw E, Maes B, Vandecauter A, et al. Zilucoplan in Patients With Acute Hypoxic Respiratory Failure Due to COVID-19 (ZILU-COV): A Structured Summary of a Study Protocol for a Randomised Controlled Trial. *Trials* (2020) 21(1):934. doi: 10.1186/s13063-020-04884-0
212. Mastaglio S, Ruggeri A, Risitano AM, Angelillo P, Yancopoulou D, Mastellos DC, et al. The First Case of COVID-19 Treated With the Complement C3 Inhibitor AMY-101. *Clin Immunol* (2020) 215:108450. doi: 10.1016/j.clim.2020.108450
213. Smith K, Pace A, Ortiz S, Kazani S, Rottinghaus S. A Phase 3 Open-Label, Randomized, Controlled Study to Evaluate the Efficacy and Safety of Intravenously Administered Ravulizumab Compared With Best Supportive Care in Patients With COVID-19 Severe Pneumonia, Acute Lung Injury, or Acute Respiratory Distress Syndrome: A Structured Summary of a Study Protocol for a Randomised Controlled Trial. *Trials* (2020) 21(1):639. doi: 10.1186/s13063-020-04548-z
214. Diurno F, Numis FG, Porta G, Cirillo F, Maddaluno S, Ragozzino A, et al. Eculizumab Treatment in Patients With COVID-19: Preliminary Results From Real Life ASL Napoli 2 Nord Experience. *Eur Rev Med Pharmacol Sci* (2020) 24(7):4040–7. doi: 10.26355/eurrev_202004_20875

215. Yan B, Freiwald T, Chauss D, Wang L, West E, Mirabelli C, et al. SARS-CoV-2 Drives JAK1/2-Dependent Local Complement Hyperactivation. *Sci Immunol* (2021) 6(58):eabg0833. doi: 10.1126/sciimmunol.abg0833
216. Rambaldi A, Gritti G, Mico MC, Frigeni M, Borleri G, Salvi A, et al. Endothelial Injury and Thrombotic Microangiopathy in COVID-19: Treatment With the Lectin-Pathway Inhibitor Narsoplimab. *Immunobiology* (2020) 225(6):152001. doi: 10.1016/j.imbio.2020.152001
217. Mastellos DC, Pires da Silva BGP, Fonseca BAL, Fonseca NP, Auxiliadora-Martins M, Mastaglio S, et al. Complement C3 vs C5 Inhibition in Severe COVID-19: Early Clinical Findings Reveal Differential Biological Efficacy. *Clin Immunol* (2020) 220:108598. doi: 10.1016/j.clim.2020.108598
218. Stoermer KA, Morrison TE. Complement and Viral Pathogenesis. *Virology* (2011) 411(2):362–73. doi: 10.1016/j.virol.2010.12.045
219. Annane D, Heming N, Grimaldi-Bensouda L, Fremeaux-Bacchi V, Vigan M, Roux AL, et al. Eculizumab as an Emergency Treatment for Adult Patients With Severe COVID-19 in the Intensive Care Unit: A Proof-of-Concept Study. *EClinicalMedicine* (2020) 28:100590. doi: 10.1016/j.eclinm.2020.100590
220. Vlaar APJ, de Bruin S, Busch M, Timmermans S, van Zeggeren IE, Koning R, et al. Anti-C5a Antibody IFX-1 (Vilobelimab) Treatment Versus Best Supportive Care for Patients With Severe COVID-19 (PANAMO): An Exploratory, Open-Label, Phase 2 Randomised Controlled Trial. *Lancet Rheumatol* (2020) 2(12):e764–73. doi: 10.1016/S2665-9913(20)30341-6
221. *Avdoralimab an Anti-C5aR Antibody, in Patients With COVID-19 Severe Pneumonia (FORCE)* (2020). Available at: https://ClinicalTrials.gov/show/NCT04371367.
222. Skendros P, Mitsios A, Chrysanthopoulou A, Mastellos DC, Metallidis S, Rafailidis P, et al. Complement and Tissue Factor-Enriched Neutrophil Extracellular Traps Are Key Drivers in COVID-19 Immunothrombosis. *J Clin Invest* (2020) 130(11):6151–7. doi: 10.1172/JCI141374
223. Urwyler P, Moser S, Charitos P, Heijnen I, Rudin M, Sommer G, et al. Treatment of COVID-19 With Conestat Alfa, a Regulator of the Complement, Contact Activation and Kallikrein-Kinin System. *Front Immunol* (2020) 11:2072. doi: 10.3389/fimmu.2020.02072

Conflict of Interest: The authors declare that the research was conducted in the absence of any commercial or financial relationships that could be construed as a potential conflict of interest.

GLOSSARY

ACE2	angiotensin-converting enzyme 2
aPLAs	anti-phospholipid antibodies
APS	anti-phospholipid syndrome
BK	bradykinin
C	complement system
C1-INH	C1-inhibitor
COVID-19	coronavirus disease 2019
CR1	complement receptor 1
DAF	decay accelerating factor
DAMPs	damage-associated molecular patterns
EC	endothelial cell
EMMPRIN	extracellular matrix metalloproteinase inducer
EOPE	early onset pre-eclampsia
F	factor
HCQ	hydroxychloroquine
HELLP	hemolysis, elevated liver enzymes and low platelets
iTCC	inactive terminal complement complex
LDA	low-dose aspirin
LMWH	low-molecular weight heparin
LOPE	late onset pre-eclampsia
MAC	membrane attack complex
MASPs	MBL-associated serine proteases
MBL	mannan-binding lectin
MCP	membrane cofactor protein
MERS	middle east respiratory syndrome
NETs	neutrophil extracellular traps
PAI-1	plasminogen activator inhibitor type-1
PAMPs	pathogen-associated molecular patterns
PARs	protease-activated receptors
PE	pre-eclampsia
PlGF	placental growth factor
RAAS	renin-angiotensin-aldosterone system
ROS	reactive oxygen species
SARS-CoV-2	severe acute respiratory syndrome coronavirus 2
sEng	soluble endoglin
sFlt-1	soluble fms-like tyrosine kinase 1
SLE	systemic lupus erythematosus
vWF	von Willebrand factor
TAFI	thrombin-activable fibrinolysis inhibitor
TCC	terminal complement complex
TF	tissue factor
TFPI	tissue factor pathway inhibitor
TM	thrombomodulin
TMPRSS2	transmembrane serine protease 2
UtAPI	uterine artery pulsatility index
VEGF	vascular-endothelial growth factor

frontiers in Immunology

MINI REVIEW
published: 27 January 2022
doi: 10.3389/fimmu.2022.827250

Train the Trainer: Hematopoietic Stem Cell Control of Trained Immunity

Marco De Zuani[1] *and Jan Frič*[1,2]*

[1] International Clinical Research Center, St. Anne's University Hospital, Brno, Czechia, [2] Institute of Hematology and Blood Transfusion, Prague, Czechia

Recent evidence shows that innate immune cells, in addition to B and T cells, can retain immunological memory of their encounters and afford long-term resistance against infections in a process known as 'trained immunity'. However, the duration of the unspecific protection observed *in vivo* is poorly compatible with the average lifespan of innate immune cells, suggesting the involvement of long-lived cells. Accordingly, recent studies demonstrate that hematopoietic stem and progenitor cells (HSPCs) lay at the foundation of trained immunity, retaining immunological memory of infections and giving rise to a "trained" myeloid progeny for a long time. In this review, we discuss the research demonstrating the involvement of HSPCs in the onset of long-lasting trained immunity. We highlight the roles of specific cytokines and Toll-like receptor ligands in influencing HSPC memory phenotypes and the molecular mechanisms underlying trained immunity HSPCs. Finally, we discuss the potential benefits and drawbacks of the long-lasting trained immune responses, and describe the challenges that the field is facing.

Keywords: trained immunity, hematopoietic stem cells, HSPCs, innate immunity, myeloid cells, progenitor cells

OPEN ACCESS

Edited by:
Francesca Granucci, University of Milano-Bicocca, Italy

Reviewed by:
María Luisa Gil, University of Valencia, Spain

***Correspondence:**
Jan Frič
jan.fric@fnusa.cz

Specialty section:
This article was submitted to Molecular Innate Immunity, a section of the journal Frontiers in Immunology

Received: *01 December 2021*
Accepted: *12 January 2022*
Published: *27 January 2022*

Citation:
De Zuani M and Frič J (2022) Train the Trainer: Hematopoietic Stem Cell Control of Trained Immunity. Front. Immunol. 13:827250. doi: 10.3389/fimmu.2022.827250

INTRODUCTION

Traditionally, the immune system of vertebrates has been binary classified into the innate and adaptive arms of immunity. While cells of the innate arm promptly recognize and respond to infections through pathogen recognition receptors (PRRs), cells of the adaptive arm rely on the somatic recombination of genes encoding immunoglobulin domains to recognise non-self molecules (1). Although immunological studies on plants and invertebrates – both lacking adaptive immune responses – have suggested that these organisms can become increasingly resistant to reinfections, it was long believed that only B and T cells can confer immunological memory to their host (2–4).

In the last 10 years, a growing body of evidence has demonstrated that innate immune cells can also develop immunological memory in vertebrates – a phenomenon that is termed 'trained immunity' or 'innate immune memory' (5). In vertebrates, certain cells have been found to develop trained immunity, i.e., monocytes (6), dendritic cells (7), neutrophils (8), and innate lymphoid cells such as NK cells (9) and ILC1s (10). This process mainly relies on the reprogramming of cellular metabolic pathways and the alteration of epigenetic markers regulating the expression of different sets of genes (6, 11–13). While trained immunity generally refers to the induction of an

hyperinflammatory phenotype, it was demonstrated that also the generation of opposite phenotypes, such as in the case of 'endotoxin tolerance', relies on similar mechanisms (12, 14, 15). Although the molecular basis of trained immunity has mostly been described *in vitro* using human monocytes and *in vivo* using murine models of infection, a few studies have demonstrated that the same mechanisms also apply *in vivo* to humans (16–18). Similarly, epidemiological studies proved that whole-organism vaccinations (such as Bacillus Calmette-Guerin [BCG], smallpox, and measles vaccines) afford unspecific protection against infections not specifically targeted by the vaccines, resulting in a reduction in all-cause mortality (19–22). Recent studies demonstrated that long-lived, self-renewing cells are involved in the onset of trained immunity and, indeed, participate in long-lasting protection against pathogens. For example, alveolar macrophages are able to replenish populations of tissue-resident macrophages in the lungs independently of bone marrow (BM)-derived monocytes and were shown to offer cross-protection against lung pathogens after an initial intranasal challenge with *Acinetobacter baumannii* (23, 24). However, the duration and extent of the unspecific peripheral protection *in vivo* (which is measured in years) is poorly compatible with the average lifespan of human monocytes (5 to 7 days), suggesting that other long-lived cells, such as hematopoietic stem and progenitor cells (HSPCs, with lifespans ranging from 10 to 60 months), might be involved in this phenomenon (25–27). In agreement with this hypothesis, several studies published in the last few years suggest that specific signals carried by HSPCs are able to induce trained immunity in these cells, which, in turn, gives rise to a pool of 'trained' myeloid progeny.

Here, we present the latest advancements in the field of trained immunity, describe the known mechanisms of trained immunity in HSPCs, and discuss the challenges and remaining controversies that the field is facing.

INDUCTION OF TRAINED IMMUNITY IN HSPCs

During infection and inflammation, immune effector cells are rapidly consumed at the sites of infection. As a result, HSPCs need to adapt their proliferation and differentiation rates to meet the increased demand of blood cells. To this end, HSPCs respond to different signals coming either from the BM niche, from distal inflamed sites, or from the infectious agents themselves (28). HSPCs have long been known to respond to multiple cytokines; however, several studies have demonstrated that both murine and human HSPCs express different Toll-like receptors (TLRs), and that direct engagement of these receptors with their ligands can alter the cell differentiation programming and, thus, their cellular output (28–32). HSPCs can also egress from the BM and migrate to tissues, where they can give rise to local populations of immune cells – a process known as 'extramedullary haematopoiesis' (33). Interestingly, different studies have reported that HSPCs can home back to the BM after migrating to peripheral tissues, increasing their chance of encountering TLR ligands and building a long-term memory of these encounters (34, 35).

In recent years, several studies have demonstrated that both human and murine HSPC compartments are at the foundation of the long-lasting 'peripheral' trained immunity observed *in vivo* (17). As we will discuss in the next chapters, some of these reports suggest that direct signaling from cytokines and microbial ligands to HSPCs play a central role in the reprogramming of HSPCs and their progeny (**Table 1**).

Cytokine Signaling on HSPCs Promote Trained Immunity

Cytokines and growth factors play crucial roles in haematopoiesis by regulating HSPC quiescence, proliferation and differentiation (44). Similarly, signaling from many cytokines, such as G-CSF, GM-CSF, M-CSF, IL-6, IL-1β, and Type-I and II IFNs, control the transition to emergency haematopoiesis, i.e., the adaptation of the hematopoietic process during infection (28).

Two recent studies demonstrated that stimulation with β-glucan (a fungal cell wall component known to be a strong inducer of trained immunity in monocytes) also induces long-term trained immunity in murine HSPCs and that IL-1β plays a key role in HSPC reprogramming (6, 36, 37). Mitroulis and colleagues showed that, in a murine model, the intraperitoneal injection of β-glucan acted on $CD41^+$ myeloid-skewed long-term hematopoietic stem cells (LT-HSCs), resulting in the expansion of granulocyte-monocyte progenitors (GMPs) and the reduction of lymphoid-skewed multipotent progenitors (MPP4). These myeloid skews in the HSPCs populations were accompanied by the profound metabolic reprogramming of $cKit^+$ progenitors, which showed increased glycolytic activity and alterations in their cholesterol biosynthesis pathway. Compared to PBS-treated animals, mice primed with β-glucan showed a protective response to a later lipopolysaccharide (LPS) injection, as demonstrated by the enhanced expansion of multipotent progenitors (MPPs) and Lin- Sca1+ cKit+ (LSK) cells in the BM and by the mitigation of DNA damage at the level of LT-HSCs. Interestingly, the authors found that IL-1β signaling was required for the metabolic reprogramming and lineage skewing of LT-HSCs following β-glucan administration, as the pharmacological inhibition of IL-1 by the IL-1 receptor antagonist Anakinra completely abrogated these effects (36). Similarly, in a study by Moorlag and colleagues, β-glucan administration caused the expansion of LT-HSCs, MPPs and GMPs, which was abolished in $IL\text{-}1R^{-/-}$ mice as well as wildtype (WT) mice that received Anakinra. Priming with β-glucan also protected the mice against pulmonary infection with virulent *Mycobacterium tuberculosis* (Mtb), possibly as a result of the enhanced expression of antimicrobial cytokines by myeloid cells. Again, the protective effect provided by β-glucan was completely abolished in $IL\text{-}1R^{-/-}$ mice and in Anakinra-treated WT mice, suggesting that IL-1 plays a key role in the induction of protective trained immunity in HSPCs (37).

IL-1 was also found to have a prominent role in the induction of innate immune reprogramming following a western diet

TABLE 1 | Experimental studies demonstrating the direct involvement of HSPCs in the induction of innate immune memory.

Mediator	Model	Effect on HSPCs	Mouse	Human	Refs
IL-1β	β-glucan i.p.	• Increased BM GMP frequency, reduction of MPP4 frequency; • β-glucan exposed LT-HSCs give rise to more $Gr1^+$ $CD11b^+$ cells, and less $CD19^+$ progeny; • Improved HSPCs chemoresistance; • Increased expression of genes involved in myeloid-skewing, immune functions and metabolic pathways (glycolysis, mevalonate) in LT-HSCs; • Increased glycolysis in ckit+ progenitors and promotes alterations in cholesterol biosynthesis pathway; • Phenotype abolished in mice treated with IL1Ra.	X		(36)
IL-1	β-glucan i.p.	• Increased BM LSK cells counts - particularly LT-HSCs, MPPs and GMPs; • Phenotype abolished in *Il1r*$^{-/-}$ mice and WT mice receiving IL1Ra.	X		(37)
IFN-γ	BCG vaccination (i.v. and s.c.)	• i.v. but not s.c. increased ST-HSC and MPP counts in BM • BCG i.v. induced the expression of genes involved in cell cycle and skew to myeloid MMP3 over MMP4 progenitors; • BCG i.v. Induced IFN-γ gene signature in HSCs; • BCG-exposed HSC afforded protection against Mtb infection; • Phenotype reverted in *Ifnγr*$^{-/-}$ mice.	X		(38)
IFNα, IFNβ	Mtb and BCG infection (i.v. and aerosol)	• BCG and Mtb increased BM LSK cells numbers and the frequency of $Ki67^+$ LSKs, ST-HSCs and MPPs; • Mtb reduced the frequency of CMPs and GMPs, increases CLPs frequency; • Mtb induced RIP3K-dependent necroptosis of CMPs and GMPs; • Mtb increased Stat1 expression in all HSPCs clusters and induces type-I IFNs gene expression; • Mtb reduced HSPCs engraftment potential, BCG enhances it.	X		(27)
Leptin (indirect)	Voluntary exercise	• Exercise reduced LSK proliferation and lineage commitment; • Decreased chromatin accessibility long after exercise; • Metabolic switch from glycolysis (sedentary) to OXPHOS (exercise); • Increased cellular output in exercised mice after LPS injection.	X		(39)
HNF1A/B (TF)	BCG intradermal vaccination	• Unaltered counts of BM progenitor counts; • Increased granulocytic/myeloid lineage transcripts in HSPCs 90 days post-vaccination; • Increased predicted activity of HNF1A/B TF.		X	(17)
Dectin-1	Depleted zymosan and *Candida albicans* i.v.	• Increased HSPCs proliferation in response to direct dectin1 ligation by depleted zymosan; • Increased output of CD11b+ F4/80++ cells with heightened *ex-vivo* production of inflammatory cytokines; • Phenotype reverted in *dectin1*$^{-/-}$ and *Myd88*$^{-/-}$ HSPCs.	X		(40)
TLR4 - C/EBPα (TF)	LPS i.p.	• Rapid and transient increase of LT-HSC, MMP2, MMP3 and GMP numbers, reduction of MPP4 numbers; • Stable change in $Flt3L^-$ LSK chromatin accessibility 12 weeks after LPS; • Increased myeloid differentiation, and OXPHOS and fatty acid metabolism gene signature during secondary LPS challenge; • Phenotype strongly reverted in *Tlr4*$^{-/-}$ HSPCs, completely abolished in C/EBPβ HSPCs.	X		(41)
Heme	Heme i.p.	• Decrease of BM LT-HSC and committed progenitors; • Long-term (28 days) changes in LSK chromatin accessibility, especially affecting binding sites for stemness-associated TFs (Runx, Nfi, Spi); • Open chromatin peaks associated to genes promoting myeloid cell differentiation and restraining megakaryocyte differentiation.	X		(42)
NLRP3	Western diet	• Increased abundance of MPPs and GMPs; • Transcriptional reprogramming of GMPs promoting cell proliferation and monocytic development, and restraining granulocytic development; • Long lasting upregulation of IFN response genes and inflammatory signaling in response to LPS challenge, compared to normal diet; • Long-lasting changes in GMP accessible chromatin landscape; • Phenotype reverted in *Nlrp3*$^{-/-}$ mice.	X		(43)

The table summarizes the response of HSPCs during the induction of innate immune memory. Each of these studies also demonstrated that the direct stimulation on HSPCs was responsible for the induction of long-lasting, specific memory phenotypes on myeloid cells. i.p., intra-peritoneal injection; i.v., intravenous; s.c., sub-cutaneous; BCG, Bacillus Calmette-Guérin; BM, bone marrow; CLP, common lymphoid progenitor; CMP, common myeloid progenitor; GMP, granulocyte-monocyte progenitor; HSC, hematopoietic stem cell, HSPC, hematopoietic stem and progenitor cell, IL1Ra, IL-1 receptor antagonist; LPS, lipopolysaccharide; LSK, Lin- Sca1+ Kit+ cells; LT-HSC, long term-HSC, MPP, multipotent progenitor; Mtb, Mycobacterium tuberculosis; OXPHOS, oxidative phosphorylation; ST-HSC, short term HSC; TF, transcription factor.

regime. This study employed the *Ldlr*$^{-/-}$ arteriosclerosis mouse model and showed that, when fed a western diet, these animals developed a systemic inflammatory response and long-lasting hyper-responsiveness of myeloid cells that continued after switching back to a chow diet. Mechanistically, the western diet induced the persistent transcriptional and epigenetic reprogramming of BM GMPs, which was mediated by NLRP3 activation and the subsequent release of IL-1. Accordingly,

this phenotype was largely blunted in *Nlrp3*$^{-/-}$ *Ldlr*$^{-/-}$ mice as well as in animals receiving a recombinant IL-1ra (43).

Type-I and II interferons (IFNs) were also reported to play a key role in the induction of protective or detrimental innate immune memory in murine HSPCs. Two recent studies employed different models of BCG or Mtb infection in mice to determine their effect on the hematopoietic compartment (27, 38). Interestingly, both studies demonstrated that, to affect HSPC biology, the bacteria had to reach the BM, although LSK cells were not directly infected, suggesting an indirect effect was involved. Kaufman and colleagues showed that HSCs isolated from mice exposed to BCG were myeloid-skewed and able to generate an epigenetically reprogrammed myeloid progeny which protected against Mtb infection *in vivo* (38). The authors suggested that INF-γ signaling by HSCs was required for the generation of this protective response, as mice lacking the IFN-γ receptor failed to generate macrophages with a protective phenotype. Similarly, Khan et al. compared the responses of the hematopoietic compartment to either BCG or virulent Mtb infection (27). They found that Mtb, but not BCG, reduced myelopoiesis by inducing the Ripk3-dependent necroptosis of common myeloid progenitors (CMPs) and GMPs, and impaired HSC engraftment potential. Compared to BCG-exposed HSCs, cells exposed to Mtb showed an upregulation of Stat1 and type-I IFN targets, thus suggesting the involvement of IFN-α or IFN-β in this process. Concordantly, mice lacking the type-I IFN receptor Ifnar1 were afforded more protection against Mtb infection comparted with WT animals. Similarly, the systemic administration of poly(I:C) – a strong inducer of type-I IFNs – recapitulated the negative impact on myelopoiesis observed in Mtb-infected animals, which was completely reverted in Ifnar1$^{-/-}$ mice. Taken together, these studies suggest that the balance between type-I and type-II IFN signaling by HSPCs plays a key role in the induction of a detrimental or protective innate immune memory *in vivo*. However, different studies demonstrated that chronic exposure of murine and human HSCs to IFN-γ impairs their maintenance and self-renewal, indicating that the route of infection and the duration of the stimulus play key roles in the regulation of HSC fate (45, 46).

Finally, using a murine model of voluntary exercise, Frodermann and colleagues showed that, by diminishing plasma levels of the hormone leptin, exercise reduced HSPC proliferation and lineage commitment, resulting in fewer circulating leukocytes (39). In particular, reduced leptin signaling resulted in the increased production of 'quiescence-inducing factors' by LepR^{+} stromal cells which, in turn, reduced the LSK chromatin accessibility of multiple genes involved in proliferation and myelopoiesis for several weeks after exercise interruption. Surprisingly, compared to sedentary mice, exercised mice were more fully protected against LPS injection and caecal ligation and puncture, as highlighted by their lower mortality and increased cellular output. Although the authors failed to identify the nature of these quiescence-inducing factors, it is likely that cytokines such as SCF are involved in the reprogramming of HSCs in the BM niche (47, 48).

Direct TLR Ligation Promotes Trained Immunity in the HSPC Pool

In the last two decades, several studies have demonstrated that both human and murine HSPCs express many PRRs (e.g., TLR-1, -2, -3, -4, -6, -7, -8, NOD2) and are able to respond to their engagement by activating specific downstream signaling pathways (29, 49, 50). TLR ligation on HSPCs, in particular, promotes their exit from quiescence and proliferation and results in a differentiation skew that favours a myeloid over a lymphoid cell fate (31, 32, 49, 50). Moreover, stimulation with TLR ligands induces cytokine secretion in virtually all HSPC subsets (50–52).

More recently, reports suggest that HSPCs stimulated with various TLR-ligands show memory-like traits, particularly those affecting the functionality of their myeloid progeny. For example, several studies from the Gil and Goodridge labs showed that *in vitro* differentiation of murine Lin-HSPCs exposed to TLR2 and TLR4 ligands (either *in vitro* or *in vivo*) generate macrophages with a decreased ability to release proinflammatory cytokines and reactive oxygen species in response to TLR ligation compared to control cells. However, HSPCs differentiated in the presence of *Candida albicans* yeast generated macrophages with a heightened production of inflammatory cytokines and improved fungicidal activity (52–55). Although they outlined a strong rationale for the involvement of HSPCs in building systemic trained immunity, these studies failed to determine the duration of these memory traits in HSPCs or conclude whether TLR ligation, rather than the production of autocrine soluble factors, is uniquely responsible for the observed phenotypes. A recent study, however, showed that the latter is likely to be the case: while direct TLR2 ligation on Lin-cells was required to promote myeloid differentiation, the differential response of macrophages derived from cells exposed to TLR2 and dectin-1 ligands was completely dependent on HSPC secretome release in response to these ligands (40). Interestingly, as LT-HSC do not express dectin-1, it is possible that myeloid-committed progenitors expressing dectin-1 are responsible for the secretion of training cytokines and factors (56).

However, it was recently reported that the exposure of HSPCs to LPS is sufficient to induce long-lasting innate memory in murine HSPCs (41). Using *in vivo* models of mixed BM chimaera and LSK cell transplantation, the authors showed that LPS-exposed LT-HSCs provide long-term protection against *Pseudomonas aeruginosa* infection for more than 12 weeks. This phenomenon relied on the persistent epigenetic reprogramming of HSCs, which showed increased chromatin accessibility, especially in myeloid enhancers, which were later re-activated during reinfection. Interestingly, direct signaling through TLR4 was fundamental to the induction of immune memory in HSCs, as TLR4$^{-/-}$ HSCs almost completely lost the epigenetic signature induced by LPS exposure in the TLR4$^{-/-}$: WT BM cell chimaera. Furthermore, the authors found that, while not necessary for inducing the initial response to LPS by HSCs, C/EBPβ transcription factor (TF) was required to maintain the long-term accessibility of regulatory elements

controlling the expression of myeloid and inflammatory genes during re-infection (41).

C/EBPβ and C/EBPα were also found to play key roles in the differentiation of human CD34+ cells towards the myeloid lineage in response to LPS *in vitro*. In this case, however, LPS activated a TLR4-MD2-MyD88 pathway that resulted in the expression of IL-6, which in turn, induced C/EBPα and C/EBPβ phosphorylation, finally promoting monocytic-macrophage differentiation (57). Direct TLR4 triggering of HSCs also plays an important role in the maintenance of HSC fitness. Research showed that the TLR4-MyD88 pathway in HSPCs seems to regulate myeloid suppression, while the TLR4-TRIF pathway plays a key role in regulating HSC proliferation (30, 58, 59). Concordantly, *in vivo* LPS and *Salmonella typhimurium* infection resulted in the strong proliferation of LT-HSCs through a TRIF-ROS-p38 pathway, which resulted in proliferative stress, DNA damage, and the long-term impairment of their repopulating ability (30).

Among non-canonical TLR4 ligands, heme was recently described to induce trained immunity in human monocytes as well as murine HSPCs (42, 60, 61). In fact, a single injection of heme protected a mouse model of polymicrobial sepsis from death when challenged 7 days post heme-administration. When sepsis was induced 28 days after the initial heme training, this protection completely vanished. A further analysis of BM HSPCs 28 days after heme training revealed that chromatin accessibility in the ST-HSC and MPP3 subsets was substantially different than that in control mice. These differences further reflected the alteration in the chromatin accessibility to TFs that are important for the maintenance of stemness and the promotion of myelopoiesis (e.g., Gata2, Runx1, Nfi) (42).

Finally, it was recently revealed that young and aged LT-HSCs display different memory traits after TLR activation. In aged LT-HSCs, but not in young cells, brief *ex vivo* exposure to TLR2 and TLR4 ligands induced the expansion of peripheral myeloid cells and a reduction in lymphoid cells 3 months after transplantation. This was possibly the result of the initial expansion of a CD61+ subset of LT-HSCs in the aged mice, which were found to be more proliferative and intrinsically prone to a myeloid output (62).

Taken together, these studies suggest that direct TLR ligation on HSPCs plays an important role in the terminal differentiation of the cells as well as the establishment of innate immune memory. Interestingly, both direct TLR signaling and the indirect signaling autocrinally induced by the production of cytokines seem to be equally involved in this complex phenomenon.

DISCUSSION

A growing body of evidence, examples of which are presented in this review, highlights the key roles of HSPCs in maintaining the long-lasting aspects of trained immunity. However, several questions remain to be addressed regarding the conundrum of trained immunity and its implications.

Diamonds Are Forever, Trained Immunity Is Not

Although most of the studies support the idea that trained immunity phenotypes are retained for a very long time, a key remaining aspect of trained immunity that still has to be clearly defined, is the specific duration of such phenotype *in vivo* in humans. This, as we will discuss later, has important implications on the possible translatability of such evidence to human health. Studies using murine models showed that BM HSPCs can retain an epigenetic memory, affecting the response of their myeloid progeny for over 1 year (27). Similarly, epidemiological studies suggest that BCG vaccination might afford unspecific protection for up to 5 years (63). Although it is still a matter of discussion and an object of ongoing clinical trials, recent epidemiological studies that aimed to assess the protective effects of BCG vaccination against SARS-CoV-2 infections showed that a history of BCG vaccination was associated with a decreased rate of infection and an overall improvement in the symptomatology (64, 65). Furthermore, a recent study suggested that HSCs can establish and retain a persistent epigenetic memory (characterised by drastic differences in DNA methylation and chromatin accessibility) imposed during their development, which eventually direct HSC functions during exposure to stressors (66). It is, therefore, likely that the duration of such an innate immune memory in HSCs can be measured in the context of years and that the additional effects of subsequent stresses and infections on such cells are maintained lifelong. Finally, a breakthrough study recently demonstrated that unspecific protection against bacterial infections afforded by a sublethal infection with *C. albicans* was transmitted intergenerationally and transgenerationally for up to two generations (67). Strikingly, the progeny of *C. albicans*-exposed mice inherited an epigenetic signature induced by the fungal insult from the HSPC populations of their parents, resulting in improved myeloid cell output and activation and increased survival following *E. coli* infection. These results are in agreement with a randomized controlled trial showing that the reduction in mortality observed in BCG-vaccinated infants was significantly improved if the mother also had a history of BGC vaccination (68). Understanding the specific duration of trained immunity induced by different agents (e.g. BCG, β-glucans) will be fundamental to design effective therapies.

All That Glitters Is Not Gold: Trained Immunity as a Double-Edged Sword in Inflammaging and Chronic Inflammation

Most of the studies performed so far have demonstrated that the typical enhancement of myeloid cell activation afforded by trained immunity leads to the cells having a protective role against unspecific infections, however, less is known about the putative side effects that proinflammatory poising of the myeloid compartment might have in other scenarios (69). The proinflammatory poising of myeloid cells can undoubtedly be useful during infection; nevertheless, there is evidence that it can contribute to inflammatory diseases. For example, NLRP3 activation and IL-1 release during a western diet are known to

cause the reprogramming of BM GMPs, resulting in proinflammatory poising of the myeloid compartment (43). Chronic exposure to IL-1 negatively affects the HSC pool, reducing their self-renewing capacity and restricting their lineage output (70). On a similar note, a single LPS injection was found to induce a trained phenotype of murine microglia; this in turn, promoted the neuropathology in a model of Alzheimer's disease, increasing both amyloid-β levels and the plaque load, and augmented IL-1β levels after brain ischaemia (71).

The hypothesis of a detrimental trained immunity response is also supported by a study on patients who were affected by hyper-IgD syndrome (HIDS), in which recurring attacks of sterile inflammation occur. Compared to healthy donors, the monocytes from these patients showed a trained immunity phenotype characterised by the enhanced production of inflammatory cytokines (both at the basal level and during infection) as well as an H3K27ac signature partially overlapping with that of *in vitro* trained monocytes. The authors speculated that this phenotype could be induced by the accumulation of mevalonate during HIDS which, in turn, activates the AKT-mTOR pathway (possibly through IGF1-R) and finally amplifies the molecular cascade that controls the epigenetic rewiring of trained monocytes (13). Similar observations linking the proinflammatory phenotype of monocytes to a characteristic epigenetic signature were made on patients affected by symptomatic arteriosclerosis (72) and coronary artery disease (73). Taken together, these studies point to a possible detrimental role of trained immunity, where monocytes (and possibly other myeloid cells) participate in the maintenance and worsening of inflammatory pathologies (**Figure 1**).

This gains even greater importance in the light of the long-lasting effect exerted on the HSPCs pool. It is, therefore, paramount to fully explore and identify these potential side effects before applying any treatment in the clinical practice. As a matter of fact, the pharmacological control of trained immunity is gaining more and more interest from the scientific community as a tool to boost the immunity of frail patients (74). Two recent clinical trials showed the promising effects of BCG re-vaccination in the elderly (75, 76). However, other researchers have speculated that continuous triggering of the immune system throughout life and, thus, the constant induction of trained immunity on HSPCs, could be the missing link between aging and the persistent low-grade inflammation observed in the elderly that is known as 'inflammaging' (77, 78). Therefore, dissecting the molecular mechanisms driving beneficial or detrimental trained immunity in HSPCs will be a fundamental step in the development of novel pharmacological strategies or towards the repurposing of already approved therapies. The induction of trained immunity can be achieved through stimulation with different PRR-ligands (especially ligands for dectin-1 and NOD2), while inhibition of trained immunity can be accomplished by interfering with metabolic pathways or epigenetic regulators (79). As such, great hope is placed on the use of small molecules as regulating epigenetic modifiers (80).

CONCLUSION

Taken together, the studies presented in this review clearly put the HSPC compartment at the foundation of the long-term effects exerted by trained immunity. Direct induction of trained immunity in HSPCs results in the production of a myeloid progeny with a trained phenotype directly inherited

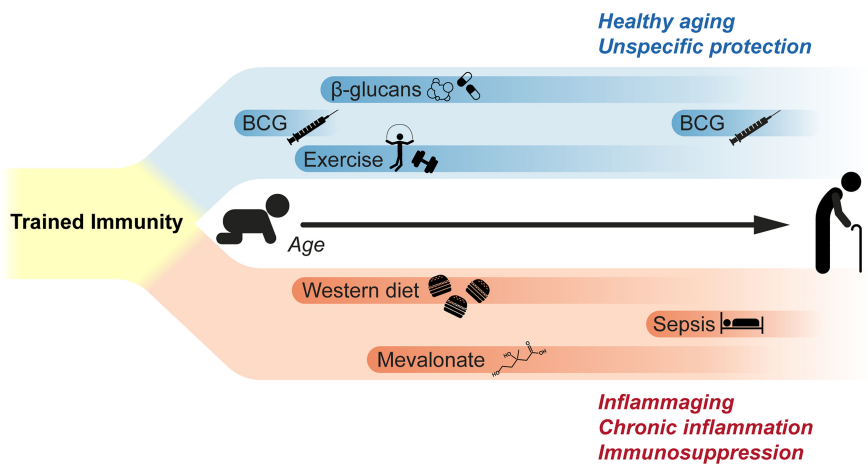

FIGURE 1 | Impact of trained immunity during lifetime. Current studies suggest that trained immunity can have both beneficial and detrimental effects. β-glucan administration is known to induce a long-lasting reprograming of myeloid cells that results in the unspecific protection against different pathogens. BCG vaccination in children is known to afford protection and reduce all-cause mortality; similarly, recent clinical trials suggest that BCG vaccination in elderly can reduce the plasma levels of inflammatory cytokines and mediators, and to afford unspecific protection against respiratory infections. Voluntary exercise also induces analogous effects, decreasing the proliferation and lineage commitment of HSPCs while affording a long-term protection during sepsis. On the other side, western diet was found to reprogram bone marrow granulocyte progenitors, increasing the reactivity of innate immune cells. Similarly, signaling by metabolic intermediates as mevalonate was suggested to be involved in the pathological hyperinflammation affecting patients suffering from hyper-IgD syndrome. Finally, sepsis is also known to induce a long-term immunosuppression in survivors, possibly through mechanisms similar to those inducing trained immunity in hematopoietic progenitors and myeloid cells.

from their progenitors. Although different studies point toward different factors, direct signaling by both cytokines (as IFNs and IL-1) and PRR ligands (as LPS and β-glucans) is fundamental for the induction of the metabolic and epigenetic rewiring in HSPCs responsible for the induction of trained immunity in HSPCs.

As the pharmaceutical control of trained immunity is gaining more and more interest by the scientific community, some aspects of this phenomenon still require thorough investigation in order to design effective therapeutic strategies. In particular, several studies report that trained immunity might participate in the onset and worsening of inflammatory pathologies such as arteriosclerosis. Knowing the derailments that can occur during the induction of trained immunity represent a key step for the development of safe treatments. Secondly, it is still not known the exact and specific duration of trained immunity induced by different factors. This would allow the design of effective 'training therapies' aimed to boost the innate response against infections without promoting an undesirable hyperinflammatory bias of the immune system which can lead to the development (or worsening) of inflammatory diseases. Finally, unravelling the common molecular pathways involved in the onset of trained immunity will allow the precise control of the balance between unspecific protection and undesirable hyperinflammation.

We believe that trained immunity represents a unique phenomenon that can be harnesser to design game changing-therapies: the direction is clear and the path paved.

AUTHOR CONTRIBUTIONS

MZ conceived and wrote the manuscript, and secured funding. JF supervised the writing and reviewed the manuscript, and secured funding. Both authors read and approved the final manuscript.

FUNDING

This work was supported by the Ministry of Health of the Czech Republic, grant no. NU21J-05-00056 and DRO (Institute of Haematology and Blood Transfusion—UHKT, 00023736), and by the European Social Fund and European Regional Development Fund—Project ENOCH (no. CZ.02.1.01/0.0/0.0/16_019/0000868). MZ was supported by the European Regional Development Fund—Project Support of MSCA IF fellowships at FNUSA-ICRC (no CZ.02.2.69/0.0/0.0/19_074/0016274).

ACKNOWLEDGMENTS

The authors would like to thank Dr Jessica Tamanini of Insight Editing London for critically reviewing the manuscript before submission.

REFERENCES

1. Cooper MD, Alder MN. The Evolution of Adaptive Immune Systems. *Cell* (2006) 124(4):815–22. doi: 10.1016/j.cell.2006.02.001
2. Gourbal B, Pinaud S, Beckers GJM, van der Meer JWM, Conrath U, Netea MG. Innate Immune Memory: An Evolutionary Perspective. *Immunol Rev* (2018) 283(1):21–40. doi: 10.1111/imr.12647
3. Melillo D, Marino R, Italiani P, Boraschi D. Innate Immune Memory in Invertebrate Metazoans: A Critical Appraisal. *Front Immunol* (2018) 9:1915. doi: 10.3389/fimmu.2018.01915
4. Reimer-Michalski EM, Conrath U. Innate Immune Memory in Plants. *Semin Immunol* (2016) 28(4):319–27. doi: 10.1016/j.smim.2016.05.006
5. Netea MG, Dominguez-Andres J, Barreiro LB, Chavakis T, Divangahi M, Fuchs E, et al. Defining Trained Immunity and Its Role in Health and Disease. *Nat Rev Immunol* (2020) 20(6):375–88. doi: 10.1038/s41577-020-0285-6
6. Quintin J, Saeed S, Martens JHA, Giamarellos-Bourboulis EJ, Ifrim DC, Logie C, et al. Candida Albicans Infection Affords Protection Against Reinfection *via* Functional Reprogramming of Monocytes. *Cell Host Microbe* (2012) 12 (2):223–32. doi: 10.1016/j.chom.2012.06.006
7. Hole CR, Wager CML, Castro-Lopez N, Campuzano A, Cai H, Wozniak KL, et al. Induction of Memory-Like Dendritic Cell Responses In Vivo. *Nat Commun* (2019) 10(1):2955. doi: 10.1038/s41467-019-10486-5
8. Moorlag SJCFM, Rodriguez-Rosales YA, Gillard J, Fanucchi S, Theunissen K, Novakovic B, et al. BCG Vaccination Induces Long-Term Functional Reprogramming of Human Neutrophils. *Cell Rep* (2020) 33(7):108387. doi: 10.1016/j.celrep.2020.108387
9. Romee R, Rosario M, Berrien-Elliott MM, Wagner JA, Jewell BA, Schappe T, et al. Cytokine-Induced Memory-Like Natural Killer Cells Exhibit Enhanced Responses Against Myeloid Leukemia. *Sci Transl Med* (2016) 8 (357):357ra123. doi: 10.1126/scitranslmed.aaf2341
10. Weizman OE, Song E, Adams NM, Hildreth AD, Riggan L, Krishna C, et al. Mouse Cytomegalovirus-Experienced ILC1s Acquire a Memory Response Dependent on the Viral Glycoprotein M12. *Nat Immunol* (2019) 20(8):1004–11. doi: 10.1038/s41590-019-0430-1
11. Cheng SC, Quintin J, Cramer RA, Shepardson KM, Saeed S, Kumar V, et al. Mtor- and HIF-1alpha-Mediated Aerobic Glycolysis as Metabolic Basis for Trained Immunity. *Science* (2014) 345(6204):1250684. doi: 10.1126/science.1250684
12. Saeed S, Quintin J, Kerstens HH, Rao NA, Aghajanirefah A, Matarese F, et al. Epigenetic Programming of Monocyte-to-Macrophage Differentiation and Trained Innate Immunity. *Science* (2014) 345(6204):1251086. doi: 10.1126/science.1251086
13. Bekkering S, Arts RJW, Novakovic B, Kourtzelis I, van der Heijden C, Li Y, et al. Metabolic Induction of Trained Immunity Through the Mevalonate Pathway. *Cell* (2018) 172(1-2):135–46.e9. doi: 10.1016/j.cell.2017.11.025
14. Foster SL, Hargreaves DC, Medzhitov R. Gene-Specific Control of Inflammation by TLR-Induced Chromatin Modifications. *Nature* (2007) 447(7147):972–8. doi: 10.1038/nature05836
15. Novakovic B, Habibi E, Wang SY, Arts RJW, Davar R, Megchelenbrink W, et al. Beta-Glucan Reverses the Epigenetic State of LPS-Induced Immunological Tolerance. *Cell* (2016) 167(5):1354–68.e14. doi: 10.1016/j.cell.2016.09.034
16. Arts RJW, Moorlag S, Novakovic B, Li Y, Wang SY, Oosting M, et al. BCG Vaccination Protects Against Experimental Viral Infection in Humans Through the Induction of Cytokines Associated With Trained Immunity. *Cell Host Microbe* (2018) 23(1):89–100.e5. doi: 10.1016/j.chom.2017.12.010
17. Cirovic B, de Bree LCJ, Groh L, Blok BA, Chan J, van der Velden W, et al. BCG Vaccination in Humans Elicits Trained Immunity *via* the Hematopoietic Progenitor Compartment. *Cell Host Microbe* (2020) 28(2):322–34.e5. doi: 10.1016/j.chom.2020.05.014
18. Kleinnijenhuis J, Quintin J, Preijers F, Joosten LA, Ifrim DC, Saeed S, et al. Bacille Calmette-Guerin Induces NOD2-Dependent Nonspecific Protection From Reinfection *via* Epigenetic Reprogramming of Monocytes. *Proc Natl Acad Sci USA* (2012) 109(43):17537–42. doi: 10.1073/pnas.1202870109
19. Aaby P, Martins CL, Garly ML, Bale C, Andersen A, Rodrigues A, et al. Non-Specific Effects of Standard Measles Vaccine at 4.5 and 9 Months of Age on Childhood Mortality: Randomised Controlled Trial. *BMJ* (2010) 341:c6495. doi: 10.1136/bmj.c6495

20. Aaby P, Roth A, Ravn H, Napirna BM, Rodrigues A, Lisse IM, et al. Randomized Trial of BCG Vaccination at Birth to Low-Birth-Weight Children: Beneficial Nonspecific Effects in the Neonatal Period? *J Infect Dis* (2011) 204(2):245–52. doi: 10.1093/infdis/jir240
21. Biering-Sorensen S, Aaby P, Napirna BM, Roth A, Ravn H, Rodrigues A, et al. Small Randomized Trial Among Low-Birth-Weight Children Receiving Bacillus Calmette-Guerin Vaccination at First Health Center Contact. *Pediatr Infect Dis J* (2012) 31(3):306–8. doi: 10.1097/INF.0b013e3182458289
22. Sorup S, Villumsen M, Ravn H, Benn CS, Sorensen TI, Aaby P, et al. Smallpox Vaccination and All-Cause Infectious Disease Hospitalization: A Danish Register-Based Cohort Study. *Int J Epidemiol* (2011) 40(4):955–63. doi: 10.1093/ije/dyr063
23. Gu H, Zeng X, Peng L, Xiang C, Zhou Y, Zhang X, et al. Vaccination Induces Rapid Protection Against Bacterial Pneumonia via Training Alveolar Macrophage in Mice. *Elife* (2021) 10:e69951. doi: 10.7554/eLife.69951
24. Hashimoto D, Chow A, Noizat C, Teo P, Beasley MB, Leboeuf M, et al. Tissue-Resident Macrophages Self-Maintain Locally Throughout Adult Life With Minimal Contribution From Circulating Monocytes. *Immunity* (2013) 38 (4):792–804. doi: 10.1016/j.immuni.2013.04.004
25. Patel AA, Zhang Y, Fullerton JN, Boelen L, Rongvaux A, Maini AA, et al. The Fate and Lifespan of Human Monocyte Subsets in Steady State and Systemic Inflammation. *J Exp Med* (2017) 214(7):1913–23. doi: 10.1084/jem.20170355
26. Sieburg HB, Rezner BD, Muller-Sieburg CE. Predicting Clonal Self-Renewal and Extinction of Hematopoietic Stem Cells. *Proc Natl Acad Sci USA* (2011) 108(11):4370–5. doi: 10.1073/pnas.1011414108
27. Khan N, Downey J, Sanz J, Kaufmann E, Blankenhaus B, Pacis A, et al. M. Tuberculosis Reprograms Hematopoietic Stem Cells to Limit Myelopoiesis and Impair Trained Immunity. *Cell* (2020) 183(3):752–70.e22. doi: 10.1016/j.cell.2020.09.062
28. Boettcher S, Manz MG. Regulation of Inflammation- and Infection-Driven Hematopoiesis. *Trends Immunol* (2017) 38(5):345–57. doi: 10.1016/j.it.2017.01.004
29. Nagai Y, Garrett KP, Ohta S, Bahrun U, Kouro T, Akira S, et al. Toll-Like Receptors on Hematopoietic Progenitor Cells Stimulate Innate Immune System Replenishment. *Immunity* (2006) 24(6):801–12. doi: 10.1016/j.immuni.2006.04.008
30. Takizawa H, Fritsch K, Kovtonyuk LV, Saito Y, Yakkala C, Jacobs K, et al. Pathogen-Induced TLR4-TRIF Innate Immune Signaling in Hematopoietic Stem Cells Promotes Proliferation But Reduces Competitive Fitness. *Cell Stem Cell* (2017) 21(2):225–40.e5. doi: 10.1016/j.stem.2017.06.013
31. Megias J, Yanez A, Moriano S, O'Connor JE, Gozalbo D, Gil ML. Direct Toll-Like Receptor-Mediated Stimulation of Hematopoietic Stem and Progenitor Cells Occurs *In Vivo* and Promotes Differentiation Toward Macrophages. *Stem Cells* (2012) 30(7):1486–95. doi: 10.1002/stem.1110
32. Sioud M, Floisand Y, Forfang L, Lund-Johansen F. Signaling Through Toll-Like Receptor 7/8 Induces the Differentiation of Human Bone Marrow CD34+ Progenitor Cells Along the Myeloid Lineage. *J Mol Biol* (2006) 364(5):945–54. doi: 10.1016/j.jmb.2006.09.054
33. Crane GM, Jeffery E, Morrison SJ. Adult Haematopoietic Stem Cell Niches. *Nat Rev Immunol* (2017) 17(9):573–90. doi: 10.1038/nri.2017.53
34. Wright DE, Wagers AJ, Gulati AP, Johnson FL, Weissman IL. Physiological Migration of Hematopoietic Stem and Progenitor Cells. *Science* (2001) 294 (5548):1933–6. doi: 10.1126/science.1064081
35. Massberg S, Schaerli P, Knezevic-Maramica I, Kollnberger M, Tubo N, Moseman EA, et al. Immunosurveillance by Hematopoietic Progenitor Cells Trafficking Through Blood, Lymph, and Peripheral Tissues. *Cell* (2007) 131 (5):994–1008. doi: 10.1016/j.cell.2007.09.047
36. Mitroulis I, Ruppova K, Wang B, Chen LS, Grzybek M, Grinenko T, et al. Modulation of Myelopoiesis Progenitors Is an Integral Component of Trained Immunity. *Cell* (2018) 172(1-2):147–61.e12. doi: 10.1016/j.cell.2017.11.034
37. Moorlag S, Khan N, Novakovic B, Kaufmann E, Jansen T, van Crevel R, et al. Beta-Glucan Induces Protective Trained Immunity Against Mycobacterium Tuberculosis Infection: A Key Role for IL-1. *Cell Rep* (2020) 31(7):107634. doi: 10.1016/j.celrep.2020.107634
38. Kaufmann E, Sanz J, Dunn JL, Khan N, Mendonca LE, Pacis A, et al. BCG Educates Hematopoietic Stem Cells to Generate Protective Innate Immunity Against Tuberculosis. *Cell* (2018) 172(1-2):176–90.e19. doi: 10.1016/j.cell.2017.12.031
39. Frodermann V, Rohde D, Courties G, Severe N, Schloss MJ, Amatullah H, et al. Exercise Reduces Inflammatory Cell Production and Cardiovascular Inflammation *via* Instruction of Hematopoietic Progenitor Cells. *Nat Med* (2019) 25(11):1761–71. doi: 10.1038/s41591-019-0633-x
40. Bono C, Martinez A, Megias J, Gozalbo D, Yanez A, Gil ML. Dectin-1 Stimulation of Hematopoietic Stem and Progenitor Cells Occurs In Vivo and Promotes Differentiation Toward Trained Macrophages *via* an Indirect Cell-Autonomous Mechanism. *mBio* (2020) 11(3):e00781–20. doi: 10.1128/mBio.00781-20
41. de Laval B, Maurizio J, Kandalla PK, Brisou G, Simonnet L, Huber C, et al. C/Ebpbeta-Dependent Epigenetic Memory Induces Trained Immunity in Hematopoietic Stem Cells. *Cell Stem Cell* (2020) 26(5):657–74.e8. doi: 10.1016/j.stem.2020.01.017
42. Jentho E, Ruiz-Moreno C, Novakovic B, Kourtzelis I, Megchelenbrink WL, Martins R, et al. Trained Innate Immunity, Long-Lasting Epigenetic Modulation, and Skewed Myelopoiesis by Heme. *Proc Natl Acad Sci USA* (2021) 118(42):e2102698118. doi: 10.1073/pnas.2102698118
43. Christ A, Gunther P, Lauterbach MAR, Duewell P, Biswas D, Pelka K, et al. Western Diet Triggers Nlrp3-Dependent Innate Immune Reprogramming. *Cell* (2018) 172(1-2):162–75.e14. doi: 10.1016/j.cell.2017.12.013
44. Kaushansky K. Lineage-Specific Hematopoietic Growth Factors. *N Engl J Med* (2006) 354(19):2034–45. doi: 10.1056/NEJMra052706
45. Yang L, Dybedal I, Bryder D, Nilsson L, Sitnicka E, Sasaki Y, et al. IFN-Gamma Negatively Modulates Self-Renewal of Repopulating Human Hemopoietic Stem Cells. *J Immunol* (2005) 174(2):752–7. doi: 10.4049/jimmunol.174.2.752
46. de Bruin AM, Demirel O, Hooibrink B, Brandts CH, Nolte MA. Interferon-Gamma Impairs Proliferation of Hematopoietic Stem Cells in Mice. *Blood* (2013) 121(18):3578–85. doi: 10.1182/blood-2012-05-432906
47. Comazzetto S, Murphy MM, Berto S, Jeffery E, Zhao Z, Morrison SJ. Restricted Hematopoietic Progenitors and Erythropoiesis Require SCF From Leptin Receptor+ Niche Cells in the Bone Marrow. *Cell Stem Cell* (2019) 24(3):477–86.e6. doi: 10.1016/j.stem.2018.11.022
48. Ding L, Saunders TL, Enikolopov G, Morrison SJ. Endothelial and Perivascular Cells Maintain Haematopoietic Stem Cells. *Nature* (2012) 481 (7382):457–62. doi: 10.1038/nature10783
49. De Luca K, Frances-Duvert V, Asensio MJ, Ihsani R, Debien E, Taillardet M, et al. The TLR1/2 Agonist PAM(3)CSK(4) Instructs Commitment of Human Hematopoietic Stem Cells to a Myeloid Cell Fate. *Leukemia* (2009) 23 (11):2063–74. doi: 10.1038/leu.2009.155
50. Sioud M, Floisand Y. NOD2/CARD15 on Bone Marrow CD34+ Hematopoietic Cells Mediates Induction of Cytokines and Cell Differentiation. *J Leukoc Biol* (2009) 85(6):939–46. doi: 10.1189/jlb.1008650
51. Zhao JL, Ma C, O'Connell RM, Mehta A, DiLoreto R, Heath JR, et al. Conversion of Danger Signals Into Cytokine Signals by Hematopoietic Stem and Progenitor Cells for Regulation of Stress-Induced Hematopoiesis. *Cell Stem Cell* (2014) 14(4):445–59. doi: 10.1016/j.stem.2014.01.007
52. Martinez A, Bono C, Megias J, Yanez A, Gozalbo D, Gil ML. Systemic Candidiasis and TLR2 Agonist Exposure Impact the Antifungal Response of Hematopoietic Stem and Progenitor Cells. *Front Cell Infect Microbiol* (2018) 8:309. doi: 10.3389/fcimb.2018.00309
53. Megias J, Martinez A, Yanez A, Goodridge HS, Gozalbo D, Gil ML. TLR2, TLR4 and Dectin-1 Signalling in Hematopoietic Stem and Progenitor Cells Determines the Antifungal Phenotype of the Macrophages They Produce. *Microbes Infect* (2016) 18(5):354–63. doi: 10.1016/j.micinf.2016.01.005
54. Martinez A, Bono C, Megias J, Yanez A, Gozalbo D, Gil ML. PRR Signaling During *In Vitro* Macrophage Differentiation From Progenitors Modulates Their Subsequent Response to Inflammatory Stimuli. *Eur Cytokine Netw* (2017) 28(3):102–10. doi: 10.1684/ecn.2017.0398
55. Yanez A, Hassanzadeh-Kiabi N, Ng MY, Megias J, Subramanian A, Liu GY, et al. Detection of a TLR2 Agonist by Hematopoietic Stem and Progenitor Cells Impacts the Function of the Macrophages They Produce. *Eur J Immunol* (2013) 43(8):2114–25. doi: 10.1002/eji.201343403
56. Yanez A, Megias J, O'Connor JE, Gozalbo D, Gil ML. Candida Albicans Induces Selective Development of Macrophages and Monocyte Derived Dendritic Cells by a TLR2 Dependent Signalling. *PloS One* (2011) 6(9): e24761. doi: 10.1371/journal.pone.0024761
57. Sasaki Y, Guo YM, Goto T, Ubukawa K, Asanuma K, Kobayashi I, et al. IL-6 Generated From Human Hematopoietic Stem and Progenitor Cells Through

TLR4 Signaling Promotes Emergency Granulopoiesis by Regulating Transcription Factor Expression. *J Immunol* (2021) 207(4):1078–86. doi: 10.4049/jimmunol.2100168
58. Zhang H, Rodriguez S, Wang L, Wang S, Serezani H, Kapur R, et al. Sepsis Induces Hematopoietic Stem Cell Exhaustion and Myelosuppression Through Distinct Contributions of TRIF and MYD88. *Stem Cell Rep* (2016) 6(6):940–56. doi: 10.1016/j.stemcr.2016.05.002
59. Liu A, Wang Y, Ding Y, Baez I, Payne KJ, Borghesi L. Cutting Edge: Hematopoietic Stem Cell Expansion and Common Lymphoid Progenitor Depletion Require Hematopoietic-Derived, Cell-Autonomous TLR4 in a Model of Chronic Endotoxin. *J Immunol* (2015) 195(6):2524–8. doi: 10.4049/jimmunol.1501231
60. Figueiredo RT, Fernandez PL, Mourao-Sa DS, Porto BN, Dutra FF, Alves LS, et al. Characterization of Heme as Activator of Toll-Like Receptor 4. *J Biol Chem* (2007) 282(28):20221–9. doi: 10.1074/jbc.M610737200
61. Janciauskiene S, Vijayan V, Immenschuh S. TLR4 Signaling by Heme and the Role of Heme-Binding Blood Proteins. *Front Immunol* (2020) 11:1964. doi: 10.3389/fimmu.2020.01964
62. Mann M, Mehta A, de Boer CG, Kowalczyk MS, Lee K, Haldeman P, et al. Heterogeneous Responses of Hematopoietic Stem Cells to Inflammatory Stimuli Are Altered With Age. *Cell Rep* (2018) 25(11):2992–3005.e5. doi: 10.1016/j.celrep.2018.11.056
63. Nankabirwa V, Tumwine JK, Mugaba PM, Tylleskar T, Sommerfelt H, Group P-ES. Child Survival and BCG Vaccination: A Community Based Prospective Cohort Study in Uganda. *BMC Public Health* (2015) 15:175. doi: 10.1186/s12889-015-1497-8
64. Moorlag S, van Deuren RC, van Werkhoven CH, Jaeger M, Debisarun P, Taks E, et al. Safety and COVID-19 Symptoms in Individuals Recently Vaccinated With BCG: A Retrospective Cohort Study. *Cell Rep Med* (2020) 1(5):100073. doi: 10.1016/j.xcrm.2020.100073
65. Rivas MN, Ebinger JE, Wu M, Sun N, Braun J, Sobhani K, et al. BCG Vaccination History Associates With Decreased SARS-Cov-2 Seroprevalence Across a Diverse Cohort of Health Care Workers. *J Clin Invest* (2021) 131(2):e145157. doi: 10.1172/JCI145157
66. Yu VWC, Yusuf RZ, Oki T, Wu J, Saez B, Wang X, et al. Epigenetic Memory Underlies Cell-Autonomous Heterogeneous Behavior of Hematopoietic Stem Cells. *Cell* (2016) 167(5):1310–22.e17. doi: 10.1016/j.cell.2016.10.045
67. Katzmarski N, Dominguez-Andres J, Cirovic B, Renieris G, Ciarlo E, Le Roy D, et al. Transmission of Trained Immunity and Heterologous Resistance to Infections Across Generations. *Nat Immunol* (2021) 22(11):1382–90. doi: 10.1038/s41590-021-01052-7
68. Berendsen MLT, Oland CB, Bles P, Jensen AKG, Kofoed PE, Whittle H, et al. Maternal Priming: Bacillus Calmette-Guerin (BCG) Vaccine Scarring in Mothers Enhances the Survival of Their Child With a BCG Vaccine Scar. *J Pediatr Infect Dis Soc* (2020) 9(2):166–72. doi: 10.1093/jpids/piy142
69. DiNardo AR, Netea MG, Musher DM. Postinfectious Epigenetic Immune Modifications - a Double-Edged Sword. *N Engl J Med* (2021) 384(3):261–70. doi: 10.1056/NEJMra2028358
70. Pietras EM, Mirantes-Barbeito C, Fong S, Loeffler D, Kovtonyuk LV, Zhang S, et al. Chronic Interleukin-1 Exposure Drives Haematopoietic Stem Cells Towards Precocious Myeloid Differentiation at the Expense of Self-Renewal. *Nat Cell Biol* (2016) 18(6):607–18. doi: 10.1038/ncb3346
71. Wendeln AC, Degenhardt K, Kaurani L, Gertig M, Ulas T, Jain G, et al. Innate Immune Memory in the Brain Shapes Neurological Disease Hallmarks. *Nature* (2018) 556(7701):332–8. doi: 10.1038/s41586-018-0023-4
72. Bekkering S, van den Munckhof I, Nielen T, Lamfers E, Dinarello C, Rutten J, et al. Innate Immune Cell Activation and Epigenetic Remodeling in Symptomatic and Asymptomatic Atherosclerosis in Humans In Vivo. *Atherosclerosis* (2016) 254:228–36. doi: 10.1016/j.atherosclerosis.2016.10.019
73. Shirai T, Nazarewicz RR, Wallis BB, Yanes RE, Watanabe R, Hilhorst M, et al. The Glycolytic Enzyme PKM2 Bridges Metabolic and Inflammatory Dysfunction in Coronary Artery Disease. *J Exp Med* (2016) 213(3):337–54. doi: 10.1084/jem.20150900
74. Bulut O, Kilic G, Dominguez-Andres J, Netea MG. Overcoming Immune Dysfunction in the Elderly: Trained Immunity as a Novel Approach. *Int Immunol* (2020) 32(12):741–53. doi: 10.1093/intimm/dxaa052
75. Giamarellos-Bourboulis EJ, Tsilika M, Moorlag S, Antonakos N, Kotsaki A, Dominguez-Andres J, et al. Activate: Randomized Clinical Trial of BCG Vaccination Against Infection in the Elderly. *Cell* (2020) 183(2):315–23.e9. doi: 10.1016/j.cell.2020.08.051
76. Pavan Kumar N, Padmapriyadarsini C, Rajamanickam A, Marinaik SB, Nancy A, Padmanaban S, et al. Effect of BCG Vaccination on Proinflammatory Responses in Elderly Individuals. *Sci Adv* (2021) 7(32):eabg7181. doi: 10.1126/sciadv.abg7181
77. Ferrucci L, Fabbri E. Inflammageing: Chronic Inflammation in Ageing, Cardiovascular Disease, and Frailty. *Nat Rev Cardiol* (2018) 15(9):505–22. doi: 10.1038/s41569-018-0064-2
78. Fulop T, Dupuis G, Baehl S, Le Page A, Bourgade K, Frost E, et al. From Inflamm-Aging to Immune-Paralysis: A Slippery Slope During Aging for Immune-Adaptation. *Biogerontology* (2016) 17(1):147–57. doi: 10.1007/s10522-015-9615-7
79. Mulder WJM, Ochando J, Joosten LAB, Fayad ZA, Netea MG. Therapeutic Targeting of Trained Immunity. *Nat Rev Drug Discovery* (2019) 18(7):553–66. doi: 10.1038/s41573-019-0025-4
80. Tough DF, Tak PP, Tarakhovsky A, Prinjha RK. Epigenetic Drug Discovery: Breaking Through the Immune Barrier. *Nat Rev Drug Discov* (2016) 15(12):835–53. doi: 10.1038/nrd.2016.185

Conflict of Interest: The authors declare that the research was conducted in the absence of any commercial or financial relationships that could be construed as a potential conflict of interest.

Publisher's Note: All claims expressed in this article are solely those of the authors and do not necessarily represent those of their affiliated organizations, or those of the publisher, the editors and the reviewers. Any product that may be evaluated in this article, or claim that may be made by its manufacturer, is not guaranteed or endorsed by the publisher.

frontiers in Immunology

ORIGINAL RESEARCH
published: 17 February 2022
doi: 10.3389/fimmu.2022.835348

LPS Guides Distinct Patterns of Training and Tolerance in Mast Cells

Marco De Zuani[1,2†], *Chiara Dal Secco*[1†], *Silvia Tonon*[1], *Alessandra Arzese*[1], *Carlo E. M. Pucillo*[1*] *and Barbara Frossi*[1]

[1] Department of Medicine, University of Udine, Udine, Italy, [2] International Clinical Research Center, St. Anne's University Hospital Brno, Brno, Czechia

Mast cells (MCs) are tissue-resident, long lived innate immune cells with important effector and immunomodulatory functions. They are equipped with an eclectic variety of receptors that enable them to sense multiple stimuli and to generate specific responses according on the type, strength and duration of the stimulation. Several studies demonstrated that myeloid cells can retain immunological memory of their encounters – a process termed 'trained immunity' or 'innate immune memory'. As MCs are among the one of first cells to come into contact with the external environment, it is possible that such mechanisms of innate immune memory might help shaping their phenotype and effector functions; however, studies on this aspect of MC biology are still scarce. In this manuscript, we investigated the ability of MCs primed with different stimuli to respond to a second stimulation with the same or different ligands, and determined the molecular and epigenetic drivers of these responses. Our results showed that, while the stimulation with IgE and β-glucan failed to induce either tolerant or trained phenotypes, LPS conditioning was able to induce a profound and long-lasting remodeling of the signaling pathways involved in the response against LPS or fungal pathogens. On one side, LPS induced a strong state of unresponsiveness to secondary LPS stimulation due to the impairment of the PI3K-AKT signaling pathway, which resulted in the reduced activation of NF-κB and the decreased release of TNF-α and IL-6, compared to naïve MCs. On the other side, LPS primed MCs showed an increased release of TNF-α upon fungal infection with live *Candida albicans*, thus suggesting a dual role of LPS in inducing both tolerance and training phenotypes depending on the secondary challenge. Interestingly, the inhibition of HDAC during LPS stimulation partially restored the response of LPS-primed MCs to a secondary challenge with LPS, but failed to revert the increased cytokine production of these cells in response to *C. albicans*. These data indicate that MCs, as other innate immune cells, can develop innate immune memory, and that different stimulatory environments can shape and direct MC specific responses towards the dampening or the propagation of the local inflammatory response.

Keywords: mast cell, trained immunity, endotoxin tolerance, cytokines, LPS, *Candida albicans*

OPEN ACCESS

Edited by:
Francesca Granucci, University of Milano-Bicocca, Italy

Reviewed by:
Ulrich Blank, Institut National de la Santé et de la Recherche Médicale (INSERM), France
Andrea Cossarizza, University of Modena and Reggio Emilia, Italy

***Correspondence:**
Carlo E. M. Pucillo
carlo.pucillo@uniud.it

†These authors share first authorship

Specialty section:
This article was submitted to Molecular Innate Immunity, a section of the journal Frontiers in Immunology

Received: *14 December 2021*
Accepted: *26 January 2022*
Published: *17 February 2022*

Citation:
De Zuani M, Dal Secco C, Tonon S, Arzese A, Pucillo CEM and Frossi B (2022) LPS Guides Distinct Patterns of Training and Tolerance in Mast Cells. Front. Immunol. 13:835348. doi: 10.3389/fimmu.2022.835348

INTRODUCTION

Despite lacking the fine antigen specificity, clonality, and longevity of adaptive lymphocytes, innate immune cells have been demonstrated to retain traits of memory of earlier challenges (e.g., infection or vaccination) and thereby display increased responsiveness upon re-challenge with the same or even unrelated stimuli (1). This enhanced state of immune activation is known as "innate immune memory" or "trained immunity" (2). Acquisition of a trained immunity state by innate immune cells involves metabolic, epigenetic and transcriptional reprogramming which is sustained for months (3, 4). Most studies have focused on changes in immune cell responses upon primary activation *via* numerous TLR ligands such as LPS, β-glucan, Pam3CSK4, CpG, and muramyl dipeptide, with training or tolerant effects depending on the type of the first stimulus received by the cells (5). This process has been described on many innate immune cells (such as monocyte/macrophages and natural killer cells) in both humans and rodents, but not completely for mast cells (MCs).

MCs belong to the innate branch of the immune system and are particularly abundant at sites where they are likely to encounter foreign molecules or microbial ligands. Both their terminal differentiation and responsiveness are highly influenced by tissue-specific stimuli. Moreover, MCs are fully equipped with an eclectic variety of receptors, and thus can be directly activated by a plethora of different stimuli (6). This plasticity, together with the strategic location in which they are normally found, makes it easy to understand why MCs are involved in different processes, from the defense against pathogens to the maintenance of tolerance and the crosstalk with other cells of the adaptive immune system (7). This versatility depends on the ability of MCs to detect pathogens and danger signals and release a unique panel of mediators to promote pro- and anti-inflammatory reactions (8).

Given the ubiquitous tissue presence of MCs and their capability to respond to a broad spectrum of stimuli, it is expected that MCs, as other innate immune cells, may also retain innate immune memory, which could explain the diverse contribution of these cells in different physiological and pathological settings (9). Consistent with this hypothesis, it has been recently demonstrated that MCs can retain a memory phenotype as a consequence of epigenetic modifications that regulate their differentiation and response to danger signals (10). Similarly, stimulation with LPS is known to induce a transient unresponsiveness in MCs (11), while IgE sensitization was described to increase their responsiveness to LPS (12). Notably, both positive and negative effects of LPS priming on FcεRI-dependent activation of MCs have been documented, suggesting a critical role of LPS in MC-dependent allergic reactions (13). However, the development of a tolerant or trained phenotype in MCs has been poorly investigated and the studies conducted so far are based on short-term experiments, with the cells being restimulated and analyzed immediately after removal of the first stimulus.

In this manuscript, we aimed to determine the long-term effect of different immunological and microenvironmental stimuli on MCs development and reactivity, by adopting an experimental panel that allowed the cells to rest for 6 days between the first stimulation and the subsequent ones. The ability of MCs primed with different stimuli (LPS, curdlan, and IgE/Ag) to respond to a secondary stimulation with the same or different triggers, was investigated at molecular and epigenetic level revealing a specific behavior of the MC that depends on the type of signal the cell received.

MATERIAL AND METHODS

Mice

C57BL/6 mice were purchased from Envigo (Netherlands) and maintained at the animal facility of the Department of Medicine, University of Udine (Italy). All animal experiments were performed according to the animal care and in accordance to institutional guidelines and national law (D.Lgs. 26/2014).

BMMCs Generation

Bone marrow-derived MCs (BMMCs) were obtained from 6- to 8- weeks-old mice by *in vitro* differentiation of bone marrow-derived progenitors obtained from mice femurs and tibiae. Precursor cells were cultivated in complete IL-3 medium [RPMI 1640 medium (Euroclone) supplemented with 20% FBS (Sigma Aldrich), 100 U/ml penicillin, 100 mg/ml Streptomycin, 2 mM Glutamine, 20 mM Hepes, non-essential aminoacids, 1 mM Sodium Pyruvate (Euroclone), 50 mM β-mercaptoethanol (Sigma Aldrich) and 20 ng/ml IL-3 (Peprotech)] at 37°C in 5% CO_2 atmosphere. After 5 weeks, BMMCs differentiation was confirmed by flow cytometry by staining with anti-FcεRIα–PE (MAR-1) and anti-cKit–PE-Cy7 (ACK2) conjugated antibodies (eBiosciences). Data were acquired with a FACScalibur cytofluorimeter (Becton Dikinson) and analyzed with FlowJo software (FlowJo LLC). BMMCs were usually more than 98% cKit and FcεRI double positive.

Candida albicans Cultures

Wild-type *Candida albicans* (*C. albicans*) SC5314 strain was a kind gift of Prof. Luigina Romani, University of Perugia (Perugia, Italy). Yeast was seeded on Sabouraud agar supplemented with 50 μg/ml chloramphenicol and incubated at 30°C for 24 hours. To generate *C. albicans hyphae*, 10^7 yeast cells were resuspended in complete RPMI medium, seeded into T-25 adhesion flasks and allowed to germinate for 3 hours at 37°C. *Hyphae* were harvested by scraping, centrifuged at 700 x g for 10 minutes and washed with PBS.

BMMCs Activation

Before all *in vitro* experiments, BMMCs were starved for 1 hour in IL-3–free complete RPMI medium. For IgE-dependent activation, BMMC were sensitized in IL-3–free complete RPMI medium for 3 hours with 1 μg/ml of dinitrophenol (DNP)-

specific IgE, washed twice and challenged with 100 ng/ml DNP (Sigma- Aldrich).

For *C. albicans* infections, BMMCs were stimulated with *C. albicans* yeast (1:1 ratio) or *hyphae* (1:10 ratio) at a final concentration of 2 x 10^6 cells/ml in IL-3–free complete RPMI medium. To limit fungal growth, Amphotericin-B (Sigma Aldrich) was added to each well at a final concentration of 10 ng/ml. RNA extraction was performed before the addition of Amphotericin-B.

For the stimulation–restimulation panel (described in **Figure 1A**), BMMCs were differentiated for 6 weeks in complete IL-3 medium and checked for purity by flow cytometry. BMMCs were left untreated or stimulated for 24 hours with 1 µg/ml LPS (LPS from *E. coli* O55:E5, Sigma Aldrich), 10 µg/ml curdlan (*In vivo*gen), IgE/Ag (100 ng/ml DNP) in IL-3–free complete RPMI medium. After the stimulation, supernatants were collected and cells were washed twice with PBS and put back in culture in fresh complete–IL-3

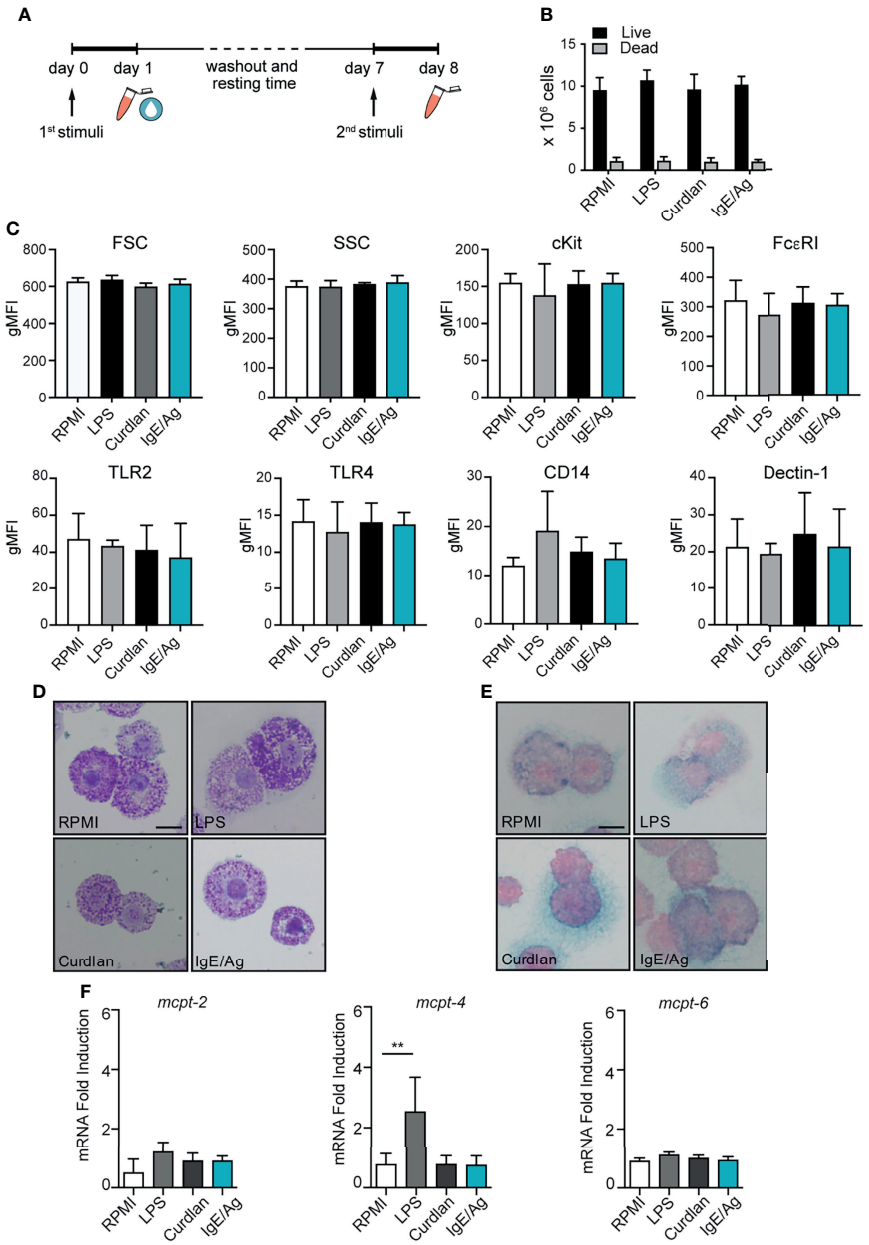

FIGURE 1 | MC vitality and phenotype after the conditioning period. **(A)** Schematic representation of experimental protocol. BMMC were first stimulated for 24h with LPS, curdlan, IgE/Ag or left untreated (RPMI). Then cells were left to recover for 6 days, countedand tested for viability by means of trypan blue exclusion **(B)**, analyzed for surface marker expression **(C)**, stained with Toluidin blue **(D)** and Alcian-blu safranin **(E)** and analyzed for connective and mucosal proteases mRNA expression **(F)**. Data are expressed as mean +SD from n>3 experiments; statistical analysis were performed with one-way Anova with Dunnet correction (**p < 0,01).

for 6 days. Each cells subset was then re-stimulated with 100 ng/ml LPS, live *C. albicans* yeasts (MOI=1) or IgE/Ag for 24 hours. In some experiments, before the addition of the first stimulus, cells were pre-treated with inhibitors of HDAC: 1nM suberoylanilide hydroxamic acid (SAHA, from Sigma Aldrich) or 10nM Trichostatin (TSA, from Sigma Aldrich).

Flow Cytometry

0.5 x 10^6 cells were harvested, washed with PBS and stained for 30 minutes at 4°C in the dark with monoclonal conjugated antibodies. All antibodies were from Biolegend: anti-FcεRI–PE (MAR-1), anti-cKit–PE-Cy7 (ACK2), anti-CD14 PE (Sa14-2), anti-TLR2 PE (6C2), anti-TLR4 APC (SA15-21), anti-Dectin-1 PE (bg1fpj). Cells were then washed twice with PBS and acquired with a FACSCalibur flow cytometer (Becton Dickinson).

Histochemical Staining

10^4 BMMCs were cytospin onto SuperFrost glass slides (Menzel) at 300 x g for 3 minutes and allowed to air-dry overnight. For toluidine blue staining, slides were incubated for 5 minutes with a solution of 1% toluidine blue [pH 5] (Sigma Aldrich), rinsed twice in PBS and once in water, then allowed to air-dry and mounted with Micro mount (Diapath). For alcian blue–safranin staining, slides were incubated for 10 minutes with a solution of 0.5% alcian blue (Sigma Aldrich) in 0.3% acetic acid [pH 3], rinsed twice in PBS then incubated for 20 minutes with a solution of 0.1% safranin-O (Sigma Aldrich) in 0.1% acetic acid [pH 4]. Slides were then rinsed and mounted as described above. Images were acquired with a Leica DM750 equipped with a Leica ICC50W camera at a magnification of 63x and processed with Fiji (ImageJ) software.

Degranulation Assay

BMMCs degranulation response was determined as the percentage of β-hexosaminidase released. 0.5 x 10^6 BMMCs were incubated in Tyrode's buffer (10 mM HEPES buffer [pH 7.4], 130 mM NaCl, 5 mM KCl, 1.4 mM $CaCl_2$, 1mM $MgCl_2$, 5.6 mM glucose, and 0.1% BSA) with or without the addition of 10% FBS, and stimulated with the same number of *C. albicans* yeasts at 37° for the indicated time points. As positive control, 0.5 x 10^6 BMMCs were sensitized in complete RPMI medium for 3 hours with 1 μg/ml of dinitrophenol (DNP)-specific IgE, then washed twice, resuspended in Tyrode's buffer and challenged with 100 ng/ml DNP (Sigma-Aldrich). The enzymatic activity of the released β-hexosaminidase was assessed by the cleavage of its synthetic substrate (p-nitrophenyl N-acetyl- glucosamide, Sigma Aldrich) in p-nitrophenol and measuring the p-nitrophenol absorbance at 405nm with a plate spectrophotometer. Results are expressed as the percentage of b-hexosaminidase released over β-hexosaminidase retained in the cytoplasm.

Cytokine ELISA Assays

Supernatants for cytokine quantitation were collected 24 hours after BMMC stimulation. Supernatants were assessed for TNF-α and IL-6, using specific ELISA kits (eBiosciences) according to the manufacturer's instructions.

RNA Extraction and Real-Time PCR Analyses

Cells were lysed with EUROGOLD TriFast (Euroclone) and total RNA extracted according to manufacturer's instructions. Total RNA was quantified using a NanoDropTM spectrophotometer (ThermoFischer) and retro-transcribed with the SensiFAST™ cDNA Synthesis kit (Bioline). Quantitative qPCR analyses were performed with SYBR Green chemistry (BioRad) using a BioRad CFX96 real-time PCR detection systems. Target genes expression were quantified with the ΔΔCt method using G3PDH (glyceraldehyde 3-phosphate dehydrogenase) as normalizer gene. The un-treated sample with the lowest expression was set to one and used to calculate the fold inductions of all other samples. Primer's sequence are:

mG3PDH_for TCAACAGCAACTCCCACTCTTCC;
mG3PDH_rev ACCCTGTTGCTGTAGCCGTATTC;
mMCPT-4_for GGGCTGGAGCTGAGGAGATTA;
mMCPT-4_rev GTCAACACAAATTGGCGGGA
mMCPT-2_for AAGCTCACCAAGGCCTCAAC;
mMCPT-2_rev ACACCACCAATAATCTCCTCAG
mMCPT-6_for CGACATTGATCCTGACGAGCCTC;
mMCPT-6_rev ACAGGTGTTTTCCACAATGG
mTNF-alpha_for AGGCACTCCCCCAAAGATG;
mTNF-alpha_rev CCATTTGGGAACTTCTCATCCC
mIL-6_for ACCACTTCACAAGTCGGAGGCTTA;
mIL-6_rev TCTGCAAGTGCATCATCGTTGTTC;
mSOCS3_for GGGAGCCCCTTTGTAGACTT;
mSOCS3_rev CATCCCGGGGAGCTAGT

Cell Lysis and Western Blot Analyses

BMMCs were stimulated with an equal number of *C. albicans* yeasts or with the indicated stimuli or left untreated for the indicated times. Cells were then incubated for 5 minutes on ice to stop the reaction and centrifuged 300 x g, 5 minutes at 4°C. Before the lysis, BMMCs were washed twice with PBS + phosphatase inhibitors (Active Motif). Cell pellet were lysed in 50 μl NP-40 buffer (25 mM Tris-HCl [pH 7.4], 150 mM NaCl, 1 mM EDTA, 1% NP-40 and 5% glycerol, 1 mM Na3VO4, 50 mM NaF (Sigma Aldrich), and COmplete Mini protease inhibitor cocktail (Roche, usage according to manufacturer)) for 10 minutes on ice. Lysates were then centrifuged at 12000 x g, 4°C for 10 minutes and supernatants were collected and stored at -80 C.

Upon western blot analyses, lysates were diluted with 4x Laemmli buffer and denatured 7 minutes at 95°C. Lysates were then separated on SDS 10% polyacrilamide gels and blotted on a nitrocellulose membrane (Amersham) at 300 V, 250 mA, 4°C for 3 hours. Membranes for phosphoproteins were blocked in TBS-T (20 mM Tris-base [pH 7.6], 150 mM NaCl, 0.05% Tween-20) +

5% BSA while membranes for total proteins were blocked in TBS-T + 5% non-fat dry milk for 1 hour at room temperature. Primary antibodies for phosphoproteins were diluted 1:1000 in TBS-T + 5% BSA and membranes probed overnight at 4°C with gentle agitation. HRP-conjugated secondary antibodies (Pierce) were incubated for 1 hour at room temperature with gentle agitation. Signals were detected using ECL substrates Luminata forte (Millipore) or SuperSignal West Femto (Thermo Scientific) and acquired with a ChemiDoc imaging system (BioRad). Densitometric analyses were performed with the Image Lab 5.2 software (BioRad). Probed membranes were stripped twice for 10 minutes at room temperature in mild stripping buffer (0.2 M glycine, 0.1% SDS (Sigma Aldrich), 1% Tween20, pH 2.2) than blocked in TBS-T + 5% non-fat dry milk for 1 hour at room temperature and reprobed overnight at 4 C with gentle agitation. Antibodies (clones, vendors): actin (C4, BD biosciences), AKT (BD bio- sciences), phospho-AKT S473 (D9E, CST), PI3K p85 (CST), phospho-PI3K p85 p55 Y459 Y199 (CST), p38 MAPK (CST), phospho-p38 MAPK T180 Y182 (CST), PI3K p110d (A-8, Santa Cruz).

NF-κB Activity

Nuclear protein fractions were obtained as described above and protein concentration was measured with the PierceTM BCA Protein Assay Kit (Thermo Scientific). 20 μg of protein extracts were used for the quantification of NF-κB p65 and p50 activity using the TransAM^{TM} NF-kB kit (Active Motif) according to manufacturer's instructions.

DNA Methylation Analysis

CpG methylation was determined by either pyrosequencing or real-time methylation specific PCR (rt-MSP). For each condition, gDNA was extracted and bisulphite-converted from up to 10^5 cells using the EpiTect Fast Bisulfite Conversion kit (Qiagen). ssDNA was quantified with NanoDrop 2000 and 20 ng were used to produce PCR amplicons. TNF-α promoter methylation was determined by pyrosequencing: PCR products from bisulphite-converted DNA were sequenced using PyroMark Q24 ID (Qiagen) while the data was analyzed with PyroMark software. In order to perform the analysis, the selected region (mm10 chr17:35201591-35202581) was divided into two subregions (primer listed in **Supplemental Material S2**). Both regions were amplified with 45 cycles: region 1 Ta=50°C while region 2 Ta= 55°C.

SOCS3 promoter methylation was determined instead by rt-MSP. The methylation status was quantified calculating the difference between unmethylated and methylated Ct values (uCt – mCt): the smaller the ΔCt value is, the greater will be the proportion of methylation in the region (14). All primers used for methylation analysis are listed in in **Supplemental Material S2**.

Statistical Analyses

Unless otherwise indicated, results are expressed as mean ± standard deviation (SD) of at least three experimental replicates. Data were analyzed using paired Student t-test or ordinary one-way ANOVA tests with Dunnet correction (GraphPad Prism v6). *$p < 0.05$, **$p < 0.01$, ***$p < 0.001$.

RESULTS

Different Priming Affect MCs Phenotype

To assess whether long-lasting trained immunity or tolerance could be induced in BMMCs, cells were differentiated for 5 weeks in IL- 3 media and then primed for 24 hours by stimulation with either LPS, curdlan (a dectin-1 agonist consisting of β-(1,3)-linked glucose residues), IgE/Ag or left untreated (RPMI). BMMCs were then washed and put back in culture in fresh IL-3 media to allow their recovery. After 6 days, each cell subset was investigated for proliferation rate and phenotype, then subjected to a second stimulation with the same or a different stimulus (LPS, IgE/Ag or live *Candida albicans*) and investigated for their responsiveness (**Figure 1A**).

As shown in **Figure 1B**, during the 6 days of resting time all the cells kept proliferating at a low rate, and the cell viability (determined by trypan-blue exclusion) was found to be comparable for all the stimulations (**Figure 1B**). The size of the cells and their granularity did not change after the stimulation, as indicated by the almost identical levels of forward scatter (FSC) and side scatter (SSC). Similarly, FcεRI and cKit levels remained constant after the resting time (**Figure 1C**) indicating that BMMCs did not lose their cellular identity after the priming. Moreover, no differences in Dectin-1, CD14, TLR2 and TLR4 protein expression were detected between unstimulated and differently primed BMMCs (**Figure 1C**).

To define whether MCs priming was responsible for a phenotypic change in MCs, 6 days after the pre-stimulation BMMCs were stained with toluidine blue and alcian blue–safranin to visualize granules. BMMCs granule content and metachromasia were comparable between the four conditions (**Figures 1D, E**). Interestingly, BMMCs that degranulated after the first challenge with IgE/Ag, recovered most of their granules and stained metachromatically with toluidine blue (**Figure 1D**).

To assess whether the expression profile of MC proteases was influenced by the priming with different stimuli, we measured the gene expression levels of connective and mucosal MC proteases in BMMCs 6 days after the pre-stimulation with LPS, curdlan, IgE/Ag and RPMI. Curdlan and IgE/Ag pre-stimulation did not modify the mRNA expression of MC proteases, while LPS priming remarkably increased *MCPT-4* (but not *MCPT-2* and *MCPT-6*) expression, -compared to untreated cells (**Figure 1F**).

These results suggest that the stimulation of BMMCs with different ligands do not alter the expression levels of TLR2, TLR4, CD14, and Dectin-1. However, BMMCs stimulated with curdlan or IgE/Ag conserve their mucosal-like phenotype, while MC priming with LPS stably modifies the composition of granule proteases with an increase in *MPCT-4* gene expression.

MCs Priming Differently Affects the Degranulation and Cytokine Response to Secondary Inflammatory Stimuli

To address whether the pre-stimulation of MCs with different stimuli could influence their ability to mount an effective degranulation response, we quantified the amount of β-hexosaminidase released by pre-stimulated MCs in response to

anaphylactic stimuli. We first studied the degranulation response to the classical Ag challenge of IgE sensitized MC: BMMC were pre-stimulated with LPS, curdlan or IgE/Ag, allowed to rest for 6 days, then sensitized with IgE and finally challenged with the specific antigen for 30 minutes. As shown in **Figure 2A**, the pre-stimulation did not affect the amount of β-hexosaminidase released following the aggregation of the high-affinity receptor for IgE. Moreover, similar degranulation responses were observed by pre-stimulated BMMCs once challenged for the same short time with the Ca^{++} ionophore ionomycin (**Figure 2B**). These results suggest that the early events that characterize the anaphylactic reaction in BMMCs are not influenced by previous conditioning of the cells.

The effect of the pre-stimulation on cytokine production induced by a second stimulation was then investigated by ELISA (**Figures 2C–J**). BMMC primed for 24h with RPMI, IgE/Ag, LPS or curdlan, were re-stimulated, after 6 days, with IgE/Ag, a 10-fold lower dose of LPS or live *C. albicans* yeasts for 24 hours (as depicted in **Figure 1A**), and the levels of TNF-α and IL-6 secretion were measured.

Single stimulations with IgE/Ag, LPS or live *C. albicans* yeasts induced the secretion of comparable levels of cytokines, while curdlan caused only a minimal release of both TNF-α and IL-6 (**Supplemental Figure S1**). Interestingly, when we investigated the cytokine secretion induced in differently primed BMMC by a second stimulation, we observed diverse responses depending

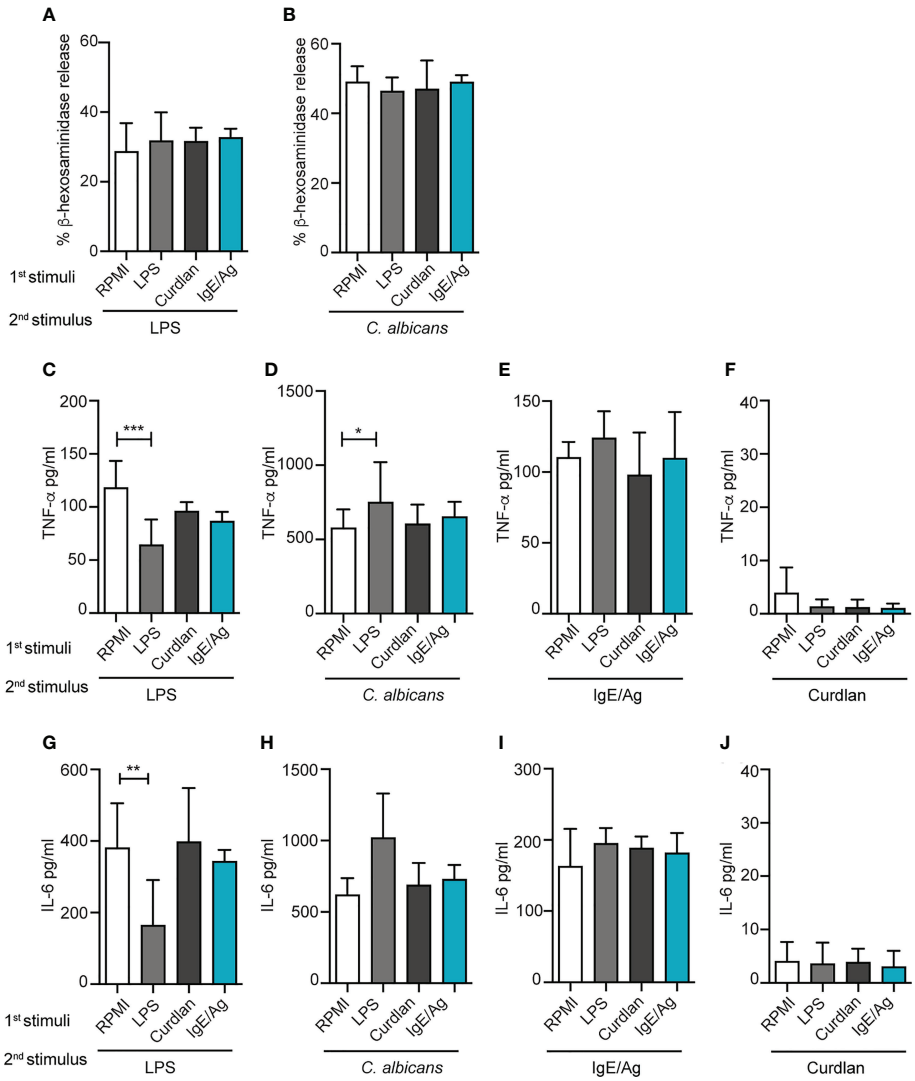

FIGURE 2 | Effect of different priming on MC degranulation and cytokine release response to a secondary challenge. Degranulation of BMMCs primed with LPS (1mg/ml), curdlan (100mg/ml), IgE/Ag or RPMI was determined 6 days after cell recovery as percentages of released β-hexosaminidase in response to 30 min of stimulation with IgE/Ag **(A)** or ionomycin **(B)**. BMMC primed with RPMI, LPS (1mg/ml), curdlan (100mg/ml) or IgE/Ag were subjected to a second stimulation with LPS **(C–G)**, live *C. Albicans* **(D–H)**, IgE/Ag **(F–I)** or curdlan **(E–J)**. TNF-α **(C–F)** and IL-6 **(G–J)** levels were detected in culture supernatants after 24 hours. Data are expressed as mean +SD from n>4 experiments; statistical analysis were performed with one-way Anova with Dunnet correction (*p < 0,05 **p < 0,01; ***p < 0,001).

both on the first and the second stimulus. As expected, the priming with LPS impaired BMMCs response to a secondary challenge with LPS as demonstrated by the lower release of TNF-α (**Figure 2C**) and IL- 6 (**Figure 2G**). On the other side, priming with curdlan or IgE/Ag did not affect MCs' responsiveness to secondary LPS challenge (**Figures 2C, G**).

To determine whether LPS priming could induce cross-tolerance also against non-TLR4 stimulations, BMMCs were restimulated either with live *C. albicans* yeasts or IgE/Ag. Strikingly, priming with LPS induced a stronger response to *C. albicans* compared to RPMI control, enhancing the release of TNF-α (**Figure 2D**) but not of IL-6 (**Figure 2H**). As for LPS, the response against *C. albicans* challenge by MCs primed with curdlan or IgE/Ag was comparable with the control (**Figures 2D, H**). By contrast, the pre-stimulation with curdlan did not affect the responsiveness to secondary stimuli. Notably, the first stimulation with LPS, curdlan and IgE/Ag did not influence the response to stimulation with the classical anaphylactoid stimulation IgE/Ag that was comparable between all the four groups, in terms of release of both TNF-α and IL-6 (**Figures 2E, I**). In our system, curdlan stimulation didn't exert any relevant training or tolerance effect (**Figures 2F, J**).

Taken together, our results indicate that LPS pre-stimulation can induce an opposite, dual response in MCs depending on the secondary trigger received by the cells.

LPS Priming Modulates Cytokines and Proteases Expression at mRNA Level

To assess whether BMMCs conditioning with LPS correlates with cytokines mRNA transcription, qPCR analyses were performed 3 hours post-restimulation. Consistent with the protein release detected by ELISA, the stimulation with a second dose of LPS resulted in the impaired expression of the transcripts for both TNF-α and IL-6 in LPS-primed BMMCs (**Figure 3**). Moreover, stimulation of LPS-primed BMMCs with *C. albicans* yeast caused an increased expression of *TNF-α* (**Figure 3A**) but not of *IL-6* (**Figure 3B**). Interestingly, LPS-primed BMMCs showed an increased basal transcription of *TNF-α*, 3.3 times higher than controls. Stimulation with *C. albicans* induced a 300-fold increase in *TNF-α* transcription levels in both LPS-primed BMMCs and controls, which were found to be 2.7 times higher in LPS-primed cells (**Figure 3A**). Taken together, these results suggest that LPS-priming induce a higher basal transcription for *TNF-α* but not *IL-6*, and that *C. albicans* challenge likely has the same effect on both LPS-primed and control cells.

LPS Conditioning Impairs the PI3K-AKT Pathway

In MCs, the regulation of TNF-α and IL-6 production during TLR-mediated stimulation involves the activation of the PI3K pathway (15). This pathway is of great importance also for MCs development and for the activation of the complimentary FYN-GAB2-PI3K signaling cascade during IgE/Ag activation. Seen that PI3K seems to play a dual role depending on the cellular context (16), the modulation of PI3K, AKT and p38 MAPK pathways in primed BMMCs was evaluated (**Figure 4**).

Strikingly, LPS-primed BMMCs showed a decreased level of total PI3K p85 and lower levels of PI3K p85 and p55 phosphorylation following *C. albicans* infection (**Figure 4A**). This phenomenon correlated with the expression of a putative isoform (or truncated version) of PI3K with an approximative molecular weight of 65 kDa (**Figure 4A**). This putative isoform was recognized both by the anti-p85 full-length antibody and to a lesser extent by the anti-phospho-PI3K antibody which recognizes the phosphorylated Tyr458 of p85 and Tyr199 of p55 (**Figure 4**). LPS-primed MCs displayed also a reduced phosphorylation of p38 MAPK 30 minutes after the re-stimulation with low-dose LPS (**Figure 4A**). Conversely, the same cells showed no impairment of p38 phosphorylation after 30 minutes of *C. albicans* challenge. All the cell expressed comparable levels of the catalytic subunit PI3K p110d (**Figure 4A**).

This phenomenon prompted us to compare the kinetics of AKT activation level during LPS- and *C. albicans*-induced activation of primed MCs (**Figures 4B, C**). Control BMMCs (RPMI) showed a strong activation of AKT already after 60 minutes of stimulation with second dose of LPS, while it was completely abolished in LPS-primed MCs. AKT activation in control cells correlated with an earlier and more sustained activation of p38 MAPK (**Figures 4B, C**). On the other side,

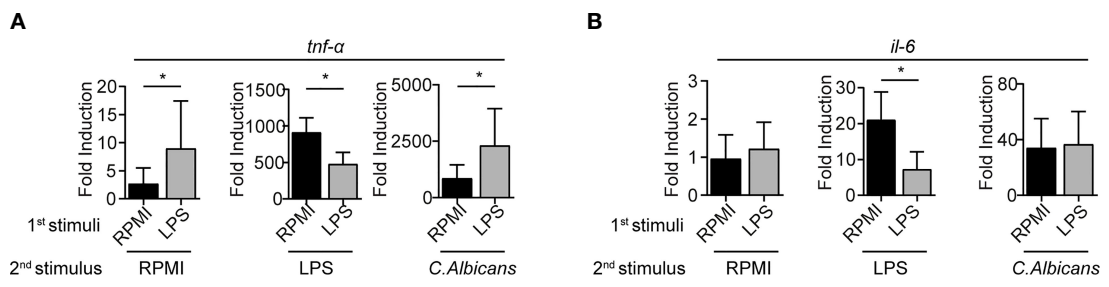

FIGURE 3 | mRNA cytokine expression levels are impaired in LPS-primed BMMCs. mRNA expression of *TNF- α* **(A)** and *IL-6* **(B)** were measured by rt-PCR on LPS-primed BMMC after 3 hours of stimulation with LPS (1mg/ml), live *C. Albicans* (MOI=1) or RPMI. Data are expressed as mean +SD from n=3 experiments. Statistical analysis were performed with paired Student t-test (*p < 0,05).

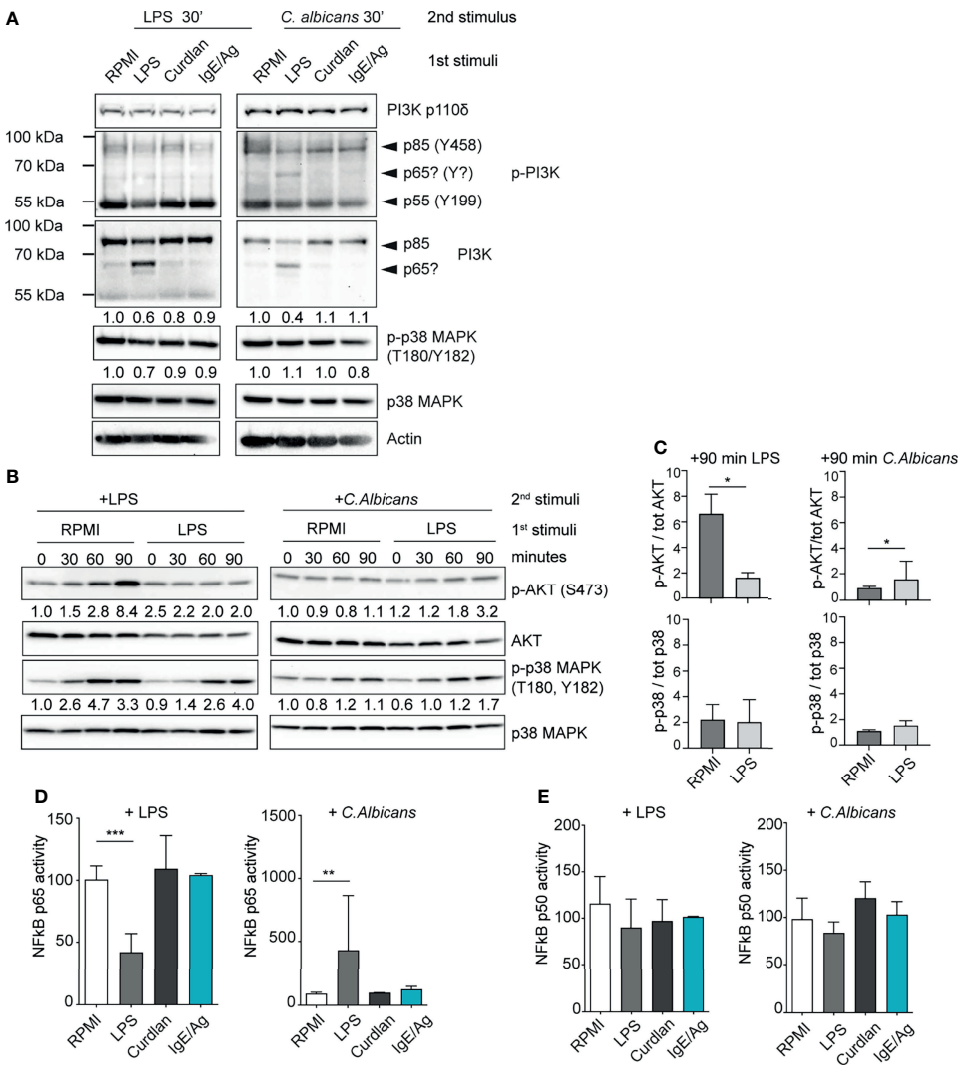

FIGURE 4 | LPS-primed MCs differently activate the PI3K-AKT pathway. **(A)** Western Blot (WB) analysis of PI3K subunits and of phosphorylated p38 in differently primed-BMMC restimulated for 30 minutes with LPS or live *C. Albicans* (MOI=1). Numbers indicate the results of densitometric analyses calculated over endogenous protein expression. **(B)** Time-course WB analysis of phosphor Akt and phospho p38 in LPS primed-BMMC restimulated with LPS or live *C. Albicans* (MOI=1). Numbers indicate the results of densitometric analyses calculated over endogenous protein expression normalized versus t=0. **(C)** Mean + SD of densitometric analysis of n=3 independent experiments are reported. Statistical analyses were performed with paired Student t-test (*=p<0,05). NF-kB p65 **(D)** and p50 **(E)** activity in LPS primed BMMC was determined after 30 minutes form addition of the second stimuli. Results were expressed as fold percentages over control (RPMI). Mean + SD of n=3 independent experiments are reported. Statistical analysis were performed with one-way Anova with Dunnet correction (*p < 0,05 **p < 0,01; ***p < 0,001).

C. albicans failed to induce the activation of AKT in both the cell populations but LPS- primed MCs displayed an enhanced activation of p38 MAPK.

To further characterize the nature of the ambivalent behavior of LPS- primed MCs, we looked at the activation status of the NF-kB transcription factor. During LPS restimulation NF-kB p65 activity was reduced in LPS-primed MCs while after challenge with *C. albicans* LPS-primed cells displayed an increase of NF-kB p65 activity (**Figure 4D**). Interestingly, NF-kB p50 activity was found to be unaltered by cell priming (**Figure 4E**).

These results indicate that the differential response following the restimulation of LPS-primed MCs with LPS or *C. albicans* is likely due to an altered activation of the downstream PI3K-AKT-p38 signaling pathway, which resulted in the impaired activation of NF-κB.

LPS Tolerance Is Partially Dependent on Histone Acetylation

Several studies demonstrated that the induction of trained immunity in myeloid cells is dependent on epigenetic

mechanism (17), including modification in the DNA methylation profile and in chromatin accessibility.

To demonstrate if similar mechanisms also happens in MCs, at first, we investigated the CpG methylation profile of the TNF-α promoter in BMMCs one week after pre-stimulation with RPMI or LPS by pyrosequencing. A total of five CpG sites were analyzed in the selected region, however, we did not detect significant differences in their level of methylation. A similar level of methylation was observed in all the CpG after the first stimulation with LPS and curdlan, as well as after the recovery period before the second stimulation (**Figure 5A**).

We then addressed the possibility that chromatin accessibility in primed MCs was differently influenced by pre-stimulation with by LPS. Therefore, we pretreated BMMC with histone deacetylase (HDAC) inhibitors, namely suberoylanilide hydroxamic (SAHA) and Trichostatin (TSA), for 1 hour before the addition of LPS or RPMI. After 6 days, we investigated the ability of these BMMCs to release cytokines in response to a re-stimulation with LPS or live *C. albicans*. We observed that both the inhibitors partially restored the secretion of TNF-α (**Figure 5B**) and IL-6 (**Figure 5C**) after LPS stimulation when compared with untreated BMMC, but failed to affect the cytokine secretion in response to *C. albicans* restimulation. These results indicate that HDAC inhibitors can interfere with cytokine production after MC activation through TLR4.

In immune cells, including MCs, the expression of cytokines is negatively controlled by the activity of the cytokine-suppressor-proteins (SOCS) (18–20). To understand whether SOCS protein could be involved in the different responses of primed MC to re-stimulation, we investigated the level of mRNA expression of SOCS3 and the methylation profile of SOCS3 promoter by rt-MSP, in BMMCs pre-stimulated with LPS. rt-MSP showed that the methylation profiles of SOCS3 promoter was comparable between unstimulated cells (RPMI) and MCs primed with LPS or curdlan, either after the first stimulation and the recovery period (**Figure 5D**). Moreover, quantitative PCR performed on MCs at day 7 (i.e. 6 days after the first stimulation and before the addition of the second stimulus) showed similar levels of SOCS3 expression in all primed cells, excluding that the observed reduction in cytokine expression was due to a different activity of SOCS3 (**Figure 5E**).

Taken together, these results suggest that histone acetylation by HDAC, but not chromatin methylation, might be partially responsible for the reduced release of TNF-α and IL-6 following LPS restimulation in LPS-primed BMMCs.

LPS Tolerance Is Long-Lasting and Induced Early in MCs Differentiation

Considering that MCs *in vivo* displays extreme heterogeneity and variability depending on the local microenvironment, the possibility to induce the maturation and skewing of immature MC towards a tolerant or pro-inflammatory phenotype could be relevant. Therefore, having established that mature BMMCs can develop a long-lasting immunological memory, we decided to investigate the effect of repetitive stimulation of MCs with LPS at early stages of maturation. 4-weeks old BMMCs were challenged for 24 h with LPS, washed and put in culture for 6 days in IL-3 containing medium. The same treatment was repeated once a week for three weeks as depicted in **Figure 6A**. BMMCs were investigated for their phenotype, the expression of *MCPT-4*, and the release of TNF-α and IL-6. As shown in **Figure 6B**, multiple stimulations with LPS did not modify the expression of surface markers, neither of TLR-2, CD14 and Dectin-1 (**Figure 6B**). However, the first stimulation with LPS induced an increased expression of *MCPT-4* mRNA after the first treatment that persisted up to 14 days (**Figure 6C**). Analysis of the cytokine released in response to repeated LPS stimulation demonstrated that the priming of BMMC with the first dose of LPS induced a tolerant phenotype that lasted for more than 2 weeks. Indeed, as shown in **Figures 6D, E**, LPS-primed BMMCs challenged with a second and a third dose of LPS did not recover the ability to fully release cytokines and their hypo-responsiveness was maintained. This effect was also confirmed by comparing the levels of cytokines released by BMMCs treated with one or more doses of LPS. LPS-primed BMMCs allowed to recover and exposed to the second dose of LPS after 2 weeks (green bar) still maintained their hyporesponsiveness and released lower amounts of TNF-α (**Figure 6F**) and IL6 (**Figure 6G**) compared to MCs challenged with a single LPS dose (red bar).

These results demonstrate that LPS tolerance in LPS-primed MCs can last for at least two weeks and can be induced already in the early stages on MC differentiation.

DISCUSSION

The fact that MCs are tissue-resident cells which can survive for up to 12 weeks, and that their terminal differentiation is highly influenced by tissue-specific stimuli, renders these cells possibly implicated in innate immune memory.

In the last decades, some studies on the nature of endotoxin tolerance demonstrated memory-like traits also in MCs. Initially, it has been reported that LPS stimulation induced endotoxin tolerance in BMMCs through the upregulation of the phosphatase SHIP (but not of SHIP2 nor PTEN) by the autocrine effect of LPS-induced release of TGF-β (11). More recent studies demonstrated the ability of MCs to respond to LPS by releasing pro-inflammatory TNF-α and IL-6 in a p38-dependent manner, and that the release of these cytokines was severely decreased upon a secondary stimulation with LPS or other TLR2 agonists, suggesting that endotoxin tolerance could also induce cross-tolerance against different stimuli (18, 21). A recent report by Poplutz et al. demonstrated that after a second stimulation with LPS, MCs displayed a decreased nuclear translocation and DNA binding ability of the canonical NF-kB p65/p50 heterodimer (17). The latter phenomenon was due to the constitutive presence of the suppressive marker H3K9me3 on the promoters of TNF-α and IL-6 which inhibited NF-kB binding to those promoters. These repression markers were transiently lost during the initial LPS stimulation (thus allowing NF-kB binding and gene transcription) but remained unchanged during the second LPS challenge. According to

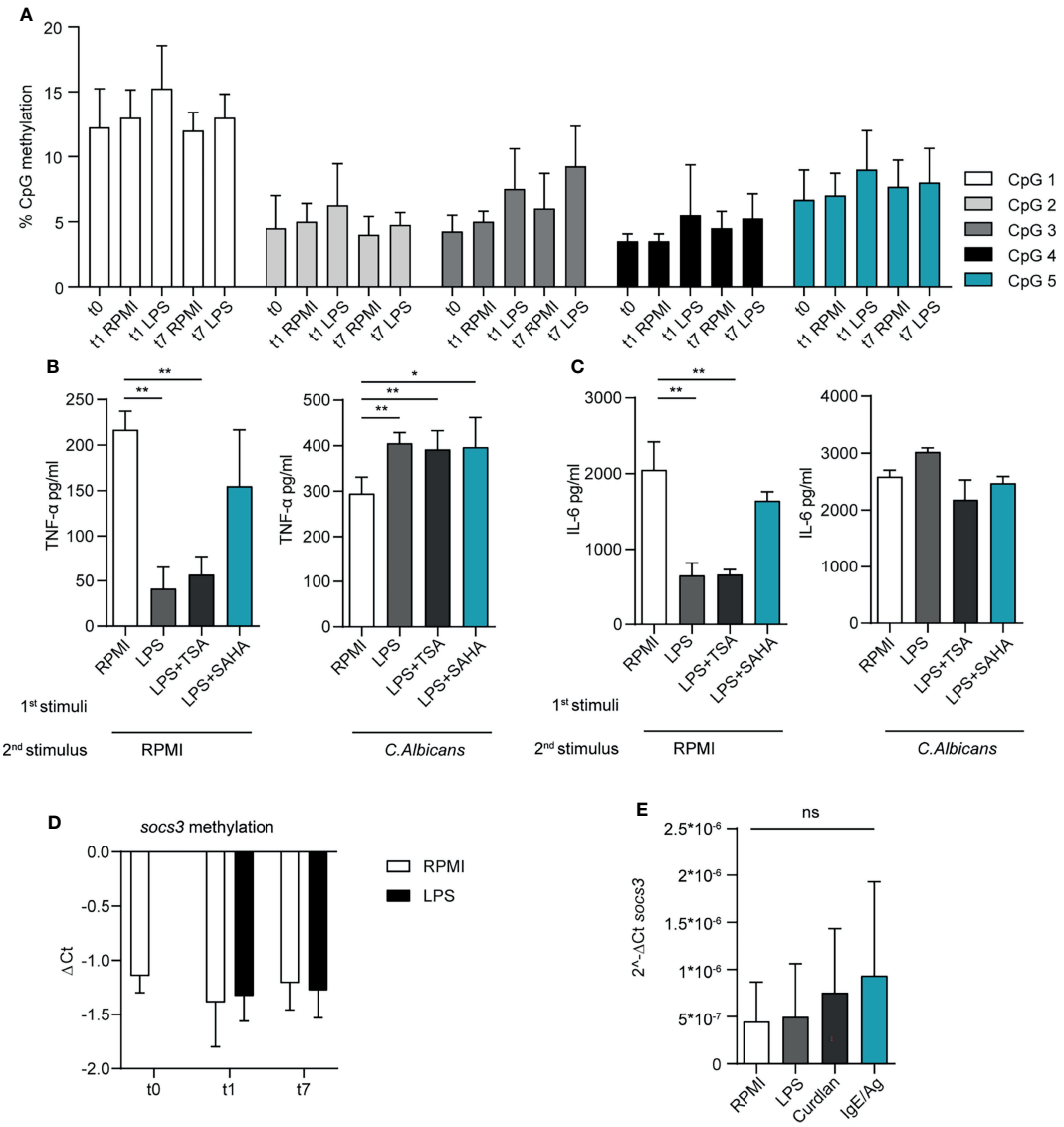

FIGURE 5 | LPS priming affects the epigenetic landscape in MCs. **(A)** CpG methylation at TNF-α promoter region. A total of five CpG sites were analysed in the selected region, their level of methylation was determined by pyrosequencing. Mean + SD of n=3-5 independent experiments are reported. BMMC were primed with LPS (1μg/ml) in presence of HDAC inhibitors (SAHA 1nM; TSA 10nM), then washed, re-stimulated and analysed for TNF-α **(B)** and IL-6 **(C)** secretion upon second stimulation with LPS or *C. albicans*. Mean + SD of n=3 independent experiments are reported. **(D)** SOCS3 promoter CpG methylation was determined by real-time MSP. Methylation was calculated as difference among Ct values of unmethylated and methylated region. Mean + SD of n=2-6 independent experiments are reported. **(E)** *SOCS3* mRNA expression in BMMC at day 7, i.e. 6 days after the first stimulation with LPS, curdlan and IgE/Ag. Mean + SD of n=3 independent experiments are reported. Statistical analysis were performed with one-way Anova with Dunnet correction (*p < 0,05 **p < 0,01; ***p < 0,001 ns, not significant).

previous reports, short pre-treatment with LPS did not affect TNF-α and IL-6 release during IgE/Ag cross-linking, possibly due to the involvement of Ca^{++}-dependent NFAT activation (13, 22). Nevertheless, all these studies were restricted to LPS pre-stimulation and were limited to a rapid *in vitro* restimulation after cell priming.

To address more in detail the possibility that different types of environmental signals might influence MC reactivity to subsequent and repetitive stimulations, we set up an experimental model which allowed the cells to rest for 6 days between the first stimulation and the subsequent restimulation. We then systematically compared the ability of different signals to either train or induce tolerance on MCs.

In line with previous findings (13, 22), the response to the classic anaphylactoid IgE/Ag stimulation was not affected by the priming with LPS, both in terms of TNF-α, IL-6 and β-hexosaminidase release. Similarly, IgE/Ag priming of BMMCs did not modify the response to a second stimulation with LPS, *C.*

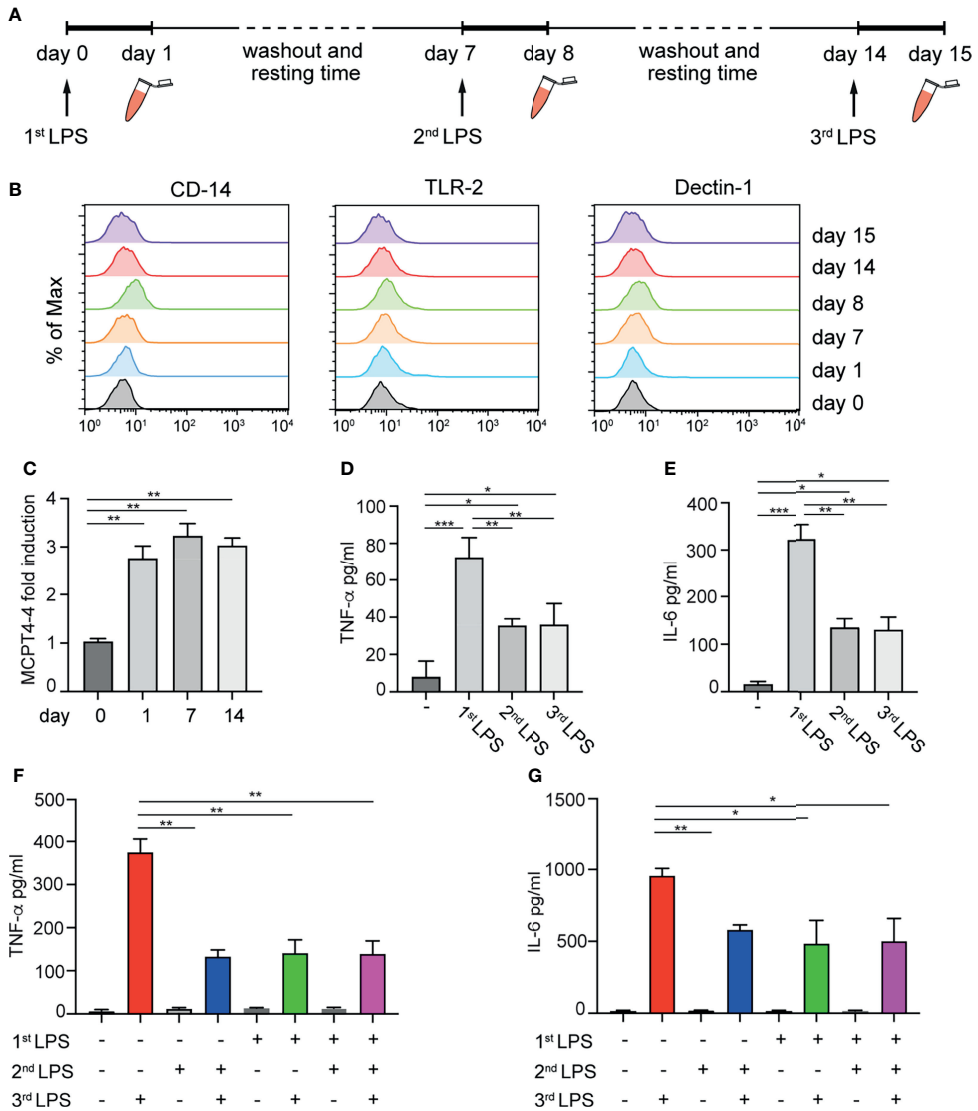

FIGURE 6 | Effect of repetitive LPS stimulation on BMMCs. Schematic representation of experimental protocol: 4-weeks old BMMCs were treated for 24h with LPS once a week for three weeks **(A)**. Surface marker expression **(B)** and *MCPT-4* mRNA expression **(C)** were evaluated at indicated times. The levels of TNF-α **(D)** and IL-6 **(E)** released by BMMC after the first, the second and the third dose of LPS are shown. The levels of TNF-α **(F)** and IL-6 **(G)** released by BMMC treated with one or more doses of LPS have been compared. Data are means +SD. Statistical analysis were performed with one-way Anova with Dunnet correction (*p < 0,05 **p < 0,01; ***p < 0,001).

albicans or to the re-engagement of the FcεRI by IgE and antigen. Unlike with monocytes and macrophages, priming of MCs with the Dectin-1 ligand curdlan did not boost cytokine secretion in response to LPS or *C. albicans* stimulation and, therefore, failed to induce a training effect in MCs. Other authors demonstrated the ability of curdlan to induce cytokine productions in MCs. However, in our hands curdlan induced only a minimal release of IL-6 and TNF-α in BMMC and seems to be unable to conditionate cells to further stimulation. This could be due to different handling procedures between laboratories, nevertheless, besides curdlan, we tried different ligands of Dectin, such as β-glucan or WPG (data not shown), but none of these has been found to induce a strong BMMC response or to influence the MC reactivity against further stimulation.

As expected, the impaired release of TNF-α and IL-6 showed by LPS-primed cells in response to LPS confirmed that MCs became tolerant to a second dose of LPS, and suggests that endotoxin tolerance can be maintained for at least 6 days. Surprisingly, the pre-stimulation of BMMCs with LPS did not modify their ability to release cytokines in response to a challenge with *C. albicans*. As a matter of fact, restimulation of LPS-primed cells with *C. albicans* caused a higher release of TNF-α compared

to naïve BMMCs, suggesting that LPS priming can induce both tolerance and training depending on the secondary stimuli. We excluded that the altered responses of re-stimulated BMMC could be mediated by the differential expression of pattern recognition receptors involved in the recognition of *C. albicans* or LPS, as the expression levels of TLR4, TLR2, and Dectin-1 were comparable between primed and naïve cells.

Interestingly, BMMCs primed with IgE/Ag or curdlan maintained the same mucosal-like phenotype of naïve unprimed BMMCs, while the exposure to a single dose of LPS induced an increased mRNA expression of the connective-tissue protease MCPT-4 that persisted for 6 days. MCPT-4 is a MC protease normally found in the cytoplasm of connective-tissue MCs, but it is also well-known for the anti-inflammatory role that can exert. For example, this protease was found to be involved in the degradation of MC-derived TNF-α in a murine model of sepsis, as MCPT-4-deficient mice exhibited increased levels of intraperitoneal TNF-α and higher numbers of peritoneal neutrophils (23). Moreover, unlike mucosal MCs, connective-tissue MCs are known to express high levels of TGF-β during fungal infections, thus contributing to mucosal immune tolerance (24). In addition, MCPT-4 is required for the cleavage and activation of TGF-β which, in turn, can activate a Th17 response that is known to be involved in fungal immunity (25, 26). Therefore, MCPT-4 could contribute on one hand to the tolerogenic response of LPS pre-stimulated MC that show a reduced TNF-α release after a second LPS stimulation, and on the other hand, it could be involved also in the enhanced response to *C. Albicans* infections. Notably, the upregulation in MCPT-4 mRNA expression and the reduced secretion of cytokine in response to the second dose of LPS was also found in BMMCs two weeks after the first stimulation with LPS, and in BMMCs exposed to repetitive LPS expositions, suggesting that a single, early priming of MCs can affect their behavior for a long time.

Although it is known that LPS can induce endotoxin tolerance or training depending on the dose used for cell priming (27), here we report an ambivalent role for LPS in the induction of both tolerance and training depending on the secondary challenge. This phenomenon is made possible by the result of the combined rewiring of intracellular signaling cascades and epigenetic changes in the regulating accessibility to the loci of TNF-α. On one hand, LPS-priming induced long-term tolerance to endotoxin by impairing the PI3K-AKT pathway possibly through the modulation of PI3K p85 expression. The lack of AKT activation correlated with an impaired p38 phosphorylation and NF-kB p65 activity, finally leading to a reduced expression of TNF-α and IL-6. On the other hand, LPS-priming induced a higher basal transcription of the *Tnf-α* gene (**Figure 3A**). We believe that this phenomenon could be the result of improved chromatin accessibility on TNF-α regulating regions or due to the constitutive presence of active enhancers/co-activators. Inhibition of HDAC activity partially restored the ability of LPS primed cells to activate a transcriptional response to second stimulation with LPS. Interestingly, inhibition of HDAC activity did not modify the amount of cytokine produced by MC in response to *C. albicans* yeast independently on the first stimulus. These results suggest that altered HDAC activity in LPS-primed cells partially accounts for the repressed transcription of inflammatory genes and that stimulation with live *C. albicans* is likely to be sufficiently different to activate transcription in tolerant cells. These results do not rule out the possibility that the combination of specific patterning of histone modifications, including methylation, phosphorylation, and acetylation, provide integral information for enhancing transcription. At the same time, it must be considered that these cells developed a profound rearrangement of the intracellular signaling network involved in TLR4 responses which could override the higher basal TNF-α transcription. Further proof of this hypothesis is given by the pattern of IL-6 expression: its reduction during LPS-restimulation indicates that the impaired signaling pathway controlling TNF-α expression also affects other pro-inflammatory cytokines. On the other side, restimulation with *C. albicans* did not affect IL-6 expression in primed cells, suggesting that the control of *TNF-α* transcription might be governed by gene-specific chromatin modification rather than by the rewiring of the signaling cascades activated by the fungus.

Taken together, our results suggest that LPS challenge induce long-term memory in MCs promoting, at the same time, tolerance towards further LPS restimulation and immune training during *C. albicans* infection. However, the exact mechanisms orchestrating a tolerogenic rather than trained response in primed MCs remains unclear, as it appears to rely on a multi-layered process that most likely involves receptor signals rewiring, chromatin modification, and gene reprogramming. Additional efforts will be required to elucidate the nature of this ambivalent phenomenon mediated by LPS. By expanding the signaling pathway involved in LPS and fungal sensing, and characterizing the putative epigenetic mechanisms controlling TNF-α expression it will be possible to describe the roles of MCs priming in both homeostatic and pathological conditions.

DATA AVAILABILITY STATEMENT

The original contributions presented in the study are included in the article/**Supplementary Material**. Further inquiries can be directed to the corresponding author.

ETHICS STATEMENT

The animal study was reviewed and approved by OPBA of University of Udine.

AUTHOR CONTRIBUTIONS

MZ, CS, CP, and BF conceived and designed the experiments. MZ, BF, CS, and ST performed the experiments. AA cultured the

fungus and performed some experiments. MZ, CS, and ST analysed the data. MZ, CS, and BF wrote the manuscript. CP and BF supervised the study. All authors read and approved the final manuscript.

FUNDING

This work was supported by Associazione Italiana Ricerca sul Cancro (AIRC) under grant IG 2014 N.15561 and Progetti di Ricerca di Interesse Nazionale (PRIN) under grant 2015YYKPNN_003 to CP. MZ was supported by the European Regional Development Fund – Project Support of MSCA IF fellowships at FNUSA-ICRC (No CZ.02.2.69/0.0/0.0/19_074/0016274).

ACKNOWLEDGMENTS

We thank Luca Bazzichetto for technical assistance.

SUPPLEMENTARY MATERIAL

The Supplementary Material for this article can be found online at: https://www.frontiersin.org/articles/10.3389/fimmu.2022.835348/full#supplementary-material

REFERENCES

1. Netea MG, Domínguez-Andrés J, Barreiro LB, Chavakis T, Divangahi M, Fuchs E, et al. Defining Trained Immunity and Its Role in Health and Disease. *Nat Rev Immunol* (2020) 20(6):375–88. doi: 10.1038/s41577-020-0285-6
2. Netea MG, van der Meer JW. Trained Immunity: An Ancient Way of Remembering. *Cell Host Microbe* (2017) 21(3):297–300. doi: 10.1016/j.chom.2017.02.003
3. Saeed S, Quintin J, Kerstens HH, Rao NA, Aghajanirefah A, Matarese F, et al. Epigenetic Programming of Monocyte-to-Macrophage Differentiation and Trained Innate Immunity. *Science* (2014) 345(6204):1251086. doi: 10.1126/science.1251086
4. Quintin J, Cheng SC, van der Meer JWM, Netea MG. Innate Immune Memory: Towards a Better Understanding of Host Defense Mechanisms. *Curr Opin Immunol* (2014) 29(1):1–7. doi: 10.1016/j.coi.2014.02.006
5. Ifrim CD, Quintin J, Joosten L, Jacobs C, Jansen T, Jacobs L, et al. Mihai G Netea. Trained Immunity or Tolerance: Opposing Functional Programs Induced in Human Monocytes After Engagement of Various Pattern Recognition Receptors. *Clin Vaccine Immunol* (2014) 21(4):534–45. doi: 10.1128/CVI.00688-13
6. Shelburne CP, Abraham SN. The Mast Cell in Innate and Adaptive Immunity. *Adv Exp Med Biol* (2011) 716:162–85. doi: 10.1007/978-1-4419-9533-9_10
7. Frossi B, Mion F, Tripodo C, Colombo MP, Pucillo CE. Rheostatic Functions of MCs in the Control of Innate and Adaptive Immune Responses. *Trends Immunol* (2017) 38(9):648–56. doi: 10.1016/j.it.2017.04.001
8. Carter MC, Metcalfe DD. Decoding the Intricacies of the MCs Compartment. *Br J Haematol* (2021) 196(2):304–15. doi: 10.1111/bjh.17714
9. Ikeda T, Funaba M. Altered Function of Murine MCs in Response to Lipopolysaccharide and Peptidoglycan. *Immunol Lett* (2003) 88(1):21–6. doi: 10.1016/s0165-2478(03)00031-2
10. Monticelli S, Leoni C. Epigenetic and Transcriptional Control of MCs Responses. *F1000Res* (2017) 29(6):2064. doi: 10.12688/f1000research.12384.1
11. Sly LM, Rauh MJ, Kalesnikoff J, Song CH, Krystal G. LPS-Induced Upregulation of Ship Is Essential for Endotoxin Tolerance. *Immunity* (2004) 21(2):227–39. doi: 10.1016/j.immuni.2004.07.010
12. Nigo YI, Yamashita M, Hirahara K, Shinnakasu R, Inami M, Kimura M, et al. Regulation of Allergic Airway Inflammation Through Toll-Like Receptor 4-Mediated Modification of MCs Function. *Proc Natl Acad Sci USA* (2006) 103(7):2286–91. doi: 10.1073/pnas.0510685103
13. Saluja R, Delin I, Nilsson GP, Adner M. FcepsilonR1-Mediated MCs Reactivity Is Amplified Through Prolonged Toll-Like Receptor-Ligand Treatment. *PloS One* (2012) 7(8):e43547. doi: 10.1371/journal.pone.0043547
14. Yoshioka M, Matsutani T, Hara A, Hirono S, Hiwasa T, Takiguchi M, et al. Real-Time Methylation-Specific PCR for the Evaluation of Methylation Status of MGMT Gene in Glioblastoma. *Oncotarget* (2018) 9(45):27728–35. doi: 10.1016/j.it.2008.07.004
15. Hochdorfer T, Kuhny M, Zorn CN, Hendriks RW, Vanhaesebroeck B, Bohnacker T, et al. Activation of the Pi3k Pathway Increases Tlr-Induced Tnf-Alpha and Il-6 But Reduces Il-1beta Production in MCs. *Cell Signal* (2011) 23(5):866–75. doi: 10.1016/j.cellsig
16. Kim MS, Rådinger M, Gilfillan AM. The Multiple Roles of Phosphoinositide 3-Kinase in Mast Cell Biology. *Trends Immunol* (2008) 29(10):493–501. doi: 10.1016/j.it.2008.07.004
17. Poplutz M, Levikova M, Lüscher-Firzlaff J, Lesina M, Algül H, Lüscher B, et al. Endotoxin Tolerance in MCs, Its Consequences for IgE-Mediated Signalling, and the Effects of BCL3 Deficiency. *Sci Rep* (2017) 7(1):4534. doi: 10.1038/s41598-017-04890-4
18. Saturnino SF, Prado RO, Cunha-Melo JR, Andrade MV. Endotoxin Tolerance and Cross-Tolerance in MCs Involves TLR4, TLR2 and FcepsilonR1 Interactions and SOCS Expression: Perspectives on Immunomodulation in Infectious and Allergic Diseases. *BMC Infect Dis* (2010) 10:240. doi: 10.1186/1471-2334-10-240
19. Jannat A, Khan M, Shabbir M, Badshah Y. Expression of Suppressor of Cytokine Signaling 3 (SOCS3) and Interleukin-6 (-174-G/C) Polymorphism in Atopic Conditions. *PloS One* (2019) 14(6):e0219084. doi: 10.1371/journal.pone.0219084
20. Kim D, Kim SH, Cho SH, Shin K, Kim S. SOCS3 Suppresses the Expression of IL-4 Cytokine by Inhibiting the Phosphorylation of C-Jun Through the ERK Signaling Pathway in Rat Mast Cell Line RBL-2h3. *Mol Immunol* (2011) 48(5):776–81. doi: 10.1016/j.molimm.2010.11.005
21. Hochdorfer T, Tiedje C, Stumpo DJ, Blackshear PJ, Gaestel M, Huber M. Lps-Induced Production of Tnf-Alpha and Il-6 in MCs Is Dependent on P38 But Independent of Ttp. *Cell Signal* (2013) 25(6):1339–47. doi: 10.1016/j.cellsig.2013.02.022
22. Medina-Tamayo J, Ibarra-Sánchez A, Padilla-Trejo A, González-Espinosa C. IgE-Dependent Sensitization Increases Responsiveness to LPS But Does Not Modify Development of Endotoxin Tolerance in Mast Cells. *Inflammation Res* (2011) 60(1):19–27. doi: 10.1007/s00011-010-0230-4
23. Piliponsky AM, Chen CC, Rios EJ, Treuting PM, Lahiri A, Abrink M, et al. The Chymase Mouse MCs Protease 4 Degrades TNF, Limits Inflammation, and Promotes Survival in a Model of Sepsis. *Am J Pathol* (2012) 181(3):875–86. doi: 10.1016/j.ajpath.2012.05.013
24. Renga G, Moretti S, Oikonomou V, Borghi M, Zelante T, Paolicelli G, et al. IL-9 and MCs Are Key Players of Candida Albicans Commensalism and Pathogenesis in the Gut. *Cell Rep* (2018) 23(6):1767–78. doi: 10.1016/j.celrep.2018.04.034
25. Taipale J, Lohi J, Saarinen J, Kovanen PT, Keski-Oja J. Human MCs Chymase and Leukocyte Elastase Release Latent Transforming Growth Factor-β1 From the Extracellular Matrix of Cultured Human Epithelial and Endothelial Cells. *J Biol Chem* (1995) 270(9):4689–96. doi: 10.1074/jbc.270.9.4689
26. Zhang S. The Role of Transforming Growth Factor β in T Helper 17 Differentiation. *Immunology* (2018) 155(1):24–35. doi: 10.1111/imm.12938
27. Deng H, Maitra U, Morris M, Li L. Molecular Mechanism Responsible for the Priming of Macrophage Activation. *J Biol Chem* (2013) 288(6):3897–906. doi: 10.1074/jbc.M112.424390

Conflict of Interest: The authors declare that the research was conducted in the absence of any commercial or financial relationships that could be construed as a potential conflict of interest.

Publisher's Note: All claims expressed in this article are solely those of the authors and do not necessarily represent those of their affiliated organizations, or those of the publisher, the editors and the reviewers. Any product that may be evaluated in

this article, or claim that may be made by its manufacturer, is not guaranteed or endorsed by the publisher.

frontiers in Immunology

ORIGINAL RESEARCH
published: 24 February 2022
doi: 10.3389/fimmu.2022.838448

SARS-CoV-2 Induces Cytokine Responses in Human Basophils

Srinivasa Reddy Bonam[1†], *Camille Chauvin*[1,2†], *Laurine Levillayer*[2†], *Mano Joseph Mathew*[3], *Anavaj Sakuntabhai*[2,4] *and Jagadeesh Bayry*[1,5*]

[1] Institut National de la Santé et de la Recherche Médicale, Centre de Recherche des Cordeliers, Sorbonne Université, Université de Paris, Paris, France, [2] Functional Genetics of Infectious Diseases Unit, Department of Global Health, Institut Pasteur, Paris, France, [3] EFREI, Villejuif, France, [4] Centre National de la Recherche Scientifique (CNRS), UMR2000, Paris, France, [5] Department of Biological Sciences & Engineering, Indian Institute of Technology Palakkad, Palakkad, India

Basophils play a key role in the orientation of immune responses. Though the interaction of SARS-CoV-2 with various immune cells has been relatively well studied, the response of basophils to this pandemic virus is not characterized yet. In this study, we report that SARS-CoV-2 induces cytokine responses and in particular IL-13, in both resting and IL-3 primed basophils. The response was prominent under IL-3 primed condition. However, either SARS-CoV-2 or SARS-CoV-2-infected epithelial cells did not alter the expression of surface markers associated with the activation of basophils, such as CD69, CD13 and/or degranulation marker CD107a. We also validate that human basophils are not permissive to SARS-CoV-2 replication. Though increased expression of immune checkpoint molecule PD-L1 has been reported on the basophils from COVID-19 patients, we observed that SARS-CoV-2 does not induce PD-L1 on the basophils. Our data suggest that basophil cytokine responses to SARS-CoV-2 might help in reducing the inflammation and also to promote antibody responses to the virus.

Keywords: basophils, SARS-CoV-2, COVID-19, IL-3, Caco-2 cells, IL-13, IL-4, epithelial cells

OPEN ACCESS

Edited by:
Uday Kishore,
Brunel University London,
United Kingdom

Reviewed by:
Taruna Madan,
National Institute for Research in Reproductive Health (ICMR), India
Chiara Agostinis,
Institute for Maternal and Child Health Burlo Garofolo (IRCCS), Italy

***Correspondence:**
Jagadeesh Bayry
Jagadeesh.bayry@crc.jussieu.fr;
bayry@iitpkd.ac.in

[†]*These authors have contributed equally to this work and share first authorship*

Specialty section:
This article was submitted to Molecular Innate Immunity, a section of the journal Frontiers in Immunology

Received: *17 December 2021*
Accepted: *31 January 2022*
Published: *24 February 2022*

Citation:
Bonam SR, Chauvin C, Levillayer L, Mathew MJ, Sakuntabhai A and Bayry J (2022) SARS-CoV-2 Induces Cytokine Responses in Human Basophils. Front. Immunol. 13:838448. doi: 10.3389/fimmu.2022.838448

INTRODUCTION

The current COVID-19 pandemic, caused by the new severe acute respiratory syndrome coronavirus 2 (SARS-CoV-2), presents an unprecedented danger to global health systems, with over 5.2 million confirmed fatalities (10th December 2021) (1). Large number of studies have dissected the spectrum of innate and adaptive immune responses in COVID-19 patients and their role in the immunopathogenesis of the disease (2–7).

Basophils are rare immune cells. In addition to mediating the protection against helminth infection, basophils are well known for their role in the pathogenesis of various allergic inflammatory diseases of respiratory tract, gastro-intestinal tract and skin (8–10). A longitudinal systems-level analyses of immune cells from the blood indicates that basophils are depleted during acute and severe phases of COVID-19 (2) and in line with the established fact that basophils regulate T and B cell responses, a correlation between anti-RBD (receptor-binding domain) IgG titers and basophil number in the circulation has been observed (2). In addition, basophils also displayed an activated phenotype in COVID-19 patients (11). However, the direct response of human basophils to SARS-CoV-2 remains unexplored.

In this study, we have investigated the response of human basophils to SARS-CoV-2 infection. We found that SARS-CoV-2 induces IL-4 and IL-13 cytokines both in resting and IL-3-primed basophils without modifying the expression of surface markers including the checkpoint molecule PD-L1. In fact, PD-L1 expression was at basal level. Our data indicate that activation of basophils by SARS-CoV-2 might support Th2 and antibody responses to the virus.

MATERIALS AND METHODS

Reagents and Antibodies

For flow cytometry, the following fluorochrome-conjugated monoclonal antibodies were used. BD Biosciences (Le Pont de Claix, France): CD13-APC (Clone: WM15), CD69-APC/Cy7 (Clone: FN50), CD274 (PD-L1)-FITC (Clone: MIH1); Miltenyi Biotec: FcεRIα-PE (Clone: CRA-1); eBioscience (Paris, France): and fixable viability dye eFluor 506. Biolegend (Amsterdam, Netherlands): CD107a-BV421 (clone H4A3). IL-3 was from ImmunoTools (Friesoythe, Germany).

Cell Lines

Vero E6 (African green monkey kidney epithelial cells, ATCC, CRL-1586) was maintained in Dulbecco's modified Eagle's medium (DMEM) containing 10% fetal bovine serum (FBS), 1% penicillin-streptomycin (PS) (5 units/mL penicillin, and 5 µg/mL streptomycin). Caco-2 (Human colon epithelial cells, ATCC, HTB-37) was maintained in DMEM containing 20% FBS, 1% penicillin-streptomycin. All cell lines were cultured at 37°C, 5% CO_2.

Virus Strains

The primary strain BetaCoV/France/IDF0372/2020 (EPI_ISL_410720 (GISAID ID); wild-type strain) was supplied by the National Reference Centre for Respiratory Viruses hosted by Institut Pasteur (Paris, France) and headed by Dr. Sylvie van der Werf, and the human sample was isolated and provided by Drs. Xavier Lescure, Yazdan Yazdanpanah from the Bichat Hospital, Paris.

Virus Production

Viral stocks were produced using Vero E6 in DMEM without FBS with a multiplicity of infection (MOI) 10^{-3} of the virus stock. After 1 h incubation at 37°C under 5% CO_2, all the medium used for infection was removed before adding fresh DMEM containing 2% FBS, 1% PS. Cells were incubated for further 72 h at 37°C, 5% CO_2.

Virus Titration

Viral titers were assessed by plaque assay in 24-well plates on Vero E6 cells ($1.5x10^5$ cells/well) in DMEM supplemented with 10% FBS and 1% penicillin-streptomycin. Ten-fold serial dilutions in DMEM without FBS and 1% PS were used for the titration. After 1 h of incubation at 37°C, 5% CO_2, the medium was replaced by overlaying the cells with carboxymethyl cellulose CMC/DMEM with 2% FBS (vol/vol). After 72 h of incubation, the CMC/DMEM was removed and a mixture of crystal violet/ethanol/formaldehyde was added for 30 min at room temperature. Experiments with live SARS-CoV-2 were performed according to Institut Pasteur guidelines for Biosafety Level 3 work.

Purification of Basophils

The buffy coats of the healthy donors (Centre Trinité, L'Établissement Français du Sang, Paris; EFS-INSERM ethical committee permission 18/EFS/041) were used to isolate peripheral blood mononuclear cells (PBMCs) by Ficoll density gradient centrifugation. Basophils were isolated from the PBMCs by negative selection using Basophil Isolation Kit II (Miltenyi Biotec, Paris, France).

Basophil Infection

Freshly isolated basophils were plated in a 96-well plate at a concentration of $0.1x10^6$ cells/100 µl/well without FBS, and directly infected with the SARS-CoV-2 (primary strain IDF0372) at a MOI of one. Non-infected cells were used as a control. In some conditions, basophils were primed with IL-3 (20 ng/ml) along with infection. Vero E6 cells were used as a control of infection. After 1 h, the medium was replaced by fresh X-Vivo medium and the cells were further incubated for 24 h at 37°C, 5% CO_2. After 24 h of culture, supernatants were collected and stored at -80°C for subsequent cytokine quantification. The cells were processed for surface staining of various markers, such as FcεR1, CD107a, CD13, CD69, and PD-L1. The cells were fixed with 4% paraformaldehyde and were acquired using LSR II (BD Biosciences). The data were analyzed by BD FACS DIVA and FlowJo software.

Coculture of Basophils With Virus Infected Caco-2

Human Caco-2 cells were plated a day before in 96-well plates. Cells were infected in DMEM without FBS with the SARS-CoV-2 primary strain IDF0372 at a MOI of one. After 1 h, the medium was replaced by fresh DMEM medium containing 2% FBS, 1% PS and cells were incubated at 37°C, 5% CO_2. After 24 h, basophils ($0.1x10^6$ cells/100 µl/well) were added on the top of infected Caco-2 ($5x10^4$ cells/100 µl/well). The basophils were assessed for the expression of various surface markers after 24 h.

ELISA

Cell culture supernatants were inactivated with Triton X-100 1% (v/v) for 2 h at room temperature. The virus inactivated supernatants were analyzed for the cytokines, such as IL-13 and IL-4 (ELISA Ready-SET-Go, eBioscience).

Statistical Analysis

As highlighted in the figure legends, the experiments were repeated in several times by using cells from independent donors. Graphs and Statistical analyses were performed by the paired Wilcoxon test (for comparison between two groups) or one-way ANOVA Friedman test with Dunn's multiple

comparisons post-test as indicated using Prism 8 (GraphPad Software Inc, CA). $P < 0.05$ was considered significant.

RESULTS

SARS-CoV-2 Induces Limited Activation of Resting Human Basophils

Basophils play a major role in the pathogenesis of various respiratory diseases (8–10). Though the phenotype of basophils was previously analyzed in COVID-19 patients (11), it was not clear whether the activated basophil phenotype observed in the COVID-19 patients was due to direct virus stimulation or a repercussion of inflammatory responses. Therefore, to address this question, we first evaluated the response of basophils to SARS-CoV-2 infection. In our study, we isolated basophils from the healthy donors' blood and were treated with SARS-CoV-2 for 1 h followed by 24 h incubation. The phenotype of basophils was analyzed by flow cytometry (**Figure 1A**). While the expression of CD13 and CD69 was not modified by SARS-CoV-2, a modest increase in the median fluorescence intensity of FcεRI was observed on SARS-CoV-2-infected basophils (**Figure 1B**). SARS-CoV-2 had no cytopathic effects on the basophils as either cell yield or viability as analyzed by fixable-viable dye were not altered.

We analyzed whether SARS-CoV-2 infection induced cytokine responses in basophils. We found that both IL-4 and IL-13 cytokines were enhanced upon SARS-CoV-2 stimulation (**Figure 1C**) thus confirming SARS-CoV-2 induces activation of human basophils. These data together indicate that resting human basophils undergo limited activation by SARS-CoV-2. Our data also suggest that higher expression of activation markers reported on basophils from COVID-19 patients was possibly not due to the direct virus stimulation (11).

SARS-CoV-2 Enhances Cytokine Production in IL-3 Primed Basophils

Under certain conditions, basophils require prior priming to undergo activation by stimuli (12). We therefore investigated if SARS-CoV-2 could induce activation of basophils if they were primed. Data from various labs including ours have shown that among various cytokines, IL-3 induces strong priming of human basophils (12–15). Therefore, we primed the basophils with IL-3 along with SARS-CoV-2 stimulation. Priming with IL-3 enhanced the expression of various surface markers (compared to unstimulated basophils, **Figure 1B**) such as CD13 and CD69 (**Figures 2A, B**). However, SARS-CoV-2 did not alter the phenotype of IL-3-primed basophils (**Figure 2B**). Also, SARS-CoV-2 did not induce degranulation of basophils as the expression of CD107a, a marker associated with basophil degranulation, was similar in both the experimental conditions. We confirmed that basophils either resting or IL-3-primed were not permissive to SARS-CoV-2 replication (**Figure 2C**).

Interestingly, SARS-CoV-2 significantly enhanced IL-4 and IL-13 cytokine production in IL-3 primed basophils (**Figure 2D**). Though significant, IL-4 enhancement was marginal compared to IL-13, which is not surprising as IL-4 induction in basophils is dependent on FcεRI-mediated signaling (16).

Lack of Basophil Activation by SARS-CoV-2 Infected Epithelial Cells

The entry of SARS-CoV-2 into the cell depends on two receptors, angiotensin-converting enzyme 2 (ACE2) and type II transmembrane serine protease (TMPRSS2), which are involved in binding to RBD of the Spike (S) protein and activation of the S protein by proteolytic priming, respectively. Epithelial cells are the major target of SARS-CoV-2 infection and several studies have highlighted cross-talk between the epithelial cells and basophils (17–19). Therefore, we surmised that epithelial cells infected with SARS-CoV-2 could affect activation of basophils. Though A549 lung epithelial cells have been reported to induce activation of human basophils (18), they lack both ACE2 and TMPRSS2 receptors (20). On the other hand, human colorectal adenocarcinoma cells (Caco-2 cells) were reported to express both ACE2 and TMPRSS2 receptors and support SARS-CoV-2 replication (20). Virus titration experiments have confirmed that Caco-2 are permissive to SARS-CoV-2 infection (**Figure 3A**). However, SARS-CoV-2-infected Caco-2 cells did not alter either phenotype of basophils (**Figure 3B**) or cytokines secreted (**Figure 3C**).

SARS-CoV-2 Does Not Induce PD-L1 on the Basophils

Immuno-phenotyping studies have revealed that programmed death receptor ligand 1 (PD-L1, CD274, B7-H1; family of B7 costimulatory molecule) is dysregulated on monocytes, neutrophils, and T cells in COVID-19 patients (21). In addition, an enhanced expression of PD-L1 was also observed on the peripheral blood basophils of severe COVID-19 patients (11, 22–24), though this observation was not confirmed by another report (11). Therefore, we investigated the repercussion of SARS-CoV-2 infection on the expression of PD-L1 on the basophils at 24 h. We found that both resting as well as SARS-CoV-2-infected basophils lacked the expression of PD-L1 (**Figure 4A**). Similar results were also obtained with IL-3-primed basophils (**Figure 4B**) and basophils co-cultured with virus-infected Caco-2 (**Figure 4C**). Our control experiments have indicated that the expression of PD-L1 on the basophils did not differ at 24 and 48 h. These data together suggest that SARS-CoV-2 does not induce PD-L1 on the basophils and altered expression of this molecule observed on the basophils from COVID-19 patients was possibly due to the inflammatory cytokine responses.

DISCUSSION

Various studies have confirmed the dysregulation of immune system, particularly cells of the innate immune system and cytokine storm in severe COVID-19 patients (25). Systems-level immuno-monitoring of adult COVID-19 patients by mass-cytometry revealed that polymorphonuclear granulocytes

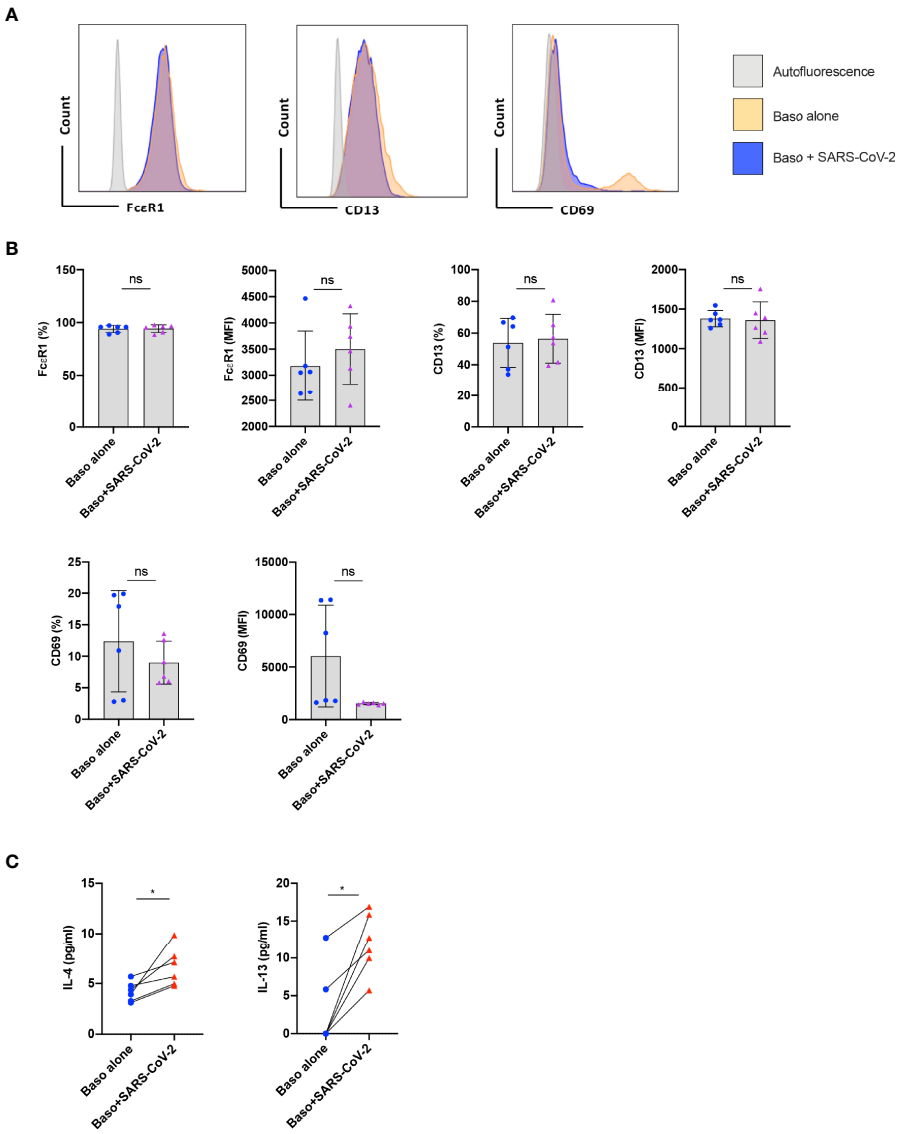

FIGURE 1 | Resting human basophils undergo limited activation upon stimulation with SARS-CoV-2. Basophils ($0.1x10^6$ cells/100 µl) isolated from PBMCs of healthy donors were cultured with or without SARS-CoV-2 at a MOI of 1. Cell phenotype was evaluated by flow cytometry after 24 h. **(A)** Representative histogram overlays displaying the expression pattern of FcεR1, CD13 and CD69 on basophils under various experimental conditions. **(B)** Expression of FcεR1, CD13 and CD69 on basophils (% positive cells and median fluorescence intensities (MFI), mean ± SD; n = 6 independent donors). **(C)** The amount (pg/ml) of secreted IL-4 and IL-13 in the cell-free supernatant from the above experiments (mean ± SD, n = 6 independent donors). ns, not significant, *P < 0.05, paired Wilcoxon test.

(neutrophils, eosinophils, and basophils) are differentially regulated in the circulation during infection (2). Both absolute count and relative frequencies of basophils are decreased in moderate and severe COVID-19 patients (11, 26). However, in contrast to neutrophils, basophils are increased from acute to recovery phase though another cohort reported no difference in the basophil count in COVID-19 patients during acute phase as compared to healthy donors (27). An activated phenotype of basophils was also documented in COVID-19 patients (11) though the underlying mechanisms are not known. In view of activation of complement pathway in COVID-19 patients (28–30) and that human basophils express C5aR and C3aR (31), indirect activation of basophils in COVID-19 patients through complement components cannot be ruled out. However, direct or indirect interaction of basophils with SARS-CoV-2 has not been investigated yet, despite their vital role in the pulmonary pathologies and regulation of immune responses. The low frequency of basophils (0.2 to 0.5% of leukocytes) in the circulation is one of the main limitations for researchers to study the basophils.

Direct capture of human immunodeficiency virus (HIV)-1 by basophils has been described (32), though the identity of pattern recognition receptor (PRR) that mediates virus capture is not clear (33). Human basophils produce histamine when cells are

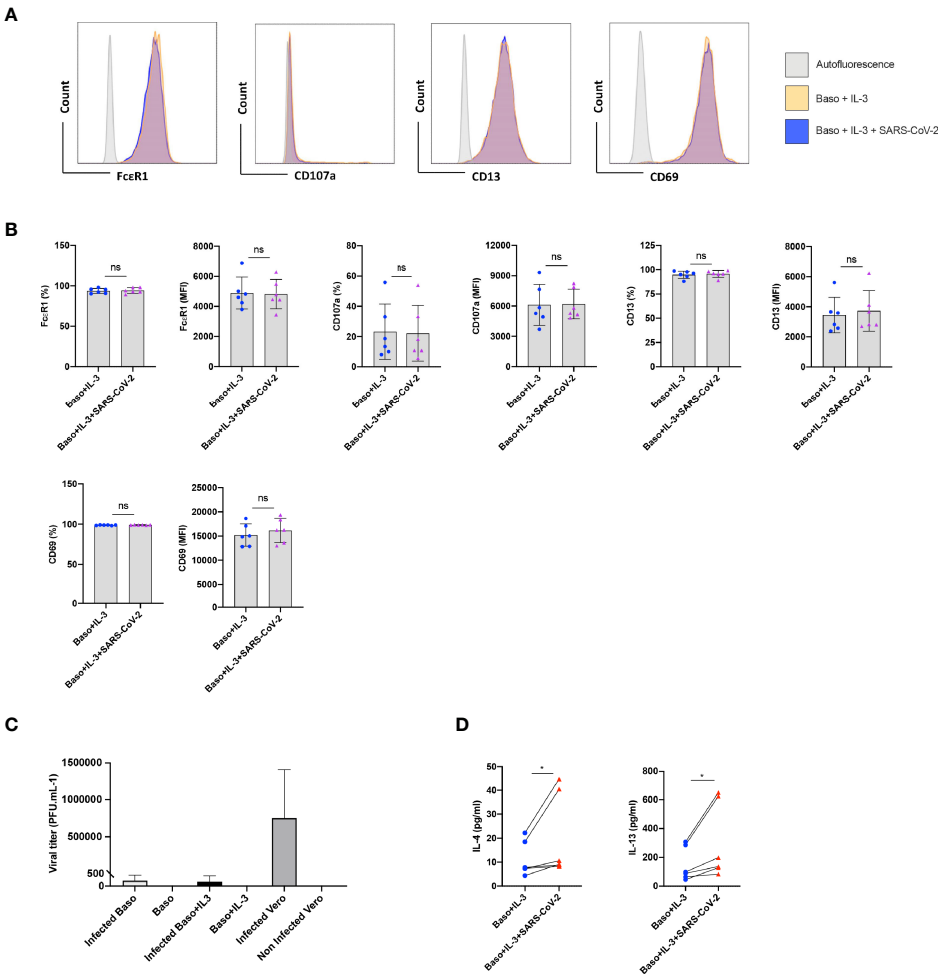

FIGURE 2 | SARS-CoV-2 enhances cytokines in IL-3-primed basophils. Basophils ($0.1x10^6$ cells/100 µl) from the healthy donors were primed with IL-3 (20 ng/ml) along with infection with SARS-CoV-2 at a MOI of 1. Non-infected basophils were used as a control. Cell phenotype was evaluated by flow cytometry after 24 h. **(A)** Representative histogram overlays displaying the expression pattern of FcεR1, CD107a, CD13 and CD69 on basophils under different experimental conditions. **(B)** Expression of FcεR1, CD107a, CD13 and CD69 on the basophils (% positive cells and median fluorescence intensities (MFI), mean ± SD; n = 6 independent donors). **(C)** Basophils are not permissive to SARS-CoV-2 replication. Either resting basophils ($0.1x10^6$ cells/well/96 well plate) or IL-3-primed basophils were infected with SARS-CoV-2 (mean ± SD, n=6 independent donors). Viral titers were evaluated after 24 h post-infection. Infected and non-infected Vero E6 cells were used as controls for the infection (n = 3). **(D)** The amount (pg/ml) of secreted IL-4 and IL-13 in the cell-free supernatant from the above experiments (mean ± SD, n = 6 independent donors). ns, not significant, *P < 0.05, paired Wilcoxon test.

incubated with paramyxoviruses, thus indicating that basophils have a capacity to respond to virus stimuli (34). In addition, human basophilic cell line (KU812) has been demonstrated to be permissive to rhinovirus infection *in vitro* (35). In view of these observations and the role of basophils in various respiratory pathologies, we investigated the cross-talk between SARS-CoV-2 and basophils. Our data suggest that SARS-CoV-2 could induce partial activation of basophils leading to the secretion of cytokines, IL-4 and IL-13, both in resting and IL-3-primed basophils. The effect of SARS-CoV-2 on IL-13 induction was particularly remarkable in IL-3 primed condition. The mechanism by which SARS-CoV-2 induces basophil activation is the subject of future investigation.

Previous data have shown inability of SARS-CoV-2 to replicate in various immune cells (36). Also, proteomic and genomic data clearly highlighted the absence of ACE2 receptor on the basophils (37). Therefore, we believe that SARS-CoV-2 could induce basophil activation by signaling through PRR in coordination with cytokines like IL-3. Activated T cells are the major source of IL-3 (14, 38, 39) and flow cytometric data showed that IL-3 in COVID-19 patients is contributed mainly by $CD4^+$ T cells (40). Of note, low levels of IL-3 in the circulation of COVID-19 patients is associated with enhanced severity of the disease and mortality (40). Mechanistically, it was proposed that IL-3 enhances the recruitment of plasmacytoid dendritic cells into the airways and hence boosts the anti-viral innate immunity.

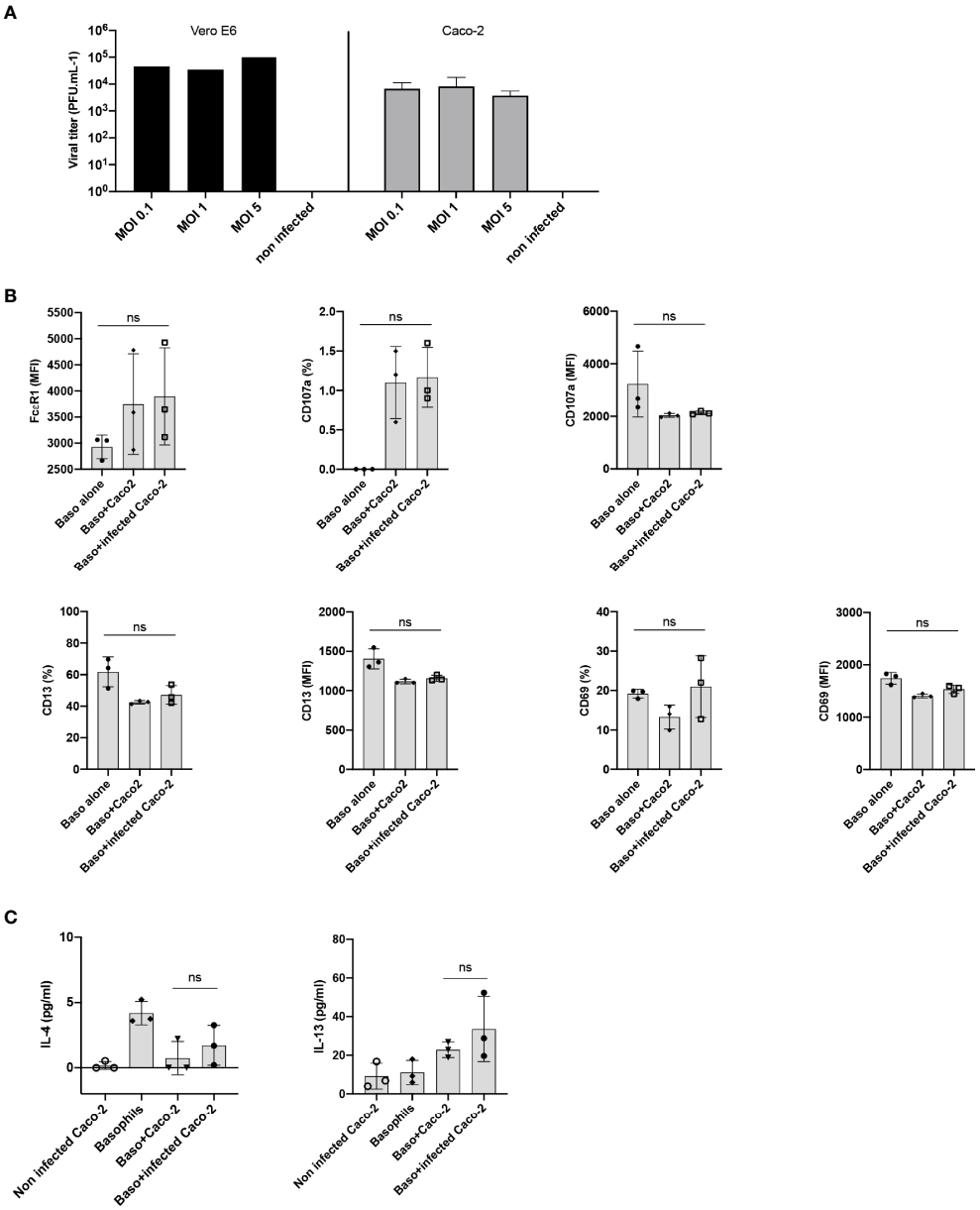

FIGURE 3 | Lack of basophil activation by SARS-CoV-2 infected epithelial cells. **(A)** Caco-2 cells permit SARS-CoV-2 replication. Caco-2 cells ($1.5x10^5$ cells per well/24 well plate) in duplicates were infected with SARS-CoV-2 at the MOI of 0.1, 1 and 5. Viral titers were evaluated after 72 h post-infection. Data were presented as mean ± SD. Infection of Vero E6 cells with SARS-CoV-2 was used as a control. **(B, C)** Basophils were cultured as follows: basophils alone ($0.1x10^6$ cells/100 µl), basophils ($0.1x10^6$ cells/100 µl) + Caco-2 ($5x10^4$ cells/100 µl), and basophils + Caco-2 infected with SARS-CoV-2. Cell phenotype was evaluated by flow cytometry after 24 h. **(B)** Expression of FcεR1, CD107a, CD13, CD69 on basophils (% positive cells and/or median fluorescence intensities (MFI), mean ± SD; n = 3 independent donors). **(C)** The amount (pg/ml) of secreted IL-4 and IL-13 in the cell-free supernatant from the above experiments (mean ± SD, n = 3 independent donors). ns, not significant, one-way ANOVA Friedman test with Dunn's multiple comparisons post-test.

Our data imply that IL-3 also primes basophils to secrete higher amounts of cytokines IL-13 and IL-4 in response to virus stimulation that might help in reducing the inflammation and also to promote antibody responses to the SARS-CoV-2.

Interaction between the checkpoint molecules programmed cell death protein PD-1 and PD-L1 plays a key role in maintaining immune tolerance (41–43). However, immune exhaustion by signaling through checkpoint molecules could prevent effective clearance of the pathogens leading to exacerbated immune responses (44, 45). PD-L1 and PD-1 interaction also supports regulatory T cell responses (46–50). Of note, PD-L1 expression was significantly higher in a group of severe COVID-19 patients as compared to milder patients and was positively correlated with the WHO and Sequential Organ

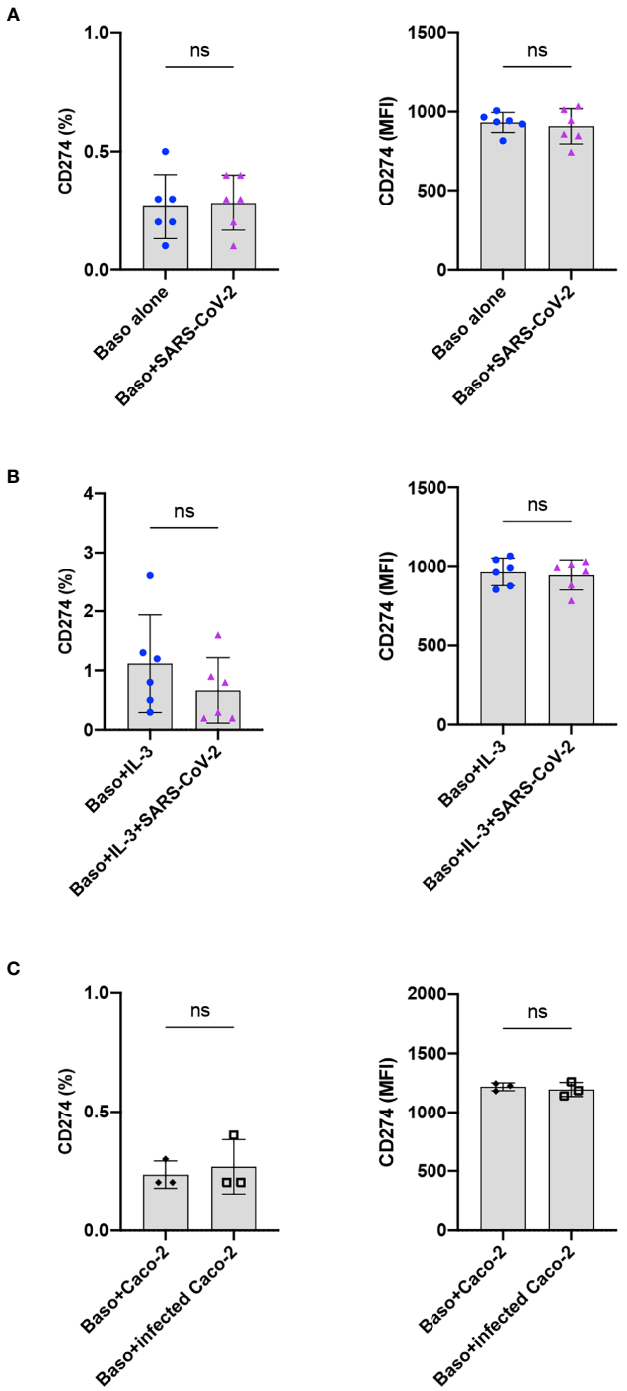

FIGURE 4 | SARS-CoV-2 does not induce PD-L1 on the basophils. The expression of PD-L1 on the basophils under various experimental conditions of SARS-CoV-2 stimulation. **(A)** Resting basophils ($0.1x10^6$ cells/100 µl) were cultured with or without SARS-CoV-2 for 24 h and the expression of PD-L1 was analyzed by flow cytometry. **(B)** Basophils were primed with IL-3 along with infection with SARS-CoV-2. Non-infected basophils were used as a control. PD-L1 was analyzed after 24 h culture. **(C)** Basophils were cultured with either non-infected or SARS-CoV-2 infected Caco-2 cells for 24 h. The data (mean ± SD) were presented as % cells positive for PD-L1 and median fluorescence intensities (MFI), and were from 3 **(C)** to 6 **(A, B)** independent donors. ns, not significant, paired Wilcoxon test.

Failure Assessment (SOFA) clinical scores (22). It is likely that the induced expression of PD-L1 in severe COVID-19 patients might be responsible for the T cell exhaustion. The trigger that induces PD-L1 on the basophils from COVID-19 patients is not known. Our data however suggest that SARS-CoV-2 infection does not induce PD-L1 on the basophils (51). However, PD-L1 on basophils may not influence the effector $CD4^+$ T cell responses as basophils lack the features of antigen presenting cells (52–56). In view of these facts, the significance of basophil-PD-L1 in the pathogenesis of COVID-19 remains unclear.

SARS-CoV-2 entry is facilitated by the presence of ACE2 and TMPRSS2 receptors on the host cells. These receptors are highly expressed by epithelial cells that are present in the lungs and gastrointestinal tract. Several innate stimuli including epithelial derived inflammatory cytokines (IL-33, IL-18, Thymic stromal lymphopoietin, and GM-CSF), growth factors (IL-3, IL-7, TGF-β, and VEGF) activate the mouse basophils (57). Also, airway epithelial cell line A549 has been reported to induce activation of human basophils (18). Whether other epithelial cells also display similar capacity to induce basophil activation is not known. Our results however suggest that Caco-2 cells lack the ability to induce basophil activation. Primary lung epithelial cells need to be used to examine the cross-talk between SARS-CoV-2-infected airway epithelial cells and basophils, and is the limitation of our study.

DATA AVAILABILITY STATEMENT

The original contributions presented in the study are included in the article/supplementary material. Further inquiries can be directed to the corresponding author.

ETHICS STATEMENT

EFS-INSERM permission (18/EFS/041) was obtained for the purchase of healthy donors buffy coats used in the study.

AUTHOR CONTRIBUTIONS

JB conceptualized, designed and coordinated the study, contributed to the interpretation of the results and wrote the paper. SB, CC, LL, and MJM performed the experiments and participated in the data interpretation and wrote the first draft of the paper. AS coordinated the study along with JB. All authors read and approved the final submitted version of the article.

FUNDING

Agence Nationale de la Recherche, France under the call "Flash COVID-19" (ANR-20-COVI-0093-COVIMUNE) and ANR-19-CE17-0021 (BASIN).

ACKNOWLEDGMENTS

We thank the staff of core facilities [Centre d'Histologie, d'Imagerie et de Cytométrie (CHIC)] at Centre de Recherche des Cordeliers for the help. We would like to thank the National Reference Centre for Respiratory Viruses hosted by Institut Pasteur (Paris, France) and headed by Dr. Sylvie van der Werf for providing the virus strain. The human sample was isolated and provided by Drs. Xavier Lescure, Yazdan Yazdanpanah from the Bichat Hospital, Paris.

REFERENCES

1. *Who Coronavirus (Covid-19) Dashboard*. Geneva, Switzerland: WHO (2021). Available at: https://covid19.who.int/.
2. Rodriguez L, Pekkarinen PT, Lakshmikanth T, Tan Z, Consiglio CR, Pou C, et al. Systems-Level Immunomonitoring From Acute to Recovery Phase of Severe Covid-19. *Cell Rep Med* (2020) 1:100078. doi: 10.1016/j.xcrm.2020.100078
3. Koutsakos M, Rowntree LC, Hensen L, Chua BY, van de Sandt CE, Habel JR, et al. Integrated Immune Dynamics Define Correlates of Covid-19 Severity and Antibody Responses. *Cell Rep Med* (2021) 2:100208. doi: 10.1016/j.xcrm.2021.100208
4. Ogbe A, Kronsteiner B, Skelly DT, Pace M, Brown A, Adland E, et al. T Cell Assays Differentiate Clinical and Subclinical Sars-Cov-2 Infections From Cross-Reactive Antiviral Responses. *Nat Commun* (2021) 12:2055. doi: 10.1038/s41467-021-21856-3
5. Gaebler C, Wang Z, Lorenzi JCC, Muecksch F, Finkin S, Tokuyama M, et al. Evolution of Antibody Immunity to Sars-Cov-2. *Nature* (2021) 591:639–44. doi: 10.1038/s41586-021-03207-w
6. Trombetta AC, Farias GB, Gomes AMC, Godinho-Santos A, Rosmaninho P, Conceicao CM, et al. Severe Covid-19 Recovery Is Associated With Timely Acquisition of a Myeloid Cell Immune-Regulatory Phenotype. *Front Immunol* (2021) 12:691725. doi: 10.3389/fimmu.2021.691725
7. Bost P, De Sanctis F, Cane S, Ugel S, Donadello K, Castellucci M, et al. Deciphering the State of Immune Silence in Fatal Covid-19 Patients. *Nat Commun* (2021) 12:1428. doi: 10.1038/s41467-021-21702-6
8. Voehringer D. Protective and Pathological Roles of Mast Cells and Basophils. *Nat Rev Immunol* (2013) 13:362–75. doi: 10.1038/nri3427
9. Karasuyama H, Miyake K, Yoshikawa S, Yamanishi Y. Multifaceted Roles of Basophils in Health and Disease. *J Allergy Clin Immunol* (2018) 142:370–80. doi: 10.1016/j.jaci.2017.10.042
10. Karasuyama H, Shibata S, Yoshikawa S, Miyake K. Basophils, a Neglected Minority in the Immune System, Have Come Into the Limelight at Last. *Int Immunol* (2021) 33:809–13. doi: 10.1093/intimm/dxab021
11. Lourda M, Dzidic M, Hertwig L, Bergsten H, Palma Medina LM, Sinha I, et al. High-Dimensional Profiling Reveals Phenotypic Heterogeneity and Disease-Specific Alterations of Granulocytes in Covid-19. *Proc Natl Acad Sci USA* (2021) 118:e2109123118. doi: 10.1073/pnas.2109123118
12. Voehringer D. Basophil Modulation by Cytokine Instruction. *Eur J Immunol* (2012) 42:2544–50. doi: 10.1002/eji.201142318
13. Yoshimura C, Yamaguchi M, Iikura M, Izumi S, Kudo K, Nagase H, et al. Activation Markers of Human Basophils: Cd69 Expression Is Strongly and Preferentially Induced by Il-3. *J Allergy Clin Immunol* (2002) 109:817–23. doi: 10.1067/mai.2002.123532
14. Sharma M, Das M, Stephen-Victor E, Galeotti C, Karnam A, Maddur MS, et al. Regulatory T Cells Induce Activation Rather Than Suppression of Human Basophils. *Sci Immunol* (2018) 3:eaan0829. doi: 10.1126/sciimmunol.aan0829
15. Galeotti C, Stephen-Victor E, Karnam A, Das M, Gilardin L, Maddur MS, et al. Intravenous Immunoglobulin Induces Il-4 in Human Basophils by Signaling Through Surface-Bound Ige. *J Allergy Clin Immunol* (2019) 144:524–35 e8. doi: 10.1016/j.jaci.2018.10.064
16. Ochensberger B, Daepp GC, Rihs S, Dahinden CA. Human Blood Basophils Produce Interleukin-13 in Response to Ige- Receptor-Dependent and -Independent Activation. *Blood* (1996) 88:3028–37. doi: 10.1182/blood.V88.8.3028.bloodjournal8883028
17. Motomura Y, Morita H, Moro K, Nakae S, Artis D, Endo TA, et al. Basophil-Derived Interleukin-4 Controls the Function of Natural Helper Cells, A Member of Ilc2s, in Lung Inflammation. *Immunity* (2014) 40:758–71. doi: 10.1016/j.immuni.2014.04.013
18. Schroeder JT, Bieneman AP. Activation of Human Basophils by A549 Lung Epithelial Cells Reveals a Novel Ige-Dependent Response Independent of Allergen. *J Immunol* (2017) 199:855–65. doi: 10.4049/jimmunol.1700055
19. Roan F, Obata-Ninomiya K, Ziegler SF. Epithelial Cell-Derived Cytokines: More Than Just Signaling the Alarm. *J Clin Invest* (2019) 129:1441–51. doi: 10.1172/JCI124606
20. Wing PAC, Keeley TP, Zhuang X, Lee JY, Prange-Barczynska M, Tsukuda S, et al. Hypoxic and Pharmacological Activation of Hif Inhibits Sars-Cov-2 Infection of Lung Epithelial Cells. *Cell Rep* (2021) 35:109020. doi: 10.1016/j.celrep.2021.109020
21. Sabbatino F, Conti V, Franci G, Sellitto C, Manzo V, Pagliano P, et al. Pd-L1 Dysregulation in Covid-19 Patients. *Front Immunol* (2021) 12:695242. doi: 10.3389/fimmu.2021.695242
22. Vitte J, Diallo AB, Boumaza A, Lopez A, Michel M, Allardet-Servent J, et al. A Granulocytic Signature Identifies Covid-19 and Its Severity. *J Infect Dis* (2020) 222:1985–96. doi: 10.1093/infdis/jiaa591
23. Vitte J, Diallo AB, Boumaza A, Lopez A, Michel M, Allardet-Servent J, et al. Reply to Chen and Vitetta. *J Infect Dis* (2021) 223:1660–2. doi: 10.1093/infdis/jiab062
24. Chen J, Vitetta L. Increased Pd-L1 Expression May Be Associated With the Cytokine Storm and Cd8+ T-Cell Exhaustion in Severe Covid-19. *J Infect Dis* (2021) 223:1659–60. doi: 10.1093/infdis/jiab061
25. Bonam SR, Kaveri SV, Sakuntabhai A, Gilardin L, Bayry J. Adjunct Immunotherapies for the Management of Severely Ill Covid-19 Patients. *Cell Rep Med* (2020) 1:100016. doi: 10.1016/j.xcrm.2020.100016
26. Laing AG, Lorenc A, Del Molino Del Barrio I, Das A, Fish M, Monin L, et al. A Dynamic Covid-19 Immune Signature Includes Associations With Poor Prognosis. *Nat Med* (2020) 26:1623–35. doi: 10.1038/s41591-020-1038-6
27. Mathew D, Giles JR, Baxter AE, Oldridge DA, Greenplate AR, Wu JE, et al. Deep Immune Profiling of Covid-19 Patients Reveals Distinct Immunotypes With Therapeutic Implications. *Science* (2020) 369:eabc8511. doi: 10.1126/science.abc8511
28. Afzali B, Noris M, Lambrecht BN, Kemper C. The State of Complement in Covid-19. *Nat Rev Immunol* (2022) 22:77–84. doi: 10.1038/s41577-021-00665-1
29. Senent Y, Inogés S, López-Díaz de Cerio A, Blanco A, Campo A, Carmona-Torre F, et al. Persistence of High Levels of Serum Complement C5a in Severe Covid-19 Cases After Hospital Discharge. *Front Immunol* (2021) 12:767376. doi: 10.3389/fimmu.2021.767376
30. Cyprian FS, Suleman M, Abdelhafez I, Doudin A, Masud Danjuma IM, Mir FA, et al. Complement C5a and Clinical Markers as Predictors of Covid-19 Disease Severity and Mortality in a Multi-Ethnic Population. *Front Immunol* (2021) 12:707159. doi: 10.3389/fimmu.2021.707159
31. Zwirner J, Gotze O, Begemann G, Kapp A, Kirchhoff K, Werfel T. Evaluation of C3a Receptor Expression on Human Leucocytes by the Use of Novel Monoclonal Antibodies. *Immunology* (1999) 97:166–72. doi: 10.1046/j.1365-2567.1999.00764.x
32. Jiang AP, Jiang JF, Guo MG, Jin YM, Li YY, Wang JH. Human Blood-Circulating Basophils Capture Hiv-1 and Mediate Viral Trans-Infection of Cd4+ T Cells. *J Virol* (2015) 89:8050–62. doi: 10.1128/JVI.01021-15
33. Das M, Galeotti C, Stephen-Victor E, Karnam A, Kaveri SV, Bayry J. Human Basophils May Not Undergo Modulation by Dc-Sign and Mannose Receptor-Targeting Immunotherapies Due to Absence of Receptors. *J Allergy Clin Immunol* (2017) 139:1403–4 e1. doi: 10.1016/j.jaci.2016.09.062
34. Sanchezlegrand F, Smith T. Interaction of Paramyxoviruses With Human Basophils and Their Effect on Histamine Release. *J Allergy Clin Immunol* (1989) 84:538–46. doi: 10.1016/0091-6749(89)90368-0
35. Hosoda M, Yamaya M, Suzuki T, Yamada N, Kamanaka M, Sekizawa K, et al. Effects of Rhinovirus Infection on Histamine and Cytokine Production by Cell

Lines From Human Mast Cells and Basophils. *J Immunol* (2002) 169:1482–91. doi: 10.4049/jimmunol.169.3.1482
36. Jiang M, Kolehmainen P, Kakkola L, Maljanen S, Melen K, Smura T, et al. Sars-Cov-2 Isolates Show Impaired Replication in Human Immune Cells But Differential Ability to Replicate and Induce Innate Immunity in Lung Epithelial Cells. *Microbiol Spectr* (2021) 9:e0077421. doi: 10.1128/Spectrum.00774-21
37. Wang Y, Wang Y, Luo W, Huang L, Xiao J, Li F, et al. A Comprehensive Investigation of the Mrna and Protein Level of Ace2, the Putative Receptor of Sars-Cov-2, in Human Tissues and Blood Cells. *Int J Med Sci* (2020) 17:1522–31. doi: 10.7150/ijms.46695
38. Sullivan BM, Liang HE, Bando JK, Wu D, Cheng LE, McKerrow JK, et al. Genetic Analysis of Basophil Function *in Vivo*. *Nat Immunol* (2011) 12:527–35. doi: 10.1038/ni.2036
39. Leyva-Castillo JM, Hener P, Michea P, Karasuyama H, Chan S, Soumelis V, et al. Skin Thymic Stromal Lymphopoietin Initiates Th2 Responses Through an Orchestrated Immune Cascade. *Nat Commun* (2013) 4:2847. doi: 10.1038/ncomms3847
40. Benard A, Jacobsen A, Brunner M, Krautz C, Klosch B, Swierzy I, et al. Interleukin-3 Is a Predictive Marker for Severity and Outcome During Sars-Cov-2 Infections. *Nat Commun* (2021) 12:1112. doi: 10.1038/s41467-021-21310-4
41. Francisco LM, Sage PT, Sharpe AH. The Pd-1 Pathway in Tolerance and Autoimmunity. *Immunol Rev* (2010) 236:219–42. doi: 10.1111/j.1600-065X.2010.00923.x
42. Tumeh PC, Harview CL, Yearley JH, Shintaku IP, Taylor EJ, Robert L, et al. Pd-1 Blockade Induces Responses by Inhibiting Adaptive Immune Resistance. *Nature* (2014) 515:568–71. doi: 10.1038/nature13954
43. Jubel JM, Barbati ZR, Burger C, Wirtz DC, Schildberg FA. The Role of Pd-1 in Acute and Chronic Infection. *Front Immunol* (2020) 11:487. doi: 10.3389/fimmu.2020.00487
44. Zinselmeyer BH, Heydari S, Sacristan C, Nayak D, Cammer M, Herz J, et al. Pd-1 Promotes Immune Exhaustion by Inducing Antiviral T Cell Motility Paralysis. *J Exp Med* (2013) 210:757–74. doi: 10.1084/jem.20121416
45. Klein S, Ghersi D, Manns MP, Prinz I, Cornberg M, Kraft ARM. Pd-L1 Checkpoint Inhibition Narrows the Antigen-Specific T Cell Receptor Repertoire in Chronic Lymphocytic Choriomeningitis Virus Infection. *J Virol* (2020) 94:e00795-20. doi: 10.1128/JVI.00795-20
46. Wang L, Pino-Lagos K, de Vries VC, Guleria I, Sayegh MH, Noelle RJ. Programmed Death 1 Ligand Signaling Regulates the Generation of Adaptive Foxp3+Cd4+ Regulatory T Cells. *Proc Natl Acad USA* (2008) 105:9331–6. doi: 10.1073/pnas.0710441105
47. Amarnath S, Mangus CW, Wang JC, Wei F, He A, Kapoor V, et al. The Pdl1-Pd1 Axis Converts Human Th1 Cells Into Regulatory T Cells. *Sci Transl Med* (2011) 3:111ra20. doi: 10.1126/scitranslmed.3003130
48. Stephen-Victor E, Karnam A, Fontaine T, Beauvais A, Das M, Hegde P, et al. Aspergillus Fumigatus Cell Wall Alpha-(1,3)-Glucan Stimulates Regulatory T-Cell Polarization by Inducing Pd-L1 Expression on Human Dendritic Cells. *J Infect Dis* (2017) 216:1281–94. doi: 10.1093/infdis/jix469
49. Fanelli G, Romano M, Nova-Lamperti E, Werner Sunderland M, Nerviani A, Scotta C, et al. Pd-L1 Signaling on Human Memory Cd4+ T Cells Induces a Regulatory Phenotype. *PloS Biol* (2021) 19:e3001199. doi: 10.1371/journal.pbio.3001199
50. Karnam A, Bonam SR, Rambabu N, Wong SSW, Aimanianda V, Bayry J. Wnt-Beta-Catenin Signaling in Human Dendritic Cells Mediates Regulatory T-Cell Responses to Fungi *Via* the Pd-L1 Pathway. *mBio* (2021) 0:e0282421. doi: 10.1128/mBio.02824-21
51. Lee SJ, Jang BC, Lee SW, Yang YI, Suh SI, Park YM, et al. Interferon Regulatory Factor-1 Is Prerequisite to the Constitutive Expression and Ifn-Gamma-Induced Upregulation of B7-H1 (Cd274). *FEBS Lett* (2006) 580:755–62. doi: 10.1016/j.febslet.2005.12.093
52. Eckl-Dorna J, Ellinger A, Blatt K, Ghanim V, Steiner I, Pavelka M, et al. Basophils Are Not the Key Antigen-Presenting Cells in Allergic Patients. *Allergy* (2012) 67:601–8. doi: 10.1111/j.1398-9995.2012.02792.x
53. Kitzmuller C, Nagl B, Deifl S, Walterskirchen C, Jahn-Schmid B, Zlabinger GJ, et al. Human Blood Basophils Do Not Act as Antigen-Presenting Cells for the Major Birch Pollen Allergen Bet V 1. *Allergy* (2012) 67:593–600. doi: 10.1111/j.1398-9995.2011.02764.x
54. Sharma M, Hegde P, Aimanianda V, Beau R, Maddur MS, Sénéchal H, et al. Circulating Human Basophils Lack the Features of Professional Antigen Presenting Cells. *Sci Rep* (2013) 3:1188. doi: 10.1038/srep01188
55. Sharma M, Stephen-Victor E, Poncet P, Kaveri SV, Bayry J. Basophils Are Inept at Promoting Human Th17 Responses. *Hum Immunol* (2015) 76:176–80. doi: 10.1016/j.humimm.2014.12.015
56. Emmanuel S-V, Mrinmoy D, Meenu S, Caroline G, Hélène F-T, Boualem S, et al. Demystification of Enigma on Antigen-Presenting Cell Features of Human Basophils: Data From Secondary Lymphoid Organs. *Haematologica* (2017) 102:e233–e7. doi: 10.3324/haematol.2016.163451
57. Pellefigues C, Mehta P, Chappell S, Yumnam B, Old S, Camberis M, et al. Diverse Innate Stimuli Activate Basophils Through Pathways Involving Syk and Ikappab Kinases. *Proc Natl Acad Sci USA* (2021) 118:e2019524118. doi: 10.1073/pnas.2019524118

Conflict of Interest: The authors declare that the research was conducted in the absence of any commercial or financial relationships that could be construed as a potential conflict of interest.

Publisher's Note: All claims expressed in this article are solely those of the authors and do not necessarily represent those of their affiliated organizations, or those of the publisher, the editors and the reviewers. Any product that may be evaluated in this article, or claim that may be made by its manufacturer, is not guaranteed or endorsed by the publisher.

frontiers in Immunology

ORIGINAL RESEARCH
published: 25 February 2022
doi: 10.3389/fimmu.2022.794776

Discordance in STING-Induced Activation and Cell Death Between Mouse and Human Dendritic Cell Populations

*Ee Shan Pang[1], Ghazal Daraj[2], Katherine R. Balka[3], Dominic De Nardo[3], Christophe Macri[1], Hubertus Hochrein[4], Kelly-Anne Masterman[2], Peck S. Tan[1], Angus Shoppee[1], Zoe Magill[1], Nazneen Jahan[1], Mariam Bafit[1], Yifan Zhan[5,6], Benjamin T. Kile[3,7], Kate E. Lawlor[8,9], Kristen J. Radford[2], Mark D. Wright[10] and Meredith O'Keeffe[1]**

[1] Department of Biochemistry and Molecular Biology, Biomedicine Discovery Institute, Monash University, Clayton, VIC, Australia, [2] Translational Research Institute, Mater Research-University of Queensland, Woolloongabba, QLD, Australia, [3] Department of Anatomy and Developmental Biology, Biomedicine Discovery Institute, Monash University, Clayton, VIC, Australia, [4] Department of Research, Bavarian Nordic GmbH, Martinsried, Germany, [5] Immunology Division, The Walter and Eliza Hall Institute of Medical Research, Parkville, VIC, Australia, [6] Department of Medical Biology, University of Melbourne, Parkville, VIC, Australia, [7] Faculty of Health and Medical Sciences, The University of Adelaide, Adelaide, SA, Australia, [8] Centre for Innate Immunity and Infectious Diseases, Hudson Institute of Medical Research, Clayton, VIC, Australia, [9] Department of Molecular and Translational Science, Monash University, Clayton, VIC, Australia, [10] Department of Immunology and Pathology, Monash University, Melbourne, VIC, Australia

OPEN ACCESS

Edited by:
Chien-Kuo Lee, National Taiwan University, Taiwan

Reviewed by:
Amiram Ariel, University of Haifa, Israel
Xavier Lhaye, U932 Immunité et Cancer (INSERM), France

***Correspondence:**
Meredith O'Keeffe
meredith.okeeffe@monash.edu

Specialty section:
This article was submitted to Molecular Innate Immunity, a section of the journal Frontiers in Immunology

Received: *14 October 2021*
Accepted: *03 February 2022*
Published: *25 February 2022*

Citation:
Pang ES, Daraj G, Balka KR, De Nardo D, Macri C, Hochrein H, Masterman K-A, Tan PS, Shoppee A, Magill Z, Jahan N, Bafit M, Zhan Y, Kile BT, Lawlor KE, Radford KJ, Wright MD and O'Keeffe M (2022) Discordance in STING-Induced Activation and Cell Death Between Mouse and Human Dendritic Cell Populations. Front. Immunol. 13:794776. doi: 10.3389/fimmu.2022.794776

Stimulator of Interferon Genes (STING) is a cytosolic sensor of cyclic dinucleotides (CDNs). The activation of dendritic cells (DC) *via* the STING pathway, and their subsequent production of type I interferon (IFN) is considered central to eradicating tumours in mouse models. However, this contribution of STING in preclinical murine studies has not translated into positive outcomes of STING agonists in phase I & II clinical trials. We therefore questioned whether a difference in human DC responses could be critical to the lack of STING agonist efficacy in human settings. This study sought to directly compare mouse and human plasmacytoid DCs and conventional DC subset responses upon STING activation. We found all mouse and human DC subsets were potently activated by STING stimulation. As expected, Type I IFNs were produced by both mouse and human plasmacytoid DCs. However, mouse and human plasmacytoid and conventional DCs all produced type III IFNs (i.e., IFN-λs) in response to STING activation. Of particular interest, all human DCs produced large amounts of IFN-λ1, not expressed in the mouse genome. Furthermore, we also found differential cell death responses upon STING activation, observing rapid ablation of mouse, but not human, plasmacytoid DCs. STING-induced cell death in murine plasmacytoid DCs occurred in a cell-intrinsic manner and involved intrinsic apoptosis. These data highlight discordance between STING IFN and cell death responses in mouse and human DCs and caution against extrapolating STING-mediated events in mouse models to equivalent human outcomes.

Keywords: STING activation, dendritic cell (DC), interferon-lambda, human dendritic cells, type III interferons, cell death, plasmacytoid dendritic cells (pDCs)

INTRODUCTION

Stimulator of IFN genes (STING, also known as TMEM173, MITA, MPYS or ERIS) is a pattern recognition receptor (PRR) that recognises cytosolic DNA in the form of cyclic dinucleotides (CDNs), such as the bacterial product cyclic-guanosine monophosphate-adenosine monophosphate (3'3' cGAMP) (1–4). In addition to bacterial components, other forms of DNA from viruses, or the host cell, that find their way into the cytosol are recognised by an enzyme c-GMP-AMP (cGAMP) synthase (cGAS). Upon cytosolic DNA binding, cGAS converts ATP and GTP into the metazoan-specific CDN 2'3'-cGAMP for STING recognition and activation (4–6). STING is a transmembrane protein that exists as dimers anchored within the endoplasmic reticulum membrane and forms a V-shaped pocket that enables cytosolic CDN binding. Ligand binding results in significant conformational changes in the C-terminal domain of STING, mediating its transport to Golgi compartments. At the Golgi, STING recruits TANK-binding kinase 1 (TBK1), which facilitates IRF3 phosphorylation, nuclear translocation and the strong induction of transcription of type I IFNs (e.g. IFN-β) (7–12). STING also triggers a robust pro-inflammatory cytokine response [e.g. tumour necrosis factor (TNF)] by activating Nuclear Factor-kappa B (NF-κB) and this part of the pathway can be mediated independent of TBK1 *via* a closely related homologue protein, IKKε (13).

STING activation, and associated type I IFN responses, are required for optimal immune responses to infectious pathogens and DNA-based vaccines (14), as well as for anti-tumour responses (15), including after DNA damage induced by radiation and chemotherapies (16–18). Thus, therapeutics directly targeting STING represent an important avenue to explore. Indeed, in mouse, the use of STING agonists has emerged as a powerful tool to eliminate tumours, both when used alone or as an adjunct to enhance checkpoint immunotherapies (15, 19–21). However, human clinical trials to date have failed to recapitulate the promising pre-clinical responses observed in animal models (22, 23). This lack of efficacy has been somewhat surprising as previous studies have suggested that STING-induced signaling pathways that lead to type I IFN and pro-inflammatory cytokine production are intact in humans and mice (13).

Dendritic cells (DCs) are important players in innate immune responses and their activation is required for the induction of specific immunity. It has been proposed that a DC type I IFN (IFN-α, β) response is essential for STING-mediated immune responses (14, 24). The current dogma garnered from mouse tumour models proposes that DC ingestion of tumour DNA, or use of STING agonist therapy, leads to STING-dependent IFN-β production that enhances conventional (c) DC function to boost subsequent anti-tumour immune responses (15, 24). However, any further detailed molecular studies focused on STING activation in cDCs have largely focused on monocyte-derived DCs generated *in vitro* with GM-CSF (9). A direct comparison of human and mouse DC responses to STING activation is therefore of critical importance, but to date has not been carried out.

DCs are categorised into different subsets with specialised functions and are conserved across species. Plasmacytoid DCs (pDCs), the original natural interferon producing cells (NIPC), are major type I IFN producers. The cDC1 subset excels at the presentation of exogenous antigen on MHCI (cross-presentation), particularly when associated as particulate or cell-associated antigen, and cDC1 are excellent at inducing and activating cytotoxic T cells (CTL). cDC2s are superior at enhancing $CD4^+$ T cell activation through MHCII presentation and are important for inducing T helper 2 (Th2) and Th17 cellular responses [reviewed in (25)]. We have previously shown that pDCs and cDC1s also have the specialized capacity to produce high levels of Type III IFNs (or IFN-λ) in response to TLR7/9 and TLR3 ligands, respectively, and to multiple viruses (26). Others have also recently shown that human pDCs produce IFN-λ in response to STING agonists, similar to TLR7 or 9 activation (27).

The IFN-λ family of genes differs between human and mouse in that the mouse genome encodes only 2 highly homologous genes, IFN-λ2 and IFN-λ3, whilst the human genome universally encodes 3 genes, IFN-λ1, -λ2 and -λ3. Moreover, polymorphisms in the IFN-λ gene locus that are more prevalent in people of African descent (28, 29) can lead to expression of a fourth IFN-λ gene, IFN-λ4, which exhibits only approximately 40% identity to the other IFN-λ genes but still signals through the IFN-λ Receptor (R) (30). IFN-λ proteins bind to the IFN-λR composed of the unique IFNLR1 (IL-28RA) and the IL-10Rβ. The IFN-λR, although distinct from the type I IFNR, similarly employs JAK-STAT signaling leading to the transcription of hundreds of interferon stimulated genes (ISGs) and antiviral activity (31). However, IFN-λR expression is mainly confined to epithelial cells and select subsets of hematopoietic cells, including DC, with much work still to be done to refine expression during health and disease settings (32). Overall, IFN-λ seems to have evolved to protect mucosal and epithelial barriers. Whilst IFN-λ1 and -λ2 induce upregulation of similar sets of ISGs, there is some evidence that IFN-λ1 lacks gene repressor function compared to IFN-λ2 (33). Whether unique function of IFN-λ1 in specific epithelial and hematopoietic cells generates differences in overall IFN-λ signaling outcomes in mouse versus humans is not yet known. In addition, expression of IFN-λ4, together with other polymorphisms within the IFN-λ locus, is strongly linked to poor clearance of Hepatitis C Virus (34). Polymorphisms within the IFN-λ gene locus have also recently been linked with the incidence and/or mortality of other diseases including liver inflammation, fibrosis and non-alcoholic fatty liver disease and certain cancers (28, 29, 35). Intriguingly, the mechanisms behind how these polymorphisms affect viral infection, inflammatory disease and cancer, as well as the involvement of high IFN-λ producing cells such as DCs in these contexts, are as yet unclear.

Here we present the first detailed comparison of STING activation in freshly isolated *ex vivo* DCs from mice and humans, and reveal divergent molecular and cellular responses. STING ligation by cyclic dinucleotides (CDNs) markedly upregulated cell surface expression markers of DC activation and maturation to levels at least as prominent as TLR activation. Moreover, STING activation elicited equivalent cell death in human blood and mouse cDC2. In contrast, while mouse pDC were rapidly ablated, human pDCs were refractory to STING-induced killing. Importantly,

in response to STING stimulation, differential IFN production was observed by DC subsets that is shared across the species. pDC of both species produced IFN-α, whilst all DC subsets produce IFN-2 and -3 proteins upon STING activation. IFN-λ1 was the most highly expressed IFN from all human DC subsets. This work places IFN-λ in the spotlight as a potential major player in DC-mediated immune responses downstream of STING activation.

RESULTS

DC Subsets Reveal Differential Signaling Upon STING Activation but IFN-λ Is Produced From All Mouse DC Subsets

The activation of STING in cDCs is reported to lead to type I IFN production (14), enabling enhanced T cell stimulation and therefore is likely to be essential for co-ordinating downstream T cell-mediated immune responses. However, the direct effects of STING activation on mouse and human DC function is less clear but remains of immense interest to understand the potential adjuvant properties of STING ligands. We therefore firstly tested the ability of an array of cyclic dinucleotide (CDN) STING ligands, c[G(3',5')pA(3',5')p] (3'3' cGAMP), 2'3' cGAMP, c di-AMP, c di-GMP, versus linearised controls, to activate and induce type I and III IFN production in mouse splenic DC cultures. All STING ligands led to upregulation of CD86 (**Figure 1A**) and MHCII (**Supplementary Figure 1A** and **Supplementary Figure 2**) on pDC and cDC subsets. In fact, cGAMP (10 nmol) induced CD86 expression on DC, most notably on pDC, that far surpassed the level seen in response to TLR activation (**Figure 1A**). Analyses of IFNs in these cultures also revealed that upon activation, STING induced appreciable levels of IFN-α and IFN-λ (**Figure 1B**), albeit at lower levels than the TLR9 ligand, CpG-A (CpG 2216). Importantly, IFN production was abrogated in DC lacking STING (**Supplementary Figure 1B**), confirming the responses were indeed STING-dependent. However, whether cell activation and IFN production was intrinsic to each of the DC subsets examined, or a bystander event upon selective DC activation, remained unclear.

Conventional DC1 (cDC1) activation has been observed *in vivo* in response to STING-activating adjuvants (36). Moreover, activation of cDC1 through STING is purported to be critical in inducing CTL responses upon immunotherapy administration (reviewed in (37)). However, in these scenarios, whether cDC1 *directly* respond to STING ligands has not been examined in detail. We therefore firstly examined levels of STING in DC subsets and found that STING (encoded by the gene *Tmem173*) is differentially expressed amongst DC subsets with expression in mouse pDC >cDC2 >cDC1 (**Supplementary Figure 3A**). Next, to determine the response of individual DC subsets to STING ligands, we sorted freshly isolated mouse splenic DCs into cDC1 ($CD11c^{hi}CD317^{lo}CD8^{+}CD11b^{-}$), cDC2 ($CD11c^{hi}CD317^{lo}CD8^{-}CD11b^{+}$) and pDC ($CD11c^{int}CD317^{hi}CD11b^{-}$) subsets (**Supplementary Figure 4A**), and stimulated them with 3'3'-cGAMP for 1.5 hours. Consistent with our gene expression data (**Supplementary Figure 3A**), Western blotting confirmed differential protein levels of total STING between DC subsets. These analyses further indicated that the cDC1 and cDC2 populations showed similar signaling events within the STING signaling pathway, with activation of NF-κB-p65, TBK1, IRF3 and STING (**Figures 2A, B**). This was commensurate with signaling events shown for other cell types (13); with the exception that we were unable to detect IKKε protein in any DC subset (not shown). Although not reaching significance, there was a trend for cDC2 to express the highest relative level of phospho (P)-STING, and the phosphorylated form of the STING-activating kinase, TBK1 (**Figures 2A, B**). Intriguingly, despite pDC exhibiting the highest levels of total STING protein they demonstrated modest STING phosphorylation and IRF3 activation, and showed little to no activation of NF-κB p65 (**Figures 2A, B**). These data strongly suggest differential regulation of the STING signaling pathways between cDCs and pDCs.

In view of the fact that all DC subsets were STING competent, we next examined the expression of co-stimulatory markers CD86 and CD80 in cultured DC subsets by FACS (**Figure 2C** and **Supplementary Figure 5**). It is worth noting that we and others routinely observe that isolated cDCs upregulate these activation markers *in vitro* in media alone (38) and that further increases are observed in cDC1 and cDC2 upon TLR3 (poly I:C) or TLR9 (CpG) activation, respectively (**Figure 2C**). Remarkably, we observed that 3'3'-cGAMP stimulation potently induced significant upregulation of CD86 (**Figure 2C**) and CD80 expression in cDC2 (**Supplementary Figure 5**), commensurate with increased STING signaling responses (**Figure 2A**). Compared to the negative controls, this upregulation was notably higher than the CD86 and CD80 expression elicited by CpG stimulation (**Figure 2C** and **Supplementary Figure 5**). Likewise, pDCs, which normally exhibit modest upregulation of CD86 and CD80 on their surface after CpG-induced activation, also expressed heightened expression of these markers after cGAMP stimulation (**Figure 2C** and **Supplementary Figure 5**). This is perhaps surprising given the relatively poor STING phosphorylation observed in pDCs upon stimulation (**Figure 2A**). Commensurate with the low levels of STING we observed in cDC1, cGAMP only slightly enhanced CD86 (**Figure 2C**) and CD80 (**Supplementary Figure 5**) levels, which were more comparable to that induced by poly I:C (**Figure 2C** and **Supplementary Figure 5**).

We have previously documented that cDC1 and pDCs produce not only large quantities of type I IFNs but also IFN-λ in response to poly I:C and CpG stimulation, respectively (26). Consequently, we tested supernatants from sorted mouse DC subsets treated with 3'3'-cGAMP for production of IFN-α and -β, as well as IFN-λ, by ELISA and bead array. In order to support the viability of sorted cDC after sorting and maximise IFN-λ production (26), we included a low concentration of GM-CSF (0.2 ng/ml) in the stimulated cultures. Interestingly, the levels of STING activation in each of the DC subsets was not directly related to levels of IFN production (**Figures 2A, D**). Consistent with their specialised IFN-I producing function, pDCs produced low levels of IFN-α in response to cGAMP stimulation (**Figure 2D**). However, cDC2 and cDC1 also produced low levels of IFN-α that was only detectable in the presence of GM-CSF (**Figure 2D** and **Supplementary Figure 6**). The major producers of IFN-β were

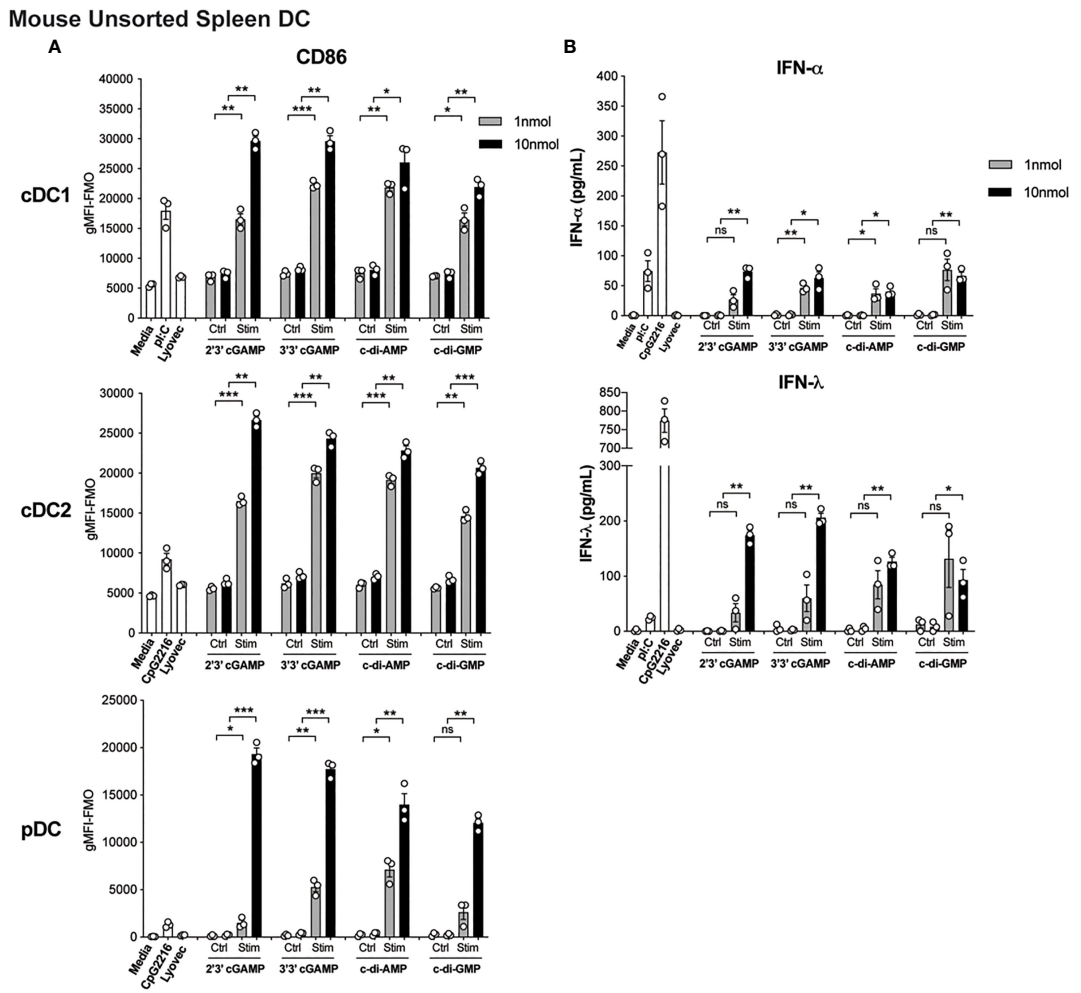

FIGURE 1 | Triggering STING with CDNs induces potent activation and IFN production in mouse DCs. Bulk splenic mouse DCs were stimulated with 1 or 10 nmol 2'3' cGAMP, 3'3' cGAMP, c-di-AMP or c-di-GMP complexed with lyovec, their respective linearized control ligands (Ctrl) complexed with lyovec, lyovec alone, 0.5 μM CpG2216 or 100 μg/mL pI:C for 18 h. **(A)** CD86 expression on DC subsets was determined using flow cytometry. Bar graphs represent the mean difference between geometric mean fluorescence intensities (gMFI) of stained samples and fluorescence minus one (FMO) controls ± SEM from 3 biological replicates (pool of 2 mice per replicate). **(B)** IFN production in cell culture supernatants were analysed by ELISA. Bar graphs represent mean ± SEM from 3 biological replicates (pool of 2 mice per replicate). Statistical analyses were performed using two-tailed Paired Student's *t* test where $^{*}P < 0.05$, $^{**}P < 0.01$, $^{***}P < 0.001$ and ns, not significant.

the cDC2 subset, while IFN-λ2/3 was produced by *all* DC subsets in response to 3'3' cGAMP–mediated STING activation (**Figure 2D**), with cDC1 producing the most, most prominently when supplemented with GM-CSF (**Figure 2D** and **Supplementary Figure 6**). Overall these data reveal that while all DC subsets activate STING upon CDN treatment they differ in their downstream signaling and IFN responses.

STING-Dependent Activation Occurs Co-Incident With Potent Killing of Mouse pDCs

It has recently been recognized that STING signaling can trigger multiple forms of cell death, including apoptosis, pyroptosis and necroptosis (39), but the effects on DCs are unknown. Given the potential importance of antigen presentation and IFN responses induced in individual DC subsets after STING activation, we set out to determine whether STING signaling induced death of DC subsets. Analyses of the total spleen mouse DCs after activation with CDNs revealed that pDC numbers were obliterated compared to stimulation with a control linearized dinucleotide ligand (**Figure 3A**). The analyses of sorted spleen DCs revealed this cGAMP-induced death was intrinsic to the pDC and not due to feedback from the other DCs in the total DC cultures (**Figure 3B**). This was in stark contrast to TLR9 activation with CpG, which enhanced survival of pDCs compared to media alone (**Figure 3B**). In addition to the depletion of pDCs, we further observed a significant reduction in sorted cDC after stimulation with cGAMP, although to a lesser extent (**Figure 3B**) and cDC1 and cDC2 population ratios remained similar in the unsorted DC (**Supplementary Figure 7**). Remarkably, pDC cell

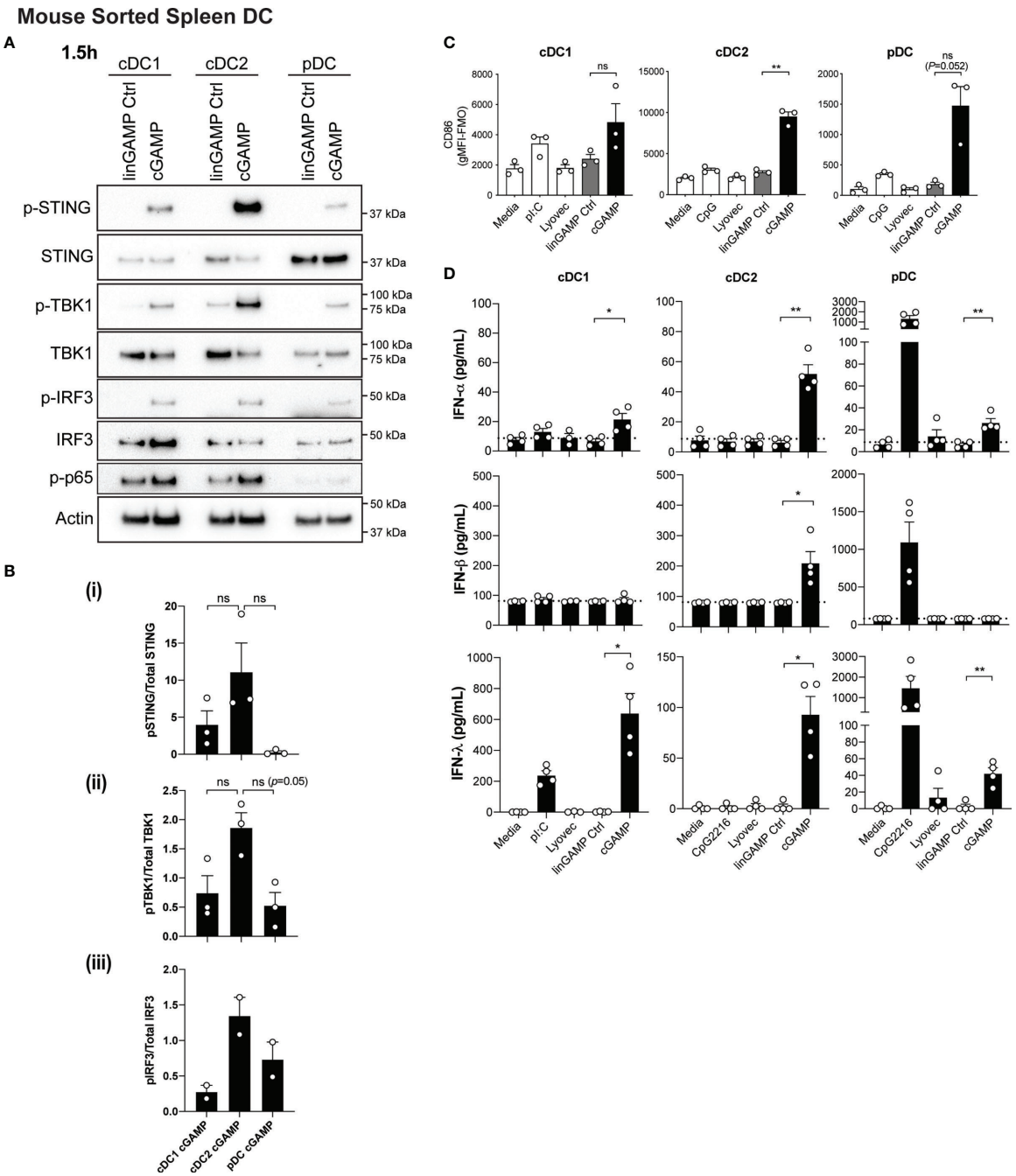

FIGURE 2 | Type I and III IFNs are differentially produced by DC subsets after cGAMP stimulation. **(A, B)** Sorted splenic mouse cDC1, cDC2 and pDCs (see **Supplementary Figure 4A** for sorting strategy) from a pool of 11-12 mice were stimulated with 10 nmol 3'3' cGAMP or its linearized control ligand (linGAMP Ctrl) complexed with lyovec for 1.5 hrs. **(A)** Cells were then lysed and blotted using the indicated antibodies. Data shown represents 1 of 2-3 independent experiments. **(B)** Densitometric analysis of (i) phosphorylated STING relative to total STING (ii) phosphorylated TBK1 relative to total TBK1 and (iii) phosphorylated IRF3 relative to total IRF3 immunoblots from 2-3 independent experiments are shown. Bar graphs show mean ± SEM. **(C)** Sorted splenic mouse cDC1, cDC2 and pDCs from a pool of 15-17 mice were stimulated with 10 nmol 3'3' cGAMP or its linearized control ligand (linGAMP Ctrl) complexed with lyovec, lyovec alone, 0.5 μM CpG2216 or 100 μg/mL pI:C for 18 h. CD86 expression on DC subsets was determined using flow cytometry. Bar graphs represent the mean difference between geometric mean fluorescence intensities (gMFI) of stained samples and fluorescence minus one (FMO) controls ± SEM from 3 independent experiments. **(D)** Sorted splenic mouse cDC1, cDC2 and pDCs from a pool of 15-17 mice were stimulated with 10 nmol 3'3' cGAMP or its linearized control ligand (linGAMP Ctrl) complexed with lyovec, lyovec alone, 0.5 μM CpG2216 or 100 μg/mL pI:C in the presence of 0.2 ng/mL GM-CSF for 18 hrs. IFN production in cell culture supernatants was analysed by ELISA (IFN-α and IFN-λ) or flow cytometric bead assay (IFN-β). Bar graphs represent mean ± SEM from 4 independent experiments. Statistical analyses were performed using two-tailed Paired Student's *t* test where $^{*}P < 0.05$, $^{**}P < 0.01$ and ns, not significant.

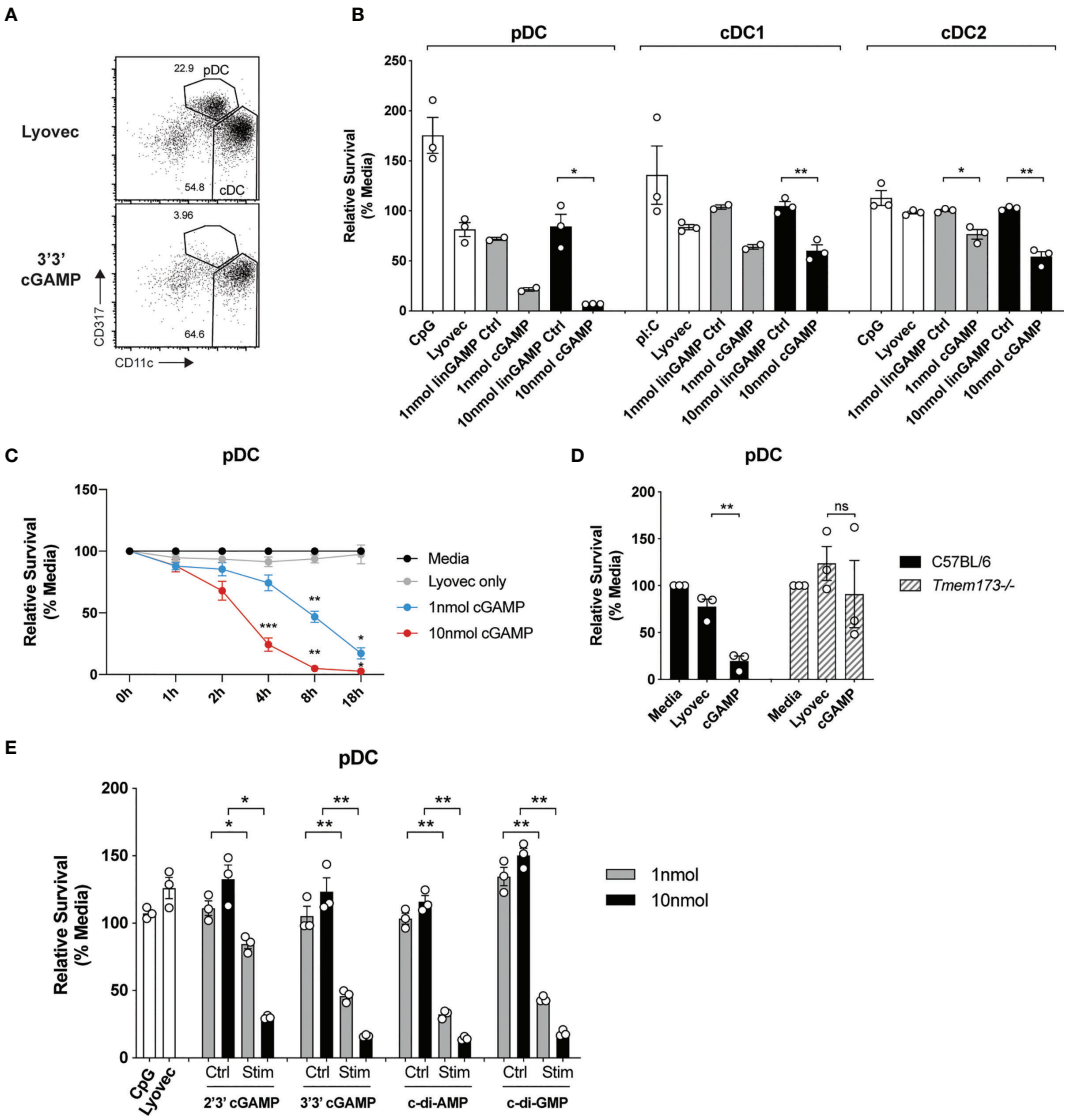

FIGURE 3 | cGAMP stimulation induces rapid, potent killing of mouse pDCs. **(A)** FACS plots showing bulk mouse splenic pDCs ($CD11c^{int}CD317^{hi}$) and cDCs ($CD11c^{hi}CD317^{lo}$) stimulated for 18 h with 10 nmol 3'3' cGAMP complexed with lyovec, or lyovec alone. **(B)** Sorted mouse splenic pDCs and cDC subsets from a pool of 15-17 mice were stimulated for 18 h with 1 or 10 nmol 3'3' cGAMP, its linearized control ligand (linGAMP Ctrl) complexed with lyovec, lyovec alone, 0.5 μM CpG2216 or 100 μg/mL pI:C. Bar graphs show the mean relative survival (compared to media alone) ± SEM compiled from 2-3 independent experiments. **(C)** Bulk splenic DCs from a pool of 5-6 mice per replicate were stimulated with 1 or 10 nmol 3'3' cGAMP complexed with lyovec or lyovec alone for the indicated time points. Line graph depicts the mean relative survival (compared to media alone) ± SEM combined from 3 independent experiments. **(D)** Bulk splenic DCs from C57BL/6 or *Tmem173*$^{-/-}$ mice were stimulated with 10 nmol 3'3' cGAMP complexed with lyovec or lyovec alone for 18 h. Bar graphs show their mean pDC relative survival ± SEM from 3 individual mice per genotype. **(E)** Bulk splenic DCs were stimulated with 1 or 10nmol 2'3' cGAMP, 3'3' cGAMP, c-di-AMP or c-di-GMP complexed with lyovec, their respective linearized control ligands (Ctrl) complexed with lyovec, lyovec alone or 0.5 μM CpG2216 for 18 h. Bar graphs represent the mean relative survival of pDCs ± SEM from 3 biological replicates (pool of 2 mice per replicate). Statistical analyses were performed using **(B, D, E)** two-tailed Paired Student's *t* test or **(C)** two-way ANOVA using Tukey's test to correct for multiple comparisons where $^{*}P < 0.05$, $^{**}P < 0.01$, $^{***}P < 0.001$ and ns, not significant.

death was rapid (significant from 4 hours onwards, **Figure 3C**) and stimulation with a 10-fold lower concentration of cGAMP (1nmol) still induced killing of pDCs, albeit reduced (**Figure 3C**). These results suggest murine pDCs are more sensitive to cell death upon STING activation than both cDC1 and cDC2s.

To determine the specificity of STING in inducing rapid pDC death we assessed pDCs viability upon the genetic deletion of STING. STING deficiency (*Tmem173*$^{-/-}$) completely protected pDCs from cell death following 3'3' cGAMP stimulation (**Figure 3D**) thereby confirming this is a STING-dependent event. Given that different CDNs bind to STING with different affinities and could potentially affect STING activation (40), we next determined whether other CDNs were able to similarly induce DC death in mixed cultures of spleen DC. Significant

pDC death occurred after stimulation with all four types of CDNs tested, although bacterial CDNs (3'3' cGAMP, c-di-AMP, c-di-GMP) were more potent at inducing cell death when compared to mammalian 2'3' cGAMP at a lower (1 nmol) dose (**Figure 3E**). For cDCs, the cDC2 subset exhibited increased death to all CDNs over the controls (**Supplementary Figure 8**), however, a drop in the cDC1 population numbers was only observed after c-di-AMP stimulation (**Supplementary Figure 8**). Overall, cell death in these mixed cultures (**Supplementary Figure 8**) was not as dramatic as seen in the sorted populations (**Figure 3B**). We did not further investigate the reason for this but propose that a combination of cell:cell crosstalk and lack of stress induced by cell sorting slightly enhanced the survival of the unsorted populations.

Soluble Mediators Induced by STING Activation Are Not Responsible for Mouse pDC Death

To clarify the mode of pDC death after STING activation, we first investigated if pDCs were dying *via* a direct, intrinsic mechanism following STING activation, or if they were producing a soluble factor that could feedback on cells and induce cell death extrinsically. Some cytokines, such as the key pro-inflammatory cytokine TNF, can bind to receptors that have death domains and trigger apoptosis (41). Therefore, we examined the cytokine and chemokine profile in the supernatants of mouse pDCs stimulated with cGAMP. Although pDCs produced large quantities of TNF, IL-6, RANTES and MIP-1β in response to CpG stimulation, they produced much lower amounts of these cytokines and chemokines after cGAMP stimulation (**Figure 4A**). Others have shown that IL-10, previously implicated in human pDC death (42), can also be produced in response to STING activation (43). We did not detect any IL-10 in the supernatants of pDCs stimulated with cGAMP (data not shown). However, other types of soluble mediators not tested here, including hormones, could be present in these supernatants and induce pDC death after STING activation (44).

To formally address if pDC death could be induced by a soluble factor produced after STING activation, we stimulated splenic DCs from wild-type (WT) C57BL/6 mice with 3'3' cGAMP/lyovec complexes then harvested the culture supernatants after 18 hours to isolate potential soluble death-inducing factors. Freshly isolated DCs from WT and *Tmem173*$^{-/-}$ mice were then stimulated with these culture supernatants alone and pDC survival was determined (**Figures 4B, C**). Use of *Tmem173*$^{-/-}$ DCs that lack STING expression eliminated the possibility that residual ecto-nucleotide pyrophosphatase phosphodiesterase degradation resistant 3'3'-cGAMP/lyovec complexes (45) present in the supernatants, and/or STING ligands released from dead and dying cells, could activate STING directly in freshly isolated DCs (**Figure 4B**). Hence, if an inducible soluble mediator was indirectly inducing pDC death both WT C57BL/6 and *Tmem173*$^{-/-}$ pDCs should die. Importantly, we observed that pDCs from WT C57BL/6, but <u>not</u> *Tmem173*$^{-/-}$, mice displayed significant cell death after stimulation with culture supernatants (**Figure 4C**), suggesting that pDC depletion after STING activation was not caused by a secreted soluble factor but rather *via* direct intracellular STING activation.

Intrinsic Apoptosis Is Indispensable or cDC Death but Only Partly Required for pDC Death Induced Upon STING Activation

Having established that mouse STING-mediated pDC death is cell intrinsic, we next investigated which programmed cell death pathway was responsible. As multiple modes of cell death have been implicated in mammalian and bacterial/viral DNA sensing (46), as well as during STING responses in myeloid cells, fibroblasts and other cell types (47) we examined the role of four major inflammatory and non-inflammatory cell death pathways in pDC demise: pyroptosis, necroptosis, extrinsic and intrinsic apoptosis. A schematic diagram displaying key signaling components of each pathway is shown in **Figure 5A**. To determine which cell death pathway was involved in STING-dependent pDC death, we used genetically modified mice that had key components of each pathway deleted or overexpressed. *Caspase-1*$^{-/-}$*Caspase-11*$^{-/-}$(*Casp1/11*$^{-/-}$) and *Ripk3*$^{-/-}$ mice were used to block pyroptosis and necroptosis, respectively. In addition to its key role in extrinsic apoptosis, caspase-8 can also cleave RIPK3 to limit necroptosis (48). Therefore, *Ripk3*$^{-/-}$*Caspase-8*$^{-/-}$ (*Ripk3*$^{-/-}$*Casp8*$^{-/-}$) mice were also used to inhibit both extrinsic apoptosis and necroptosis simultaneously. We isolated DCs from these knockout mice and stimulated them with cGAMP for 18 hours. We observed pDC depletion of comparable severity to C57BL/6 mice in *Casp1/11*$^{-/-}$, *Ripk3*$^{-/-}$ and *Ripk3*$^{-/-}$*Casp8*$^{-/-}$ mice after cGAMP stimulation, thus eliminating the involvement of pyroptosis, necroptosis and extrinsic apoptosis, respectively, in STING-mediated pDC death (**Figures 5B, C**).

Next, to determine any involvement of intrinsic "mitochondrial BCL-2 family regulated" apoptosis in STING-dependent pDC death, we used Bcl2 transgenic mice that overexpress anti-apoptotic protein BCL-2 under the haematopoietic-restricted Vav promoter (*Bcl2Tg*). Importantly, BCL-2 has previously been shown to be a key baseline pro-survival factor in pDCs but not cDCs (49, 50). We isolated splenic DCs from WT non-transgenic or *Bcl2Tg* mice and stimulated them with 3'3' cGAMP *in vitro*. Consistent with our previous findings (49, 50), there was a greater percentage of pDCs in the *Bcl2Tg* spleens (**Figure 5D**). Moreover, whilst we recovered more pDCs back from cultures of *Bcl2Tg* pDC treated with cGAMP, there was still a 72% decrease in pDC number compared to stimulation with its control ligand, suggesting that the major mechanism of pDC death post-STING activation is not rescued by BCL-2 overexpression (**Figure 5E**). Likewise, the cell death seen in STING-activated cDC populations was also not rescued by BCL-2 overexpression (**Figure 5F**).

Although BCL-2 is a crucial regulator of pDC survival, or at least its transgenic expression is able to support pDC survival (49), there are other anti- and pro-apoptotic signals (e.g. BH3-only proteins) that can influence the activation of intrinsic

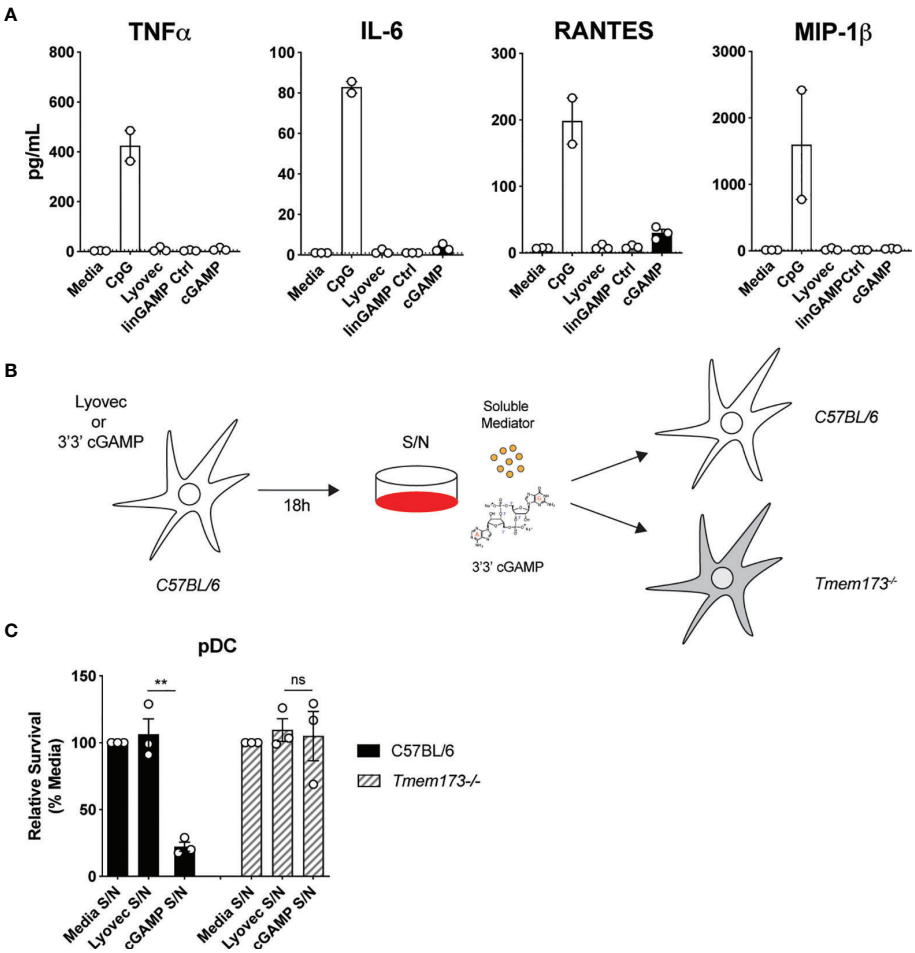

FIGURE 4 | Soluble mediators induced by STING activation are not responsible for pDC death. **(A)** Sorted splenic pDC from a pool of 15-17 mice were stimulated for 18 hrs with 10 nmol 3'3' cGAMP or its linearized control ligand (linGAMP Ctrl) complexed with lyovec, lyovec alone or 0.5 μM CpG1668. Cytokine and chemokine production in supernatants were measured by flow cytometric bead assay. Bar graphs depict data from 2-3 independent experiments showing mean ± SEM. **(B, C)** Supernatants harvested 18 h after bulk C57BL/6 DCs were stimulated with 10 nmol 3'3' cGAMP complexed with lyovec, lyovec alone or media were diluted 1/5 in media and were used to stimulate freshly isolated DCs from C57BL/6 or *Tmem173*$^{-/-}$ mice for 18 h. **(B)** Schematic diagram showing experimental design. **(C)** Bar graphs show mean relative survival (compared to media supernatant alone) ± SEM from 3 individual mice per genotype. Statistical analysis was performed using two-tailed Paired Student's *t* test where $^{**}P < 0.01$ and ns, not significant.

apoptosis. Hence, to more definitively determine if intrinsic apoptosis is involved in STING-dependent pDC death, we examined STING-mediated cell death in mice lacking the intrinsic apoptosis effector proteins, BAX and BAK. BAX and BAK activation and pore formation in the mitochondrial outer membrane is the 'point of no return' in apoptosis (recently reviewed in (51, 52)). Mice harbouring global genetic deletion of both *Bax* and *Bak* genes are embryonically lethal and therefore viable $Vav^{cre}Bax^{lox/lox}Bak^{-/-}$ mice were used to generate bone marrow (BM) chimeras lacking BAX and BAK specifically in haematopoietic cells (53). As per prior experiments, we isolated splenic DCs from these mice and stimulated them with 3'3' cGAMP. The BM chimera splenic DC responded to cGAMP stimulation, in fact trending higher in the production of IFN-λ, IFN-α and TNF than the WT chimeras (**Supplementary Figure 9A**). As expected, the pDC population was depleted in the WT BM chimera spleen cultures after cGAMP stimulation, illustrating that STING-dependent pDC death still occurred in these BM chimeric mice (**Figure 5G**). However, in line with our *Bcl2Tg* results, pDCs from the $Bax^{-/-}/Bak^{-/-}$ BM chimeras were partially rescued from cell death after cGAMP stimulation (**Figure 5H**), with survival increased about 40% in pDC deficient in expression of BAX and BAK. The trend of increased IFN-α from the STING-activated BAX/BAK deficient DC cultures (**Supplementary Figure 9A**) is likely due to the increased survival of these cells. Indeed, the $Bax^{-/-}/Bak^{-/-}$ pDC also showed clear STING-dependent activation with upregulation of both CD69 and CD86 on these increased numbers of surviving cells (**Supplementary Figure 9B**). These data are in line with publicly available RNA sequencing data indicating normal levels of STING pathway genes (e.g., *Tmem173*, *Tbk1*, *Irf3*) in immune cells deficient in expression

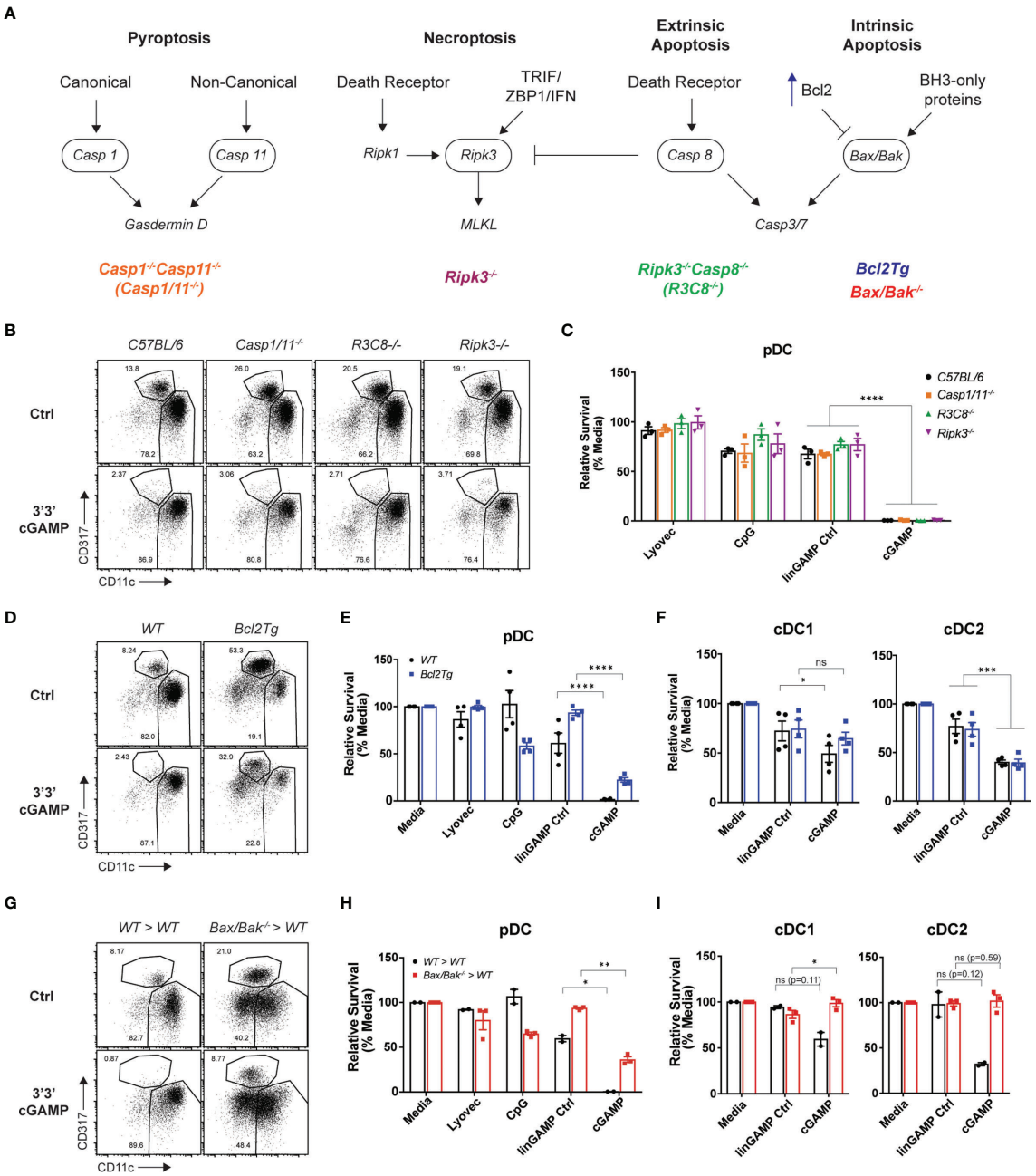

FIGURE 5 | Blocking intrinsic apoptosis partially inhibits STING-dependent pDC death and rescues cDC death. **(A)** Schematic diagram showing death signaling pathways: encircled components highlight deleted genes in mice upstream of effector proteins gasdermin D, mixed lineage kinase domain-like (MLKL) protein and caspase-3 and caspase-7. **(B)** FACS plots or **(C)** bar graphs show mean relative survival ± SEM from 3 individual mice per genotype from C57BL/6, *Casp1/11*$^{-/-}$, *Ripk3*$^{-/-}$*Casp8*$^{-/-}$ *(R3C8*$^{-/-}$*)* and *Ripk3*$^{-/-}$ bulk splenic DCs stimulated with 10 nmol 3'3' cGAMP or its linearized control ligand (linGAMP Ctrl) complexed with lyovec, lyovec alone or 0.5 µM CpG2216 for 18h. **(D)** FACS plots or **(E, F)** bar graphs from WT or *Bcl2Tg* bulk splenic DCs cultured with stimuli conditions as per **(B)**. Bar graph shows mean relative survival of **(E)** pDCs or **(F)** cDC subsets, mean ± SEM from 4 individual mice per genotype compiled from 2 independent experiments. **(G)** FACS plots and **(H, I)** bar graphs showing bulk splenic DCs from BM chimeras generated using Ly5.2 WT or *Vav-Cre Bax*$^{-/-}$*/Bak*$^{-/-}$ mice cultured with stimuli conditions as per **(B)**. Bar graphs show Ly5.2^{+} relative survival of **(H)** pDCs or **(I)** cDC subsets, mean ± SEM from 2-3 individual mice per genotype. Statistical analysis was performed using **(C)** two-way ANOVA using Tukey's test to correct for multiple comparisons or **(E, F, H, I)** two-tailed Paired Student's *t* test where *$P < 0.05$, **$P < 0.01$, ***$P < 0.001$, ****$P < 0.0001$ and ns, not significant.

of BAX and BAK (54). These results confirm a partial contribution of intrinsic apoptosis to STING-dependent pDC death. The rigour of this finding was highlighted by the fact that, in contrast to the partial rescue of mouse pDC death observed in *Bax*$^{-/-}$/*Bak*$^{-/-}$ BM chimeras after cGAMP stimulation, a complete rescue of the moderate levels of cell death in both cDC1 and cDC2 was observed, identifying that intrinsic apoptosis is the main mechanism of STING-dependent death of cDC (**Figure 5I**). These data further demonstrate that, similar to our findings relating to differential IFN production from cDCs and pDCs, it appears these subsets may elicit alternative (at least in part) modes of cell death.

To further substantiate our findings showing intrinsic apoptosis was involved in the rapid STING-induced death of pDC, we first treated DC with the pan-caspase inhibitor Q-VD-OPh (55). The pDC were rescued from cell death induced in just media alone or STING-induced (**Supplementary Figure 9C**). The cleavage of caspase 3 occurs downstream of BAX/BAK activation and at 1.5 h we show that caspase 3, although expressed at low levels, is indeed cleaved in pDC (**Supplementary Figure 9D**). Moreover, caspase 3/7 activity in the cGAMP-stimulated pDC was illustrated using the caspase 3/7 Glo-assay (Promega, **Supplementary Figure 9E**).

Human DCs Display Divergent Responses to STING Activation

Our data thus far indicated that STING activation in mouse DC subsets induces DC activation and differential type I IFN production between subsets, and IFN-λ production from all subsets examined. cDC1 and cDC2 were also susceptible to STING-driven cell death and this was completely dependent on intrinsic apoptosis. We therefore turned to the human immune system to determine whether human DC subsets displayed similar phenotypes. Interrogation of publicly available microarray and RNA sequencing data sets revealed that, similar to mouse DC subsets, human cDC1 (CD141^{+}) expressed the lowest levels of STING transcripts (**Supplementary Figure 3B–E**). The human cDC2 (CD1c^{+}) expressed the highest level of STING amongst the DC subsets of human blood, with blood pDCs displaying intermediate STING expression between cDC1 and cDC2 subsets (**Supplementary Figure 3B**). Expression of STING transcripts in humanised mice DC subsets was similar, although pDC tended to have expression levels closer to cDC2 (**Supplementary Figure 3B–E**).

Recently, Pratik et al. (27) demonstrated that human pDC, in line with their mouse counterparts, also produced type I IFN and IFN-λ, specifically IFN-λ1, upon STING activation. To determine whether STING stimulation with cGAMP also induces potent activation of *all* human DCs, cDC and pDC populations were isolated from human blood (**Supplementary Figure 4B**) and were stimulated with 2'3' cGAMP, which has been reported to be the most stimulatory STING ligand for human cells (56). Upon cGAMP stimulation the levels of activation marker CD86 on cDCs (**Figure 6A**) and CD69 on pDCs were upregulated (**Figure 6B**). Examination of DCs from humanised mice, previously shown to be functionally akin to their human blood counterparts (57), also demonstrated a potent increase in CD80 expression by pDCs and cDC subsets (**Supplementary Figure 10A**). Therefore, as we observed in mouse DC subsets (**Figure 1**), 2'3' cGAMP is a strong activator of all human DC subsets.

To investigate whether human DCs similarly responded with IFN production to STING ligands, we isolated total DCs from human blood and stimulated them with 2'3' cGAMP and controls and measured IFN production. Like mouse splenic DCs, human DCs produced IFN-α, IFN-β and IFN-λ2/3 in response to the cGAMP (**Figure 6C**). However, IFN-λ1 (IL-29), an isotype of IFN-λ that is a pseudogene in the mouse genome, was produced at extremely high levels in response to cGAMP (**Figure 6C**). As with mouse DCs (**Figure 1**), we observed human blood DC IFN-β responses were also much greater than IFN-α responses to STING ligand (**Figure 6C**).

We have previously shown that the activation of humanised mice DC subsets closely mirrors that of *ex vivo* blood DC of human donors (57–61), and using these mice is far more practical to obtain enough human DC numbers suitable for analyses of individual subset function. Therefore, to determine the specific human DC subsets responsible for IFN production in response to STING ligand, we examined 2'3' cGAMP-induced IFN production in sorted DC subsets from humanised mice. pDC were the only subset found to produce detectable levels of IFN-α2, whilst all subsets produced low levels of IFN-β in response to 2'3'cGAMP (**Figure 6D**). Strikingly, all humanised mice DC subsets also produced large amounts of IFN-λ1 after stimulation with 2'3'cGAMP (**Figure 6D**), although this was found to be statistically not significant due to human cord blood derived-DC donor-to-donor variation in STING responses. This variation in the absolute amount of cytokines produced by human DC in response to STING activation was also observed in the enriched blood DC responses (**Figure 6C**). In most experiments, the production of IFN-λ2/3 was not detected above background in response to cGAMP stimulation of the sorted humanised mice DC subsets (not shown). Thus, our data reveal for the first time that *all* mouse and human DC subsets produce IFN-λ in response to ligands of the cytoplasmic CDN sensor, STING. Of note, we have discovered that the human restricted IFN-λ1 is the IFN produced most highly by *all* human DC subsets.

Human pDCs Are Resistant to STING-Induced Cell Death

We uncovered that STING activation causes rapid death of mouse pDCs that was partially dependent on intrinsic apoptosis. Intriguingly, enumeration of DC subsets from human blood DC cultures or isolated DCs from humanised mice after 18 hours stimulation with 2'3' cGAMP or its linearized control, indicated that the obliteration observed for murine pDCs upon STING activation was *not* translated in the human system (**Figure 6E** and **Supplementary Figure 10B**). In fact, pDC death was actually rescued by activation with 2'3' cGAMP in most human donors (**Figure 6E**). The CD141^{+} cDC1 subset showed little survival difference between the control and 2'3'

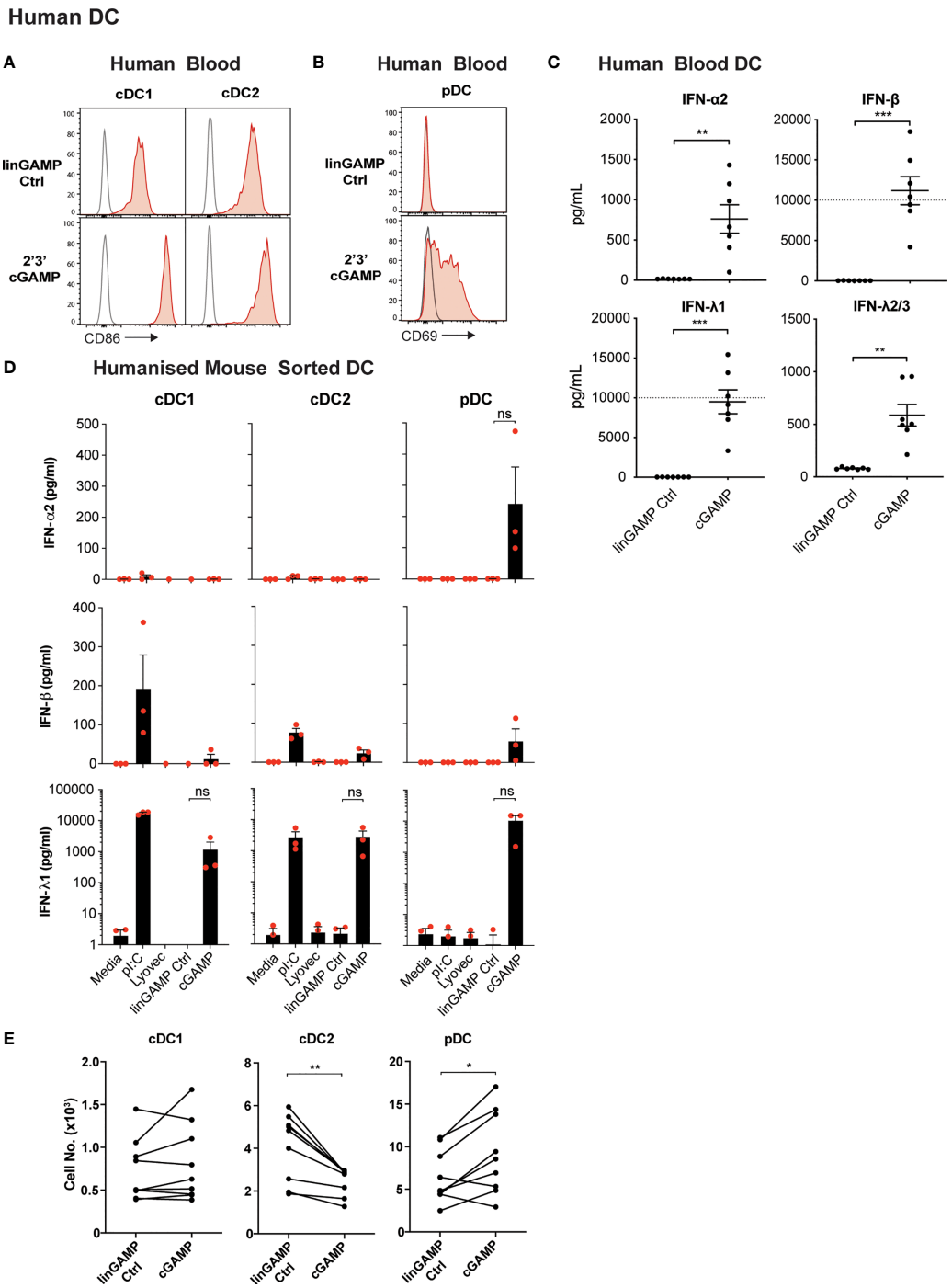

FIGURE 6 | Human DCs demonstrate potent activation and differential IFN production, but not pDC death, after cGAMP stimulation. **(A–C)** Human blood DCs were stimulated with 5 nmol 2'3' cGAMP or its linearized control ligand (linGAMP Ctrl) complexed with lyovec for 18 hrs. Histograms show activation marker expression on human blood **(A)** cDCs or **(B)** pDCs. Grey unfilled lines represent isotype control and red filled lines represent Ab stain. **(C)** Dots represent IFN production by DCs from each donor and lines show mean ± SEM of 7 donors from 3 independent experiments. Dotted line represents upper limit of quantification. **(D)** Sorted humanised mice DCs from BM were stimulated with 10 μg/mL pI:C, 10 nmol 2'3' cGAMP or its linearized control ligand (linGAMP Ctrl) complexed with lyovec or lyovec alone for 18h. Bar graphs depict IFN production by each humanised mice DC subset showing mean ± SEM from 3 independent experiments. Human DC IFN production was analysed by flow cytometric bead assay. **(E)** Human blood DCs were stimulated with 5 nmol 2'3' cGAMP or its linearized control ligand complexed with lyovec for 18 h and DC numbers enumerated by flow cytometry. Line graphs show paired individual cell numbers for each donor for each DC subset (n=9). Statistical analyses were performed using two-tailed Paired Student's *t* test where $^{*}P < 0.05$, $^{**}P < 0.01$, $^{***}P < 0.001$ and ns, not significant.

cGAMP stimulation conditions, with minor variations between donors (**Figure 6E** and **Supplementary Figure 10B**). However, the blood cDC2 subset exhibited significantly enhanced cell death in the presence of 2'3' cGAMP in all donors tested (**Figure 6E**). Interestingly, the observed death of human blood cDC2 was not conserved in the cDC2 of humanised mice that were similarly challenged with 2'3' cGAMP (**Supplementary Figure 10B**). Thus, our data reveal strong species differences between DC responses to STING activation, with heightened cell death exhibited by mouse but not human pDCs.

An open question here was whether the IFN-λ1, only produced by the human DC, could have been protecting the human pDC from STING-induced death. However, experiments which stimulated human DC with STING ligands in the presence of IFN-λ1 neutralising antibodies, did not lead to enhanced cell death of human pDC (**Supplementary Figure 10C**). These results suggested that survival of human pDC after STING activation was independent of their production of IFN-λ1. However, the IFN-λ1 neutralising antibodies did abrogate the upregulation of CD69 on the human pDC, indicating that the upregulation of this ISG is dependent on active IFN-λ signaling in the cultures (**Supplementary Figure 10D**).

DISCUSSION

A protective role of IFN-λ in protecting against mucosal anti-viral responses is clear. Potential roles of IFN-λ in many other diseases have been proposed by GWAS studies revealing associations with polymorphisms in the IFN-λ locus. In this study, we show for the first time that all major subsets of mouse and human DC, key professional antigen presenting cells linking innate and adaptive immunity, produce IFN-λ in response to direct STING activation. STING signaling is implicated in many different diseases, raising the possibility that IFN-λ production from DC underpins at least some phenotypes of STING-mediated disease.

IFN-λ2/3 are the only IFN-λs expressed in mouse and mouse cDC1 were the prominent producers in response to STING activation (**Figure 2D**), although cDC2 and pDC also produced low levels. In the human DC, where IFN-λ1, 2 and 3 genes are present, IFN-λ1 was by far the *predominant* IFN produced in response to STING ligands (**Figures 6C, D**). Strikingly, we were also able to show that distinct type I IFNs are produced by human and mouse DCs to STING ligands. Namely, IFN-α is produced at low levels by all mouse DC but solely by human pDCs in response to STING activation (**Figures 2D**, **6D**), while amongst the mouse DC, only mouse cDC2 produce IFN-β (**Figure 2D**) and all human DC subsets produce low levels of IFN-β (**Figure 6D**).

We have provided evidence that STING-mediated signaling, at least in the mouse DC, differs between cDC and pDC subsets. The signaling downstream of STING activation in the mouse DC subsets included the characteristic TBK1 phosphorylation, STING phosphorylation and IRF3 activation in all subsets (**Figure 2A**). However, surprisingly, STING-mediated NF-κB activation (read out as phosphorylation of the NF-κB p65 subunit) and associated cytokine production was very weak in the STING competent pDC subset despite these cells expressing the highest levels of total STING protein. Of note, this difference in STING activation was concomitant with rapid death of the mouse pDC (significant by 4 hours after stimulation), involving intrinsic apoptosis. We have previously found differential reliance on NF-κB subunits for pDC activation and cytokine production compared to cDC (49). This, together with the high basal IRF7 expression by pDC (62) may explain the lack of NF-κB p65 activation, but requires further investigation.

The human IFN-λ response to STING activation was unusual in that it was predominated by IFN-λ1. Depending on the donor, 10–30-fold more IFN-λ than IFN-λ2/3 was produced by human DC in response to STING activation (**Figure 6C**). We have not previously seen this predominant IFN-λ1 production when examining human DC responses to TLR3 stimulation, where IFN-λ1 and IFN-λ2/3 were produced at similarly high levels (26). IFN-λ1 production by cDC1, proposed to be *via* TLR3, has recently been associated with positive clinical outcomes and local Th1 immune responses in breast cancer patients (63). In these patients, IFN-λ1 transcripts were produced at similar levels to the combined IFN-λ2/3 transcripts, aligning with what we have previously seen at the protein level with poly I:C stimulation in human DCs (26). The downstream immune response elicited by STING activation of DCs, with a predominance of IFN-λ1 over IFN-λ2/3 production by *all* DC subsets is not yet clear. Previous work indicated a potential lack of gene repressor function by IFN-λ1 compared with IFN-λ2 on epithelial cells (33). Our findings certainly warrant future examination of the effects of IFN-λ1 production in the context of STING activation.

The role of the cytosolic CDN sensor STING in anti-tumour immunity has been attributed to its recognition of tumour DNA within cDC1s, which consequently triggers type I IFN production and enhances DC cross-priming of tumour antigen to cytotoxic T cells (24). As a result, STING agonists have been promoted as potent adjuvants in cancer immunotherapies. However, not only does the cDC1 subset have the lowest expression of STING amongst the DC subsets (**Supplementary Figure 2**), they also do not produce high quantities of IFN-I after STING activation (**Figures 2D**, **6D**). Our results suggest that cDC2 and pDCs could contribute to IFN-I production in the anti-tumour cytokine milieu, which has been previously postulated (64). In contrast to the well documented role for STING-induced type I IFNs in anti-tumour immunity, the role of IFN-λ has not been investigated up until this point. We have previously shown that TLR3-induced IFN-λ production is blunted in DCs lacking the Type I IFN receptor (IFNAR) (26), thus studies showing a requirement for IFNAR signaling in the efficacy of STING responses could also be masking the involvement of downstream IFN-λ signaling. An anti-tumour role for IFN-λ is an attractive idea, as IFN-λR is expressed on neutrophils, DCs, throughout the mucosal epithelia, within epithelial cells of the liver, kidney and brain, as well as on various tumours (31, 65). Moreover, IFN-λ treatment has been shown to synergise with the kinase inhibitor sorafenib to inhibit

Hepatocellular carcinoma cell growth and induce apoptosis (66), and a strong correlation between IFN-λ1, 2, and 3 producing cDC1 and beneficial outcomes in breast cancer has recently been described (63). Therefore, the fact a large amount of IFN-λ is produced by DCs in response to STING activation warrants further investigation in the realms of cancer immunotherapy. However, as the IFN-λ locus has been shown to be polymorphic in a subset of cancer patients and patients suffering from infectious diseases (8, 29, 65, 66), moving forward, polymorphisms and differences in IFN-λ gene expression will need to be taken into account when considering clinical STING immunotherapeutic approaches (29, 35, 67, 68).

It is of interest that some studies have implicated STING-induced IL-10 as having an inhibitory effect on anti-tumour immunity (69, 70) and in some cases, a protective effect to avoid continued inflammation and development of colorectal cancer (43). Our studies show that DCs do not produce IL-10 in response to cGAMP stimulation but it is worth noting that the IFN-λ1 receptor shares with the IL-10 family the use of IL-10 R2. Whether the extremely high levels of IFN-λ1 expressed by human DC in response to STING stimulation could lead to a usurping of the IL-10R2 to the IFN-λR complex, and thus result in a decrease of available IL10R2 for IL-10 signaling, remains to be elucidated.

Importantly, mouse and human pDC survival in response to STING activation was divergent, with human pDC showing equivalent or enhanced survival *in vitro* to STING activation (**Figure 6E** and **Supplementary Figure 10B, C**), whereas mouse pDC were rapidly and potently killed *in vitro* (**Figure 3**). This death was STING-dependent (**Figure 3D**) and involved the intrinsic apoptotic pathway, although it was not the sole mechanism for STING-induced killing of pDCs (**Figure 5** and **Supplementary Figure 9**). This finding contradicts the pathways reported to mediate STING-dependent cell death observed in malignant lymphocytes and other myeloid cell types (71–77). Lysosomal rupture or other forms of phagocytic cell death may be compensatory mechanisms, given the co-localisation between STING and autophagy-related proteins (10). Alternatively, the rapid death of the murine pDC may be a novel form of cell lysis. A further cell death anomaly we observed was that both mouse splenic (**Figure 3B**) and human blood (**Figure 6E**) cDC2 but not humanised BM cDC2 were sensitised to STING-mediated intrinsic apoptotic cell death (**Figure 5I** and **Supplementary Figure 10B**). The lack of death in the humanised mice cDC2 of BM origin suggests that the non-haematopoietic niche may contribute to priming of these cells for STING-mediated death. Whether this is mediated by soluble factors or cell-mediated interactions remains to be elucidated.

Divergent outcomes in DC viability and high production of IFN-λ1 after STING activation mark major points of difference between species and need to be considered when translating experimental results from mouse models to human clinical trials. Of particular importance, pDC in the tumour environment are often associated with poor prognosis (78–81). Our data would suggest that in mouse tumour models, exposure to STING ligand adjuvants would eliminate pDCs. In humans treated with STING adjuvants, activated pDCs would potentially persist in a tumour environment. Hubert et al. (63) recently demonstrated a correlation between pDC infiltration in breast tumours and Treg accumulation. This suggests that pDCs activated by STING could similarly lead to an immunosuppressive microenvironment, although this remains to be elucidated. We are yet to define what the key mediators directing differental STING signaling outcomes between mouse and human pDCs are, however elucidating these molecular differences could lend insight into discrete mechanisms of inducing rapid pDC death, tools that could potentially be harnessed to improve cancer immunotherapies or alter viral immune responses.

In summary, this work places IFN-λ in the spotlight as a potential major player in DC-mediated immune responses downstream of STING activation. It also highlights the need to re-evaluate STING responses in mice, in particular, does the direct killing of murine pDC have beneficial anti-tumour effects, or indeed anti-viral effects, that are not recapitulated in the human setting?

METHODS

Mice

All mice were housed under specific pathogen free conditions and all animal experimental procedures were approved by either Monash University or Walter and Eliza Hall Institute (WEHI) animal ethics committees. C57BL/6 (WT) mice were obtained from either Monash Animal Research Platform or WEHI and all transgenic mice were obtained from WEHI. *Tmem173*$^{-/-}$ mice (9) were provided by Benjamin Kile (Biomedicine Discovery Institute, Monash University, Australia). *Vav-Bcl-2* transgenic mice (*Bcl2Tg*) (82) were provided by Yifan Zhan (WEHI, Australia). *Ripk3*$^{-/-}$, *Ripk3*$^{-/-}$*Casp8*$^{-/-}$ mice (83) and *Vav-Cre Bax*$^{lox/lox}$*Bak*$^{-/-}$ (*Bax*$^{-/-}$/*Bak*$^{-/-}$) BM chimeras (84) were provided by Kate Lawlor (Hudson Institute of Medical Research, Australia) and James Vince (WEHI). *Casp1*$^{-/-}$*Casp11*$^{-/-}$ mice (85) were provided by Seth Masters (WEHI, Australia). Mice used were 6-12 weeks old except for *Bax*$^{-/-}$/*Bak*$^{-/-}$ BM chimeric mice that were 10 months old.

Mouse DC Purification

DCs from spleen were isolated using a previously described method (86). In brief, spleens were digested using DNase/Collagenase (Roche Diagnostics, Basel, Switzerland/Worthington Biochemical Corporation, Lakewood, New Jersey) at room temperature (RT) for 20 min and filtered to create a single cell suspension. Light density cells were isolated by centrifugation in a 1.077 g/cm^3 NycoPrep^{TM} medium (AXIS Shield PoC AS, Dundee, Scotland). Negative selection using a rat monoclonal Ab cocktail against CD3-ϵ (KT3-1.1), Thy-1 (T24/31.7), Ly6G/Ly6C (1A8), CD19 (ID3) and erythrocytes (TER-119) together with anti-rat immunoglobulin immunomagnetic beads (Qiagen, Hilden, Germany) was used to isolate DCs. For sorted DCs, these isolated cells were then labelled with the following fluorophore-conjugated mAbs:

CD11c (N418), CD45RA (14.8), CD8 (53-6.7), CD11b (M1/70), CD49b (DX5) (Becton Dickinson, Franklin Lakes, New Jersey; eBioscience, San Diego, California; BioLegend, San Diego, California; TONBO, San Diego, California) and sorted on BD Influx machine according to gating strategy provided (**Supplementary Figure 4A**).

Human Blood DC Purification

Human blood (15-20 mL) collected in heparin tubes was diluted with PBS (human osmolarity) and underlayed with 10 mL Ficoll-Hypaque 1.077 g/mL density medium (Thermofisher Scientific, Waltham, Massachusetts) at RT. Samples were then centrifuged at 400 g for 30 min at 20°C with the brake off. The peripheral blood mononuclear cell (PBMC) layer was then collected, washed twice and counted. DCs were negatively selected from PBMCs using EasySep™ Human Pan-DC pre-enrichment kit (STEMCELL™ Technologies, Tullamarine, Victoria) according to manufacturer's instructions.

Humanized Mouse DC Purification

Human $CD141^+$ DC, $CD1c^+$ DCs and pDCs were isolated from the bone marrow and spleens of humanised mice as described previously (57). Briefly, humanised mice were generated by engrafting immunodeficient neonatal NSG mice with human cord blood $CD34^+$ haematopoietic progenitor cells (HSC), leading to multi-lineage human immune reconstitution, including functional human DC subsets, from 12 weeks of age (57). Cord blood was obtained from the Queensland Cord Blood Bank following written informed consent in accordance with Mater Adult Hospital Human Ethics Committee approval. Mice were housed and treated in accordance with approval by the University of Queensland Animal Ethics Committee and under TRI Biological Resources Facility (BRF) operations. Following immune reconstitution, DC populations were expanded with 2 *s.c.* injections with 50 μg Flt3L (Bio-X Cell, Lebanon, New Hampshire) 4 days apart. Where indicated, gene expression data were obtained from humanised DC that were activated *in vivo* by administration of HBSS (control) 50 μg high molecular weight poly I:C (*In vivo*Gen), 20 μg R848 (*In vivo*Gen), or poly I:C and R848 combined, as previously described (57).

Humanised mouse DC were enriched by magnetic bead depletion of mouse CD45, using rat anti-mouse CD45 (Beckman Coulter, Pasadena, California, 30-F11) and TER-119 and rat anti-human CD14 (Beckman Coulter, RMO52), CD19 (Beckman Coulter, J3-119), CD3 (Scientific support, OKT3) and CD34 (Beckton Dickson, MY10) Abs and rat anti-mouse TER-119 (BioLegend, TER-119) followed by sheep anti-rat IgG Dynabeads (Thermofisher Scientific) separation. Obtained single cell suspension was then stained for flow cytometry sorting using: LIVE/DEAD Fixable Aqua (Thermofisher Scientific), huCD45 APC Cy7 (BioLegend), Lineage (CD3, CD14, CD16, CD19, CD20 and CD56) PacBlue (BioLegend), HLA-DR PE-Cy7 (BioLegend), CD123 PerCP5.5 (BioLegend), CD141 APC (BioLegend), CD1c PE (BioLegend). Human DCs were gated on a live cell gate as $huCD45^+huHLA^-DR^+Lineage^-$. cDC1 were further defined as $CD141^+CD1c^-$, cDC2 as $CD141^-CD1c^+$ and pDC as $CD141^-CD1c^-CD123^+$ (**Supplementary Figure 4B**).

In Vitro Stimulations

Mouse spleen and human blood DCs were resuspended in RPMI-1640 Glutamax (Thermofisher Scientific) with 10% FCS (*In vitro* Technologies™, Noble Park, Victoria), 100μM 2-Mercaptoethanol (Thermofisher Scientific) and 0.01% Penicillin/Streptomycin (Thermofisher Scientific) and humanized mice DCs were resuspended in RPMI containing 10% FCS, 10 mM HEPES, 1mM sodium pyruvate, penicillin, streptomycin, 2 mM L glutamine, NEAA and 50 μM β-mercaptoethanol and were plated at a concentration of $0.5x10^6$/mL in 96-well round bottom plates. They were stimulated with 0.5 or 10 μM cytosine-phosphate guanosine (CpG) oligonucleotides 2216 or 1668 (Geneworks, Thebarton, South Australia; Miltenyi Biotech, Bergisch Gladbach, Germany), 10-100 μg/mL high molecular weight polyinosinic: polycytidylic acid (poly I:C) (*In vivo*Gen) or 10 nmol transfected 3'3' cGAMP (c[G(3',5')pA(3',5')p]), 2'3' cGAMP (c[G(2',5')pA(3',5')p]), c-di-AMP, c-di-GMP (*In vivo*Gen) or their respective linearized control ligands 3'5'-pGpA, 2'5'-GpAp, 5'-pApA and 5'-pGpG (*In vivo*Gen) at 37°C, 10% CO_2 for 18 hrs unless indicated otherwise. The following reagents were included in some experimental cultures as indicated in the figure legends: 0.2ng/mL recombinant mouse GM-CSF (Peprotech, East Windsor, New Jersey), 5μM Q-VD-Oph (Selleck Chemicals, Houston, Texas), 30ng/mL recombinant human IL-29 (R&D Systems, Minneapolis, Minnesota), 5μg/mL anti-human IL-29 (neutralising Clone MAB15981, R&D systems).

CDN Transfection

Cyclic dinucleotides (CDNs) were incubated with Lyovec (*In vivo*Gen) at RT for 15min before being used for stimulations.

Flow Cytometry

Single cell suspensions were incubated with Fc Block (FcγRIII/II, 2.4G2) for 10 min before labelling with the following anti-mouse fluorophore-conjugated mAbs (BD, eBiosciences, BioLegend, TONBO, in house): CD11c (N418), CD11b (M1/70), CD317 (120.G8 or 927), CD8 (53-6.7), CCR9 (CW-1.2), CD3-ϵ (17A2), CD49b (DX5), CD86 (GL1), CD80 (16-10A1) and MHCII (M5/114.15.2) or anti-human fluorophore-conjugated mAbs (BD, eBiosciences, BioLegend, Miltenyi, in house): CD1c (L161), CD3-ϵ (BC3), CD11c (B-ly6), CD14 (FMC17), CD16 (3G8), CD19 (FMC63), CD20 (B1), CD34 (AC133), CD57 (HNK1.1), CD69 (FN50), CD86 (IT2.2), CD123 (7G3), CD141 (AD5-14H12), Glycophorin A (10F7MN) and HLA-DR (REA332). Sorted humanised mouse DCs were labelled with FITC-conjugated CD80 (BioLegend). Dead cells were excluded using propidium iodide (Merck Millipore, Darmstadt, Germany) or LIVE/DEAD Fixable Aqua (Thermofisher Scientific) dyes and samples were acquired on either Fortessa or LSRII flow cytometer (BD). Sphero or TruCOUNT beads (BD) were used to determine cell counts for human DCs. Analysis was conducted using FlowJo software (Tree Star, Ashland, Oregon).

IFN ELISAs

Murine IFN-λ and IFN-α in supernatants were assayed using sandwich ELISA mAbs from RnD Systems, Minneapolis, Minnesota (IFN-λ) or *In vivo*Gen (IFN-α). Immunosorbent plates (Thermofisher Scientific) were coated with 1 μg/mL rat IgG2b anti-mouse IL-28a/b or 2 μg/mL anti-mouse IFN-α capture mAbs at 4°C overnight in a humidified box. Plates were washed between each step using 0.05% Tween (Sigma-Aldrich, St Louis, Missouri)/PBS and 1% bovine serum albumin (Sigma-Aldrich)/PBS was used for blocking at RT for 1 hr. Supernatants were added to plates and incubated at 4°C overnight. Recombinant mouse IL-28a/b (Cat No: 1789-ML-025) or IFN-α (Cat No: re-mifna) were used as standards. 0.25 μg/mL rat IgG2b anti-mouse IL-28a/b or 30 ng/mL anti-mouse IFN-α biotinylated detection mAbs were added to plates and incubated for 2 hr at room temperature. Streptavidin-horseradish peroxidase (GE Healthcare, Chicago, Illinois) was used to develop ELISA substrate containing 0.1 M citric acid, 548 μg/mL 2,2′-azino-bis(3-ethylbenz-thiazoline-6- sulfonic acid (ABTS), Sigma-Aldrich) and H_2O_2. ELISA results were read at 405-490 nm wavelength reduction.

Cytokine Analysis

All cytokines and chemokines, except for murine IFN-λ and IFN-α, in supernatants were analysed using flow cytometric bead-based assay LEGENDplex™ kit (BioLegend) according to manufacturer's instructions and software.

RNA-Sequencing and Bioinformatics Analysis

RNA from sorted mouse splenic DC subsets was isolated using an RNeasy Mini Kit (Qiagen) and residual genomic DNA removed using RNase-free DNase (Qiagen). Sample libraries were constructed using Illumina TruSeq Stranded mRNA kit according to manufacturer's instructions. Libraries were quantitated using Qubit DNA HS kit (Thermofisher Scientific) and checked for adaptor contamination using Bioanalyzer 2100 (Agilent Technologies, Santa Clara, California). Sample libraries were then sequenced by Micromon on NextSeq500 using High-Output SBS chemistry (Illumina, San Diego, California) at 1.8pM library concentration and 1x75b read length. RNA-seq data analysis was performed in Degust (http://degust.erc.monash.edu/; version 4.1.1) by the Monash Bioinformatics Platform personnel, D.R Powell and A. Barugahare.

Quantitative RT-PCR

Total RNA was extracted from sorted DC subsets and cDNA synthesized using SuperScript® IV First-Strand Synthesis System (Thermofisher Scientific) according to the manufacturer's protocol. The expression of genes was determined using quantitative real-time PCR. STING (*TMEM173*) and cGAS (*MB21D1*) qPCR Primers were purchased from QIAGEN. Each cDNA sample was amplified using SYBR Green Master Mix (Rox) (Thermofisher Scientific) on the Real-time PCR Viaa 7 system using cycles conditions as: 95˚C for 10 min, 45–50 cycles at 95˚C for 15 sec, and 60˚C for 60 sec. Reactions were run in triplicates for four independent experiments. The Ct (cycle threshold) values were normalized to the geometric mean of GAPDH as the housekeeping gene to control the variability in expression levels and were analyzed using the $2^{-\Delta\Delta CT}$ method (87).

Western Blotting

Western blotting of sorted DC lysates was performed according to a recently published protocol (13). The primary and secondary antibodies used in this assay were: Rabbit monoclonal anti-STING (D2P2F) (Cell Signaling Technology, Danvers, Massachusetts; Cat#13647), rabbit monoclonal anti-P-STING Ser^{365} (D8F4W) antibody (Cell Signaling Technology, Cat#72971), rabbit polyclonal anti-TBK1 antibody (Cell Signaling Technology, Cat#3013), rabbit monoclonal anti-TBK1 Ser^{172} (D52C2) antibody (Cell Signaling Technology, Cat#5483), rabbit monoclonal anti-IRF3 (D83B9) antibody (Cell Signaling Technology, Cat#4302), rabbit monoclonal anti-P-IRF3 Ser^{396} (4D4G) (Cell Signaling Technology, Cat#4947), rabbit monoclonal anti-NF-kappa-B p65 (C22B4) antibody (Cell Signaling Technology, Cat#4764), rabbit monoclonal anti-NF-kappa-B P-p65 Ser^{536} (93H1) antibody (Cell Signaling Technology, Cat#3033), rabbit polyclonal anti-cleaved caspase 3 (Asp175) antibody (Cell Signaling Technology, Cat#9661), mouse monoclonal anti-beta ACTIN, HRP (AC-15) (Abcam, Cambridge, Massachusetts; Cat#Ab49900) and Peroxidase-AffiniPure Goat Anti-Rabbit IgG (H+L) secondary antibody (Jackson ImmunoResearch Labs, West Grove, Pennsylvania, Cat#111-035-003).

Caspase3/7 Detection Assay

Caspase3/7 activity was measured using Caspase-Glo®3/7 Assay (Promega, Madison, WI) according to manufacturer's instructions.

Statistical Analysis

Paired and unpaired two-tailed Student's *t* tests, one- or two-way ANOVA was performed using Prism 7.0 (GraphPad software) where $*P < 0.05$, $**P < 0.01$, $***P < 0.001$ and $****P < 0.0001$.

DATA AVAILABILITY STATEMENT

The datasets presented in this study can be found in online repositories. The names of the repository/repositories and accession number(s) can be found below: GEO, GSE188992.

ETHICS STATEMENT

The studies involving human participants were reviewed and approved by Monash University Human Research Ethics Committee Monash University, Clayton, Victoria, Australia. The patients/participants provided their written informed consent to participate in this study. The animal study was reviewed and approved by Monash Animal Ethics Committee MARP-2, Monash University, Clayton, Victoria, Australia.

AUTHOR CONTRIBUTIONS

ESP, GD, PT, AS, ZM, NJ, KB, and KAM performed the experiments. EP, GD, KB, PT, MB, KR, MW, and MO'K analyzed and interpreted results. EP, MO'K, HH, MW, CM, BK, DDN, and KL contributed to the experimental design. YZ, BK, and KL provided genetically modified mice. EP, GD, KR, and MO'K wrote the manuscript. All authors reviewed the manuscript. All authors contributed to the article and approved the submitted version.

FUNDING

MO'K was supported by a National Health and Medical Research Council (NHMRC) Senior Research Fellowship (1077633), NHMRC Project grant (1085934) and Worldwide Cancer Research Grant (14-0281) and Worldwide Cancer Research / Cancer Australia Grant (20-0300). KR was supported by NHMRC project grants (1085934) and Mater Foundation grants; KL was funded by NHMRC project grants 1145788, 1162765 and 11801089 and is supported by an ARC Future Fellowship (FT190100266). DDN was supported by a Monash University FMNHS Senior Postdoctoral Fellowship. ESP was supported by a Monash University PhD scholarship and Worldwide Cancer Research / Cancer Australia Grant (20-0300) and GD was supported by a Griffith University PhD Scholarship. AS, MB, ZM were supported through Australian Government Research Training Program (RTP) scholarships. NJ was supported through a Monash University Faculty International Tuition Scholarship (FITS) and Co-funded Monash Graduate Scholarship (Co-MGS). KB was supported by a Monash Silver Jubilee Postgraduate Research scholarship (MSJS) and a Monash Graduate Excellence scholarship. The Translational Research Institute is supported by a grant from the Australian Government.

ACKNOWLEDGMENTS

We thank the Monash Animal Research Platform and Flowcore facility for their technical assistance. We also acknowledge the use of services, facilities and support of Micromon at Monash University and Monash Bioinformatics Platform for this work. We also acknowledge Seth Masters and James Vince (WEHI) for access to genetically modified mice.

SUPPLEMENTARY MATERIAL

The Supplementary Material for this article can be found online at: https://www.frontiersin.org/articles/10.3389/fimmu.2022.794776/full#supplementary-material

Supplementary Figure 1 | Mouse DCs are potently activated by CDNs and produce IFN-λ that is STING-dependent. **(A)** Bulk splenic mouse DCs were stimulated with 1 or 10nmol 2'3' cGAMP, 3'3' cGAMP, c-di-AMP or c-di-GMP complexed with lyovec, their respective linearized control ligands (Ctrl) complexed with lyovec, lyovec alone, 0.5 μM CpG2216 or 100 μg/mL pI:C for 18h. MHCII expression on DC subsets was determined using flow cytometry. Bar graphs represent the mean difference between geometric mean fluorescence intensities (gMFI) of stained samples and fluorescence minus one (FMO) controls ± SEM from 3 biological replicates (pool of 2 mice per replicate). **(B)** Bulk splenic mouse DCs from C57BL/6 or Tmem173-/- were stimulated with 10nmol 3'3' cGAMP complexed with lyovec, lyovec alone or 0.5 μM CpG2216 for 18h. IFN-λ production in cell culture supernatants were analysed by ELISA. Bar graphs represent mean ± SEM from 3 individual mice per genotype. Statistical analyses were performed using two-tailed Paired Student's t test where *P < 0.05, ** P < 0.01and ns, not significant.

Supplementary Figure 2 | Mouse DCs upregulate activation markers CD86 and MHCII after CDN stimulation. Bulk splenic mouse DCs were stimulated with 1 or 10nmol 2'3' cGAMP, 3'3' cGAMP, c-di-AMP or c-di-GMP complexed with lyovec, their respective linearized control ligands (linGAMP Ctrl) complexed with lyovec, lyovec alone, 0.5 μM CpG2216 or 100 μg/mL pI:C for 18h. Histograms show CD86 and MHCII expression on DC determined using flow cytometry. Dotted lines represent fluorescence minus one (FMO) control and filled in lines represent Ab stain. Grey lines represent linGAMP Ctrl and red lines represent cGAMP samples. Histograms represent 1 of 3 biological replicates (pool of 2 mice per replicate).

Supplementary Figure 3 | STING transcripts in mouse and human DCs. **(A)** *Tmem173* transcript expression (counts per million) from RNA-sequencing analysis of steady state sorted mouse splenic DCs. Bar graphs represent mean ± SEM from 3 independent samples of 10-14 mice pooled per sample. **(B)** Publicly available microarray data sets [www.stemformatics.org] represent expression levels of STING in human immune cells isolated from different organs (Heidkamp, 2016). **(C)** Microarray data demonstrating the changes in gene expression levels of STING in human cDCs when treated with polyI:C (TLR3 agonist), R848 (TLR7/8 agonist) and the combo (polyI:C+R848) (Minoda, 2017). **(D, E)** Quantitative PCR analysis was performed on immune cell subsets isolated from humanised mouse bone marrow to determine the pattern of STING expression in the steady state **(D)** as well as the expression levels after activation **(E)** in each DC subset. Gene expression levels were normalised to GAPDH. Each experiment was performed for 4 independent samples (n = 4) and the error bars represent mean ± SEM.

Supplementary Figure 4 | Gating strategies for mouse and human DC subsets. **(A)** Bulk splenic DCs pooled from $15^{+}17$ C57BL/6 mice were labelled with the following fluorophore^{+}conjugated mAbs: CD11c (N418), CD45RA (14.8), CD8 ($53^{+}6.7$), CD11b (M1/70), CD49b (DX5). They were then sorted by first removing NK cells using junk gate and sorted into pDC ($CD11c^{int}CD317^{hi}CD11b^{-}$), cDC1 ($CD11c^{hi}CD317^{lo}CD8^{+}CD11b^{-}$) and cDC2 ($CD11c^{hi}CD317^{lo}CD8^{-}CD11b^{-}$) subsets. **(B)** Purified human blood DCs were labelled with the following fluorophore^{+}conjugated mAbs: CD1c (L161), $CD3^{-}\varepsilon$ (BC3), CD11c ($B^{+}ly6$), CD14 (FMC17), CD16 (3G8), CD19 (FMC63), CD20 (B1), CD34 (AC133), CD57 (HNK1.1), CD69 (FN50), CD86 (IT2.2), CD123 (7G3), CD141 ($AD5^{+}14H12$), Glycophorin A (10F7MN) and $HLA^{+}DR$ (REA332). DCs were first gated on $HLA^{-}DR^{+}Lin^{-}$ cells followed by separation into cDC1 ($CD11c^{+}CD141^{+}CD1c^{-}CD123^{-}$), cDC2 ($CD11c^{+}CD1c^{+}$) and pDC ($CD11c^{-}CD123^{+}$).

Supplementary Figure 5 | Sorted mouse DCs upregulate CD80 and CD86 expression after cGAMP stimulation. Sorted splenic mouse cDC1, cDC2 and pDCs from a pool of 15-17 mice were stimulated with 10 nmol 3'3' cGAMP or its linearized control ligand (linGAMP Ctrl) complexed with lyovec, lyovec alone, 0.5 μM CpG2216 or 100 μg/mL pI:C for 18h. CD80 and CD86 expression on DC subsets was determined using flow cytometry. **(A)** Bar graphs represent the mean difference between geometric mean fluorescence intensities (gMFI) of stained samples and fluorescence minus one (FMO) controls ± SEM from 3 independent experiments. **(B)** Representative histograms showing CD80 and CD86 expression on all sorted DC subsets after stimulations. Grey unfilled lines represent FMO control and red filled lines represent Ab stain. Histograms represent 1 of 3 independent experiments. Statistical analyses were performed using two-tailed Paired Student's t test where *P < 0.05 and ns, not significant.

Supplementary Figure 6 | Type I and III IFNs are differentially produced by DC subsets after cGAMP stimulation. Sorted splenic mouse cDC1, cDC2 and pDCs from a pool of 15-17 mice were stimulated with 10 nmol 3'3' cGAMP or its linearized control ligand (linGAMP Ctrl) complexed with lyovec, lyovec alone, 0.5 μM CpG2216 or 100 μg/mL pI:C for 18 hrs. IFN production in cell culture supernatants was analysed by ELISA (IFN-α and IFN-λ) or flow cytometric bead assay (IFN-β). Bar

graphs represent mean ± SEM from 3 independent experiments. Statistical analyses were performed using two-tailed Paired Student's t test where *P < 0.05 and ns, not significant.

Supplementary Figure 7 | cDC subsets after cGAMP stimulation. FACS plots showing bulk mouse splenic cDC1 ($CD11c^{hi}CD317^{lo}CD8^{+}CD11b^{lo}$) and cDC2 ($CD11c^{hi}CD317^{lo}CD8^{-}CD11b^{hi}$) subsets stimulated for 18 h with 10 nmol 3'3' cGAMP complexed with lyovec, or lyovec alone.

Supplementary Figure 8 | cDC2 are partially killed after CDN stimulation. Bulk splenic DCs were stimulated with 1 or 10 nmol 2'3' cGAMP, 3'3' cGAMP, c-di-AMP or c-di-GMP complexed with lyovec, their respective linearized control ligands (Ctrl) complexed with lyovec, lyovec alone or 0.5 μM CpG2216 for 18h. Bar graphs represent the mean relative survival of cDC subsets ± SEM from 3 biological replicates (pool of 2 mice per replicate). Statistical analyses were performed using two-tailed Paired Student's t test where *P < 0.05 and **P < 0.01 and ns, not significant.

Supplementary Figure 9 | Caspase 3 is involved in cGAMP-mediated pDC death. **(A, B)** Bulk splenic DCs from BM chimeras generated using Ly5.2 WT or Vav-Cre Bax-/-/Bak-/- mice were stimulated with 10 nmol 3'3' cGAMP or its linearized control ligand (linGAMP Ctrl) complexed with lyovec, lyovec alone or 0.5 μM CpG2216 for 18h. **(A)** Cytokine production in cell supernatants was analysed by ELISA (IFN-λ and IFN-α) or flow cytometric bead assay (TNF-α). Dotted lines represent upper limit of detection. Bar graphs show mean ± SEM from 2-3 individual mice per genotype. **(B)** Activation markers CD86 and CD69 were determined by flow cytometry. (i) Histograms show CD86 expression on pDCs. Dotted unfilled lines represent fluorescence minus one (FMO) control and solid filled lines represent Ab stain. Black and red lines represent WT and Vav-Cre Bax-/-/Bak-/- BM chimeric mice respectively. (ii) Bar graphs show the mean difference between geometric mean fluorescence intensities (gMFI) of stained samples and FMO controls ± SEM from 2-3 individual mice per genotype. **(C)** Bulk splenic DCs from a pool of 8-14 mice per replicate were treated with or without 5 μM pan-caspase inhibitor Q-VD-OPh for 1h before stimulations with 10 nmol 3'3' cGAMP or its linearized control ligand (linGAMP Ctrl) complexed with lyovec or media alone for 4h. pDC numbers were enumerated using flow cytometry and bar graphs show mean relative survival (compared to media alone) ± SEM compiled from 3 independent experiments. **(D)** Sorted splenic mouse cDC1, cDC2 and pDCs (see **Supplementary Figure 4A** for sorting strategy) from a pool of 11-12 mice per replicate were stimulated with 10 nmol 3'3' cGAMP or its linearized control ligand (linGAMP Ctrl) complexed with lyovec for 1.5 h. Cells were then lysed and blotted using antibodies specific for cleaved caspase 3 and actin. (i) Immunoblot shown represents 1 of 3 independent experiments. (ii) Densitometric analysis of cleaved caspase 3 relative to actin compiled from the immunoblots of 3 independent experiments. Bar graphs show mean ± SEM. **(E)** Sorted splenic mouse pDCs from a pool of 7-14 mice per replicate were stimulated with 10 nmol 3'3' cGAMP or its linearized control ligand (linGAMP Ctrl) complexed with lyovec for 1.5 h. Caspase 3/7 activity was determined using Caspase-Glo 3/7® Assay according to manufacturer's instructions. Bar graphs show mean relative caspase 3/7 activity (compared to linGAMP Ctrl) ± SEM compiled from 2-3 independent experiments. Statistical analyses were performed using two-tailed Paired Student's t test where *P < 0.05 and ns, not significant.

Supplementary Figure 10 | Humanised mice DC are activated, but not killed, after cGAMP stimulation. Enriched, unsorted humanised mice DCs from BM were stimulated with 25 μg/mL pI:C, 10 μM CpG2216, 10 nmol 2'3' cGAMP or its linearized control ligand complexed (linGAMP Ctrl) with lyovec for 18h. **(A)** Bar graphs represent the average change in CD80 gMFI values in stimulated samples compared to media only samples ± SEM from 3 independent experiments. **(B)** Bar graphs represent the mean relative survival (compared to media alone) ± SEM compiled from 3 independent experiments. **(C, D)** Human blood DC from 4 independent donors were stimulated with 5 nmol 2'3' cGAMP or its linearized control ligand (linGAMP Ctrl) complexed with lyovec in the presence or absence of 5 μg/mL neutralising anti-IFN-λ1 antibody (anti-IL-29, MAB15981, R&D Systems) or antibody control for 18 h. **(C)** pDC numbers were enumerated using flow cytometry. Bar graphs show mean ± SEM and each dot represents individual human blood donors (n=4). **(D)** CD69 expression on pDC were determined using flow cytometry. Bar graphs shown mean difference between geometric mean fluorescence intensities (gMFI) of stained samples and FMO controls ± SEM and each dot represents individual human blood donors (n=4). Statistical analyses were performed using two-tailed Paired Student's t test where *P < 0.05, **P < 0.01 and ns, not significant.

REFERENCES

1. Ishikawa H, Barber GN. STING is an Endoplasmic Reticulum Adaptor That Facilitates Innate Immune Signalling. *Nature* (2008) 455:674. doi: 10.1038/nature07317
2. Zhong B, Yang Y, Li S, Wang Y-Y, Li Y, Diao F, et al. The Adaptor Protein MITA Links Virus-Sensing Receptors to IRF3 Transcription Factor Activation. *Immunity* (2008) 29(4):538–50. doi: 10.1016/j.immuni.2008.09.003
3. Sun W, Li Y, Chen L, Chen H, You F, Zhou X, et al. ERIS, an Endoplasmic Reticulum IFN Stimulator, Activates Innate Immune Signaling Through Dimerization. *Proc Natl Acad Sci* (2009) 106(21):8653. doi: 10.1073/pnas.0900850106
4. Burdette DL, Monroe KM, Sotelo-Troha K, Iwig JS, Eckert B, Hyodo M, et al. STING is a Direct Innate Immune Sensor of Cyclic Di-GMP. *Nature* (2011) 478:515. doi: 10.1038/nature10429
5. Ablasser A, Goldeck M, Cavlar T, Deimling T, Witte G, Röhl I, et al. cGAS Produces a 2′-5′-Linked Cyclic Dinucleotide Second Messenger That Activates STING. *Nature* (2013) 498:380. doi: 10.1038/nature12306
6. Sun L, Wu J, Du F, Chen X, Chen ZJ. Cyclic GMP-AMP Synthase Is a Cytosolic DNA Sensor That Activates the Type I Interferon Pathway. *Science* (2013) 339(6121):786. doi: 10.1126/science.1232458
7. Abe T, Barber GN. Cytosolic-DNA-Mediated, STING-Dependent Proinflammatory Gene Induction Necessitates Canonical NF-κb Activation Through TBK1. *J Virol* (2014) 88(10):5328. doi: 10.1128/JVI.00037-14
8. Balka KR, De Nardo D. Molecular and Spatial Mechanisms Governing STING Signalling. *FEBS J* (2021) 288(19):5504–29. doi: 10.1111/febs.15640. pub ahead of print Nov 25.
9. Jin L, Hill KK, Filak H, Mogan J, Knowles H, Zhang B, et al. MPYS Is Required for IFN Response Factor 3 Activation and Type I IFN Production in the Response of Cultured Phagocytes to Bacterial Second Messengers Cyclic-Di-AMP and Cyclic-Di-GMP. *J Immunol* (2011) 187(5):2595. doi: 10.4049/jimmunol.1100088
10. Saitoh T, Fujita N, Hayashi T, Takahara K, Satoh T, Lee H, et al. Atg9a Controls dsDNA-Driven Dynamic Translocation of STING and the Innate Immune Response. *Proc Natl Acad Sci* (2009) 106(49):20842. doi: 10.1073/pnas.0911267106
11. Tanaka Y, Chen ZJ. STING Specifies IRF3 Phosphorylation by TBK1 in the Cytosolic DNA Signaling Pathway. *Sci Signaling* (2012) 5(214):ra20–0. doi: 10.1126/scisignal.2002521
12. Zhang X, Shi H, Wu J, Zhang X, Sun L, Chen C, et al. Cyclic GMP-AMP Containing Mixed Phosphodiester Linkages Is An Endogenous High-Affinity Ligand for STING. *Mol Cell* (2013) 51(2):226–35. doi: 10.1016/j.molcel.2013.05.022
13. Balka KR, Louis C, Saunders TL, Smith AM, Calleja DJ, D'Silva DB, et al. TBK1 and Ikkε Act Redundantly to Mediate STING-Induced NF-κb Responses in Myeloid Cells. *Cell Rep* (2020) 31(1):107492. doi: 10.1016/j.celrep.2020.03.056
14. Ishikawa H, Ma Z, Barber GN. STING Regulates Intracellular DNA-Mediated, Type I Interferon-Dependent Innate Immunity. *Nature* (2009) 461(7265):788–92. doi: 10.1038/nature08476
15. Woo S-R, Fuertes Mercedes B, Corrales L, Spranger S, Furdyna Michael J, Leung Michael YK, et al. STING-Dependent Cytosolic DNA Sensing Mediates Innate Immune Recognition of Immunogenic Tumors. *Immunity* (2014) 41(5):830–42. doi: 10.1016/j.immuni.2014.10.017
16. Liu Y, Jesus AA, Marrero B, Yang D, Ramsey SE, Montealegre Sanchez GA, et al. Activated STING in a Vascular and Pulmonary Syndrome. *N Engl J Med* (2014) 371(6):507–18. doi: 10.1056/NEJMoa1312625
17. Glück S, Ablasser A. Innate Immunosensing of DNA in Cellular Senescence. *Curr Opin Immunol* (2019) 56:31–6. doi: 10.1016/j.coi.2018.09.013
18. Barber GN. STING: Infection, Inflammation and Cancer. *Nat Rev Immunol* (2015) 15:760. doi: 10.1038/nri3921

19. Deng L, Liang H, Xu M, Yang X, Burnette B, Arina A, et al. STING-Dependent Cytosolic DNA Sensing Promotes Radiation-Induced Type I Interferon-Dependent Antitumor Immunity in Immunogenic Tumors. *Immunity* (2014) 41(5):843–52. doi: 10.1016/j.immuni.2014.10.019
20. Li T, Cheng H, Yuan H, Xu Q, Shu C, Zhang Y, et al. Antitumor Activity of cGAMP *via* Stimulation of cGAS-cGAMP-STING-IRF3 Mediated Innate Immune Response. *Sci Rep* (2016) 6:19049–9. doi: 10.1038/srep19049
21. Wang H, Hu S, Chen X, Shi H, Chen C, Sun L, et al. cGAS is Essential for the Antitumor Effect of Immune Checkpoint Blockade. *Proc Natl Acad Sci USA* (2017) 114(7):1637–42. doi: 10.1073/pnas.1621363114
22. Le Naour J, Zitvogel L, Galluzzi L, Vacchelli E, Kroemer G. Trial Watch: STING Agonists in Cancer Therapy. *Oncoimmunology* (2020) 9(1):1777624. doi: 10.1080/2162402X.2020.1777624
23. Sheridan C. Drug Developers Switch Gears to Inhibit STING. *Nat Biotechnol* (2019) 37(3):199–201. doi: 10.1038/s41587-019-0060-z
24. Chen Q, Sun L, Chen ZJ. Regulation and Function of the cGAS–STING Pathway of Cytosolic DNA Sensing. *Nat Immunol* (2016) 17:1142. doi: 10.1038/ni.3558
25. Macri C, Pang ES, Patton T, O'Keeffe M. Dendritic Cell Subsets. *Semin Cell Dev Biol* (2018) 84:11–21. doi: 10.1016/j.semcdb.2017.12.009
26. Lauterbach H, Bathke B, Gilles S, Traidl-Hoffmann C, Luber CA, Fejer G, et al. Mouse Cd8α≪Sup<+≪/Sup< DCs and Human BDCA3<sup<+</sup< DCs are Major Producers of IFN-λ in Response to Poly IC. *J Exp Med* (2010) 207(12):2703. doi: 10.1084/jem.20092720
27. Deb P, Dai J, Singh S, Kalyoussef E, Fitzgerald-Bocarsly P. Triggering of the cGAS–STING Pathway in Human Plasmacytoid Dendritic Cells Inhibits TLR9-Mediated IFN Production. *J Immunol* (2020) 205(1):223–36. doi: 10.4049/jimmunol.1800933
28. Prokunina-Olsson L. Genetics of the Human Interferon Lambda Region. *J Interferon Cytokine Res* (2019) 39(10):599–608. doi: 10.1089/jir.2019.0043
29. Fang MZ, Jackson SS, O'Brien TR. IFNL4: Notable Variants and Associated Phenotypes. *Gene* (2020) 730:144289. doi: 10.1016/j.gene.2019.144289
30. Hamming OJ, Terczyńska-Dyla E, Vieyres G, Dijkman R, Jørgensen SE, Akhtar H, et al. Interferon Lambda 4 Signals *via* the Ifnλ Receptor to Regulate Antiviral Activity Against HCV and Coronaviruses. *EMBO J* (2013) 32(23):3055. doi: 10.1038/emboj.2013.232
31. Donnelly RP, Kotenko SV. Interferon-Lambda: A New Addition to an Old Family. *J Interferon Cytokine Res* (2010) 30(8):555–64. doi: 10.1089/jir.2010.0078
32. Ye L, Schnepf D, Staeheli P. Interferon-Lambda Orchestrates Innate and Adaptive Mucosal Immune Responses. *Nat Rev Immunol* (2019) 19(10):614–25. doi: 10.1038/s41577-019-0182-z
33. Diegelmann J, Beigel F, Zitzmann K, Kaul A, Goke B, Auernhammer CJ, et al. Comparative Analysis of the Lambda-Interferons IL-28A and IL-29 Regarding Their Transcriptome and Their Antiviral Properties Against Hepatitis C Virus. *PloS One* (2010) 5(12):e15200. doi: 10.1371/journal.pone.0015200
34. Wack A, Terczynska-Dyla E, Hartmann R. Guarding the Frontiers: The Biology of Type III Interferons. *Nat Immunol* (2015) 16:802+. doi: 10.1038/ni.3212
35. Tang W, Wallace TA, Yi M, Magi-Galluzzi C, Dorsey TH, Onabajo OO, et al. ≪Em<IFNL4</em<-Δg Allele Is Associated With an Interferon Signature in Tumors and Survival of African-American Men With Prostate Cancer. *Clin Cancer Res* (2018) 24(21):5471. doi: 10.1158/1078-0432
36. Luo M, Wang H, Wang Z, Cai H, Lu Z, Li Y, et al. A STING-Activating Nanovaccine for Cancer Immunotherapy. *Nat Nanotechnol* (2017) 12(7):648–54. doi: 10.1038/nnano.2017.52
37. Chen Q, Sun L, Chen ZJ. Regulation and Function of the cGAS-STING Pathway of Cytosolic DNA Sensing. *Nat Immunol* (2016) 17(10):1142–9. doi: 10.1038/ni.3558
38. Vremec D, O'Keeffe M, Wilson A, Ferrero I, Koch U, Radtke F, et al. Factors Determining the Spontaneous Activation of Splenic Dendritic Cells in Culture. *Innate Immun* (2011) 17(3):338–52. doi: 10.1177/1753425910371396
39. Sun F, Liu Z, Yang Z, Liu S, Guan W. The Emerging Role of STING-Dependent Signaling on Cell Death. *Immunol Res* (2019) 67(2):290–6. doi: 10.1007/s12026-019-09073-z
40. Gao P, Ascano M, Zillinger T, Wang W, Dai P, Serganov Artem A, et al. Structure-Function Analysis of STING Activation by C[G(2′,5′)pA(3′,5′)p] and Targeting by Antiviral DMXAA. *Cell* (2013) 154(4):748–62. doi: 10.1016/j.cell.2013.07.023
41. Green DR, Llambi F. Cell Death Signaling. *Cold Spring Harbor Perspect Biol* (2015) 7(12):1–24. doi: 10.1101/cshperspect.a006080
42. Payvandi F, Amrute S, Fitzgerald-Bocarsly P. Exogenous and Endogenous IL-10 Regulate IFN-α Production by Peripheral Blood Mononuclear Cells in Response to Viral Stimulation. *J Immunol* (1998) 160(12):5861.
43. Ahn J, Son S, Oliveira SC, Barber GN. STING-Dependent Signaling Underlies IL-10 Controlled Inflammatory Colitis. *Cell Rep* (2017) 21(13):3873–84. doi: 10.1016/j.celrep.2017.11.101
44. Rocamora-Reverte L, Reichardt HM, Villunger A, Wiegers G. T-Cell Autonomous Death Induced by Regeneration of Inert Glucocorticoid Metabolites. *Cell Death Dis* (2017) 8:e2948. doi: 10.1038/cddis.2017.344
45. Li L, Yin Q, Kuss P, Maliga Z, Millán JL, Wu H, et al. Hydrolysis of 2′3′-cGAMP by ENPP1 and Design of Nonhydrolyzable Analogs. *Nat Chem Biol* (2014) 10:1043. doi: 10.1038/nchembio.1661
46. Sagulenko V, Vitak N, Vajjhala PR, Vince JE, Stacey KJ. Caspase-1 Is an Apical Caspase Leading to Caspase-3 Cleavage in the AIM2 Inflammasome Response, Independent of Caspase-8. *J Mol Biol* (2018) 430(2):238–47. doi: 10.1016/j.jmb.2017.10.028
47. Murthy AMV, Robinson N, Kumar S. Crosstalk Between cGAS-STING Signaling and Cell Death. *Cell Death Differ* (2020) 27(11):2989–3003. doi: 10.1038/s41418-020-00624-8
48. Newton K, Wickliffe KE, Dugger DL, Maltzman A, Roose-Girma M, Dohse M, et al. Cleavage of RIPK1 by Caspase-8 is Crucial for Limiting Apoptosis and Necroptosis. *Nature* (2019) 574(7778):428–31. doi: 10.1038/s41586-019-1548-x
49. O'Keeffe M, Grumont RJ, Hochrein H, Fuchsberger M, Gugasyan R, Vremec D, et al. Distinct Roles for the NF-κb1 and C-Rel Transcription Factors in the Differentiation and Survival of Plasmacytoid and Conventional Dendritic Cells Activated by TLR-9 Signals. *Blood* (2005) 106(10):3457. doi: 10.1182/blood-2004-12-4965
50. Carrington EM, Zhang J-G, Sutherland RM, Vikstrom IB, Brady JL, Soo P, et al. Prosurvival Bcl-2 Family Members Reveal a Distinct Apoptotic Identity Between Conventional and Plasmacytoid Dendritic Cells. *Proc Natl Acad Sci* (2015) 112(13):4044. doi: 10.1073/pnas.1417620112
51. Birkinshaw RW, Czabotar PE. The BCL-2 Family of Proteins and Mitochondrial Outer Membrane Permeabilisation. *Semin Cell Dev Biol* (2017) 72:152–62. doi: 10.1016/j.semcdb.2017.04.001
52. Flores-Romero H, Ros U, Garcia-Saez AJ. Pore Formation in Regulated Cell Death. *EMBO J* (2020) 39(23):e105753. doi: 10.15252/embj.2020105753
53. Vince JE, De Nardo D, Gao W, Vince AJ, Hall C, McArthur K, et al. The Mitochondrial Apoptotic Effectors BAX/BAK Activate Caspase-3 and -7 to Trigger NLRP3 Inflammasome and Caspase-8 Driven IL-1beta Activation. *Cell Rep* (2018) 25(9):2339–53:e2334. doi: 10.1016/j.celrep.2018.10.103
54. Chappaz S, McArthur K, Kealy L, Law CW, Tailler M, Lane RM, et al. Homeostatic Apoptosis Prevents Competition-Induced Atrophy in Follicular B Cells. *Cell Rep* (2021) 36(3):109430. doi: 10.1016/j.celrep.2021.109430
55. Caserta TM, Smith AN, Gultice AD, Reedy MA, Brown TL. Q-VD-OPh, a Broad Spectrum Caspase Inhibitor With Potent Antiapoptotic Properties. *Apoptosis* (2003) 8(4):345–52. doi: 10.1023/A:1024116916932
56. Kranzusch Philip J, Wilson Stephen C, Lee Amy SY, Berger James M, Doudna Jennifer A, Vance Russell E. Ancient Origin of cGAS-STING Reveals Mechanism of Universal 2′,3′ cGAMP Signaling. *Mol Cell* (2015) 59(6):891–903. doi: 10.1016/j.molcel.2015.07.022
57. Minoda Y, Virshup I, Leal Rojas I, Haigh O, Wong Y, Miles JJ, et al. Human CD141+ Dendritic Cell and CD1c+ Dendritic Cell Undergo Concordant Early Genetic Programming After Activation in Humanized Mice In Vivo. *Front Immunol* (2017) 8:1419. doi: 10.3389/fimmu.2017.01419
58. Chiang M-C, Tullett KM, Lee YS, Idris A, Ding Y, McDonald KJ, et al. Differential Uptake and Cross-Presentation of Soluble and Necrotic Cell Antigen by Human DC Subsets. *Eur J Immunol* (2016) 46(2):329–39. doi: 10.1002/eji.201546023
59. Ding Y, Wilkinson A, Idris A, Fancke B, O'Keeffe M, Khalil D, et al. FLT3-Ligand Treatment of Humanized Mice Results in the Generation of Large Numbers of $CD141^+$ and $CD1c^+$ Dendritic Cells *In Vivo*. *J Immunol* (2014) 192(4):1982. doi: 10.4049/jimmunol.1302391

60. Pearson FE, Tullett KM, Leal-Rojas IM, Haigh OL, Masterman KA, Walpole C, et al. Human CLEC9A Antibodies Deliver Wilms' Tumor 1 (WT1) Antigen to CD141(+) Dendritic Cells to Activate Naïve and Memory WT1-Specific CD8(+) T Cells. *Clin Transl Immunol* (2020) 9(6):e1141. doi: 10.1002/cti2.1141
61. Tullett KM, Leal Rojas IM, Minoda Y, Tan PS, Zhang J-G, Smith C, et al. Targeting CLEC9A Delivers Antigen to Human CD141(+) DC for CD4(+) and CD8(+)T Cell Recognition. *JCI Insight* (2016) 1(7):e87102–2. doi: 10.1172/jci.insight.87102
62. Luber CA, Cox J, Lauterbach H, Fancke B, Selbach M, Tschopp J, et al. Quantitative Proteomics Reveals Subset-Specific Viral Recognition in Dendritic Cells. *Immunity* (2010) 32(2):279–89. doi: 10.1016/j.immuni.2010.01.013
63. Hubert M, Gobbini E, Couillault C, Manh TV, Doffin AC, Berthet J, et al. IFN-III is Selectively Produced by Cdc1 and Predicts Good Clinical Outcome in Breast Cancer. *Sci Immunol* (2020) 5(46):1–14. doi: 10.1126/sciimmunol.aav3942
64. Fuertes MB, Kacha AK, Kline J, Woo S-R, Kranz DM, Murphy KM, et al. Host Type I IFN Signals are Required for Antitumor CD8+ T Cell Responses Through CD8α+ Dendritic Cells. *J Exp Med* (2011) 208(10):2005. doi: 10.1084/jem.20101159
65. Syedbasha M, Egli A. Interferon Lambda: Modulating Immunity in Infectious Diseases. *Front Immunol* (2017) 8:119. doi: 10.3389/fimmu.2017.00119
66. Yan Y, Wang L, He J, Liu P, Lv X, Zhang Y, et al. Synergy With Interferon-Lambda 3 and Sorafenib Suppresses Hepatocellular Carcinoma Proliferation. *Biomed Pharmacother = Biomed Pharmacother* (2017) 88:395–402. doi: 10.1016/j.biopha.2017.01.077
67. Hausmann LD, de Almeida BS, de Souza IR, Drehmer MN, Fernandes BL, Wilkens RS, et al. Association of TNFRSF1A and IFNLR1 Gene Polymorphisms With the Risk of Developing Breast Cancer and Clinical Pathologic Features. *Biochem Genet* (2021) 59(5):1233–46. doi: 10.1007/s10528-021-10060-z. e-pub ahead of print 2021/03/22.
68. Huschka H, Mihm S. Interferon-Lambda (IFNL) Germline Variations and Their Significance for HCC and PDAC Progression: An Analysis of The Cancer Genome Atlas (TCGA) Data. *BMC Cancer* (2020) 20(1):1131–1. doi: 10.1186/s12885-020-07589-4
69. Lemos H, Mohamed E, Huang L, Ou R, Pacholczyk G, Arbab AS, et al. STING Promotes the Growth of Tumors Characterized by Low Antigenicity *via* IDO Activation. *Cancer Res* (2016) 76(8):2076–81. doi: 10.1158/0008-5472.CAN-15-1456
70. Liang D, Xiao-Feng H, Guan-Jun D, Er-Ling H, Sheng C, Ting-Ting W, et al. Activated STING Enhances Tregs Infiltration in the HPV-Related Carcinogenesis of Tongue Squamous Cells *via* the C-Jun/CCL22 Signal. *Biochim Biophys Acta* (2015) 1852(11):2494–503. doi: 10.1016/j.bbadis.2015.08.011
71. Tang C-HA, Zundell JA, Ranatunga S, Lin C, Nefedova Y, Del Valle JR, et al. Agonist-Mediated Activation of STING Induces Apoptosis in Malignant B Cells. *Cancer Res* (2016) 76(8):2137. doi: 10.1158/0008-5472.CAN-15-1885
72. Larkin B, Ilyukha V, Sorokin M, Buzdin A, Vannier E, Poltorak A. Cutting Edge: Activation of STING in T Cells Induces Type I IFN Responses and Cell Death. *J Immunol* (2017) 199(2):397. doi: 10.4049/jimmunol.1601999
73. Gulen MF, Koch U, Haag SM, Schuler F, Apetoh L, Villunger A, et al. Signalling Strength Determines Proapoptotic Functions of STING. *Nat Commun* (2017) 8(1):427. doi: 10.1038/s41467-017-00573-w
74. Sarhan J, Liu BC, Muendlein HI, Weindel CG, Smirnova I, Tang AY, et al. Constitutive Interferon Signaling Maintains Critical Threshold of MLKL Expression to License Necroptosis. *Cell Death Different* (2019) 26(2):332–47. doi: 10.1038/s41418-018-0122-7
75. Brault M, Olsen TM, Martinez J, Stetson DB, Oberst A. Intracellular Nucleic Acid Sensing Triggers Necroptosis Through Synergistic Type I IFN and TNF Signaling. *J Immunol* (2018) 200(8):2748. doi: 10.4049/jimmunol.1701492
76. Swanson KV, Junkins RD, Kurkjian CJ, Holley-Guthrie E, Pendse AA, El Morabiti R, et al. A Noncanonical Function of cGAMP in Inflammasome Priming and Activation. *J Exp Med* (2017) 214(12):3611. doi: 10.1084/jem.20171749
77. Gaidt MM, Ebert TS, Chauhan D, Ramshorn K, Pinci F, Zuber S, et al. The DNA Inflammasome in Human Myeloid Cells Is Initiated by a STING-Cell Death Program Upstream of NLRP3. *Cell* (2017) 171(5):1110–1124.e1118. doi: 10.1016/j.cell.2017.09.039
78. Conrad C, Gregorio J, Wang YH, Ito T, Meller S, Hanabuchi S, et al. Plasmacytoid Dendritic Cells Promote Immunosuppression in Ovarian Cancer *via* ICOS Costimulation of Foxp3(+) T-Regulatory Cells. *Cancer Res* (2012) 72(20):5240–9. doi: 10.1158/0008-5472.CAN-12-2271
79. Mitchell D, Chintala S, Dey M. Plasmacytoid Dendritic Cell in Immunity and Cancer. *J Neuroimmunol* (2018) 322:63–73. doi: 10.1016/j.jneuroim.2018.06.012
80. Sisirak V, Faget J, Gobert M, Goutagny N, Vey N, Treilleux I, et al. Impaired IFN-α Production by Plasmacytoid Dendritic Cells Favors Regulatory T-Cell Expansion That May Contribute to Breast Cancer Progression. *Cancer Res* (2012) 72(20):5188. doi: 10.1158/0008-5472.CAN-11-3468
81. Treilleux I, Blay J-Y, Bendriss-Vermare N, Ray-Coquard I, Bachelot T, Guastalla J-P, et al. Dendritic Cell Infiltration and Prognosis of Early Stage Breast Cancer. *Clin Cancer Res* (2004) 10(22):7466. doi: 10.1158/1078-0432.CCR-04-0684
82. Ogilvy S, Metcalf D, Print CG, Bath ML, Harris AW, Adams JM. Constitutive Bcl-2 Expression Throughout the Hematopoietic Compartment Affects Multiple Lineages and Enhances Progenitor Cell Survival. *Proc Natl Acad Sci U.S.A.* (1999) 96(26):14943–8. doi: 10.1073/pnas.96.26.14943
83. Rickard JA, O'Donnell JA, Evans JM, Lalaoui N, Poh AR, Rogers T, et al. RIPK1 Regulates RIPK3-MLKL-Driven Systemic Inflammation and Emergency Hematopoiesis. *Cell* (2014) 157(5):1175–88. doi: 10.1016/j.cell.2014.04.019
84. Takeuchi O, Fisher J, Suh H, Harada H, Malynn BA, Korsmeyer SJ. Essential Role of BAX,BAK in B Cell Homeostasis and Prevention of Autoimmune Disease. *Proc Natl Acad Sci U.S.A.* (2005) 102(32):11272–7. doi: 10.1073/pnas.0504783102
85. Kuida K, Lippke JA, Ku G, Harding MW, Livingston DJ, Su MS, et al. Altered Cytokine Export and Apoptosis in Mice Deficient in Interleukin-1 Beta Converting Enzyme. *Science* (1995) 267(5206):2000–3. doi: 10.1126/science.7535475
86. Vremec D, Pooley J, Hochrein H, Wu L, Shortman K. CD4 and CD8 Expression by Dendritic Cell Subtypes in Mouse Thymus and Spleen. *J Immunol* (2000) 164(6):2978. doi: 10.4049/jimmunol.164.6.2978
87. Livak KJ, Schmittgen TD. Analysis of Relative Gene Expression Data Using Real-Time Quantitative PCR and the 2–ΔΔct Method. *Methods* (2001) 25(4):402–8. doi: 10.1006/meth.2001.1262

Conflict of Interest: HH is an employee of Bavarian Nordic GmbH.

The remaining authors declare that the research was conducted in the absence of any commercial or financial relationships that could be construed as a potential conflict of interest.

Publisher's Note: All claims expressed in this article are solely those of the authors and do not necessarily represent those of their affiliated organizations, or those of the publisher, the editors and the reviewers. Any product that may be evaluated in this article, or claim that may be made by its manufacturer, is not guaranteed or endorsed by the publisher.

frontiers in Immunology

ORIGINAL RESEARCH
published: 10 March 2022
doi: 10.3389/fimmu.2022.840861

Domain-Dependent Evolution Explains Functional Homology of Protostome and Deuterostome Complement C3-Like Proteins

Maoxiao Peng[1,2†], Zhi Li[1,2†], João C. R. Cardoso[2], Donghong Niu[1,3,4], Xiaojun Liu[5], Zhiguo Dong[4], Jiale Li[1,3,4] and Deborah M. Power[2,6*]*

[1] Key Laboratory of Exploration and Utilization of Aquatic Genetic Resources, Ministry of Education, Shanghai Ocean University, Shanghai, China, [2] Comparative Endocrinology and Integrative Biology, Centre of Marine Sciences, Universidade do Algarve, Faro, Portugal, [3] Shanghai Engineering Research Center of Aquaculture, Shanghai Ocean University (SHOU), Shanghai, China, [4] Co-Innovation Center of Jiangsu Marine Bio-industry Technology, Jiangsu Ocean University, Lianyungang, China, [5] Department of Biotechnology and Biomedicine, Yangtze Delta Region Institute of Tsinghua University, Jiaxing, China, [6] Shanghai Ocean University International Center for Marine Studies, Shanghai, China

OPEN ACCESS

Edited by:
Uday Kishore, Brunel University London, United Kingdom

Reviewed by:
Jing Xing, Ocean University of China, China
Miki Nakao, Kyushu University, Japan

***Correspondence:**
Jiale Li
jlli2009@126.com
Deborah M. Power
dpower@ualg.pt

[†]These authors have contributed equally to this work

Specialty section:
This article was submitted to Molecular Innate Immunity, a section of the journal Frontiers in Immunology

Received: *21 December 2021*
Accepted: *10 February 2022*
Published: *10 March 2022*

Citation:
Peng M, Li Z, Cardoso JCR, Niu D, Liu X, Dong Z, Li J and Power DM (2022) Domain-Dependent Evolution Explains Functional Homology of Protostome and Deuterostome Complement C3-Like Proteins. Front. Immunol. 13:840861. doi: 10.3389/fimmu.2022.840861

Complement proteins emerged early in evolution but outside the vertebrate clade they are poorly characterized. An evolutionary model of C3 family members revealed that in contrast to vertebrates the evolutionary trajectory of *C3-like* genes in cnidarian, protostomes and invertebrate deuterostomes was highly divergent due to independent lineage and species-specific duplications. The deduced *C3-like* and vertebrate C3, C4 and C5 proteins had low sequence conservation, but extraordinarily high structural conservation and 2-chain and 3-chain protein isoforms repeatedly emerged. Functional characterization of three *C3-like* isoforms in a bivalve representative revealed that in common with vertebrates complement proteins they were cleaved into two subunits, b and a, and the latter regulated inflammation-related genes, chemotaxis and phagocytosis. Changes within the thioester bond cleavage sites and the a-subunit protein (ANATO domain) explained the functional differentiation of bivalve *C3-like*. The emergence of domain-related functions early during evolution explains the overlapping functions of bivalve *C3-like* and vertebrate C3, C4 and C5, despite low sequence conservation and indicates that evolutionary pressure acted to conserve protein domain organization rather than the primary sequence.

Keywords: conserved domain, functional homologues, parallel evolution, complement C3/C4/C5 family, C3-like protein a-subunit

INTRODUCTION

The complement system is of central importance for immunity and complement 3 (*C3*) is at the core of its function (1–3). C3 belongs to the thioester bond containing protein (TEP) superfamily (4) that also includes α_2-macroglobulin (A2M) (5), pregnancy zone protein (PZP) (6), CD109 (7) and PZP-like A2M domain-containing 8 (CPAMD8) (8). The appearance and differentiation of C3, A2M and CD109 occurred after the divergence of the sponges and before the divergence of cnidaria from the

bilaterian lineage (9, 10). The *C3* gene has been identified in all deuterostomes studied so far (1). Studies directed at deciphering the evolution of the complement system suggest a common ancestral molecule gave rise to *C3* and to two others complement molecules *C4* and *C5* in vertebrates (11–15). The *C3* prototype gene underwent several rounds of duplication before the cyclostome (lampreys and hagfish) divergence and in the vertebrates *C3*, *C4* and *C5* gene members emerged (11, 13). Evolution and function of the complement pathway in the species rich protostome clade is less well resolved (16–20).

The complement system in vertebrates straddles the innate and acquired immune response. It is activated by three pathways [the classical, alternative and mannose binding lectin (MBL)] and all converge on *C3* (21, 22). Complement activation causes proteolytic cleavage of C3, C4 and C5 and generates a smaller anaphylatoxin "a" protein subunit and larger "b" subunit in vertebrates. The end point of the cascade is the formation of the membrane attack complex (MAC, C5bC6C7C8C9) that causes cell lysis (2, 23–25).

We hypothesized that the non-vertebrate prototype *C3* gene, designated *C3-like* in this study, is the functional homologue of vertebrate *C3*, *C4* and *C5* genes. Available evidence indicates that complement activation *via* both the lectin and alternative pathways is possible in protostomes and emerged in a similar evolutionary timeframe in cnidarians (10, 26–29). MAC complex homologues (C6 and C7/C8/C9) have not been identified in protostomes and the main activity assigned to complement is opsonization (30). Nonetheless, genes encoding MAC-type domain containing proteins (MACPF) have been identified in a marine gastropod, the periwinkle (*Littorina littorea*) (31). Moreover, gastropod and bivalve hemolymph has cytotoxic activity (32) and duplicate *C3-like* (*C3-like-1* and *C3-like 2*) genes with hemolytic activity have been identified in the Chinese razor clam (*Sinonovacula constricta*) (14, 33, 34).

Exploiting the burgeoning availability of genomes and transcriptomes for cnidarian, protostomes and invertebrate deuterostomes we establish a model for complement evolution focused on *C3-like* genes and reveal a common origin with vertebrate genes but with highly divergent evolutionary trajectories. The primary amino acid sequence of the deduced C3-like and vertebrate C3, C4 and C5 proteins has low sequence conservation but a well conserved domain structure. Homologues of vertebrate two-chain structural isoforms typical of mature C3 and C5 proteins (composed of α and β subunits) and 3-chain isoforms typical of mature C4 protein (with α, β and γ subunits) (3, 35) repeatedly emerged in the protostomes and other non-vertebrate phyla and share common activities.

RESULTS

C3-Like Genes Evolved by Lineage and Species-Specific Events

Database searches identified *C3-like* genes in 56 species representatives of different phyla (5 Cnidaria, 1 Nemertea, 31 Mollusca, 12 Arthropoda, 4 Echinodermata, 2 Hemichordata, 1 Cephalochordata) and revealed that gene number was variable across species. Phylogenetic analysis (**Figure 1** and **Supplementary Figure 1**) suggested that the metazoan *C3-like* ancestral molecule underwent distinct evolutionary trajectories in different phyla. Although since most sequences were obtained from transcriptomes and not genomes it was unclear if all forms of *C3-like* that exist were retrieved for all species (**Supplementary Table 1**). No clustering with the vertebrate *C3*, *C4* and *C5* was found but phyla specific clustering of the modern *C3-like* genes occurred and the diverse gene number in cnidaria, protostomes and invertebrate deuterostomes resulted from: a) lineage-specific and b) species-specific duplications events. Clustering of the invertebrate deuterostomes (Hemichordata, Echinodermata and Cephalochordata phyla) *C3-like* genes suggest that evolution was similar to the protostome model, but their early radiation prior to the protostome and vertebrate clades explains the greater gene sequence divergence (**Figure 1** and **Supplementary Figure 1**). The *C3-like* gene first emerged in the Cnidaria phylum but was subsequently lost from representative species of the phyla of Annelida, Dicyemida, Platyhelminthes, Nematoda and in some subphylum of Arthropoda (Hexapoda and Crustacea). Lineage duplication events led to multiple *C3-like* genes in Cnidaria (Hexacorallia, subclass), Arthropods (Ixodes and Sarcoptiformes orders) and Mollusca (Gastropoda class) phyla generating two types of *C3-like* (Type I and Type II). Species-specific duplications of the *C3-like* gene were also identified in species of the Arthropoda (Scolopendromorpha and Ixodida order), Mollusca (Cardiida, Venerida, Myida and Unionida orders) and in the deuterostome Echinodermata (Forcipulatida, Valvatida, Aspidochirotida, Camarodonta orders) phyla (**Figure 1**).

C3-Like Proteins Share Conserved Sequence Motifs and Similar Protein Chains With Vertebrates

The 13 characteristic domains of the vertebrate C3, C4 and C5 proteins (3, 36, 37) such as the eight macroglobulin domains (MG1-8); the link domain (LNK), anaphylatoxin domain (ANATO), the complement C1r/C1s, Uegf, Bmp1 domain (CUB), the thioester-containing domain (TED) and the carboxy-terminal domain (C345C) are present in the deduced cnidaria, protostome and invertebrate deuterostome C3-like proteins. The deduced protein structure of C3-like also contained the two enzymatic cleavage sites (α-β and α-γ) (**Figure 2** and **Supplementary Figure 2A**) responsible for the release of β, α and γ protein chains that generate the functional structure. More specifically the "RXXR" motif (where X is K, P, Q, M or T) in the α-β cleavage site and the α-γ cleavage site was highly conserved in C3-like from Cnidaria and other phyla up to the vertebrate C3, C4 and C5 (**Figure 2**). The α-γ cleavage site was absent from some forms of C3-like for example in the Cnidarian, the cauliflower coral *Pocillopora damicornis* C3-like-2 (PdaC3-like-2), in the Arthropoda, the Chinese red-headed centipede *Scolopendra japonica* C3-like-1 (SjaC3-like-1), in the Mollusca, the Chinese razor clam *S. constricta* C3-like-3 (ScoC3-like-3) and in the Echinodermata, the sea urchin *Strongylocentrostus purpuratus* C3-like-1 (SpuC3-like-1). In the ANATO domain, six cysteine (Cys) residues and a C-terminal

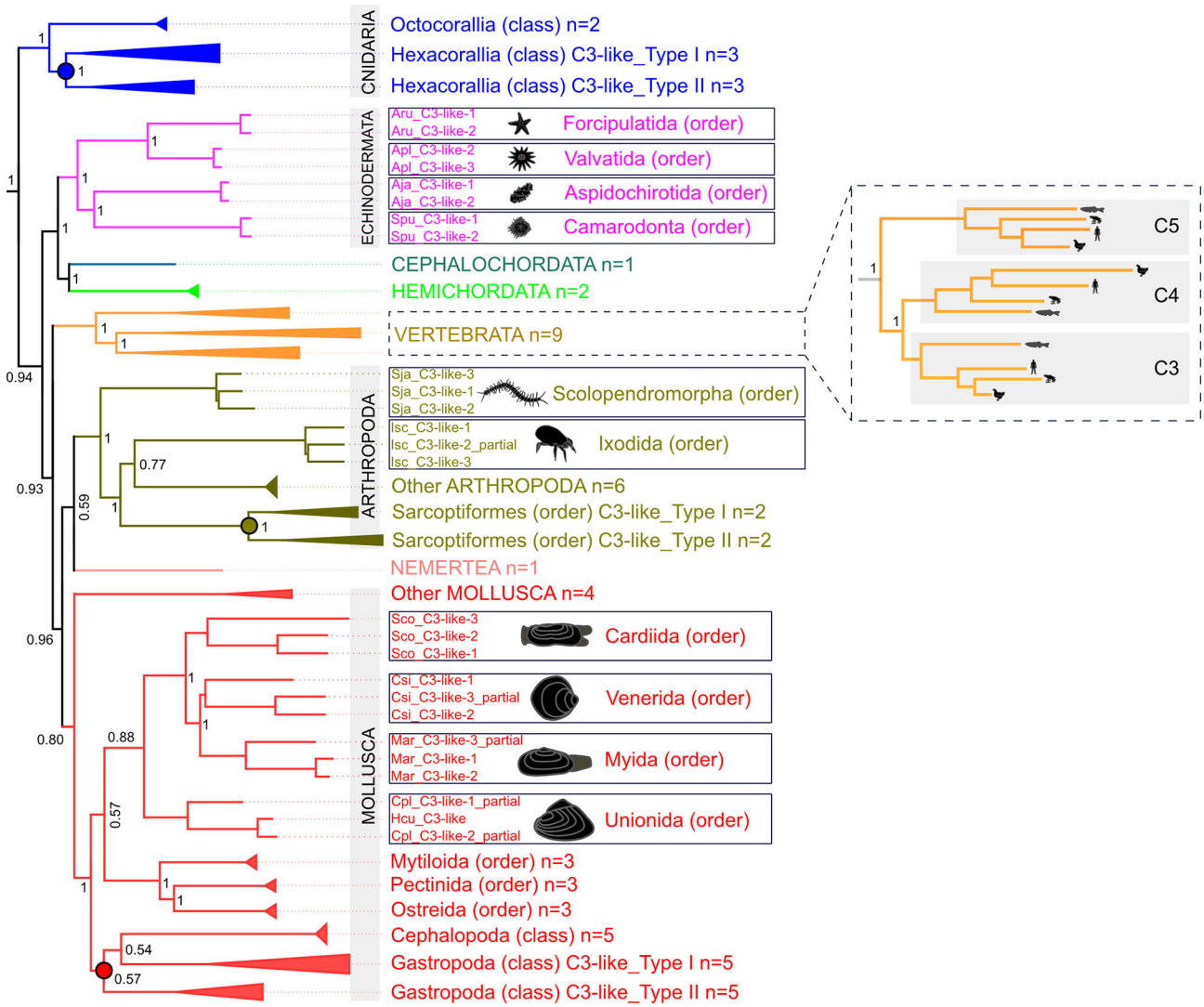

FIGURE 1 | Collapsed phylogenetic tree of the cnidaria, protostomes and invertebrate deuterostomes *C3-like* genes. The phylogenetic tree was constructed using the Bayesian Inference (BI) method and posterior probability values for the main branches are represented. Sequences from 56 species of diverse non-vertebrate phyla and with representatives of different orders and classes were used. Analysis included C3, C4 and C5 from 9 vertebrates for comparisons. To facilitate visualization some branches were collapsed. The tree was rooted with human CD109 and A2MG but these sequences are not shown in the figure. The unedited phylogenetic tree is available as **Supplementary Figure 1A**. Branches with different colors indicate the species of different phyla: Cnidarian (deep blue), Nemertean (pink), Mollusca (red), Arthropoda (olive green), Echinodermata (purple), Cephalochordata (green), Hemichordata (light blue) and Vertebrata (orange). Circles in the branches indicate lineage-specific duplication events. The boxes highlight the sequences that arose by species-specific events and a silhouette of the different animals is presented. The number of species (n) collapsed within each tree branch is indicated. An ML tree with a similar topology is available as **Supplementary Figure 1B**. The source and accession numbers of the sequences used are in **Supplementary Table 1**.

arginine (Arg) residue which are responsible for the activity of the vertebrate protein a-subunit were highly conserved from Cnidaria C3-like up to vertebrate C3, C4 and C5 (**Figure 3** and **Supplementary Figure 2B**). But species-specific *C3-like* gene duplication events in Mollusca and Arthropoda produced a gene isoform with a non-conserved thioester "GCGEQ" bond analogous to what occurs in vertebrate C5. In the gastropods, *C3-like* type I gene encoded a protein that lost the α-β cleavage site, the ANATO domain and had a non-conserved thioester bond.

Mollusca Duplicate C3-Like Isoform Function

The function of protostome *C3-like* isoforms was explored in, a bivalve mollusk (the Chinese razor clam) and their highly conserved domain structure across protostomes favors functional inference. Three *C3-like* gene members exist in the Chinese razor clam (*ScoC3-like-1* to *3*) and arose by species specific gene duplications and their deduced protein structure contained the 13 characteristic motifs, and the conserved α-β (^{665}RVKR^{668}) cleavage site and the ANATO

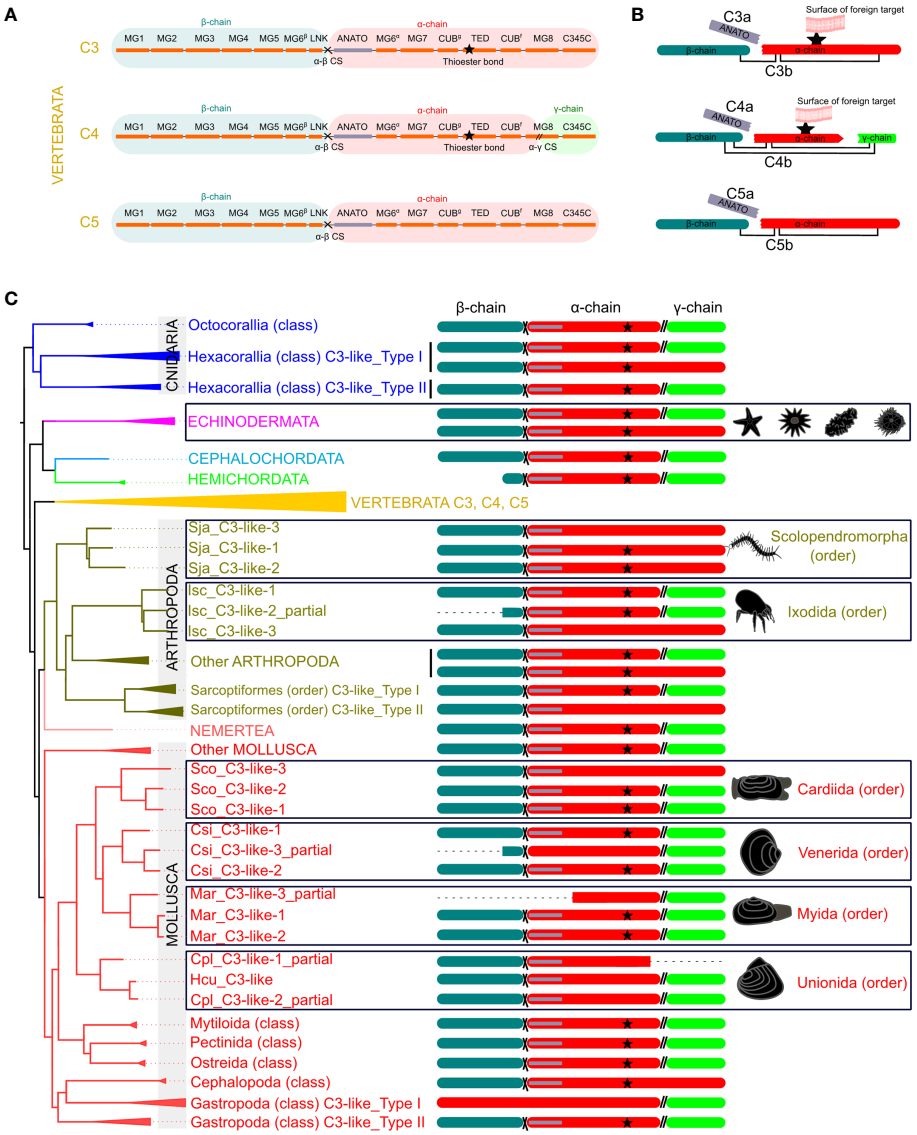

FIGURE 2 | Schematic representation of the protein domains of the vertebrate C3, C4 and C5 and the non-vertebrate C3-like deduced proteins. **(A)** Linear representation of the human C3, C4 and C5 structure with the localization of the 13 domains elucidated from the crystallographic structure of human C3 (3, 36, 37) [eight MG- macroglobulin domains (MG1-8); the link domain (LNK), anaphylatoxin domain (ANATO), the complement C1r/C1s, Uegf, Bmp1 domain (CUB), thioester-containing domain (TED) and the carboxy-terminal domain (C345C)]; the α-β (cross symbol) and α-γ (parallel lines symbol), cleavage sites and the three protein chains (β (blue), α (red) and γ (green) -chain). **(B)** Predicted mature protein structure of human C3, C4 and C5. The two mature protein subunits, "a" (only with the ANATO domain) and "b" for each protein is represented. The star represents the thioester bond, and the connecting lines represent the disulphide bridges that connect the different protein chains. **(C)** Mature protein structure predicted for C3-like. Only the predicted chains and ANATO domains, cleavage sites and thioester bond are represented. The dashed line represents incomplete sequences. The phylogenetic tree represented is a simplified version of **Figure 1** and branches with different colors indicate different phyla. The deduced structure of the C3-like proteins that are proposed to have emerged from species-specific duplication events are boxed to highlight their predicted structural diversity. The detailed figure with all species and protein motifs is available in **Supplementary Figure 2A**. The source and accession numbers of the sequences are given in **Supplementary Table 1**.

domain with six conserved cysteine (Cys) residues (14, 33) (**Figure 3** and **Supplementary Figure 2B**). In ScoC3-like-3, the thioester bond structure (^{1038}GCVSQ^{1042}) was poorly conserved (**Figure 3**). ScoC3-like-1 and ScoC3-like-2 deduced proteins had the three-chain structure (α-β cleavage site and α-γ cleavage site) typical of vertebrate C4 and ScoC3-like-3 had the two-chain structure (α-β cleavage site only) typical of vertebrate C5. All three *C3-like* genes in the Chinese razor clam had a similar tissue distribution and were present in liver, hemocytes, siphon, mantle, foot, gill, and gonad (**Supplementary Figure 3A**). *ScoC3-like-3* was significantly more abundant ($p < 0.001$) in the liver compared to *ScoC3-like-1* and *ScoC3-like-2*.

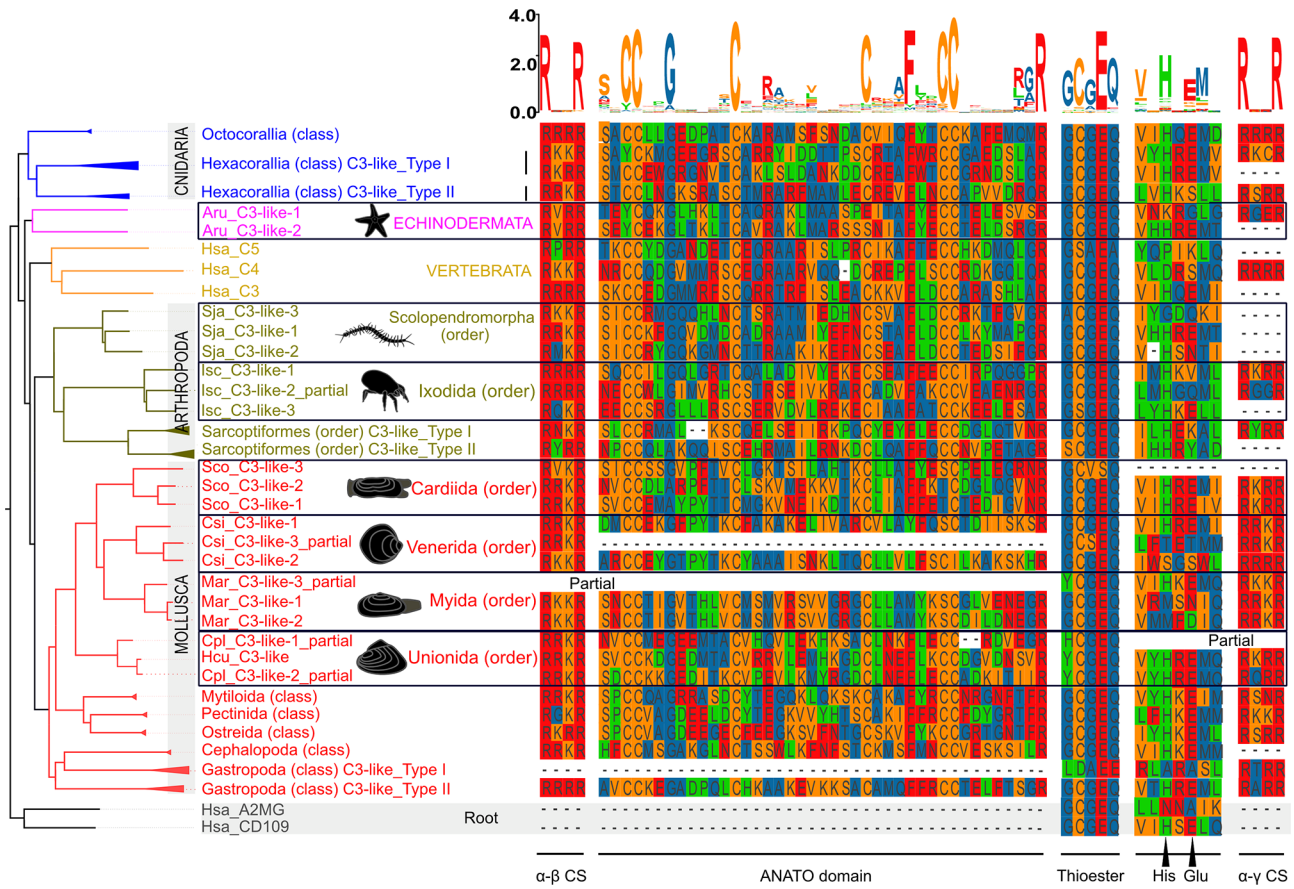

FIGURE 3 | Sequence conservation of the C3-like functional domains and motifs. The alignment of the predicted amino acid sequences for the ANATO domain (a-subunit), the thioester bond and His-Glu amino acid residues essential for the binding of C3 and C4 to the surface of foreign targets, and the two cleavage sites: α-γ(CS) and α-β are represented. This figure is a summary version of the full figure available in **Supplementary Figure 2B**. The different protein domains and motifs represented were deduced from the C3-like sequence alignment containing all collected sequences. Amino acids were colored using the MSA default settings and letters of different heights are indicative of amino acid residue conservation across sequences (the bigger the letter, the higher the sequence conservation). The dashed line indicates the regions where no sequence overlap was found. The sequences of the Echinodermata, Arthropoda and Mollusca species-specific C3-like proteins are boxed. The ANATO domain represented is the automatic trimmed sequence alignment of the most conserved regions using the Multiple alignment trimming tool with a site coverage cut-off= 0.95 in the TBtools software (38). The source and accession numbers of the sequences used are listed in **Supplementary Table 1**.

Cleavage of Bivalve C3-Like Into "a and b" Functional Subunits

ScoC3-like circulates in the hemolymph (**Supplementary Figure 4**). To confirm if ScoC3-like is cleaved into two subunits (a-subunit and b-subunit) as occurs for vertebrate C3, native ScoC3-like-1, ScoC3-like-2 and ScoC3-like-3 in LPS activated razor clam hemolymph (SCH) were analyzed by Mass Spectrometry (MS). The C-like peptide sequences obtained confirmed the presence of the N-terminal a-subunit cleavage site (^{661}RRKR^{664}, ^{661}RRKR^{664} and ^{665}RVKR^{668} in ScoC3-like-1, ScoC3-like-2 and ScoC3-like-3, respectively) and the C-terminal site (^{754}VNR^{756}, ^{754}VNR^{756} and ^{760}RNR^{762} was identified in ScoC3-like-1, ScoC3-like-2 and ScoC3-like-3, respectively) (**Supplementary Table 2**). The theoretical molecular weight of the a-subunit for each ScoC3-like protein isoform (**Supplementary Table 3**) matched the predicted size of the deduced protein sequence indicating that in razor clam the three C3-like isoforms are cleaved, to generate functional "a" and "b" subunits that circulate in SCH.

Functional Divergence of Bivalve C3-Like Subunits

The function of the two C3-like protein subunits (a and b) of the three different razor clam C3-like isoforms was characterized.

C3-Like-b Subunit

A hemolysis-inhibition assay with antisera specific for each ScoC3-like-b isoform was used to determine, which b-subunits provoked significant hemolysis of rabbit erythrocytes (**Figure 4A**). Antisera specific for ScoC3-like-3b did not significantly modify the hemolysis rate ($p > 0.05$). Antisera specific for ScoC3-like-1b (33) and ScoC3-like-2b subunits (14)

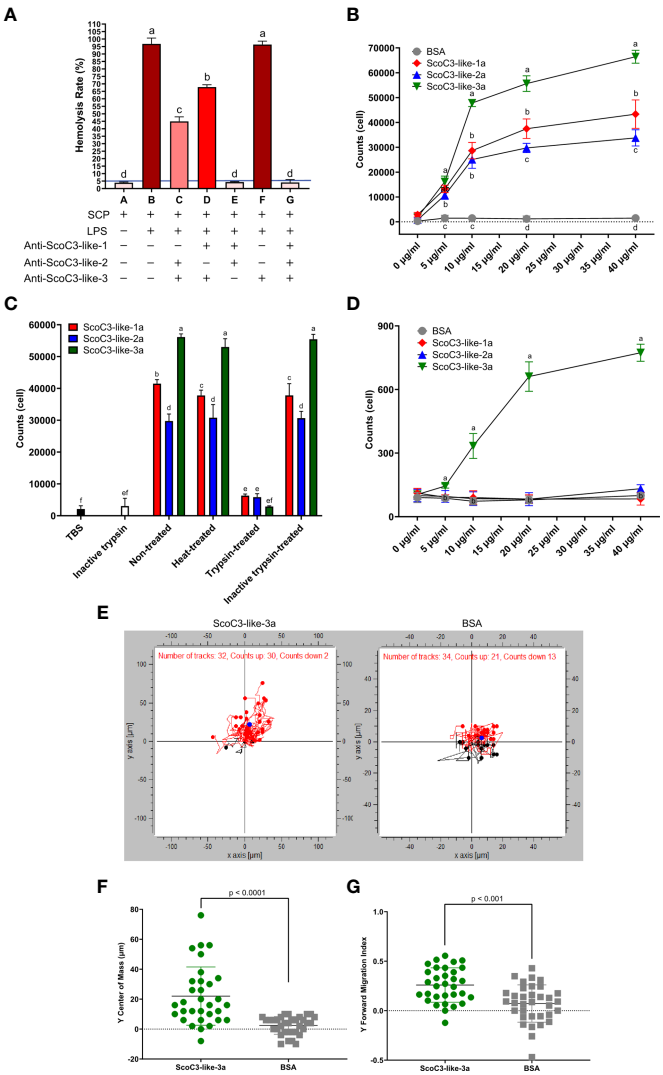

FIGURE 4 | Razor clam C3-like protein functional assays. **(A)** Hemolytic activity. Rabbit erythrocytes were used. The blue line represents the threshold of hemolysis. Results are shown as the mean ± the standard error (SEM, n = 3 assays). "+" means the reagent was added and "-" means the reagent was not added. The increase in color tone of the bars represents the intensity of hemolysis. One-Way Anova was used, and different letters indicate the significantly different groups ($p < 0.001$). **(B)** Chemotaxis response of SCHC to recombinant *S. constricta* a-protein subunits. Values represent the mean ± SEM (n = 3 assays). Different letters indicate significantly different groups ($p < 0.05$). **(C)** Effect of heat and trypsinization of recombinant *S. constricta* a-protein subunits. Bars represent the mean ± SEM (n = 3 assays). One-Way Anova was used, and different letters indicate significantly different groups ($p < 0.05$). **(D)** Effect of recombinant ScoC3-like-a subunits on chemotaxis of J774A.1 cells. BSA was used as the positive control. Values represent the mean ± SEM (n = 3 assays). One-Way Anova was used and groups with different letters are significantly different ($p < 0.05$). **(E)** Migration of J774A.1 cells in response to ScoC3-like-3a. Dark points represent the center of mass (COM), red dots represent the upwards-migrating cells (red lines) and blue dots the downwards-migrating cells (black lines). BSA was used as the negative control. The chemotaxic factors (ScoC3-like-3a or BSA) were added to the lower chamber. The number of cells for which migration was tracked using the automatic setting is indicated: C3-like-3a (exposed group, n=32) and BSA (control group, n=34). **(F)** Scatter plot of the displacement of center of mass (COM) of the J774A.1 cells. Values represent the mean ± SEM (n = 32, automatic detection setting). A students t-test was used to identify significant differences between groups. The p value for the pairwise comparison is shown. **(G)** Scatter plot of the forward migration index (FMI) of the J774A.1 cells. Values represent the mean ± SEM (n = 34, automatic detection setting). A student t-test was used to identify significant differences between groups. The p value for the pairwise comparison is shown.

both caused a significant ($p < 0.05$) reduction in the hemolysis rate. Addition of anti-ScoC3-like-1b serum and anti-ScoC3-like-2b serum to the hemolytic positive control (B) ablated hemolysis, revealing that ScoC3-like-1b and ScoC3-like-2b were hemolytic factors but ScoC3-like-3b was not.

C3-Like-a Subunit

Cell chemotaxis assays and phagocytosis assays were used to characterize the function of the C3-like protein a-subunits. Chemotaxis assays using either razor clam hemocytes (SCHC) or mammalian J774A.1 cells revealed that the recombinant ScoC3-

like-3a was the most active protein isoform in both assays. In the SCHC assay all recombinant ScoC3-like-a forms significantly stimulated cell migration ($p < 0.001$) but ScoC3-like-3a was significantly more active ($p < 0.001$) than the other ScoC3-like a-subunits (**Figure 4B**). Heat-treatment of ScoC3-like-a protein subunits did not significantly modify their capacity to promote SCHC migration and ScoC3-like-3a was still significantly more active ($p < 0.001$) (**Figure 4C**). Treatment of all recombinant ScoC3-like-a protein subunits with trypsin ablated their action.

ScoC3-like-3a was the only protein tested that significantly induced J774A.1 cell chemotaxis ($p < 0.001$) (**Figure 4D**). The induced trajectory of J774A.1 cell chemotaxis towards ScoC3-like-3a and BSA (**Figure 4E**) was 94% and ~62%, respectively. The greater number of J774A.1 cells that migrated towards ScoC3-like-3a, was revealed by the significant upward shift ($p < 0.0001$) of the center mass [COM (blue circle)](**Figure 4F**) and by the induced ($p < 0.001$) Forward Migration Index (FMI) on the Y axis (**Figure 4G**).

The SCHC phagocytic activity against *Staphylococcus aureus* and *Vibrio anguillarum* revealed that all recombinant ScoC3-like a-protein subunits significantly increased ($p < 0.05$) phagocytosis compared to the negative control (TBS) and positive control (bovine serum albumin BSA) (**Figures 5A, B** and **Supplementary Figure 5**). SCHC phagocytic ability was significantly higher in the presence of ScoC3-like-3a ($p < 0.001$ and $p < 0.05$) compared to ScoC3-like-1a and ScoC3-like-2a.

Bivalve C3-Like-a Subunit Induces an Inflammatory Response

The consequences of high circulating levels of ScoC3-like-a in razor clams was assessed by measuring a candidate gene of the inflammatory response (*NF-κB*) and a proinflammatory cytokine (*TNF-α*) *in vivo*. Injection of Sco-C3-like-1a significantly up-regulated ($p < 0.001$) *ScNF-κB* in the liver 4 and 8 h post injection and *ScTNF-α*, 1, 2 and 4 h post injection (**Figures 5C, D**). Injection of ScoC3-like-2a significantly up-regulated ($p < 0.001$) *ScNF-κB*, 1, 2, 4 and 8 h post injection and *ScTNF-α* at 4 and 8 h post injection. ScoC3-like-3a injections provoked a significant up-regulation ($p < 0.001$) of *ScNF-κB* and *ScTNF-α* at 1, 2, 4 and 8 h post injection (**Figures 5C, D**).

DISCUSSION

The phylogenetic analysis in the present study indicates the appearance of multiple *C3-like* genes in cnidaria, protostomes and invertebrate deuterostomes was independent of the process that gave rise to the *C3, C4* and *C5* genes in vertebrates. In phyla where innate immunity is the main defense mechanism appearance of multiple C3-like genes is the prevalent evolutionary model. A putative *C3-like* prototype gene emerged early in evolution after Porifera and during the species radiation it was lost from some species genomes while in others, lineage and species-specific gene duplications occurred which probably contributed to structural and functional diversity (**Figure 6**). In the bivalve mollusk, the Chinese razor clam, three paralogue *C3-like* genes emerged by species-specific gene duplication and shared functions with the vertebrate orthologues.

The complexity of mapping C3 evolution is associated with the greater importance of protein domains and protein structure for function and family member assignment than the primary amino acid sequence. The elucidation of the crystalline structure of mammalian C3 (3), which uncovered high domain/structural similarities with C4 and C5 despite substantial primary sequence divergence consolidated this concept (10). This may explain why evolutionary models based on the comparison of the primary amino acid sequence of non-vertebrate *C3-like* genes fail to cluster gene isoforms within phyla and generate ambiguous evolutionary models. Nonetheless, as observed for vertebrate C3, C4 and C5 high domain/structural similarities existed between the deduced proteins of different *C3-like* gene isoforms (**Figure 6**).

Common structural features of vertebrate C3 and C4 were identified in C3-like isoforms including in the Cnidaria phylum where it first emerged (9, 27, 39). This suggests that the ancestral gene already contained the structural elements responsible for the modern proteins functions and explains the structure/function conservation between vertebrate C3, C4 and C5 and cnidarian, protostome and invertebrate deuterostomes C3-like despite their evolutionary distance (**Figure 6**). In the case of the Chinese razor clam, duplication led to divergence of C3-like isoforms with secondary loss of some structural domains in ScoC3-like-3 and associated functional modifications, which echoes what occurred to vertebrate C4 and C5. The characteristic three-chain structure, α-β cleavage site and α-γ cleavage site of vertebrate C4 was identified in ScoC3-like-1 and ScoC3-like-2 deduced proteins and the two-chain structure, α-β cleavage site and absence of the α-γ cleavage site characteristic of C5 (2, 15) was identified in ScoC3-like-3. In other Mollusks two other C3-like structural isoforms, specific to this phylum, were also predicted. These were found in several gastropods and the deduced proteins had lost important functional domains including the ANATO domain that is responsible for the function of the protein a-subunit raising question about their function (**Figure 6**).

With few exceptions (Gastropods and Scolopendromorpha) a stable and conserved multi-chain structure is the main characteristic of C3-like proteins, which contrasts with the members of the A2M superfamily where no α-β cleavage site exists (11). The structural similarities between deduced C3-like proteins and the TEP superfamily are consistent with its proposed origin from the TEP gene family duplication (1, 9, 40). The *C3-like* gene duplication in Hexacorallia and loss of the α-γ cleavage site in one of the duplicates is reminiscent of the situation that arose in the vertebrate duplication that generated the *C3*, *C4* and *C5* genes (11–15). Although in early vertebrates like the hagfish (*Eptatretus burgeri*), the α-γ cleavage site is still evident in the deduced C3 protein (41, 42) and generates a mature protein with 3 chains. The loss of the α-γ cleavage site in non-vertebrates and vertebrates, was a crucial step in the functional differentiation of the gene duplicates.

The loss of the α-γ cleavage site in *C3-like* occurred independently many times in cnidaria, protostomes and invertebrate deuterostomes during lineage or species-specific gene duplications (**Figure 3**). This was clearly exemplified by the genes and their deduced proteins in the razor clam. *ScoC3-like-*

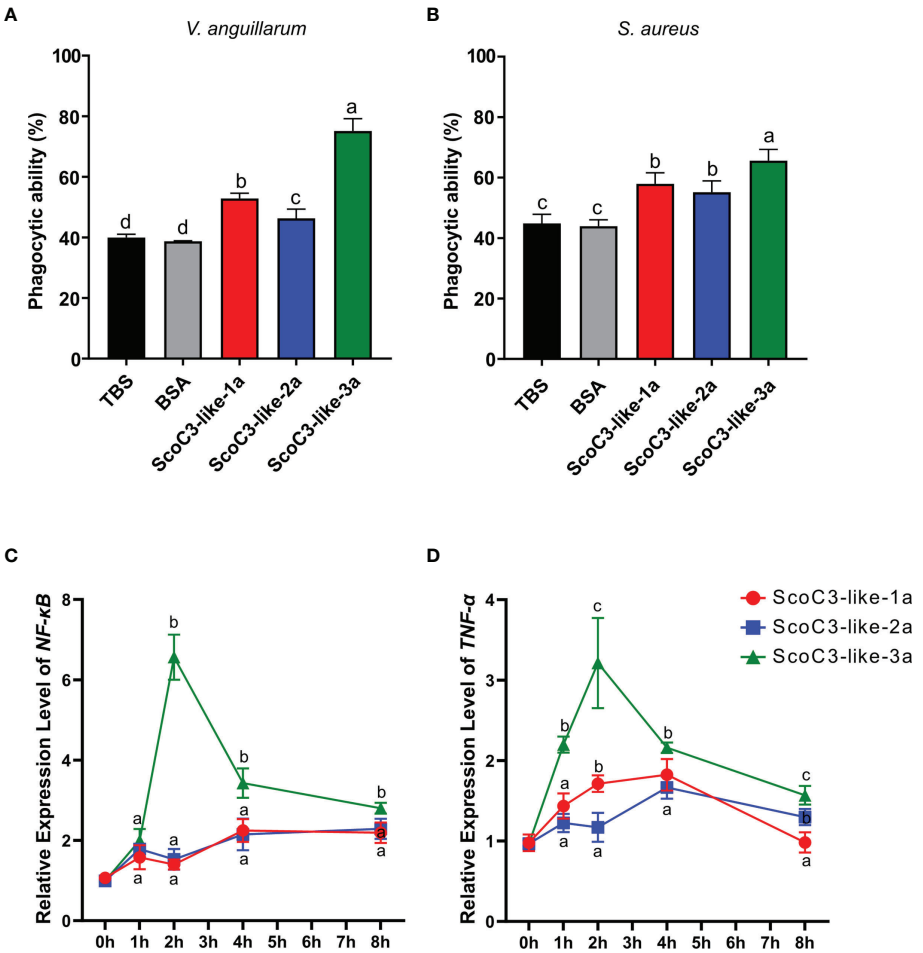

FIGURE 5 | Capacity of the recombinant ScoC3-like-a subunit to induce SCHC phagocytic activity and their role in the regulation of the expression of immune inflammatory factors. For the phagocytosis assays two types of bacteria were used **(A)** *V. anguillarum* and **(B)** *S. aureus* and analysis were performed by flow cytometry. One-Way Anova was used and the groups with different letters are significantly different ($p < 0.05$). Quantitative expression analysis of NF-κB **(C)** and TNF-α **(D)** in Chinese razor clam hemocytes after exposure to recombinant ScoC3-like-a protein subunits. Relative expression level is expressed as fold-change in comparison to the control groups (TBS and BSA treated group). Values represent the mean ± SEM (n = 3 pools composed of 3 individuals/pool). One-Way Anova was performed, and different letters represent significant differences ($p < 0.05$) in relation to the control.

1 and *ScoC3-like-2* generated the more ancient three-chain type protein, while *ScoC3-like-3*, lost the α-γ cleavage site and belongs to the two-chain type. Functional characterization of the razor clam C3-like isoforms generating three-chain or two-chain proteins unveiled the activities of the a-protein subunit, which were reminiscent of vertebrate C4 and C3/C5, respectively (43, 44). Furthermore, the *C3* gene (encoding a two-chain protein) in advanced vertebrates has a specific functional role in the complement signaling pathway, however the *C3* gene of cyclostomes (encoding a three-chain protein) still exhibits a broad activity spectrum (45–47). The functional studies of C3-like isoforms and C3, C4 and C5 in vertebrates fully support the notion that the loss of the α-γ cleavage site contributed to functional differentiation of C3, C4 and C5 family genes (48–50).

From a functional perspective the thioester bond directly interacts with the surface of foreign targets in vertebrate C3 and C4 but not C5 (5, 40) and C3-like in the horseshoe crab (Crustacean, Arthropoda phylum) that retains the thioester bond also bind to the surface of bacteria (30, 39). In vertebrate C3 the thioester bond and the two conserved amino acid residues (His and Glu) in proximity guide foreign target binding and the lack of a thioester bond in C5 explains its functional divergence (5, 40). The results of the phylogenetic and sequence analysis revealed that secondary loss of the thioester bond in C3-like occurred independently many times in cnidarian, protostomes and invertebrate deuterostomes during lineage or species-specific gene duplications. The consequences of *C3-like* gene duplication on the function of the complement system in Mollusca have not previously been described and infrequent reports of *C3-like* genes and immunological activity exist in protostomes (17, 18, 30, 39, 51). The functional significance of the structural changes in the non-vertebrate C3-like proteins exemplified by the results

of the razor clam is reported for the first time. Based on structure/function relationships the razor clam genes were divided into 2 groups (ScoC3-like1/2 and ScoC3-like-3) that mirrored the modified protein structure found in vertebrate C4 and C5 (**Figure 6**) and both ScoC3-like-1 and 2 were potent hemolytic factors that bind to the surface of pathogens (14, 33). In vertebrates, even though C5 lost the thioester bond, C5b is part of the MAC complex that causes cell lysis. ScoC3-like-3b also lacks the thioester bond but is not a hemolytic factor and its function in the mollusca complement pathway remains to be established.

The complement a-protein subunit is produced from the ANATO domain, which contains six conserved cysteine residues and one cleavage site (35). The convertase cleavage site of the ANATO region (L-R) was conserved across most vertebrates (35, 44) and was missing from the sea cucumber (*A. japonicus*, R-R) (20), Ciona (*C. intestinalis*, Q-G-R) (43) and sea squirt (*Halocynthia roretzi*, T-S-R) (52). Nonetheless, although the L-R site was missing in cnidaria, protostomes and invertebrate deuterostomes LC-MS of razor clam C3-like revealed cleavage occurred at non-consensus sites (e.g V-N-R, R-N-R) to generate the a and b-protein subunit. The anaphylactic activity of the C3-like-a protein subunits in razor clam differed in potency (ScoC3-like-3a > ScoC3-like-1a, ScoC3-like-3a > ScoC3-like-2a) much like the human C3/C4/C5-a protein subunit (35, 53). The chemotactic activity of the razor

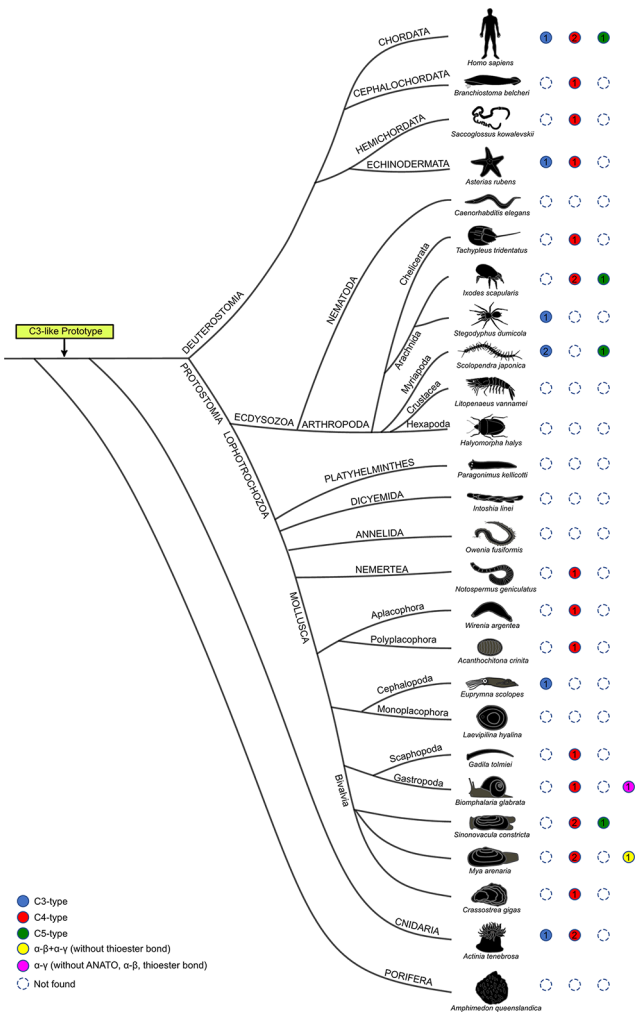

FIGURE 6 | Structural homology of the predicted non-vertebrate C3-like proteins with the vertebrate C3, C4 and C5 proteins. Circles of different color represent the distinct structural isoforms predicted. Human C3, C4 and C5 are represented at the top for comparison. Dashed circles represent gene absence and the numbers inside the colored circles indicate the number of proteins with similar structure found in the species. Blue circles, indicate that a C3-like protein is predicted with a functional structure consistent with the vertebrate C3 (which contains the α-β cleavage site, ANATO and thioester bond); Red circles, indicate that a C3-like isoform is predicted with a functional structure similar to vertebrate C4 (α-β and α-γ cleavage sites, ANATO and thioester bond); Green circles, indicate that a C3-like isoform is predicted with a functional structure similar to vertebrate C5 (α-β cleavage site and ANATO). Two other C3-like protein structures (colored yellow and pink) that have no representatives in vertebrates were identified in Mollusca.

clam C3-like-a protein subunits on hemocytes and mice macrophage was coherant with their structural and functional conservation with vertebrate C5a activity on neutrophils, monocytes, and macrophages (54) and C3a on eosinophils and mast cells (54, 56, 57). A C3-like-a protein subunit that induces chemotaxis of ascidian (*Pyura stolonifera*) hemocytes was proposed to act *via* a C3aR-dependent mechanism due to the conserved high-level structure of ascidian C3-like-a and vertebrate C3a (58). The recent identification of a complement a-subunit receptor protein in the Heterodonta clade (29) leads us to speculate that the mechanisms determining ScoC3-like-3a induced chemotaxis of bivalve hemocytes may also be *via* a C3aR-like dependent pathway.

CONCLUSION

An evolutionary model for the C3 gene family in metazoans was developed and revealed gene family expansion occurred by both lineage and species-specific duplications in cnidarian, protostomes and invertebrate deuterostomes. The main structural domains characteristic of vertebrate C3, C4 and C5 were already present in the ancestral genes and differentiated independently during the evolution of *C3-like* genes. Conservation of the ancestral prototype C3 protein domains in cnidarian, protostomes, invertebrate deuterostomes and vertebrates were associated with functional homology and indicates parallel evolution occurred. The complement system provides an example of how proteins with a strong link between domain structure and function influence gene evolution.

We demonstrate that the parallel functional evolution of the C3, C4, C5 and C3-like genes resulted from a common process, the secondary loss of specific functional domains due to gene duplication, which corroborates the *secondary loss evolutionary model* of Nonaka and Kimura (10).

The detailed evolutionary and functional analysis of C3-like in bivalves leads us to propose that overall, the complement system in mollusks shares the core functions of C3, C4 and C5 in vertebrates. The results of the present study, taken with data from other studies (14, 28, 33, 34) indicate the complement system in cnidarian, protostomes and invertebrate deuterostomes acquired unique characteristics: 1) it does not rely on a MAC structure to cause lysis and 2) novel reaction cascade pathways are triggered by C3-like.

MATERIALS AND METHODS

Animals, Experimental Conditions, and Tissue Sampling

Chinese razor clam (*Sinonovacula constricta*) is a non-endangered species. Adult razor clams (body weight 8.5 ± 0.5 g, length 5.0 ± 0.3 cm) were collected from Donghang Farm (Zhejiang Province, China) and used in the experiments. Approximately 300 adult razor clams were maintained in a 40 L tank (80×50×30cm) with oxygenated freshwater at 24 – 25°C and 20 ‰ salinity. Half of the tank water was renewed daily. Experimental animals were anesthetized on ice before tissue collection and were opened by cutting the adductor mussel and hinge with a blade. The SCH was collected from the cardiocoelom using a sterile 1000 μL syringe (14) and each sample represents a pools of 9 animals. The SCH was centrifuged to separate the SCHC and filtered twice (0.22 μm) to remove any cells, bacteria, or other debris. The collected SCH was used in: Western blot (WB), immunoprecipitation (IP), hemolysis assays and mass spectrometry (MS). The pelleted SCHCs were washed and resuspended in Tris Buffered Saline (TBS, 50 mM; Tris-Cl pH 8.0; 300 mM NaCl) before determination of cell migration and phagocytic activity. All tissues collected were immediately frozen in Liquid nitrogen and stored at -80°C.

Database Searches, Phylogeny Analysis and Protein Motif Annotation

Human C3, C4 and C5 sequences were used as queries to retrieve putative C3-like genes/transcripts (*e-value* ≤ $1e^{-40}$) from 66 species representative of different animal phyla (Anthozoa, Nemertea, Mollusca, Arthropoda, Echinodermata, Chordata) in public databases (**Supplementary Table 1**). The identity of retrieved sequences was confirmed by searching against NCBI (nr, taxid:9606). Multiple sequence alignments (MSA) were made using the MUSCLE algorithm (59) and the deduced amino acid sequence (60). For the phylogenetic analysis removal of gaps and improvement of alignments was achieved by manual editing of the MSA and two tree-building methods were used: Maximum Likelihood (ML) and Bayesian Inference (BI). The BI tree was built in the CIPRES Science Gateway v3 using a WAG substitution model (selected using model test-ng 0.1.5) and run on XSEDE v3.2.7a with 1.000.000 generation sampling and probability values to support tree branching. The ML tree was built in PhyML 3.0 from the ATGC bioinformatics platform (http://www.atgc-montpellier.fr/phyml/ with the same model and 100 bootstrap replicates. Trees were displayed in FigTree 1.4.3 (http://tree.bio.ed.ac.uk/software/figtree), rooted with human CD109 and A2MG and edited in the Inkscape program (https://inkscape.org). An MSA of the full length deduced amino acid sequence of vertebrate C3, C4 and C5 and non-vertebrate C3-like was used to identify common protein domain structures according to (3, 36, 37) and specific motifs/domains that included the α-β cleavage site, ANATO domain, the α-γ cleavage site, Thioester bond site and the downstream His-Glu amino acid residues were analyzed in detail. MSA were displayed using TBtools (38) software.

Mass Spectroscopy

Mass spectroscopy (MS) was used to determine if ScoC3-like-3 was cleaved and if cleavage liberated C3-like3a and C3-like-3b protein subunits. Complement activation reactions were carried out by adding LPS (0.2 μg) to SCH (200 μL) and incubating for 1h at room temperature. The reaction mix (20 μL of the reaction mix) was analyzed on a 10% SDS-PAGE polyacrylamide gel stained with Coomassie Brilliant Blue. The region of the gel between 7-15 kDa (corresponding to the predicted size of C3-like-3a) and between 60-135 kDa (corresponding to the predicted size of C3-like-3b) were

excised and analyzed by MS (UHPLC Systems, UltiMate 3000, Thermo Fisher, USA) and the output data analyzed using Mascot 2.2 software (see **Supplementary Methods**).

Hemolytic Activity

The hemolytic activity of three ScoC3-like isoforms was determined using rabbit erythrocytes in TBS and protein specific antisera (ScoC3-like-1b and ScoC3-like-2b (34) and ScoC3-like-3b antisera). For the hemolysis assays, triplicate 200 µL reactions were set-up for each treatment and incubated at 28°C with occasional mixing for 5 h (**Supplementary Table 4**, see **Supplementary Methods**). The experiment was repeated on two other independent occasions. The hemolysis rate was calculated using the formula: (Sample OD − PBS OD) × 100/ (water OD − PBS OD). A hemolysis rate of less than 5% was taken to indicate no hemolysis occurred [Mayer (61)].

Cell Chemotaxis Assay

The capacity of each isoform of ScoC3-like-a (0, 5, 10, 20 and 40 µg/ml) to stimulate chemotaxis was tested with SCHC and with a mammalian monocyte macrophage cell line (J774A.1) derived from tumors of BALB/c mice (FH0329, FuHeng Cell Center, Shanghai, China). Three independent assays were performed. Cells were activated by exposure for 12 h to 200 nm/ml LPS (from *Escherichia coli* O111:B4, Sigma-Aldrich, USA) and Transwell chemotaxis assays were performed at 28°C for 3 h with the SCHC cells and at 37°C for 2 h with the J774A.1 cells (see **Supplementary Methods**). Cells that migrated to the lower chamber were analyzed with a flow cytometer (BD C6Plus, BD Biosciences, USA). Control assays included the use of C3-like-a proteins exposed to heat-treated, trypsin-treated, or heat inactivated trypsin. A µ-Slide Chemotaxis assay (µ-Slide Chemotaxis ibiTreat, Ibidi, Germany) (62, 63), was used to confirm the observed effects of ScoC3-like-3a (see **Supplementary Methods**). The µ-Slide was observed using an inverted microscope (DMI8, Leica, Germany) and the cell migration captured by photographing preparations every 2 min over 90 min. Cell trajectories (32 and 34 cells in C3-like-a exposed and BSA group, respectively) of the three assays were analyzed using the ImageJ (NIH, Bethesda, MD) program and the Ibidi chemotaxis with the migration tool. Displacement of center of mass (COM) and the forward migration index (FMI) was determined (64).

Phagocytosis Assay

Phagocytosis by SCHC of heat killed bacteria (*S. aureus* and *V. anguillarum*) labelled with FITC was assessed in the presence and absence of the recombinant ScoC3-like-a proteins by flow cytometry (BD C6Plus) and dot plots collected (see **Supplementary Material**). Three independent assays were set up. The phagocytic ratio of SCHC was established by applying the formula: 100% × (total SCHC – non-phagocytic SCHC)/total SCHC.

In Vivo Injection of ScoC3-Like-a Protein Subunit

The consequences of high circulating levels of each of the 3 isoforms of ScoC3-like-a subunits *in vivo* was analyzed. Approximately 175 adult razor clams acclimated to the experimental conditions (outlined above) were used and divided into 5 groups (35 animals per group). The control group was injected with 100 µL TBS into the foot and four treatment groups were injected with either 40 µg of BSA or the recombinant ScoC3-like-1a, ScoC3-like-2a, or ScoC3-like-3a (see **Supplementary Methods** for recombinant protein production). After injection six individuals from each group were killed at 0, 1, 2, 4 and 8 h and the liver was dissected out and stored at -80°C until analysis. The candidate genes chosen to monitor the immune response were *TNF-α* and *NF-κB* obtained from a cDNA library (65) (**Supplementary Table 5**). Total RNA, cDNA and expression analysis were performed as described above.

DATA ANALYSIS

SPSS 19.0 statistical software was used for data analysis. Data from qRT-PCR and functional assays were analyzed using a Fisher LSD one-way ANOVA to determines significant differences between groups ($p < 0.05$). The data in **Figures 4F, G** were analyzed using a Student *t*-test to determine the existence of significant differences between groups ($p < 0.05$). Data are presented as the mean ± SEM. Figures were plotted using GraphPad Prism software (V8.0.2, USA).

DATA AVAILABILITY STATEMENT

The datasets presented in this study can be found in online repositories. The names of the repository/repositories and accession number(s) can be found in the article/**Supplementary Material**.

AUTHOR CONTRIBUTIONS

JL, DN, XL, ZD, and DP planned and supervised the study. MP and JC performed the bioinformatic and comparative analysis. MP and ZL performed the experimental work. MP, JC, and DP analyzed the results and wrote the manuscript. All authors contributed to the article and approved the submitted version.

FUNDING

This work was supported by a National Key R & D plan "Blue Granary Science and Technology Innovation" special project (grant number 2019YFD0900700), the National Natural Science Foundation of China (grant number 31472278), the National Natural Science Foundation of China (grant number 32072975) and by the Portuguese Foundation for Science and Technology (FCT) through project UIDB/04326/2020 and from CRESC Algarve 2020 and COMPETE 2020 through the project EMBRC.PT ALG-01-0145-FEDER-022121. ZL was supported by a PhD scholarship from the China Scholarship Council.

SUPPLEMENTARY MATERIAL

The Supplementary Material for this article can be found online at: https://www.frontiersin.org/articles/10.3389/fimmu.2022.840861/full#supplementary-material

REFERENCES

1. Nonaka M. Evolution of the Complement System. *SubCell Biochem* (2014) 80:31–43. doi: 10.1007/978-94-017-8881-6_3
2. Liszewski MK, Farries TC, Lublin DM, Rooney IA, Atkinson JP. Control of the Complement System. *Adv Immunol* (1996) 61:201–83. doi: 10.1016/S0065-2776(08)60868-8
3. Janssen BJC, Huizinga EG, Raaijmakers HCA, Roos A, Daha MR, Nilsson-Ekdahl K, et al. Structures of Complement Component C3 Provide Insights Into the Function and Evolution of Immunity. *Nature* (2005) 437:505–11. doi: 10.1038/nature04005
4. Gehring M, Shiels B, Northemann W, De Bruijn M, Kan CC, Chain A, et al. Sequence of Rat Liver Alpha 2-Macroglobulin and Acute Phase Control of Its Messenger RNA. *J Biol Chem* (1987) 262:446–45. doi: 10.1016/S0021-9258(19)75947-X
5. Dodds MW, Alex LS. The Phylogeny and Evolution of the Thioester Bond-Containing Proteins C3, C4 and α2–Macroglobulin. *Immunol Rev* (1998) 166:15–26. doi: 10.1111/j.1600-065X.1998.tb01249.x
6. Sottrup-Jensen L, Folkersen J, Kristensen T, Tack BF. Partial Primary Structure of Human Pregnancy Zone Protein: Extensive Sequence Homology With Human Alpha 2-Macroglobulin. *Proc Natl Acad Sci* (1984) 81:7353–7. doi: 10.1073/pnas.81.23.7353
7. Lin M, Sutherland DR, Horsfall W, Totty N, Yeo E, Nayar R, et al. Cell Surface Antigen CD109 Is a Novel Member of the Alpha(2) Macroglobulin/C3, C4, C5 Family of Thioester-Containing Proteins. *Blood* (2002) 99:1683–91. doi: 10.1182/blood.V99.5.1683
8. Li Z, Wu X, Engvall E. Identification and Characterization of CPAMD8, a Novel Member of the Complement 3/Alpha2-Macroglobulin Family With a C-Terminal Kazal Domain. *Genomics* (2004) 83:1083–93. doi: 10.1016/j.ygeno.2003.12.005
9. Fujito NT, Sugimoto S, Nonaka M. Evolution of Thioester-Containing Proteins Revealed by Cloning and Characterization of Their Genes From a Cnidarian Sea Anemone, *Haliplanella Lineate*. *Dev Comp Immunol* (2010) 34:775–84. doi: 10.1016/j.dci.2010.02.011
10. Nonaka M, Kimura A. Genomic View of the Evolution of the Complement System. *Immunogenetics* (2006) 58:701–13. doi: 10.1007/s00251-006-0142-1
11. Hughes AL. Phylogeny of the C3/C4/C5 Complement-Component Gene Family Indicates That C5 Diverged First. *Mol Biol Evol* (1994) 11:417–25. doi: 10.1093/oxfordjournals.molbev.a040123
12. Marino R, Kimura Y, De Santis R, Lambris JD, Pinto M. Complement in Urochordates: Cloning and Characterization of Two C3-Like Genes in the Ascidian *Ciona Intestinalis*. *Immunogenetics* (2002) 53:1055–64. doi: 10.1007/s00251-001-0421-9
13. Najafpour B, Cardoso JCR, Canário AVM, Power DM. Specific Evolution and Gene Family Expansion of Complement 3 and Regulatory Factor H in Fish. *Front Immunol* (2020) 2020:568631. doi: 10.3389/fimmu.2020.568631
14. Peng M, Niu D, Chen Z, Lan T, Dong Z, Tran T-N, et al. Expression of a Novel Complement C3 Gene in the Razor Clam *Sinonovacula Constricta* and Its Role in Innate Immune Response and Hemolysis. *Dev Comp Immunol* (2017) 73:184–92. doi: 10.1016/j.dci.2017.03.027
15. Reid K, Bentley D, Campbell R, Chung L, Sim R, Kristensen T, et al. Complement System Proteins Which Interact With C3b or C4b A Superfamily of Structurally Related Proteins. *Immunol Today* (1986) 7:230–4. doi: 10.1016/0167-5699(86)90110-6
16. Gross PS, Clow LA, Smith LC. SpC3, the Complement Homologue From the Purple Sea Urchin, *Strongylocentrotus Purpuratus*, Is Expressed in Two Subpopulations of the Phagocytic Coelomocytes. *Immunogenetics* (2000) 51:1034–44. doi: 10.1007/s002510000234
17. Prado-Álvarez M, Rotllant J, Gestal C, Novoa B, Figueras A. Characterization of a C3 and a Factor B-Like in the Carpet-Shell Clam, *Ruditapes Decussatus*. *Fish Shellfish Immunol* (2009) 26:305–15. doi: 10.1016/j.fsi.2008.11.015
18. Castillo MG, Goodson MS, McFall-Ngai M. Identification and Molecular Characterization of a Complement C3 Molecule in a Lophotrochozoan, the Hawaiian Bobtail Squid *Euprymna Scolopes*. *Dev Comp Immunol* (2009) 33:69–76. doi: 10.1016/j.dci.2008.07.013
19. Sekiguchi R, Nonaka M. Evolution of the Complement System in Protostomes Revealed by *De Novo* Transcriptome Analysis of Six Species of Arthropoda. *Dev Comp Immunol* (2015) 50:58–67. doi: 10.1016/j.dci.2014.12.008
20. Zhou Z, Sun D, Yang A, Dong Y, Chen Z, Wang X, et al. Molecular Characterization and Expression Analysis of a Complement Component 3 in the Sea Cucumber (*Apostichopus Japonicus*). *Fish Shellfish Immunol* (2011) 31:540–7. doi: 10.1016/j.fsi.2011.06.023
21. Sarma JV, Ward PA. The Complement System. *Cell Tissue Res* (2010) 343:227–35. doi: 10.1007/s00441-010-1034-0
22. Merle NS, Church SE, Fremeaux-Bacchi V, Roumenina LT. Complement System Part I–molecular Mechanisms of Activation and Regulation. *Front Immunol* (2015) 6:262. doi: 10.3389/fimmu.2015.00262
23. Weigle WO, Morgan EL, Goodman MG, Chenoweth DE, Hugli TE. Modulation of the Immune Response by Anaphylatoxin in the Microenvironment of the Interacting Cells. *Fed Proc* (1982) 41:3099–103.
24. Pangburn MK, Rawal N. Structure and Function of Complement C5 Convertase Enzymes. *Biochem Soc Trans* (2002) 30:1006–10. doi: 10.1042/bst0301006
25. Muller-Eberhard HJ. The Membrane Attack Complex of Complement. *Annu Rev Immunol* (1986) 4:503–28. doi: 10.1146/annurev.iy.04.040186.002443
26. Zhu Y, Thangamani S, Ho B, Ding JL. The Ancient Origin of the Complement System. *EMBO J* (2005) 24:382–94. doi: 10.1038/sj.emboj.7600533
27. Kimura A, Sakaguchi E, Nonaka M. Multi-Component Complement System of Cnidaria: C3, Bf, and MASP Genes Expressed in the Endodermal Tissues of a Sea Anemone, *Nematostella Vectensis*. *Immunobiology* (2009) 214:165–78. doi: 10.1016/j.imbio.2009.01.003
28. Peng M, Li Z, Niu D, Liu X, Dong Z, Li J. Complement Factor B/C2 in Mollusks Regulates Agglutination and Illuminates Evolution of the Bf/C2 Family. *FASEB J* (2019) 33:13323–33. doi: 10.1096/fj.201901142RR
29. Yan X, Nie H, Huo Z, Ding J, Li Z, Yan L, et al. Clam Genome Sequence Clarifies the Molecular Basis of Its Benthic Adaptation and Extraordinary Shell Color Diversity. *Iscience* (2019) 19:1225–37. doi: 10.1016/j.isci.2019.08.049
30. Cerenius L, Kawabata S-I, BL L, Nonaka M, Söderhäll K. Proteolytic Cascades and Their Involvement in Invertebrate Immunity. *Trends Biochem Sci* (2010) 35:575–83. doi: 10.1016/j.tibs.2010.04.006
31. Gorbushin AM. Membrane Attack Complex/Perforin Domain-Containing Proteins in a Dual-Species Transcriptome of Caenogastropoda *Littorina Littorea* and Its Trematode Parasite *Himasthla Elongata*. *Fish Shellfish Immunol* (2016) 54:254–6. doi: 10.1016/j.fsi.2016.04.015
32. Klimovich AV, Gorbushin AM. Evolutionary Radiation of Cytotoxic Effects in Bivalve and Gastropod Haemolymph. *J Evol Biochem Physiol* (2017) 53:470–9. doi: 10.1134/S0022093017060047
33. Peng M, Niu D, Wang F, Chen Z, Li J. Complement C3 Gene: Expression Characterization and Innate Immune Response in Razor Clam *Sinonovacula Constricta*. *Fish Shellfish Immunol* (2016) 55:223–32. doi: 10.1016/j.fsi.2016.05.024
34. Niu D, Xiong Y, Peng M, Meng X, Lan T, Li J. Hemolytic Reactions in the Hemolymph of Bivalve *Sinonovacula Constricta* Show Complement-Like Activity. *Fish ShellFish Immunol* (2018) 79:11–7. doi: 10.1016/j.fsi.2018.04.062
35. Hugh TE. Structure and Function of the Anaphylatoxins. *Springer Semin Immunopathol* (1984) 7:193–219. doi: 10.1007/BF01893020
36. Mortensen S, Kidmose RT, Petersen SV, Szilágyi A, Prohászka Z, Andersen GR. Structural Basis for the Function of Complement Component C4 Within the Classical and Lectin Pathways of Complement. *J Immunol* (2015) 194:5488–96. doi: 10.4049/jimmunol.1500087
37. Fredslund F, Laursen NS, Roversi P, Jenner L, Oliveira CLP, Pedersen JS, et al. Structure of and Influence of a Tick Complement Inhibitor on Human Complement Component 5. *Nat Immunol* (2008) 9:753–60. doi: 10.1038/ni.1625
38. Chen C, Chen H, Zhang Y, Thomas HR, Frank MH, He Y, et al. TBtools: An Integrative Toolkit Developed for Interactive Analyses of Big Biological Data. *Mol Plant* (2020) 13:1194–202. doi: 10.1016/j.molp.2020.06.009
39. Ariki S, Takahara S, Shibata T, Fukuoka T, Ozaki A, Endo Y, et al. Factor C Acts as a Lipopolysaccharide-Responsive C3 Convertase in Horseshoe Crab Complement Activation. *J Immunol* (2008) 181:7994–8001. doi: 10.4049/jimmunol.181.11.7994
40. Pinto MR, Melillo D, Giacomelli S, Sfyroera G, Lambris JD. Ancient Origin of the Complement System: Emerging Invertebrate Models. (2007), 372–88. In. Current Topics in Innate Immunity: Springer. Advances in Experimental Medicine and Biology, vol. 598. doi: 10.1007/978-0-387-71767-8_26

41. Fujii T, Kunisada S. The Association of the Subunits of Component C3 of Hagfish Complement Is Unstable and Leads to Novel Degradation During Electrophoresis. *Immunol Cell Biol* (1997) 75:568–74. doi: 10.1038/icb.1997.88
42. Fujii T, Nakamura T, Tomonaga S. Component C3 of Hagfish Complement has a Unique Structure: Identification of Native C3 and Its Degradation Products. *Mol Immunol* (1995) 32:633–42. doi: 10.1016/0161-5890(95)00033-B
43. Pinto MR, Chinnici CM, Kimura Y, Melillo D, Marino R, Spruce LA, et al. CiC3-1a-Mediated Chemotaxis in the Deuterostome Invertebrate *Ciona Intestinalis* (Urochordata). *J Immunol* (2003) 171:5521–8. doi: 10.4049/jimmunol.171.10.5521
44. Gao Z, Li M, Wu J, Zhang S. Interplay Between Invertebrate C3a With Vertebrate Macrophages: Functional Characterization of Immune Activities of Amphioxus C3a. *Fish Shellfish Immunol* (2013) 35:1249–59. doi: 10.1016/j.fsi.2013.07.049
45. Li J, Liu H, Ma Q, Song X, Pang Y, Su P, et al. VLRs Expression Were Significantly Affected by Complement C3 Knockdown Morphants in *Lampetra Morii*. *Fish Shellfish Immunol* (2020) 106:307–17. doi: 10.1016/j.fsi.2020.07.013
46. Lv W, Ma A, Chi X, Li Q, Pang Y, Su P. A Novel Complement Factor I Involving in the Complement System Immune Response From *Lampetra Morii*. *Fish Shellfish Immunol* (2020) 98:988–94. doi: 10.1016/j.fsi.2019.11.017
47. Dodds AW, Matsushita M. The Phylogeny of the Complement System and the Origins of the Classical Pathway. *Immunobiology* (2007) 212:233–43. doi: 10.1016/j.imbio.2006.11.009
48. Nonaka M. Molecular Analysis of the Lamprey Complement System. *Fish Shellfish Immunol* (1994) 4:437–46. doi: 10.1006/fsim.1994.1039
49. Matsushita M. The Complement System of Agnathans. *Front Immunol* (2018) 9:1405. doi: 10.3389/fimmu.2018.01405
50. Nonaka M, Kuroda N, Naruse K, Shima A. Molecular Genetics of the Complement C3 Convertases in Lower Vertebrates. *Immunol Rev* (1998) 166:59–65. doi: 10.1111/j.1600-065X.1998.tb01252.x
51. Chen Y, Xu K, Li J, Wang X, Ye Y, Qi P. Molecular Characterization of Complement Component 3 (C3) in *Mytilus Coruscus* Improves Our Understanding of Bivalve Complement System. *Fish Shellfish Immunol* (2018) 76:41–7. doi: 10.1016/j.fsi.2018.02.044
52. Nonaka M, Azumi K, Ji X, Namikawa-Yamada C, Sasaki M, Saiga H, et al. Opsonic Complement Component C3 in the Solitary Ascidian, *Halocynthia Roretzi*. *J Immunol* (1999) 162:387–91.
53. Hugli T. The Structural Basis for Anaphylatoxin and Chemotactic Functions of C3a, C4a, and C5a. *Crit Rev Immunol* (1981) 1:321–66.
54. Daffern PJ, Pfeifer PH, Ember JA, Hugli TE. C3a Is a Chemotaxin for Human Eosinophils But Not for Neutrophils. I. C3a Stimulation of Neutrophils Is Secondary to Eosinophil Activation. *J Exp Med* (1995) 181:2119–27. doi: 10.1084/jem.181.6.2119
55. Ember JA, Hugli TE. Complement Factors and Their Receptors. *Immunopharmacology* (1997) 38:3–15. doi: 10.1016/S0162-3109(97)00088-X
56. Hartmann K, Henz BM, Krüger-Krasagakes S, Köhl J, Burger R, Guhl S, et al. C3a and C5a Stimulate Chemotaxis of Human Mast Cells. *Blood* (1997) 89:2863–70. doi: 10.1182/blood.V89.8.2863
57. Nilsson G, Johnell M, Hammer CH, Tiffany HL, Nilsson K, Metcalfe DD, et al. C3a and C5a Are Chemotaxins for Human Mast Cells and Act Through Distinct Receptors *via* a Pertussis Toxin-Sensitive Signal Transduction Pathway. *J Immunol* (1996) 157:1693–8.
58. Raftos DA, Robbins J, Newton RA, Nair SV. A Complement Component C3a-Like Peptide Stimulates Chemotaxis by Hemocytes From an Invertebrate Chordate—the Tunicate, *Pyura Stolonifera*. *Comp Biochem Physiol A Mol Integr Physiol* (2003) 134:377–86. doi: 10.1016/S1095-6433(02)00287-8
59. Edgar RC. MUSCLE: Multiple Sequence Alignment With High Accuracy and High Throughput. *Nucleic Acids Res* (2004) 32:1792–7. doi: 10.1093/nar/gkh340
60. Larsson A. AliView: A Fast and Lightweight Alignment Viewer and Editor for Large Datasets. *Bioinformatics* (2014) 30:3276–8. doi: 10.1093/bioinformatics/btu531
61. Zhu Z. Modified Mayer's Assay for Total Complement Activity (Single Tube Colorimetric Method). *Chin J Clin Lab Sci* (1986) 4:71–3.
62. Ocaña-Morgner C, Reichardt P, Chopin M, Braungart S, Wahren C, Gunzer M, et al. Sphingosine 1-Phosphate-Induced Motility and Endocytosis of Dendritic Cells Is Regulated by SWAP-70 Through RhoA. *J Immunol* (2011) 186:5345–55. doi: 10.4049/jimmunol.1003461
63. Pepperell E, Watt S. A Novel Application for a 3-Dimensional Timelapse Assay That Distinguishes Chemotactic From Chemokinetic Responses of Hematopoietic CD133+ Stem/Progenitor Cells. *Stem Cell Res* (2013) 11:707–20. doi: 10.1016/j.scr.2013.04.006
64. Chmilewsky F, Jeanneau C, Laurent P, About I. Pulp Fibroblasts Synthesize Functional Complement Proteins Involved in Initiating Dentin–Pulp Regeneration. *Am J Pathol* (2014) 184:1991–2000. doi: 10.1016/j.ajpath.2014.04.003
65. Niu D, Wang L, Sun F, Liu Z, Li J. Development of Molecular Resources for an Intertidal Clam, *Sinonovacula Constricta*, Using 454 Transcriptome Sequencing. *PloS One* (2013) 8:e67456. doi: 10.1371/journal.pone.0067456

Conflict of Interest: The authors declare that the research was conducted in the absence of any commercial or financial relationships that could be construed as a potential conflict of interest.

Publisher's Note: All claims expressed in this article are solely those of the authors and do not necessarily represent those of their affiliated organizations, or those of the publisher, the editors and the reviewers. Any product that may be evaluated in this article, or claim that may be made by its manufacturer, is not guaranteed or endorsed by the publisher.

frontiers in Immunology

REVIEW
published: 16 March 2022
doi: 10.3389/fimmu.2022.866747

Targeting Neutrophils for Promoting the Resolution of Inflammation

János G. Filep [1,2*]

[1] Department of Pathology and Cell Biology, University of Montreal, Montreal, QC, Canada, [2] Research Center, Maisonneuve-Rosemont Hospital, Montreal, QC, Canada

Acute inflammation is a localized and self-limited innate host-defense mechanism against invading pathogens and tissue injury. Neutrophils, the most abundant immune cells in humans, play pivotal roles in host defense by eradicating invading pathogens and debris. Ideally, elimination of the offending insult prompts repair and return to homeostasis. However, the neutrophils` powerful weaponry to combat microbes can also cause tissue damage and neutrophil-driven inflammation is a unifying mechanism for many diseases. For timely resolution of inflammation, in addition to stopping neutrophil recruitment, emigrated neutrophils need to be disarmed and removed from the affected site. Accumulating evidence documents the phenotypic and functional versatility of neutrophils far beyond their antimicrobial functions. Hence, understanding the receptors that integrate opposing cues and checkpoints that determine the fate of neutrophils in inflamed tissues provides insight into the mechanisms that distinguish protective and dysregulated, excessive inflammation and govern resolution. This review aims to provide a brief overview and update with key points from recent advances on neutrophil heterogeneity, functional versatility and signaling, and discusses challenges and emerging therapeutic approaches that target neutrophils to enhance the resolution of inflammation.

Keywords: neutrophil, neutrophil trafficking, apoptosis, neutrophil extracellular trap, pro-resolving mediators, GPCRs, resolution of inflammation

OPEN ACCESS

Edited by:
Francesca Granucci, University of Milano-Bicocca, Italy

Reviewed by:
Nicola Tamassia, University of Verona, Italy
Maria Rosaria Galdiero, University of Naples Federico II, Italy

***Correspondence:**
János G. Filep
janos.g.filep@umontreal.ca

Specialty section:
This article was submitted to Molecular Innate Immunity, a section of the journal Frontiers in Immunology

Received: *31 January 2022*
Accepted: *21 February 2022*
Published: *16 March 2022*

Citation:
Filep JG (2022) Targeting Neutrophils for Promoting the Resolution of Inflammation. Front. Immunol. 13:866747. doi: 10.3389/fimmu.2022.866747

INTRODUCTION

Acute inflammation is a localized, self-limited, multicellular innate host-defense mechanism against invading pathogens and tissue injury. Polymorphonuclear neutrophil granulocytes play pivotal roles in host defense and are rapidly deployed to the affected sites, where they engage in immediate and intense antimicrobial responses (1–3). Elimination of the offending insult ideally prompts repair of the collateral tissue damage, restoration of tissue function and return to homeostasis (4). However, the neutrophils` powerful weaponry to combat pathogens can cause collateral damage to the host (5). This will then amplifies the initial response through feed-forward inflammatory mechanisms, leading to loss of functional tissue and ultimately to organ dysfunction (6). Neutrophil-driven inflammation is a common mechanism for many diseases, including reperfusion injury, atherosclerosis, cancer, autoimmune diseases, neurodegeneration, and obesity (1, 5, 7). The capacity of neutrophils to augment tissue damage beyond that evoked by the initial infection or tissue injury itself, suggest that early checkpoints control neutrophil kinetics and fate within the

inflamed tissue to prevent secondary tissue damage by these effector cells. To assure timely resolution of inflammation, neutrophil influx needs to be stopped, and emigrated neutrophils need to be disarmed and removed from the affected sites.

Neutrophils sense and integrate signals from the inflammatory microenvironment, which modulate their survival and function, and generate cues that can orchestrate innate or adaptive immune effector responses (1, 8). These include secretion of granular proteins (9, 10) cytokines (11), extracellular vesicles (12), neutrophil extracellular traps (13) and formation of membrane tethers (named cytonemes) (14). The role of neutrophils in initiation and progression of a wide range of pathologies makes neutrophils attractive therapeutic targets. However, the critical requirement of neutrophils for antibacterial host defense limits the usefulness of therapies that globally reduce neutrophil numbers or functional responses. Current treatments that target single mediators of inflammation may have limited efficacy because of the redundancy within the innate immune system and many eventually become immunosuppressive (15). Arguably, an ideal therapeutic strategy would be to prevent or reverse neutrophil-mediated tissue injury without impairing their ability to control microbial invasion. One way to develop innovative approaches for the treatment of inflammatory pathologies is to exploit neutrophil biology to enhance the resolution of inflammation. We provide here a brief overview and update with key points from recent advances on neutrophil heterogeneity, functional versatility and signaling, which can be exploited to enhance resolution of inflammation.

NEUTROPHILS IN HOMEOSTASIS AND PATHOGENESIS

Protective Versus Uncontrolled Inflammation

The acute inflammatory response is protective and resolves on their own. Neutrophils are the most abundant leukocytes in blood and form the first line of cellular defense against invading pathogens (1, 2). Neutrophils deploys a potent enzymatic and chemical arsenal to neutralize and clear invaders and necrotic tissues (2, 3) and to facilitate repair (16). Neutrophil trafficking into tissues is a multistep, tightly controlled process (17–19). Aberrant neutrophil recruitment and activation causes tissue damage that amplifies the initial inflammatory response and may continue to chronicity (3, 5, 9).

Preclinical data indicate that impaired neutrophil removal from inflamed tissues results in aggravation and prolongation of the inflammatory responses (5). Accumulating evidence indicates that ongoing inflammation is a prominent component of many diseases, including cardiovascular, acute respiratory, neurodegenerative, metabolic, and autoimmune diseases, arthritis, inflammatory bowel disease, periodontitis and sepsis (7, 18).

The resolution of inflammation is an active process, integrating mechanisms that lead to the restoration of normal tissue function. This process is governed by specialized pro-resolving lipid mediators (lipoxins, resolvins, protectins and maresins), proteins (e.g., annexin A1and galectins) and gaseous mediators (e.g. hydrogen sulfite and carbon monoxide) produced during resolution of self-limited inflammation (15, 20, 21).These mediators act predominantly on phagocytes and other immune cells to instruct repair. Their biosynthesis, receptors, cellular targets, signaling pathways and networks have been described in several excellent reviews (15, 20), and mapped into the searchable Atlas of Inflammation Resolution (21), hence will not be reviewed here. Low grade ongoing inflammation is thought to impair activation of the resolution process (5, 22). Defect in resolution mechanism is increasingly being recognized as an important trigger for acute exacerbation of chronic inflammatory conditions as reported for atherosclerotic plaque rupture (23, 24) or propagation of bacterial infection in mice (25).

While pro-resolving mediators signal through several distinct receptors, two receptors, the β2 integrin Mac-1 (CD11b/CD18) and formyl peptide receptor 2/lipoxin A_4 receptor (ALX/FPR2) have emerged as master regulators of neutrophil responses and fates.

Mac-1 functions as a bidirectional allosteric "signaling machine" (26). Mac-1 is best known for mediating neutrophil adherence to the activated endothelium and the extracellular matrix (17, 18) and phagocytosis of complement C3b-opsonized bacteria (27). Mac-1 binding to platelets, immune complexes or myeloperoxidase generates survival signals (28), leading to preservation of Mcl-1, the central regulator of lifespan of human neutrophils (29). Phagocytosis of opsonized bacteria induces ROS-dependent activation of caspase-8, which overrides Mac-1 ligation-activated survival signals, resulting in apoptosis (30, 31). Caspase-8 forms a complex with FLIP (FLICE-inhibitory protein), which inhibits RIPK3-dependent necrosis and prevents degranulation (32, 33). Mac-1 also binds neutrophil elastase that directs reverse transendothelial migration (34).

ALX/FPR2 is a member of the formyl peptide receptor family, consisting of three class A G-protein-coupled receptors that share significant sequence homology (35). Formyl peptide receptors recognize pathogen-associated molecular patterns (PAMPs) and damage-associated molecular patterns (DAMPs) to initiate innate immunity. ALX/FPR2 binds an unusually large number of structurally diverse ligands, including proteins, peptides and lipids, and conveys contrasting biological effects (35, 36). For example, ligation of ALX/FPR2 with the acute-phase protein serum amyloid A or the antimicrobial peptide LL-37 activates proinflammatory circuits (37, 38). Annexin A1, annexin A1-derived peptide Ac2-26, lipoxin A_4, aspirin-triggered 15-epi-LXA_4 and 17-epi-RvD1 also signal through ALX/FPR2 to limit neutrophil trafficking and lifespan and to promote efferocytosis (25, 39, 40), critical events in the resolution of inflammation. Interestingly, opposing ALX/FPR2 ligands, such as serum amyloid A and lipoxin A_4, allosterically inhibit each other to bias ALX/FPR2 signaling to promote either inflammation or resolution (37, 41). ALX/FPR2 can form homodimers and heterodimers with FPR1 receptor in ligand-dependent manner, resulting in alternate patterns of downstream signal coupling that dictate neutrophil functional responses (42–45). Recent data suggest that lipoxin A_4

may act as a biased allosteric modulator, exerting a dual regulatory mechanism on intracellular cAMP accumulation and Ca^{2+} mobilization (45). Binding of serum amyloid A to ALX/FPR2 decreases formation of homodimers and induces phosphorylation of ERK and Akt, whereas lipoxin A_4 engagement increases heterodimerization with FPR1 with activation of the JNK-caspase-3 pathway, leading to apoptosis in neutrophils (42, 43). While the structural basis of diverse downstream signaling remains largely unexplored, ALX/FPR2 contains a C-terminal motif that mediates receptor recycling following endocytosis and provides protection against apoptosis (46).

Evolving evidence suggest that neutrophils also contribute to wound healing, revascularization and tissue repair (16, 47, 48). Infiltrating neutrophils provide fibronectin as "emergency extracellular matrix" to promote early bone fracture healing (49) and neutrophil-derived matrix metalloprotease 9 facilitates tissue repair in acute lung injury (50). Neutrophil gelatinase-associated lipocalin (NGAL) was reported to orchestrate post-myocardial infarction by increasing the capacity of cardiac macrophages to clear apoptotic cells in mice (51). Conversely, defect in phagocytosis or neutrophil-induced genomic instability in epithelial cells impedes resolution of inflammation and wound healing (12).

Neutrophil Heterogeneity

Neutrophils are traditionally viewed as a relatively homogeneous cell population with highly conserved function. This perception is, however, rapidly evolving as accumulating data indicate heterogeneity in morphology, phenotype or function under homeostatic and a variety of pathological conditions (52–57). Neutrophil classification has traditionally relied on morphology, gradient separation or surface markers. However, the exact function of some neutrophil subpopulations remain elusive. Single cell RNA sequencing revealed transcriptomically distinct neutrophil populations, even amongst mature peripheral neutrophils (58, 59) and neutrophils associated with chronic inflammatory states (58, 60–62). Different neutrophil states in healthy mice and humans can be projected onto a signal development continuum (termed neutrotime) characterized by clearly defined poles separated by a smooth transcriptome shift (63). Linking the neutrophil transcriptome to the neutrophil phenotype or functional properties will, however, require further investigations. For instance, expression of $CD177^+$ (together with membrane-bound proteinase 3) on a subset of human neutrophils facilitates their transmigration (64), hence antimicrobial defense, whereas the elevated frequency of $CD117^+$ neutrophils is associated with increased risk of relapse in patients with ANCA-dependent vasculitis (65, 66). VEGF-A recruits a distinct subset of neutrophils with proangiogenic properties into transplanted hypoxic tissues to facilitate restoration of blood supply (67). Reduced CD62L expression on circulating neutrophils defines "senescent" or "aged" neutrophils, which are destined for clearance (68). Neutrophil senescence is controlled by circadian oscillations in the hematopoietic niche (69), the microbiome (70) and the clock-related genes, such as Bmal1 and the CXCR2 signaling pathway (68). Functional heterogeneity, such as competitive phagocytosis (71), in the human circulating neutrophil pool has also been reported, though linking functional responses to phenotype remains challenging.

The widely used term "low density neutrophils" ("low density granulocytes" or "granulocytic myeloid-derived suppressor cells") also refers to a heterogeneous population of $CD66b^+$mature and immature neutrophils with both proinflammatory and immunosuppressive properties (53). Both immature (banded neutrophils) and hypersegmented neutrophils have been identified in this neutrophil subset (53). Hence, the buoyant density of neutrophils is partially coupled to maturation and may rather reflect a spectrum of different densities found in healthy individuals (72). Since mature neutrophils decrease their density when activated *in vitro*, circulating low density neutrophils have been suggested to acquire the activated phenotype within the tissue, perhaps indicating neutrophils that underwent reverse transmigration (72, 73). Consistently, homing neutrophils to the lung was found to switch to an activated phenotype irrespective of the inflammatory disease (74). Low density neutrophils have been implicated in the pathogenesis of systemic lupus erythematosus, albeit it is uncertain whether they are premature neutrophils released from the bone marrow (75) or represent a distinct lineage of neutrophils caused by genomic damage (76). CD10 was suggested as a marker to distinguish proinflammatory and immunosuppressive neutrophils within heterogeneous neutrophil populations in patients with acute or chronic inflammatory diseases (77). A recent study has identified two neutrophil subsets, $CD123^+$ immature neutrophils and programmed death-ligand 1 $(PD\text{-}L1)^+/CD10^-$ neutrophils as potential biomarkers for patients with sepsis (78). Future studies are needed to elucidate the contribution of these subsets to the pathogenesis of sepsis.

Distinct subsets of tumor infiltrating neutrophils have also been identified. The N1 subset, characterized by hypersegmented nuclei possesses potent tumor killing capacity, whereas the N2 subset that displays an immature phenotype favors tumor growth in mice (79). Although the origin of the N1 and N2 populations is uncertain (80), TGF-β and IFN-β have been implied in polarizing neutrophils toward the N1 phenotype (81, 82). Another subset of tumor-associated neutrophils with antigen-presenting cell features has been found to trigger an anti-tumor T cell response in early-stage of human lung cancer (83). Tumor growth is associated with loss of this neutrophil subset and functional divergence of tumor-associated neutrophils (83, 84).

Mature neutrophils exhibit transcriptional and translational plasticity in response to signals from the inflammatory environment (11) and display a cell-specific pattern of non-coding regulatory regions (85). Thus, *de novo* synthesis of cytokines and membrane receptors, e.g. program death ligand 1 (PD-L1), may alter neutrophil function and contribute to heterogeneity. The importance of gene expression regulation of neutrophils is illustrated by the association of altered methylation profiles with susceptibility to lupus erythematosus (86). Metabolic

reprogramming also occurs during the neutrophil life cycle. Neutrophils may utilize glycogen for fuel during phagocytosis or under hypoglycemic conditions (87, 88), and glycogen levels may directly control their lifespan (89). Furthermore, neutrophils exposed to PGE_2 or PGD_2 induces a phenotype switch from LTB_4 production to lipoxin production, which marks the resolution phase (15, 90), further highlighting the functional diversity of these cells.

Fate of Emigrated Neutrophils

Neutrophils recruited to the site of infection or tissue injury engage in different activities to respond to the initial insult, which will also determine that fate and govern their ultimate removal from the inflamed area, critical for protective inflammation and return to homeostasis. By contrast, suppression of certain neutrophil functions or excessive neutrophil responses contribute to uncontrolled inflammation and may lead to chronicity. These responses are discussed in the following sections and summarized on **Figure 1**.

Neutrophil Swarming

Following transendothelial migration, neutrophils congregate or swarm in tissues, forming clusters around the infected or damaged core to seal off the affected site (90–93). Neutrophil contact with necrotic cells is critical to initiate swarming (94), followed by coordinated LTB_4 release form neutrophils (91, 95), leading to formation of a stable LTB_4 gradient that drives concerted waves of neutrophil migration (91, 95). Microscale protein arrays have identified numerous protein mediators, including galectin-3, CXCL8, lipocalin-2 and pentraxin-3that can further enhance LTB_4-driven neutrophil swarming (95). Mac-1 (CD11b) and LFA-1 (CD11a) mediate neutrophil

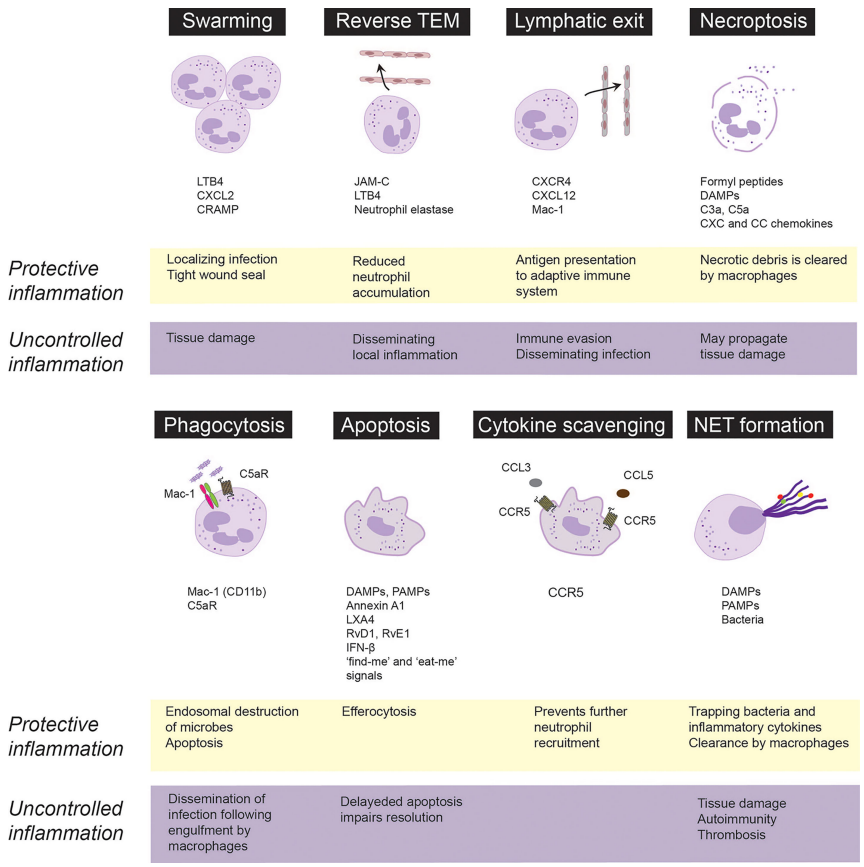

FIGURE 1 | Fate and roles of emigrated neutrophils in protective vs. uncontrolled inflammation. Neutrophils are rapidly recruited from the circulation to the infected or injured tissues. Following extravasation, neutrophils swarm toward the infected sites to localize infection and from a tight wound seal. Neutrophils may trap, neutralize and kill invading pathogens through necroptosis, phagocytosis or release of extracellular traps (NETs). Phagocytosis of opsonized bacteria usually induces apoptosis followed by phagocytosis of apoptotic cells by macrophages *via* efferocytosis. Neutrophils integrate pro-survival and apoptosis-promoting cues from the inflammatory environment, which governs their lifespan. Apoptotic neutrophils express CCR5, which by binding chemokines prevents further neutrophil recruitment. Excessive swarming and necroptosis may aggravate and perpetuate tissue damage. Neutrophils may egress from the inflammatory locus through reverse transendothelial migration (TEM) or lymphatic vessels, which dampen neutrophil accumulation, but may also lead to immune evasion and dissemination of local inflammation. Neutrophils carrying bacteria that they cannot destroy, may serve as "Trojan horses" to disseminate the infection on phagocytosis of apoptotic neutrophils by macrophages. CRAMP, cathelin-related antimicrobial peptide; DAMPs, damage-associated molecular patterns, JAM-C, junctional adhesion molecules C; LTB_4, leukotriene B_4; LXA_4, lipoxin A_4; PAMPs, pathogen-associated molecular patterns; RvD1, resolvin D1; RvE1, resolvin E1.

accumulation in the collagen-free injury center (91). Chemokine receptor trafficking and the LTB_4 receptor BLT1 coordinate dense neutrophils clusters to form a tight wound seal (91, 96). Development of human neutrophil swarms is associated with lipid mediator class-switching, leading to generation of lipoxin A_4 and resolvin E3, which, in turn, can limit swarm size (95). By cloaking the injured area (sensing and removing debris as well as damage-associated alarmins), tissue-resident macrophages also contribute to sealing off the damage by preventing initiation of the LTB_4-driven feedforward signaling cascade that results in neutrophil swarms (94).

Neutrophil swarming has been found to limit tissue damage and contain pathogens in a variety of preclinical models (91, 94, 97, 98), indicating a protective role. Swarming behavior of neutrophils from patients following major trauma or patients receiving immunosuppressive therapy is deficient and is associated with increased susceptibility and reduced ability to clear bacterial (99) or fungal infections (100). Excessive neutrophil swarming leads to collateral tissue damage through release of neutrophil granule content *via* frustrated phagocytosis or necrosis (3, 101) as exemplified by pulmonary ischemia reperfusion injury in mice (97) and inflammation flares around uric acid crystals in gout (102).

Reverse Transendothelial Migration and Lymphatic Exit

Advances in intravital imaging technologies have revealed that transmigrated neutrophils can also exhibit motility away from inflamed sites, return across the endothelium and re-enter circulation (34, 103–106). Neutrophil reverse transmigration is most prevalent in tissues subjected to ischemia-reperfusion injury (106, 107). Luminal to abluminal transendothelial migration is regulated by various junctional proteins, including VE-cadherin, platelet endothelial cell adhesion molecule-1 and CD99, whereas reverse transmigration predominantly depends on junctional adhesion molecule-C (JAM-C) (106). Under ischemic conditions, excessive production of LTB_4 induces neutrophil degranulation, expression of neutrophil elastase on Mac-1, which leads to JAM-C degradation and reverse transmigration (34). Reverse transmigrated neutrophils display a different phenotype, characterized by high ICAM-1 and low CXCR1 expression, increased capacity to produce superoxide and prolonged lifespan (103, 106), thereby contributing to the heterogeneity of circulating neutrophils. The biological consequences of reverse transmigration are unclear and may depend on the circumstances. As reverse transendothelial migration leads to removal of neutrophils from the inflamed site, it may function as a protective mechanism that limits the inflammatory response (104, 108). On the contrary, reverse transmigration could lead to systemic propagation of inflammation or distant organ injury in mice subjected to cremaster muscle or lower-limb ischemia-reperfusion injury (34, 106).

An alternative way of neutrophil egress from the inflamed site may involve the exit through the lymphatic vessels. During infection, neutrophils were detected carrying living bacteria from the infected tissue to draining lymph nodes in mice (109–112). Skin egress of neutrophils *via* lymphatic vessels depends on CXCR4 and its ligand CXCL12 expressed by lymphatic endothelial cells as well as on Mac-1 (111, 113), though the counter-ligand for Mac-1 remains to be identified. *Staphylococcus aureus*-pulsed neutrophils recruited into the lymph node acquire the phenotype (expression of major histocompatibility complex (MHC) II and the costimulatory molecules CD80 and CD86) and functionality of antigen-presenting cells to initiate adaptive immunity (111, 114). By contrast, other studies have proposed that neutrophils carrying bacteria or viruses may lead to immune evasion and permit the dissemination of the infection upon engulfment by macrophages (115, 116).

Neutrophil Lifespan, Apoptosis and Efferocytosis

Mature neutrophils have a short half-life in the circulation (117, 118) and die rapidly *via* apoptosis (119). Following recruitment to inflamed tissues, neutrophil lifespan is increased through delaying apoptosis in response to PAMPs, DAMPs and environmental signals, though the extent of increased lifespan remains unknown (120, 121). Neutrophils contribute to interstitial acidosis, which serves as a danger signal (121) that extends neutrophil lifespan by preserving the expression of the anti-apoptotic protein Mcl-1 (122). Hypoxia or bacterial infections even under normoxia were shown to induce release of HIF-1α and HIF-2α, which generates survival cues for neutrophils and enhances their bactericidal activity to restrict systemic spread of infection (123, 124). Activated neutrophils release myeloperoxidase that activates a Mac-1-centered feed-forward loop to induce degranulation and generate survival signals, thereby perpetuating the inflammatory response (28). Conversely, genetic deletion of myeloperoxidase or disruption of the myeloperoxidase-triggered feedforward loop with 15-epi-LXA_4 limits neutrophil-evoked tissue damage and facilitates resolution (40, 125, 126).

Extended neutrophil lifespan through delayed apoptosis is a common feature of many inflammatory diseases, including sepsis (127, 128), acute respiratory distress syndrome (129), severe asthma (130) and acute coronary syndrome (131), and is associated with disease severity. In experimental models, suppressing neutrophil apoptosis prolongs and aggravates the inflammatory response (28, 132), whereas promoting neutrophil apoptosis with cyclin-dependent kinase inhibitors (133), 15-epi-LXA_4 (40), or IFN-β (134) accelerates the resolution of inflammation. Consistently, genetic deletion of the pro-apoptotic ARTS protein hinders the execution of the intrinsic apoptosis program in neutrophils and delays activation of resolution programs (135).

Phagocytosis of complement-opsonized bacteria or necrotic cells overrides survival signals generated by Mac-1 ligation and accelerates neutrophil apoptosis (also known as phagocytosis-induced cell death or PICD) (30, 31). Complement-mediated phagocytosis is governed by a delicate balance between Mac-1 and the complement C5a receptor (C5aR or CD88) (136, 137). Thus, reduced Mac-1 expression or genetic deletion of C5aR disables phagocytosis and reduces bacterial killing (136, 138).

Bacterial or mitochondrial DNA signaling through TLR-9 upregulates Mac-1 expression and induces neutrophil elastase and proteinase 3-mediated shedding of C5aR, leading to reduced phagocytosis of *E. coli*, suppressed PICD and efferocytosis, thereby prolonging acute lung injury in mice (25). Conversely, by preventing TLR9 activation-mediated Mac-1 upregulation and C5aR shedding, aspirin-triggered 15-epi-LXA_4 and 17-epi-RvD1 restore the balance between Mac-1 and C5aR and consequently enhance phagocytosis, bacterial killing, PICD and the resolution of lung injury (25). Of note, the pro-resolving lipid mediators resolvin E1 and resolvin D5, which signals through the LTB_4 receptor BLT1 (31) and GPR32 (139), respectively, can also enhance phagocytosis of bacteria by naïve neutrophils.

Removal of apoptotic neutrophils (and other cell types) by macrophages is critical for restoring tissue homeostasis. The detection and elimination of apoptotic cells are orchestrated by "find-me" and "keep-out" signals that regulates recruitment of phagocytes to the vicinity of apoptotic cells and "eat-me" signals that allow recognition and engulfment (139–143). Apoptotic cells release nucleotides, such as ATP and UTP through caspase-mediated activation of pannexin 1 channels, which act as key "find-me" signals (144, 145). By contrast, lactoferrin released by apoptotic cells inhibits neutrophil chemotaxis without hindering monocyte recruitment (146), thereby assuring the recruitment of appropriate phagocytes for clearance of apoptotic cells and limit inflammation. Efferocytosis induces a metabolic switch in engulfing macrophages, leading to glycolysis and lactate release through SLC16A1 and reprograms macrophages from the inflammatory phenotype to an anti-inflammatory phenotype (22, 147, 148) and subsequently to a $CD11b^{low}$ subset with minimal phagocytic activity, increased oxidative phosphorylation and expression of IFN-β-related gene signature (134, 149). By promoting neutrophil apoptosis and efferocytosis as well as reprogramming macrophages to the $CD11b^{low}$ phenotype, IFN-β orchestrates bidirectional cross-talk between neutrophils and macrophages to accelerate resolution (134). Genetic deletion or pharmacological inhibition of cyclin-dependent kinases 5 and 9 drives neutrophil apoptosis and reprograms macrophages, thereby facilitating neutrophil clearance and resolution (133, 150).

Neutrophils carrying *Toxoplasma gondii* or *Leishmania donovani*, which they cannot destroy, may serve as "Trojan horses" to disseminate the infection following macrophage engulfment (115, 116). The Gram-negative intracellular coccobacillus *Francisella tularensis* can evade phagosomal elimination and replicates in the cytosol (151) parallel with sustaining mitochondrial integrity and delaying neutrophil apoptosis (152, 153). Continued accumulation of dysfunctional neutrophils at the infection site is thought to contribute to disease exacerbation.

NETosis

Among the neutrophil defense armory is the release of extracellular traps (NETs), consisting of a nucleic acid scaffold decorated with histones and granular proteins to entrap and kill bacteria, viruses and fungi (13, 154, 155). Suicidal NET release (commonly referred to as NETosis) occurs in response to various stimuli and classically involves activation of protein kinase C and the Raf-MEK-ERK pathway, NADPH-dependent translocation of neutrophil elastase and myeloperoxidase from cytosolic granules into the nucleus, leading to the breakdown of chromatin and the nuclear envelop. NETs are extruded following the rupture of the neutrophil cell membrane (13). Hence, NETosis may be considered as a distinct form of necrotic cell death (156). Differences in NET composition have also been reported (157, 158), though the implications of these differences remain to be investigated. NET release may also occur in the absence of cellular suicide (also known as vital NETosis) in response to recognition of certain bacteria or PAMPs (154). For example, HMGB1 released from activated platelets or necrotic cells evokes NET release through interactions with TLR4, independent of NADPH oxidase (159), while suppressing phagocytosis (160). Vital NETosis requires vesicular trafficking of DNA for delivering the NET out of the cell without requiring membrane perforation (161). NET caused by extrusion of mitochondrial rather than nuclear DNA does not cause lytic cell death (162). Reports also exist that neutrophils that had already underwent vital NETosis were still capable of chasing and imprisoning live *Staphylococcus aureus* or *Candida albicans*, whereas NETs recruited additional neutrophils in a swarming-like behavior (161, 163). Although limited information is available on the molecular switches that trigger phagocytosis, NETosis or degranulation, it is plausible that selective activation of these processes assures the most effective neutrophil response to an insult. One possible control mechanism is ALX/FPR2, as genetic deletion of Fpr2 (the equivalent of human ALX/FPR2) in mice is associated with excess NET production and more severe lung injury following bacterial infection (164).

NETs are eventually degraded by macrophages and dendritic cells through DNase 1 that cleaves chromatin within NETs (165) or the cytosolic exonuclease TREX1 (DNase III) following endocytosis (166, 167). The antibacterial protein LL-37 facilitates NET uptake by macrophages, while protecting NETs against degradation by bacterial nucleases (167). A recent study reported that the thirteen-series (or T-series) resolvins, present in resolution exudates, enhance NET uptake by macrophages through the cAMP-PKA-MAPK pathway (168). The receptor for T-series resolvins remains to be identified.

NETs effectively capture a large range of microbes, exert direct antimicrobial activities and demarcate the infected locus (169, 170). However, since the effects of NET components are not restricted to invading pathogens, excessive or uncontrolled NET formation can inflict damage to the surrounding tissue, maintaining a pro-inflammatory and pro-thrombotic environment that underlies various pathologies. For example, extracellular histone components through TLR-mediated generation of thrombin can evoke microaggregation, and endothelial and tissue injury (169, 171, 172), whereas neutrophil granule constituents expressed on NETs, such as proteinase 3 or myeloperoxidase can trigger autoimmunity when NET degradation is impaired (165, 173). Clinical studies have also reported an association between NET generation and disease severity in sepsis-induced (164, 174) or COVID-19-associated acute respiratory distress syndrome (175–177).

Albeit wide-ranging differences in intrapulmonary neutrophils were reported in COVID-19 autopsies (178), intense neutrophilic inflammation and NET release contribute to progression of the disease and higher mortality (175, 179–181). NETs infiltrate the airways, pulmonary interstitial space and vasculature in severe COVID-19 (182), leading to tissue damage and formation of microthrombi in pulmonary capillaries (175, 177, 179–181). Activated neutrophils secrete ROS and proteases, which in turn, enhance NETosis and inactivate plasma antiproteases that protect against neutrophil proteases (183). These create a vicious cycle to propagate tissue destruction. Enhancing NET degradation by DNase I or partial genetic deletion of peptidyl arginine deiminase 4 ($PAD4^{+/-}$) reduced the severity of bacterial lung injury in mice (164). Complete PAD4 deficiency markedly suppressed NET formation and lung injury, but increased bacterial burden, indicating a shift in the balance between the protective and deleterious actions of NETs during bacterial infections.

Accumulating evidence indicates dual role for NETs in cancer (184). NETs were found to inhibit proliferation of colon carcinoma cells (185) and exert cytotoxic activity on malignant melanoma cells (186). Accumulation of NET producing $CD16^{high}$ $CD62L^{dim}$ neutrophils in tumor sites was reported to predict improved survival in patients with head and neck squamous cell carcinoma (187). In contrast, tumor cells can prime neutrophils to release NETs (188), forming an amplifying loop that links NET formation to tumor progression. As an example, NET-associated neutrophil elastase and matrix metallopeptidase 9 (MMP9) could awaken dormant cancer cells, thereby promoting invasion and metastases (189, 190). NETs may shield tumor cells against NK cells and cytotoxic T cells (191), exert pro-angiogenic activities that support tumor growth (192), and contribute to tumor-associated thrombosis (193, 194) and hypercoagulability (195). Furthermore, NETs can also capture tumor cells and carry them in the circulation, thus favoring tumor dissemination (196). NET-DNA was also shown to act as a chemotactic factor to attract tumor cells through binding to the transmembrane protein CCDC25 expressed on primary cancer cells, thereby promoting metastasis (197).

Necrosis and Necroptosis

At sites of inflammation, neutrophils can undergo necrotic cell death, which occurs in a disorderly manner following cell injury, or necroptosis, a programmed form of necrosis (198). Necrotic cell death is associated with the release of DAMPs and cell debris, which are potent inducers of inflammation (198). TNFα or ligation of the adhesion receptors Mac-1, CD18, CD15 or CD44 in GM-CSF-primed neutrophils activates the receptor-interacting protein kinase 1 (RIPK1)-RIPK3- mixed lineage kinase domain-like protein (MLKL) signaling pathway (199, 200), leading to translocation of MLKL1 to the inner leaflet of plasma membrane and membrane permeabilization (201). X-linked IAP (XIAP) ubiquitinylates RIPK1 (202) and thus functions as a switch to direct neutrophils to either necroptosis or apoptosis (201). NADPH oxidase-mediated generation of ROS is essential for necroptosis (199, 200). Consistently, neutrophils from patients with chronic granulomatous disease (caused by a genetic defect in NADPH oxidase) do not undergo necroptosis (200). Some studies reported association of necroptosis with NET formation in a mouse model of gouty arthritis (203), though NET release occurred independently of RIPK3 and MLKL signaling (204). Phagocytosis of methicillin-resistant *Staphylococcus aureus* redirects neutrophils from phagocytosis-induced apoptosis to necroptosis, which may allow the escape of viable bacteria from dead neutrophils, thereby persisting infection (205, 206). This requires RIPK3, but not RIPK1 and MLKL, and is associated with RIPK3- and protease-mediated production of IL-1β (205, 207). Neutrophil necroptosis, evidenced by the activation of RIPK3 and MLKL, was detected in tissue samples from patients with neutrophilic diseases (200). The pathological significance of these observations remains elusive.

Dying cells release DAMPs, including mitochondrial formyl peptides, purines, LTB_4, cytokines and chemokines, and triggers generation of C3a and C5a, which collectively function as "find-me" signals for phagocytes (208–210). Similar to apoptotic cells, necrotic cells also express "eat-me" signals, such as externalization of phosphatidylserine and LTB_4, which facilitate their clearance by macrophages (209). "Eat-me" cues unique to necrotic cells include deposition of complement C1q on the cell membrane (211) and cell surface externalization of annexin A1 (212). The importance of removing necrotic neutrophils is illustrated by the role of the neutrophil granule constituent proteinase 3 in autoimmune vasculitis (65, 66) and chronic obstructive pulmonary disease (213).

THERAPEUTIC OPPORTUNITIES

Given the central role of neutrophils in inflammation, it is paramount to seek novel therapeutic approaches controlling neutrophil-mediated collateral tissue damage and/or facilitating clearance of neutrophils from the inflamed site upon fulfillment of their immediate mission. Indeed, a variety of strategies have been developed to prevent the detrimental effects of neutrophils, with some approaches entering clinical trials (**Figure 2**).

Beta-2 Integrin-Targeted Therapeutic Approaches

Mac-1 conformations and broad ligand recognition specificity shape neutrophil responses and contribute to neutrophil functional heterogeneity (30, 214). Hence, β2 integrins have attracted considerable interest as potential therapeutic targets. Indeed, currently available monoclonal antibodies and small molecule inhibitors that block the ligand-binding site and a broad repertoire of β2 integrin functionality efficiently reduced neutrophil-driven inflammation in numerous experimental models (7, 18, 214). However, global β2 integrin blockade lacks functional selectivity, and can impair phagocytosis and antibacterial defense (215). Conventional β2 integrin blockade may also increase the risk of development of LAD-like symptoms. Alternative approaches include targeting Mac-1

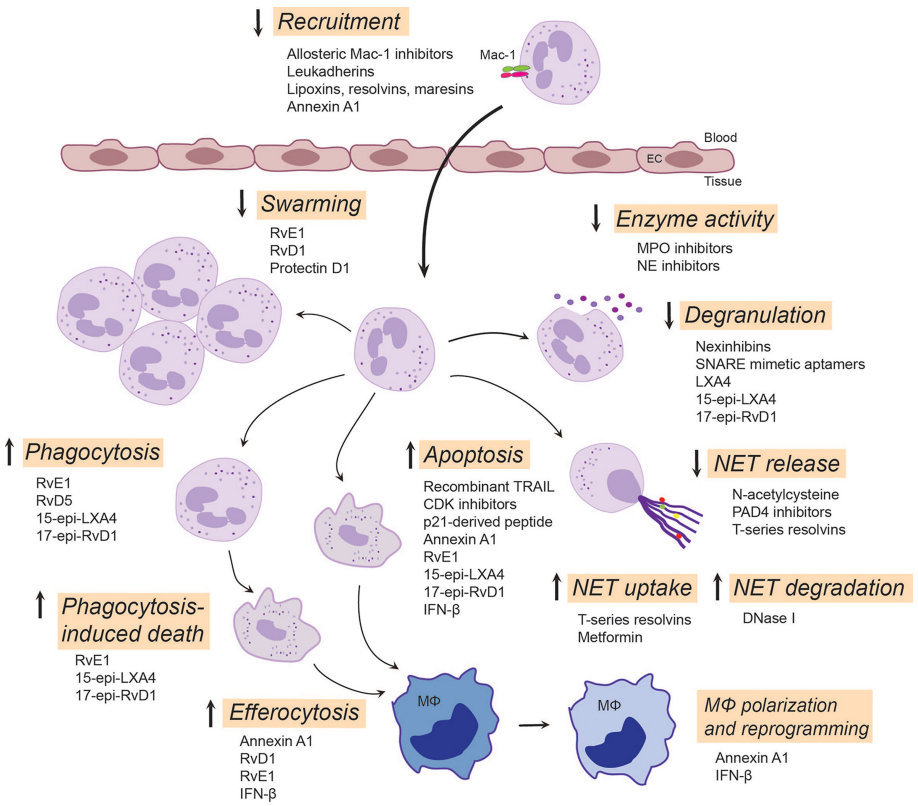

FIGURE 2 | Emerging neutrophil-targeted therapeutic approaches to promote the resolution of inflammation. The strategies include blocking, restoring or activating neutrophil functions. Thus, blocking function of Mac-1 or upregulation of Mac-1expression dampens neutrophil accumulation, a critical component of terminating the inflammatory response. LXA_4, RvE3 and protectin D1 serve as stop signals for swarming. Inhibition of degranulation or the activity of secreted enzymes, such as MPO and NE, could reduce tissue injury and alter composition of NETs. Enhancing NET degradation by DNase I or promoting NET uptake by T-series resolvins or metformin may prevent the deleterious actions of excessive NET formation. RvD5 and RvE1 facilitates phagocytosis, whereas 15-epi-LXA_4 and 17-epi-RvD1 restore impaired phagocytosis, facilitate clearance of bacteria and phagocytosis-induced apoptotic cell death. By countering survival cues, many molecules, including CDK inhibitors, annexin A1, IFN-β and lipid SPMs, can redirect neutrophils to apoptosis and promote their uptake by macrophages through efferocytosis. This leads to reprogramming and polarization of macrophages toward a pro-resolution, regenerative phenotype that promotes further removal of neutrophils. Annexin A1, RvE1, RvD1 and IFN-β play pivotal roles in mediating feedforward resolution programs. Of note, although most of these data are from experimental models, some strategies (e.g. LXA_4 mimetics, NE inhibitors or DNase I) are currently being investigated in clinical trials. C5aR, complement C5a receptor; CDK, cyclin-dependent kinase; EC, endothelial cell; IFN-β, interferon-β; LXA_4, lipoxin A_4; 15-epi-LXA_4, 15-epi-lipoxin A_4; MPO, myeloperoxidase; NE, neutrophil elastase; NET, neutrophil extracellular traps; PAD4, peptidyl arginine deiminase 4; 17-epi-RvD1, 17-epi-resolvin D1; RvE1, resolvin E1; RvE3, resolvin E3; RvD5, resolvin D5; SNARE, soluble N-ethylmaleimide-sensitive-factor attachment protein receptor; SPMs, specialized pro-resolving mediators; TRAIL, TNF-related apoptosis-inducing ligand.

conformation or ligand-specific signaling mechanisms without compromising host defense. Selective inhibition of Mac-1 binding of its ligand CD40L with the M7 monoclonal antibody reduced inflammation without affecting protective immunity (19, 216). Allosteric inhibitors that stabilize β2 integrins in the high affinity bent conformation efficiently blocked neutrophil adherence (217) and restricted neutrophil accumulation in murine models (218, 219). Selective targeting of discrete glycan motifs present on Mac-1 with plant lectins was reported to reduce neutrophil adhesion and trans-epithelial migration, while enhancing phagocytosis and neutrophil apoptosis (220). Other studies have reported that activation of Mac-1 with the small molecule agonists leukadherins reduced neutrophil trafficking into the kidney, while augmented leukocyte adherence to the endothelium in murine models (221). These resulted in attenuation of arterial narrowing and improved renal function. Leukadherin-1 was reported to activate microRNA Let7a and induce polarization of M0 macrophages toward the pro-inflammatory M1 phenotype that drives anti-tumor immunity (222). Thus, leukadherins likely exert context-dependent actions. Hence, additional studies are required to explore their effects on macrophage polarization and the resolution of inflammation.

Among the mechanisms by which specialized pro-resolving mediators (SPMs) facilitate resolution of inflammation is inhibition of neutrophil trafficking into the inflamed site by decreasing their adhesion and transmigration. SPMs signal through stereospecific binding to cellular receptors (223) to prevent upregulation of Mac-1 expression on neutrophils and to reduce Mac-1-mediated neutrophil adhesion and

transendothelial migration, consequently limiting their tissue accumulation (15, 21). Thus, annexin A1, lipoxin A_4 and resolvin D1 interact with ALX/FPR2, resolvin E1 binds ERV1 and resolvin D2 binds to DRV2 to repress Mac-1 expression (20, 223). In a feedforward mechanism for resolution, SPM receptor signaling by one mediator can trigger mobilization or synthesis of other SPMs for other receptors, exemplified by LXA_4 mobilization of annexin A1 to limit neutrophil trafficking into the inflamed microvasculature (224), resolvin D1-triggered LXA_4 generation in periodontal wound healing (225), and resolvin E1-ERV1-induced biosynthesis of LXA_4 for ALX/FPR2-mediated resolution of allergic lung inflammation (226). Of note, the gaseous mediator hydrogen sulfide and mast cell-stabilizing drug nedocronil also mobilize annexin A1 to control leukocyte trafficking in the mouse mesenteric circulation (224, 227).

FPR2 Agonists: Shifting the Balance Towards Resolution

As the pleiotropic receptor ALX/FPR2 conveys ligand-specific pro- or anti-inflammatory actions, it has been proposed to function as a master switch to initiate the resolution of inflammation. A unique feature of ALX/FPR2 is that ligation of this receptor can to activate several, if not all of the processes that are critical for inflammation resolution, including blocking neutrophil trafficking into tissues, promoting neutrophil apoptosis and macrophage efferocytosis (15, 20, 25, 31, 40). As an example, annexin A1 and its mimetic peptide Ac2-26 induce the detachment of adherent neutrophils from the endothelium and inhibit neutrophil chemotaxis, thereby controlling neutrophil accumulation within the inflammatory locus (228), regulate phagocytosis of bacteria and fungi (229) and accelerate neutrophil apoptosis (39). Annexin A1 released from apoptotic neutrophils recruits monocytes to clear apoptotic cells (230), promotes their polarization towards the M2 phenotype (231), thereby protecting the surrounding healthy tissue and accelerating muscle regeneration through AMPK activation (232). Activated neutrophils releases annexin A1-containing microparticles and exosomes, which mediate its anti-inflammatory activity (233) and orchestrate epithelial wound repair through ALX/FPR2 and FPR1 (234). Neutrophil-derived microvesicles can enter cartilage and protect the joint in inflammatory arthritis (235). These findings raise the possibility of harnessing annexin A1-loaded microvesicles as a therapeutic strategy for reducing neutrophil infiltration and protection against tissue damage.

Ligation of ALX/FPR2 with LXA_4, resolvin D1 and aspirin-triggered 15-epi-LXA_4 and 17-epi-RvD1 activates mechanisms that partially overlap those stimulated by annexin A1, but also distinct patterns of activation for intracellular pathways, including ERK and NF-κB phosphorylation (15, 31). In addition to ALX/FPR2, to date, three other surface receptors, ERV1, DRV1 and DRV2 have been identified mediate cell-specific actions of SPMs (15, 223). A common feature of ligation of these receptors is attenuation of neutrophil activation and trafficking into inflamed tissues (15, 20, 223). SPM binding to ALX/FPR2 decreases NF-κB activity and cytokine production (31, 236), disrupts the myeloperoxidase-centered feedforward loop and redirects neutrophils to apoptosis (40), and restores TLR9-impaired phagocytosis of bacteria and promotes phagocytosis-induced neutrophil death (25). Consistently, 15-lipoxin A_4 was found to accelerate the resolution of inflammation in a variety of experimental models, including asthma (237), peritonitis (238, 239), cystic fibrosis (240), ischemia-reperfusion (139), and myeloperoxidase and *E. coli*-induced acute lung injury in mice (25, 40). By reducing bacterial burden, ALX/FPR2 agonists may also be used to lower reduce antibiotic requirements or used in conjunction with antibiotics to strengthen host defense against infections (241, 242). Most SPMs are metabolically inactivated within the inflammatory site, some SPMs reach circulation (242, 243). To circumvent rapid inactivation, several metabolically stable analogs, such as benzo-RvD1, were synthesized (15) and nanomedicines were designed to deliver SPMs and their analogs to promote wound healing (244). Furthermore, the lipoxin A_4 analog BLXA4-ME is currently in trial for periodontal inflammation (245), whereas other molecules are in clinical development program (15). Nanomedicine delivery of SPMs to correct resolution deficits represents a fascinating novel avenue for preventing the progression of chronic diseases, as exemplified by the decreases in tissue SPMs immediately before plaque rupture (23, 24).

The intriguing biology of the ALX/FPR2 receptor has initiated numerous medicinal chemistry programs to develop small-molecule agonists to activate resolution programs (15, 246). Relevant examples here are the beneficial actions of synthetic lipoxin mimetics and the prototype peptide agonist WKYMVM in various preclinical models (247, 248). Phase I clinical trials reported promising tissue protective actions with other small-molecule ALX/FPR2 agonists, such as compound ACT-389949 (Actelion) (249), and compound BMS986235 (Bristol –Myers Squibb) (250) in heart failure. However, since ALX/FPR2 expression is not restricted to myeloid cells, further studies are required to identify the cellular targets (e.g. endothelium, smooth muscle cells or fibroblasts) mediating the beneficial actions of these compounds.

Targeting Neutrophil Lifespan and Apoptosis

Several preclinical studies indicate the therapeutic potential of targeting neutrophil apoptosis for facilitating the resolution of inflammation. Thus, pharmacologic blockade of cyclin-dependent kinases (CDKs), which principally inhibit CDK9-mediated transcription of Mcl-1 (150, 251) has been shown to exert potent anti-inflammatory effects in experimental models of neutrophil-dominated inflammation and enhance resolution of severe lung injury models (133, 251, 252). Interestingly, the CDK inhibitor drug R-roscovitine also increased bacterial clearance (251) through a yet unidentified mechanism. *Ex vivo* studies showed that the CDK inhibitor AT7519 efficiently overrides the delayed neutrophil apoptosis in patients with sepsis-associated ARDS concurrent with reduced expression of Mcl-1 (253). Studies in preclinical models indicate that several SPMs, including 15-epi-lipoxin A_4 and resolvin E1, signaling through ALX/FPR2 and the LTB_4 receptor BLT1, respectively, can also override pro-survival cues and redirect neutrophils to apoptosis in part by reducing Mcl-1 expression (31, 40). In line with these

observations, the annexin A1 mimetic peptide Ac2-26 induces neutrophil apoptosis (254, 255). Furthermore, IFN-β, produced by resolution phase macrophages, drives neutrophil apoptosis through the IFNαR1-STAT3 signaling pathway and acceleration of Mcl-1 degradation (134). These findings identify Mcl-1as a promising target for resolution therapy.

Another potential mechanism to accelerate neutrophil apoptosis is restoring impaired phagocytosis. Indeed, bacterial and mitochondrial DNA were shown to reduce phagocytosis and consequently bacterial clearance as well as phagocytosis-induced death by inducing the cleavage of complement C5a receptor, which acts in concert with Mac-1 to mediate phagocytosis (10, 256). By preventing cleavage of C5a receptor, aspirin-triggered 15-epi-lipoxin A_4 and 17-epi-resolvin D1 restore impaired phagocytosis, enhances bacterial clearance, drive phagocytosis-induced death and consequently attenuate *E. coli*-evoked lung injury in mice (25).

Other strategies to modulate neutrophil apoptosis include activating the extrinsic pathway of apoptosis by TNF-related apoptosis-inducing ligand (TRAIL) and the use of peptides derived from the cyclin-dependent kinase inhibitor p21. While TRAIL appears to have no role in constitutive neutrophil apoptosis, treatment with recombinant TRAIL was shown to enhance neutrophil apoptosis and limit the inflammatory response to LPS in mice (257). The p21 peptide binds and sequesters proliferating cell nuclear antigen (PCNA), which acts as a cytoplasmic platform to control the lifespan of human neutrophils (258). Consistently, a p21-derived peptide was shown to induce apoptosis in neutrophils isolated from patients with *Pseudomonas aeruginosa* infection (259), highlighting PCNA as a novel target to modulate pathological inflammation. Apoptotic neutrophils and T cells sequester chemokines, such as CCL3 and CCL5, through modulation of CCR5 expression, thereby reducing the availability of proinflammatory cytokines for other neutrophils and preventing further neutrophil recruitment (260). An interesting approach emerged from these observations is that administration of apoptotic cells markedly reduced the cytokine/chemokine storm and protected against acute lung and kidney injury in a mouse model of severe sepsis (261).

Macrophages play a crucial role in the clearance of apoptotic and necrotic cells, including neutrophils (140, 209, 262). Various pathologies, including ARDS is associated with impaired macrophage phagocytic function (263, 264). Thus, restoring macrophage function represents another avenue of potential therapy. As an example, IFN-β, produced by resolution phase macrophages, mediates a feedforward loop to promote neutrophil apoptosis and efferocytosis, which contributes to macrophage reprogramming and production of additional IFN-β (134). Several clinical trials reported favorable response to early IFN-β use to mitigate SARS-CoV2 infection-associated severe ARDS and other studies are underway testing the clinical efficacies of type I interferons (265).

Modulation of Degranulation, NET Release and Clearance

As excessive or aberrant NET formation has been implicated in the pathogenesis of many pathologies, inhibiting NET release or enhancing NET clearance open promising avenues for therapy. Preclinical studies showed that ROS scavengers, such as N-acetyl cysteine (266), myeloperoxidase inhibitors (267) and PAD4 inhibitors (268–270) could inhibit NET release and dampen tissue injury in experimental models of arthritis, arteriosclerosis and autoimmune diseases. Likewise, the reversible PAD4 inhibitor GSK484 was shown to inhibit suicidal NETosis (271) and to prevent cancer-associated neutrophil-mediated renal injury in mice (272). Studies in PAD4-knockout mice suggest that bacterial infections may shift the balance of the protective and deleterious effects of NETs in host defense (273, 274). Select lipid SPMs, such as resolvin D4 (275) and T-series resolvins (168) also limit NET formation, though the underlying molecular mechanisms are incompletely understood.

Another potential therapeutic approach is blocking neutrophil degranulation or the effects of granule enzymes. Neutrophil-specific exocytosis inhibitors, termed Nexinhibs, and SNARE domain-derived peptide aptamers have been developed. Nexinhibs selectively inhibit release of azurophil granule contents by interrupting the Rab27a-JFC1 interaction without affecting phagocytosis (276, 277), and reduce neutrophil accumulation in the kidney and liver in a mouse model of systemic inflammation (277). Intrapulmonary delivery of Nexinhib20-loaded nanoparticles, which release Nexinhib20 upon cleavage by neutrophil elastase, was shown to dampen neutrophil recruitment and degranulation within the lower airways (278). SNARE mimicking peptide aptamers exhibit varying selectivity towards neutrophil granule subsets (276). As an example, TAT-SNAP-23 (a fusion protein containing the N-terminal SNAP-23 SNARE domain fused with the cell penetrating HIV peptide TAT) was reported to attenuate lung injury evoked by pulmonary immune complex deposition (279) or sepsis (280). However, since SNARE expression is not restricted to neutrophils, further studies are needed to distinguish their actions of neutrophils and other cell types *in vivo*. Several SPMs, including lipoxin A_4, resolvin D1 and aspirin-triggered 15-epi-LXA_4 and 17-epi-RvD1, acting through ALX/FPR2, also block myeloperoxidase- or TLR9 activation evoked release of myeloperoxidase, neutrophil elastase and proteinase 3 and consequently accelerate resolution of sterile (40) and *E. coli*-induced lung injury in mice (25). Several synthetic inhibitors and natural compounds became available over the past years, in particular compounds that target neutrophil elastase (281). Neutrophil elastase inhibition was reported to prevent progression of lung injury in various experimental models (282). However, the synthetic selective neutrophil elastase inhibitor, sivelastat failed to improve 28-day mortality in patients with ARDS (283). It remains to be investigated whether this was due to its toxic or off-target effects.

Promoting NET degradation by treatment with DNase I attenuated tissue injury and increased survival in mouse models of severe bacterial pneumonia/acute lung injury (164, 174), transplantation-associated lung injury (284), tumor (285) and lupus (286). Furthermore, an ongoing phase III clinical trial is investigating the effectiveness of inhaled dornase-α

(recombinant human DNase I) in reducing the incidence of ARDS in severe trauma patients (287). Other bioengineered DNases, such as actin-resistant DNase (alidornase-α) (288, 289) or DNase 1-like 3 (290) have been developed and some are currently being tested in phase I and II trials (288, 289). Macrophages from ARDS patients exhibit reduced capacity to clear NETs as well as apoptotic cells (263). Treatment of bronchoalveolar lavage fluid macrophages from ARDS patients *ex vivo* with the AMPK activator metformin (264) enhanced NET clearance and efferocytosis (263). In addition to blocking suicidal NET formation, T-series resolvins, and RvT2 in particular, were shown to facilitate NET uptake by monocyte-derived M0 macrophages *in vitro* as well as by peritoneal macrophages in mice (168), indicating the therapeutic potential of RvT2 in the *in vivo* setting.

CONCLUDING REMARKS

Timely removal of neutrophils from the inflamed area is of outmost importance to efficient resolution of inflammation and return to homeostasis. Failure to clear neutrophils may lead to perpetuation of the inflammatory response and persisting tissue damage. Thus, exploring the fate of emigrated neutrophils and their contribution to mechanisms that distinguish self-limiting or protective inflammation from aggravated and chronic inflammation is critical to improve current therapies. The phenotypic heterogeneity and functional versatility of neutrophils and their diverse roles in innate and adaptive immune responses provide important cues for development of neutrophil-targeting therapies. However, whether the neutrophil`s actions are mediated by different polarization states of mature neutrophils or distinct neutrophil subsets remains unclear. A simple "one size fit all" anti-neutrophil approach is perhaps naïve and outdated (282). Indeed, over the past years numerous strategies have been developed, which show promising results in preclinical models to prevent the detrimental effects of neutrophils. These include molecules that can inhibit, restore or enhance specific neutrophil functions. Use of pro-resolving agonists, such as lipoxins, resolvins and annexin A1, which activate endogenous resolution programs and would serve as immunoresolvants rather than immunosuppressant (15), represent a conceptual change for the treatment of inflammatory pathologies as well as the emergence of "resolution pharmacology" (291). Although large-scale clinical studies with these compounds seem distant, some strategies, e.g. topical application of a LXA_4 mimetic and degrading NETs within the lung with inhaled dornase-α, are currently being investigated in clinical trials. This ongoing research highlights the importance of targeting neutrophils, and distinct neutrophil subsets in particular, and will likely spur further advances in neutrophil-targeted therapies to dampen inflammation to favor reparative processes without comprising antimicrobial host defense.

AUTHOR CONTRIBUTIONS

The author confirms being the sole contributor of this work and has approved it for publication.

FUNDING

This study was supported by grants from the Canadian Institutes of Health Research (MOP-97742 and MOP-102619).

REFERENCES

1. Mantovani A, Cassatella MA, Costantini C, Jaillon S. Neutrophils in the Activation and Regulation of Innate and Adaptive Immunity. *Nat Rev Immunol* (2011) 11:519–31. doi: 10.1038/nri3024
2. Nauseef WM, Borregaard N. Neutrophils at Work. *Nat Immunol* (2014) 15:602–11. doi: 10.1038/ni.2921
3. Gordon S. Phagocytosis: An Immunobiologic Process. *Immunity* (2016) 44:463–75. doi: 10.1016/j.immuni.2016.02.026
4. Medzhitov R. Origin and Physiological Roles of Inflammation. *Nature* (2008) 454:428–35. doi: 10.1038/nature07201
5. Nathan C, Ding A. Nonresolving Inflammation. *Cell* (2010) 140:871–82. doi: 10.1016/j.cell.2010.02.029
6. Brandes M, Klauschen F, Kuchen S, Germain RN. A Systems Analysis Identifies a Feedforward Inflammatory Circuit Leading to Lethal Influenza Infection. *Cell* (2013) 154:197–212. doi: 10.1016/j.cell.2013.06.013
7. Liew PX, Kubes P. The Neutrophil's Role During Health and Disease. *Physiol Rev* (2019) 99:1223–48. doi: 10.1152/physrev.00012.2018
8. Nicolás-Ávila JÁ, Adrover JM, Hidalgo A. Neutrophils in Homeostasis, Immunity, and Cancer. *Immunity* (2017) 46:15–28. doi: 10.1016/j.immuni.2016.12.012
9. Klebanoff SJ. Myeloperoxidase: Friend and Foe. *J Leukoc Biol* (2005) 77:598–625. doi: 10.1189/jlb.1204697
10. Othman A, Sekheri M, Filep JG. Roles of Neutrophil Granule Protein in Orchestrating Inflammation and Immunity. *FEBS J* (2021) 2021. doi: 10.1111/febs.15803
11. Cassatella MA, Östberg NK, Tamassia N, Soehnlein O. Biological Roles of Neutrophil-Derived Granule Proteins and Cytokines. *Trends Immunol* (2019) 40:648–64. doi: 10.1016/j.it.2019.05.003
12. Butin-Israeli V, Bui TM, Wiesolek HL, Mascarenhas L, Lee JJ, Mehl LC, et al. Neutrophil-Induced Genomic Instability Impedes Resolution of Inflammation and Wound Healing. *J Clin Invest* (2019) 129:712–26. doi: 10.1172/JCI122085
13. Brinkmann V, Reichard U, Goosmann C, Fauler B, Uhlemann Y, Weiss DS, et al. Neutrophil Extracellular Traps Kill Bacteria. *Science* (2004) 303:1532–5. doi: 10.1126/science.1092385
14. Galkina SI, Fedorova NV, Serebryakova MV, Romanova JM, Golyshev SA, Stadnichuk VI, et al. Proteome Analysis Identified Human Neutrophil Membrane Tubulovesicular Extensions (Cytonemes, Membrane Tethers) as Bactericide Trafficking. *Biochim Biophys Acta* (2012) 1820:1705–14. doi: 10.1016/j.bbagen.2012.06.016
15. Serhan CN, Levy BD. Resolvins in Inflammation: Emergence of the Pro-Resolving Superfamily of Mediators. *J Clin Invest* (2018) 128:2657–69. doi: 10.1172/JCI97943
16. Peiseler M, Kubes P. More Friend Than Foe: The Emerging Role of Neutrophils in Tissue Repair. *J Clin Invest* (2019) 129:2629–39. doi: 10.1171/JCI124616
17. Ley K, Laudanna C, Cybulsky MI, Nourshargh S. Getting to the Site of Inflammation: The Leukocyte Adhesion Cascade Updated. *Nat Rev Immunol* (2007) 7:678–89. doi: 10.1038/nri2156
18. Kolaczkowska E, Kubes P. Neutrophil Recruitment and Function in Health and Inflammation. *Nat Rev Immunol* (2013) 13:159–75. doi: 10.1038/nri3399

19. Nourshargh S, Alon R. Leukocyte Migration Into Inflamed Tissues. *Immunity* (2014) 41:694–707. doi: 10.1016/j.immuni.2014.10.008
20. Perretti M, Cooper D, Dalli J, Norling LV. Immune Resolution Mechanisms in Inflammatory Arthritis. *Nat Rev Rheumatol* (2017) 13:87–99. doi: 10.1038/nrrheum.2016.193
21. Serhan CN, Gupta SK, Perretti M, Godson C, Brennan E, Li Y, et al. The Atlas of Inflammation Resolution (AIR). *Mol Aspects Med* (2020) 74:100894. doi: 10.1016/j.mam.2020.100894
22. Serhan CN, Savill J. Resolution of Inflammation: The Beginning Programs the End. *Nat Immunol* (2005) 6:1191–7. doi: 10.1038/ni1276
23. Fredman G, Hellmann J, Proto JD, Kuriakose G, Colas RA, Dorweiler B, et al. An Imbalance Between Specialized Pro-Resolving Lipid Mediators and Pro-Inflammatory Leukotrienes Promotes Instability of Atherosclerotic Plaques. *Nat Commun* (2016) 7:12859. doi: 10.1038/ncomms12859
24. Fredman G, Tabas I. Boosting Inflammation Resolution in Atherosclerosis: The Next Frontiers for Therapy. *Am J Pathol* (2017) 187:1211–21. doi: 10.1016/j.ajpath.2017.01.018
25. Sekheri M, El Kebir D, Edner N, Filep JG. 15-Epi-LXA $_4$ and 17-Epi-RvD1 Restore TLR9-Mediated Impaired Neutrophil Phagocytosis and Accelerate Resolution of Lung Inflammation. *Proc Natl Acad Sci USA* (2020) 117:7971–80. doi: 10.1073/pnas.1920193117
26. Hynes RO. Integrins: Bidirectional, Allosteric Signaling Machines. *Cell* (2002) 110:673–87. doi: 10.1016/S0092-8674(02)00971-6
27. Dupuy AG, Caron E. Integrin-Dependent Phagocytosis: Spreading From Microadhesion to New Concepts. *J Cell Sci* (2008) 121:1773–83. doi: 10.1242/jcs.018036
28. El Kebir D, József L, Pan W, Filep JG. Myeloperoxidase Delays Neutrophil Apoptosis Through CD11b/CD18 Integrins and Prolongs Inflammation. *Circ Res* (2008) 103:352–9. doi: 10.1161/01.RES.0000326772.76822.7a
29. Dzhagalov I, St. John A, He YW. The Antiapoptotic Protein Mcl-1 Is Essential for the Survival of Neutrophils But Not Macrophages. *Blood* (2007) 109:1620–6. doi: 10.1182/blood-2006-03-013771
30. Mayadas TN, Cullere X. Neutrophil β2 Integrins: Moderators of Life or Death Decisions. *Trends Immunol* (2005) 26:388–95. doi: 10.1016/j.it.2005.05.002
31. El Kebir D, Gjorstrup P, Filep JG. Resolvin E1 Promotes Phagocytosis-Induced Neutrophil Apoptosis and Accelerates Resolution of Pulmonary Inflammation. *Proc Natl Acad Sci USA* (2012) 109:14983–8. doi: 10.1073/pnas.1206641109
32. Oberst A, Dillon CP, Weinlich R, McCormick LL, Fitzgerald P, Pop C, et al. Catalytic Activity of the Caspase-8-FLIP(L) Complex Inhibits RIPK3-Dependent Necrosis. *Nature* (2011) 471:363–7. doi: 10.1038/nature09852
33. Oberst A, Green DR. It Cuts Both Ways: Reconciling the Dual Roles of Caspase 8 in Cell Death and Survival. *Nat Rev Mol Cell Biol* (2011) 12:757–63. doi: 10.1038/nrm3214
34. Colom B, Bodkin JV, Beyrau M, Woodfin A, Ody C, Rourke C, et al. Leukotriene B4-Neutrophil Elastase Axis Drives Neutrophil Reverse Transendothelial Cell Migration *In Vivo*. *Immunity* (2015) 42:1075–86. doi: 10.1016/j.immuni.2015.05.010
35. Ye RD, Boulay F, Wang JM, Dahlgren C, Gerard C, Parmentier M, et al. International Union of Basic and Clinical Pharmacology. LXXIII. Nomenclature for the Formyl Peptide Receptor (FPR) Family. *Pharmacol Rev* (2009) 61:119–61. doi: 10.1124/pr.109.001578
36. Chiang N, Serhan CN, Dahlén SE, Drazen JM, Hay DWP, Rovati GE, et al. The Lipoxin Receptor ALX: Potent Ligand-Specific and Stereoselective Actions *in Vivo*. *Pharmacol Rev* (2006) 58:463–87. doi: 10.1124/pr.58.3.4
37. El Kebir D, József L, Khreiss T, Pan W, Petasis NA, Serhan CN, et al. Aspirin-Triggered Lipoxins Override the Apoptosis-Delaying Action of Serum Amyloid A in Human Neutrophils: A Novel Mechanism for Resolution of Inflammation. *J Immunol* (2007) 179:616–22. doi: 10.4049/jimmunol.179.1.616
38. Wan M, Godson C, Guiry PJ, Agerberth B, Haeggstrom JZ. Leukotriene B4/antimicrobial Peptide LL-37 Pro-Inflammatory Circuits are Mediated by BLT1 and FPR2/ALX and are Counterregulated by Lipoxin A4 and Resolvin E1. *FASEB J* (2011) 25:1697–705. doi: 10.1096/fj.10-175687
39. Leoni G, Nusrat A. Annexin A1: Shifting the Balance Towards Resolution and Repair. *Biol Chem* (2016) 397:971–9. doi: 10.1515/hsz-2016-0180
40. El Kebir D, József L, Pan W, Wang L, Petasis NA, Serhan CN, et al. 15-Epi-Lipoxin A4 Inhibits Myeloperoxidase Signaling and Enhances Resolution of Acute Lung Injury. *Am J Respir Crit Care Med* (2009) 180:311–9. doi: 10.1164/rccm.200810-1601OC
41. Bozinovski S, Uddin M, Vlahos R, Thompson M, McQualter JL, Merritt AS, et al. Serum Amyloid A Opposes Lipoxin A_4 to Mediate Glucocorticoid Refractory Lung Inflammation in Chronic Obstructive Pulmonary Disease. *Proc Natl Acad Sci USA* (2012) 109:935–40. doi: 10.1073/pnas.1109382109
42. Cooray SN, Gobbetti T, Montero-Melendez T, McArthur S, Thompson D, Clark AJL, et al. Ligand-Specific Conformational Change of the G-Protein-Coupled Receptor ALX/FPR2 Determines Proresolving Functional Responses. *Proc Natl Acad Sci USA* (2013) 110:18232–7. doi: 10.1073/pnas.1308253110
43. Filep JG. Biasing the Lipoxin A4/formyl Peptide Receptor 2 Pushes Inflammatory Resolution. *Proc Natl Acad Sci USA* (2013) 110:18033–4. doi: 10.1073/pnas.1317798110
44. Chen T, Xiong M, Zong X, Ge Y, Zhang H, Wang M, et al. Structural Basis of Ligand Binding Modes at the Human Formyl Peptide Receptor 2. *Nat Commun* (2020) 11:1208. doi: 10.1038/s41467-020-15009-1
45. Ge Y, Zhang S, Wang J, Xia F, Wan J, Lu J, et al. Dual Modulation of Formyl Peptide Receptor 2 by Aspirin-Triggered Lipoxin Contributes to Its Anti-Inflammatory Activity. *FASEB J* (2020) 34:6920–33. doi: 10.1096./fj.201903206R
46. Thompson D, McArthur S, Hislop JN, Flower RJ, Perretti M. Identification of a Novel Recycling Sequence in the C-Tail of FPR2/ALX: Association With Cell Protection From Apoptosis. *J Biol Chem* (2014) 289:36166–78. doi: 10.1074/jbc.M114.612630
47. Soehnlein O, Wantha S, Simsekyilmaz S, Döring Y, Megens RT, Mause SF, et al. Neutrophil-Derived Cathelicidin Protects From Neointimal Hyperplasia. *Sci Transl Med* (2011) 3:103a98. doi: 10.1126/scitranslmed.3002531
48. Jones HR, Robb CT, Perretti M, Rossi AG. The Role of Neutrophils in Inflammation Resolution. *Semin Immunol* (2016) 28:137–45. doi: 10.1016/j.smim.2016.03.007
49. Bastian OW, Koenderman L, Alblas J, Leenen LP, Blokhuis TJ. Neutrophils Contribute to Fracture Healing by Synthesizing Fibronectin+ Extracellular Matrix Rapidly After Injury. *Clin Immunol* (2016) 164:78–84. doi: 10.1016/j.clim.2016.02.001
50. Blázquez-Prieto J, López-Alonso I, Amado-Rodríguez L, Huidobro C, González-López A, Kuebler WM, et al. Impaired Lung Repair During Neutropenia Can be Reverted by Matrix Metalloproteinase-9. *Thorax* (2018) 73:321–30. doi: 10.1136/thoraxjnl-2017-210105
51. Horckmans M, Ring L, Duchene J, Santovito D, Schloss MJ, Drechsler M, et al. Neutrophils Orchestrate Post-Myocardial Infarction Healing by Polarizing Macrophages Towards a Reparative Phenotype. *Eur Heart J* (2017) 38:187–97. doi: 10.1093/eurheartj/ehw002
52. Kruger P, Saffarzadeh M, Weber AN, Rieber W, Radsak M, von Bernuth H, et al. Neutrophils: Between Host Defence, Immune Modulation, and Tissue Injury. *PloS Pathog* (2015) 11:e1004651. doi: 10.1371/journal.ppat.1004651
53. Scapini P, Marini O, Tecchio C, Cassatella MA. Human Neutrophils in the Saga of Cellular Heterogeneity: Insights and Open Questions. *Immunol Rev* (2016) 273:48–60. doi: 10.1111/imr.12448
54. Silvestre-Roig C, Hidalgo A, Soehnlein O. Neutrophil Heterogeneity: Implications for Homeostasis and Pathogenesis. *Blood* (2016) 127:2173–81. doi: 10.1182/blood-2016-01-688887
55. Ng LG, Ostuni R, Hidalgo A. Heterogeneity of Neutrophils. *Nat Rev Immunol* (2019) 19:255–65. doi: 10.1038/s41577-019-0141-8
56. Hidalgo A, Casanova-Ascebes M. Dimensions of Neutrophil Life and Fate. *Semin Immunol* (2021) 25:101506. doi: 10.1016/j.smim.2021.101506
57. Silvestre-Roig C, Friedlander ZG, Glogauer M, Scapini P. Neutrophil Diversity in Health and Disease. *Trends Immunol* (2019) 40:565–83. doi: 10.1016/j.it.2019.04.012
58. Xie X, Shi Q, Wu P, Zhang X, Kambara H, Su J, et al. Single-Cell Transcriptome Profiling Reveals Neutrophil Heterogeneity in Homeostasis and Infection. *Nat Immunol* (2020) 21:1119–33. doi: 10.1038/s41590-020-0736-z
59. Garratt LW. Current Understanding of the Neutrophil Transcriptome in Health and Disease. *Cells* (2021) 10:2406. doi: 10.3390/cells10092406
60. Jiang K, Sun X, Chen Y, Shen Y, Jarvis JN. RNA Sequencing From Human Neutrophils Reveals Distinct Transcriptional Differences Associated With

Chronic Inflammatory States. *BMC Med Genomics* (2015) 8:55. doi: 10.1186/s12920-015-0128-7
61. Gomez GC, Dang H, Kanke M, Hagan RS, Mock JR, Kelada SNP, et al. Predicted Effects of Observed Changes in the mRNA and microRNA Transcriptome of Lung Neutrophils During S. Pneumoniae Pneumonia in Mice. *Sci Rep* (2017) 7:11258. doi: 10.1038/s41598-017-11638-7
62. Ai Z, Udalova IA. Transcriptional Regulation of Neutrophil Differentiation and Function During Inflammation. *J Leukoc Biol* (2020) 107:419–30. doi: 10.1002/JLB.1RU1219-504RR
63. Grieshaber-Bouyer R, Radtke FA, Cunin P, Stifano G, Levescot A, Vijaykumar B, et al. The Neutrotime Transcriptional Signature Defines a Single Continuum of Neutrophils Across Biological Compartments. *Nat Commun* (2021) 12:2856. doi: 10.1038/s41467-021-22973-9
64. Kuckleburg CJ, Tilkens SB, Santoso S, Newman PJ. Proteinase 3 Contributes to Transendothelial Migration of NB1-Positive Neutrophils. *J Immunol* (2012) 188:2419–26. doi: 10.4049/jimmunol.1102540
65. Hu N, Westra J, Huitema MG, Bijl M, Brouwer E, Stegeman CA, et al. Coexpression of CD177 and Membrane Proteinase 3 on Neutrophils in Antineutrophil Cytoplasmic Autoantibody-Associated Systemic Vasculitis: Anti-Proteinase 3-Mediated Neutrophil Activation Is Independent of the Role of CD177-Expressing Neutrophils. *Arthritis Rheum* (2009) 60:1548–57. doi: 10.1002/art.24442
66. Rarok AA, Stegeman CA, Limburg PC, Kallenberg CG. Neutrophil Membrane Expression of Proteinase 3 (PR3) is Related to Relapse in PR3-ANCA-Associated Vasculitis. *J Am Soc Nephrol* (2002) 13:2232–8. doi: 10.1097/01.ASN.0000028642.26222.00
67. Christofferson G, Vågesjö E, Vandooren J, Lidén M, Massena S, Reinert RB, et al. VEGF-A Recruits a Proangiogenic MMP-9-Delivering Neutrophil Subset That Induces Angiogenesis in Transplanted Hypoxic Tissue. *Blood* (2012) 120:4653–62. doi: 10.1182/blood-2012-04-421040
68. Adrover JM, del Fresno C, Crainiciuc G, Cuartero MI, Casanova-Acebes M, Weiss LA, et al. A Neutrophil Timer Coordinates Immune Defense and Vascular Protection. *Immunity* (2019) 50:390–402. doi: 10.1016/j.immuni.2019.01.002
69. Casanova-Acebes M, Pitaval C, Weiss LA, Nombela-Arrieta C, Chèvre R, A-González N, et al. Rhythmic Modulation of the Hematopoietic Niche Through Neutrophil Clearance. *Cell* (2013) 153:1025–35. doi: 10.1016/j.cell.2013.04.040
70. Zhang D, Chen G, Manwani D, Mortha A, Xu C, Faith JJ, et al. Neutrophil Ageing is Regulated by the Microbiome. *Nature* (2015) 525:528–32. doi: 10.1038/nature15367
71. Hellebrekers P, Hietbrink F, Vrisekoop, Leenen LPH, Koenderman L. Neutrophil Functional Heterogeneity: Identification of Competitive Phagocytosis. *Front Immunol* (2017) 8:1498. doi: 10.3389/fimmu.2017.01498
72. Hassani M, Hellebrekers P, Chen N, van Aalst C, Bongers S, Hietbrink F, et al. On the Origin of Low Density Neutrophils. *J Leukoc Biol* (2020) 107:809–18. doi: 10.1002/JLB.5HR0120-459R
73. Buckley CD, Ross EA, McGettrick HM, Osborne CE, Haworth O, Schmutz C, et al. Identification of a Phenotypically and Functionally Distinct Population of Long-Lived Neutrophils in a Model of Reverse Endothelial Transmigration. *J Leukoc Biol* (2006) 79:303–11. doi: 10.1189/jlb.0905496
74. Fortunati E, Kazemier KM, Grutters JC, Koenderman L, Van den Bosch van JMM. Human Neutrophils Switch to an Activated Phenotype After Homing to the Lung Irrespective of Inflammatory Disease. *Clin Exp Immunol* (2009) 155:559–66. doi: 10.1111/j.1365-2249.2008.03791.x
75. Carmona-Rivera C, Kaplan MJ. Low Density Granulocytes a Distinct Class of Neutrophils in Systemic Autoimmunity. *Semin Immunopathol* (2013) 35:455–63. doi: 10.1007/s00281-013-0375-7
76. Singh N, Traisak P, Martin KA, Kaplan MJ, Cohen PL, Denny MF. Genomic Alterations in Abnormal Neutrophils Isolated From Adult Patients With Systemic Lupus Erythematosus. *Arthritis Res Ther* (2014) 16:R165. doi: 10.1186/ar4681
77. Marini O, Costa S, Bevilacqua D, Calzetti F, Tamassia N, Spina C, et al. Mature $CD10^+$ and Immature CD1- Neutrophils Present in G-CSF-Treated Donors Display Opposite Effects on T Cells. *Blood* (2017) 129:1343–56. doi: 10.1182/blood-2016-04-713206
78. Meghraoui-Kheddar A, Chousterman BG, Guillou N, Barone SM, Granjeaud S, Vallet H, et al. Two New Neutrophil Subsets Define a Discriminating Sepsis Signature. *Am J Respir Crit Care Med* (2022) 205:46–59. doi: 10.1164/rccm.202104-1027OC
79. Fridlender ZG, Sun J, Kim S, Kapoor V, Cheng G, Ling L, et al. Polarization of Tumor-Associated Neutrophil Phenotype by TGF-Beta: "N1" Versus "N2" TAN. *Cancer Cell* (2009) 16:183–94. doi: 10.1016/j.ccr.2009.06.017
80. Fridlender ZG, Sun J, Mishalian I, Singhal S, Cheng G, Kapoor V, et al. Transcriptomic Analysis of Comparing Tumor-Associated Neutrophils With Granulocytic Myeloid-Derived Suppressor Cells and Normal Neutrophils. *PloS One* (2012) 7:e31524. doi: 10.1371/journal.pone.0031524
81. Jablonska J, Leschner S, Westphal K, Lienenklaus S, Weiss S. Neutrophils Responsive to Endogenous IFN-Beta Regulate Tumor Angiogenesis and Growth in a Mouse Tumor Model. *J Clin Invest* (2010) 120:1151–64. doi: 10.1172/JCI37223
82. Andzinski L, Kasnitz N, Stahnke S, Wu CF, Gereke M, von Köckritz-Blickwede M, et al. Type I IFNs Induce Anti-Tumor Polarization of Tumor-Associated Neutrophils in Mice and Human. *Int J Cancer* (2016) 138:1982–93. doi: 10.1002/ijc.29945
83. Singhal S, Bhojnagarwala PS, O'Brien S, Moon EK, Garfall AL, Rao AS, et al. Origin and Role of a Subset of Tumor-Associated Neutrophils With Antigen-Presenting Cell Features in Early Stage Human Lung Cancer. *Cancer Cell* (2016) 30:120–35. doi: 10.1016/j.ccell.2016.06.001
84. Saha S, Biswas SK. Tumor-Associated Neutrophils Show Phenotypic and Functional Divergence in Human Lung Cancer. *Cancer Cell* (2016) 30:11–3. doi: 10.1016/j.ccell.2016.06.016
85. Naranbhai V, Fairfax BP, Makino S, Humburg P, Wong D, Ng E, et al. Genomic Modulators of Gene Expression in Human Neutrophils. *Nat Commun* (2015) 6:7545. doi: 10.1038/ncomms8545
86. Coit P, Yalavarthi S, Ognenovski M, Zhao W, Hasni S, Wren JD, et al. Epigenome Profiling Reveals Significant DNA Demethylation of Interferon Signature Genes in Lupus Neutrophils. *J Autoimmun* (2015) 58:59–66. doi: 10.1016/j.jaut.2015.01.004
87. Injarabian L, Devin A, Ransac S, Marteyn BS. Neutrophil Metabolic Shift During Their Lifecycle: Impact on Their Survival and Activation. *Int J Mol Sci* (2019) 21:287. doi: 10.3390/ijms21010287
88. Curi R, Levada-Pires AC, Silva EBD, Poma SO, Zambonatto RF, Domenech P, et al. The Critical Role of Cell Metabolism for Essential Neutrophil Functions. *Cell Physiol Biochem* (2020) 54:629–47. doi: 10.33594/000000245
89. Sadiku P, Willson JA, Ryan EM, Sammut D, Coelho P, Watts ER, et al. Neutrophils Fuel Effective Immune Responses Through Gluconeogenesis and Glycogenesis. *Cell Metab* (2021) 33:1062–4. doi: 10.1016/j.cmet.2020.11.016
90. Levy BD, Clish CB, Schmidt B, Gronert K, Serhan CN. Lipid Mediator Class Switching During Acute Inflammation: Signals in Resolution. *Nat Immunol* (2001) 2:612–9. doi: 10.1038/89759
91. Lämmermann T, Afonso PV, Angermann BR, Wang JM, Kastenmüller W, Parent CA, et al. Neutrophil Swarms Require LTB4 and Integrins at Sites of Cell Death *In Vivo*. *Nature* (2013) 498:371–5. doi: 10.1038/nature12175
92. Kienle K, Lämmermann T. Neutrophil Swarming: An Essential Process of the Neutrophil Tissue Response. *Immunol Rev* (2016) 273:76–93. doi: 10.1111/imr.12458
93. Lämmermann T. In the Eye of the Neutrophil Swarm-Navigation Signals That Bring Neutrophils Together in Inflamed and Infected Tissues. *J Leukoc Biol* (2016) 100:55–63. doi: 10.1189/jlb.1MR0915-403
94. Uderhardt S, Martins AJ, Tsang JS, Lämmermann T, Germain RN. Resident Macrophages Cloak Tissue Microlesions to Prevent Neutrophil Driven Inflammatory Damage. *Cell* (2019) 177:541–55.e17. doi: 10.1016/j.cell.2019.02.028
95. Reátegui E, Jalali F, Khankhel AH, Wong E, Cho H, Lee J, et al. Microscale Arrays for the Profiling of Start and Stop Signals Coordinating Human-Neutrophil Swarming. *Nat BioMed Eng* (2017) 1:0094. doi: 10.1038/s41551-017-0094
96. Coombs C, Georgantzoglou A, Walker HA, Patt J, Merten N, Poplimont H, et al. Chemokine Receptor Trafficking Coordinates Neutrophil Clustering and Dispersal at Wounds in Zebrafish. *Nat Commun* (2019) 10:5166. doi: 10.1038/s41467-019-13107-3
97. Kreisel D, Nava RG, Li W, Zinselmeyer BH, Wang B, Lai J, et al. *In Vivo* Two-Photon Imaging Reveals Monocyte-Dependent Neutrophil Extravasation During Pulmonary Inflammation. *Proc Natl Acad Sci USA* (2010) 107:18073–8. doi: 10.1073/pnas.1008737107

98. Kamenyeva O, Boularan C, Kabat J, Cheung GY, Cicala C, Yeh AJ, et al. Neutrophil Recruitment to Lymph Nodes Limits Local Humoral Response to *Staphylococcus Aureus*. *PloS Pathog* (2015) 11:e1004827. doi: 10.1371/journal.ppat.1004827
99. Leliefeld PHC, Wessels CM, Leenen LPH, Koenderman L, Pillay J. The Role of Neutrophils in Immune Dysfunction During Severe Inflammation. *Crit Care* (2016) 20:73. doi: 10.1186/s13054-016-1250-4
100. Jones CN, Dimisko L, Forrest K, Judice K, Poznansky MC, Markmann JF, et al. Human Neutrophils are Primed by Chemoattractant Gradients for Blocking the Growth of *Aspergillus Fumigatus*. *J Infect Dis* (2016) 213:465–75. doi: 10.1093/infdis/jiv419
101. Malawista SE, de Boisfleury Chevance A, van Damme J, Serhan CN. Tonic Inhibition of Chemotaxis in Human Plasma. *Proc Natl Acad Sci USA* (2008) 105:17949–54. doi: 10.1073/pnas.0802572105
102. Malawista SE, de Boisfleury AC, Naccache PH. Inflammatory Gout: Observations Over a Half-Century. *FASEB J* (2011) 25:4073–8. doi: 10.1096/fj.11-1201ufm
103. Buckley CD, Ross EA, McGettrick HM, Osborne CE, Haworth O, Schmutz C, et al. Identification of a Phenotypically and Functionally Distinct Population of Long-Lived Neutrophils in a Model of Reverse Endothelial Migration. *J Leukoc Biol* (2006) 79:303–11. doi: 10.1189/jlb.0905496
104. Mathias JR, Perrin BJ, Liu TX, Kanki J, Look AT, Huttenlocher A. Resolution of Inflammation by Retrograde Chemotaxis of Neutrophils in Transgenic Zebrafish. *J Leukoc Biol* (2006) 80:1281–8. doi: 10.1189/jlb.0506346
105. Lambris JD, Ricklin D, Geisbrecht BV. Complement Evasion by Human Pathogens. *Nat Rev Microbiol* (2008) 6:132–42. doi: 10.1038/nrmicro1824
106. Woodfin A, Voisin MB, Beyrau M, Colom B, Caille D, Diapouli FM, et al. The Junctional Adhesion Molecule JAM-C Regulates Polarized Transendothelial Migration of Neutrophils *In Vivo*. *Nat Immunol* (2011) 12:761–9. doi: 10.1038/ni.2062
107. Scheiermann C, Colom B, Meda P, Patel NS, Voisin MB, Marrelli A, et al. Junctional Adhesion Molecule-C Mediates Leukocyte Infiltration in Response to Ischemia Reperfusion Injury. *Arterioscler Thromb Vasc Biol* (2009) 29:1509–15. doi: 10.1161/ATVBAHA.109.187559
108. Nourshargh S, Renshaw SA, Imhof BA. Reverse Migration of Neutrophils: Where, When, How and Why? *Trends Immunol* (2016) 37:273–86. doi: 10.1016/j.it.2016.03.006
109. Abadie V, Badell E, Douillard P, Ensergueix D, Leenen PJ, Tanguy M, et al. Neutrophils Rapidly Migrate *via* Lymphatics After *Mycobacterium Bovis* BCG Intradermal Vaccination and Shuttle Live Bacilli to the Draining Lymph Nodes. *Blood* (2005) 106:1843–50. doi: 10.1182/blood-2005-03-1281
110. Chtanova T, Schaeffer M, Han SJ, van Dooren GG, Nollmann M, Herzmark P, et al. Dynamics of Neutrophil Migration in Lymph Nodes During Infection. *Immunity* (2008) 29:487–96. doi: 10.1016/j.immuni.2008.07.012
111. Hampton HR, Bailey J, Tomura M, Brink R, Chtanova T. Microbe Dependent Lymphatic Migration of Neutrophils Modulates Lymphocyte Proliferation in Lymph Nodes. *Nat Commun* (2015) 6:7139. doi: 10.1038/ncomms8139
112. Hampton HR, Chtanova T. The Lymph Node Neutrophil. *Semin Immunol* (2016) 28:129–36. doi: 10.1016/j.smim.2016.03.008
113. Rigby DA, Ferguson DJ, Johnson LA, Jackson DG. Neutrophils Rapidly Transit Inflamed Lymphatic Vessel Endothelium *via* Integrin-Dependent Proteolysis and Lipoxin-Induced Junctional Retraction. *J Leukoc Biol* (2015) 98:897–912. doi: 10.1189/jlb.1HI0415-149R
114. Takashima A, Yao Y. Neutrophil Plasticity: Acquisition of Phenotype and Functionality of Antigen-Presenting Cell. *J Leukoc Biol* (2015) 98:489–96. doi: 10.1189/jlb.1MR1014-502R
115. Peters NC, Egen JG, Secundino N, Debrabant A, Kimblin N, Kamhawi S, et al. *In Vivo* Imaging Reveals an Essential Role for Neutrophils in Leishmaniosis Transmitted by Sand Flies. *Science* (2008) 321:970–4. doi: 10.1126/science.1159194
116. Coombes JL, Charsar BA, Han SJ, Halkias J, Chan SW, Koshy AA, et al. Motile Invaded Neutrophils in the Small Intestine of *Toxoplasma Gondii*-Infected Mice Reveal a Potential Mechanism for Parasite Spread. *Proc Natl Acad Sci USA* (2013) 110:E1913–22. doi: 10.1073/pnas.1220272110
117. Lahoz-Beneytez J, Elemans M, Zhang Y, Ahmed R, Salam A, Block M, et al. Human Neutrophil Kinetics: Modeling of Stable Isotope Labeling Data Supports Short Blood Neutrophil Half-Lives. *Blood* (2016) 127:3431–8. doi: 10.1182/blood-2016-03-700336
118. Tak T, Tesselaar K, Pillay J, Borghans JA, Koenderman L. What's Your Age Again? Determination of Human Neutrophil Half-Lives Revisited. *J Leukoc Biol* (2013) 94:595–601. doi: 10.1189/jlb.1112571
119. Savill JS, Wyllie AH, Henson JE, Walport MJ, Henson PM, Haslett C. Macrophage Phagocytosis of Aging Neutrophils in Inflammation. Programmed Cell Death in the Neutrophil Leads to its Recognition by Macrophages. *J Clin Invest* (1989) 83:865–75. doi: 10.1172/JCI113970
120. József L, Khreiss T, Filep JG. CpG Motifs in Bacterial DNA Delay Apoptosis of Neutrophil Granulocytes. *FASEB J* (2004) 18:1776–8. doi: 10.1096/fj.04-2048fje
121. Rajamäki K, Nordström T, Nurmi K, Åkerman KE, Kovanen PT, Öörni K, et al. Extracellular Acidosis is a Novel Danger Signal Alerting Innate Immunity *via* the NLRP3 Inflammasome. *J Biol Chem* (2013) 288:13410–9. doi: 10.1074/jbc.M112.426254
122. El Kebir D, de Oliveira Lima Dos Santos E, Mansouri S, Sekheri M, Filep JG. Mild Acidosis Delays Neutrophil Apoptosis *via* Multiple Signaling Pathways and Acts in Concert With Inflammatory Mediators. *J Leukoc Biol* (2017) 102:1389–400. doi: 10.1189/jlb.3A0117-041R
123. Peyssonnaux C, Datta V, Cramer T, Doedens A, Theodorakis EA, Gallo RL, et al. HIF-1α Expression Regulates the Bactericidal Capacity of Phagocytes. *J Clin Invest* (2005) 115:1806–15. doi: 10.1172/JCI23865
124. Thompson AA, Elks PM, Marriott HM, Eamsamarng S, Higgins KR, Lewis A, et al. Hypoxia-Inducible Factor 2α Regulates Key Neutrophil Functions in Humans, Mice, and Zebrafish. *Blood* (2014) 123:366–76. doi: 10.1182/blood-2013-05-500207
125. Matthijsen RA, Huugen D, Hoebers NT, de Vries B, Peutz-Kootstra CJ, Aratani Y, et al. Myeloperoxidase is Critically Involved in the Induction of Organ Damage After Renal Ischemia Reperfusion. *Am J Pathol* (2007) 171:1743–52. doi: 10.2353/ajpath.2007.070184
126. Brovkovych V, Gao XP, Ong E, Brovkovych S, Brennan ML, Su X, et al. Augmented Inducible Nitric Oxide Synthase Expression and Increased NO Production Reduce Sepsis-Induced Lung Injury and Mortality in Myeloperoxidase-Null Mice. *Am J Physiol Lung Cell Mol Physiol* (2008) 295:L96–L103. doi: 10.1152/ajplung.00450.2007
127. Jia SH, Li Y, Parodo J, Kapus A, Fan L, Rotstein OD, et al. Pre-B Cell Colony-Enhancing Factor Inhibits Neutrophil Apoptosis in Experimental Inflammation and Clinical Sepsis. *J Clin Invest* (2004) 113:1318–27. doi: 10.1172/JCI19930
128. Keel M, Ungethüm U, Steckholzer U, Niederer E, Hartung T, Trentz O, et al. Interleukin-10 Counterregulates Proinflammatory Cytokine Induced Inhibition of Neutrophil Apoptosis During Severe Sepsis. *Blood* (1997) 90:3356–63. doi: 10.1182/blood.V90.9.3356
129. Matute-Bello G, Liles WC, Radella F II, Steinberg KP, Ruzinski JT, Jonas M, et al. Neutrophil Apoptosis in the Acute Respiratory Distress Syndrome. *Am J Respir Crit Care Med* (1997) 156:1969–77. doi: 10.1164/ajrccm.156.6.96-12081
130. Uddin M, Nong G, Ward J, Seumois G, Prince LR, Wilson SJ, et al. Prosurvival Activity for Airway Neutrophils in Severe Asthma. *Thorax* (2010) 65:684–9. doi: 10.1136/thx.2009.120741
131. Garlichs CD, Eskafi S, Cicha I, Schmeisser A, Walzog B, Raaz D, et al. Delay of Neutrophil Apoptosis in Acute Coronary Syndromes. *J Leukoc Biol* (2004) 75:828–35. doi: 10.1189/jlb.0703358
132. Jonsson H, Allen P, Peng SL. Inflammatory Arthritis Requires Foxo3a to Prevent Fas Ligand-Induced Neutrophil Apoptosis. *Nat Med* (2005) 11:666–71. doi: 10.1038/nm1248
133. Rossi AG, Sawatzky DA, Walker A, Ward C, Sheldrake TA, Riley NA, et al. Cyclin-Dependent Kinase Inhibitors Enhance the Resolution of Inflammation by Promoting Inflammatory Cell Apoptosis. *Nat Med* (2006) 12:1056–64. doi: 10.1038/nm1468
134. Kumaran Satyanarayanan S, El Kebir D, Soboh S, Butenko S, Sekheri M, Saadi J, et al. IFN-β Is a Macrophage-Derived Effector Cytokine Facilitating the Resolution of Bacterial Inflammation. *Nat Commun* (2019) 10:3471. doi: 10.1038/s41467-019-10903-9
135. Maimon N, Zamir ZZ, Kalkar P, Zeytuni-Timor O, Schif-Zuck S, Larisch S, et al. The Pro-Apoptotic ARTS Protein Promotes Neutrophil Apoptosis, Efferocytosis and Macrophage Reprogramming in Resolving Inflammation. *Apoptosis* (2020) 25:558–73. doi: 10.1007/s10495-020-01615-3
136. Mollnes TE, Brekke OL, Fung M, Fure H, Christiansen D, Bergseth G, et al. Essential Role of the C5a Receptor in *E. Coli*-Induced Oxidative Burst and

Phagocytosis Revealed by a Novel Lepirudin-Based Human Whole Blood Model of Inflammation. *Blood* (2002) 100:1869–77.
137. Freeman SA, Goyette J, Furuya W, Woods EC, Bertozzi CR, Bergmeier W, et al. Integrins Form an Expanding Diffusion Barrier That Coordinates Phagocytosis. *Cell* (2016) 164:128–40. doi: 10.1016/j.cell.2015.11.048
138. Berger M, Sorensen RU, Tosi MF, Dearborn DG, Döring G. Complement Receptor Expression on Neutrophils at an Inflammatory Site, the *Pseudomonas*-Infected Lung in Cystic Fibrosis. *J Clin Invest* (1989) 84:1302–13. doi: 10.1172/JCI114298
139. Chiang N, Fredman G, Bäckhed F, Oh SF, Vickery T, Schmidt BA, et al. Infection Regulates Pro-Resolving Mediators That Lower Antibiotic Requirements. *Nature* (2012) 484:524–8. doi: 10.1038/nature11042
140. Doran AC, Yurdagul A Jr, Tabas I. Efferocytosis in Health and Disease. *Nat Rev Immunol* (2020) 20:254–67. doi: 10.1038/s41577-019-0240-6
141. Kourtzelis I, Hajishengallis G, Chavakis T. Phagocytosis of Apoptotic Cells in Resolution of Inflammation. *Front Immunol* (2020) 11:553. doi: 10.3389/fimmu.2020.00553
142. Morioka S, Maueröder C, Ravichandran KS. Living on the Edge: Efferocytosis at the Interface of Homeostasis and Pathology. *Immunity* (2019) 50:1149–62. doi: 10.1016/j.immuni.2019.04.018
143. Sugimoto MA, Vago JP, Perretti M, Teixeira MM. Mediators of the Resolution of the Inflammatory Response. *Trends Immunol* (2019) 40:212–27. doi: 10.1016/j.it.2019.01.007
144. Elliott MR, Chekeni FB, Trampont PC, Lazarowski ER, Kadl A, Walk SF, et al. Nucleotides Released by Apoptotic Cells Acts as a Find-Me Signal to Promote Phagocytic Clearance. *Nature* (2009) 461:282–6. doi: 10.1038/nature08296
145. Chekeni FB, Elliott MR, Sandilos JK, Walk SF, Kinchen JM, Lazarowski ER, et al. Pannexin 1 Channels Mediate 'Find-Me' Signal Release and Membrane Permeability During Apoptosis. *Nature* (2010) 467:863–7. doi: 10.1038/nature09413
146. Bournazou I, Pound JD, Duffin R, Bournazos S, Melville LA, Brown SB, et al. Apoptotic Human Cells Inhibit Migration of Granulocytes *via* Release of Lactoferrin. *J Clin Invest* (2009) 119:20–32. doi: 10.1172/JCI36226
147. Ariel A, Serhan CN. New Lives Given by Cell Death: Macrophage Differentiation Following Their Encounter With Apoptotic Leukocytes During the Resolution of Inflammation. *Front Immunol* (2012) 3:4. doi: 10.3389/fimmu.2012.00004
148. Morioka S, Perry JSA, Raymond MH, Medina CB, Zhu Y, Zhao L, et al. Efferocytosis Induces a Novel SLC Program to Promote Glucose Uptake and Lactate Release. *Nature* (2018) 563:714–8. doi: 10.1038/s41586-018-0735-5
149. Schif-Zuck S, Gross N, Assi S, Rostoker R, Serhan CN, Ariel A. Saturated-Efferocytosis Generates Pro-Resolving CD11blow Macrophages: Modulation by Resolvins and Glucocorticoids. *Eur J Immunol* (2011) 41:366–79. doi: 10.1002/eji.201040801
150. Hoodless LJ, Lucas CD, Duffin R, Denvir MA, Haslett C, Tucker CS, et al. Genetic and Pharmacological Inhibition of CDK9 Drives Neutrophil Apoptosis to Resolve Inflammation in Zebrafish *In Vivo*. *Sci Rep* (2016) 5:36980. doi: 10.1038/srep36980
151. Kinkead LC, Allen LA. Multifaceted Effects of *Francisella Tularensis* on Human Neutrophil Function and Lifespan. *Immunol Rev* (2016) 273:266–81. doi: 10.1111/imr.12445
152. Schwartz JT, Bandyopadhyay S, Kobayashi SD, McCracken J, Whitney AR, De Leo FR, et al. *Francisella Tularensis* Alters Human Neutrophil Gene Expression: Insights Into the Molecular Basis of Delayed Neutrophil Apoptosis. *J Innate Immun* (2013) 5:124–36. doi: 10.1159/000342430
153. McCracken JM, Kinkead LC, McCaffrey RL, Allen L-AH. *Francisella Tularensis* Modulates a Distinct Subset of Regulatory Factors and Sustains Mitochondrial Integrity to Impair Human Neutrophil Apoptosis. *J Innate Immun* (2016) 8:299–313. doi: 10.1159/000443882
154. Yipp BG, Kubes P. NETosis: How Vital Is It? *Blood* (2013) 122:2784–94. doi: 10.1182/blood-2013-04-457671
155. Bardoel BW, Kenny EF, Sollberger G, Zychlinsky A. The Balancing Act of Neutrophils. *Cell Host Microbe* (2014) 15:526–36. doi: 10.1016/j.chom.2014.04.011
156. Metzler KD, Goosmann C, Lubojemska A, Zychlinsky A. Papayannopoulos V. A Myeloperoxidase-Containing Complex Regulates Neutrophil Elastase Release and Actin Dynamics During NETosis. *Cell Rep* (2014) 8:883–96. doi: 10.1016/j.celrep.2014.06.044
157. Sørensen OE, Borregaard N. Neutrophil Extracellular Traps - the Dark Side of Neutrophils. *J Clin Invest* (2016) 126:1612–20. doi: 10.1172/JCI84538
158. Papayannopoulos V. Neutrophil Extracellular Traps in Immunity and Disease. *Nat Rev Immunol* (2018) 18:134–47. doi: 10.1038/nri.2017.105
159. Tadie JM, Bae HB, Jiang S, Park DW, Bell CP, Yang H, et al. HMGB1promotes Neutrophil Extracellular Trap Formation Through Interactions With Toll-Like Receptor 4. *Am J Physiol Lung Cell Mol Physiol* (2013) 304:L342–9. doi: 10.1152/ajplung.00151.2012
160. Banerjee S, de Freitas A, Friggeri A, Zmijewski JW, Liu G, Abraham E. Intracellular HMGB1 Negatively Regulates Efferocytosis. *J Immunol* (2011) 187:4686–94. doi: 10.4049/jimmunol.1101500
161. Pilsczek FH, Salina D, Poon KK, Fahey C, Yipp BG, Sibley CD, et al. A Novel Mechanism of Rapid Nuclear Neutrophil Extracellular Trap Formation in Response to *Staphylococcus Aureus*. *J Immunol* (2010) 185:7413–25. doi: 10.4049/jimmunol.1000675
162. Yousefi S, Mihalache C, Kozlowski E, Schmid I, Simon HU. Viable Neutrophils Release Mitochondrial DNA to Form Neutrophil Extracellular Traps. *Cell Death Differ* (2009) 16:1438–44. doi: 10.1038/cdd.2009.96
163. Byrd AS, O'Brien XM, Johnson CM, Lavigne LM, Reichner JS. An Extracellular Matrix-Based Mechanism of Rapid Neutrophil Extracellular Trap Formation in Response to *Candida Albicans*. *J Immunol* (2013) 190:4136–48. doi: 10.4049/jimmunol.1202671
164. Lefrançais E, Mallavia B, Zhuo H, Calfee CS, Looney MR. Maladaptive Role of Neutrophil Extracellular Traps in Pathogen-Induced Lung Injury. *JCI Insight* (2018) 3:e98178. doi: 10.1172/jci.insight.98178
165. Hakkim A, Fürnrohr BG, Amann K, Laube B, Abed UA, Brinkmann V, et al. Impairment of Neutrophil Extracellular Trap Degradation Is Associated With Lupus Nephritis. *Proc Natl Acad Sci USA* (2010) 107:9813–8. doi: 10.1073/pnas.0909927107
166. Farrera C, Fadeel B. Macrophage Clearance of Neutrophil Extracellular Traps is a Silent Process. *J Immunol* (2013) 191:2647–56. doi: 10.4049/jimmunol.1300436
167. Lazzaretto B, Fadeel B. Intra- and Extracellular Degradation of Neutrophil Extracellular Traps by Macrophages and Dendritic Cells. *J Immunol* (2019) 203:2276–90. doi: 10.4049/jimmunol.1800159
168. Chiang N, Sakuma M, Rodriguez AR, Spur BW, Irimia D, Serhan CN. Resolvin T-Series Reduce Neutrophil Extracellular Traps. *Blood* (2022) 139:1222–33. doi: 10.1182/blood.2021013422
169. Clark SR, Ma AC, Tavener SA, McDonald B, Goodarzi Z, Kelly MM, et al. Platelet TLR4 Activates Neutrophil Extracellular Traps to Ensnare Bacteria in Septic Blood. *Nat Med* (2007) 13:463–9. doi: 10.1038/nm1565
170. Fuchs TA, Brill A, Duerschmied D, Schatzberg D, Monestier M, Myers DD Jr, et al. Extracellular DNA Traps Promote Thrombosis. *Proc Natl Acad Sci USA* (2010) 107:15880–5. doi: 10.1073/pnas.1005743107
171. Semeraro F, Ammollo CT, Morrissey JH, Dale GL, Friese P, Esmon NL, et al. Extracellular Histones Promote Thrombin Generation Through Platelet-Dependent Mechanisms: Involvement of Platelet TLR2 Andtlr4. *Blood* (2011) 118:1952–61. doi: 10.1182/blood-2011-03-343061
172. Xu J, Zhang X, Monestier M, Esmon NL, Esmon CT. Extracellular Histones are Mediators of Death Through TLR2 and TLR4 in Mouse Fatal Liver Injury. *J Immunol* (2011) 187:2626–31. doi: 10.4049/jimmunol.1003930
173. Gupta S, Kaplan MJ. The Role of Neutrophils and NETosis in Autoimmune and Renal Diseases. *Nat Rev Nephrol* (2016) 12:402–13. doi: 10.1038/nrneph.2016.71
174. Li H, Zhou X, Tan H, Hu Y, Zhang L, Liu S, et al. Neutrophil Extracellular Traps Contribute to the Pathogenesis of Acid-Aspiration-Induced ALI/ARDS. *Oncotarget* (2018) 9:1772–84. doi: 10.18632/oncotarget.22744
175. Barnes BJ, Adrover JM, Baxter-Stoltzfus A, Borczuk A, Cools-Lartigue J, Crawford JM, et al. Targeting Potential Drivers of COVID-19: Neutrophil Extracellular Traps. *J Exp Med* (2020) 217:e20200652. doi: 10.1084/jem.20200652
176. Zuo Y, Yalavarthi S, Shi H, Gockman K, Zuo M, Madison JA, et al. Neutrophil Extracellular Traps in COVID-19. *JCI Insight* (2020) 5:e138999. doi: 10.1172/jci.insight.138999
177. Middleton EA, He X-Y, Denorme F, Campbell RA, Ng D, Salvatore SP, et al. Neutrophil Extracellular Traps Contribute to Immunothrombosis in COVID-19 Acute Respiratory Distress Syndrome. *Blood* (2020) 136:1169–79. doi: 10.1182/blood.2020007008

178. Nathan C. Neutrophils and COVID-19: Nots, NETs, and Knots. *J Exp Med* (2020) 217:e20201439. doi: 10.1084./jem.20201439
179. Tomar B, Anders H-J, Desai J, Mulay SR. Neutrophils and Neutrophil Extracellular Traps Drive Necroinflammation in COVID-19. *Cells* (2020) 9:1383. doi: 10.3390/cells9061383
180. Schönrich G, Raftery MJ, Samstag Y. Devilishly Radical NETwork in COVID-19: Oxidative Stress, Neutrophil Extracellular Traps (NETs), and T Cell Suppression. *Rev Adv Biol Regul* (2020) 77:100741. doi: 10.1016/j.jbior.2020.100741
181. Zhou Z, Ren L, Zhang L, Zhong J, Xiao Y, Jia Z, et al. Heightened Innate Immune Responses in the Respiratory Tract of COVID-19 Patients. *Cell Host Microbe* (2020) 27:883–90.e2. doi: 10.1016/j.chom.2020.04.017
182. Radermecker C, Detrembleur N, Guiot J, Cavalier E, Henket M, d'Emal C, et al. Neutrophil Extracellular Traps Infiltrate the Lung Airway, Interstitial, and Vascular Compartments in Severe COVID-19. *J Exp Med* (2020) 217: e20201012. doi: 10.1084/jem.20201012
183. Nathan C. Neutrophils and Immunity: Challenges and Opportunities. *Nat Rev Immunol* (2006) 6:173–82. doi: 10.1038/nri1785
184. Cristinziano L, Modestino L, Antonelli A, Marone G, Simon H-U, Varricchi G, et al. Neutrophil Extracellular Traps in Cancer. *Semin Cancer Biol* (2022) 79:91–204. doi: 10.1016/j.semcancer.2021.07.011
185. Arelaki S, Arampatzioglou A, Kambas K, Papagoras C, Miltiades P, Angelidou I, et al. Gradient Infiltration of Neutrophil Extracellular Traps in Colon Cancer and Evidence for Their Involvement in Tumour Growth. *PloS One* (2016) 11:e0154484. doi: 10.1371/journal.pone.0154484
186. Schedel F, Mayer-Hain S, Pappelbaum KI, Metze D, Stock M, Goerge T, et al. Evidence and Impact of Neutrophil Extracellular Traps in Malignant Melanoma. *Pigment Cell Melanoma Res* (2020) 33:63–73. doi: 10.1111/pcmr.12818
187. Millrud CR, Kågedal Å, Kumlien Georén S, Winqvist O, Uddman R, Razavi R, et al. NET-Producing CD16^{high} CD62L^{dim} Neutrophils Migrate to Tumor Sites and Predict Improved Survival in Patients With HNSCC. *Int J Cancer* (2017) 140:2557–67. doi: 10.1002/ijc.30671
188. Erpenbeck L, Schon MP. Neutrophil Extracellular Traps: Protagonists of Cancer Progression? *Oncogene* (2017) 36:2483–90. doi: 10.1038/onc.2016.406
189. Barkan D, El Touny LH, Michalowski AM, Smith JA, Chu I, Davis AS, et al. Metastatic Growth From Dormant Cells Induced by a Col-I Enriched Fibrotic Environment. *Cancer Res* (2010) 70:5706–16. doi: 10.1158/0008-5472.CAN-09-2356
190. Pierce BL, Ballard-Barbash R, Bernstein L, Baumgartner RN, Neuhouser ML, Wener MH, et al. Elevated Biomarkers of Inflammation Are Associated With Reduced Survival Among Breast Cancer Patients. *J Clin Oncol* (2009) 27:3437–44. doi: 10.1200/JCO.2008.18.9068
191. Teijeira Á, Garasa S, Gato M, Alfaro C, Migueliz I, Cirella A, et al. CXCR1 and CXCR2 Chemokine Receptor Agonists Produced by Tumors Induce Neutrophil Extracellular Traps That Interfere With Immune Cytotoxicity. *Immunity* (2020) 52:856–71.e8. doi: 10.1016/j.immuni.2020.03.001
192. Cristinziano L, Modestino L, Loffredo S, Varricchi G, Braile M, Ferrara AL, et al. Anaplastic Thyroid Cancer Cells Induce the Release of Mitochondrial Extracellular DNA Traps by Viable Neutrophils. *J Immunol* (2020) 204:1362–72. doi: 10.4049/jimmunol.1900543
193. Seo JD, Gu J-Y, Jung HS, Kim YJ, Kim HK. Contact System Activation and Neutrophil Extracellular Trap Markers: Risk Factors for Portal Vein Thrombosis in Patients With Hepatocellular Carcinoma. *Clin Appl Thromb Hemost* (2019) 25:1076029618825310. doi: 10.1177/1076029618825310
194. Bang OY, Chung J-W, Cho YH, Oh MJ, Seo W-K, Kim G-M, et al. Circulating DNAs, a Marker of Neutrophil Extracellular Traposis and Cancer-Related Stroke: The OASIS-Cancer Study. *Stroke* (2019) 50:2944–7. doi: 10.1161/STROKEAHA.119.026373
195. Boone BA, Murthy P, Miller-Ocuin J, Doerfler WR, Ellis JT, Liang X, et al. Chloroquine Reduces Hypercoagulability in Pancreatic Cancer Through Inhibition of Neutrophil Extracellular Traps. *BMC Cancer* (2018) 18:678. doi: 10.1186/s12885-018-4584-2
196. McDonald B, Spicer J, Giannais B, Fallavollita L, Brodt P, Ferri LE. Systemic Inflammation Increases Cancer Cell Adhesion to Hepatic Sinusoids by Neutrophil Mediated Mechanisms. *Int J Cancer* (2009) 125:1298–305. doi: 10.1002/ijc.24409
197. Yang L, Liu Q, Zhang X, Liu X, Zhou B, Chen J, et al. DNA of Neutrophil Extracellular Traps Promotes Cancer Metastasis *via* CCDC25. *Nature* (2020) 583:133–8. doi: 10.1038/s41586-020-2394-6
198. Pasparakis M, Vandenabeele P. Necroptosis and its Role in Inflammation. *Nature* (2015) 517:311–20. doi: 10.1038/nature14191
199. Benarafa C, Simon HU. Role of Granule Proteases in the Life and Death of Neutrophils. *Biochem Biophys Res Commun* (2017) 482:473–81. doi: 10.1016/j.bbrc.2016.11.086
200. Wang X, He Z, Liu H, Yousefi S, Simon HU. Neutrophil Necroptosis is Triggered by Ligation of Adhesion Molecules Following GM-CSF Priming. *J Immunol* (2016) 197:4090–100. doi: 10.4049/jimmunol.1600051
201. Wicki S, Gurzeler U, Wei-Lynn Wong W, Jost PJ, Bachmann D, Kaufmann T. Loss of XIAP Facilitates Switch to Tnfα-Induced Necroptosis in Mouse Neutrophils. *Cell Death Dis* (2016) 7:e2422. doi: 10.1038/cddis.2016.311
202. Weinlich R, Oberst A, Beere HM, Green DR. Necroptosis in Development, Inflammation, and Disease. *Nat Rev Mol Cell Biol* (2017) 18:127–36. doi: 10.1038/nrm.2016.149
203. Desai J, Kumar SV, Mulay SR, Konrad L, Romoli S, Schauer C, et al. PMA and Crystal-Induced Neutrophil Extracellular Trap Formation Involves RIPK1-RIPK3-MLKL Signaling. *Eur J Immunol* (2016) 46:223–9. doi: 10.1002/eji.201545605
204. Amini P, Stojkov D, Wang X, Wicki S, Kaufmann T, Wong WW, et al. NET Formation can Occur Independently of RIPK3 and MLKL Signaling. *Eur J Immunol* (2016) 46:178–84. doi: 10.1002/eji.201545615
205. Greenlee-Wacker MC, Kremserová S, Nauseef WM. Lysis of Human Neutrophils by Community-Associated Methicillin-Resistant *Staphylococcus Aureus*. *Blood* (2017) 129:3237–44. doi: 10.1182/blood-2017-02-766253
206. Greenlee-Wacker MC, Rigby KM, Kobayashi SD, Porter AR, De Leo FR, Nauseef WM. Phagocytosis of *Staphylococcus Aureus* by Human Neutrophils Prevents Macrophage Efferocytosis and Induces Programmed Necrosis. *J Immunol* (2014) 192:4709–17. doi: 10.4049/jimmunol.1302692
207. Kremserova S, Nauseef WM. Frontline Science: *Staphylococcus Aureus* Promotes Receptor-Interacting Protein Kinase 3- and Protease-Dependent Production of IL-1β in Human Neutrophils. *J Leukoc Biol* (2019) 105:437–47. doi: 10.1002/JLB.4HI0918-346R
208. Chen GY, Nuñez G. Sterile Inflammation: Sensing and Reacting to Damage. *Nat Rev Immunol* (2010) 10:826–37. doi: 10.1038/nri2873
209. Westman J, Grinstein S, Marques PE. Phagocytosis of Necrotic Debris at Sites of Injury and Inflammation. *Front Immunol* (2020) 10:3030. doi: 10.3389/fimmu.2019.03030
210. McDonald B, Pittman K, Menezes GB, Hirota SA, Slaba I, Waterhouse CC, et al. Intravascular Danger Signals Guide Neutrophils to Sites of Sterile Inflammation. *Science* (2010) 330:362–6. doi: 10.1126/science.1195491
211. Gaipl US, Kuenkele S, Voll RE, Beyer TD, Kolowos W, Heyder P, et al. Complement Binding is an Early Feature of Necrotic and a Rather Late Event During Apoptotic Cell Death. *Cell Death Differ* (2001) 8:327–34. doi: 10.1038/sj.cdd.4400826
212. Blume KE, Soeroes S, Waibel M, Keppeler H, Wesselborg S, Herrmann M, et al. Cell Surface Externalization of Annexin A1 as a Failsafe Mechanism Preventing Inflammatory Responses During Secondary Necrosis. *J Immunol* (2009) 183:8138–47. doi: 10.4049/jimmunol.0902250
213. Crisford H, Sapey E, Stockley RA. Proteinase 3; a Potential Target in Chronic Obstructive Pulmonary Disease and Other Chronic Inflammatory Diseases. *Respir Res* (2018) 19:180. doi: 10.1186/s12931-018-0883-z
214. Ley K, Rivera-Nieves J, Sandborn WJ, Shattil S. Integrin-Based Therapeutics: Biological Basis, Clinical Use, and New Drugs. *Nat Rev Drug Discov* (2016) 15:173–83. doi: 10.1038/nrd.2015.10
215. Wolf D, Anto-Michel N, Blankenbach H, Wiedermann A, Buscher K, Hohmann JD, et al. A Ligand-Specific Blockade of the Integrin Mac-1selectively Targets Pathologic Inflammation While Maintaining Protective Host-Defense. *Nat Commun* (2018) 9:525. doi: 10.1038/s41467-018-02896-8
216. Wolf D, Hohmann J-D, Wiedermann A, Bledzka K, Blankenbach H, Marchini T, et al. Binding of CD40L to Mac-1's I-Domain Involves the EQLKKSKTL Motif and Mediates Leukocyte Recruitment and Atherosclerosis–But Does Not Affect Immunity and Thrombosis in Mice. *Circ Res* (2011) 109:1269–79. doi: 10.1161/CIRCRESAHA.111.247684

217. Fan Z, McArdle S, Marki A, Mikulski Z, Gutierrez E, Engelhardt B, et al. Neutrophil Recruitment Limited by High Affinity Bent β2 Integrin Binding Ligand in Cis. *Nat Commun* (2016) 7:12658. doi: 10.1038/ncomms12658
218. Wilson ZS, Ahn LB, Serratelli WS, Belley MD, Lomas-Nera J, Sen M, et al. Activated β2 Integrins Restrict Neutrophil Recruitment During Murine Acute Pseudomonal Pneumonia. *Am J Respir Cell Mol Biol* (2017) 56:620–7. doi: 10.1165/rcmb.2016-0215OC
219. Saggu G, Okubo K, Chen Y, Vattepu R, Tsuboi N, Rosetti F, et al. Cis Interaction Between Sialylated FcgRIIA and the aI-Domain of Mac-1 Limits Antibody-Mediated Neutrophil Recruitment. *Nat Commun* (2018) 9:5058. doi: 10.1038/s41467-018-07506-1
220. Kelm M, Lehoux S, Azcutia V, Cummings RD, Nusrat A, Parkos CA, et al. Regulation of Neutrophil Function by Selective Targeting of Glycan Epitopes Expressed on the Integrin CD11b/Cd18. *FASEB J* (2020) 34:2326–43. doi: 10.1096/fj.201902542R
221. Maiguel D, Faridi MH, Wei C, Kuwano Y, Balla KM, Hernandez D, et al. Small Molecule–Mediated Activation of the Integrin CD11b/CD18 Reduces Inflammatory Disease. *Sci Signal* (2011) 4:ra57. doi: 10.1126/scisignal.2001811
222. Schmid MC, Khan SQ, Kaneda MM, Pathria P, Shephard R, Louis TL, et al. Integrin CD11b Activation Drives Anti-Tumor Innate Immunity. *Nat Commun* (2018) 9:5379. doi: 10.1038/s41467-018-07387-4
223. Chiang N, Serhan CN. Structural Elucidation and Physiologic Functions of Specialized Pro-Resolving Mediators and Their Receptors. *Mol Aspects Med* (2017) 58:114–29. doi: 10.1016/j.mam.2017.03.005
224. Brancaleone V, Mitidieri E, Flower RJ, Cirino G, Perretti M. Annexin A1 Mediates Hydrogen Sulfide Properties in the Control of Inflammation. *J Pharmacol Exp Ther* (2014) 351:96–104. doi: 10.1124/jpet.114.217034
225. Mustafa M, Zarrough A, Bolstad AI, Lygre H, Mustafa K, Hasturk H, et al. Resolvin D1 Protects Periodontal Ligament. *Am J Physiol Cell Physiol* (2013) 305:C673–9. doi: 10.1152/ajpcell.00242.2012
226. Haworth O, Cernadas M, Yang R, Serhan CN, Levy BD. Resolvin E1 Regulates Interleukin 23, Interferon-Gamma and Lipoxin A4 to Promote the Resolution of Allergic Inflammation. *Nat Immunol* (2008) 9:873–9. doi: 10.1038/ni.1627
227. Yazid S, Leoni G, Getting SJ, Cooper D, Solito E, Perretti M, et al. Antiallergic Cromones Inhibit Neutrophil Recruitment Onto Vascular Endothelium *via* Annexin-A1mobilization. *Arterioscler Thromb Vasc Biol* (2010) 30:1718–24. doi: 10.1161/ATVBAHA.110.209536
228. Perretti M, D'Acquisto F. Annexin A1 and Glucocorticoids as Effectors of the Resolution of Inflammation. *Nat Rev Immunol* (2009) 9:62–70. doi: 10.1038/nri2470
229. Yona S, Heinsbroek SE, Peiser L, Gordon S, Perretti M, Flower RJ. Impaired Phagocytic Mechanism in Annexin 1 Null Macrophages. *Br J Pharmacol* (2006) 148:469–77. doi: 10.1038/sj.bjp.0706730
230. McArthur S, Gobbetti T, Kusters DH, Reutelingsperger CP, Flower RJ, Perretti M. Definition of a Novel Pathway Centered on Lysophosphatidic Acid to Recruit Monocytes During the Resolution Phase of Tissue Inflammation. *J Immunol* (2015) 195:1139–51. doi: 10.4049/jimmunol.1500733
231. Li Y, Cai L, Wang H, Wu P, Gu W, Chen Y, et al. Pleiotropic Regulation of Macrophage Polarization and Tumorigenesis by Formyl Peptide Receptor-2. *Oncogene* (2011) 30:3887–99. doi: 10.1038/onc.2011.112
232. McArthur S, Juban G, Gobbetti T, Desgorges T, Theret M, Gondin J, et al. Annexin A1 Drives Macrophage Skewing to Accelerate Muscle Regeneration Through AMPK Activation. *J Clin Invest* (2020) 130:1156–67. doi: 10.1172/JCI124635
233. Tsai WH, Chien HY, Shih CH, Lai SL, Li IT, Hsu SC, et al. Annexin A1 Mediates the Anti-Inflammatory Effects During the Granulocytic Differentiation Process in All-Trans Retinoic Acid-Treated Acute Promyleocytic Leukemic Cells. *J Cell Physiol* (2012) 227:3661–9. doi: 10.1002/jcp.24073
234. Leoni G, Neumann PA, Kamaly N, Quiros M, Nishio H, Jones HR, et al. Annexin A1-Containing Extracellular Vesicles and Polymeric Nanoparticles Promote Epithelial Wound Repair. *J Clin Invest* (2015) 125:1215–27. doi: 10.1172/JCI76693
235. Headland SE, Jones HR, Norling LV, Kim A, Souza PR, Corsiero E, et al. Neutrophil-Derived Microvesicles Enter Cartilage and Protect the Joint in Inflammatory Arthritis. *Sci Transl Med* (2015) 7:315ra190. doi: 10.1126/scitranslmed.aac5608
236. József L, Zouki C, Petasis NA, Serhan CN, Filep JG. Lipoxin A_4 and Aspirin-Triggered 15-Epi-Lipoxin A_4 Inhibit Peroxynitrite Formation, NF-κb and AP-1 Activation, and IL-8 Gene Expression in Human Leukocytes. *Proc Natl Acad Sci USA* (2002) 99:13266–71. doi: 10.1073/pnas.202296999
237. Levy BD, De Sanctis GT, Devchand PR, Kim E, Ackerman K, Schmidt BA, et al. Multi-Pronged Inhibition of Airway Hyper-Responsiveness and Inflammation by Lipoxin A_4. *Nat Med* (2002) 8:1018–23. doi: 10.1038/nm748
238. Godson C, Mitchell S, Harvey K, Petasis NA, Hogg N, Brady HR. Cutting Edge: Lipoxins Rapidly Stimulate Nonphlogistic Phagocytosis of Apoptotic Neutrophils by Monocyte-Derived Macrophages. *J Immunol* (2000) 164:1663–7. doi: 10.4049/jimmunol.164.4.1663
239. Schwab JM, Chiang N, Arita M, Serhan CN. Resolvin E1 and Protectin D1 Activate Inflammation-Resolution Programmes. *Nature* (2007) 447:869–74. doi: 10.1038/nature05877
240. Karp CL, Flick LM, Park KW, Softic S, Greer TM, Keledjian R, et al. Defective Lipoxin-Mediated Anti-Inflammatory Activity in the Cystic Fibrosis Airway. *Nat Immunol* (2004) 5:388–92. doi: 10.1038/ni1056
241. Morita M, Kuba K, Ichikawa A, Nakayama M, Katahira J, Iwamoto R, et al. The Lipid Mediator Protectin D1 Inhibits Influenza Virus Replication and Improves Severe Influenza. *Cell* (2013) 153:112–25. doi: 10.1016/j.cell.2013.02.027
242. Colas RA, Shinohara M, Dalli J, Chiang N, Serhan CN. Identification and Signature Profiles for Pro-Resolving and Inflammatory Lipid Mediators in Human Tissue. *Am J Physiol Cell Physiol* (2014) 307:C39–54. doi: 10.1152/ajpcell.00024.2014
243. Dalli J, Colas RA, Quintana C, Barragan-Bradford D, Huwitz S, Levy BD, et al. Human Sepsis Eicosanoid and Proresolving Lipid Mediator Temporal Profiles: Correlations With Survival and Clinical Outcomes. *Crit Care Med* (2017) 45:58–68. doi: 10.1097/CCM.0000000000002014
244. Norling LV, Spite M, Yang R, Flower RJ, Perretti M, Serhan CN. Cutting Edge: Humanized Nano-Proresolving Medicines Mimic Inflammation-Resolution and Enhance Wound Healing. *J Immunol* (2011) 186:5543–7. doi: 10.4049/jimmunol.1003865
245. The Forsyth Institute. *Safety and Preliminary Efficacy of Lipoxin Analog BLXA4-ME Oral Rinse for the Treatment of Gingivitis (Blxa4)*. Available at: https://clinicaltrials.gov/ct2/show/NCT02342691 (Accessed January 25, 2022).
246. Corminboeuf O, Leroy X. FPR2/ALXR Agonists and the Resolution of Inflammation. *J Med Chem* (2015) 58:537–59. doi: 10.1021/jm501051x
247. de Gaetano M, Butler E, Gahan K, Zanetti A, Marai M, Chen J, et al. Asymmetric Synthesis and Biological Evaluation of Imidazole- and Oxazole-Containing Synthetic Lipoxin A_4 Mimetics (Slxms). *Eur J Med Chem* (2019) 162:80–108. doi: 10.1016/j.ejmech.2018.10.049
248. Heo SC, Kwon YW, Jang IH, Jeong GO, Lee TW, Yoon JW, et al. Formyl Peptide Receptor 2 is Involved in Cardiac Repair After Myocardial Infarction Through Mobilization of Circulating Angiogenic Cells. *Stem Cells* (2017) 35:654–65. doi: 10.1002/stem.2535
249. Stalder AK, Lott D, Strasser DS, Cruz HG, Krause A, Groenen PMA, et al. Biomarker-Guided Clinical Development of the First-in-Class Anti-Inflammatory FPR2/ALX Agonist ACT-389949. *Br J Clin Pharmacol* (2017) 83:476–86. doi: 10.1111/bcp.13149
250. Asahina Y, Wurtz NR, Arakawa K, Carson N, Fujii K, Fukuchi K, et al. Discovery of BMS-986235/LAR-1219: A Potent Formyl Peptide Receptor 2 (FPR2) Selective Agonist for the Prevention of Heart Failure. *J Med Chem* (2020) 63:9003–19. doi: 10.1021/acs.jmedchem.9b02101
251. Lucas CD, Dorward DA, Tait MA, Fox S, Marwick JA, Allen KC, et al. Downregulation of Mcl-1 has Anti-Inflammatory Pro-Resolution Effects and Enhances Bacterial Clearance From the Lung. *Mucosal Immunol* (2014) 7:857–68. doi: 10.1038/mi.2013.102
252. Leitch AE, Lucas CD, Marwick JA, Duffin R, Haslett C, Rossi AG. Cyclin-Dependent Kinases 7 and 9 Specifically Regulate Neutrophil Transcription and Their Inhibition Drives Apoptosis to Promote Resolution of Inflammation. *Cell Death Differ* (2012) 19:1950–61. doi: 10.1038/cdd.2012.80
253. Dorward DA, Felton JM, Robb CT, Craven T, Kipari T, Walsh TS, et al. The Cyclin-Dependent Kinase Inhibitor AT7519 Accelerates Neutrophil

Apoptosis in Sepsis-Related Acute Respiratory Distress Syndrome. *Thorax* (2017) 72:182–5. doi: 10.1136/thoraxjnl-2016-209229
254. Teixeira RAP, Mimura KK, Araujo LP, Greco KV, Oliani SM. The Essential Role of Annexin A1 Mimetic Peptide in the Skin Allograft Survival. *J Tissue Eng Regener Med* (2016) 10:E44–53. doi: 10.1002/term.1773
255. Vago JP, Nogueira CR, Tavares LP, Soriani FM, Lopes F, Russo RC, et al. Annexin A1 Modulates Natural and Glucocorticoid-Induced Resolution of Inflammation by Enhancing Neutrophil Apoptosis. *J Leukoc Biol* (2012) 92:249–58. doi: 10.1189/jlb.0112008
256. Guo RF, Ward PA. Role of C5a in Inflammatory Responses. *Annu Rev Immunol* (2005) 23:821–52. doi: 10.1146/annurev.immunol.23.021704.115835
257. McGrath EE, Marriott HM, Lawrie A, Francis SE, Sabroe I, Renshaw SA, et al. TNF-Related Apoptosis-Inducing Ligand (TRAIL) Regulates Inflammatory Neutrophil Apoptosis and Enhances Resolution of Inflammation. *J Leukoc Biol* (2011) 90:855–65. doi: 10.1189/jlb.0211062
258. Witko-Sarsat V, Mocek J, Bouayad D, Tamassia N, Ribeil JA, Candalh C, et al. Proliferating Cell Nuclear Antigen Acts as a Cytoplasmic Platform Controlling Human Neutrophil Survival. *J Exp Med* (2010) 207:2631–45. doi: 10.1084/jem.20092241
259. Martin C, Ohayon D, Alkan M, Mocek J, Pederzoli-Ribeil M, Candalh C, et al. Neutrophil-Expressed P21/Waf1 Favors Inflammation Resolution in *Pseudomonas Aeruginosa* Infection. *Am J Respir Cell Mol Biol* (2016) 54:740–50. doi: 10.1165/rcmb.2015-0047OC
260. Arial A, Fredman G, Sun Y-P, Kantarci A, Van Dyke TE, Luster AD, et al. Apoptotic Neutrophils and T Cells Sequester Chemokines During Immune Response Resolution Through Modulation of CCR5 Expression. *Nat Immunol* (2006) 7:1209–16. doi: 10.1038/ni1392
261. Karbian N, Abutbul A, el-Amore R, Eliaz R, Beeri R, Reicher B, et al. Apoptotic Cell Therapy for Cytokine Storm Associated With Acute Severe Sepsis. *Cell Death Dis* (2020) 11:535. doi: 10.1038/s41419-020-02748-8
262. Krysko DV, Denecker G, Festjens N, Gabriels S, Parthoens E, D'Herde K, et al. Macrophages Use Different Internalization Mechanisms to Clear Apoptotic and Necrotic Cells. *Cell Death Differ* (2006) 13:2011–22. doi: 10.1038/sj.cdd.4401900
263. Grégoire M, Uhel F, Lesouhaitier M, Gacouin A, Guirriec M, Mourcin F, et al. Impaired Efferocytosis and Neutrophil Extracellular Trap Clearance by Macrophages in ARDS. *Eur Respir J* (2018) 52:1702590. doi: 10.1183/13993003.02590-2017
264. Bae H-B, Zmijewski JW, Deshane JS, Tadie JM, Chaplin DD, Takashima S, et al. AMP-Activated Protein Kinase Enhances the Phagocytic Ability of Macrophages and Neutrophils. *FASEB J* (2011) 25:4358–68. doi: 10.1096/fj.11-190587
265. Lee JS, Shin E-C. The Type I Interferon Response in COVID-19: Implications for Treatment. *Nat Rev Immunol* (2020) 20:585–6. doi: 10.1038/s41577-020-00429-3
266. Patel S, Kumar S, Jyoti A, Srinag BS, Keshari RS, Saluja R, et al. Nitric Oxide Donors Release Extracellular Traps From Human Neutrophils by Augmenting Free Radical Generation. *Nitric Oxide* (2010) 22:226–34. doi: 10.1016/j.niox.2010.01.001
267. Zheng W, Warner R, Ruggeri R, Su C, Cortes C, Skoura A, et al. PF-1355, a Mechanism-Based Myeloperoxidase Inhibitor, Prevents Immune Complex Vasculitis and Anti-Glomerular-Basement Membrane Glomerulonephritis. *J Pharmacol Exp Ther* (2015) 353:288–98. doi: 10.1124/jpet.114.221788
268. Willis VC, Gizinski AM, Banda NK, Causey CP, Knuckley B, Cordova KN, et al. N-α-Benzoyl-N5-(2-Chloro-1-Iminoethyl)-L-Ornithine Amide, a Protein Arginine Deiminase Inhibitor, Reduces the Severity of Murine Collagen-Induced Arthritis. *J Immunol* (2011) 186:4396–404. doi: 10.4049/jimmunol.1001620
269. Knight JS, Zhao W, Luo W, Subramanian V, O'Dell AA, Yalavarthi S, et al. Peptidylarginine Deiminase Inhibition is Immunomodulatory and Vasoprotective in Murine Lupus. *J Clin Invest* (2012) 123:2981–93. doi: 10.1172/JCI67390
270. Knight JS, Luo W, O'Dell AA, Yalavarthi S, Zhao W, Subramanian V, et al. Peptidylarginine Deiminase Inhibition Reduces Vascular Damage and Modulates Innate Immune Responses in Murine Models of Atherosclerosis. *Circ Res* (2014) 114:947–56. doi: 10.1161/CIRCRESAHA.114.303312
271. Lewis HD, Liddle J, Coote JE, Atkinson SJ, Barker MD, Bax BD, et al. Inhibition of PAD4 Activity Is Sufficient to Disrupt Mouse and Human NET Formation. *Nat Chem Biol* (2015) 11:189–91. doi: 10.1038/nchembio.1735
272. Cedervall J, Dragomir A, Saupe F, Zhang Y, Ärnlöv J, Larsson E, et al. Pharmacological Targeting of Peptidylarginine Deiminase 4 Prevents Cancer-Associated Kidney Injury in Mice. *Oncoimmunology* (2017) 6:e1320009. doi: 10.1080/2162402X.2017.1320009
273. Li P, Li M, Lindberg MR, Kennett MJ, Xiong N, Wang Y. PAD4 is Essential for Antibacterial Innate Immunity Mediated by Neutrophil Extracellular Traps. *J Exp Med* (2010) 207:1853–62. doi: 10.1084/jem.20100239
274. Martinod K, Fuchs TA, Zitomersky NL, Wong SL, Demers M, Gallant M, et al. PAD4-Deficiency Does Not Affect Bacteremia in Polymicrobial Sepsis and Ameliorates Endotoxemic Shock. *Blood* (2015) 125:1948–56. doi: 10.1182/blood-2014-07-587709
275. Cherpokova D, Jouvene CC, Libreros S, DeRoo EP, Chu L, de la Rosa X, et al. Resolvin D4 Attenuates the Severity of Pathological Thrombosis in Mice. *Blood* (2019) 134:1458–68. doi: 10.1182/blood.2018886317
276. Catz SD, McLeish KR. Therapeutic Targeting of Neutrophil Exocytosis. *J Leukoc Biol* (2020) 107:393–408. doi: 10.1002/JLB.3RI0120-645R
277. Johnson JL, Ramadass M, He J, Brown SJ, Zhang J, Abgaryan L, et al. Identification of Neutrophil Exocytosis Inhibitors (Nexinhibs), Small Molecule Inhibitors of Neutrophil Exocytosis and Inflammation: Druggability of the Small GTPase Rab27a. *J Biol Chem* (2016) 291:25965–82. doi: 10.1074/jbc.M116.741884
278. Mejias JC, Forrest OA, Margaroli C, Frey Rubio DA, Viera L, Li J, et al. Neutrophil-Targeted, Protease-Activated Pulmonary Drug Delivery Blocks Airway and Systemic Inflammation. *JCI Insight* (2019) 4:e131468. doi: 10.1172/jci.insight.131468
279. Uriarte SM, Rane MJ, Merchant ML, Jin S, Lentsch AB, Ward RA, et al. Inhibition of Neutrophil Exocytosis Ameliorates Acute Lung Injury in Rats. *Shock* (2015) 39:286–92. doi: 10.1097/SHK.0b013e318282c9a1
280. Bai J, Tang L, Lomas-Neira J, Chen Y, McLeish KR, Uriarte SM, et al. TAT-SNAP-23 Treatment Inhibits the Priming of Neutrophil Functions Contributing to Shock and/or Sepsis-Induced Extra-Pulmonary Acute Lung Injury. *Innate Immun* (2015) 21:42–54. doi: 10.1177/1753425913516524
281. Tremblay GM, Jenelle MF, Bourbonnais Y. Anti-Inflammatory Activity of Neutrophil Elastase Inhibitors. *Curr Opin Investig Drugs* (2003) 4:556–65.
282. Potey PMD, Rossi AG, Lucas CD, Dorward DA. Neutrophils in the Initiation and Resolution of Acute Pulmonary Inflammation: Understanding Biological Function and Therapeutic Potential. *J Pathol* (2019) 247:672–85. doi: 10.1002/path.5221
283. Pu S, Wang D, Liu D, Zhao Y, Qi D, He J, et al. Effect of Sivelastat Sodium in Patients With Acute Lung Injury or Acute Respiratory Distress Syndrome: A Meta-Analysis of Randomized Controlled Trials. *BMC Pulm Med* (2017) 17:148. doi: 10.1186/s12890-017-0498-z
284. Sayah DM, Mallavia B, Liu F, Ortiz-Muñoz G, Caudrillier A, Der Hovanessian A, et al. Neutrophil Extracellular Traps are Pathogenic in Primary Graft Dysfunction After Lung Transplantation. *Am J Respir Crit Care Med* (2015) 191:455–63. doi: 10.1164/rccm.201406-1086OC
285. Cedervall J, Zhang Y, Huang H, Zhang L, Femel J, Dimberg A, et al. Neutrophil Extracellular Traps Accumulate in Peripheral Blood Vessels and Compromise Organ Function in Tumor-Bearing Animals. *Cancer Res* (2015) 75:2653–62. doi: 10.1158/0008-5472.CAN-14-3299
286. Macanovic M, Sinicropi D, Shak S, Baughman S, Thiru S, Lachmann PJ. The Treatment of Systemic Lupus Erythematosus (SLE) in NZB/W F1 Hybrid Mice: Studies With Recombinant Murine DNase and With Dexamethasone. *Clin Exp Immunol* (1996) 106:243–52. doi: 10.1046/j.1365-2249.1996.d01-839.x
287. Pottecher J. *Inhaled Dornase Alpha to Reduce Respiratory Failure After Severe Trauma*. Available at: https://clinicaltrials.gov/ct2/show/NCT03368092 (Accessed January 20, 2022).
288. Sponsor. *Protalix. Safety, Tolerability and Pharmacokinetics Study of AIR DNAse Administered by Inhalation to Healthy Adult Volunteers*. Available at: https://clinicaltrials.gov/ct2/show/NCT02605590 (Accessed February 15, 2022).
289. Sponsor. *Protalix. Study to Evaluate the Safety Tolerability Pharmacokinetics and Exploratory Efficacy Parameters of AIR DNase in Patients With Cystic Fibrosis Previously Treated With Pulmozyme*. Available at: https://clinicaltrials.gov/ct2/show/NCT02722122 (Accessed February 15, 2022).
290. Fuchs TA, Jiménez-Alcázar M, Göbel J, Englert H. US patent application US 2020/0024585 A1 (2019).

291. Perretti M, Godson C. Formyl Peptide Receptor Type 2 Agonists to Kick-Start Resolution Pharmacology. *Br J Pharmacol* (2020) 177:4595–600. doi: 10.1111/bph.15212

Conflict of Interest: The author declares that the research was conducted in the absence of any commercial or financial relationships that could be construed as a potential conflict of interest.

Publisher's Note: All claims expressed in this article are solely those of the authors and do not necessarily represent those of their affiliated organizations, or those of the publisher, the editors and the reviewers. Any product that may be evaluated in this article, or claim that may be made by its manufacturer, is not guaranteed or endorsed by the publisher.

frontiers | Frontiers in Immunology

REVIEW
published: 28 April 2022
doi: 10.3389/fimmu.2022.869720

Complement System and Alarmin HMGB1 Crosstalk: For Better or Worse

Christine Gaboriaud[1]*, *Marie Lorvellec*[1], *Véronique Rossi*[1], *Chantal Dumestre-Pérard*[1,2] *and Nicole M. Thielens*[1]

[1] Univ. Grenoble Alpes, CEA, CNRS, IBS, Grenoble, France, [2] Laboratoire d'Immunologie, Pôle de Biologie, CHU Grenoble Alpes, Grenoble, France

Our immune system responds to infectious (PAMPs) and tissue damage (DAMPs) signals. The complement system and alarmin High-Mobility Group Box 1 (HMGB1) are two powerful soluble actors of human host defense and immune surveillance. These systems involve molecular cascades and amplification loops for their signaling or activation. Initially activated as alarm raising systems, their function can be finally switched towards inflammation resolution, where they sustain immune maturation and orchestrate repair mechanisms, opening the way back to homeostasis. However, when getting out of control, these defense systems can become deleterious and trigger serious cellular and tissue damage. Therefore, they can be considered as double-edged swords. The close interaction between the complement and HMGB1 pathways is described here, as well as their traditional and non-canonical roles, their functioning at different locations and their independent and collective impact in different systems both in health and disease. Starting from these systems and interplay at the molecular level (when elucidated), we then provide disease examples to better illustrate the signs and consequences of their roles and interaction, highlighting their importance and possible vicious circles in alarm raising and inflammation, both individually or in combination. Although this integrated view may open new therapeutic strategies, future challenges have to be faced because of the remaining unknowns regarding the molecular mechanisms underlying the fragile molecular balance which can drift towards disease or return to homeostasis, as briefly discussed at the end.

Keywords: complement system, interplay, HMGB1, auto-immunity, lupus, inflammation, periodontitis

OPEN ACCESS

Edited by:
Uday Kishore,
Brunel University London,
United Kingdom

Reviewed by:
József Dobó,
Hungarian Academy of Sciences (MTA), Hungary
Jessy J. Alexander,
University at Buffalo, United States

***Correspondence:**
Christine Gaboriaud
christine.gaboriaud@ibs.fr

Specialty section:
This article was submitted to Molecular Innate Immunity, a section of the journal Frontiers in Immunology

Received: *04 February 2022*
Accepted: *04 April 2022*
Published: *28 April 2022*

Citation:
Gaboriaud C, Lorvellec M, Rossi V, Dumestre-Pérard C and Thielens NM (2022) Complement System and Alarmin HMGB1 Crosstalk: For Better or Worse. Front. Immunol. 13:869720. doi: 10.3389/fimmu.2022.869720

1 INTRODUCTION: COMPLEMENT C1, C3 AND HMGB1 ARE CONSTITUTIVE MULTIFUNCTIONAL COMPONENTS

Several physiological processes keep us healthy, and are modulated throughout the human life, with major variations occurring at the early and late (>65y) stages. Some processes may act silently and get discovered only when they malfunction or drift towards a disequilibrium inducing disease. This idea will be illustrated through two examples of important molecular immune players which are constitutively expressed. This review will mainly focus on the C1 and C3 components of the complement system, a major front line in the host defense, and on the nuclear protein HMGB1,

which functions as an alarmin in the extracellular space. Interestingly, these molecules are always present, except in some very rare cases of deficiency. HMGB1 is strongly conserved through evolution (99 % sequence identity within mammals), and it is lethal when completely missing. Complement C1s and C1q sequence alterations are also quite rare. The classical function of these proteins has been elucidated independently, and will only be briefly summed up, since this review will focus on possible molecular crosstalk that has recently come to light.

We will first shortly describe how alarm signals are raised and amplified through these systems independently, and possibly amplified or down-regulated by their crosstalk. Alert signals are raised by the detection of molecular motifs (associated molecular patterns, AMPs) associated with infectious (pathogens, PAMPs), tissue damage (DAMPS) or cell death (apoptotic cell, ACAMPs) context. Among similarities between the two systems, we aim to illustrate amplification mechanisms as well as the plethora of receptors and signaling pathways involved, their effect thus depending on the local tissues and environment.

The modular assembly of the smallest (HMGB1) and largest (C1q) proteins in the focus of this review are presented in **Figure 1**. Within these structures, multiple interaction sites, with various ligands and receptors (**Figures 1A, B**), lead to a large spectrum of functional facets. Since HMGB1 and the complement proteins in the focus of the present study turn to be multifunctional, the reader will be referred to complementary reviews describing each molecular system in more detail.

2 MOLECULAR BASES ON COMPLEMENT AND HMGB1 MULTIPLE FUNCTIONS, WITH A COMPLEMENTARY FOCUS ON ALARM RAISING, AMPLIFICATION AND DAMPENING

2.1 Alarm Signals Raised by Early Steps of Complement Activation and Its Immediate Amplification Loop at the C3 Convertase Level

The main canonical extracellular functions of the complement system are illustrated in a simplified way in **Figure 2**. According to this "classical" view, this system stands as a central component of the early, innate immune response against pathogens, characterized by the initiation of an extracellular proteolytic cascade (6). It comprises more than 50 soluble and surface proteins, the latter including regulators and receptors. Within the activation cascade, which needs to be locally activated and tightly controlled, many of the soluble proteins are produced as inactive precursors, which need a specific enzymatic cleavage to get activated. In terms of biological activities, the complement proteolytic cascade ultimately results in opsonization and degradation of the recognized target as well as signaling towards local and immune cells through surface receptors. There are three complement pathways that differ in their initiation mechanism: the classical, lectin and alternative pathways. Initiation of the classical pathway (CP) is triggered by the interaction of the recognition molecule C1q with the Fc constant domain of immunoglobulins IgM or IgG or with other target patterns on pathogens or altered cells (7, 8). C1q is associated with a duplet of two proteases, C1r and C1s to form the C1 complex (C1qC1r2C1s2). Upon binding of C1 to a target surface, C1r will autoactivate and cleave C1s (7). Activated C1s is then able to trigger the CP proteolytic cascade by cleavage of its canonical substrates C2 and C4. This will lead to C3 cleavage (by the CP C3 convertase) and finally to immune activation, inflammation, opsonization and eventually lysis of the pathogen. Covalent attachment of the large C3b cleavage product to the target surface through a thioester bond ensures the spatiotemporal control of the opsonization, whereas the smaller soluble C3a fragment will mediate more distant chemotactic and inflammatory signaling. C3 is the central element common to all pathways and the starting point of an amplification loop (9) (**Figure 2**). The principle of the amplification is that C3 convertases cleave many C3 molecules, and that the multiple surface C3b produced bind complement factor B (FB), which will then be cleaved by factor D (FD), to generate more C3 convertases. Amplification at this level is very effective since, at a concentration of about 1.2 mg/ml, C3 is among the most abundant plasma proteins in circulation. Therefore, the regulation of the C3 convertase amplification process is essential for the control of complement activation and its dysregulation can have pathological consequences (10). Several receptors mediate complement signaling and complement regulators modulate its trigger (e.g; C1inhibitor) or amplification, by down-regulating of the C3 or C5 convertases (see **Figure 2**). Since the complement system and its activation have already been presented in an article on the present research topic (11), and extensively reviewed previously, the reader may learn more functional and molecular details elsewhere (6, 10–16).

In addition to the "classical" functions which were briefly mentioned above, new functions of the complement proteins are being discovered (17), which are independent of the extracellular activation of the complement cascades. Initially discovered in immune T cells (18, 19), these non-canonical functions are now becoming a wider set of exciting discoveries (20). As will be later cited, some of these new functions include crosstalk with HMGB1, Toll-Like receptors (TLRs), the inflammasome, the coagulation and contact systems, etc…

2.2 Alarm Signals Associated With HMGB1 And Their Delayed Paracrine/Autocrine Amplification Mechanisms

HMGB1 is a major intracellular protein, initially discovered as part of a family of DNA-binding proteins remodeling chromatin, involved in the regulation of transcription, replication and repair (21). The spectrum of its functional facets is now largely extended (22). For example in the context of septic shock, its determinant impact has been early observed since HMGB1 injection was fatal whereas its neutralization by antibodies

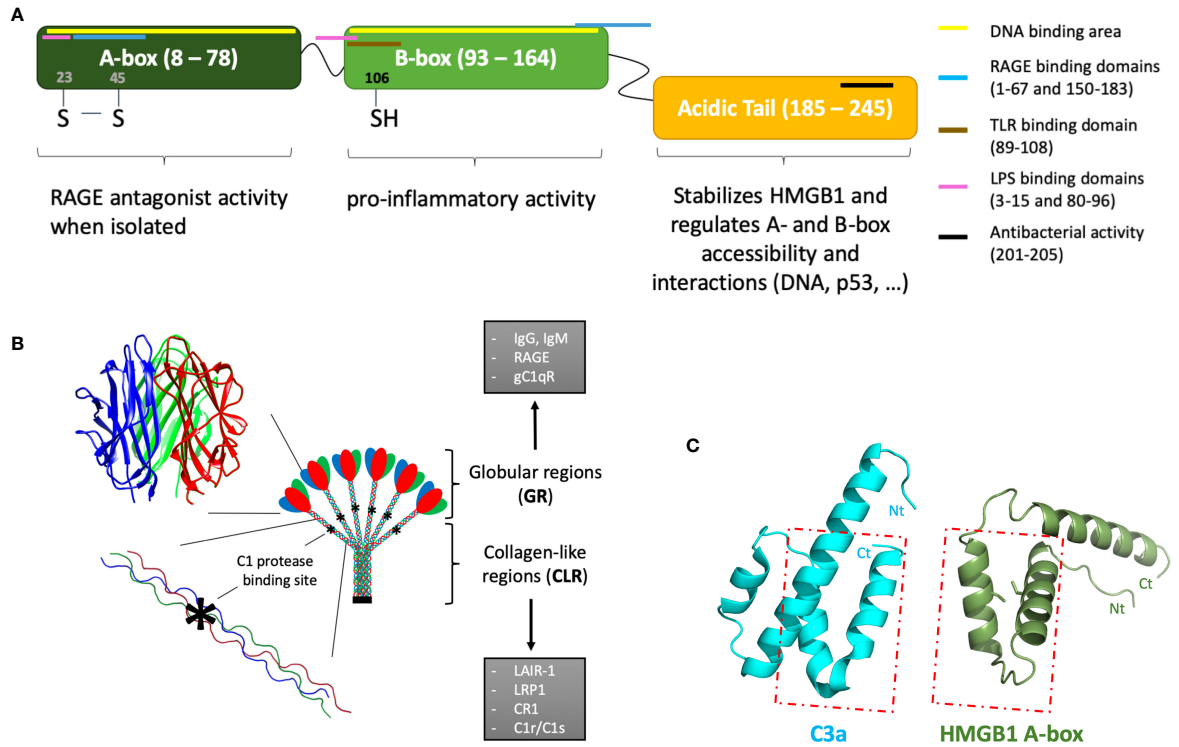

FIGURE 1 | Introductory molecular schemes on HMGB1, C1q, and C3a underlying their multiple functions. **(A)** HMGB1 function is modulated by its two DNA-binding boxes (A-box and B-box) and an acidic C-terminal tail. By binding to different receptors, targets and partners (see color bars), HMGB1 can play multiple extracellular functions. Interactions restricted to intracellular functions are not shown. The X-ray structure of the A-box is shown in **(C)**, with its two cysteines shown as sticks. HMGB1 location within cells depends on its nuclear localization signals (NLS), located in the A-box (24–44) and B-box (179–185). **(B)** The largest multivalent C1q molecule can bridge different receptors or partner molecules through two regions with strongly different structural shapes and interaction properties. C1q is assembled from three different chains (red, blue, green), with numerous post-translational modifications, especially in the collagen-like regions (CLR). The globular regions (GRs) are mostly involved in the multivalent binding of target surfaces. Its main target ligands are surfaces opsonized by IgG, IgM, CRP, PTX3. C1q GR can also directly bind to DNA, phosphatidylserine, annexins, GAPDH, as well as to lipopolysaccharides (LPS) or virus surface proteins (HIV-1 gp41, HTLV-1 gp21). Some surface receptors bind to C1q GR, such as RAGE, gC1qR, DC-SIGN or Siglec 3 (CD33). C1q CLR mostly binds effector molecules, such as the C1r and C1s proteases, or LAIR-1, CR1, LRP1 surface receptors. These latter interactions are almost exclusive, because the proteases compete with receptor binding. The C1r/C1s protease binding site (*) has been finely investigated by C1q site-directed mutagenesis (1). **(C)** The similarity between HMGB1 A-box and C3a is very limited, despite the fact that both are small helical domains which can bind RAGE. The C3a and C5a anaphylatoxins are the smallest fragments released upon C3 and C5 cleavage. They are composed of helices, which is a feature common to HMGB1 boxes. However, only the two C-terminal helices of the A-box can roughly be superimposed to the two N-terminal helices of C3a (see box), in the opposite direction: therefore, the similarity between the two molecules is very limited [PDB codes 1ckt (2) and 4hw5 (3) for A-box and C3a, respectively].

could rescue mice challenged with LPS (23–25). Extracellular HMGB1 is therefore recognized as one of the DAMPs which act as major mediators in immunity (26). Indeed, HMGB1 may be passively released from damaged tissues, late-apoptotic and necrotic cells, as well as actively produced (through a non-canonical secretion pathway) by activated immune cells or even by neurons, as part of inflammatory processes (27–29). In contrast to the immediate activation of the complement system, the secretion of HMGB1 is often delayed, hours after the initial stimulation (23, 30), and its level often remains elevated days after in contexts of chronic inflammation associated with auto-immunity, infection and cancer. HMGB1 persistence maintains and worsens inflammatory disorders, contributing to disease progression through distinct pathways, which depend on its location and diseases context (31). HGMB1 was also the first convincing determinant identified for sterile inflammation, and a key player at the crossroad between innate and adaptive immunity, through the HMGB1 secretion by dendritic cells in response to an initial maturation stimulus, in order to sustain their maturation, and for activation of T lymphocytes (32).

On a molecular side, the HMGB1 modular structure contains two DNA-binding boxes (A-box and B-box) as well as a C-terminal negatively charged 'acidic' tail, strongly enriched in aspartic and glutamic acid residues (**Figure 1A**). HMGB1 action is finely tuned by its associations and localization, which are modulated by post-translational modifications (33, 34). For example, the oxidation state of its cysteines (two in the A-box, one in the B-box) modulates its biological activity in the extracellular environment (**Figures 1**, **3**) (35). Only fully reduced HMGB1 and the non-oxidizable HMGB1 mutant 3S, in which three serine residues replace cysteines, induce chemotaxis by binding CXCL12 through the CXCR4 receptor

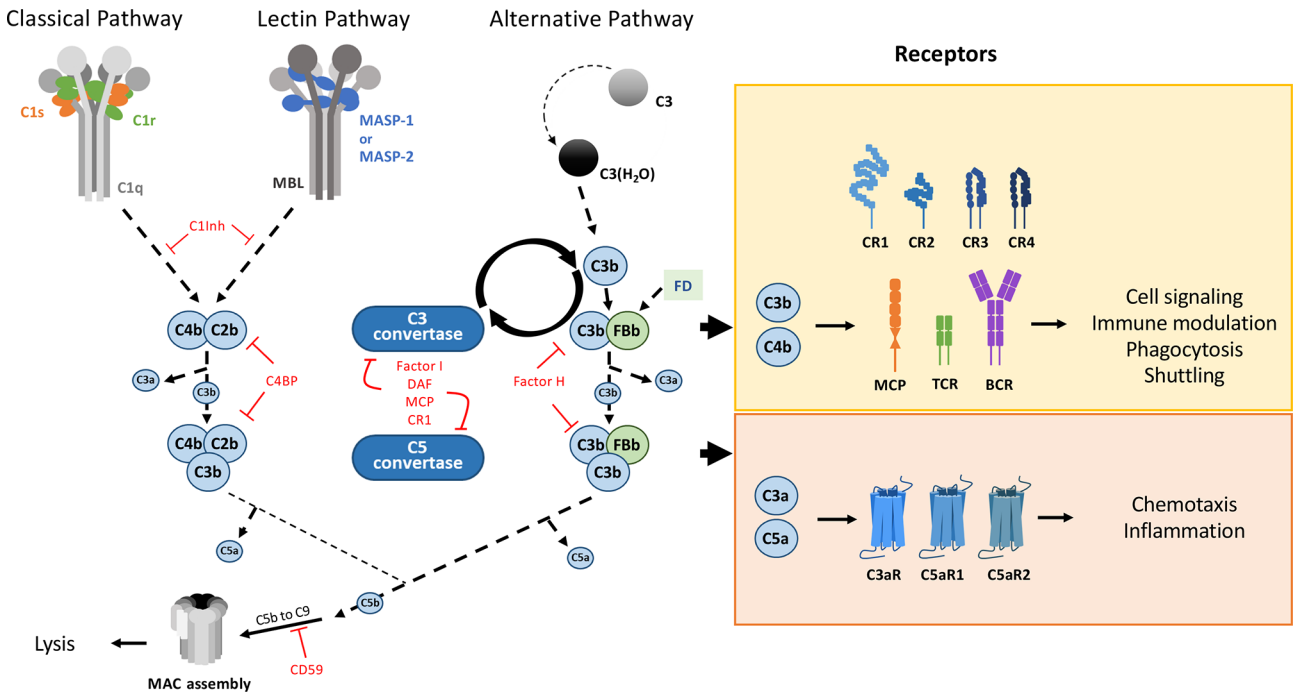

FIGURE 2 | The complement system main pathways and 'classical' canonical functions. Triggered by proteolytic cascades, this defense system gets activated and amplified 'on site', raising alarm signals through different specific receptors, under the control of numerous regulators. The classical pathway (CP) and lectin pathway (LP) are activated by the C1 complex and the collectin-MASPs complexes, respectively. Collectins (CL) are pattern recognition molecules with collagen-like domains that recognize specific carbohydrate or acetylated surface motifs: MBL, ficolins or collectins recently discovered in the liver (CL-10), kidney (CL-11) or placenta (CL-12) (4). By cleaving C4 and C2, C1s (CP) and MASP-2 (LP) generate a C3 convertase. The (AP) is activated by the spontaneous hydrolysis of C3. All three pathways lead to the formation of the C3 convertase (C4b2b for CP and LP and C3bBb for AP), thus cleaving C3 into C3a and C3b. The amplification loop of the AP C3 convertase leads to massive C3b deposition, covalently bound to the surfaces, targeting them for phagocytosis. The cascade further proceeds to the formation of the C5 convertase, which allows the formation of the Membrane Attack Complex (MAC) on the target surface leading to its lysis. The complement cascade is modulated by various inhibitors (C4BP, C1inh), regulators such as factor H (FH), factor I (FI) that destabilize the C3 convertase (FH, DAF) or cleave C3b (FI assisted by CR1 and MCP (CD46) co-factors). Other regulators limit the final MAC assembly, such as CD59, vitronectin, clusterin … Almost all fragments produced by this enzymatic cascade are bioactive. The C3a and C5a anaphylatoxins mediate chemotaxis and inflammation through their respective receptors, C3aR and C5aR1, C5aR2. Receptors involved in immune modulation depend on the immune cell: CR1, CD46 and TCR on T cells, CR2 and BCR on B cells, recognizing inactivated C3b derivatives. CR1/2/3/4 are also involved in adhesion/shuttling from red blood cells towards the liver and spleen, for example. Only the cleavage products are shown on this simplified scheme, and they follow here the recent recommendation regarding C2 nomenclature (5). Molecule schemes are not adjusted to the same scale.

[maintained at the surface by the CXCL12/HMGB1 heterodimer (36)], and recruit stem cells to orchestrate tissue regeneration (37) (**Figure 3**). Besides this particular activity, the signaling activity of HMGB1 and its complexes (with nucleic acids, LPS, …) is mainly mediated by the receptor for advanced glycation end products (RAGE) and TLRs, although a larger range of receptors may be considered (38, 39). Regarding the proinflammatory function, it is interesting to note that the two HMGB1 boxes have opposing effects when administered separately: the B-box stimulates cytokine secretion whereas the A-box inhibits this effect (30, 39) (**Figure 1A**). Consistently, a recent study observed anti-HMGB1 IgM neutralizing antibodies directed against the B-box in healthy individuals (human and mouse), suggesting a possible feedback loop limiting the level of its pro-inflammatory effect in a healthy state (40). Because HMGB1 can be internalized, and thus reach internal TLRs, it is seen as both a major inside- and outside-cell alarmin (41). Internalization of HMGB1 and HMGB1-partner molecule complexes depends on RAGE and, notably, is inhibited by the recombinant HMGB1 A-box protein (27).

Autocrine or paracrine positive feedback loops involving potent HMGB1-mediated signal amplifications are observed in a variety of contexts (42) (**Figure 3B**). For example, TNFα is secreted by endothelial cells or macrophages stimulated by HMGB1, and, in turn, TNFα will induce HMGB1 secretion from these cells. Similarly, smooth muscle cells, which are normally not HMGB1 producers, can start to secrete HMGB1 when challenged with cholesterol. In turn, once activated by HMGB1, the smooth muscle cells proliferate, migrate and … secrete more HMGB1! (43). Positive feedback loops may involve NFκB activation by HMGB1 through RAGE and/or TLRs. In turn, NFκB will increase the surface expression of these HMGB1 receptors and the production of cytokines, including HMGB1 (42) (**Figure 3C**). Local amplification can also proceed through infiltrated macrophages and leucocytes which, upon HMGB1-

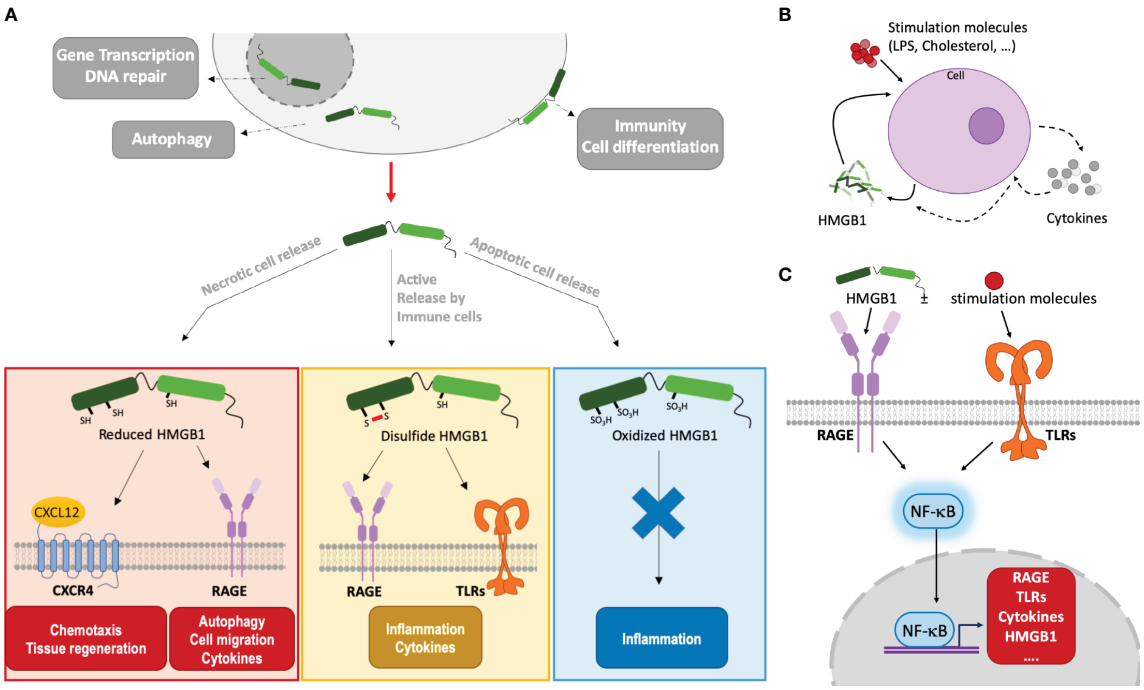

FIGURE 3 | HMGB1 functions depend on its localization/environment, oxidation state and its alarm signaling involves autocrine and paracrine amplification loops. **(A)** HMGB1 effects depend on its localization and oxidation state. Mainly located inside the nucleus, HMGB1 binds DNA and modulates nucleosome stability, thus regulating gene transcription. In the cytoplasm, it plays a role in autophagy. When actively or passively released outside cells, HMGB1 takes part in immunity, inflammation and cell differentiation. HMGB1 can stimulate immune cells (leukocytes, macrophages…). The HMGB1 redox state evolves in relation to its context. Fully reduced, HMGB1 binds to CXCL12 to promote cell recruitment and migration by activation of CXCR4 at the cell membrane. Or, by binding RAGE, it is internalized and it can promote autophagy, cell migration and cytokines synthesis. Through RAGE and TLRs signalization, disulfide HMGB1 induces inflammation and cytokines secretion. When fully oxidized, HMGB1 does not interact anymore with the receptors and may enhance immune tolerance. **(B)** HMGB1 amplifying feedback loop. Under different stimuli, a cell (macrophage, leukocyte, smooth muscle cell, …) can produce and secrete HMGB1 and its receptors directly or *via* the production of cytokines. Once HMGB1 is produced and released, a positive feedback loop is created to enhance its production at the protein level by the initial cell or by neighboring cells, hereby amplifying its effects. This is associated to the secretion of cytokines and other inflammatory molecules. **(C)** NF-κB mediated amplification of HMGB1 and its receptors. By interacting with RAGE and TLR receptors, HMGB1, often in complex with stimulating molecules, will activate the NF-κB pathway. This will induce the transcription of HMGB1, its receptors, and cytokines, leading to an amplification of the inflammatory response.

mediated activation, will secrete more HMGB1 (and TNFα) (42). In a context of sterile inflammation through acetaminophen challenge, the amplification may also be driven by neutrophils, which are massively attracted to the necrotic site in an HMGB1- and RAGE-dependent manner and exacerbate tissue injury (44).

2.3 Possible Cross-Amplification Through Enhancement of HMGB1 Secretion by C3a/C5a Anaphylatoxins, HMGB1-Mediated CP Activation and More Indirect Processes

As seen above, several feedback loops tend to auto-amplify the alarm signals generated at the levels of HMGB1 and C3a. Whether further cross-amplification may occur between the two systems is, therefore, the next question to address (**Figure 4**). Although this certainly depends on the specific context, it is interesting to note that several independent publications mention C3a or C5a mediated enhancement of HMGB1 secretion. Intriguingly, C3a was shown to tightly bind the RAGE receptor (45). Since C3a and the HMGB1 A-box are small helical domains (**Figure 1C**), and share this RAGE binding property, it was tempting to look for some 3D similarity between the two, but in fact the overall similarity is very limited (**Figure 1C**). Furthermore, the reported functional impact of this C3a-RAGE interaction was to increase IFN-α production by human peripheral blood mononuclear cells in response to unmethylated cytosine-guanine-rich DNA (45), but this remains quite poorly explored (10).

A so-called "C3/HMGB1/TGF-β1 pathway" was reported in two publications investigating the pathogenesis of diabetic nephropathy and its associated chronic renal fibrosis (46, 47). In response to C3a stimulation (provided by macrophage infiltration into renal interstitial tissues), HMGB1 translocates from nucleus to cytoplasm in primary renal tubular epithelial cells, and expression of HMGB1 and its receptor TLR4 gradually increases in their cytoplasm from 24 to 48 h after C3a stimulation. This will trigger epithelial to mesenchymal transition through the HMGB1/TLR4/p65/TGF-β1 signaling pathway (46). These effects have been inhibited by the grapefruit component GSPE (46) or the specific MiR-92d-3p miRNA in a renal tubular epithelial cell line (HK2) (47).

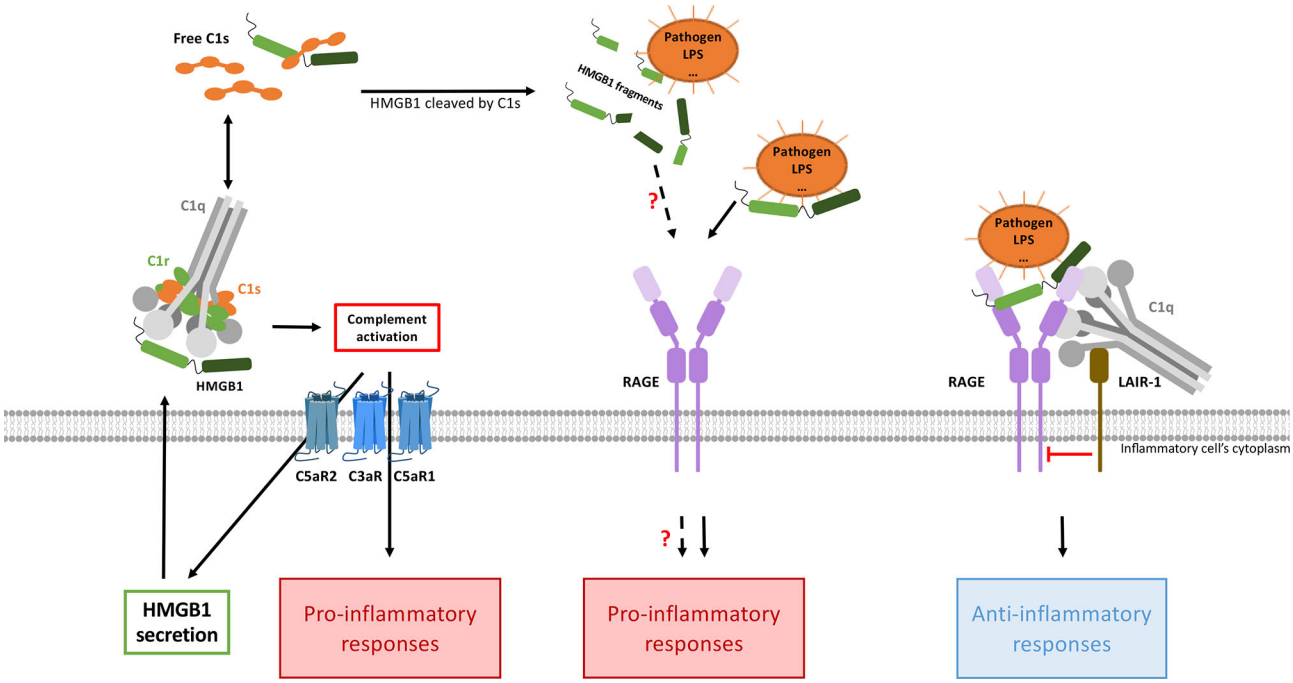

FIGURE 4 | HMGB1 and complement interplays combine pro- and anti-inflammatory responses. CP activation (possibly directly mediated by HMGB1) will produce anaphylatoxins, which enhance HMGB1 secretion (left). In this context, the pro-inflammatory responses triggered by the two pathways are additive and cross-amplified. On the other hand (right), when C1q bridges LAIR-1 and HMGB1-RAGE, then LAIR-1 recruits the SHP-1 phosphatase which will shut down the RAGE-mediated inflammatory signaling, thereby dampening inflammation. Activated C1s can also cleave HMGB1, but the functional impact of the HMGB1 cleavage fragments need to be investigated. By inhibiting HMGB1internalization through RAGE (not shown here), C1q can also limit the extent of intracellular TLR activation.

Although the role of the C5aR2 receptor in inflammation and disease remains a less studied and controversial topic, several independent publications describe that C5aR2 is critically involved in LPS-induced HMGB1 secretion (48). Indeed, macrophages that only express C5aR2, without C5aR1, show a marked HMGB1 production upon C5a stimulation, associated with signaling through MEK1/2, JNK1/2, and PI3K/Akt activation pathways. The critical role of C5a/C5aR2 interaction was later deciphered as activating the NLRP3 inflammasome and then HMGB1 release by macrophages by raising the expression of PKR *via* MEK/ERK and interferon (IFN) pathways (49). Reversely, an anti-HMGB1 antibody (Ab) reduced the C5a/C5aR2 interaction–mediated caspase-1 activation and IL-1β secretion by macrophages (50). C5a also triggers the release of HMGB1 by primary human neutrophils and plays, together with HMGB1, significant roles in the context of antineutrophil cytoplasmic Ab-induced neutrophil activation (51).

In turn, HMGB1 has been shown to activate the classical complement pathway in an Ab-independent manner, by directly binding to C1q. This process may drive sterile inflammation (52) and contributes to cross-activation in the complement C1/HMGB1 interplay (**Figure 4**).

Several lines of evidence suggest that cross-amplification may also be indirectly mediated by cytokines, such as IFNγ or TNFα. For example, Ab-mediated complement activation or HMGB1 can contribute to enhance IFNγ secretion (53, 54), which in turn can enhance C1s secretion (55, 56) or NLRP3 inflammasome signaling (53). TNFα, which is amplified by HMGB1 in response to LPS (57), may trigger C3 or C1s secretion (58, 59). Of note, it was early shown that IFNγ and TNFα are both secreted by human T cells as a response to C1q-bearing immune complexes, but not by non-opsonized complexes (60). This is also true for C3a and C3b, which are decisive drivers for a Th1 response in CD4+ T cells, with the induced secretion of IFNγ and TNFα (61). It was also shown that a crosstalk between TLRs and anaphylatoxins or C3b-coated antigens shape antigen-presenting cells towards inducing such a Th1 effector response (61).

2.4 Dampening Inflammation Through a Regulatory Anti-Inflammatory Feedback Loop Involving Complement C1, LAIR-1 And HMGB1

Inhibitory pathways are needed to dampen inflammation and limit inadequate autoreactivity. Interestingly, recent discoveries have opened a historical entry point for a non-inflammatory crosstalk between C1q and HMGB1 (62, 63). Such studies contribute to better understand the complex disease processes in systemic lupus erythematosus (SLE), the first disease context that will be taken as an example in the next section.

These regulatory roles of C1q are mostly mediated through its interaction with Leukocyte-Associated Immunoglobulin-like Receptor-1 (LAIR-1). LAIR-1 is an inhibitory receptor expressed on a wide range of human immune cells such as NK

cells, T cells, B cells, monocytes, neutrophils, basophils and mast cells (64–71). Its cytoplasmic region contains two amino acid sequences corresponding to immune receptor tyrosine-based inhibitory motifs (ITIMs), which mediate its immune inhibitory activity (64). C1q can interact with LAIR-1 through its collagen-like region (CLR) (72) (**Figure 1B**). As a first major interplay, the combined action of C1q and HMGB1 was shown to regulate human macrophages polarization (62): in lipid rafts at the monocyte surface, the multivalent C1q molecule can bridge RAGE/HMGB1 on one side, and LAIR-1 on the other side, which triggers the phosphorylation of the two ITIMs in LAIR-1, and the consequent recruitment of the SHP-1 phosphatase (**Figure 4**). Although HMGB1 alone polarizes macrophages to the M1-like inflammatory type, through RAGE phosphorylation, the recruitment of SHP-1 in the cross-talk with C1q and LAIR-1 will dephosphorylate the proximal RAGE receptor, and macrophages get polarized into a M2-like type. If C1q is too low, because of rare genetic deficiencies or immune-complexes-driven consumption, and if HMGB1 level is high, then this inhibitory control of the macrophage is ineffective, leading to M1 polarization, impaired clearance of apoptotic cells, and exposition of the adaptive immune system to numerous autoantigens, therefore generating auto-Abs. Further studies from the group of Betty Diamond have shown that HMGB1 plus C1q increase the secretion of pro-resolving lipid mediators by activated monocytes (63). On the same line, C1q/LAIR-1 interaction was shown to inhibit TLR activating signals to maintain monocyte tolerance (73), to inhibit monocyte to dendritic cell differentiation and to suppress INF-α production by plasmacytoid dendritic cells (pDC) (74).

On another line, C1q was shown to inhibit RAGE-mediated internalization of HMGB1, which may also directly contribute to its regulatory role (62). C1s was also shown to cleave HMGB1, which may reduce its immunogenicity. This proteolytic cleavage also reduces the HMGB1 property to amplify LPS-mediated proinflammatory cytokine secretion from monocytes, macrophages and dendritic cells (57, 75). All these properties may contribute to the non-inflammatory role of the C1 subunits in its cross-talk with HMGB1, but the underlying molecular mechanisms remain partly unexplored.

Altogether, these observations suggest that the interplay between HMGB1 and C1q/C1s can raise and amplify initial alarm signals, and then dampen the raised inflammation.

3 EXAMPLES OF HMGB1 AND COMPLEMENT DYSFUNCTIONS AND CROSSTALK IN INFLAMMATORY DISEASES

3.1 Exacerbating Instead of Dampening Inflammation in SLE Through HMGB1 and Complement Crosstalk

SLE is an emblematic chronic multifactorial auto-immune disease where the two alarm systems likely crosstalk and contribute to immune dysregulation (62). This disease is characterized by the production of multiple autoantibodies (auto-Abs). Regarding its etiology, it combines genetic predisposition and environmental factors that alter immune regulatory processes. It presents alternative periods of illness (flares) and wellness, and may affect different tissues. The clinical symptoms thus range from skin rashes, chronic fatigue, and arthritis to the more severe nephritic and neurological involvements (12). Disease evolution into lupus nephritis (LN) is the most common cause of morbidity and mortality, by progressing to end-stage renal failure (76). LN remains scientifically challenging to understand and predict, since it involves multiple pathogenic pathways including altered cell death, auto-immune complexes deposition, complement activation, and inflammatory flares (77).

3.1.1 SLE, Autoantibodies and Complement

Defining the role of the CP proteins in SLE is complex and has been recognized as a classical paradox in the field (78) since the system dysfunctions when these proteins are deficient (genetically or by consumption) or over-activated (12).

Since the discovery that deficiencies in CP proteins are the strongest genetic risk factors for developing SLE (79, 80), a link has been established between CP protein abnormalities and this complex disease. Cases of complete C1q, C1s, or C1r deficiencies (79–81), or of mutated C1q, which can no longer associate with its cognate C1r and C1s proteases (82), are all associated with human SLE with mortality or morbidity at a young age. This was initially explained by the impaired role of the CP components in the clearance of immune complexes and "self" debris such as apoptotic cells, known as the waste disposal hypothesis (83). More than 100 cases of complete C1q deficiency are described now, with variable clinical presentations, often sharing SLE or SLE-like disease and recurrent bacterial infections (84). Fewer (dozen) cases are described with complete C1s deficiency, maybe because recurrent infections and mortality at a young age are common in these patients. Altogether, these clinical data suggest that the CP proteins are protective from developing SLE.

However, since SLE is the disease with the largest number of identified auto-Abs, auto-immune complexes deposited on the renal surface can over-activate the complement CP, inducing strong tissue damage and profound C1q, C3 and C4 consumption (**Figure 5**). Moreover, anti-C1q auto-Abs, which are found in more than 40% of the LN patients (85), can alter C1q functions and contribute to the intrarenal complement over-activation and tissue damage (86, 87).

Although anti-C1q auto-Abs are often associated with LN, anti-C3b auto-Abs were found more specific, but less sensitive, suggesting the possible use of a combination of both auto-Abs as biomarkers to follow LN activity in SLE patients (77). More recently, C3 and C4 activation products, present in plasma and/or at the surface of blood cells, have been proposed as diagnostic markers with a tight correlation with SLE disease activity (88).

Although apparently contradictory, these different observations reveal that the function of the CP proteins is essential but needs to be tightly balanced and controlled. Exploring this paradox has led to the discovery of many other

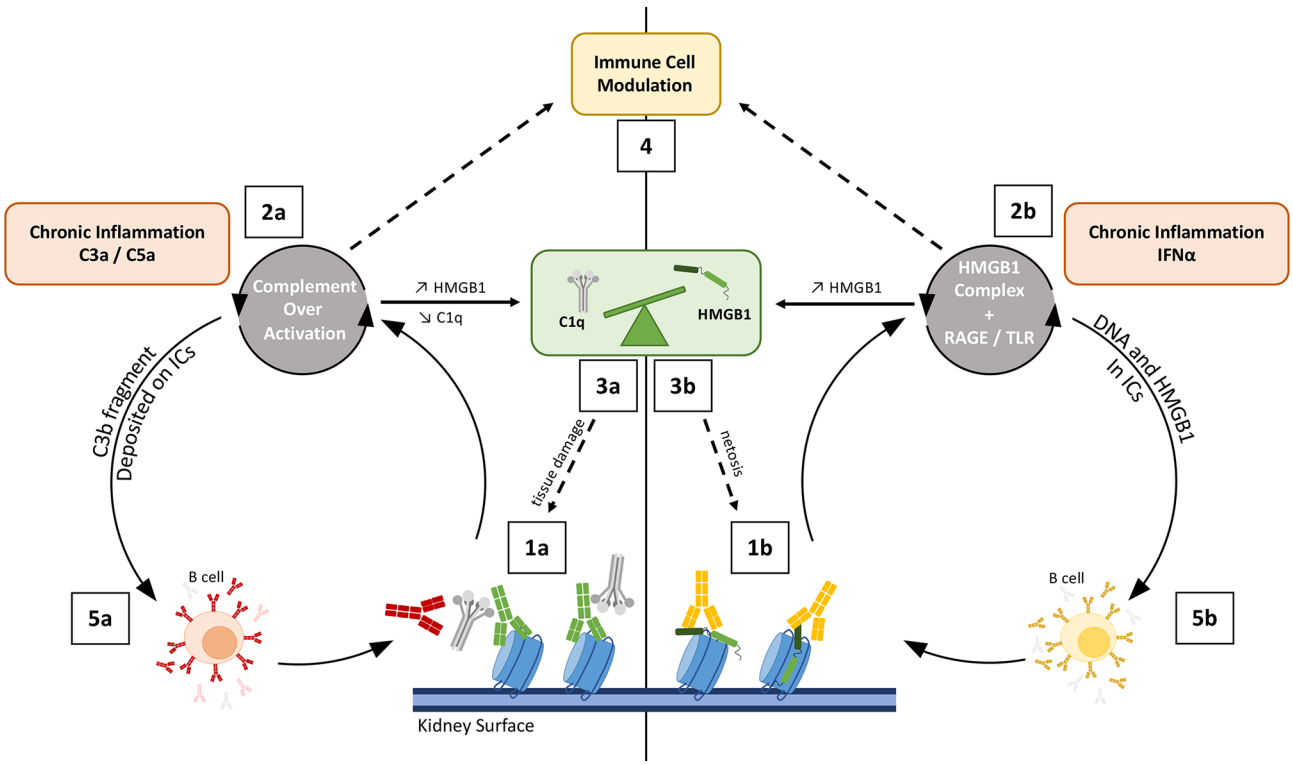

FIGURE 5 | Schematic view on how complement and HMGB1 may co-amplify tissue damaging feedback loops in SLE/LN. Left: Complement overactivation (1a to 5a); Right: HMGB1-mediated impact (1b to 5b). On the left side, complement over-activation (through C1r/s, not shown) by intrarenal deposited immune complexes is enhanced by anti-C1q (red) (1a). This leads to C3a-C5a driven inflammation (2a) and renal tissue damage, with impaired clearance because of C1q and C3 depletion, therefore releasing more nucleosomes (3). On the right side, HMGB1 forms complexes with nucleosomes (1b), LPS or cytokines. These HMGB1 complexes enhance inflammation in the kidney or in the skin of lupus patients, and activate IFN-α production (a driving cytokine in lupus pathogenesis, 2b). Both HMGB1 and C3a/C5a can stimulate HMGB1 release by activated cells (2a, 2b); HMGB1 is also passively released by complement-damaged cells (3a), and through increased netosis induced by HMGB1 (3b). The consequent imbalance effect on C1q and HMGB1 hampers proper inflammation resolution (see **Figure 6**) (4). On both sides, the process stimulates B-cells to produce more auto-Abs, which fuels the two combined vicious circles at the first steps (5a, 5b). Different types of auto-Abs are illustrated, with possible functional interference: anti-nucleosome (green), anti-C1q (red), anti-HMGB1 (orange).

functional facets of the C1q molecule (89), as reviewed recently in (90–92). The role of the C1 proteases is also to be deciphered outside of their classical role, where complement-C3d deposition on immune complexes (ICs) results in enhanced auto-Abs production by B cells (93, 94) (**Figure 5**).

3.1.2 SLE, Autoantibodies and HMGB1

Pathological roles in SLE for the alarmin HMGB1 and anti-HMGB1 auto-Abs were proposed recently (95). For more details, the reader is referred to a recent mini-review and references therein (96).

In SLE patients, higher HMGB1 serum concentrations are reported, increasing during active disease and remaining elevated even during anti-inflammatory treatments (97). A significant, positive correlation was found between HMGB1 mRNA and SLE disease activity index (SLEDAI) (98). Besides its global contribution to the pathogenesis of SLE, HMGB1 was reported to play a particular role in LN, possibly serving as a marker of disease activity in patients with renal impairment (95). In keeping with this question, it has been proposed recently that serum HMGB1 (in a context of pediatric SLE) or microparticles containing HMGB1 observed in the urine of patients may be useful as biomarkers of LN (99, 100). Interestingly, another study focusing on auto-Abs directed against HMGB1 A-box concluded about their potential interest as a biomarker for SLE, especially for the prediction of disease activity, and not specifically related to the kidney (101).

As for C1q, it is proposed that HMGB1 impacts both the innate and adaptive immune cells in SLE (96). HMGB1 may impair apoptotic cells clearance, strongly stimulating the secretion of proinflammatory cytokines like IFN-I by pDCs. It can impact cell death processes (e.g. increase neutrophil netosis).

We will mainly refer here to further observations not reported in the reviews cited above. In the particular context of LN, TLR2 has been shown to regulate glomerular mesangial matrix deposition through the activation of the MyD88/NF-κB pathway though interactions with HMGB1 (102). HMGB1 upregulation in SLE correlates with the activation of dendritic cells, targeting myeloid dendritic cells *via* the upregulation of the mTOR pathway, for example. This signaling pathway leads to the

exposure of HLA-DR, CD40, and CD86 on dendritic cells and enhances the secretion of IL-1β, IL-6, and TNF-α cytokines (103). Intriguingly, high molecular weight covalent complexes including HMGB1 circulate in the blood of SLE patients at a significantly higher concentration than in healthy patients (104).

HMGB1 also takes part in the stimulation of BAFF (B-Cell-Activating Factor) and thus auto-Ab production (105, 106), introducing a vicious circle as illustrated in **Figure 5**. Indeed, ICs containing DNA and HMGB1 can promote TNF-α and BAFF production through RAGE, leading to B cell hyperactivity (105). HMGB1 gene and protein expression is significantly increased in SLE CD4(+) T cells compared to controls, and it could impact the DNA methylation level (98).

3.1.3 HMGB1 and C1q or C1s Crosstalk in SLE

Numerous studies have contributed to elucidate the role of C1q in SLE. Among them, two reported a C1q interplay with HMGB1 towards inflammation resolution and immune balance, involving the LAIR-1 and RAGE receptors (62, 63), as described previously (**Figure 4**). In addition, the cleavage of HMGB1 by C1s was proposed to suppress surface autoantigen epitopes (57). The simplified integrated overview presented in **Figure 5** illustrates the interconnections between the functional effects of CP proteins and HMGB1, with possible cross-amplification of inflammatory vicious circles in a LN disease context. For example, in correlation with disease severity, elevated circulating HMGB1 seen in SLE patients can bind to nucleosomes released from damaged cells, and be part of ICs (because of anti-HMGB1 and anti-DNA auto-Abs) (107). These ICs will trigger complement activation, which consumes C1q and releases anaphylatoxins, which upregulates HMGB1. This process induces a molecular imbalance between HMGB1 and C1q (**Figure 5**). This imbalance (**Figure 6**), together with the downregulation of LAIR-1 on pDC in pediatric SLE (108) or at the surface of B cells (109), will limit the feedback control through these molecules shown in **Figure 4**. C3 fragments deposited on the surface of ICs and HMGB1 present in nucleosomes complexes will stimulate B cells to produce more auto-Abs.

Hyperactive T cell responses occur in SLE patients, with different co-signals. Indeed, ICs and late complement activation components trigger the activation of Syk tyrosine kinase co-signal in CD4+ T-cells through FcγRIIIa, which up-regulates TLR and HMGB1 expression, as well as the expression of IFN pathway genes (110). In addition, the deficit of spatial memory in neuro-SLE patients is a consequence of dendrite destruction by microglia. HMGB1, decorating synapses on neurons damaged by anti-neuron antibodies, enhances C1q binding which activates the microglia and targets the dendrite for destruction and remodeling (111). Both the central and peripheral nervous systems can be affected, leading to cognitive impairments.

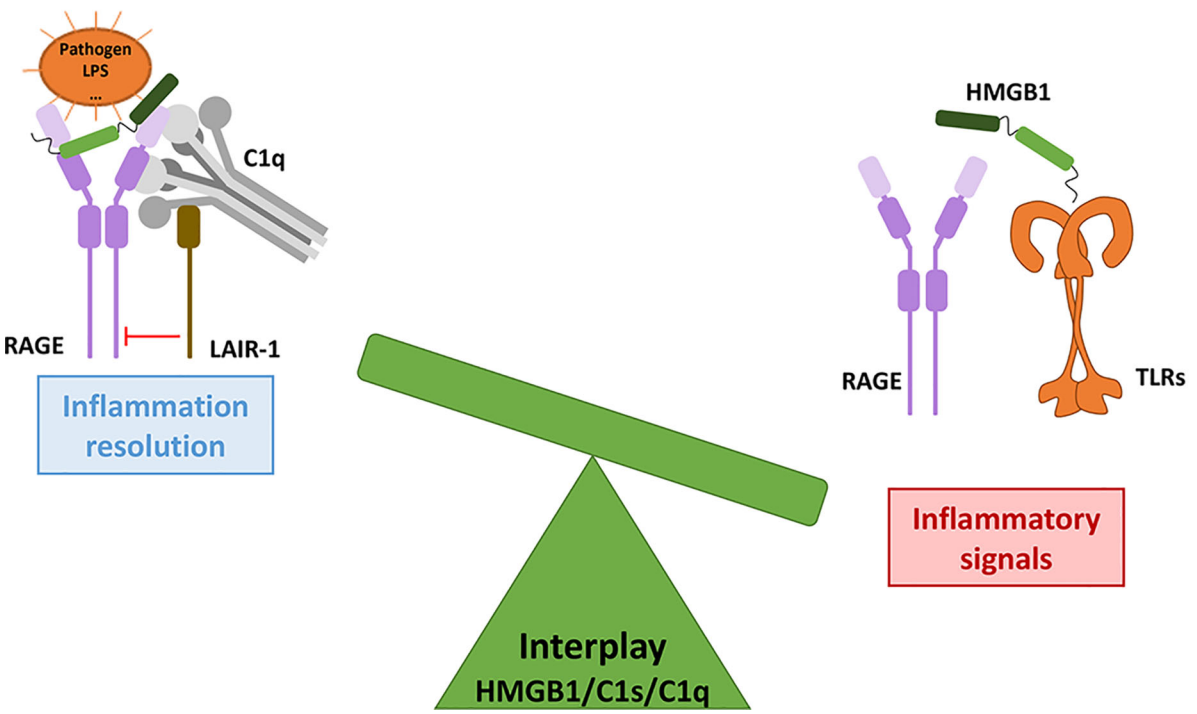

FIGURE 6 | The HMGB1/C1s/C1q interplay modulates the inflammatory signals from initiation to resolution. As a molecular switch, C1q can dampen the inflammatory signals triggered by RAGE/HMGB1, through LAIR-1 inhibitory signaling. The role of C1s in this interplay remains to be further investigated.

3.2 C1, Complement or HMGB1 Dysfunction and Possible Crosstalk in Severe Periodontitis-Like Diseases, With Tissue Degradation Associated With Chronic Inflammation and Dysbiosis

We now come to a context of inflammatory disorders which affect the periodontium, which is the tissue supporting the teeth, which includes different structures such as gingiva, cementum, periodontal ligament and alveolar bone. Periodontitis is the prototype of disease where destructive inflammation and microbial dysbiosis are reciprocally reinforced in a complex interplay. In severe cases, when inflammation persists unresolved, the exacerbated host reaction can lead to the degradation of the periodontium, namely periodontitis. Connective tissue damage and loss of alveolar bone are mediated by a dysregulated and excessive inflammatory response, which involves components of both innate and adaptive immunity, including the complement system (112, 113). Persistent inflammation leads to microbial dysbiosis in favor of bacteria surviving in these conditions and using tissue breakdown products as nutrients. Within a vicious circle, the imbalanced composition of oral bacteria will trigger more inflammation, leading to tissue permeability. Therefore, oral bacteria may disseminate in the whole body, which will extend the location of microbial dysbiosis disorders. Importantly, this chronic inflammatory context is associated with an elevated risk of systemic conditions, which reinforces the need to better understand and treat periodontitis-like diseases (114).

3.2.1 Complement in Ehlers-Danlos Syndrome Periodontal Subtype and in Periodontitis

Our interest in this disease context opened through a collaboration with scientists from Innsbruck Medical University, who discovered heterozygous mutations in C1 subunit genes *C1R* and *C1S*, which were clearly associated with a specific periodontal subtype of Ehlers-Danlos Syndromes (EDS) (115). EDS is an umbrella term for a group of inherited connective tissue disorders, characterized by joint hypermobility, skin hyperextensibility, and tissue fragility. A predominant clinical feature of periodontal EDS (pEDS) is early severe periodontitis and tooth loss or resorption. During childhood, before the onset of periodontitis, a common manifestation for this very rare disorder is the lack of attached gingiva, consistently observed only in children who inherited the familial pathogenic pEDS variant (116). Early bruising was another symptom commonly associated with children inheriting the pathogenic pEDS variant.

Identifying mutations in the *C1R* or *C1S* genes is among the criteria needed to diagnose pEDS (117). What could be the link between the heterozygous mutations in the *C1S* and *C1R* genes and this very rare syndrome? Interestingly, periodontitis can occur in this particular pEDS context without strong pathogenic colonization in gingival pockets. This observation therefore suggests that alterations in C1r or C1s functions might trigger sterile inflammation in this specific pEDS context. Two studies aimed to explore the molecular consequences of these specific mutations in C1r and C1s (118, 119). Defective secretion of these proteases is always observed in the presence of all pEDS mutations, with the only exception of a particular mutation in C1r which affects a C1q-binding residue (118). A common feature is that the altered C1r or C1s proteases, if secreted, will not assemble into the extracellular C1 complex. Therefore, this suggests that their activation and activity will escape from the physiological control associated with the C1 context. In cases of the mutations affecting the C1r coding sequence in pEDS patients, the C1s protease is intact but its level of activation is significantly increased in the supernatant of patient fibroblasts as compared to controls (without activation), which suggests that C1s activity may be involved in the pathological process (118). Further *in vitro* studies, analyzing the impact of the mutations affecting the C1s coding sequence in pEDS patients, unexpectedly revealed that only a C-terminal fragment was secreted during recombinant C1s variant expression in HEK cells. Importantly, this C1s C-terminal fragment was lacking the capacity to cleave C4, which led us to check if this fragment retained the capacity to cleave the non-canonical HMGB1 target, which was the case, although the generated fragments may slightly differ in proportion (119). As a first conclusion to these studies on pEDS mutations, the common observation is that the C1s protease gets constitutively activated, without the need of the canonical C1 trigger, and we suggest that C1s constitutive activity may thus be at least partly responsible for the observed dominant inheritance.

Consistently, we will recapitulate below the current observations on the involvement of complement (and HMGB1 in the next section) in severe periodontitis. Complement proteins are present and produced in the oral cavity. Several clinical observations and pre-clinical intervention studies that collectively suggest that complement is hyperactivated in periodontitis have been recently reviewed (112). In healthy conditions, complement split products are either absent or present in low concentrations in the gingival crevicular fluid. In contrast, complement C1q, FB, Bb, C3, C3a, C3b, C3c, C3d, C4, C5, C5a, C5b and C9 have all been detected in diseased periodontal tissue and in the gingival crevicular fluid from patients with established periodontitis (120). Increased local activation of complement in the periodontal tissues enhances the local inflammatory response, as well as loss of tooth attachment and ultimately bone resorption among the associated clinical manifestations (120). The formation of osteoclasts, the cells responsible for the removal of mineralized tissue, is modulated by C3a and C5a anaphylatoxins, in synergy with IL-1ß (121). Recent studies suggested that the complement system and mast cells are associated with the destructive periodontitis processes of alveolar bone and tooth resorption in cats (121).

In the childhood context, characterized by decidual teeth, we can note that decidual ligaments have been observed to express significantly more complement C1s than permanent ligaments, as well as more laminins extracellular matrix components, with morphological differences between the two types of periodontal ligament tissues (122). Coming back to the pEDS disease context,

there may therefore be a possible link between the above observations and the absence of attached gingiva observed in the children who inherited from the pathogenic variant in pEDS families (116).

3.2.2 HMGB1-RAGE Axis and Interplay Between the TLR/Complement Crosstalk and Pathogens in Periodontitis

As recently reviewed (123), it has been proposed that HMGB1 plays a role in the exacerbation and propagation of the oral inflammatory disorders. Infection promotes HMGB1 secretion from periodontal tissue, and the secreted HMGB1 is involved in the lingering or aggravation of periodontitis. Anti-HMGB1 antibodies were shown to attenuate periodontal inflammation and bone resorption in a murine periodontitis model (124). Several oral cells secrete HMGB1 in response to bacterial infections (for example *P. gingivalis*) or stimuli like LPS, butyric acid (which is a metabolite of periodontal pathogens), IL-1β, TNF-α. These include gingival epithelial cells, gingival fibroblasts, human periodontal ligament fibroblasts and of course macrophages. Elevated concentrations of HMGB1 in the gingival crevicular fluid were observed in periodontitis patients, with significant positive correlations between these HMGB1 levels and all periodontal parameters, including plaque index, bleeding index, probing depth, and clinical attachment level. Thus, infection and inflammation promote HMGB1 secretion from periodontal tissue, which further promotes pro-inflammatory cytokine production and osteoclast generation, aggravating periodontitis. RAGE is also highly upregulated in patients with combined type 2 diabetes and periodontitis, as compared to patients with chronic periodontitis. The two occurences of the word patients were not appropriately positioned (125).

Subversion of the complement/TLR crosstalk by pathogens was also described in the context of periodontitis (126). For example, *P. gingivalis* is a strict anaerobic bacterium that requires peptides and hemin for its growth, and thus depends on the continuous flow of inflammatory serum exudates to obtain essential nutrients for survival in the periodontal niche. Its proteases, gingipains, directly cleave C5 to generate C5a, but also degrade C3 and C5b, which inhibits membrane attack complex (MAC) formation. By another subversive mechanism involving TLR2 and C5aR1, the bacteria suppress the macrophage and neutrophil immune functions (126). This C5aR1–TLR2 crosstalk upregulates the production of proinflammatory cytokines (IL-1β, IL-6, and TNF-α), which appear to mediate inflammatory bone loss in a murine model of experimental periodontitis, as well as dysbiosis. Finally, deepening of the periodontal pockets provides nutrients and more room for bacterial growth. What about HMGB1 in this TLR/complement crosstalk? In the signaling cascade proposed by (123), HMGB1 is secreted by gingival epithelial cells in response to LPS by TLR2/4 and in response to butyric acid by other receptors. In a paracrine/autocrine mode, extracellular HMGB1 then induces signaling through TLR2, MD2/TLR4 and RAGE in the gingival epithelium, macrophages and periodontal ligaments. As seen before, the complement anaphylatoxins might up-regulate HMGB1 secretion through C5aR2. However, this interplay remains ill-defined for the moment and no figure will be proposed here. Coming back to the context of the C1s mutations studied in the pEDS disease, if the inherited pEDS mutation induces pathological effect because of uncontrolled C1s activity, we suggest that a dysfunction in the C1/HMGB1 crosstalk might be involved in this context, although the details of possible molecular mechanisms remain to be solved (119).

4 CONCLUDING REMARKS

Complement and HMGB1 are major actors of our defense systems, involving various amplification mechanisms as well as a wide range of surface receptors. Together, they first provide effective danger signals and front lines against external as well as internal insults, and can then switch towards inflammation resolution and repair. Reflecting some contradictory issues in the field, we aimed here to illustrate how their interplay may reciprocally be reinforced for the bad, in disease states, or also for the best, when repair is effective. As suggested in **Figures 5**, **6**, the molecular switch towards inflammation resolution, which involves LAIR1, depends on a fine molecular balance between C1 components and HMGB1, likely a key element in the SLE context.

Complement proteins are mainly and traditionally seen as extracellular factors, but a huge interest has been recently raised in the discovery of intracellular new functions. Conversely, HMGB1 is traditionally seen as an intracellular protein (nuclear, cytoplasmic, …) but various extracellular functions have now been deciphered in the last decades. C1q, HMGB1, C3 (and its activation products) are all therefore multitasking effectors (10, 90, 127). Their different tasks critically depend on the location, post-translational modifications (including proteolytic cleavages) and interacting partners, which the larger C1q molecule can locally bridge. Since these multiple tasks are assigned to different compartments or different steps in the processes, we choose here to avoid the 'dual role' or 'double edged-sword' mention often used in the case of C1q and HMGB1, although it is clear that in certain pathological dysregulated contexts they may be involved in strong pathological amplification of inflammation and tissue injury.

The reader may find complementary details and further inspiration in previous reviews close to this subject, from the different angles of the complement and TLR crosstalk (126, 128), complement-inflammasome crosstalk (129, 130), complement and cell death (75) or complement and SLE (92). Part of this subject is also related to reviews including non-canonical functions of complement (14, 90) or HMGB1/alarmins (31, 131) or C3 multiple functions (10).

Beyond C5aR2-stimulated HMGB1 secretion (132), publications referring to both HMGB1 and complement remain rare but their number increased recently. They are focused on a specific aspect of the crosstalk, or associated with very severe conditions, as for example Gulf War Illness (133) or

hemorrhagic shock (134), or may also relate to the field of neuroinflammation (135). This latter aspect of neurological disorders has not been fully addressed in this review, although alteration of the brain white matter has been observed for at least two pEDS families, which raises the question of the possible impact on the central nervous system (136). On a larger scale, cognitive impairment occurs in 40–90% of SLE patients (111, 137). To better understand the latter condition, the group of Betty Diamond has further explored in a mouse model how C1q and HMGB1 target together neuronal dendrites for destruction, which translates into deficits in spatial memory (137).

Hopefully, this review will shed light on new perspectives on molecular dominos and possible vicious circles combining the two systems. The disease examples cited in this review are likely 'the tip of the iceberg'. SLE is clearly the more established example, thanks to numerous studies trying to elucidate the paradoxical observation that C1q deficiency is such a high-risk factor to develop this disease. The interplay between complement and HMGB1 could likely play a key role in several other severe disease contexts, in particular inflammatory diseases where the immune pathology is host-driven, including cancer, sepsis, senescence. Even in the current pandemic COVID-19, increased circulating HMGB1 levels were observed (138) and crosstalk between the complement, contact, and coagulation systems contributed to severe pathological consequences of the infection (11).

Many challenges remain ahead. These soluble mediators may be easily 'invisible' in studies focused on immune cells. How to decipher the occurrence and impact of various post-translational modifications of HMGB1 in physiological but also pathological contexts? These modifications are not limited to the oxidation state of the cysteines (34). Experimental tricks are needed to deconvolute the impact of extracellular and intracellular contributions, as well as their local or systemic origin. Deciphering new non-canonical functions remains challenging although impressive recent progresses were made on this side. Lastly, a better understanding of these interrelated systems will open the door to new personalized therapeutic strategies including adjunctive treatment, for example to downregulate HMGB1 (139), while new drug developments are performed to control complement and HMGB1 pathological effects, as discussed in recent reviews or research papers (9, 10, 27, 33, 63, 112, 140).

AUTHOR CONTRIBUTIONS

CG, ML, NT, and CD-P reviewed the literature or wrote sections of the review article. ML created figures, supervised by CG and VR. CG organized and wrote the main part of the text. All authors contributed to the article and approved the submitted version.

FUNDING

Interest in the topic reviewed here and related research work are/were supported by three grants from the French National Research Agency (ANR): DYSALARM (ANR-21-CE14-0066), C1rsinEDS (ANR-16-CE91-0004) and C1qEffero (ANR-16-CE11-0019). ML is funded by a fellowship from the University Grenoble Alpes graduate school (Ecoles Universitaires de Recherche) CBH-EUR-GS (ANR-17-EURE-0003).

ACKNOWLEDGMENTS

This review paper relies on numerous studies performed in the field of complement and HMGB1/alarmin and all contributors in these fields are acknowledged, even if they are not directly cited, but indirectly through reviews. IBS acknowledges integration into the Interdisciplinary Research Institute of Grenoble (IRIG, CEA).

REFERENCES

1. Bally I, Ancelet S, Moriscot C, Gonnet F, Mantovani A, Daniel R, et al. Expression of Recombinant Human Complement C1q Allows Identification of the C1r/C1s-Binding Sites. *Proc Natl Acad Sci USA*. (2013) 110:8650–5. doi: 10.1073/pnas.1304894110
2. Ohndorf UM, Rould MA, He Q, Pabo CO, Lippard SJ. Basis for Recognition of Cisplatin-Modified DNA by High-Mobility-Group Proteins. *Nature* (1999) 399:708–12. doi: 10.1038/21460
3. Bajic G, Yatime L, Klos A, Andersen GR. Human C3a and C3a Desarg Anaphylatoxins Have Conserved Structures, in Contrast to C5a and C5a Desarg. *Protein Sci Publ Protein Soc* (2013) 22:204–12. doi: 10.1002/pro.2200
4. Hansen SWK, Ohtani K, Roy N, Wakamiya N. The Collectins CL-L1, CL-K1 and CL-P1, and Their Roles in Complement and Innate Immunity. *Immunobiology* (2016) 221:1058–67. doi: 10.1016/j.imbio.2016.05.012
5. Bohlson SS, Garred P, Kemper C, Tenner AJ. Complement Nomenclature—Deconvoluted. *Front Immunol* (2019) 10:1308. doi: 10.3389/fimmu.2019.01308
6. Merle NS, Church SE, Fremeaux-Bacchi V, Roumenina LT. Complement System Part I - Molecular Mechanisms of Activation and Regulation. *Front Immunol* (2015) 6:262. doi: 10.3389/fimmu.2015.00262
7. Gaboriaud C, Ling WL, Thielens NM, Bally I, Rossi V. Deciphering the Fine Details of C1 Assembly and Activation Mechanisms: "Mission Impossible"? *Front Immunol* (2014) 5:565. doi: 10.3389/fimmu.2014.00565
8. Gaboriaud C, Frachet P, Thielens NM, Arlaud GJ. The Human C1q Globular Domain: Structure and Recognition of Non-Immune Self Ligands. *Front Immunol* (2011) 2:92. doi: 10.3389/fimmu.2011.00092
9. Lachmann PJ. The Amplification Loop of the Complement Pathways. *Adv Immunol* (2009). 104:115–49. doi: 10.1016/S0065-2776(08)04004-2
10. Ricklin D, Reis ES, Mastellos DC, Gros P, Lambris JD. Complement Component C3 – The "Swiss Army Knife" of Innate Immunity and Host Defense. *Immunol Rev* (2016) 274:33–58. doi: 10.1111/imr.12500
11. Agostinis C, Mangogna A, Balduit A, Aghamajidi A, Ricci G, Kishore U, et al. COVID-19, Pre-Eclampsia, and Complement System. *Front Immunol* (2021) 12:775168. doi: 10.3389/fimmu.2021.775168
12. Merle NS, Noe R, Halbwachs-Mecarelli L, Fremeaux-Bacchi V, Roumenina LT. Complement System Part II: Role in Immunity. *Front Immunol* (2015) 6:257. doi: 10.3389/fimmu.2015.00257
13. Gasque P. Complement: A Unique Innate Immune Sensor for Danger Signals. *Mol Immunol* (2004) 41:1089–98. doi: 10.1016/j.molimm.2004.06.011

14. Ricklin D, Hajishengallis G, Yang K, Lambris JD. Complement: A Key System for Immune Surveillance and Homeostasis. *Nat Immunol* (2010) 11:785–97. doi: 10.1038/ni.1923
15. Mathern DR, Heeger PS. Molecules Great and Small: The Complement System. *Clin J Am Soc Nephrol CJASN* (2015) 10:1636–50. doi: 10.2215/CJN.06230614
16. Pouw RB, Ricklin D. Tipping the Balance: Intricate Roles of the Complement System in Disease and Therapy. *Semin Immunopathol* (2021) 43:757–71. doi: 10.1007/s00281-021-00892-7
17. Leslie M. Immunology. The New View of Complement. *Science* (2012) 337:1034–7. doi: 10.1126/science.337.6098.1034
18. Heeger PS, Kemper C. Novel Roles of Complement in T Effector Cell Regulation. *Immunobiology* (2012) 217:216–24. doi: 10.1016/j.imbio.2011.06.004
19. West EE, Kolev M, Kemper C. Complement and the Regulation of T Cell Responses. *Annu Rev Immunol* (2018) 36:309–38. doi: 10.1146/annurev-immunol-042617-053245
20. Kemper C, Köhl J. Back to the Future – Non-Canonical Functions of Complement. *Semin Immunol* (2018) 37:1–3. doi: 10.1016/j.smim.2018.05.002
21. Kang R, Chen R, Zhang Q, Hou W, Wu S, Cao L, et al. HMGB1 in Health and Disease. *Mol Aspects Med* (2014) 40:1–116. doi: 10.1016/j.mam.2014.05.001
22. Chikhirzhina E, Starkova T, Beljajev A, Polyanichko A, Tomilin A. Functional Diversity of Non-Histone Chromosomal Protein Hmgb1. *Int J Mol Sci* (2020) 21:E7948. doi: 10.3390/ijms21217948
23. Wang H, Bloom O, Zhang M, Vishnubhakat JM, Ombrellino M, Che J, et al. HMG-1 as a Late Mediator of Endotoxin Lethality in Mice. *Science* (1999) 285:248–51. doi: 10.1126/science.285.5425.248
24. Stevens NE, Chapman MJ, Fraser CK, Kuchel TR, Hayball JD, Diener KR. Therapeutic Targeting of HMGB1 During Experimental Sepsis Modulates the Inflammatory Cytokine Profile to One Associated With Improved Clinical Outcomes. *Sci Rep* (2017) 7:5850. doi: 10.1038/s41598-017-06205-z
25. Zhu CS, Wang W, Qiang X, Chen W, Lan X, Li J, et al. Endogenous Regulation and Pharmacological Modulation of Sepsis-Induced HMGB1 Release and Action: An Updated Review. *Cells* (2021) 10:2220. doi: 10.3390/cells10092220
26. Yang H, Wang H, Chavan SS, Andersson U. High Mobility Group Box Protein 1 (HMGB1): The Prototypical Endogenous Danger Molecule. *Mol Med Camb Mass* (2015) 21 Suppl 1:S6–S12. doi: 10.2119/molmed.2015.00087
27. Yang H, Wang H, Andersson U. Targeting Inflammation Driven by HMGB1. *Front Immunol* (2020) 11:484. doi: 10.3389/fimmu.2020.00484
28. Chen R, Kang R, Tang D. The Mechanism of HMGB1 Secretion and Release. *Exp Mol Med* (2022) 54:91–102. doi: 10.1038/s12276-022-00736-w
29. Yang H, Andersson U, Brines M. Neurons Are a Primary Driver of Inflammation *via* Release of HMGB1. *Cells* (2021) 10:2791. doi: 10.3390/cells10102791
30. Li J, Kokkola R, Tabibzadeh S, Yang R, Ochani M, Qiang X, et al. Structural Basis for the Proinflammatory Cytokine Activity of High Mobility Group Box 1. *Mol Med Camb Mass* (2003) 9:37–45. doi: 10.1007/BF03402105
31. Gorgulho CM, Romagnoli GG, Bharthi R, Lotze MT. Johnny on the Spot-Chronic Inflammation Is Driven by HMGB1. *Front Immunol* (2019) 10:1561. doi: 10.3389/fimmu.2019.01561
32. Bianchi ME, Manfredi AA. High-Mobility Group Box 1 (HMGB1) Protein at the Crossroads Between Innate and Adaptive Immunity. *Immunol Rev* (2007) 220:35–46. doi: 10.1111/j.1600-065X.2007.00574.x
33. Andersson U, Tracey KJ, Yang H. Post-Translational Modification of HMGB1 Disulfide Bonds in Stimulating and Inhibiting Inflammation. *Cells* (2021) 10:3323. doi: 10.3390/cells10123323
34. Kwak MS, Kim HS, Lee B, Kim YH, Son M, Shin J-S. Immunological Significance of HMGB1 Post-Translational Modification and Redox Biology. *Front Immunol* (2020) 11:1189. doi: 10.3389/fimmu.2020.01189
35. Ferrara M, Chialli G, Ferreira LM, Ruggieri E, Careccia G, Preti A, et al. Oxidation of HMGB1 Is a Dynamically Regulated Process in Physiological and Pathological Conditions. *Front Immunol* (2020) 11:1122. doi: 10.3389/fimmu.2020.01122
36. D'Agostino G, Artinger M, Locati M, Perez L, Legler DF, Bianchi ME, et al. β-Arrestin1 and β-Arrestin2 Are Required to Support the Activity of the CXCL12/HMGB1 Heterocomplex on CXCR4. *Front Immunol* (2020) 11:550824:550824. doi: 10.3389/fimmu.2020.550824
37. Tirone M, Tran NL, Ceriotti C, Gorzanelli A, Canepari M, Bottinelli R, et al. High Mobility Group Box 1 Orchestrates Tissue Regeneration *via* CXCR4. *J Exp Med* (2018) 215:303–18. doi: 10.1084/jem.20160217
38. Paudel YN, Angelopoulou E, Piperi C, Balasubramaniam VRMT, Othman I, Shaikh MF. Enlightening the Role of High Mobility Group Box 1 (HMGB1) in Inflammation: Updates on Receptor Signalling. *Eur J Pharmacol* (2019) 858:172487. doi: 10.1016/j.ejphar.2019.172487
39. Ge Y, Huang M, Yao Y. The Effect and Regulatory Mechanism of High Mobility Group Box-1 Protein on Immune Cells in Inflammatory Diseases. *Cells* (2021) 10:1044. doi: 10.3390/cells10051044
40. Geng Y, Munirathinam G, Palani S, Ross JE, Wang B, Chen A, et al. HMGB1-Neutralizing IgM Antibody Is a Normal Component of Blood Plasma. *J Immunol* (2020) 205:407–13. doi: 10.4049/jimmunol.2000014
41. Andersson U, Yang H, Harris H. High-Mobility Group Box 1 Protein (HMGB1) Operates as an Alarmin Outside as Well as Inside Cells. *Semin Immunol* (2018) 38:40–8. doi: 10.1016/j.smim.2018.02.011
42. van Beijnum JR, Buurman WA, Griffioen AW. Convergence and Amplification of Toll-Like Receptor (TLR) and Receptor for Advanced Glycation End Products (RAGE) Signaling Pathways *via* High Mobility Group B1 (Hmgb1). *Angiogenesis* (2008) 11:91–9. doi: 10.1007/s10456-008-9093-5
43. Porto A, Palumbo R, Pieroni M, Aprigliano G, Chiesa R, Sanvito F, et al. Smooth Muscle Cells in Human Atherosclerotic Plaques Secrete and Proliferate in Response to High Mobility Group Box 1 Protein. *FASEB J Off Publ Fed Am Soc Exp Biol* (2006) 20:2565–6. doi: 10.1096/fj.06-5867fje
44. Huebener P, Pradere J-P, Hernandez C, Gwak G-Y, Caviglia JM, Mu X, et al. The HMGB1/RAGE Axis Triggers Neutrophil-Mediated Injury Amplification Following Necrosis. *J Clin Invest* (2019) 130:1802. doi: 10.1172/JCI126976
45. Ruan BH, Li X, Winkler AR, Cunningham KM, Kuai J, Greco RM, et al. Complement C3a, CpG Oligos, and DNA/C3a Complex Stimulate IFN-α Production in a Receptor for Advanced Glycation End Product-Dependent Manner. *J Immunol* (2010) 185:4213–22. doi: 10.4049/jimmunol.1000863
46. Wang K, Wei H, Zhan J, Liang X, Zhang C, Liu Y, et al. GSPE Alleviates Renal Fibrosis by Inhibiting the Activation of C3/ HMGB1/ TGF-β1 Pathway. *Chem Biol Interact* (2020) 316:108926. doi: 10.1016/j.cbi.2019.108926
47. Zhang Y. MiR-92d-3p Suppresses the Progression of Diabetic Nephropathy Renal Fibrosis by Inhibiting the C3/HMGB1/TGF-β1 Pathway. *Biosci Rep* (2021) 41:BSR20203131. doi: 10.1042/BSR20203131
48. Rittirsch D, Flierl MA, Nadeau BA, Day DE, Huber-Lang M, Mackay CR, et al. Functional Roles for C5a Receptors in Sepsis. *Nat Med* (2008) 14:551–7. doi: 10.1038/nm1753
49. Yu S, Wang D, Huang L, Zhang Y, Luo R, Adah D, et al. The Complement Receptor C5aR2 Promotes Protein Kinase R Expression and Contributes to NLRP3 Inflammasome Activation and HMGB1 Release From Macrophages. *J Biol Chem* (2019) 294:8384–94. doi: 10.1074/jbc.RA118.006508
50. Zhang T, Wu K-Y, Ma N, Wei L-L, Garstka M, Zhou W, et al. The C5a/C5aR2 Axis Promotes Renal Inflammation and Tissue Damage. *JCI Insight* (2020) 5:134081. doi: 10.1172/jci.insight.134081
51. Wang C, Wang H, Hao J, Chang D-Y, Zhao M-H, Chen M. Involvement of High Mobility Group Box 1 in the Activation of C5a-Primed Neutrophils Induced by ANCA. *Clin Immunol Orlando Fla* (2015) 159:47–57. doi: 10.1016/j.clim.2015.04.008
52. Kim SY, Son M, Lee SE, Park IH, Kwak MS, Han M, et al. High-Mobility Group Box 1-Induced Complement Activation Causes Sterile Inflammation. *Front Immunol* (2018) 9:705. doi: 10.3389/fimmu.2018.00705
53. Xie CB, Qin L, Li G, Fang C, Kirkiles-Smith NC, Tellides G, et al. Complement Membrane Attack Complexes Assemble NLRP3 Inflammasomes Triggering IL-1 Activation of IFN-γ-Primed Human Endothelium. *Circ Res* (2019) 124:1747–59. doi: 10.1161/CIRCRESAHA.119.314845
54. Feng X, Hao J, Liu Q, Yang L, Lv X, Zhang Y, et al. HMGB1 Mediates IFN-γ-Induced Cell Proliferation in MMC Cells Through Regulation of Cyclin D1/

CDK4/p16 Pathway. *J Cell Biochem* (2012) 113:2009–19. doi: 10.1002/jcb.24071
55. Katz Y, Strunk RC. Synthesis and Regulation of C1 Inhibitor in Human Skin Fibroblasts. *J Immunol* (1989) 142:2041–5.
56. Daugan MV, Revel M, Russick J, Dragon-Durey M-A, Gaboriaud C, Robe-Rybkine T, et al. Complement C1s and C4d as Prognostic Biomarkers in Renal Cancer: Emergence of Noncanonical Functions of C1s. *Cancer Immunol Res* (2021) 9:891–908. doi: 10.1158/2326-6066.CIR-20-0532
57. Yeo JG, Leong J, Arkachaisri T, Cai Y, Teo BHD, Tan JHT, et al. Proteolytic Inactivation of Nuclear Alarmin High-Mobility Group Box 1 by Complement Protease C1s During Apoptosis. *Cell Death Discov* (2016) 2:16069. doi: 10.1038/cddiscovery.2016.69
58. Efstathiou NE, Moustafa GA, Maidana DE, Konstantinou EK, Notomi S, Barbisan PRT, et al. Acadesine Suppresses TNF-α Induced Complement Component 3 (C3), in Retinal Pigment Epithelial (RPE) Cells. *PloS One* (2020) 15:e0244307. doi: 10.1371/journal.pone.0244307
59. Nakagawa K, Sakiyama H, Tsuchida T, Yamaguchi K, Toyoguchi T, Masuda R, et al. Complement C1s Activation in Degenerating Articular Cartilage of Rheumatoid Arthritis Patients: Immunohistochemical Studies With an Active Form Specific Antibody. *Ann Rheum Dis* (1999) 58:175–81. doi: 10.1136/ard.58.3.175
60. Jiang K, Chen Y, Xu C-S, Jarvis JN. T Cell Activation by Soluble C1q-Bearing Immune Complexes: Implications for the Pathogenesis of Rheumatoid Arthritis. *Clin Exp Immunol* (2003) 131:61–7. doi: 10.1046/j.1365-2249.2003.02046.x
61. Fante MA, Decking S-M, Bruss C, Schreml S, Siska PJ, Kreutz M, et al. Heat-Inactivation of Human Serum Destroys C1 Inhibitor, Pro-Motes Immune Complex Formation, and Improves Human T Cell Function. *Int J Mol Sci* (2021) 22:2646. doi: 10.3390/ijms22052646
62. Son M, Porat A, He M, Suurmond J, Santiago-Schwarz F, Andersson U, et al. C1q and HMGB1 Reciprocally Regulate Human Macrophage Polarization. *Blood* (2016) 128:2218–28. doi: 10.1182/blood-2016-05-719757
63. Liu T, Xiang A, Peng T, Doran AC, Tracey KJ, Barnes BJ, et al. HMGB1–C1q Complexes Regulate Macrophage Function by Switching Between Leukotriene and Specialized Proresolving Mediator Biosynthesis. *Proc Natl Acad Sci* (2019) 116:23254–63. doi: 10.1073/pnas.1907490116
64. Meyaard L, Adema GJ, Chang C, Woollatt E, Sutherland GR, Lanier LL, et al. LAIR-1, a Novel Inhibitory Receptor Expressed on Human Mononuclear Leukocytes. *Immunity* (1997) 7:283–90. doi: 10.1016/S1074-7613(00)80530-0
65. Meyaard L, Hurenkamp J, Clevers H, Lanier LL, Phillips JH. Leukocyte-Associated Ig-Like Receptor-1 Functions as an Inhibitory Receptor on Cytotoxic T Cells. *J Immunol* (1999) 162:5800–4.
66. van der Vuurst de Vries AR, Clevers H, Logtenberg T, Meyaard L. Leukocyte-Associated Immunoglobulin-Like Receptor-1 (LAIR-1) Is Differentially Expressed During Human B Cell Differentiation and Inhibits B Cell Receptor-Mediated Signaling. *Eur J Immunol* (1999) 29:3160–7. doi: 10.1002/(SICI)1521-4141(199910)29:10<3160::AID-IMMU3160>3.0.CO;2-S
67. Saverino D, Fabbi M, Merlo A, Ravera G, Grossi CE, Ciccone E. Surface Density Expression of the Leukocyte-Associated Ig-Like Receptor-1 Is Directly Related to Inhibition of Human T-Cell Functions. *Hum Immunol* (2002) 63:534–46. doi: 10.1016/s0198-8859(02)00409-3
68. Verbrugge A, de Ruiter T, Geest C, Coffer PJ, Meyaard L. Differential Expression of Leukocyte-Associated Ig-Like Receptor-1 During Neutrophil Differentiation and Activation. *J Leukoc Biol* (2006) 79:828–36. doi: 10.1189/jlb.0705370
69. Florian S, Sonneck K, Czerny M, Hennersdorf F, Hauswirth AW, Bühring H-J, et al. Detection of Novel Leukocyte Differentiation Antigens on Basophils and Mast Cells by HLDA8 Antibodies. *Allergy* (2006) 61:1054–62. doi: 10.1111/j.1398-9995.2006.01171.x
70. Jansen CA, Cruijsen CWA, de Ruiter T, Nanlohy N, Willems N, Janssens-Korpela P-L, et al. Regulated Expression of the Inhibitory Receptor LAIR-1 on Human Peripheral T Cells During T Cell Activation and Differentiation. *Eur J Immunol* (2007) 37:914–24. doi: 10.1002/eji.200636678
71. Zhang Y, Lv K, Zhang CM, Jin BQ, Zhuang R, Ding Y. The Role of LAIR-1 (CD305) in T Cells and Monocytes/Macrophages in Patients With Rheumatoid Arthritis. *Cell Immunol* (2014) 287:46–52. doi: 10.1016/j.cellimm.2013.12.005
72. Fouët G, Bally I, Chouquet A, Reiser J-B, Thielens NM, Gaboriaud C, et al. Molecular Basis of Complement C1q Collagen-Like Region Interaction With the Immunoglobulin-Like Receptor LAIR-1. *Int J Mol Sci* (2021) 22:5125. doi: 10.3390/ijms22105125
73. Son M, Diamond B. C1q-Mediated Repression of Human Monocytes Is Regulated by Leukocyte-Associated Ig-Like Receptor 1 (LAIR-1). *Mol Med* (2015) 20:559–68. doi: 10.2119/molmed.2014.00185
74. Son M, Santiago-Schwarz F, Al-Abed Y, Diamond B. C1q Limits Dendritic Cell Differentiation and Activation by Engaging LAIR-1. *Proc Natl Acad Sci USA*. (2012) 109:E3160–3167. doi: 10.1073/pnas.1212753109
75. Yeo JG, Leong J, Lu J. Complement the Cell Death. *Cell Death Dis* (2016) 7: e2465–5. doi: 10.1038/cddis.2016.369
76. Yu F, Haas M, Glassock R, Zhao M-H. Redefining Lupus Nephritis: Clinical Implications of Pathophysiologic Subtypes. *Nat Rev Nephrol* (2017) 13:483–95. doi: 10.1038/nrneph.2017.85
77. Dumestre-Pérard C, Clavarino G, Colliard S, Cesbron J-Y, Thielens NM. Antibodies Targeting Circulating Protective Molecules in Lupus Nephritis: Interest as Serological Biomarkers. *Autoimmun Rev* (2018) 17:890–9. doi: 10.1016/j.autrev.2018.03.013
78. Pickering MC, Walport MJ. Links Between Complement Abnormalities and Systemic Lupus Erythematosus. *Rheumatology* (2000) 39:133–41. doi: 10.1093/rheumatology/39.2.133
79. Lintner KE, Wu YL, Yang Y, Spencer CH, Hauptmann G, Hebert LA, et al. Early Components of the Complement Classical Activation Pathway in Human Systemic Autoimmune Diseases. *Front Immunol* (2016) 7:36. doi: 10.3389/fimmu.2016.00036
80. Macedo ACL, Isaac L. Systemic Lupus Erythematosus and Deficiencies of Early Components of the Complement Classical Pathway. *Front Immunol* (2016) 7:55. doi: 10.3389/fimmu.2016.00055
81. Dragon-Durey MA, Quartier P, Frémeaux-Bacchi V, Blouin J, de Barace C, Prieur AM, et al. Molecular Basis of a Selective C1s Deficiency Associated With Early Onset Multiple Autoimmune Diseases. *J Immunol* (2001) 166:7612–6. doi: 10.4049/jimmunol.166.12.7612
82. Roumenina LT, Sene D, Radanova M, Blouin J, Halbwachs-Mecarelli L, Dragon-Durey M-A, et al. Functional Complement C1q Abnormality Leads to Impaired Immune Complexes and Apoptotic Cell Clearance. *J Immunol* (2011) 187:4369–73. doi: 10.4049/jimmunol.1101749
83. Walport MJ. Complement. Second of Two Parts. *N Engl J Med* (2001) 344:1140–4. doi: 10.1056/NEJM200104123441506
84. Batu ED, Koşukcu C, Taşkıran E, Sahin S, Akman S, Sözeri B, et al. Whole Exome Sequencing in Early-Onset Systemic Lupus Erythematosus. *J Rheumatol* (2018) 45:1671–9. doi: 10.3899/jrheum.171358
85. Beurskens FJ, van Schaarenburg RA, Trouw LA. C1q, Antibodies and Anti-C1q Autoantibodies. *Mol Immunol* (2015) 68:6–13. doi: 10.1016/j.molimm.2015.05.010
86. Picard C, Lega J-C, Ranchin B, Cochat P, Cabrera N, Fabien N, et al. Anti-C1q Autoantibodies as Markers of Renal Involvement in Childhood-Onset Systemic Lupus Erythematosus. *Pediatr Nephrol* (2017) 32:1537–45. doi: 10.1007/s00467-017-3646-z
87. Trendelenburg M. Autoantibodies Against Complement Component C1q in Systemic Lupus Erythematosus. *Clin Transl Immunol* (2021) 10:e1279. doi: 10.1002/cti2.1279
88. Weinstein A, Alexander RV, Zack DJ. A Review of Complement Activation in SLE. *Curr Rheumatol Rep* (2021) 23:16. doi: 10.1007/s11926-021-00984-1
89. Ling GS, Crawford G, Buang N, Bartok I, Tian K, Thielens NM, et al. C1q Restrains Autoimmunity and Viral Infection by Regulating CD8 $^+$ T Cell Metabolism. *Science* (2018) 360:558–63. doi: 10.1126/science.aao4555
90. Thielens NM, Tedesco F, Bohlson SS, Gaboriaud C, Tenner AJ. C1q: A Fresh Look Upon an Old Molecule. *Mol Immunol* (2017) 89:73–83. doi: 10.1016/j.molimm.2017.05.025
91. Scott D, Botto M. The Paradoxical Roles of C1q and C3 in Autoimmunity. *Immunobiology* (2016) 221:719–25. doi: 10.1016/j.imbio.2015.05.001
92. Hosszu KK, Valentino A, Peerschke EI, Ghebrehiwet B. SLE: Novel Postulates for Therapeutic Options. *Front Immunol* (2020) 11:583853:583853. doi: 10.3389/fimmu.2020.583853

93. Kulik L, Laskowski J, Renner B, Woolaver R, Zhang L, Lyubchenko T, et al. Targeting the Immune Complex–Bound Complement C3d Ligand as a Novel Therapy for Lupus. *J Immunol* (2019) 203:3136–47. doi: 10.4049/jimmunol.1900620
94. Nikitin PA, Rose EL, Byun TS, Parry GC, Panicker S. C1s Inhibition by BIVV009 (Sutimlimab) Prevents Complement-Enhanced Activation of Autoimmune Human B Cells *In Vitro*. *J Immunol* (2019) 202:1200–9. doi: 10.4049/jimmunol.1800998
95. Schaper F, Westra J, Bijl M. Recent Developments in the Role of High-Mobility Group Box 1 in Systemic Lupus Erythematosus. *Mol Med* (2014) 20:72. doi: 10.2119/molmed.2014.00019
96. Liu T, Son M, Diamond B. HMGB1 in Systemic Lupus Erythematosus. *Front Immunol* (2020) 11:1057. doi: 10.3389/fimmu.2020.01057
97. Zhu B, Zhu Q, Li N, Wu T, Liu S, Liu S. Association of Serum/Plasma High Mobility Group Box 1 With Autoimmune Diseases: A Systematic Review and Meta-Analysis. *Med (Baltimore)* (2018) 97:e11531. doi: 10.1097/MD.0000000000011531
98. Li Y, Huang C, Zhao M, Liang G, Xiao R, Yung S, et al. A Possible Role of HMGB1 in DNA Demethylation in CD4+ T Cells From Patients With Systemic Lupus Erythematosus. *Clin Dev Immunol* (2013) 2013:206298. doi: 10.1155/2013/206298
99. Hossny E, El-Ghoneimy D, Soliman DA, Ashour A. Diagnostic Value of Serum High-Mobility Group Box-1 in Pediatric Systemic Lupus Erythematosus. *Int J Rheum Dis* (2019) 22:1402–9. doi: 10.1111/1756-185X.13556
100. Burbano C, Gómez-Puerta JA, Muñoz-Vahos C, Vanegas-García A, Rojas M, Vásquez G, et al. HMGB1+ Microparticles Present in Urine are Hallmarks of Nephritis in Patients With Systemic Lupus Erythematosus. *Eur J Immunol* (2019) 49:323–35. doi: 10.1002/eji.201847747
101. Schaper F, Leeuw K, Horst G, Maas F, Bootsma H, Heeringa P, et al. Autoantibodies to Box A of High Mobility Group Box 1 in Systemic Lupus Erythematosus. *Clin Exp Immunol* (2017) 188:412–9. doi: 10.1111/cei.12951
102. Feng X, Yang R, Tian Y, Miao X, Guo H, Gao F, et al. HMGB1 Protein Promotes Glomerular Mesangial Matrix Deposition *via* TLR2 in Lupus Nephritis. *J Cell Physiol* (2020) 235:5111–9. doi: 10.1002/jcp.29379
103. Song X, Zhang H, Zhao Y, Lin Y, Tang Q, Zhou X, et al. HMGB1 Activates Myeloid Dendritic Cells by Up-Regulating mTOR Pathway in Systemic Lupus Erythematosus. *Front Med* (2021) 8:636188:636188. doi: 10.3389/fmed.2021.636188
104. Willis WL, Wang L, Wada TT, Gardner M, Abdouni O, Hampton J, et al. The Proinflammatory Protein HMGB1 Is a Substrate of Transglutaminase-2 and Forms High-Molecular Weight Complexes With Autoantigens. *J Biol Chem* (2018) 293:8394–409. doi: 10.1074/jbc.RA117.001078
105. Gao X-J, Qu Y-Y, Liu X-W, Zhu M, Ma C-Y, Jiao Y-L, et al. Immune Complexes Induce TNF-α and BAFF Production From U937 Cells by HMGB1 and RAGE. *Eur Rev Med Pharmacol Sci* (2017) 21:1810–9.
106. Urbonaviciute V, Fürnrohr BG, Meister S, Munoz L, Heyder P, Marchis FD, et al. Induction of Inflammatory and Immune Responses by HMGB1–Nucleosome Complexes: Implications for the Pathogenesis of SLE. *J Exp Med* (2008) 205:3007. doi: 10.1084/jem.20081165
107. Abdulahad DA, Westra J, Bijzet J, Limburg PC, Kallenberg CGM, Bijl M. High Mobility Group Box 1 (HMGB1) and Anti-HMGB1 Antibodies and Their Relation to Disease Characteristics in Systemic Lupus Erythematosus. *Arthritis Res Ther* (2011) 13:R71. doi: 10.1186/ar3332
108. Kanakoudi-Tsakalidou F, Farmaki E, Tzimouli V, Taparkou A, Paterakis G, Trachana M, et al. Simultaneous Changes in Serum HMGB1 and IFN-α Levels and in LAIR-1 Expression on Plasmatoid Dendritic Cells of Patients With Juvenile SLE. New Therapeutic Options? *Lupus* (2014) 23:305–12. doi: 10.1177/0961203313519157
109. Colombo BM, Canevali P, Magnani O, Rossi E, Puppo F, Zocchi MR, et al. Defective Expression and Function of the Leukocyte Associated Ig-Like Receptor 1 in B Lymphocytes From Systemic Lupus Erythematosus Patients. *PloS One* (2012) 7:e31903. doi: 10.1371/journal.pone.0031903
110. Chauhan AK, Moore TL, Bi Y, Chen C. Fcγriiia-Syk Co-Signal Modulates CD4+ T-Cell Response and Up-Regulates Toll-Like Receptor (TLR) Expression. *J Biol Chem* (2016) 291:1368–86. doi: 10.1074/jbc.M115.684795
111. Arinuma Y, Yamaoka K. Developmental Process in Diffuse Psychological/Neuropsychiatric Manifestations of Neuropsychiatric Systemic Lupus Erythematosus. *Immunol Med* (2021) 44:16–22. doi: 10.1080/25785826.2020.1791401
112. Hajishengallis G, Kajikawa T, Hajishengallis E, Maekawa T, Reis ES, Mastellos DC, et al. Complement-Dependent Mechanisms and Interventions in Periodontal Disease. *Front Immunol* (2019) 10:406. doi: 10.3389/fimmu.2019.00406
113. Martínez-García M, Hernández-Lemus E. Periodontal Inflammation and Systemic Diseases: An Overview. *Front Physiol* (2021) 12:709438:709438. doi: 10.3389/fphys.2021.709438
114. Li L, Zhang Y-L, Liu X-Y, Meng X, Zhao R-Q, Ou L-L, et al. Periodontitis Exacerbates and Promotes the Progression of Chronic Kidney Disease Through Oral Flora, Cytokines, and Oxidative Stress. *Front Microbiol* (2021) 12:656372:656372. doi: 10.3389/fmicb.2021.656372
115. Kapferer-Seebacher I, Pepin M, Werner R, Aitman TJ, Nordgren A, Stoiber H, et al. Periodontal Ehlers-Danlos Syndrome Is Caused by Mutations in C1R and C1S, Which Encode Subcomponents C1r and C1s of Complement. *Am J Hum Genet* (2016) 99:1005–14. doi: 10.1016/j.ajhg.2016.08.019
116. Kapferer-Seebacher I, Oakley-Hannibal E, Lepperdinger U, Johnson D, Ghali N, Brady AF, et al. Prospective Clinical Investigations of Children With Periodontal Ehlers–Danlos Syndrome Identify Generalized Lack of Attached Gingiva as a Pathognomonic Feature. *Genet Med* (2021) 23:316–322. doi: 10.1038/s41436-020-00985-y
117. Kapferer-Seebacher I, Lundberg P, Malfait F, Zschocke J. Periodontal Manifestations of Ehlers-Danlos Syndromes: A Systematic Review. *J Clin Periodontol* (2017) 44:1088–100. doi: 10.1111/jcpe.12807
118. Gröbner R, Kapferer-Seebacher I, Amberger A, Redolfi R, Dalonneau F, Björck E, et al. C1R Mutations Trigger Constitutive Complement 1 Activation in Periodontal Ehlers-Danlos Syndrome. *Front Immunol* (2019) 10:2537. doi: 10.3389/fimmu.2019.02537
119. Bally I, Dalonneau F, Chouquet A, Gröbner R, Amberger A, Kapferer-Seebacher I, et al. Two Different Missense C1S Mutations, Associated to Periodontal Ehlers-Danlos Syndrome, Lead to Identical Molecular Outcomes. *Front Immunol* (2019) 10:2962. doi: 10.3389/fimmu.2019.02962
120. Damgaard C, Holmstrup P, Van Dyke TE, Nielsen CH. The Complement System and Its Role in the Pathogenesis of Periodontitis: Current Concepts. *J Periodontal Res* (2015) 50:283–93. doi: 10.1111/jre.12209
121. Luntzer K, Lackner I, Weber B, Mödinger Y, Ignatius A, Gebhard F, et al. Increased Presence of Complement Factors and Mast Cells in Alveolar Bone and Tooth Resorption. *Int J Mol Sci* (2021) 22:2759. doi: 10.3390/ijms22052759
122. Giovani PA, Salmon CR, Martins L, Leme AFP, Rebouças P, Rontani RMP, et al. Secretome Profiling of Periodontal Ligament From Deciduous and Permanent Teeth Reveals a Distinct Expression Pattern of Laminin Chains. *PloS One* (2016) 11:e0154957. doi: 10.1371/journal.pone.0154957
123. Yamashiro K, Ideguchi H, Aoyagi H, Yoshihara-Hirata C, Hirai A, Suzuki-Kyoshima R, et al. High Mobility Group Box 1 Expression in Oral Inflammation and Regeneration. *Front Immunol* (2020) 11:1461. doi: 10.3389/fimmu.2020.01461
124. Yoshihara-Hirata C, Yamashiro K, Yamamoto T, Aoyagi H, Ideguchi H, Kawamura M, et al. Anti-HMGB1 Neutralizing Antibody Attenuates Periodontal Inflammation and Bone Resorption in a Murine Periodontitis Model. *Infect Immun* (2018) 86:e00111-18. doi: 10.1128/IAI.00111-18
125. Morimoto-Yamashita Y, Ito T, Kawahara K-I, Kikuchi K, Tatsuyama-Nagayama S, Kawakami-Morizono Y, et al. Periodontal Disease and Type 2 Diabetes Mellitus: Is the HMGB1-RAGE Axis the Missing Link? *Med Hypotheses* (2012) 79:452–5. doi: 10.1016/j.mehy.2012.06.020
126. Hajishengallis G, Lambris JD. More Than Complementing Tolls: Complement-Toll-Like Receptor Synergy and Crosstalk in Innate Immunity and Inflammation. *Immunol Rev* (2016) 274:233–44. doi: 10.1111/imr.12467
127. Kapurniotu A, Gokce O, Bernhagen J. The Multitasking Potential of Alarmins and Atypical Chemokines. *Front Med* (2019) 6:3. doi: 10.3389/fmed.2019.00003
128. Yang J, Wise L, Fukuchi K-I. TLR4 Cross-Talk With NLRP3 Inflammasome and Complement Signaling Pathways in Alzheimer's Disease. *Front Immunol* (2020) 11:724. doi: 10.3389/fimmu.2020.00724
129. Triantafilou M, Hughes TR, Morgan BP, Triantafilou K. Complementing the Inflammasome. *Immunology* (2016) 147:152–64. doi: 10.1111/imm.12556

130. Arbore G, Kemper C. A Novel "Complement–Metabolism–Inflammasome Axis" as a Key Regulator of Immune Cell Effector Function. *Eur J Immunol* (2016) 46:1563–73. doi: 10.1002/eji.201546131
131. Bertheloot D, Latz E. HMGB1, IL-1α, IL-33 and S100 Proteins: Dual-Function Alarmins. *Cell Mol Immunol* (2017) 14:43–64. doi: 10.1038/cmi.2016.34
132. Watanabe H, Son M. The Immune Tolerance Role of the HMGB1-RAGE Axis. *Cells* (2021) 10:564. doi: 10.3390/cells10030564
133. Madhu LN, Attaluri S, Kodali M, Shuai B, Upadhya R, Gitai D, et al. Neuroinflammation in Gulf War Illness Is Linked With HMGB1 and Complement Activation, Which Can Be Discerned From Brain-Derived Extracellular Vesicles in the Blood. *Brain Behav Immun* (2019) 81:430–43. doi: 10.1016/j.bbi.2019.06.040
134. Ehrnthaller C, Schultze A, Wakileh G, Neff T, Hafner S, Radermacher P, et al. Hemorrhagic Shock Induces Renal Complement Activation. *Eur J Trauma Emerg Surg Off Publ Eur Trauma Soc* (2021) 47:373–80. doi: 10.1007/s00068-019-01187-1
135. Griffiths M, Neal JW, Gasque P. Innate Immunity and Protective Neuroinflammation: New Emphasis on the Role of Neuroimmune Regulatory Proteins. *Int Rev Neurobiol* (2007) 82:29–55. doi: 10.1016/S0074-7742(07)82002-2
136. Kapferer-Seebacher I, Waisfisz Q, Boesch S, Bronk M, van Tintelen P, Gizewski ER, et al. Periodontal Ehlers–Danlos Syndrome Is Associated With Leukoencephalopathy. *neurogenetics* (2020) 20:1–8. doi: 10.1007/s10048-018-0560-x
137. Nestor J, Arinuma Y, Huerta TS, Kowal C, Nasiri E, Kello N, et al. Lupus Antibodies Induce Behavioral Changes Mediated by Microglia and Blocked by ACE Inhibitors. *J Exp Med* (2018) 215:2554–66. doi: 10.1084/jem.20180776
138. Andersson U, Ottestad W, Tracey KJ. Extracellular HMGB1: A Therapeutic Target in Severe Pulmonary Inflammation Including COVID-19? *Mol Med* (2020) 26:42. doi: 10.1186/s10020-020-00172-4
139. Diao L, Tao J, Wang Y, Hu Y, He W. Co-Delivery Of Dihydroartemisinin And HMGB1 siRNA By TAT-Modified Cationic Liposomes Through The TLR4 Signaling Pathway For Treatment Of Lupus Nephritis. *Int J Nanomed* (2019) 14:8627–45. doi: 10.2147/IJN.S220754
140. Hajishengallis G, Hasturk H, Lambris JD, Apatzidou DA, Belibasakis GN, Bostanci N, et al. C3-Targeted Therapy in Periodontal Disease: Moving Closer to the Clinic. *Trends Immunol* (2021) 42:856–64. doi: 10.1016/j.it.2021.08.001

Conflict of Interest: The authors declare that the research was conducted in the absence of any commercial or financial relationships that could be construed as a potential conflict of interest.

Publisher's Note: All claims expressed in this article are solely those of the authors and do not necessarily represent those of their affiliated organizations, or those of the publisher, the editors and the reviewers. Any product that may be evaluated in this article, or claim that may be made by its manufacturer, is not guaranteed or endorsed by the publisher.

GLOSSARY

Abs	antibodies
ACAMPs	apoptotic cell-associated molecular patterns
Akt	protein kinase B
AMPs	associated molecular patterns
AP	complement alternative pathway
auto-Abs	autoantibodies
BAFF	B-cell activating factor
BCR	B-cell receptor
C1	complement component 1 (C1q, C1r, C1s sub-units)
C1inh	C1 inhibitor
C2	complement component 2 (and its split products C2a, C2b)
C3	complement component 3 (and its split products C3a, C3b, C3c, C3d)
C3aR	complement C3a receptor
C4	complement component 4 (and its split products C4a, C4b)
C4BP	C4b-binding protein
C5	complement component 5
C5aR1	complement C5a receptor 1
C5aR2	complement C5a receptor 2
C9	complement component 9
CD	cluster of differentiation
CLR	collagen-like regions (of C1q)
COVID-19	corona virus disease 2019
CP	complement classical pathway
CR1	complement receptor 1
CR2	complement receptor 2
CR3	complement receptor 3
CR4	complement receptor 4
DAF	decay accelerating factor
DAMPs	damage-associated molecular patterns
DNA	deoxyribonucleic acid
EDS	Ehlers-Danlos syndromes
ERK	extracellular signal-regulated kinases
FB	complement factor B (and its split products FBa, FBb)
FD	complement factor D
FcγRIIIa	low affinity immunoglobulin gamma Fc region receptor III-A
FH	complement factor H
FI	complement factor I
GADPH	glyceraldehyde 3-phosphate deshydrogenase
gC1qR	globular C1q receptor
GR	globular regions (of C1q)
GSPE	grape seed procyanidins extract
HLA-DR	human leukocyte antigen – DR isotype
HMGB1	high-mobility group box 1
ICs	Immune complexes
IFN	interferons
IFNγ	interferon gamma
IgG	immunoglobulin G
IgM	immunoglobulin M
IL-1β	interleukin 1 beta
IL-6	interleukin 6
ITIM	immune receptor tyrosine-based inhibitory motifs
JNK	c-Jun N-terminal kinase
LAIR-1	leukocyte-associated immunoglobulin-like receptor-1
LN	lupus nephritis
LP	complement lectin pathway
LPS	lipopolysaccharide
MASP-1	mannose-binding lectin associated serine protease 1
MASP-2	mannose-binding lectin associated serine protease 2
MD2	myeloid differentiation protein 2
MEK	Mitogen-activated protein kinase
miRNA	micro ribonucleic acid
MCP	membrane cofactor protein
MyD88	myeloid differentiation primary response 88
NF-κB	nuclear factor-kappa B
NK	natural killer
NLRP3	NOD-like receptor family pyrin domain containing 3
P. gingivalis	*Porphyromonas gingivalis*
PAMPs	pathogen-associated molecular patterns
pDC	plasmacytoid dendritic cells
pEDS	periodontal Ehlers-Danlos syndromes
PI3K	phosphoinositide 3-kinase
PKR	protein kinase R
RAGE	receptor for advanced glycation end products
SHP1	tyrosine phosphatase containing SH2 domain
SLE	systemic lupus erythematosus
SLEDAI	systemic lupus erythematosus disease activity index
SYK	spleen tyrosine kinase
TCR	T-cell receptor
TGF-β1	transforming growth factor beta 1
Th1	T helper cells 1
TLR2	toll-like receptor 2
TLR4	toll-like receptor 4
TLRs	toll-like receptors
TNF	tumor necrosis factors
TNFα	tumor necrosis factor alpha.

frontiers | Frontiers in Immunology

MINI REVIEW
published: 13 May 2022
doi: 10.3389/fimmu.2022.868225

Helicobacter pylori and the Role of Lipopolysaccharide Variation in Innate Immune Evasion

Daniel Sijmons[1], *Andrew J. Guy*[1,2], *Anna K. Walduck*[1] *and Paul A. Ramsland*[1,3,4*]

[1] School of Science, RMIT University, Melbourne, VIC, Australia, [2] ZiP Diagnostics, Collingwood, VIC, Australia, [3] Department of Immunology, Monash University, Melbourne, VIC, Australia, [4] Department of Surgery, Austin Health, University of Melbourne, Heidelberg, VIC, Australia

Helicobacter pylori is an important human pathogen that infects half the human population and can lead to significant clinical outcomes such as acute and chronic gastritis, duodenal ulcer, and gastric adenocarcinoma. To establish infection, *H. pylori* employs several mechanisms to overcome the innate and adaptive immune systems. *H. pylori* can modulate interleukin (IL) secretion and innate immune cell function by the action of several virulence factors such as VacA, CagA and the type IV secretion system. Additionally, *H. pylori* can modulate local dendritic cells (DC) negatively impacting the function of these cells, reducing the secretion of immune signaling molecules, and influencing the differentiation of $CD4^+$ T helper cells causing a bias to Th1 type cells. Furthermore, the lipopolysaccharide (LPS) of *H. pylori* displays a high degree of phase variation and contains human blood group carbohydrate determinants such as the Lewis system antigens, which are proposed to be involved in molecular mimicry of the host. Lastly, the *H. pylori* group of outer membrane proteins such as BabA play an important role in attachment and interaction with host Lewis and other carbohydrate antigens. This review examines the various mechanisms that *H. pylori* utilises to evade the innate immune system as well as discussing how the structure of the *H. pylori* LPS plays a role in immune evasion.

Keywords: *H. pylori*, innate immunity, lipopolysaccharide, dendritic cells, Lewis system antigens, molecular mimicry, adhesion, inflammation

OPEN ACCESS

Edited by:
Uday Kishore,
Brunel University London,
United Kingdom

Reviewed by:
Peter Kraiczy,
Goethe University Frankfurt, Germany
Marco De Zuani,
Wellcome Sanger Institute (WT),
United Kingdom

***Correspondence:**
Paul A. Ramsland
paul.ramsland@rmit.edu.au

Specialty section:
This article was submitted to Molecular Innate Immunity, a section of the journal Frontiers in Immunology

Received: *02 February 2022*
Accepted: *04 April 2022*
Published: *13 May 2022*

Citation:
Sijmons D, Guy AJ, Walduck AK and Ramsland PA (2022) Helicobacter pylori and the Role of Lipopolysaccharide Variation in Innate Immune Evasion. Front. Immunol. 13:868225. doi: 10.3389/fimmu.2022.868225

INTRODUCTION

Helicobacter pylori is a gram-negative, spiral shaped bacterium that infects the stomach of up to half the world's population. The prevalence is dependent on country and can vary between 20% to 80% (1). *H. pylori* also has a high rate of clinically asymptomatic infection, with some studies reporting a prevalence as high as 67% in entirely asymptomatic populations (2, 3). However, chronic infection with *H. pylori* can result in severe clinical conditions, and colonisation induces chronic inflammation in all infected individuals (4). These conditions are thought to be caused by damage to the gastric epithelium and prolonged inflammation associated with chronic infection and immune action (3).

Antibiotics are the mainstay of treatment for confirmed infections, and quadruple antibiotic therapy is currently recommended (5). *H. pylori* strains are however increasingly found to be resistant and treatment failure is not uncommon (6). The outcome of *H. pylori* infection is strongly influenced by both the bacterial genotype as well as host polymorphisms and is driven by an array of virulence factors possessed by *H. pylori* (7). Approximately 15% of cases result in symptomatic gastric disease including acute gastritis, chronic gastritis, and peptic ulcer (8). Furthermore, 1-2% of infections result in malignant neoplastic diseases such as mucosal-associated lymphoid tissue (MALT) lymphoma and gastric adenocarcinoma (8). As a result of this *H. pylori* is classified as a type one carcinogen by the World Health Organisation (WHO) (9). The severity of *H. pylori* disease, and the increasing incidence of antibiotic resistance means there is an urgent need for new therapies and vaccines.

H. pylori employs several mechanisms to evade innate immunity allowing the bacterium to establish chronic infection. Firstly, *H. pylori* occupies a unique infective niche in the hostile conditions of the human stomach, using the secretion of the enzyme urease to survive the natural barrier of the stomach's acidity, coupled with the motility *via* its unipolar flagella (10). The motility of *H. pylori* allows it to maintain position and reside in the gastric mucous gel layer where it triggers inflammation. The net effect of *H. pylori*-induced inflammation is damage to the epithelial barrier, which presumably releases nutrients to promote bacterial growth.

Despite chronic infection, inflammatory responses to *H. pylori* infection remain relatively controlled in most cases due to a series of mechanisms that manipulate the host response, promoting persistent infection. *H. pylori* is able to adhere to mucins such as MUC5AC (11), as well as interacting with Lewis system antigens expressed on gastric epithelial cells (12), this allows it to maintain its position in the mucus gel layer and crypt isthmus and prevent its removal by the stomachs churning movement (10). Secondly, *H. pylori* can interact with and manipulate interleukin (IL) secretion of local dendritic cells (DC), negatively regulating the functions of these cells and suppressing cytokine release (13), influencing the differentiation of $CD4^+$ T helper cells towards Th1 type cells (14). Finally, the lipopolysaccharide (LPS) of *H. pylori* displays a high degree of phase variation and contains human blood group carbohydrate determinants such as the Lewis system antigens (15–17). This review examines the various mechanisms *H. pylori* utilises to evade the innate immune system as well as discussing how the structure of the *H. pylori* LPS plays a prominent role in immune evasion.

OVERVIEW OF INNATE IMMUNITY IN THE CONTEXT OF BACTERIAL INFECTION

The innate immune system is the first line of defence against the many potential pathogens humans are exposed to daily (18). Epithelial surfaces and mucous membranes provide a physical barrier between internal organs and the external environment (19). The innate immune system also employs various antimicrobial peptides within the mucosal layer which have the ability to kill or inhibit microorganisms and viruses in the area (20). These initial defences are supported by more complex innate immune mechanisms. For example, pathogen-associated molecular patterns (PAMP) can be discerned from host molecular patterns by innate and adaptive immune cells allowing the triggering of a more extensive immune response (21). PAMP frequently include molecules such as glycans and glycoconjugates which may be expressed in structures like the LPS of a gram-negative bacterium (22). Detection of these structures are commonly associated with two classes of proteins known as toll-like receptors (TLR) and nucleotide-binding oligomerization domain-like receptors (NLR), as well as complement components circulating in the blood (23). The TLR expressed in humans are particularly well characterised, with TLR2, TLR4 and TLR5 commonly associated with the detection of lipopolysaccharide structures such as a bacterial LPS or flagella, whereas TLR3, TLR7, TLR8 and TLR9 are associated with the detection of foreign nucleic acids (24). Nod-Like Receptors recognise components of the bacterial cell wall, their activation triggers the release of pro-inflammatory cytokines and have synergistic effects with TLR in immune system signaling pathways (25).

Pathogen recognition triggers several supporting immune functions such as the activation of proinflammatory effector molecules. Inflammation is an important part of the immune response and inflammasomes are a system of innate immune receptors that activate the cystine protease caspase-1 and induce inflammation in response to the presence of infectious microbes (26). Additionally, inflammasomes contribute to the activation of proinflammatory cytokines IL-1β and IL-18, which induce an influx of innate immune cells into a potentially infected area, resulting in the secretion of further inflammatory cytokines, including IL-8, IL-6, IL-12, IL-17 and TNF-α, allowing for improved clearance of infection (26–28). Recognition of infectious bacteria often results in the engulfment of the bacterium by phagocytes including macrophages and monocytes. Engulfed bacteria are encased in an intracellular vesicle, the phagosome, where the phagocytic cells concentrate molecules which are deadly to bacterial cells, including antimicrobial substances, reactive oxygen species and reactive nitrogen intermediates. As well as immediate destruction, the engulfment, or phagocytosis of bacteria can also function as a form of antigen presentation for the activation of the adaptive immune system (29). A specialised type of phagocyte known as the dendritic cell (DC) plays a primary role in the activation of the adaptive immune system. Once a DC engulfs a bacterium, it processes the bacterial cell and presents its antigens in complex with major histocompatibility molecules (MHC) to lymphocytes to induce T cell and B cell maturation and differentiation, triggering the adaptive immune response (30).

IMMUNE RESPONSE AGAINST *H. PYLORI*

Various innate immune mechanisms are activated by the colonisation of *H. pylori.* Toll-like receptors (TLR) 2, 4 and 5 can recognise PAMP of *H. pylori* (31), triggering immune pathways that activate NF-κB and IL-8 inducing a local proinflammatory response (32). *H. pylori* are extracellular and

generally non-invasive, but secretion of urease and the VacA toxin trigger local inflammatory responses. The most researched virulence factor is the type IV secretion system (TIVSS) encoded by the *Cag* pathogenicity island carried by type I strains (33). After bacterial adherence the TIVSS delivers the cytotoxin CagA to the cytoplasm where it initiates intracellular signaling cascades that activate NF-κB (34), contributing to the local inflammatory response. The combined effect of this inflammation results in erosion of the epithelium, releasing nutrients for the bacteria to grow and colonise (35). Furthermore, intracellular pathogen recognising molecules such as NOD1 can bind *H. pylori* peptidoglycans that are introduced into epithelial cells *via* the TIVSS and trigger the release of other anti-microbial proteins in response, restricting bacterial growth and initiating additional immune action (36). While additional macrophages may be stimulated, *H. pylori* is able to neutralise macrophage nitric oxide production reducing the immune action of the cell (37). Once *H. pylori* has overcome the initial epithelial response, persistent infection drives an adaptive immune response triggered by dendritic cells. The local response consists of humoral and T cell (particularly Th1 and Th17) activation. Overall there is an influx of plasma cells, lymphocytes, neutrophils and other immune cells into the gastric mucosa during *H. pylori* infection, however this rarely results in complete clearance of the bacterium, and over time a significant population of regulatory T cells become established (38). This control of inflammation by *H. pylori* probably explains why many *H. pylori* infected individuals remain asymptomatic.

The stomach has relatively few polymeric immunoglobulin receptors (pIgR), the receptor responsible for IgA transportation, in comparison to the rest of the gastrointestinal tract (39). This is altered in chronic *H. pylori* infection with upregulation of the pIgR caused by raised γ-interferon levels associated with prolonged inflammation (40). Upregulation of pIgR does not result in a corresponding increase in local secretory IgA levels, with monomeric non-secretory IgA predominating in the stomach of those infected with *H. pylori* (41). In contrast, secretory IgA is commonly observed in response to intestinal commensals and pathogens, suggesting a different mode of action of pIgR in the stomach. Systemic *H. pylori* specific IgG is also produced in adults experiencing chronic infection (42).

Role of *H. pylori* Virulence Factors in Induction of Innate Immune Responses and Immune Evasion

The natural immune response against *H. pylori* does not effectively clear infection and a combination of immune evasion techniques and bacterial factors leads to a persistent infection (**Figure 1** and **Table 1**). Initial Type 1 inflammatory responses in most infected persons become biased over time towards Th2 and Treg that acts in a kind of damage control measure, which does not clear infection but reduces damage to the host (59–61).

An important feature of *H. pylori* is its ability to overcome natural barriers preventing most microbes from colonising the human stomach (62, 63). Early studies concluded that *H. pylori* flagellin evades TLR5 recognition and recombinant *H. pylori* flagellin was considerably less stimulatory than *Salmonella* flagellin for example (64). Furthermore, a series of residues within the CD0 domain of *H. pylori* flagella protein FlaA has recently been found to enable evasion of TLR5 (**Figure 1**), these are speculated to be a result of point mutations not present in flagella proteins from other bacterium (65). However, a number of studies have now reported that *H. pylori* activates both TLR2 and 5 on epithelial cells, but not TLR4 (66). A recent report revealed that TLR5 activation is *via* interaction with the CagY protein which forms part of the TIVSS (67).

CagA is one of the most studied and most important virulence factors possessed by *H. pylori*. Contact and adherence of *H. pylori* to host gastric epithelial cells upregulates the expression of both CagA and VacA, as well as inducing the synthesis and assembly of the TIVSS (**Figure 2**) (71). Both CagA and the TIVSS are encoded by the *cag* PAI which is an approximately 40 kb chromosomal DNA region present in the most virulent strains of *H. pylori*. The TIVSS is a pilus-based "molecular syringe" structure that translocates CagA protein into host epithelial cells. The Type IV pilus binds epithelial cells *via* interaction with β1 integrin on the basolateral side (72). The bacteria gain access to the basolateral side through secretion of the HtrA enzyme which breaks down tight junctions (33).

Once in the cytoplasm, translocated CagA associates with Src and c-Abl family kinases which phosphorylate the CagA carboxyl-terminal EPIYA motif in the inner host cell membrane. Phosphorylated CagA then interferes with host cell signaling pathways, disrupting cell-cell junctions (73). In addition, CagA targets and causes the ubiquitination of the upstream kinase TAK1 (74). The downstream effects of CagA induce signaling cascades that activate NF-κB and downstream proinflammatory signaling (IL-8 secretion), cytoskeletal rearrangements, and changes to tight junctions (31, 33, 75) and inducing apoptosis (70, 76). Higher levels of CagA were shown to cause nuclear translocation of the AP-1 transcription factor and nuclear factor of activated T-cells (NFAT) (77). Furthermore, CagA is directly related to *H. pylori* carcinogenesis, enhancing DNA double strand breaks, and disabling homologous recombination-mediated DNA repair as well as stimulating Hippo signaling *via* the inhibition of PAR1b-mediated BRCA1 phosphorylation (78). Additionally, recent work has indicated that CagA initiates the oncogenic YAP pathway, further contributing to the association between CagA and gastric cancer risk (79, 80).

Infection with CagA positive *H. pylori* strains is one of the strongest risk factors for the development of gastric cancer (75). In addition, multiple *H. pylori* outer membrane proteins are associated with proinflammatory cytokine induction (**Figure 2**), these include OipA and BabA, which can induce IL-6, IL-8 and IL-11 (44, 45, 81). Like many bacteria, *H. pylori* have also been shown to release outer membrane vesicles (OMV) which contain various components, notably including portions of the *H. pylori* LPS as well as Hop family proteins including BabA and SabA along with other major virulence factors such as VacA and CagA

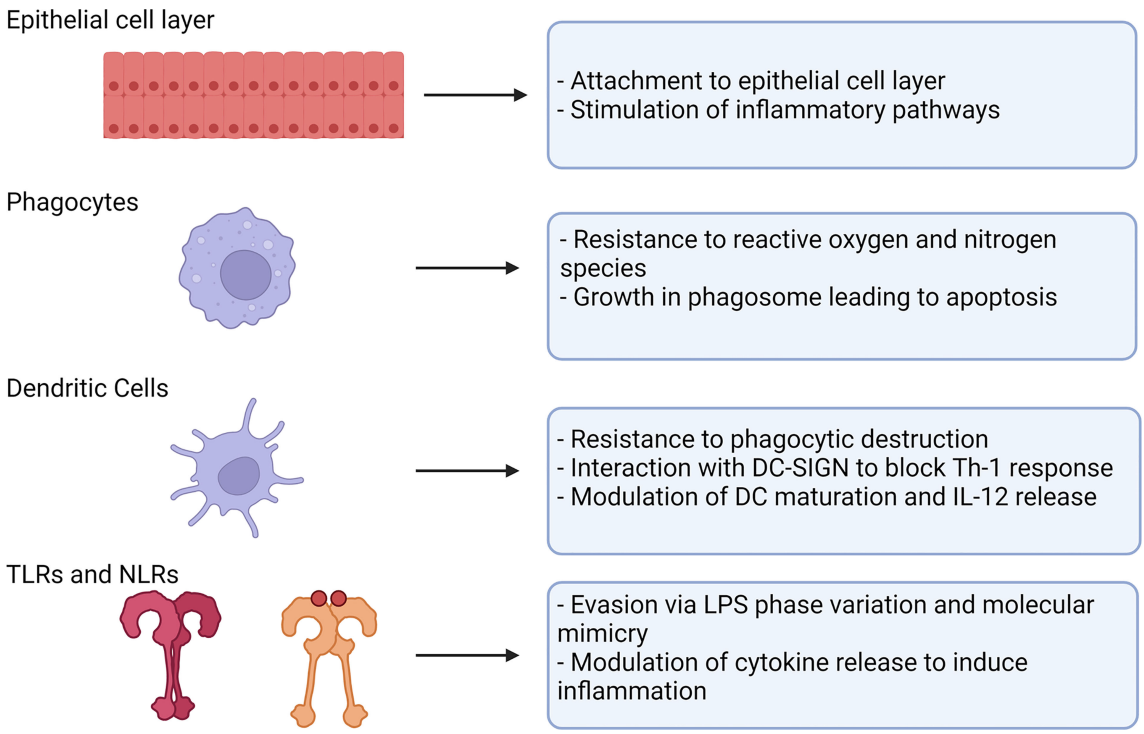

FIGURE 1 | Strategies used by *H. pylori* to evade innate immune mechanisms. *H. pylori* uses a number of mechanisms to evade the innate immune system. Various components of the innate immune system present barriers to or respond to *H. pylori* infection (left). *H. pylori* is able to overcome these by mechanisms described (right). Created with BioRender.com.

TABLE 1 | Effect of *H. pylori* virulence factors on the immune response.

Virulence factor	Immune evasion mechanisms	References
LPS	Evasion of pattern recognition receptors (TLR and NLR), inhibition of DC-SIGN.	(43)
BabA	Influences inflammasome activation. Prevention of removal by peristalsis and gastric shedding. Stimulation of inflammatory cytokines.	(44–47)
cag pathogenicity island and CagA	Prevention of phagocytosis and macrophage killing, regulation of DC cytokine production and inhibition of $CD4^+$ T cell proliferation.	(13, 48, 49)
Flagellin	Evasion of TLR, evasion of peristalsis.	(50)
Urease	Neutralisation of acidity surrounding the bacterium, apoptosis of gastric epithelial cells.	(51, 52)
VacA	Prevention of phagocytosis and macrophage killing, interference with cytokines, alteration of antigen presentation, apoptosis of monocytes, inhibition of DC maturation, apoptosis of gastric epithelial cells.	(14, 49, 53–55)
H. pylori Neutrophil-activating protein (HP-NAP)	Neutrophil activation, increased production of inflammatory cytokines from neutrophils and monocytes and interference with Th2 responses.	(56, 57)
OipA	Induction of inflammatory cytokines.	(44, 45)
SabA	Nonopsonic activation of neutrophils, upregulation allowing for enhanced adhesion in inflamed gastric environments, down regulating enabling bacterial escape from strong host immune response.	(12, 58)

(**Figure 2**) (74, 82). Interestingly, it appears that *H. pylori* is also able to regulate cytokine release from host epithelial cells *via* small noncoding RNAs that have been detected in OMV. These OMV have been shown to suppress IL-8 stimulation from AGS cells in cell culture, presumably by targeting host cell mRNAs, effectively reducing the overall immunostimulatory response to *H. pylori* LPS and outer membrane proteins (83). Consequently, OMV may play a role in immune modulation and disease progression. Regulation of cytokine release by *H. pylori* has also been investigated in relation to inflammasomes. *H. pylori* can modulate NLRP3, a regulator important for inflammasome activation, by inducing secretion of IL-10 in THP-1 monocytic leukemia cell lines, and through the action of miRNAs such as has-miR-223-3p (84). Furthermore, *H. pylori* infection was reported to suppress the secretion of mature IL-1β from human THP1 monocytes, in spite of upregulation of pro-IL-1β, potentially promoting bacterial persistence (85). Interestingly, cytokine expression has been seen to differ between children and adults, with Il-1β, IL17A, IL-23, IL2, IL-12p70 and IFN-γ upregulated in adults and downregulated in children, and IL-6,

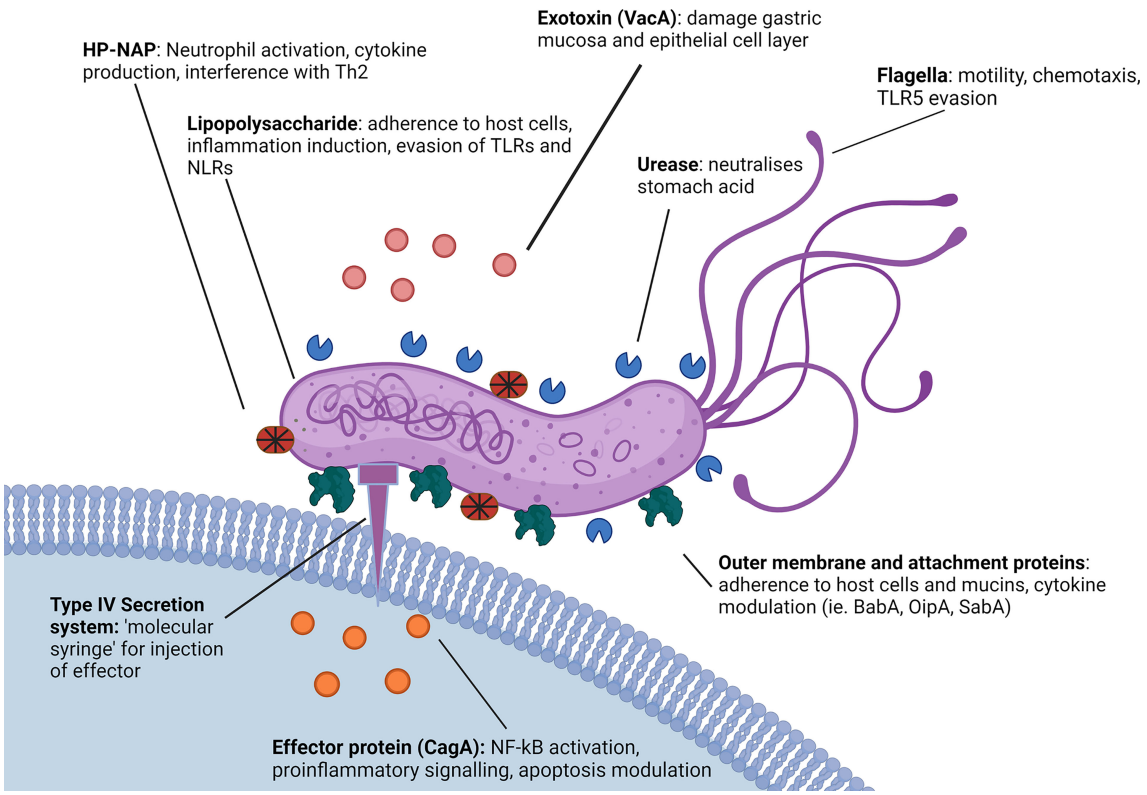

FIGURE 2 | Role of *H. pylori* virulence factors in innate immune evasion. *H. pylori* utilises a number of virulence factors to enable immune evasion. *H. pylori* possesses a less immunogenic LPS in comparison to other gram-negative microbes and both the LPS and several *H. pylori* virulence proteins such as SabA and OipA demonstrate variable expression patterns affecting the immune response (68, 69). Additionally, *H. pylori* expresses proteins such as HP-NAP, VacA and CagA that actively modulate cytokine and inflammatory signaling, as well as DC and macrophage function (56, 70). *H. pylori* flagella protein FlaA also evades detection by TLR5 *via* a series of complex point mutations (65). Created with BioRender.com.

TGF-β1, IL-10, TNF-α and IL-1a downregulated in adults and upregulated in children. As a result of these differences, children display a Treg primary response as opposed to the Th1 and Th17 response seen in adults (86–88).

The virulence factor HP-NAP also plays a major role in inducing and modulating host inflammation, recruiting neutrophils to the site of infection and causing a large increase in the neutrophil secretion of reactive nitrogen species, as well as stimulating the release of IL-12 and IL-23 from both neutrophils and monocytes (89). *In vitro* studies using cloned $CD4^+$ T cells from allergen induced T cell lines have shown HP-NAP acts as a Th2 agonist, redirecting Th2 responses into Th1 to drive further inflammation through cytotoxic Th1 responses characterised by increased TNF-α and interferon-γ (**Figure 2**) (56).

H. pylori is able to adhere to both the secreted gastric mucin MUC5AC (90) and gastric epithelial cells *via* several surface proteins, such as the blood group binding adhesin (BabA) and the sialic acid binding adhesin (SabA). These surface proteins interact with carbohydrate determinants such as the host Lewis system antigens, again providing a mechanism by which *H. pylori* prevents its removal by peristalsis as well as gastric shedding (**Figure 2**) (46).

H. pylori also expresses Lewis system antigens within the LPS, that is thought to represent a form of molecular mimicry which subverts the host immune response. Indeed, there is also evidence suggesting the expression of Lewis determinants is involved in *H. pylori* interacting with the DC calcium dependent (C-type) lectin DC-SIGN (**Table 1**) (91). Upon phagocytosis by an innate immune cell, *H. pylori* can also avoid destruction by interfering with phagosome maturation (**Figure 2**) (92). Another method of immune evasion used by *H. pylori* involves the interaction with DC (**Figure 1**). While *H. pylori* inhabits a unique niche in the stomach where few cells have access, there has been strong evidence of DC interaction, with DC maturation and function heavily affected in mouse models (93). Furthermore, there is evidence of *H. pylori* having the capability to infect DC in cell culture (48). *H. pylori* is capable of modulating IL-12 secretion by DC affecting the maturation and differentiation of $CD4^+$ T cells and causing Th1 bias in mice (94). *In-vitro* studies have supported this, with *H. pylori* demonstrating the ability to modulate expression of IL-12 and TNF-α in cultured DC (95).

In addition to manipulating DC responses, other virulence factors including VacA (96) along with γ-glutamyltranspeptidase

(GGT) (97) and CagA (98) have been reported to interfere with the T cell response to *H. pylori*, causing a characteristic hyposensitivity of $CD4^+$ T cells and suppressing mucosal effector T cells (99). Notably, VacA has been found to have an influence on both DC cytokine expression and T cell differentiation, with VacA positive *H. pylori* strains showing the ability to supress IL-23 secretion by DC resulting in increased proliferation of Th17 cells. VacA plays additional roles in immune mediation including showing the ability to impair lysosomes and autophagosomes, a function with which VacA shares a synergistic effect with CagA, impairing the ability of both macrophages and gastric epithelial cells to remove internalised or invading bacteria. Specifically, *H. pylori* is able to inhibit the functions of lysosomal enzymes acid phosphatase, N-acetyl-β-d-glucosaminidase, and cathepsin D, prevent autolysosomal acidification, interfere with retrograde trafficking of mannose-6-phosphate receptors and inhibit autophagosome formation to promote intracellular survival of the bacterium (100).

It is likely *H. pylori* is highly resistant to destruction by phagocytes, although this has only been seen *in-vitro* (101). Even though *H. pylori* is frequently engulfed by phagocytes *in vitro*, it is proficient at neutralising and resisting the reactive oxygen and nitrate species released by monocytes and macrophages. This allows the bacteria to continue to replicate inside the phagosome, eventually inducing apoptosis of the host cell (49, 101). *H. pylori* possessing the *cag* pathogenicity island (*cag*PI) are even more resistant to phagocytosis than other strains (102), with isogenic mutants of *H. pylori* lacking *cag*PI far more readily taken up by phagocytes (49). The mechanism for this appears to be the ability of *H. pylori* to activate the reverse transsulfuration pathway to induce cystathionine γ-lyase (CTH) in host macrophages, promoting bacterial growth and enhancing bacterial survival in macrophages. *H. pylori* does this *via* the CagA-dependant induction of the PI3K/AKT1 pathway, the CagA-independent induction of the MTOR pathway and activation of SP1, increasing macrophage production of CTH (103) Furthermore, it has been shown that *H. pylori* is able to upregulate the metabolism of macrophage-associated polyamines, impairing M1 macrophage function (104).

Antibody Activity and Humoral Immune Evasion by *H. pylori*

The mechanisms of humoral immune evasion by *H. pylori* are somewhat less clear. Most immunocompetent individuals who are infected with *H. pylori* develop a specific IgG and IgA response, in many cases high antibody titres to the pathogen, however, this often is not enough to clear infection (53, 105). Furthermore, it has been reported that the type of antibody produced correlates with the outcome of infection, with patients experiencing gastritis and duodenal ulcers having greater titres of IgG, and patients suffering from gastric cancers often having greater titres of IgA (106). Other studies have suggested that a weaker overall antibody response is linked to the development of gastric cancers, and patients who had a weak but still detectable antibody response to *H. pylori* had a higher rate of gastric cancer than those with a stronger antibody response (107–109).

H. PYLORI LPS AND LEWIS ANTIGENS

H. pylori both interacts with host Lewis system antigens and displays Lewis antigens in its LPS. The expression of Lewis antigens by *H. pylori* is associated with immune evasion and a reduced immunogenicity of its LPS when compared to other bacteria (110, 111). The reduced immunogenicity of *H. pylori* LPS is related to its structure, much like that of other gram-negative bacterium, the *H. pylori* LPS contains 3 domains: a hydrophobic lipid A domain on the outer bacterial membrane, a core oligosaccharide and a repetitive oligosaccharide termed the O chain (111). The O chain of the *H. pylori* LPS is the main location where Lewis system antigens are displayed by the organism (112). The *H. pylori* O antigen is typically composed of a Gal-GlcNAc backbone chain which is divided into two types based on its linkage (**Figure 3**). Type 1 chains are composed of Galβ1-3GlcNAc, which forms the core saccharide for Le^a, sialyl-Le^a and Le^b. Type 2 chains are composed of Galβ1-4GlcNAc or LacNAc, which forms the core saccharide for Le^x, sialyl-Le^x and Le^y (63). In humans, Lewis system antigens like ABO blood group antigens are expressed in fluids and tissue including the gastric mucosa and endothelium. Le^a and Le^b are commonly expressed on various cell types from red blood cells to gastric epithelial cells, with Le^b in particular associated with various pathologies (113). In the human stomach, Le^a and Le^b are predominantly expressed on the surface and foveolar epithelia, whereas Le^x and Le^y are predominantly expressed in the mucus as well as the chief and parietal cells of the gastric glands. More specifically, non-secretory cells in the surface and foveolar epithelia express Le^a while Le^b and Le^y are expressed in secretory cells (114). Clinical isolates of *H. pylori* typically have a poly-LacNAc with several α-L-fucose residues forming internal Le^x determinants with terminal Le^x and Le^y determinants, while other strains have been described as displaying Le^a, Le^b and sialyl-Le^x as well as group A, B and H-1 determinants (111). As many as 90% of clinical isolates of *H. pylori* contain Lewis antigens in the O antigen portion of the LPS. This expression has been found to be relatively stable after subculturing using methods such as immunoblot. However, it is possible for cultured *H. pylori* strains to lose Lewis antigen expression over time (68, 115).

H. pylori LPS Structure, Phase Variation, and Diversity

As described above, the O antigen portion of the *H. pylori* LPS is associated with the expression of various Lewis antigens in addition to playing a role in the adhesion and immune evasion of the bacterium (116). The O antigen chain is comprised of a glucan group (saccharide composed of glucose), a D-glycerol-D-manno-heptan (DD-heptan) group and a highly conserved trisaccharide (trio) (115). Variability in the O antigen is derived from phase variation, whereby *H. pylori* uses an on/off system to regulate its biosynthetic genes, including the fucosyltransferase genes FutA, FutB, and FutC (117), allowing the bacterium to adjust the carbohydrate expression of the O

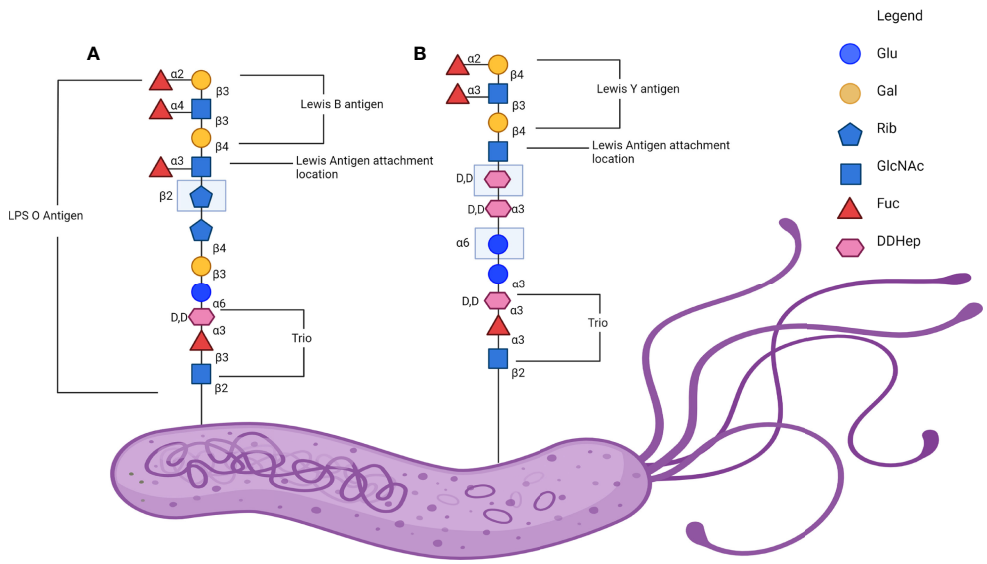

FIGURE 3 | Lewis antigen expression on *H. pylori* lipopolysaccharide (LPS) O antigen. **(A)** A representative linear glycan chain of the *H. pylori* SS1 strain O antigen with the Le^b in comparison to **(B)** a representative linear glycan chain of *H. pylori* 26695 and G27 O antigen with the Le^y antigen attached. Adapted from the established structure in Li et al., 2018. Note that the exact structure and the Lewis determinate expressed is variable and dependant on isolate (115). Created with BioRender.com.

antigen with the changing environment of the stomach and gastric mucosa (16). Additionally, phase variation of the *H. pylori* LPS allows for a greater range of phenotypes and gives *H. pylori* the ability to modify the expression of Lewis system antigens in its LPS. Additionally, it has been indicated that the *H. pylori* LPS induces lower biological responses when compared to other gram-negative organisms such as *E. coli* and *Salmonella* spp., with *in vivo* mouse and rabbit studies showing 500 to 1000 fold lower mitogenic and pyrogenic responses (118).

The genes encoding the glycotransferases responsible for the construction of this LPS vary between different regional strains, with the common European strain of *H. pylori* G27 possessing the trisaccharide fucosyltransferase (HP0102), heptan transferase (HP1283) and GlcNAc transferase (HP1578), the last of which is responsible for initiating synthesis of Lewis system antigens onto a heptan motif (111). In addition to this, a comparison between the European model strain G27 and East Asian strains found that the East Asian strains lacked the genes encoding for heptan transferase and GlcNAc transferase (119). Furthermore, East Asian strains instead express additional copies of other genes, HP1105 and JHP0562, which may act as GlcNAc transferases as well as Gal transferase in place of HP1578 (119). This was identified as an area of interest due to the higher rates of gastric cancer in East Asia and the potential to further characterise the role of the *H. pylori* LPS heptan in pathogenesis (119). **Figure 3** illustrates an abbreviated version of the established structure of the O antigen structure from the mouse-adapted *H. pylori* SS1 strain including the trio, attachment site and the Lewis antigenic determinants.

H. pylori LPS Structural Diversity in Infection and Immune Evasion

The *H. pylori* LPS is generally considered less immunogenic in comparison to enterobacterial LPS, with early studies showing significant reductions in pyrogenicity, mitogenicity and toxicity, as well as a reduced cytokine and chemokine response (118, 120, 121). Previous studies have shown that synthesised partial *H. pylori* LPS structures, specifically lipid A compounds and Kdo-lipid A compounds, can modulate cytokine production by host cells. All lipid A and Kdo-lipid A *H. pylori* LPS structures synthesised either failed to induce, or induced very low levels of IL-1β, IL-6 and IL-8, and conversely stimulated high levels of cytokines IL-12 and IL-18 in heparinised human peripheral whole blood (122, 123). IL-12 induction by *H. pylori* is generally linked to MyD88 expression in macrophages (124). Furthermore, *H. pylori* modifies the lipid A portion of the LPS by *via* dephosphorylation of the 1- and 4-'positions of the lipid A backbone. Mutations to the lpxE/F machinery required for this modification have shown an increased susceptibility of *H. pylori* to the antimicrobial peptide polymyxin B, as well as reducing the ability of *H. pylori* to colonise mice (125). Knockout studies on *H. pylori* genes *HP0044* and *HP1275* demonstrated the production of a truncated *H. pylori* LPS missing fucose residues found in both the trio and Lewis antigen portions of the *H. pylori* LPS O antigen, resulting in the loss of a significant portion of the *H. pylori* LPS. This in turn affected the growth of the bacterium, increased its susceptibility to both the detergent SDS, promoted bacterial autoaggregation, increased surface hydrophobicity and affected bacterial virulence and OMV protein sorting (126). Notably, phase variation of *H. pylori*

fucosyltransferases, and consequently the glycosylation pattern of the LPS has previously been identified to occur in high frequencies, with *in-vitro* studies demonstrating the expression of Le^x can vary at a frequency of 0.2-0.5% resulting in differing LPS variants in the same population. Variation of Lewis antigen expression, particularly between Le^x and Le^y has been suggested to be influenced by relative pH in liquid medium. The function for this has not been fully identified, but is hypothesised to aid in bacterial persistence (127). On a molecular level the variation in *H. pylori* fucosylation has previously been attributed to slipped-strand mispairing as a result of differing numbers of polyC repeats in fucosyltransferase genes *futA*, *futB* and *futC*. However, a recent study has described a role for small RNAs (sRNA) in the regulation of the *H. pylori* LPS biosynthesis. The sRNA RepG modulate *HP0102* and *TlpB*, providing post-transcriptional regulation to LPS biosynthesis potentially indicating further means by which *H. pylori* is able to adapt to host immune response (128).

ROLE OF *H. PYLORI* ADHESINS IN IMMUNE EVASION

In addition to *H. pylori* commonly expressing Lewis determinants in its LPS, *H. pylori* also binds to host Lewis determinants, assisting in the attachment of the bacterium to the gastric epithelium (129, 130). Binding is facilitated by a group of outer membrane proteins, including BabA and SabA.

BabA

H. pylori binds to the various Lewis system antigens expressed on the surface of gastric epithelial cells, including Le^b and sialyl-Le^x (131). Chronic inflammation also leads to upregulation of Le^x and Le^y in the host, further enhancing bacterial colonisation (131). Furthermore, *H. pylori* has a range of adhesive proteins that have been identified and examined. The first identified was BabA, a protein that commonly binds the Le^b determinant as well as mucin proteins and the H1 blood group antigen (132). Specifically, BabA binds the lacto series of glycans containing a terminal fucose molecule with an α1,2 linkage attached to a Galβ1-3GlcNAc core (133). This includes H1 blood group antigen as well as other H neoglycoconjugates and Le^b. However, BabA binds to Le^b with as much as a two-fold increase in affinity in comparison to H neoglycoconjugates (134). The BabA encoding gene(s) can be found in three separate loci on the *H. pylori* genome with the binding pattern of the protein differing based on the specific loci expressed (135). For example, strains containing locus A BabA (BabA2) bind the classically associated Le^b whereas strains with locus B BabA (BabA1) do not bind to Le^b (136). Furthermore, some strains may contain more than one BabA encoding gene allowing expression of proteins with varying binding characteristics (137). BabA in general is a highly polymorphic protein with variable expression, which may be lost during laboratory cultivation. Additionally about one quarter of strains isolated from chronically infected hosts tend to lose BabA expression (69, 138). This suggests that BabA is a specific adhesin that is advantageous in the colonisation of a human host that is unnecessary on solid media (137). There has been evidence of numerous binding molecules for BabA in addition to the Le^b molecules expressed by gastric epithelia. Several salivary proteins have also been identified to interact with BabA, such as the mucin MUC5B, the agglutinin glycoprotein-340 and the proline-rich glycoprotein containing the Fucα1-2Galβ motif. In addition to this, fucose-containing oligosaccharides present in secretory IgA also play a role in binding BabA, however this is not universal to all secretory IgA (132). It has been observed that BabA presence in a *H. pylori* strain is associated with expression of VacA, CagA and OipA among other common but variable virulence factors, particularly in the outcome of gastric metaplasia. An *in-vitro* study found that Le^b-positive AGS cells expressed increased levels of mRNA for the cytokines CCL5 and IL-8 as well as precancer related factors CDX2 and MUC2 in the presence of wild type *H. pylori*, however this was not the case for *H. pylori* mutants with either BabA genes or TIVSS deleted (139).

SabA

SabA is an additional adhesion molecule associated with the binding of Lewis system determinants by *H. pylori.* More specifically, SabA binds sialylated molecules such as sialyl-Le^x and some gangliosides characterised by Neu5Acα3-neolactohexaosylceramide and Neu5Acα3-neolactooctaosylceramide molecules (58). The gastric inflammation caused by *H. pylori* infection is essential for changes in glycosylation patterns within the gastric mucosa, promoting the expression of sialyl-Le^x as well as sialyl-Le^a, which in turn increases the adhesive properties of SabA (140). Similar to BabA, the expression of SabA is highly variable and is often subject to phase variation. It has been suggested that *H. pylori* may have multiple means of modulating the expression of SabA, with one such method being an acid-responsive ArsRS two-component signal transduction system, and an alternative involving the slipped-strand mispairing of SabA alleles during chromosomal replication in various *H. pylori* subpopulations (141). Additionally, SabA is commonly subject to homologous recombination and gene conversion due to changing environmental pressures (142). Deactivation of the SabA encoding gene may further assist in bacterial escape as cytotoxic activity by neutrophils is in part triggered by SabA binding to gangliosides. Neutrophil action has been shown to be defective against SabA deleted *H. pylori* cells (58).

OipA

OipA is also a member of the Hop family of outer membrane proteins possessed by *H. pylori.* There is currently no available crystal structure for OipA, limiting detailed studies of its binding (143). OipA is known to be closely associated with the *cag* PAI and CagA, with the *oipA* locus approximately 100 kb from the *cag* PAI. OipA is regulated by slipped-strand mispairing and displays on/off states which are closely associated with the expression of CagA. Alleles of *oipA* have been demonstrated in up to 96% of *cag* PAI positive *H. pylori* strains, solidifying the relationship of the two virulence factors (144). With the exception of CagA, OipA is typically independent of other *H. pylori* virulence factors. OipA is associated with the induction of

IL-8 from host epithelial cells, inhibition of apoptosis and enhanced adhesion to gastric cells *in vitro* (144). Induction of IL-8 and its subsequent role in inducing gastritis has been associated with a synergistic effect from *H. pylori* strains possessing both the *cag* PAI and a functional *oipA* gene (145). In contrast *oipA* "off" strains can down-regulate anti-apoptotic processes in AGS cells, more regularly inducing apoptosis on infection than *oipA* "on" strains *in-vitro* (146).

CONCLUSIONS

H. pylori is a very successful global pathogen and has adopted a range of adaptions to evade the innate immune system. These mechanisms include both active systems, such as the neutralisation of reactive oxygen and nitrogen species released by macrophages, the modulation of cytokine secretion and the maturation of dendritic cells, and more passive systems such as the variability and the uniquely low immunogenicity of its LPS (15, 53). In addition, the expression of Lewis antigens in the LPS of *H. pylori* gives the bacterium the ability to mimic host antigens and thereby hide from the immune system (147). Notably, several of the immune evasion mechanisms *H. pylori* employs are yet to be fully explained. For example, knowledge of *H. pylori* activation and modulation of innate immunity outside of interactions with dendritic cells and DC-SIGN is surprisingly limited. It is also known that outer membrane proteins such as BabA, SabA and OipA play a role in the induction of inflammatory cytokines, although the molecular mechanism is still unclear (44, 144). Further study into ways to circumvent the methods *H. pylori* uses for immune evasion could allow for improved treatment and vaccination options. Additionally, blocking the activity of *H. pylori* adhesins to prevent attachment in the gastric mucosal gel layer and to epithelial cells has potential for new treatment options in an environment of increased antibiotic resistance.

AUTHOR CONTRIBUTIONS

DS, prepared figures and wrote the manuscript; AG, critically reviewed and commented on the manuscript; AW, critically reviewed and commented on the manuscript; PR, critically reviewed and commented on the manuscript. All authors conceived and discussed the topic of the review. All authors read and approved the final manuscript.

FUNDING

DS is supported by a Research Training Program Stipend Scholarship from the Australian Government, Department of Education and Training.

REFERENCES

1. Venerito M, Link A, Rokkas T, Malfertheiner P. Review: Gastric Cancer—Clinical Aspects. *Helicobacter* (2019) 24(S1):e12643. doi: 10.1111/hel.12643
2. Mungazi SG, Chihaka OB, Muguti GI. Prevalence of Helicobacter Pylori in Asymptomatic Patients at Surgical Outpatient Department: Harare Hospitals. *Ann Med Surg (Lond)* (2018) 35:153–7. doi: 10.1016/j.amsu.2018.09.040
3. Lim SH, Kwon J-W, Kim N, Kim GH, Kang JM, Park MJ, et al. Prevalence and Risk Factors of Helicobacter Pylori Infection in Korea: Nationwide Multicenter Study Over 13 Years. *BMC Gastroenterol* (2013) 13:104. doi: 10.1186/1471-230X-13-104
4. Dunne C, Dolan B, Clyne M. Factors That Mediate Colonization of the Human Stomach by Helicobacter Pylori. *World J Gastroenterol* (2014) 20 (19):5610–24. doi: 10.3748/wjg.v20.i19.5610
5. Malfertheiner P, Megraud F, O'Morain CA, Gisbert JP, Kuipers EJ, Axon AT, et al. Management of Helicobacter Pylori Infection-the Maastricht V/Florence Consensus Report. *Gut* (2017) 66(1):6–30. doi: 10.1136/gutjnl-2016-312288
6. Tshibangu-Kabamba E, Yamaoka Y. Helicobacter Pylori Infection and Antibiotic Resistance - From Biology to Clinical Implications. *Nat Rev Gastroenterol Hepatol* (2021) 18(9):613–29. doi: 10.1038/s41575-021-00449-x
7. Roszczenko-Jasińska P, Wojtyś MI, Jagusztyn-Krynicka EK. Helicobacter Pylori Treatment in the Post-Antibiotics Era-Searching for New Drug Targets. *Appl Microbiol Biotechnol* (2020) 104(23):9891–905. doi: 10.1007/s00253-020-10945-w
8. Testerman TL, Morris J. Beyond the Stomach: An Updated View of Helicobacter Pylori Pathogenesis, Diagnosis, and Treatment. *World J Gastroenterol* (2014) 20(36):12781–808. doi: 10.3748/wjg.v20.i36.12781
9. Parkin DM, Bray F, Ferlay J, Pisani P. Global Cancer Statistics, 2002. *CA Cancer J Clin* (2005) 55(2):74–108. doi: 10.3322/canjclin.55.2.74
10. Kusters JG, van Vliet AHM, Kuipers EJ. Pathogenesis of Helicobacter Pylori Infection. *Clin Microbiol Rev* (2006) 19(3):449–90. doi: 10.1128/CMR.00054-05
11. Van den Brink GR, Tytgat KM, van der Hulst RW, van der Loos CM, Einerhand AW, Büller HA, et al. H Pylori Colocalises With MUC5AC in the Human Stomach. *Gut* (2000) 46(5):601–7. doi: 10.1136/gut.46.5.601
12. Doohan D, Rezkitha YAA, Waskito LA, Yamaoka Y, Miftahussurur M. Helicobacter Pylori BabA-SabA Key Roles in the Adherence Phase: The Synergic Mechanism for Successful Colonization and Disease Development. *Toxins (Basel)* (2021) 13(7):485. doi: 10.3390/toxins13070485
13. Tanaka H, Yoshida M, Nishiumi S, Ohnishi N, Kobayashi K, Yamamoto K, et al. The CagA Protein of Helicobacter Pylori Suppresses the Functions of Dendritic Cell in Mice. *Arch Biochem Biophys* (2010) 498(1):35–42. doi: 10.1016/j.abb.2010.03.021
14. Kim JM, Kim JS, Yoo DY, Ko SH, Kim N, Kim H, et al. Stimulation of Dendritic Cells With Helicobacter Pylori Vacuolating Cytotoxin Negatively Regulates Their Maturation *via* the Restoration of E2F1. *Clin Exp Immunol* (2011) 166(1):34–45. doi: 10.1111/j.1365-2249.2011.04447.x
15. Pece S, Giuliani G, Di Leo A, Fumarola D, Antonaci S, Jirillo E. Role of Lipopolysaccharide and Related Cytokines in Helicobacter Pylori Infection. *Recenti Prog Med* (1997) 88(5):237–41.
16. Appelmelk BJ, Martino MC, Veenhof E, Monteiro MA, Maaskant JJ, Negrini R, et al. Phase Variation in H Type I and Lewis a Epitopes of Helicobacter Pylori Lipopolysaccharide. *Infect Immun* (2000) 68(10):5928–32. doi: 10.1128/iai.68.10.5928-5932.2000
17. Perepelov AV, Senchenkova SN, Knirel YA. Variations in the Expression of Terminal Oligosaccharide Units and Glycosylation of Poly(N-Acetyllactosamine) Chain in the Helicobacter Pylori Lipopolysaccharide Upon Colonization of Rhesus Macaques. *Biochem (Moscow)* (2020) 85 (2):234–40. doi: 10.1134/S0006297920020108
18. Alberts B, Johnson A, Lewis J, Raff M, Roberts K, Walter P. Innate Immunity. In: *Molecular Biology of the Cell*. New York: Garland Science (2002).

19. Muñoz-Carrillo JL, Rodríguez F, Gutierrez O, Moreno Garcìa M, Cordero J. Physiology and Pathology of Innate Immune Response Against Pathogens. In: Rezaei N, editor. *Physiology and Pathology of Immunology*. London: IntechOpen. (2017) p. 99–134. doi: 10.5772/intechopen.70556
20. Pasupuleti M, Schmidtchen A, Malmsten M. Antimicrobial Peptides: Key Components of the Innate Immune System. *Crit Rev Biotechnol* (2012) 32 (2):143–71. doi: 10.3109/07388551.2011.594423
21. Maverakis E, Kim K, Shimoda M, Gershwin ME, Patel F, Wilken R, et al. Glycans in the Immune System and The Altered Glycan Theory of Autoimmunity: A Critical Review. *J Autoimmun* (2015) 57:1–13. doi: 10.1016/j.jaut.2014.12.002
22. Akira S, Uematsu S, Takeuchi O. Pathogen Recognition and Innate Immunity. *Cell* (2006) 124(4):783–801. doi: 10.1016/j.cell.2006.02.015
23. Medzhitov R. Recognition of Microorganisms and Activation of the Immune Response. *Nature* (2007) 449(7164):819–26. doi: 10.1038/nature06246
24. Diacovich L, Gorvel J-P. Bacterial Manipulation of Innate Immunity to Promote Infection. *Nat Rev Microbiol* (2010) 8(2):117–28. doi: 10.1038/nrmicro2295
25. Fritz JH, Ferrero RL, Philpott DJ, Girardin SE. Nod-Like Proteins in Immunity, Inflammation and Disease. *Nat Immunol* (2006) 7(12):1250–7. doi: 10.1038/ni1412
26. Guo H, Callaway JB, Ting JPY. Inflammasomes: Mechanism of Action, Role in Disease, and Therapeutics. *Nat Med* (2015) 21(7):677–87. doi: 10.1038/nm.3893
27. Luo Y, Zheng SG. Hall of Fame Among Pro-Inflammatory Cytokines: Interleukin-6 Gene and Its Transcriptional Regulation Mechanisms. *Front Immunol* (2016) 7:604(604). doi: 10.3389/fimmu.2016.00604
28. Tran LS, Chonwerawong M, Ferrero RL. Regulation and Functions of Inflammasome-Mediated Cytokines in Helicobacter Pylori Infection. *Microbes Infect* (2017) 19(9-10):449–58. doi: 10.1016/j.micinf.2017.06.005
29. Ramachandra L, Simmons D, Harding CV. MHC Molecules and Microbial Antigen Processing in Phagosomes. *Curr Opin Immunol* (2009) 21(1):98–104. doi: 10.1016/j.coi.2009.01.001
30. Salcedo SP, Marchesini MI, Lelouard H, Fugier E, Jolly G, Balor S, et al. Brucella Control of Dendritic Cell Maturation Is Dependent on the TIR-Containing Protein Btp1. *PloS Pathog* (2008) 4(2):e21–e. doi: 10.1371/journal.ppat.0040021
31. Viala J, Chaput C, Boneca IG, Cardona A, Girardin SE, Moran AP, et al. Nod1 Responds to Peptidoglycan Delivered by the Helicobacter Pylori Cag Pathogenicity Island. *Nat Immunol* (2004) 5(11):1166–74. doi: 10.1038/ni1131
32. Crabtree JE, Kersulyte D, Li SD, Lindley IJ, Berg DE. Modulation of Helicobacter Pylori Induced Interleukin-8 Synthesis in Gastric Epithelial Cells Mediated by Cag PAI Encoded VirD4 Homologue. *J Clin Pathol* (1999) 52(9):653–7. doi: 10.1136/jcp.52.9.653
33. Backert S, Haas R, Gerhard M, Naumann M. The Helicobacter Pylori Type IV Secretion System Encoded by the Cag Pathogenicity Island: Architecture, Function, and Signaling. In: S Backert and E Grohmann, editors. *Type IV Secretion in Gram-Negative and Gram-Positive Bacteria*. Cham: Springer International Publishing (2017). p. 187–220.
34. Tafreshi M, Guan J, Gorrell RJ, Chew N, Xin Y, Deswaerte V, et al. Helicobacter Pylori Type IV Secretion System and Its Adhesin Subunit, CagL, Mediate Potent Inflammatory Responses in Primary Human Endothelial Cells. *Front Cell Infect Microbiol* (2018) 8:22. doi: 10.3389/fcimb.2018.00022
35. Huang Y, Wang Q-l, Cheng D-d, Xu W-t, Lu N-h. Adhesion and Invasion of Gastric Mucosa Epithelial Cells by Helicobacter Pylori. *Front Cell Infect Microbiol* (2016) 6:159(159). doi: 10.3389/fcimb.2016.00159
36. Grubman A, Kaparakis M, Viala J, Allison C, Badea L, Karrar A, et al. The Innate Immune Molecule, NOD1, Regulates Direct Killing of Helicobacter Pylori by Antimicrobial Peptides. *Cell Microbiol* (2010) 12(5):626–39. doi: 10.1111/j.1462-5822.2009.01421.x
37. Lamarque D, Moran AP, Szepes Z, Delchier JC, Whittle BJ. Cytotoxicity Associated With Induction of Nitric Oxide Synthase in Rat Duodenal Epithelial Cells *In Vivo* by Lipopolysaccharide of Helicobacter Pylori: Inhibition by Superoxide Dismutase. *Br J Pharmacol* (2000) 130(7):1531–8. doi: 10.1038/sj.bjp.0703468
38. O'Keeffe J, Moran AP. Conventional, Regulatory, and Unconventional T Cells in the Immunologic Response to Helicobacter Pylori. *Helicobacter* (2008) 13(1):1–19. doi: 10.1111/j.1523-5378.2008.00559.x
39. Kaneko T, Ota H, Hayama M, Akamatsu T, Katsuyama T. Helicobacter Pylori Infection Produces Expression of a Secretory Component in Gastric Mucous Cells. *Virchows Archiv* (2000) 437(5):514–20. doi: 10.1007/s004280000285
40. Gorrell RJ, Wijburg OLC, Pedersen JS, Walduck AK, Kwok T, Strugnell RA, et al. Contribution of Secretory Antibodies to Intestinal Mucosal Immunity Against Helicobacter Pylori. *Infect Immun* (2013) 81(10):3880–93. doi: 10.1128/IAI.01424-12
41. Moyat M, Velin D. Immune Responses to Helicobacter Pylori Infection. *World J Gastroenterol* (2014) 20(19):5583–93. doi: 10.3748/wjg.v20.i19.5583
42. Blanchard TG, Nedrud JG, Czinn SJ. Local and Systemic Antibody Responses in Humans With Helicobacter Pylori Infection. *Can J Gastroenterol* (1999) 13(7):591–4. doi: 10.1155/1999/142457
43. van Kooyk Y, Geijtenbeek TB. DC-SIGN: Escape Mechanism for Pathogens. *Nat Rev Immunol* (2003) 3(9):697–709. doi: 10.1038/nri1182
44. Sugimoto M, Ohno T, Graham DY, Yamaoka Y. Helicobacter Pylori Outer Membrane Proteins on Gastric Mucosal Interleukin 6 and 11 Expression in Mongolian Gerbils. *J Gastroenterol Hepatol* (2011) 26(11):1677–84. doi: 10.1111/j.1440-1746.2011.06817.x
45. Lamb A, Chen L-F. Role of the Helicobacter Pylori-Induced Inflammatory Response in the Development of Gastric Cancer. *J Cell Biochem* (2013) 114 (3):491–7. doi: 10.1002/jcb.24389
46. Yamaoka Y. Roles of Helicobacter Pylori BabA in Gastroduodenal Pathogenesis. *World J Gastroenterol* (2008) 14(27):4265–72. doi: 10.3748/wjg.14.4265
47. Semper RP, Mejías-Luque R, Groß C, Anderl F, Müller A, Vieth M, et al. Helicobacter Pylori–Induced IL-1β Secretion in Innate Immune Cells Is Regulated by the NLRP3 Inflammasome and Requires the Cag Pathogenicity Island. *J Immunol* (2014) 193(7):3566–76. doi: 10.4049/jimmunol.1400362
48. Mitchell P, Germain C, Fiori PL, Khamri W, Foster GR, Ghosh S, et al. Chronic Exposure to Helicobacter Pylori Impairs Dendritic Cell Function and Inhibits Th1 Development. *Infect Immun* (2007) 75(2):810–9. doi: 10.1128/iai.00228-06
49. Ramarao N, Meyer TF. Helicobacter Pylori Resists Phagocytosis by Macrophages: Quantitative Assessment by Confocal Microscopy and Fluorescence-Activated Cell Sorting. *Infect Immun* (2001) 69(4):2604–11. doi: 10.1128/IAI.69.4.2604-2611.2001
50. Ottemann KM, Lowenthal AC. Helicobacter Pylori Uses Motility for Initial Colonization and to Attain Robust Infection. *Infect Immun* (2002) 70 (4):1984–90. doi: 10.1128/iai.70.4.1984-1990.2002
51. Tsuda M, Karita M, Morshed MG, Okita K, Nakazawa T. A Urease-Negative Mutant of Helicobacter Pylori Constructed by Allelic Exchange Mutagenesis Lacks the Ability to Colonize the Nude Mouse Stomach. *Infect Immun* (1994) 62(8):3586–9. doi: 10.1128/iai.62.8.3586-3589.1994
52. Fan X, Gunasena H, Cheng Z, Espejo R, Crowe SE, Ernst PB, et al. Helicobacter Pylori Urease Binds to Class II MHC on Gastric Epithelial Cells and Induces Their Apoptosis. *J Immunol* (2000) 165(4):1918–24. doi: 10.4049/jimmunol.165.4.1918
53. Lina TT, Alzahrani S, Gonzalez J, Pinchuk IV, Beswick EJ, Reyes VE. Immune Evasion Strategies Used by Helicobacter Pylori. *World J Gastroenterol* (2014) 20(36):12753–66. doi: 10.3748/wjg.v20.i36.12753
54. Junaid M, Linn AK, Javadi MB, Al-Gubare S, Ali N, Katzenmeier G. Vacuolating Cytotoxin A (VacA) - A Multi-Talented Pore-Forming Toxin From Helicobacter Pylori. *Toxicon* (2016) 118:27–35. doi: 10.1016/j.toxicon.2016.04.037
55. Guo Y, Feinberg H, Conroy E, Mitchell DA, Alvarez R, Blixt O, et al. Structural Basis for Distinct Ligand-Binding and Targeting Properties of the Receptors DC-SIGN and DC-SIGNR. *Nat Struct Mol Biol* (2004) 11(7):591–8. doi: 10.1038/nsmb784
56. D'Elios MM, Amedei A, Cappon A, Del Prete G, de Bernard M. The Neutrophil-Activating Protein of Helicobacter Pylori (HP-NAP) as an Immune Modulating Agent. *FEMS Immunol Med Microbiol* (2007) 50 (2):157–64. doi: 10.1111/j.1574-695X.2007.00258.x
57. Amedei A, Cappon A, Codolo G, Cabrelle A, Polenghi A, Benagiano M, et al. The Neutrophil-Activating Protein of Helicobacter Pylori Promotes Th1 Immune Responses. *J Clin Invest* (2006) 116(4):1092–101. doi: 10.1172/jci27177
58. Benktander J, Barone A, Johansson MM, Teneberg S. Helicobacter Pylori SabA Binding Gangliosides of Human Stomach. *Virulence* (2018) 9(1):738–51. doi: 10.1080/21505594.2018.1440171

59. Blaser N, Backert S, Pachathundikandi SK. Immune Cell Signaling by Helicobacter Pylori: Impact on Gastric Pathology. *Adv Exp Med Biol* (2019) 1149:77–106. doi: 10.1007/5584_2019_360
60. Ren Z, Pang G, Clancy R, Li LC, Lee CS, Batey R, et al. Shift of the Gastric T-Cell Response in Gastric Carcinoma. *J Gastroenterol Hepatol* (2001) 16 (2):142–8. doi: 10.1046/j.1440-1746.2001.02385.x
61. Wang S-K, Zhu H-F, He B-S, Zhang Z-Y, Chen Z-T, Wang Z-Z, et al. CagA+ H Pylori Infection is Associated With Polarization of T Helper Cell Immune Responses in Gastric Carcinogenesis. *World J Gastroenterol* (2007) 13 (21):2923–31. doi: 10.3748/wjg.v13.i21.2923
62. Olivera-Severo D, Uberti AF, Marques MS, Pinto MT, Gomez-Lazaro M, Figueiredo C, et al. A New Role for Helicobacter Pylori Urease: Contributions to Angiogenesis. *Front Microbiol* (2017) 8:1883(1883). doi: 10.3389/fmicb.2017.01883
63. Sheu B-S, Yang H-B, Yeh Y-C, Wu J-J. Helicobacter Pylori Colonization of the Human Gastric Epithelium: A Bug's First Step is a Novel Target for Us. *J Gastroenterol Hepatol* (2010) 25(1):26–32. doi: 10.1111/j.1440-1746.2009.06141.x
64. Sanders CJ, Yu Y, Moore DA3rd, Williams IR, Gewirtz AT. Humoral Immune Response to Flagellin Requires T Cells and Activation of Innate Immunity. *J Immunol* (2006) 177(5):2810–8. doi: 10.4049/jimmunol.177.5.2810
65. Forstnerič V, Ivičak-Kocjan K, Plaper T, Jerala R, Benčina M. The Role of the C-Terminal D0 Domain of Flagellin in Activation of Toll Like Receptor 5. *PloS Pathog* (2017) 13(8):e1006574–e. doi: 10.1371/journal.ppat.1006574
66. Smith SM. Role of Toll-Like Receptors in Helicobacter Pylori Infection and Immunity. *World J Gastrointest Pathophysiol* (2014) 5(3):133–46. doi: 10.4291/wjgp.v5.i3.133
67. Tegtmeyer N, Neddermann M, Lind J, Pachathundikandi SK, Sharafutdinov I, Gutiérrez-Escobar AJ, et al. Toll-Like Receptor 5 Activation by the CagY Repeat Domains of Helicobacter Pylori. *Cell Rep* (2020) 32(11):108159. doi: 10.1016/j.celrep.2020.108159
68. Nilsson C, Skoglund A, Moran AP, Annuk H, Engstrand L, Normark S. Lipopolysaccharide Diversity Evolving in Helicobacter Pylori Communities Through Genetic Modifications in Fucosyltransferases. *PloS One* (2008) 3 (11):e3811–e. doi: 10.1371/journal.pone.0003811
69. Solnick JV, Hansen LM, Salama NR, Boonjakuakul JK, Syvanen M. Modification of Helicobacter Pylori Outer Membrane Protein Expression During Experimental Infection of Rhesus Macaques. *Proc Natl Acad Sci USA* (2004) 101(7):2106–11. doi: 10.1073/pnas.0308573100
70. Sharndama HC, Mba IE. Helicobacter Pylori: An Up-to-Date Overview on the Virulence and Pathogenesis Mechanisms. *Braz J Microbiol* (2022) 53 (1):33–50. doi: 10.1007/s42770-021-00675-0
71. Raghwan, Chowdhury R. Host Cell Contact Induces Fur-Dependent Expression of Virulence Factors CagA and VacA in Helicobacter Pylori. *Helicobacter* (2014) 19(1):17–25. doi: 10.1111/hel.12087
72. Kwok T, Zabler D, Urman S, Rohde M, Hartig R, Wessler S, et al. Helicobacter Exploits Integrin for Type IV Secretion and Kinase Activation. *Nature* (2007) 449(7164):862–6. doi: 10.1038/nature06187
73. Prashar A, Capurro MI, Jones NL. Under the Radar: Strategies Used by Helicobacter Pylori to Evade Host Responses. *Annu Rev Physiol* (2022) 84 (1):485–506. doi: 10.1146/annurev-physiol-061121-035930
74. Lamb A, Yang X-D, Tsang Y-HN, Li J-D, Higashi H, Hatakeyama M, et al. Helicobacter Pylori CagA Activates NF-kappaB by Targeting TAK1 for TRAF6-Mediated Lys 63 Ubiquitination. *EMBO Rep* (2009) 10(11):1242–9. doi: 10.1038/embor.2009.210
75. Hatakeyama M. Structure and Function of Helicobacter Pylori CagA, the First-Identified Bacterial Protein Involved in Human Cancer. *Proc Jpn Acad Ser B Phys Biol Sci* (2017) 93(4):196–219. doi: 10.2183/pjab.93.013
76. Baj J, Forma A, Sitarz M, Portincasa P, Garruti G, Krasowska D, et al. Helicobacter Pylori Virulence Factors-Mechanisms of Bacterial Pathogenicity in the Gastric Microenvironment. *Cells* (2020) 10(1):27. doi: 10.3390/cells10010027
77. Backert S, Naumann M. What a Disorder: Proinflammatory Signaling Pathways Induced by Helicobacter Pylori. *Trends Microbiol* (2010) 18 (11):479–86. doi: 10.1016/j.tim.2010.08.003
78. Imai S, Ooki T, Murata-Kamiya N, Komura D, Tahmina K, Wu W, et al. Helicobacter Pylori CagA Elicits BRCAness to Induce Genome Instability That may Underlie Bacterial Gastric Carcinogenesis. *Cell Host Microbe* (2021) 29(6):941–58.e10. doi: 10.1016/j.chom.2021.04.006
79. Li N, Feng Y, Hu Y, He C, Xie C, Ouyang Y, et al. Helicobacter Pylori CagA Promotes Epithelial Mesenchymal Transition in Gastric Carcinogenesis *via* Triggering Oncogenic YAP Pathway. *J Exp Clin Cancer Res* (2018) 37(1):280. doi: 10.1186/s13046-018-0962-5
80. Cheok YY, Lee CYQ, Cheong HC, Vadivelu J, Looi CY, Abdullah S, et al. An Overview of Helicobacter Pylori Survival Tactics in the Hostile Human Stomach Environment. *Microorganisms* (2021) 9(12):2502. doi: 10.3390/microorganisms9122502
81. Yamaoka Y, Kwon DH, Graham DY. A M(r) 34,000 Proinflammatory Outer Membrane Protein (Oipa) of Helicobacter Pylori. *Proc Natl Acad Sci USA* (2000) 97(13):7533–8. doi: 10.1073/pnas.130079797
82. Chmiela M, Walczak N, Rudnicka K. Helicobacter Pylori Outer Membrane Vesicles Involvement in the Infection Development and Helicobacter Pylori-Related Diseases. *J BioMed Sci* (2018) 25(1):78–. doi: 10.1186/s12929-018-0480-y
83. Zhang H, Zhang Y, Song Z, Li R, Ruan H, Liu Q, et al. sncRNAs Packaged by Helicobacter Pylori Outer Membrane Vesicles Attenuate IL-8 Secretion in Human Cells. *Int J Med Microbiol* (2020) 310(1):151356. doi: 10.1016/j.ijmm.2019.151356
84. Pachathundikandi SK, Backert S. Helicobacter Pylori Controls NLRP3 Expression by Regulating hsa-miR-223-3p and IL-10 in Cultured and Primary Human Immune Cells. *Innate Immun* (2017) 24(1):11–23. doi: 10.1177/1753425917738043
85. Pachathundikandi SK, Blaser N, Bruns H, Backert S. Helicobacter Pylori Avoids the Critical Activation of NLRP3 Inflammasome-Mediated Production of Oncogenic Mature IL-1β in Human Immune Cells. *Cancers (Basel)* (2020) 12(4):803. doi: 10.3390/cancers12040803
86. Altobelli A, Bauer M, Velez K, Cover TL, Müller A. Helicobacter Pylori VacA Targets Myeloid Cells in the Gastric Lamina Propria To Promote Peripherally Induced Regulatory T-Cell Differentiation and Persistent Infection. *mBio* (2019) 10(2):e00261–19, 1–13. doi: 10.1128/mBio.00261-19
87. Araújo GRL, Marques HS, Santos MLC, da Silva FAF, da Brito BB, Correa Santos GL, et al. Helicobacter Pylori Infection: How Does Age Influence the Inflammatory Pattern? *World J Gastroenterol* (2022) 28(4):402–11. doi: 10.3748/wjg.v28.i4.402
88. Freire de Melo F, Rocha AM, Rocha GA, Pedroso SH, de Assis Batista S, Fonseca de Castro LP, et al. A Regulatory Instead of an IL-17 T Response Predominates in Helicobacter Pylori-Associated Gastritis in Children. *Microbes Infect* (2012) 14(4):341–7. doi: 10.1016/j.micinf.2011.11.008
89. de Bernard M, D'Elios MM. The Immune Modulating Activity of the Helicobacter Pylori HP-NAP: Friend or Foe? *Toxicon* (2010) 56(7):1186–92. doi: 10.1016/j.toxicon.2009.09.020
90. Lindén S, Nordman H, Hedenbro J, Hurtig M, Borén T, Carlstedt I. Strain- and Blood Group-Dependent Binding of Helicobacter Pylori to Human Gastric MUC5AC Glycoforms. *Gastroenterology* (2002) 123(6):1923–30. doi: 10.1053/gast.2002.37076
91. Miszczyk E, Rudnicka K, Moran AP, Fol M, Kowalewicz-Kulbat M, Druszczyńska M, et al. Interaction of Helicobacter Pylori With C-Type Lectin Dendritic Cell-Specific ICAM Grabbing Nonintegrin. *J BioMed Biotechnol* (2012) 2012:206463. doi: 10.1155/2012/206463
92. Abadi ATB. Strategies Used by Helicobacter Pylori to Establish Persistent Infection. *World J Gastroenterol* (2017) 23(16):2870–82. doi: 10.3748/wjg.v23.i16.2870
93. Oertli M, Sundquist M, Hitzler I, Engler DB, Arnold IC, Reuter S, et al. DC-Derived IL-18 Drives Treg Differentiation, Murine Helicobacter Pylori-Specific Immune Tolerance, and Asthma Protection. *J Clin Invest* (2012) 122(3):1082–96. doi: 10.1172/JCI61029
94. Bergman MP, Engering A, Smits HH, van Vliet SJ, van Bodegraven AA, Wirth H-P, et al. Helicobacter Pylori Modulates the T Helper Cell 1/T Helper Cell 2 Balance Through Phase-Variable Interaction Between Lipopolysaccharide and DC-SIGN. *J Exp Med* (2004) 200(8):979–90. doi: 10.1084/jem.20041061
95. Sarajlic M, Neuper T, Vetter J, Schaller S, Klicznik MM, Gratz IK, et al. H. Pylorimodulates DC Functions *via* T4SS/Tnfα/P38-Dependent SOCS3 Expression. *Cell Communication Signaling* (2020) 18(1):160. doi: 10.1186/s12964-020-00655-1

96. Cover TL, Vaughn SG, Cao P, Blaser MJ. Potentiation of Helicobacter Pylori Vacuolating Toxin Activity by Nicotine and Other Weak Bases. *J Infect Dis* (1992) 166(5):1073–8. doi: 10.1093/infdis/166.5.1073
97. Chevalier C, Thiberge JM, Ferrero RL, Labigne A. Essential Role of Helicobacter Pylori Gamma-Glutamyltranspeptidase for the Colonization of the Gastric Mucosa of Mice. *Mol Microbiol* (1999) 31(5):1359–72. doi: 10.1046/j.1365-2958.1999.01271.x
98. Yokoyama K, Higashi H, Ishikawa S, Fujii Y, Kondo S, Kato H, et al. Functional Antagonism Between Helicobacter Pylori CagA and Vacuolating Toxin VacA in Control of the NFAT Signaling Pathway in Gastric Epithelial Cells. *Proc Natl Acad Sci USA* (2005) 102(27):9661–6. doi: 10.1073/pnas.0502529102
99. Ling SSM, Khoo LHB, Hwang L-A, Yeoh KG, Ho B. Instrumental Role of Helicobacter Pylori γ-Glutamyl Transpeptidase in VacA-Dependent Vacuolation in Gastric Epithelial Cells. *PloS One* (2015) 10(6):e0131460. doi: 10.1371/journal.pone.0131460
100. Zhang L, Hu W, Cho CH, Chan FK, Yu J, Fitzgerald JR, et al. Reduced Lysosomal Clearance of Autophagosomes Promotes Survival and Colonization of Helicobacter Pylori. *J Pathol* (2018) 244(4):432–44. doi: 10.1002/path.5033
101. Lekmeechai S, Su Y-C, Brant M, Alvarado-Kristensson M, Vallström A, Obi I, et al. Helicobacter Pylori Outer Membrane Vesicles Protect the Pathogen From Reactive Oxygen Species of the Respiratory Burst. *Front Microbiol* (2018) 9:1837. doi: 10.3389/fmicb.2018.01837
102. Borlace GN, Butler RN, Brooks DA. Monocyte and Macrophage Killing of Helicobacter Pylori: Relationship to Bacterial Virulence Factors. *Helicobacter* (2008) 13(5):380–7. doi: 10.1111/j.1523-5378.2008.00625.x
103. Gobert AP, Latour YL, Asim M, Finley JL, Verriere TG, Barry DP, et al. Bacterial Pathogens Hijack the Innate Immune Response by Activation of the Reverse Transsulfuration Pathway. *mBio* (2019) 10(5): e02174–19, 1–18. doi: 10.1128/mBio.02174-19
104. Latour YL, Gobert AP, Wilson KT. The Role of Polyamines in the Regulation of Macrophage Polarization and Function. *Amino Acids* (2020) 52(2):151–60. doi: 10.1007/s00726-019-02719-0
105. Darwin PE, Sztein MB, Zheng QX, James SP, Fantry GT. Immune Evasion by Helicobacter Pylori: Gastric Spiral Bacteria Lack Surface Immunoglobulin Deposition and Reactivity With Homologous Antibodies. *Helicobacter* (1996) 1(1):20–7. doi: 10.1111/j.1523-5378.1996.tb00004.x
106. Manojlovic N, Nikolic L, Pilcevic D, Josifovski J, Babic D. Systemic Humoral Anti-Helicobacter Pylori Immune Response in Patients With Gastric Malignancies and Benign Gastroduodenal Disease. *Hepatogastroenterology* (2004) 51(55):282–4.
107. Yamaji Y, Mitsushima T, Ikuma H, Okamoto M, Yoshida H, Kawabe T, et al. Weak Response of Helicobacter Pylori Antibody is High Risk for Gastric Cancer: A Cross-Sectional Study of 10,234 Endoscoped Japanese. *Scand J Gastroenterol* (2002) 37(2):148–53. doi: 10.1080/003655202753416795
108. Toyoshima O, Nishizawa T, Sakitani K, Yamakawa T, Takahashi Y, Yamamichi N, et al. Serum Anti-Helicobacter Pylori Antibody Titer and Its Association With Gastric Nodularity, Atrophy, and Age: A Cross-Sectional Study. *World J Gastroenterol* (2018) 24(35):4061–8. doi: 10.3748/wjg.v24.i35.4061
109. Kishikawa H, Kimura K, Takarabe S, Kaida S, Nishida J. Helicobacter Pylori Antibody Titer and Gastric Cancer Screening. *Dis Markers* (2015) 2015:156719–. doi: 10.1155/2015/156719
110. Nielsen H, Birkholz S, Andersen LP, Moran AP. Neutrophil Activation by Helicobacter Pylori Lipopolysaccharides. *J Infect Dis* (1994) 170(1):135–9. doi: 10.1093/infdis/170.1.135
111. Li H, Liao T, Debowski AW, Tang H, Nilsson H-O, Stubbs KA, et al. Lipopolysaccharide Structure and Biosynthesis in Helicobacter Pylori. *Helicobacter* (2016) 21(6):445–61. doi: 10.1111/hel.12301
112. Sherburne R, Taylor DE. Helicobacter Pylori Expresses a Complex Surface Carbohydrate, Lewis X. *Infect Immun* (1995) 63(12):4564–8. doi: 10.1128/iai.63.12.4564-4568.1995
113. Xue J, Li L, Li F, Li N, Li T, Li C. Expression of Lewis (B) Blood Group Antigen Interferes With Oral Dienogest Therapy Among Women With Adenomyosis. *J Reprod Immunol* (2020) 137:103079. doi: 10.1016/j.jri.2019.103079
114. de Mattos LC. Structural Diversity and Biological Importance of ABO, H, Lewis and Secretor Histo-Blood Group Carbohydrates. *Rev Bras Hematol Hemoter* (2016) 38(4):331–40. doi: 10.1016/j.bjhh.2016.07.005
115. Li H, Tang H, Debowski AW, Stubbs KA, Marshall BJ, Benghezal M. Lipopolysaccharide Structural Differences Between Western and Asian Helicobacter Pylori Strains. *Toxins (Basel)* (2018) 10(9):364. doi: 10.3390/toxins10090364
116. Moran A. The Role of Lipopolysaccharide in Helicobacter Pylori Pathogenesis. *Alimentary Pharmacol Ther* (1996) 10(Sup1):39–50. doi: 10.1046/j.1365-2036.1996.22164004.x
117. Nilsson C, Skoglund A, Moran AP, Annuk H, Engstrand L, Normark S. An Enzymatic Ruler Modulates Lewis Antigen Glycosylation of Helicobacter Pylori LPS During Persistent Infection. *Proc Natl Acad Sci USA* (2006) 103(8):2863–8. doi: 10.1073/pnas.0511119103
118. Muotiala A, Helander IM, Pyhälä L, Kosunen TU, Moran AP. Low Biological Activity of Helicobacter Pylori Lipopolysaccharide. *Infect Immun* (1992) 60(4):1714–6. doi: 10.1128/iai.60.4.1714-1716.1992
119. Li H, Marceau M, Yang T, Liao T, Tang X, Hu R, et al. East-Asian Helicobacter Pylori Strains Synthesize Heptan-Deficient Lipopolysaccharide. *PloS Genet* (2019) 15(11):e1008497–e. doi: 10.1371/journal.pgen.1008497
120. Pece S, Fumarola D, Giuliani G, Jirillo E, Moran AP. Activity in the Limulus Amebocyte Lysate Assay and Induction of Tumor Necrosis Factor-α by Diverse Helicobacter Pylori Lipopolysaccharide Preparations. *J Endotoxin Res* (1995) 2(6):455–62. doi: 10.1177/096805199600200609
121. Moran AP. Lipopolysaccharide in Bacterial Chronic Infection: Insights From Helicobacter Pylori Lipopolysaccharide and Lipid a. *Int J Med Microbiol* (2007) 297(5):307–19. doi: 10.1016/j.ijmm.2007.03.008
122. Shimoyama A, Saeki A, Tanimura N, Tsutsui H, Miyake K, Suda Y, et al. Chemical Synthesis of Helicobacter Pylori Lipopolysaccharide Partial Structures and Their Selective Proinflammatory Responses. *Chem A Eur J* (2011) 17(51):14464–74. doi: 10.1002/chem.201003581
123. Fujimoto Y, Shimoyama A, Suda Y, Fukase K. Synthesis and Immunomodulatory Activities of Helicobacter Pylori Lipophilic Terminus of Lipopolysaccharide Including Lipid a. *Carbohydr Res* (2012) 356:37–43. doi: 10.1016/j.carres.2012.03.013
124. Obonyo M, Sabet M, Cole SP, Ebmeyer J, Uematsu S, Akira S, et al. Deficiencies of Myeloid Differentiation Factor 88, Toll-Like Receptor 2 (TLR2), or TLR4 Produce Specific Defects in Macrophage Cytokine Secretion Induced by Helicobacter Pylori. *Infect Immun* (2007) 75(5):2408–14. doi: 10.1128/IAI.01794-06
125. Cullen TW, Giles DK, Wolf LN, Ecobichon C, Boneca IG, Trent MS. Helicobacter Pylori Versus the Host: Remodeling of the Bacterial Outer Membrane Is Required for Survival in the Gastric Mucosa. *PloS Pathog* (2011) 7(12):e1002454–e. doi: 10.1371/journal.ppat.1002454
126. Liu A-N, Teng K-W, Chew Y, Wang P-C, Nguyen TTH, Kao M-C. The Effects of HP0044 and HP1275 Knockout Mutations on the Structure and Function of Lipopolysaccharide in Helicobacter Pylori Strain 26695. *Biomedicines* (2022) 10(1):145. doi: 10.3390/biomedicines10010145
127. Moran AP, Knirel YA, Senchenkova SN, Widmalm G, Hynes SO, Jansson PE. Phenotypic Variation in Molecular Mimicry Between Helicobacter Pylori Lipopolysaccharides and Human Gastric Epithelial Cell Surface Glycoforms. Acid-Induced Phase Variation in Lewis(x) and Lewis(y) Expression by H. Pylori Lipopolysaccharides. *J Biol Chem* (2002) 277(8):5785–95. doi: 10.1074/jbc.M108574200
128. Pernitzsch SR, Alzheimer M, Bremer BU, Robbe-Saule M, De Reuse H, Sharma CM. Small RNA Mediated Gradual Control of Lipopolysaccharide Biosynthesis Affects Antibiotic Resistance in Helicobacter Pylori. *Nat Commun* (2021) 12(1):4433–. doi: 10.1038/s41467-021-24689-2
129. Monteiro MA, Appelmelk BJ, Rasko DA, Moran AP, Hynes SO, MacLean LL, et al. Lipopolysaccharide Structures of Helicobacter Pylori Genomic Strains 26695 and J99, Mouse Model H. Pylori Sydney Strain, H. Pylori P466 Carrying Sialyl Lewis X, and H. Pylori UA915 Expressing Lewis B Classification of H. Pylori Lipopolysaccharides Into Glycotype Families. *Eur J Biochem* (2000) 267(2):305–20. doi: 10.1046/j.1432-1327.2000.01007.x
130. Lozniewski A, Haristoy X, Rasko DA, Hatier R, Plénat F, Taylor DE, et al. Influence of Lewis Antigen Expression by Helicobacter Pylori on Bacterial

Internalization by Gastric Epithelial Cells. *Infect Immun* (2003) 71(5):2902–6. doi: 10.1128/iai.71.5.2902-2906.2003
131. Gonciarz W, Walencka M, Moran AP, Hinc K, Obuchowski M, Chmiela M. Upregulation of MUC5AC Production and Deposition of LEWIS Determinants by HELICOBACTER PYLORI Facilitate Gastric Tissue Colonization and the Maintenance of Infection. *J Biomed Sci* (2019) 26 (1):23. doi: 10.1186/s12929-019-0515-z
132. Boren T, Falk P, Roth KA, Larson G, Normark S. Attachment of Helicobacter Pylori to Human Gastric Epithelium Mediated by Blood Group Antigens. *Science* (1993) 262(5141):1892. doi: 10.1126/science.8018146
133. Ilver D, Arnqvist A, Ogren J, Frick IM, Kersulyte D, Incecik ET, et al. Helicobacter Pylori Adhesin Binding Fucosylated Histo-Blood Group Antigens Revealed by Retagging. *Science* (1998) 279(5349):373–7. doi: 10.1126/science.279.5349.373
134. Moonens K, Gideonsson P, Subedi S, Bugaytsova J, Romaõ E, Mendez M, et al. Structural Insights Into Polymorphic ABO Glycan Binding by Helicobacter Pylori. *Cell Host Microbe* (2016) 19(1):55–66. doi: 10.1016/j.chom.2015.12.004
135. Matteo MJ, Armitano RI, Romeo M, Wonaga A, Olmos M, Catalano M. Helicobacter Pylori Bab Genes During Chronic Colonization. *Int J Mol Epidemiol Genet* (2011) 2(3):286–91.
136. Bäckström A, Lundberg C, Kersulyte D, Berg DE, Borén T, Arnqvist A. Metastability of Helicobacter Pylori Bab Adhesin Genes and Dynamics in Lewis B Antigen Binding. *Proc Natl Acad Sci USA* (2004) 101(48):16923–8. doi: 10.1073/pnas.0404817101
137. Ansari S, Yamaoka Y. Helicobacter Pylori BabA in Adaptation for Gastric Colonization. *World J Gastroenterol* (2017) 23(23):4158–69. doi: 10.3748/wjg.v23.i23.4158
138. Styer CM, Hansen LM, Cooke CL, Gundersen AM, Choi SS, Berg DE, et al. Expression of the BabA Adhesin During Experimental Infection With Helicobacter Pylori. *Infect Immun* (2010) 78(4):1593–600. doi: 10.1128/IAI.01297-09
139. Ishijima N, Suzuki M, Ashida H, Ichikawa Y, Kanegae Y, Saito I, et al. BabA-Mediated Adherence Is a Potentiator of the Helicobacter Pylori Type IV Secretion System Activity. *J Biol Chem* (2011) 286(28):25256–64. doi: 10.1074/jbc.M111.233601
140. Mahdavi J, Sondén B, Hurtig M, Olfat FO, Forsberg L, Roche N, et al. Helicobacter Pylori SabA Adhesin in Persistent Infection and Chronic Inflammation. *Science* (2002) 297(5581):573–8. doi: 10.1126/science.1069076
141. Goodwin AC, Weinberger DM, Ford CB, Nelson JC, Snider JD, Hall JD, et al. Expression of the Helicobacter Pylori Adhesin SabA Is Controlled via Phase Variation and the ArsRS Signal Transduction System. *Microbiology* (2008) 154(Pt 8):2231–40. doi: 10.1099/mic.0.2007/016055-0
142. Talarico S, Whitefield SE, Fero J, Haas R, Salama NR. Regulation of Helicobacter Pylori Adherence by Gene Conversion. *Mol Microbiol* (2012) 84(6):1050–61. doi: 10.1111/j.1365-2958.2012.08073.x
143. Xu C, Soyfoo DM, Wu Y, Xu S. Virulence of Helicobacter Pylori Outer Membrane Proteins: An Updated Review. *Eur J Clin Microbiol Infect Dis* (2020) 39(10):1821–30. doi: 10.1007/s10096-020-03948-y
144. Horridge DN, Begley AA, Kim J, Aravindan N, Fan K, Forsyth MH. Outer Inflammatory Protein a (OipA) of Helicobacter Pylori is Regulated by Host Cell Contact and Mediates CagA Translocation and Interleukin-8 Response Only in the Presence of a Functional Cag Pathogenicity Island Type IV Secretion System. *Pathog Dis* (2017) 75(8):ftx113. doi: 10.1093/femspd/ftx113
145. Farzi N, Yadegar A, Aghdaei HA, Yamaoka Y, Zali MR. Genetic Diversity and Functional Analysis of oipA Gene in Association With Other Virulence Factors Among Helicobacter Pylori Isolates From Iranian Patients With Different Gastric Diseases. *Infect Genet Evol* (2018) 60:26–34. doi: 10.1016/j.meegid.2018.02.017
146. Al-Maleki AR, Loke MF, Lui SY, Ramli NSK, Khosravi Y, Ng CG, et al. Helicobacter Pylori Outer Inflammatory Protein A (OipA) Suppresses Apoptosis of AGS Gastric Cells. *Vitro Cell Microbiol* (2017) 19(12):e12771. doi: 10.1111/cmi.12771
147. Negrini R, Savio A, Poiesi C, Appelmelk BJ, Buffoli F, Paterlini A, et al. Antigenic Mimicry Between Helicobacter Pylori and Gastric Mucosa in the Pathogenesis of Body Atrophic Gastritis. *Gastroenterology* (1996) 111 (3):655–65. doi: 10.1053/gast.1996.v111.pm8780570

Conflict of Interest: Author AG was employed by company ZiP Diagnostics.

The remaining authors declare that the research was conducted in the absence of any commercial or financial relationships that could be construed as a potential conflict of interest.

frontiers | Frontiers in Immunology

REVIEW
published: 17 May 2022
doi: 10.3389/fimmu.2022.888897

Dysregulated Interferon Response and Immune Hyperactivation in Severe COVID-19: Targeting STATs as a Novel Therapeutic Strategy

*Mahdi Eskandarian Boroujeni[1], Agata Sekrecka[1], Aleksandra Antonczyk[1], Sanaz Hassani[1], Michal Sekrecki[1], Hanna Nowicka[1], Natalia Lopacinska[1], Arta Olya[1], Katarzyna Kluzek[1], Joanna Wesoly[2] and Hans A. R. Bluyssen[1]**

[1] Laboratory of Human Molecular Genetics, Institute of Molecular Biology and Biotechnology, Faculty of Biology, Adam Mickiewicz University, Poznań, Poland, [2] Laboratory of High Throughput Technologies, Institute of Molecular Biology and Biotechnology, Faculty of Biology, Adam Mickiewicz University, Poznań, Poland

OPEN ACCESS

Edited by:
Uday Kishore,
Brunel University London,
United Kingdom

Reviewed by:
Béatrice Nal,
INSERM U1104 Centre d'immunologie de Marseille-Luminy (CIML), France
Taruna Madan,
National Institute for Research in Reproductive Health (ICMR), India

***Correspondence:**
Hans A. R. Bluyssen
h.bluyss@amu.edu.pl

Specialty section:
This article was submitted to Molecular Innate Immunity, a section of the journal Frontiers in Immunology

Received: 03 March 2022
Accepted: 13 April 2022
Published: 17 May 2022

Citation:
Eskandarian Boroujeni M, Sekrecka A, Antonczyk A, Hassani S, Sekrecki M, Nowicka H, Lopacinska N, Olya A, Kluzek K, Wesoly J and Bluyssen HAR (2022) Dysregulated Interferon Response and Immune Hyperactivation in Severe COVID-19: Targeting STATs as a Novel Therapeutic Strategy. Front. Immunol. 13:888897. doi: 10.3389/fimmu.2022.888897

A disease outbreak in December 2019, caused by a novel coronavirus SARS-CoV-2, was named COVID-19. SARS-CoV-2 infects cells from the upper and lower respiratory tract system and is transmitted by inhalation or contact with infected droplets. Common clinical symptoms include fatigue, fever, and cough, but also shortness of breath and lung abnormalities. Still, some 5% of SARS-CoV-2 infections progress to severe pneumonia and acute respiratory distress syndrome (ARDS), with pulmonary edema, acute kidney injury, and/or multiple organ failure as important consequences, which can lead to death. The innate immune system recognizes viral RNAs and triggers the expression of interferons (IFN). IFNs activate anti-viral effectors and components of the adaptive immune system by activating members of the STAT and IRF families that induce the expression of IFN-stimulated genes (ISG)s. Among other coronaviruses, such as Middle East respiratory syndrome coronavirus (MERS-CoV) and SARS-CoV, common strategies have been identified to antagonize IFN signaling. This typically coincides with hyperactive inflammatory host responses known as the "cytokine storm" that mediate severe lung damage. Likewise, SARS-CoV-2 infection combines a dysregulated IFN response with excessive production of inflammatory cytokines in the lungs. This excessive inflammatory response in the lungs is associated with the local recruitment of immune cells that create a pathogenic inflammatory loop. Together, it causes severe lung pathology, including ARDS, as well as damage to other vulnerable organs, like the heart, spleen, lymph nodes, and kidney, as well as the brain. This can rapidly progress to multiple organ exhaustion and correlates with a poor prognosis in COVID-19 patients. In this review, we focus on the crucial role of different types of IFN that underlies the progression of SARS-CoV-2 infection and leads to immune cell hyper-activation in the lungs, exuberant systemic inflammation, and multiple organ damage. Consequently, to protect from systemic inflammation, it will be critical to interfere with signaling cascades activated by

IFNs and other inflammatory cytokines. Targeting members of the STAT family could therefore be proposed as a novel therapeutic strategy in patients with severe COVID-19.

Keywords: COVID – 19, interferon response, immune hyperactivation, multiple organ damage, STAT signaling, Statinhib, therapy

INTRODUCTION

Since the end of 2019, a novel coronavirus (SARS-CoV-2) caused a respiratory disease outbreak in Wuhan, that quickly spread in China and subsequently worldwide. Soon after that, the WHO declared SARS-CoV-2 infection a global health threat and named it coronavirus disease-19 (COVID-19). Clinically, COVID-19 varied from mild to severe symptoms, including acute respiratory distress syndrome (ARDS), as observed after SARS-CoV infection. As of February 2022, more than 350 million confirmed cases, including 5.6 million deaths have been reported.

SARS-CoV-2 is a SARS-CoV-like β-lineage coronavirus originating from bats, that initially infects cells from the upper and lower respiratory tract system through inhalation or contact with infected droplets (1, 2). Common clinical symptoms include fatigue, fever, and cough, but also shortness of breath and lung abnormalities. Still, some 5% of SARS-CoV-2 infections progress to severe pneumonia and ARDS, with pulmonary edema, acute kidney injury, and/or multiple organ failure as important consequences, which can lead to death (3–6).

The innate immune system recognizes viral RNAs *via* endosomal and cytosolic pattern recognition receptors, including TLRs or RIG-1 and MDA5. This triggers the expression of interferons (IFN), which are the mediators of cellular homeostatic responses to virus infection. IFNs comprise a family of antiviral cytokines, classified as type I, II, and III. Through binding to their cognate cellular receptors, they activate transcription factors of the STAT and IRF family and expression of IFN-stimulated genes (ISG)s, which turn on the anti-viral state and render cells more resistant to virus infection and thereby limit virus spread (7, 8). Among other coronaviruses, such as Middle East respiratory syndrome coronavirus (MERS-CoV) and SARS-CoV, common strategies have been identified to antagonize IFN signaling. This typically coincides with hyperactive inflammatory host responses known as the "cytokine storm" that mediate severe lung damage.

Based on recent COVID-19 patient and animal studies it can be concluded that early during SARS-CoV-2 infection of the upper airways a dysregulated IFN response, mediated by antagonizing IFN induced signaling pathways, is a hallmark of SARS-CoV-2 infections. Later in the lungs, this is accompanied by the production of inflammatory cytokines, together with excessive IFN production, known as the "cytokine storm". The excessive inflammatory response in the lungs is associated with the local recruitment of immune cells, including macrophages, effector T-cells, dendritic cells, and neutrophils that create a pathogenic inflammatory loop (9, 10). Together, it causes severe lung pathology, including ARDS, as well as damage to other vulnerable organs, like the heart, spleen, lymph nodes, and kidney, as well as the brain. This can rapidly progress to multiple organ exhaustion and correlates with a poor prognosis in COVID-19 patients (6, 9, 10).

So far, several effective vaccines have been generated to prevent infection and transmission. On the other hand, efforts to increase our understanding of the biology of SARS-CoV-2 infection and the host immune response are urgently pursued to design therapeutic strategies that reduce the risk of severe COVID-19 and the overall mortality rate.

SARS-COV-2 INFECTION, EXUBERANT INFLAMMATION, AND CLINICAL OUTCOME

SARS-CoV-2 infection starts with its entrance into human cells. Like SARS-CoV, SARS-CoV-2 engages angiotensin-converting enzyme-2 (ACE2) as a cellular entry receptor. In addition, it uses the cellular serine protease TMPRSS2 for S protein priming, whereas Neuropilin1 (NRP1) serves as a co-factor in cell entry (11–14). Thus, effective SARS-CoV-2 transmission requires high co-expression of ACE2 and TMPRSS2 in target cells, including nasal epithelial cells and type II alveolar cells (AT2) of the lungs (15). Viral-Track was developed as a new computational pipeline, to detect viral RNA in single-cell transcriptome data of bronchoalveolar lavage fluid (BALF) from COVID-19 patients. Detecting viral RNA only in severe disease (16), particularly in ciliated and epithelial progenitors and in a subset of macrophages (SPP1+ macrophages), suggested differential progression of infection in the lung (16, 17).

In addition to the nose and lung, the extrapulmonary spread of SARS-CoV-2 was observed (13). Interestingly, Zou et al. recently analyzed single-cell RNA sequencing datasets combined with ACE2 expression and identified potential risk organs, including the lung, heart, kidney, ileum, esophagus, and bladder (18). At the same time, specific cell types could be located (i.e., ileum and esophagus epithelial cells, bladder urothelial cells, AT2, myocardial cells, and proximal tubule cells of the kidney), being sensitive to SARS-CoV-2 infection (19). In fact, ACE2 distribution in the host organism importantly correlated with organ injury. Likewise, expression differences and/or ACE2 polymorphisms determine SARS-CoV-2 infection susceptibility and clinical manifestations. As part of the renin-angiotensin-aldosterone system (RAAS), ACE2 converts angiotensin II (Ang II) to Ang (1–7). Therefore, ACE2 has a dual role in both SARS-CoV and SARS-CoV-2 infection. On the one hand, it acts as the host cell virus entry receptor, but on the other by protecting the lungs and other organs from Ang II-mediated vasoconstrictive, pro-inflammatory, and pro-fibrotic injury on pulmonary vascular and epithelial cells (6, 20).

Common clinical symptoms of SARS-CoV-2 infection include fatigue, fever, and cough, but also shortness of breath and lung abnormalities. A mere 20% of COVID-19 patients require hospitalization and about 1 in 4 of these progress to severe pneumonia and ARDS, with pulmonary edema, acute kidney injury, and/or multiple organ failure as important consequences, that require invasive mechanical ventilation (3–5). In common with SARS-CoV and MERS-CoV infections, ARDS causes similar immunopathogenic features and is the main cause of death in COVID-19 disease (4). Advanced age and the presence of certain comorbidities, such as coronary heart disease, hypertension, chronic obstructive pulmonary disease, and diabetes mellitus, are among the risk factors for the development of severe COVID-19 and poor outcome (3, 21–25).

An important hallmark of ARDS is the cytokine storm - an excessive inflammatory response of immune effector cells combined with the release of pro-inflammatory cytokines and chemokines (4). Indeed, SARS-CoV-2 infected individuals with severe symptoms display increased serum concentrations of many pro-inflammatory mediators, including interferon (IFN)-g-induced protein 10 (IP-10), monocyte chemoattractant protein 1 (MCP1), macrophage inflammatory protein (MIP)-1a, platelet-derived growth factor (PDGF), TNF-a, vascular endothelial growth factor (VEGF), granulocyte colony-stimulating factor (G-CFS), IL-1b, IL-2, IL-6, IL-7, IL-8 (4, 26–29). Also, recent single-cell expression profiling studies in bronchoalveolar cells, PBMCs, and airway epithelium from COVID-19 patients, have shown that upregulation of pro-inflammatory pathways correlates with severe symptoms (17, 30). Therefore, an excessive inflammatory response, associated with high levels of circulating pro-inflammatory cytokines and chemokines, profound lymphopenia, and substantial infiltration of hyper-active mononuclear cells in the lungs, is a major cause of disease severity and death in patients with COVID-19. In addition, it has also become clear that SARS-CoV-2 infected individuals can rapidly progress to a multiple organ dysfunction syndrome (MODS). In this respect, increased fibrin degradation products (identified as D- dimers) and coagulation abnormalities (i.e, apparent thrombotic manifestations and prolonged prothrombin time) as well as lower platelets counts, promote vascular leakage and disseminated intravascular coagulation. These vascular abnormalities could lead to organ failure and death and are a clear link with poor prognosis in patients with severe COVID-19 (3–5, 31, 32).

SARS-COV-2 INFECTION AND DYSREGULATED IFN RESPONSES

The innate immune system recognizes viral RNAs *via* endosomal and cytosolic pattern recognition receptors, including Toll-like receptor (TLR) 3 and TLR7 or retinoic acid–inducible gene I (RIG-I) and melanoma differentiation-associated protein 5 (MDA5) (33, 34). After infection of the target cells, they trigger the activation of the downstream transcription factors, namely interferon regulatory factor (IRF)3 and IRF7 and nuclear factor-kappa B (NF-κB). These factors collectively induce the production of IFNs, the main mediators of cellular homeostatic responses to virus infection (7, 8).

IFNs consist of three sub-types, including IFN-I, IFN-II, and IFN-III. IFN-II, also known as IFNγ, mediates broad immune responses to pathogens by binding to the IFNγ receptor (IFNGR) complex. In response to foreign antigens or mitogens, IFN-II is mainly produced by T lymphocytes and Natural Killer (NK) cells, to modulate adaptive immunity as well as inflammation. Although IFN-II exhibits anti-viral activity, IFN-I is the main anti-viral IFN subtype, predominantly consisting of IFNα and IFNβ subtypes. IFN-I can be produced by many cell types and collectively bind to the IFNα receptor (IFNAR) to potently inhibit viral infection as part of a robust innate immune response. IFN-III (consisting of IFNΛ1 to -4 subtypes) is largely produced by epithelial cells, hepatocytes, and dendritic cells, in a tissue-specific manner. All IFNΛ subtypes bind the heterodimeric IFN-Λ receptor (IFNLR) (35), which is restricted to certain cell types and tissues, including macrophages, conventional dendritic cells (DCs), and plasmacytoid dendritic cells (pDCs), neutrophils, and respiratory epithelial cells. IFN-Λ responses, therefore, confer more localized antiviral protection at the site of infection. In addition to antiviral and pro-inflammatory activity, IFNs exert anti-proliferative and pro-apoptotic functions (7, 8).

As potent IFN-producing cells also plasmacytoid (p)DCs are important cellular mediators of the antiviral response by producing massive amounts of IFN-I and IFN-III. In addition, they produce other pro-inflammatory cytokines, which modulate the function of innate and adaptive immune cells (35).

Coronaviruses, such as SARS-CoV and MERS-CoV, have developed strategies to antagonize IFN responses. This typically coincides with hyperactive inflammatory host responses that lead to severe lung damage. Using mice infected with SARS-CoV, it was shown that robust virus replication accompanied by delayed IFN-I signaling triggers hyperinflammatory and severe immune pathology of the lungs as well as reduced survival. This dysregulated IFN-I signaling promoted the infiltration of pathogenic inflammatory monocyte macrophages (IMM), leading to increased lung cytokine/chemokine levels, and resulting in vascular leakage and impaired virus-specific T cell responses (30). Likewise, robust and persistent expression of IFN and IFN-stimulated genes (ISGs) in association with impaired T cell and antibody responses was observed in fatal SARS in humans (36). Thus, during SARS-CoV and MERS-CoV infection, an ineffective IFN-I response, accompanied by excessive production of inflammatory cytokines, correlates with disease severity and poor prognosis and appears to be a hallmark of coronavirus infections (37–39).

As stated by Zhang et al: "Combined immunodeficiencies, immune dysregulation disorders and defects of innate immunity impairing type I interferon responses show a higher rate of severe disease and higher mortality. In addition, inborn errors of type I interferon responses and inborn errors of immunity in which patients harbor autoantibodies against these cytokines, confer a high risk for critical COVID-19" (40). Together, this reflects the

key role of IFN-I in the host defense against SARS-CoV-2 (**Figure 1**). Using peripheral blood mononuclear cells (PBMCs), Lee et al. (30) performed single-cell RNA-seq to identify driving factors of COVID-19 progression. By comparing healthy donors, patients with mild or severe COVID-19, and patients with severe influenza, they observed that all PBMC cell types of COVID-19 displayed hyper-inflammatory signatures, marked by a TNF/IL-1β-mediated inflammatory response, as compared to severe influenza. Moreover, classical monocytes from severe COVID-19 patients displayed a type I IFN response together with the TNF/IL-1β-mediated inflammation, being absent in mild COVID-19 patients. Remarkably, patients with severe influenza also presented these type I IFN-dependent inflammatory features. Consequently, it was proposed that the type I IFN response plays an important role in the excessive inflammation seen in severe COVID-19 patients (30) (**Figure 1**).

Conversely, by studying peripheral blood responses of COVID-19 patients, Hadjadj et al. (41) observed reduced IFN responses in critically ill patients paired with a pro-inflammatory response. By comparing the transcriptional responses of several respiratory viruses, including SARS-CoV-2, Blanco-Melo et al. demonstrated *in vitro* that the host response to SARS-CoV-2 is unable to activate a robust IFN-I and -III response whereas high levels of chemokines were presented for the recruitment of immune cells (42). Along the same lines, Broggi and colleagues evaluated the ability of SARS-CoV-2 to induce IFNs in the upper or lower airways of COVID-19 patients. Importantly, they observed that IFN levels in the upper respiratory tract of COVID-19 patients did not significantly differ from healthy individuals. But bronchoalveolar lavage fluid from these patients exhibited increased levels of inflammatory cytokines, IFN-I, and IFN-III. This indicated that in the upper airways interferon production is inhibited by SARS-CoV-2, diminishing the immune response and promoting virus survival (**Figure 1**). But by the time the virus enters the lower respiratory tract, an excessive immune response is activated, together with upregulation of interferons that at this point is harmful. In conclusion, both early-stage deficiencies in type I IFN responses and late stage IFN hyper-responsiveness are a characteristic of severe COVID-19 (43, 44). Indeed, an early transient response of IFNa and IFNΛ was observed in mild-to-moderate COVID-19, whereas in severe patients, levels further enhanced towards the second week (45). The longitudinal dynamic changes of IFN-I production in severe patients correlate with experiments in a mouse SARS-CoV-2 model, further proving *in vivo* that IFN-I is unable to control SARS-CoV-2 replication but importantly drives hyperactive immune responses (46).

Therefore, it is tempting to propose that during early SARS-CoV-2 infection of the upper respiratory tract, intervention with

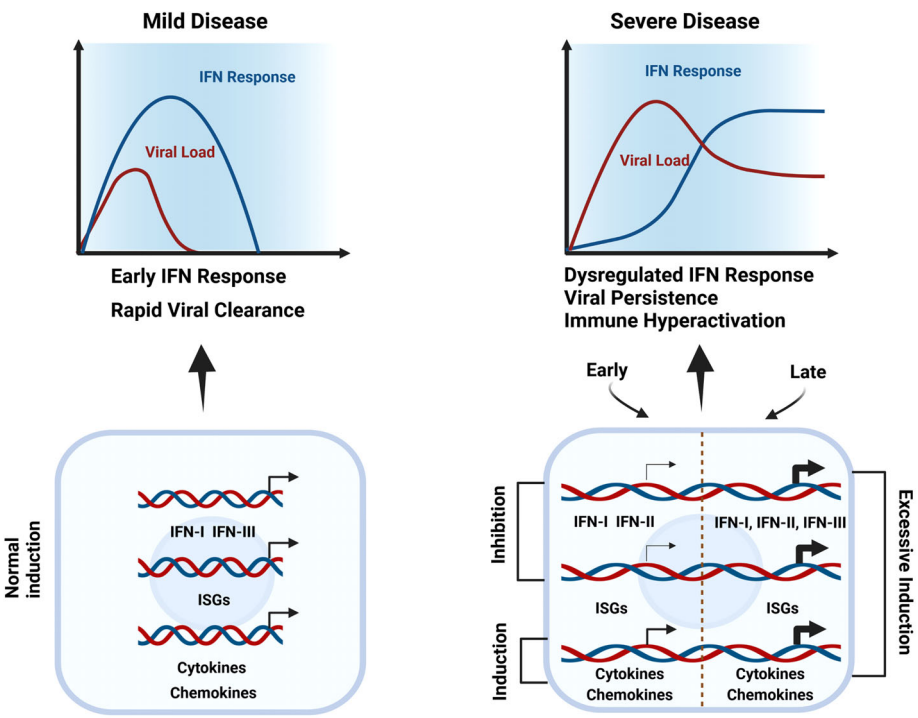

FIGURE 1 | Dysregulated IFN responses & immune hyper-activation in severe COVID-19. During mild disease, the initial viral burden is low and IFNs, together with cytokines, chemokines, and other ISGs are induced early and rapidly to mediate effective viral clearance (left). In severe COVID-19 (right), in the upper respiratory tract interferon production and ISG expression are inhibited by SARS-CoV-2, diminishing the immune response and promoting virus survival (Early). But by the time the virus enters the lower respiratory tract, an exuberant immune response is activated, including excessive upregulation of interferons, cytokines, chemokines, and other ISGs that at this point are harmful (Late). Thus, both early-stage deficiencies in type I IFN responses and late-stage IFN hyper-responsiveness are clear characteristics of severe COVID-19.

recombinant interferons and other antivirals offer important solutions. However, during hyper-inflammation in the lower respiratory tract, it will be critical to interfere with signaling cascades activated by IFNs and other inflammatory cytokines, probably with anti-inflammatory drugs.

SARS-COV-2 EVOLVED STRATEGIES TO TARGET IFN SIGNALING

As mentioned above, after infection of target cells, RNA viruses trigger the activation of downstream IRF3 and IRF7 and NF-κB transcription factors and the production of IFNs. Subsequently, through binding to their cognate cellular receptors and Janus kinase (JAK)-dependent phosphorylation, IFNs activate transcription factors of the Signal Transducer and Activator of Transcription (STAT) family and IFN-stimulated gene (ISG) expression, which turn on the anti-viral state and render cells more resistant to virus infection and thereby limits virus spread. Thus, IFN-I, IFN-II, and IFN-III induce ISG expression by phosphorylating STAT1 and/or STAT2. IFN-II-induced STAT1 homodimers regulate gene expression of IFN-II activation site (GAS) containing genes. The association of IRF9 with STAT1/2 heterodimers (known as ISGF3), expands the range of enhancer elements targeted by IFN-I and IFN-III to IFN-stimulated response element (ISRE) (**Figure 2**). Similarly, IRF family members, including IRF1, IRF7 and IRF8, can regulate ISG expression in response to all three types of IFN by binding the ISRE. Together, this leads to the transcriptional activation of hundreds of ISGs, such as MX1 and 2, ISG15, IFIT1, IFIT2 and IFIT3, and OAS1, OAS2, and OAS3 that importantly participate in the antiviral response (7, 8).

Among coronaviruses, such as MERS-CoV and SARS-CoV, common strategies have been identified to antagonize IFN production and inhibit IFN signaling (39, 47, 48). For example, SARS-CoV was shown to antagonize the IFN response using nsp1, papain-like protease (PLpro), nsp7, nsp15, ORF3b, M, ORF6, and N proteins (49, 50). Thus, several antagonizing mechanisms have been identified, including inhibition of IRF3 and IRF7 activation, blocking expression of STAT1, and interaction with ISG15.

Concerning SARS-CoV-2 infection and dysregulated IFN-I responses, likewise, nsp1, nsp12, nsp13, nsp14, and, nsp15 and orf6 and the M protein (51–53) were among potent IFN-I inhibitors. In addition, Li et al. observed that ORF6, ORF8, and nucleocapsid proteins significantly inhibited IFN-I production, and the IFN-I-mediated innate immune response (53). The same was true for ORF3b (54). A more detailed functional analysis of these proteins in relation to COVID-19 progression was performed by Xia et al. Importantly, they found that nsp6 suppressed IRF3 phosphorylation by binding TANK binding kinase 1 (TBK1), nsp13 blocked and bound TBK1 phosphorylation, and ORF6 inhibited IRF3 nuclear translocation by binding importin Karyopherin a 2 (KPNA2). They also identified nsp1 and nsp6 to block IFN-I signaling by interfering with the phosphorylation of STAT1/STAT2 or their

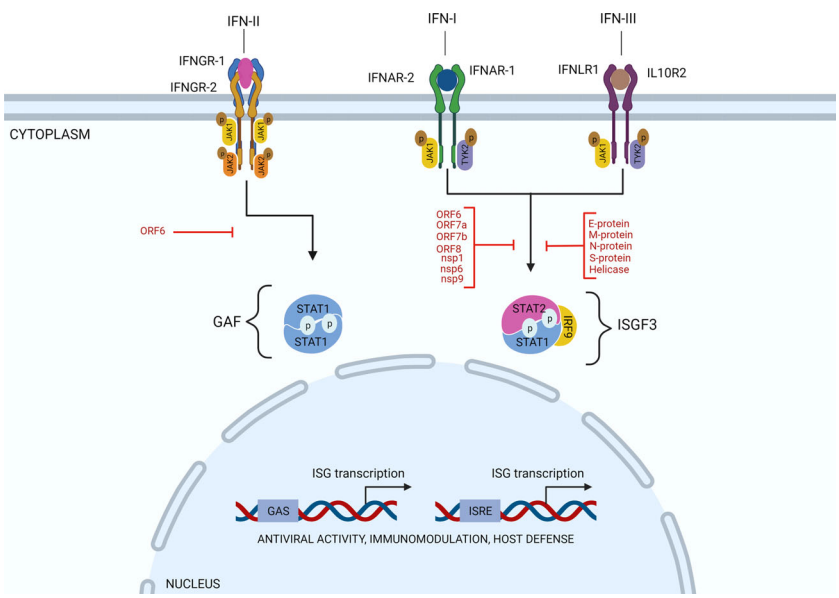

FIGURE 2 | SARS-CoV-2 evolved strategies to target IFN signaling. Through binding to their cognate cellular receptors and Janus kinase (JAK)-dependent phosphorylation, IFNs activate transcription factors of the Signal Transducer and Activator of Transcription (STAT) family and expression of IFN-stimulated genes (ISG)s. Thus, IFN-I, IFN-II, and IFN-III induce ISG expression by phosphorylating STAT1 and/or STAT2. IFN-II-induced STAT1 homodimers regulate gene expression of IFN-II activation site (GAS) containing genes. The association of IRF9 with STAT1/2 heterodimers (known as ISGF3), expands the range of enhancer elements targeted by IFN-I and IFN-III to IFN-stimulated response element (ISRE). Various SARS-CoV-2 proteins, as indicated (in red), have been identified to inhibit the IFN response. Particularly, by interfering with STAT1 and/or STAT2 activation and ISG expression, as explained in the text.

nuclear translocation (**Figure 2**). Interestingly, nsp1 and nsp6 proteins of SARS-CoV-2 antagonized IFN-I signaling more efficiently than the counterparts of SARS-CoV and MERS-CoV suggesting that SARS-CoV and SARS-CoV-2 use different mechanisms to affect disease onset and progression (55). Along the same lines, Zhang et al. observed that the SARS-CoV-2 M protein did not significantly affect IRF3 phosphorylation, but blocked its nuclear translocation. Likewise, the S protein was found to suppress STAT1 phosphorylation and nuclear translocation by intervening with JAK1-STAT1 interaction (56). On the other hand, without directly influencing STAT1 and STAT2 activation, nsp7 and ORF7a clearly inhibited ISRE promoter activity (56). Nsp9 and ORF8 exhibited inhibition of STAT1 activation, whereas Helicase and E protein intervened with STAT1 and STAT2 activation (56). The same was shown by Shi et al. with the M protein significantly blocking STAT1 phosphorylation and ISG expression (55). This study by Shi et al. also provided evidence to suggest that ORF7a inhibited STAT2 phosphorylation, whereas ORF7b inhibited phosphorylation of both STAT1 and STAT2 (55). In a separate study, Mu et al. found that SARS-CoV-2 replication was efficiently enhanced upon N protein overexpression in infected human cells, by interacting with STAT1 and STAT2 and inhibiting their phosphorylation and nuclear translocation (57). (**Figure 2**). Finally, the S protein also interfered with IFN-I signaling, however with a currently unknown mechanism (51, 57).

Analysis of gene expression profiles from COVID-19 patient airway epithelial cells together with epithelial cell lines infected with SARS-CoV-2 revealed that also IFN-II signaling is antagonized in a SARS-CoV-2 dependent manner (58). Particularly, it was shown that the SARS-CoV-2 ORF6 protein suppressed NLRC5, an MHC class I trans-activator, both transcriptionally and functionally (**Figure 2**). This was mediated by blocking type II interferon-mediated STAT1 signaling, and subsequent NLRC5 and IRF1 gene expression. At the same time, ORF6 was shown to inhibit NLRC5 nuclear import, uncovering a novel immune evasion mechanism toward modulation of the MHC class I pathway.

Finally, it was assessed how JAK/STAT signaling was altered in immune cells in COVID-19 patients and if an imbalance in JAK/STAT signaling contributed to disease severity. Rincon-Arevalo et al. reported increased expression in mild and severe COVID-19 patients of STAT1 and IRF9, in correlation with peripheral monocytes exhibiting IFN signatures [marked by Siglec-1 [CD169] expression (59)]. Remarkably, CD14+ monocytes and plasmablasts in severe patients displayed reduced expression of STAT1 and Siglec-1 in comparison to mild patients. In contrast, STAT1 phosphorylation was increased in severe COVID-19 cases, pointing to an imbalanced JAK/STAT signaling and lack of ISG induced transcription. This defect was still present in PBMCs isolated from severe COVID-19 patients stimulated with IFN-α and IFN-γ. This strongly implies that impaired JAK/STAT signaling could serve as a potential predictive biomarker of severe COVID-19 in combination with patient stratification and IFN response targeted therapy.

Together a picture emerges in which multiple components of the type I, II and III IFN systems are targeted by SARS-CoV-2, including members of the STAT family (**Figure 2**) and also IRFs. This affects important aspects of the innate and adaptive immune system and leads to a dysregulated immune response.

IFNS AND IMMUNE CELL HYPERACTIVATION IN LUNG PATHOLOGY OF SEVERE COVID-19

As with SARS-CoV and MERS-CoV infected patients, acute pneumonia is the most frequent and critical clinical manifestation presented among severe COVID-19 patients (2–6). Severe lung pathology after MERS-CoV and SARS-CoV infection is a consequence of dysregulated IFN-I responses and rapid virus replication, which promote the accumulation of pathogenic inflammatory monocyte macrophages (IMM) and IFN-producing pDCs, and the release of elevated lung cytokine/chemokine levels. Subsequently increased influx of IMM resulted in exuberant inflammation. In addition, T cell responses are reduced through IFN-I-mediated T cell apoptosis. Together, this causes severe lung pathology that correlated with poor outcome of patients infected with MERS-CoV and SARS-CoV (60–63).

Likewise, SARS-CoV-2 infection combines a dysregulated IFN response with excessive production of inflammatory cytokines in the lungs. In COVID-19 patients, this also has proven to be a main cause of disease severity and death and is associated with high levels of circulating pro-inflammatory cytokines and chemokines and the local recruitment of immune cells (6, 10, 64, 65). A current model suggests that upon upper airway entry, SARS-CoV-2 impregnates the lower lungs, where it infects a number of target cells, including the alveolar type 2 cells (AT2), alveolar macrophages, and vascular endothelial cells (**Figure 3**). Virus cell entry recognition *via* endosomal and cytosolic pattern recognition receptors (as TLR3 and TLR7) triggers the activation of downstream IRF3 and IRF7 and NF-κB transcription factors and the production of IFNs and proinflammatory mediators. Severe COVID-19 also displays increased CD4+ and CD8+ T cell activation. Yet, with the observed lymphopenia in these patients it is anticipated that in response to the virus, effector T cells are recruited to the lung. In this respect, lymphopenia has been recognized as a hallmark of severe COVID-19 (4, 5, 10), whereas an elevated neutrophil/lymphocyte ratio has been shown to serve as a biomarker of disease severity (65–68). Interestingly, plasmacytoid DC (pDCs), the main source of IFN-I and IFN-III, were also reduced in abundance in the circulation (65, 69).

Together, the local recruitment of immune cells further perpetuates proinflammatory cytokine and chemokine expression in BALF (CCL2, CCL3, CCL4, and CXCL10) but also in the circulation (IL-1, IFN-I, IFN-II, and IFN-III, IL-17, TNF, IP-10, MCP-1, G-CSF, GM-CSF, IL-1RA, CCL2, CCL3, CCL5, CCL8, CXCL2, CXCL8, CXCL9, and CXCL16) (4–6, 41, 42, 64, 70–72). Consequently, this further augments damage to

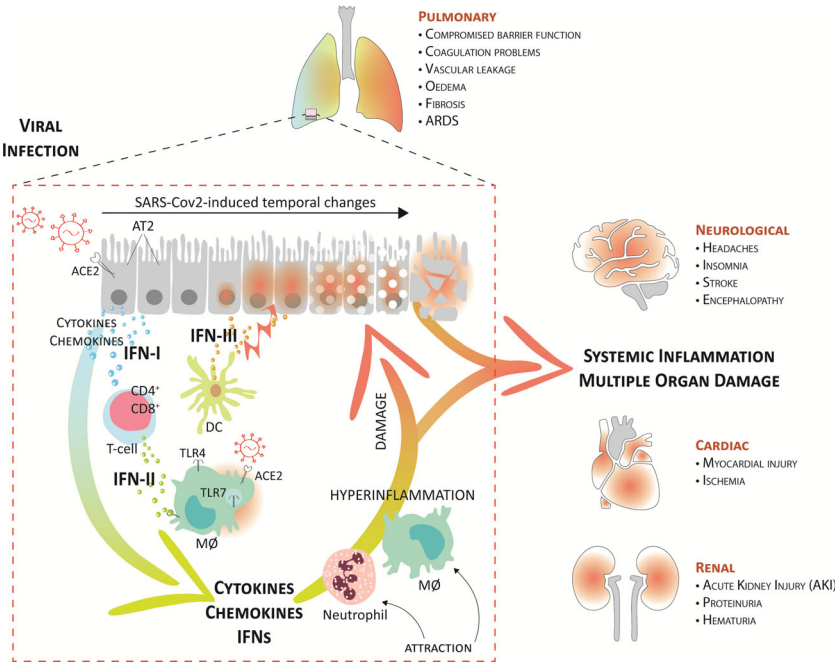

FIGURE 3 | Systemic inflammation and multiple organ damage in severe COVID-19. A current model suggests that upon upper airway entry, SARS-CoV-2 impregnates the lower lungs *via* ACE2, where it infects several target cells, including the alveolar type 2 cells (AT2), alveolar macrophages (MØ), and vascular endothelial cells. Virus cell entry recognition *via* endosomal and cytosolic pattern recognition receptors (as TLR3 and TLR7) trigger the production of IFNs and proinflammatory mediators. Together, the local recruitment of effector T-cells (CD4+ and CD8+) and dendritic cells (DCs), further perpetuates higher proinflammatory cytokines, IFNs, and chemokines in the lung fluid. Consequently, this further augments damage to the lung tissue, mediated by endothelial dysfunction and vasodilation, and leads to the attraction of more inflammatory neutrophils and macrophages that create a pathogenic inflammatory loop in the lung. On the one hand, this leads to respiratory/organ failure and on the other hand, it also results in a "systemic cytokine storm" that causes widespread inflammation and damage to other vulnerable organs, like the heart, kidney, and brain. This can rapidly progress to multiple organ exhaustion, which correlates with a poor prognosis in COVID-19 patients.

the lung tissue, mediated by endothelial dysfunction and vasodilation, and leads to the attraction of more inflammatory neutrophils and macrophages that create a pathogenic inflammatory loop in the lung (**Figure 3**). These systemic cytokine profiles show overlap with cytokine release syndromes, and this highly suggests that COVID-19-associated hyper-inflammation is mediated by an over-activated mononuclear phagocyte (MNP) compartment (73, 74).

Interestingly, excessive IFN production, especially IFN-III, has shown to be an important factor impairing lung epithelial regeneration. IFN-III, unlike other IFNs, activates antiviral response and at the same time limits tissue-damaging functions of neutrophils. Major et al. (75) and Broggi et al. (43) showed that both IFN-I and IFN-III, produced by lung-resident dendritic cells through TLR-3 stimulation, disrupt lung epithelial cell repair during influenza recovery in mice in lower airways. IFN-λ is prevalent compared to IFN-I in virus-infected lungs. Specifically, IFN-λ directly affects epithelial cell proliferation and viability to inhibit tissue repair. With the presence of IFN-I and IFN-III in the lower, but not upper, airways of patients with COVID-19, it is therefore proposed that also during SARS-CoV-2 infection, especially IFN-III produced by activated DCs, acts on lung epithelial cells to compromise lung barrier function (76, 77) (**Figure 3**).

Recently, the cyclic GMP-AMP synthase (cGAS)–stimulator of interferon genes (STING) pathway was implicated in the pathological type I IFN responses in COVID-19. Indeed, a STING-dependent type I IFN signature was observed primarily in macrophages adjacent to areas of endothelial cell damage of COVID-19 skin manifestations. Under these conditions, SARS-CoV-2 infection activated cGAS–STING signaling in endothelial cells through mitochondrial DNA release, resulting in cell death and type I IFN production. Likewise, in lung samples from patients with COVID-19 with prominent tissue destruction, cGAS–STING activity was associated with type I IFN responses. Finally, in SARS-CoV-2 infected epithelial cell lines, such as Calu-3 and A549-ACE2, cGAS–STING activation was also linked to the production of pro-inflammatory cytokines. Together, this potentially identified the cGAS–STING pathway, activated by damaged mitochondrial DNA and not SARS-CoV-2, as a major driver of pathological type I IFN and pro-inflammatory cytokine responses in severe COVID-19 (78–80).

The excessive infiltration of inflammatory immune cells and the amplified production of cytokines, chemokines, and IFNs,

observed in severe COVID-19, result in vascular leakage, coagulation abnormalities, and diminished lung barrier function, which stimulate endotheliitis and lung edema. This limits oxygen exchange and promotes hypoxia, leading to lung failure (81, 82). On the other hand, these excessive inflammatory conditions also result in a "systemic cytokine storm" that causes widespread inflammation and damage to other vulnerable organs, like the heart, spleen, lymph nodes, and kidney, as well as the brain. This can rapidly progress to multiple organ exhaustion, which correlates with a poor prognosis in COVID-19 patients (6, 9, 10) (**Figure 3**).

It is important to realize that under these COVID-19 associated excessive inflammatory conditions, immune cell activation and cytokine and IFN release is tightly regulated by IFN and TLR signaling. Accordingly, maximum expression of many of these pro-inflammatory cytokines and IFN-stimulated genes has shown to depend on combinatorial actions of transcription factors of the STAT, IRF, and NF-kB families. This identifies STATs as potential therapeutic targets in severe COVID-19 (83–88) (**Figure 4**).

Further evidence for this was proposed in one publication where hyperactivation of STAT3 was linked to COVID-19-associated coagulopathy and lung damage. Specifically, plasminogen activator inhibitor-1 (PAI-1) upregulation, as an important STAT3 target, was linked to coagulopathy. TLR4 bound PAI-1 on macrophages could also induce the local production of proinflammatory cytokines and chemokines. This leads to the influx of active innate immune cells to the SARS-CoV-2 infected lung and drives the destruction of lung architecture. Based on this, STAT3 inhibition was proposed as a treatment strategy for COVID- 19 (89). In another study, in Syrian hamsters, which are highly sensitive to SARS-CoV-2 infection and virus-induced lung pathology (90), a STAT2-mediated dysregulated immune response was identified as the driving force. In particular STAT2-dependent type I and III IFN signaling was shown to restrict infection and systemic dissemination of SARS-CoV-2. This was in agreement with the effect of STAT1 in a mouse SARS-CoV infection model (91). Surprisingly, the severe lung damage presented in SARS-CoV-2 infected WT hamsters was absent in STAT2 KO hamsters, contrary to general observations of viral infections in STAT2 −/− mice (92) or STAT2−/− hamsters (93–95). Indeed, pneumonia was absent in SARS-CoV-2 infected STAT2−/− hamsters. Accordingly, this points to an important role of STAT2 in systemic inflammation and severe COVID-19 and identifies it as a novel therapeutic target. Moreover, hamsters could serve as a preferred infection model for the preclinical assessment of vaccines or antiviral therapies, and of anti-inflammatory strategies controlling the hyperactive immune response in severe COVID-19 (96, 97).

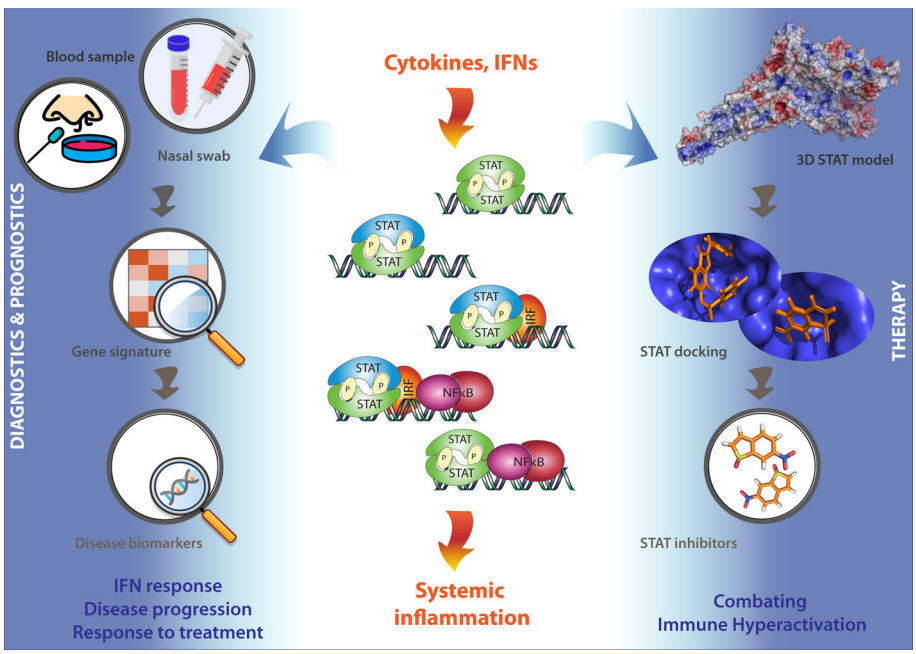

FIGURE 4 | STATs as potential therapeutic targets in COVID-19 patients. Under conditions of excessive inflammation, maximum expression of many pro-inflammatory cytokine and IFN-stimulated genes has shown to depend on combinatorial actions of transcription factors of the STAT, IRF, and NF-kB families. This identifies STATs as potential therapeutic targets in severe COVID-19. Thus, a STAT-dependent pro-inflammatory gene signature could serve as a novel diagnostic tool to monitor and diagnose IFN responses, disease progression, and responses to treatment using blood or nasal swabs from COVID-19 patients (Left). On the other hand, the further testing and optimizing of already available Statinhibs, together with the identification of new Statinhibs using *in silico* 3D STAT modeling, virtual docking and screening, and *in vitro* validation, may offer new clinical benefits in combating immune hyper-activation during severe COVID-19 (Right).

SYSTEMIC INFLAMMATION AND MULTIPLE ORGAN DAMAGE IN SEVERE COVID-19

As shown above, SARS-CoV-2 mainly infects the upper and lower respiratory system but also targets extrapulmonary organs. An important cause of death in COVID-19 disease is ARDS, which is characterized by the "cytokine storm". This results from the release of pro-inflammatory cytokines and chemokines and IFNs by immune effector cells, which mediates widespread inflammation and damage to other vulnerable organs. This can rapidly progress to multiple organ damage, which correlates with a poor prognosis in COVID-19 patients. So far several molecular mechanisms have been described that cause widespread inflammation and damage to vulnerable organs, including cardiovascular, renal, and neurological systems, and contribute to multiple organ exhaustion and death in COVID-19.

Cardiovascular System

With the growing number of COVID-19 infected cases and accumulating clinical data, COVID-19 related cardiovascular diseases have attracted a great deal of concern over an associated mortality rise among infected patients. Likewise, the strong correlation of risk factors such as hypertension and cardiovascular disease with the severity of COVID-19 outcome has already been well established (98). In this aspect, the cardiovascular manifestations in patients with COVID-19 encompass a wide range of complications including myocardial infarction, arrhythmias, heart failure, and hypercoagulation (99). It is well known that ACE2 is abundant in the heart, especially in pericytes, coronary endothelial cells, cardiomyocytes, and cardiac fibroblasts (100). Following SARS-CoV-2 infection and downregulation of ACE2, RAAS is over-activated and may contribute to thrombotic events and inflammatory responses and ultimately leading to microvascular dysfunction and injury (101). Coagulation abnormalities are evidently seen in nearly 20%–55% of hospitalized patients with COVID-19 (102). For instance, in a cohort study of confirmed COVID-19 patients, the elevated levels of D-dimer and fibrin degradation product (FDP) along with prolonged prothrombin time and activated partial thromboplastin time were frequently seen in COVID-19 non-survivors (103). This observation indicates the high incidence of thromboembolic events in COVID-19 cases which might impact vascular homeostasis (104).

In a recent systemic review investigating the potential contribution of hyper-inflammation in the induction of cardiac injuries in the COVID-19 context, the authors concluded that systematic hyper-inflammatory response may trigger cardiac injury in COVID-19 patients including children and adolescents without having pre-existing cardiovascular abnormalities (105). For the hyperinflammation assessment, the markers C-reactive protein(CRP) and/or ferritin and/or IL-6 were employed in their investigation, as both ferritin and IL-6 have been previously shown increases in severe COVID-19 cases in contrast to survivors (106). A retrospective study that explored the relationship between SARS-CoV-2-induced hyperinflammatory response in 317 patients with COVID-19, reported that 14 out of 39 patients with a myocardial injury who showed immune dysregulation, developed myocardial injury nine days after admission (107). This finding may imply that cardiac injury is elicited by the development of inflammatory storms in severe COVID-19 cases. In other words, cytokine storms may contribute to apoptosis or necrosis of the myocardial cells, compromising the hemodynamics of coronary circulation, destabilizing coronary plaque, and instigating vascular microthrombosis (108).

Urinary System

Kidney injury in a quarter of hospitalized patients with COVID-19 has been described in several studies. Indeed, COVID-19 associated acute kidney injury (AKI) is reported with a high mortality rate, particularly in critically ill patients with comorbidities such as hypertension and diabetes (109). Urine analysis of COVID-19 patients displayed alterations in urine sediments including proteinuria and hematuria which is linked with elevated mortality in hospitalized COVID-19 patients (110). Moreover, adequate evidence for the presence of SARS-CoV-2 RNA in the urine of COVID-19-positive patients does not seem robust to accurately predict renal dysfunction (111).

The pathophysiological mechanisms underlying COVID-19 associated AKI remains to be clarified. However, there are COVID-19-specific mechanisms that might play a role in renal dysfunction. Among all, the relationship between ACE2 and the renin-angiotensin-aldosterone system (RAAS) which is disturbed by COVID-19 infection is regarded as a major mechanism engaged in kidney injury (112). In fact, ACE2 as the main receptor for SARS-CoV-2 and highly expressed in kidney (113), is able to convert angiotensin II to angiotensin 1–7, down-regulating RAAS-mediated platelet and endothelial activation, vasoconstriction and release of proinflammatory mediators. However, upon binding of SARS-CoV-2 to ACE2, followed by accumulation of angiotensin II and overactivation of RAAS, leading subsequently to hypercoagulability, endothelial injury, and inflammatory response (114). Based on this understanding, drugs that inhibit RAAS have been suggested as a potential treatment for COVID-19 (115), but it still demands more tailor-made prospective randomized controlled studies to confirm the efficacy of these drugs.

Cytokine storm syndrome which is portrayed as a hyperactive state of the immune system through extensive recruitment of immune cells, is believed to substantially contribute to the severity of COVID-19 infection (116). Likewise, upregulation of cytokines namely IL-6 which is a key element in multi-organ damage including kidney injury, has been frequently recorded in COVID-19 patients (117). It was shown that IFN-α and IFN-β display mutual and differential effects on podocytes and parietal epithelial cells, which collectively advance glomerulosclerosis by inducing podocyte loss and also restricting podocyte regeneration from local progenitors (118). This is of considerable importance since inflammation-induced proteinuria is mediated by podocyte injury and aberrant type I interferon response can further aggravate proteinuric kidney disease (119). Moreover, a growing body of evidence showed the renal levels of C5b-9 which engaged in the complement membrane attack complex, were elevated in severe COVID-19

patients compared with healthy controls. Similarly, C5a triggers abnormal epigenetic changes in renal tubular epithelial cells causing tubular senescence. In addition, C5b–9 is involved in endotheliopathy and thromboinflammation (117, 120). In light of these findings, complement activation might drive inflammation associated with coagulation and thrombosis in the context of COVID-19, exacerbating kidney dysfunction towards to progression of AKI.

Nervous System

There is also a growing body of evidence pointing to complications of the nervous system in patients with COVID-19. These neurological and neuropsychiatric symptoms range from smell and taste alterations to infectious encephalitis. The underlying mechanisms involved in these neurological manifestations are not entirely understood. However, it seems systemic inflammation and deregulated immune activity might cast new light on the causes of SARS-CoV-2-associated neuropathogenesis.

There are conflicting reports about the direct invasion of SARS-CoV-2 to the brain (121–123). Indeed, the varied expression levels of SARS-CoV-2 entry receptors in the central nervous system propose potential routes including the olfactory system and blood-brain barrier (BBB) for direct viral infection. For instance, it was shown that ACE2 and TMPRSS2 are expressed in the cells located in the olfactory epithelium, except for olfactory sensory neurons (124). Likewise, the expression of ACE2 is detected in pericytes which is a part of the neurovascular unit in BBB (125).

According to a meta-analysis of postmortem examinations in COVID-19 patients with neurological manifestations, the main neuropathological features that were documented among over 190 cases were gliosis including astrogliosis and microgliosis, hypoxic alterations, infiltration of inflammatory cells such as macrophages and T- lymphocytes, cerebral microthrombosis, ischaemic brain lesions. In light of these observations, it seems that systemic inflammation and dysregulated coagulation substantially drive neuropathological outcomes including hemorrhages and microthrombi in the context of COVID-19 infection, compared with the injuries caused directly by SARS-CoV-2 infection (126). The contribution of gliosis is further supported by the neuropathological examinations of 43 patients with COVID-19, in which the interplay between activated immune response and nervous system was of considerable note in all examined brain regions where reactive astrogliosis was detectable at varying levels of intensity (122). In fact, reactive astrocytes are regarded to be an indispensable part of the neuroimmune system by promoting neuroprotection in infectious diseases. However, following SARS-CoV-2 infection, the expression levels of glial fibrillary acidic protein (GFAP), as an astrogliosis marker, are highly induced in patients with moderate to severe COVID-19 (127, 128), suggesting the possible role of reactive astrocytes along with aberrant microglial functions in shaping COVID-19-induced cytokine storm, leading ultimately to multiple-organ failure.

Current research on dysregulated immune activity in COVID-19 shows the upregulation of circulating cytokines such as TNF-α, IL-6, and IL-10 (4, 129), suggesting peripheral inflammation induced by COVID-19 might be disseminated to brain parenchyma through compromised BBB and severely affect neurons and glial cells. In this regard, we recently showed the increased levels of neuroinflammatory genes along with gliosis and neuronal death in the cerebral cortex of COVID-19 patients (127), as also reported in (130). Additionally in our study, upon the close histopathologic examination of the post-mortem cerebral cortex of patients with COVID-19, inflammation of blood vessels (vasculitis) was detected, which might pave the way for lymphocytic infiltration and neuronal damage, as already documented in a case report of COVID-19 (131). Thus, disrupted BBB undermines the regulation of BBB permeability and makes the brain vulnerable to the invasion of pathogens and entry of pro-inflammatory mediators, leading to severe systemic disease.

STATS AS POTENTIAL THERAPEUTIC TARGETS IN COVID-19 PATIENTS

Implications for recombinant IFN therapy have strictly been proposed in the early stages of COVID-19 disease, especially during upper respiratory tract infection of SARS-CoV-2. In this respect, the kinetics of IFN-I secretion versus the kinetics of viral replication should help in identifying the window of therapeutic opportunity.

On the other hand, significant progress has been made on therapeutic approaches that can manage the systemic inflammation and hyperactive immune response in severe COVID-19 patients (29, 132–134). Currently, at clinicaltrials.gov over one hundred clinical trials are registered connected to inflammatory cytokine blocking medications as potential treatment strategy in COVID-19 patients.

As the JAK/STAT pathway modulates important inflammatory and immunological pathways, JAKs and STATs serve as potential therapeutic targets in severe COVID-19. Anti-IL6 antibodies (Tocilizumab), BTK inhibition with ibrutinib and acalabrutinib, as well as the known JAK inhibitors- Ruxolitinib, Fedratinib, and Baricitinib are part of potential treatment strategies against COVID-19 that combine antiviral and anti-inflammatory agents (135–139). Ruxolitinib entered phase III clinical trials (NCT04120090, NCT03533790) and Fedratinib phase II, both were used in connection with pneumonia-associated COVID-19 disease.

Strategies to inhibit the JAK-STAT pathway identified numerous JAK inhibitors (Jakinibs), which mostly are known as pan-JAK inhibitors. For example, the FDA approved Tofacitinib, Ruxolitinib, Fedratinib, and Baricitinib, which inhibit multiple JAKs. Likewise, a high number of small molecules have been identified that target the pTyr-SH2 interaction area of STAT3, and in analogy to Jakinhibs indicated as Statinibs (140, 141). They were recently compiled by our group in SINBAD, a curated open-access database of more than 175 Statinhibs which have been published and described in scientific articles providing proof of their inhibitory properties. It is a tool allowing user-friendly analysis

of experimental conditions and provides detailed information about known STAT inhibitory compounds (142); datasets are available at http://sinbad.amu.edu.pl as well as through the public repository https://doi.org/10.6084/m9.figshare.14975136.v1 (142).

Among the first reported Statinhibs was STA-21, which was shown to inhibit STAT3 dimerization, DNA binding, and STAT3-dependent transcription in breast cancer cells (143). Similarly, the known Statinhibs STATTIC and STX-0119 inhibited phosphorylation, dimerization and nuclear translocation of STAT3, leading to increased apoptosis of cancer cells [reviewed in (87, 144, 145)].

As part of a novel strategy to characterize and understand STAT-inhibition, we combined comparative *in silico* docking and virtual screening of multiple STAT-SH2 models with *in vitro* validation of STAT inhibition (146, 147). This led to the identification of a novel class of multi-STAT or pan-STAT inhibitor, C01L_F03 that commonly and with equal affinity targets the SH2 domain of STAT1, 2, and 3. Interestingly, STATTIC and STX-0119 displayed similar STAT cross-binding characteristics. During anti-microbial and inflammatory responses, macrophage activation, and cytokine release is tightly regulated by IFN and TLR signaling. Accordingly, maximum expression of important pro-inflammatory and chemokine genes depends on cross-talk between IFNs and TLR signaling through collaborative actions of STATs, IRFs, and NF-kB. Recently, we further proved that in macrophages, dendritic cells and vascular smooth muscle cells, under conditions of IFN and TLR cross-talk, the above-mentioned novel pan-STAT inhibitors (with STATTIC being the most potent one) managed genome-wide inhibition of multiple cytokines, chemokines and anti-viral products. Accordingly, a novel STAT-inhibitory strategy was developed for the inhibition of pro-inflammatory cytokine-dependent migration of endothelial cells, adhesion of leukocytes to endothelial cells, and loss of contractility of mesenteric arteries (148).

Promising results for several FDA-approved inhibitors [Tofacitinib: pan-JAK inhibition; Ruxolitinib: JAK1/2-inhibition; Tocilizumab: IL6 receptor antibody); or (pre)Clinical Trial tested [sb1578: JAK2-inhibition; WP1066: JAK2-inhibition; STA-21: STAT3-SH2 inhibition; STATTIC: STAT3-SH2 inhibition], promises entry of Statinhibs to the clinic shortly (87). So far, Statinhibs have not been implicated in connection to COVID-19. However, the further testing and optimizing of already available Statinhibs, together with the identification of new Statinhibs, may offer new clinical benefits in combating immune hyperactivation during severe COVID-19. In this context, according to Toubiana et al., "care must be taken to apply STAT targeting therapeutic strategies in a stage-appropriate manner, because some approaches that may help in the earlier stages of the disease could be detrimental if used in its later stages. With the potential use for COVID-19 treatment of existing drugs that enhance STAT1 or inhibit STAT3 functions, problems could arise. For example, chronic mucocutaneous candidiasis (CMC) was present in 98% of patients with gain of function (GOF) mutations in STAT1 in one study of 274 individuals, and the few that did not have CMC, had invasive fungal or bacterial infections. Generally, the immune profile was relatively normal, but 82% had decreased Th17 cells" (149). Conversely, a STAT-dependent pro-inflammatory gene signature could serve as a novel diagnostic tool to monitor and diagnose IFN responses, disease progression, and responses to treatment using blood or nasal swabs from COVID-19 patients (**Figure 4**).

AUTHOR CONTRIBUTIONS

MEB was involved in concept development and writing and editing of the manuscript. AS, AA and SH designed figures. MS, HN, NL, AO, KK, and JW participated in the development of the concept and critically evaluated and edited the manuscript. HB developed the concept and was involved in writing and editing the manuscript and coordinated input from all co-authors. All authors contributed to the article and approved the submitted version.

FUNDING

This publication was supported by grant UMO 2016/23/B/NZ2/00623 (HAR.B.) from the National Science Centre Poland and grant 7/2020 (HAR.B.) from the Adam Mickiewicz University in Poznan.

REFERENCES

1. Wu F, Zhao S, Yu B, Chen Y-M, Wang W, Song Z-G, et al. A New Coronavirus Associated With Human Respiratory Disease in China. *Nature* (2020) 579(7798):265–9. doi: 10.1038/s41586-020-2008-3
2. Zhou P, Yang X-L, Wang X-G, Hu B, Zhang L, Zhang W, et al. A Pneumonia Outbreak Associated With a New Coronavirus of Probable Bat Origin. *Nature* (2020) 579(7798):270–3. doi: 10.1038/s41586-020-2012-7
3. Guan W-J, Ni Z-Y, Hu Y, Liang W-H, Ou C-Q, He J-X, et al. Clinical Characteristics of Coronavirus Disease 2019 in China. *N Engl J Med* (2020) 382(18):1708–20. doi: 10.1056/NEJMoa2002032
4. Huang C, Wang Y, Li X, Ren L, Zhao J, Hu Y, et al. Clinical Features of Patients Infected With 2019 Novel Coronavirus in Wuhan, China. *Lancet* (2020) 395(10223):497–506. doi: 10.1016/S0140-6736(20)30183-5
5. Wang D, Hu B, Hu C, Zhu F, Liu X, Zhang J, et al. Clinical Characteristics of 138 Hospitalized Patients With 2019 Novel Coronavirus–Infected Pneumonia in Wuhan, China. *Jama* (2020) 323(11):1061–9. doi: 10.1001/jama.2020.1585
6. Lopes-Pacheco M, Silva PL, Cruz FF, Battaglini D, Robba C, Pelosi P, et al. Pathogenesis of Multiple Organ Injury in Covid-19 and Potential Therapeutic Strategies. *Front Physiol* (2021) 29. doi: 10.3389/fphys.2021.593223
7. Antonczyk A, Krist B, Sajek M, Michalska A, Piaszyk-Borychowska A, Plens-Galaska M, et al. Direct Inhibition of Irf-Dependent Transcriptional Regulatory Mechanisms Associated With Disease. *Front Immunol* (2019) 10:1176. doi: 10.3389/fimmu.2019.01176
8. Michalska A, Blaszczyk K, Wesoly J, Bluyssen HA. A Positive Feedback Amplifier Circuit That Regulates Interferon (Ifn)-Stimulated Gene Expression and Controls Type I and Type Ii Ifn Responses. *Front Immunol* (2018) 9:1135. doi: 10.3389/fimmu.2018.01135

9. Park A, Iwasaki A. Type I and Type Iii Interferons–Induction, Signaling, Evasion, and Application to Combat Covid-19. *Cell Host Microbe* (2020) 27 (6):870–8. doi: 10.1016/j.chom.2020.05.008
10. Schultze JL, Aschenbrenner AC. Covid-19 and the Human Innate Immune System. *Cell* (2021) 184(7):1671–92. doi: 10.1016/j.cell.2021.02.029
11. Li W, Moore MJ, Vasilieva N, Sui J, Wong SK, Berne MA, et al. Angiotensin-Converting Enzyme 2 Is a Functional Receptor for the Sars Coronavirus. *Nature* (2003) 426(6965):450–4. doi: 10.1038/nature02145
12. Wan Y, Shang J, Graham R, Baric RS, Li F. Receptor Recognition by the Novel Coronavirus From Wuhan: An Analysis Based on Decade-Long Structural Studies of Sars Coronavirus. *J Virol* (2020) 94(7):e00127–20. doi: 10.1128/JVI.00127-20
13. Hoffmann M, Kleine-Weber H, Schroeder S, Krüger N, Herrler T, Erichsen S, et al. Sars-Cov-2 Cell Entry Depends on Ace2 and Tmprss2 and Is Blocked by a Clinically Proven Protease Inhibitor. *cell* (2020) 181(2):271–80. doi: 10.1016/j.cell.2020.02.052
14. Matsuyama S, Nagata N, Shirato K, Kawase M, Takeda M, Taguchi F. Efficient Activation of the Severe Acute Respiratory Syndrome Coronavirus Spike Protein by the Transmembrane Protease Tmprss2. *J Virol* (2010) 84 (24):12658–64. doi: 10.1128/JVI.01542-10
15. Cantuti-Castelvetri L, Ojha R, Pedro LD, Djannatian M, Franz J, Kuivanen S, et al. Neuropilin-1 Facilitates Sars-Cov-2 Cell Entry and Infectivity. *Science* (2020) 370(6518):856–60. doi: 10.1126/science.abd2985
16. Bost P, Giladi A, Liu Y, Bendjelal Y, Xu G, David E, et al. Host-Viral Infection Maps Reveal Signatures of Severe Covid-19 Patients. *Cell* (2020) 181(7):1475–88. doi: 10.1016/j.cell.2020.05.006
17. Chua RL, Lukassen S, Trump S, Hennig BP, Wendisch D, Pott F, et al. Covid-19 Severity Correlates With Airway Epithelium–Immune Cell Interactions Identified by Single-Cell Analysis. *Nat Biotechnol* (2020) 38 (8):970–9. doi: 10.1038/s41587-020-0602-4
18. Zou X, Chen K, Zou J, Han P, Hao J, Han Z. Single-Cell Rna-Seq Data Analysis on the Receptor Ace2 Expression Reveals the Potential Risk of Different Human Organs Vulnerable to 2019-Ncov Infection. *Front Med* (2020) 14(2):185–92. doi: 10.1007/s11684-020-0754-0
19. Barbry P, Muus C, Luecken M, Eraslan G, Waghray A, Heimberg G, et al. Integrated Analyses of Single-Cell Atlases Reveal Age, Gender, and Smoking Status Associations With Cell Type-Specific Expression of Mediators of Sars-Cov-2 Viral Entry and Highlights Inflammatory Programs in Putative Target Cells. *bioRxiv* (2020) 2020.04.19.049254. doi: 10.1101/2020.04.19.049254
20. Gheblawi M, Wang K, Viveiros A, Nguyen Q, Zhong J-C, Turner AJ, et al. Angiotensin-Converting Enzyme 2: Sars-Cov-2 Receptor and Regulator of the Renin-Angiotensin System: Celebrating the 20th Anniversary of the Discovery of Ace2. *Circ Res* (2020) 126(10):1456–74. doi: 10.1161/CIRCRESAHA.120.317015
21. Leung JM, Yang CX, Tam A, Shaipanich T, Hackett T-L, Singhera GK, et al. Ace-2 Expression in the Small Airway Epithelia of Smokers and Copd Patients: Implications for Covid-19. *Eur Respir J* (2020) 55(5):2000688. doi: 10.1183/13993003.00688-2020
22. Iaccarino G, Grassi G, Borghi C, Ferri C, Salvetti M, Volpe M. Age and Multimorbidity Predict Death Among Covid-19 Patients: Results of the Sars-Ras Study of the Italian Society of Hypertension. *Hypertension* (2020) 76(2):366–72. doi: 10.1161/HYPERTENSIONAHA.120.15324
23. Williamson EJ, Walker AJ, Bhaskaran K, Bacon S, Bates C, Morton CE, et al. Opensafely: Factors Associated With Covid-19 Death in 17 Million Patients. *Nature* 584:430–36 (2020). doi: 10.1038/s41586-020-2521-4
24. Wu Z, McGoogan JM. Characteristics of and Important Lessons From the Coronavirus Disease 2019 (Covid-19) Outbreak in China: Summary of a Report of 72 314 Cases From the Chinese Center for Disease Control and Prevention. *JAMA* (2020) 323(13):1239–42. doi: 10.1001/jama.2020.2648
25. Zhou F, Yu T, Du R, Fan G, Liu Y, Liu Z, et al. Clinical Course and Risk Factors for Mortality of Adult Inpatients With Covid-19 in Wuhan, China: A Retrospective Cohort Study. *Lancet* (2020) 395(10229):1054–62. doi: 10.1016/S0140-6736(20)30566-3
26. Ackermann M, Verleden SE, Kuehnel M, Haverich A, Welte T, Laenger F, et al. Pulmonary Vascular Endothelialitis, Thrombosis, and Angiogenesis in Covid-19. *N Engl J Med* (2020) 383(2):120–8. doi: 10.1056/NEJMoa2015432
27. Chen N, Zhou M, Dong X, Qu J, Gong F, Han Y, et al. Epidemiological and Clinical Characteristics of 99 Cases of 2019 Novel Coronavirus Pneumonia in Wuhan, China: A Descriptive Study. *Lancet* (2020) 395(10223):507–13. doi: 10.1016/S0140-6736(20)30211-7
28. Liu J, Li S, Liu J, Liang B, Wang X, Wang H, et al. Longitudinal Characteristics of Lymphocyte Responses and Cytokine Profiles in the Peripheral Blood of Sars-Cov-2 Infected Patients. *EBioMedicine* (2020) 55:102763. doi: 10.1016/j.ebiom.2020.102763
29. Zhang C, Wu Z, Li J-W, Zhao H, Wang G-Q. Cytokine Release Syndrome in Severe Covid-19: Interleukin-6 Receptor Antagonist Tocilizumab May Be the Key to Reduce Mortality. *Int J Antimicrob Agents* (2020) 55(5):105954. doi: 10.1016/j.ijantimicag.2020.105954
30. Lee JS, Park S, Jeong HW, Ahn JY, Choi SJ, Lee H, et al. Immunophenotyping of Covid-19 and Influenza Highlights the Role of Type I Interferons in Development of Severe Covid-19. *Sci Immunol* (2020) 5(49):eabd1554. doi: 10.1126/sciimmunol.abd1554
31. Helms J, Tacquard C, Severac F, Leonard-Lorant I, Ohana M, Delabranche X, et al. High Risk of Thrombosis in Patients With Severe Sars-Cov-2 Infection: A Multicenter Prospective Cohort Study. *Intensive Care Med* (2020) 46(6):1089–98. doi: 10.1007/s00134-020-06062-x
32. Tang N, Bai H, Chen X, Gong J, Li D, Sun Z. Anticoagulant Treatment Is Associated With Decreased Mortality in Severe Coronavirus Disease 2019 Patients With Coagulopathy. *J Thromb Haemostasis* (2020) 18(5):1094–9. doi: 10.1111/jth.14817
33. Mazaleuskaya L, Veltrop R, Ikpeze N, Martin-Garcia J, Navas-Martin S. Protective Role of Toll-Like Receptor 3-Induced Type I Interferon in Murine Coronavirus Infection of Macrophages. *Viruses* (2012) 4(5):901–23. doi: 10.3390/v4050901
34. Sa Ribero M, Jouvenet N, Dreux M, Nisole S. Interplay Between Sars-Cov-2 and the Type I Interferon Response. *PloS Pathog* (2020) 16(7):e1008737. doi: 10.1371/journal.ppat.1008737
35. Gilliet M, Cao W, Liu Y-J. Plasmacytoid Dendritic Cells: Sensing Nucleic Acids in Viral Infection and Autoimmune Diseases. *Nat Rev Immunol* (2008) 8(8):594–606. doi: 10.1038/nri2358
36. Cameron MJ, Bermejo-Martin JF, Danesh A, Muller MP, Kelvin DJ. Human Immunopathogenesis of Severe Acute Respiratory Syndrome (Sars). *Virus Res* (2008) 133(1):13–9. doi: 10.1016/j.virusres.2007.02.014
37. Lim YX, Ng YL, Tam JP, Liu DX. Human Coronaviruses: A Review of Virus–Host Interactions. *Diseases* (2016) 4(3):26. doi: 10.3390/diseases4030026
38. Nelemans T, Kikkert M. Viral Innate Immune Evasion and the Pathogenesis of Emerging Rna Virus Infections. *Viruses* (2019) 11(10):961. doi: 10.3390/v11100961
39. Totura AL, Baric RS. Sars Coronavirus Pathogenesis: Host Innate Immune Responses and Viral Antagonism of Interferon. *Curr Opin Virol* (2012) 2 (3):264–75. doi: 10.1016/j.coviro.2012.04.004
40. Zhang Q, Bastard P, Cobat A, Casanova J-L. Human Genetic and Immunological Determinants of Critical Covid-19 Pneumonia. *Nature* (2022) 603:587–98. doi: 10.1038/s41586-022-04447-0
41. Hadjadj J, Yatim N, Barnabei L, Corneau A, Boussier J, Smith N, et al. Impaired Type I Interferon Activity and Inflammatory Responses in Severe Covid-19 Patients. *Science* (2020) 369(6504):718–24. doi: 10.1126/science.abc6027
42. Blanco-Melo D, Nilsson-Payant BE, Liu W-C, Uhl S, Hoagland D, Møller R, et al. Imbalanced Host Response to Sars-Cov-2 Drives Development of Covid-19. *Cell* (2020) 181(5):1036–45. doi: 10.1016/j.cell.2020.04.026
43. Broggi A, Ghosh S, Sposito B, Spreafico R, Balzarini F, Lo Cascio A, et al. Type Iii Interferons Disrupt the Lung Epithelial Barrier Upon Viral Recognition. *Science* (2020) 369(6504):706–12. doi: 10.1126/science.abc3545
44. King C, Sprent J. Dual Nature of Type I Interferons in Sars-Cov-2-Induced Inflammation. *Trends Immunol* (2021) 42(4):312–22. doi: 10.1016/j.it.2021.02.003
45. Lucas C, Wong P, Klein J, Castro TB, Silva J, Sundaram M, et al. Longitudinal Analyses Reveal Immunological Misfiring in Severe Covid-19. *Nature* (2020) 584(7821):463–9. doi: 10.1038/s41586-020-2588-y
46. Israelow B, Song E, Mao T, Lu P, Meir A, Liu F, et al. Mouse Model of Sars-Cov-2 Reveals Inflammatory Role of Type I Interferon Signaling. *J Exp Med* (2020) 217(12):e20201241. doi: 10.1084/jem.20201241

47. R Channappanavar and S Perlman eds. Pathogenic Human Coronavirus Infections: Causes and Consequences of Cytokine Storm and Immunopathology. *Semin Immunopathol* (2017) 39:529–39. doi: 10.1007/s00281-017-0629-x
48. Kindler E, Thiel V, Weber F. Interaction of Sars and Mers Coronaviruses With the Antiviral Interferon Response. *Adv Virus Res* (2016) 96:219–43. doi: 10.1016/bs.aivir.2016.08.006
49. Frieman M, Ratia K, Johnston RE, Mesecar AD, Baric RS. Severe Acute Respiratory Syndrome Coronavirus Papain-Like Protease Ubiquitin-Like Domain and Catalytic Domain Regulate Antagonism of Irf3 and Nf-Kb Signaling. *J Virol* (2009) 83(13):6689–705. doi: 10.1128/JVI.02220-08
50. Niemeyer D, Mösbauer K, Klein EM, Sieberg A, Mettelman RC, Mielech AM, et al. The Papain-Like Protease Determines a Virulence Trait That Varies Among Members of the Sars-Coronavirus Species. *PloS Pathog* (2018) 14(9):e1007296. doi: 10.1371/journal.ppat.1007296
51. Lei X, Dong X, Ma R, Wang W, Xiao X, Tian Z, et al. Activation and Evasion of Type I Interferon Responses by Sars-Cov-2. *Nat Commun* (2020) 11(1):1–12. doi: 10.1038/s41467-020-17665-9
52. Yuen C-K, Lam J-Y, Wong W-M, Mak L-F, Wang X, Chu H, et al. Sars-Cov-2 Nsp13, Nsp14, Nsp15 and Orf6 Function as Potent Interferon Antagonists. *Emerging Microbes Infect* (2020) 9(1):1418–28. doi: 10.1080/22221751.2020.1780953
53. Li G, Fan Y, Lai Y, Han T, Li Z, Zhou P, et al. Coronavirus Infections and Immune Responses. *J Med Virol* (2020) 92(4):424–32. doi: 10.1002/jmv.25685
54. Konno Y, Kimura I, Uriu K, Fukushi M, Irie T, Koyanagi Y, et al. Sars-Cov-2 Orf3b Is a Potent Interferon Antagonist Whose Activity Is Increased by a Naturally Occurring Elongation Variant. *Cell Rep* (2020) 32(12):108185. doi: 10.1016/j.celrep.2020.108185
55. Xia H, Cao Z, Xie X, Zhang X, Chen JY-C, Wang H, et al. Evasion of Type I Interferon by Sars-Cov-2. *Cell Rep* (2020) 33(1):108234. doi: 10.1016/j.celrep.2020.108234
56. Zhang Q, Chen Z, Huang C, Sun J, Xue M, Feng T, et al. Severe Acute Respiratory Syndrome Coronavirus 2 (Sars-Cov-2) Membrane (M) and Spike (S) Proteins Antagonize Host Type I Interferon Response. *Front Cell Infect Microbiol* (2021) 1242. doi: 10.3389/fcimb.2021.766922
57. Mu J, Fang Y, Yang Q, Shu T, Wang A, Huang M, et al. Sars-Cov-2 N Protein Antagonizes Type I Interferon Signaling by Suppressing Phosphorylation and Nuclear Translocation of Stat1 and Stat2. *Cell Discov* (2020) 6(1):1–4. doi: 10.1038/s41421-020-00208-3
58. Yoo J-S, Sasaki M, Cho SX, Kasuga Y, Zhu B, Ouda R, et al. Sars-Cov-2 Inhibits Induction of the Mhc Class I Pathway by Targeting the Stat1-Irf1-Nlrc5 Axis. *Nat Commun* (2021) 12(1):1–17. doi: 10.1038/s41467-021-26910-8
59. Rincon-Arevalo H, Aue A, Ritter J, Szelinski F, Khadzhynov D, Zickler D, et al. Altered Increase in Stat1 Expression and Phosphorylation in Severe Covid-19. *Eur J Immunol* (2022) 52(1):138–48. doi: 10.1002/eji.202149575
60. De Wit E, Van Doremalen N, Falzarano D, Munster VJ. Sars and Mers: Recent Insights Into Emerging Coronaviruses. *Nat Rev Microbiol* (2016) 14(8):523–34. doi: 10.1038/nrmicro.2016.81
61. Fehr AR, Channappanavar R, Perlman S. Middle East Respiratory Syndrome: Emergence of a Pathogenic Human Coronavirus. *Annu Rev Med* (2017) 68:387–99. doi: 10.1146/annurev-med-051215-031152
62. Newton AH, Cardani A, Braciale TJ. The Host Immune Response in Respiratory Virus Infection: Balancing Virus Clearance and Immunopathology. *Semin Immunopathol* 38(4):471–82 (2016). doi: 10.1007/s00281-016-0558-0
63. Channappanavar R, Fehr AR, Vijay R, Mack M, Zhao J, Meyerholz DK, et al. Dysregulated Type I Interferon and Inflammatory Monocyte-Macrophage Responses Cause Lethal Pneumonia in Sars-Cov-Infected Mice. *Cell Host Microbe* (2016) 19(2):181–93. doi: 10.1016/j.chom.2016.01.007
64. Harrison AG, Lin T, Wang P. Mechanisms of Sars-Cov-2 Transmission and Pathogenesis. *Trends Immunol* (2020) 41(12):1100–15. doi: 10.1016/j.it.2020.10.004
65. Kuri-Cervantes L, Pampena MB, Meng W, Rosenfeld AM, Ittner CA, Weisman AR, et al. Comprehensive Mapping of Immune Perturbations Associated With Severe Covid-19. *Sci Immunol* (2020) 5(49):eabd7114. doi: 10.1126/sciimmunol.abd7114
66. Lagunas-Rangel FA. Neutrophil-To-Lymphocyte Ratio and Lymphocyte-To-C-Reactive Protein Ratio in Patients With Severe Coronavirus Disease 2019 (Covid-19): A Meta-Analysis. *J Med Virol* 92(10):1733–34. (2020). doi: 10.1002/jmv.25819
67. Liu Y, Du X, Chen J, Jin Y, Peng L, Wang HH, et al. Neutrophil-To-Lymphocyte Ratio as an Independent Risk Factor for Mortality in Hospitalized Patients With Covid-19. *J Infect* (2020) 81(1):e6–e12. doi: 10.1016/j.jinf.2020.04.002
68. Qin C, Zhou L, Hu Z, Zhang S, Yang S, Tao Y, et al. Dysregulation of Immune Response in Patients With Coronavirus 2019 (Covid-19) in Wuhan, China. *Clin Infect Dis* (2020) 71(15):762–8. doi: 10.1093/cid/ciaa248
69. Arunachalam PS, Wimmers F, Mok CKP, Perera RA, Scott M, Hagan T, et al. Systems Biological Assessment of Immunity to Mild Versus Severe Covid-19 Infection in Humans. *Science* (2020) 369(6508):1210–20. doi: 10.1126/science.abc6261
70. Xiong Y, Liu Y, Cao L, Wang D, Guo M, Jiang A, et al. Transcriptomic Characteristics of Bronchoalveolar Lavage Fluid and Peripheral Blood Mononuclear Cells in Covid-19 Patients. *Emerging Microbes Infect* (2020) 9(1):761–70. doi: 10.1080/22221751.2020.1747363
71. Stephenson E, Reynolds G, Botting RA, Calero-Nieto FJ, Morgan MD, Tuong ZK, et al. Single-Cell Multi-Omics Analysis of the Immune Response in Covid-19. *Nat Med* (2021) 27(5):904–16. doi: 10.1038/s41591-021-01329-2
72. Merad M, Martin JC. Pathological Inflammation in Patients With Covid-19: A Key Role for Monocytes and Macrophages. *Nat Rev Immunol* (2020) 20(6):355–62. doi: 10.1038/s41577-020-0331-4
73. Mehta P, McAuley DF, Brown M, Sanchez E, Tattersall RS, Manson JJ. Covid-19: Consider Cytokine Storm Syndromes and Immunosuppression. *Lancet* (2020) 395(10229):1033–4. doi: 10.1016/S0140-6736(20)30628-0
74. Schulert GS, Grom AA. Pathogenesis of Macrophage Activation Syndrome and Potential for Cytokine-Directed Therapies. *Annu Rev Med* (2015) 66:145–59. doi: 10.1146/annurev-med-061813-012806
75. Major J, Crotta S, Llorian M, McCabe TM, Gad HH, Priestnall SL, et al. Type I and Iii Interferons Disrupt Lung Epithelial Repair During Recovery From Viral Infection. *Science* (2020) 369(6504):712–7. doi: 10.1126/science.abc2061
76. Broggi A, Granucci F, Zanoni I. Type Iii Interferons: Balancing Tissue Tolerance and Resistance to Pathogen Invasion. *J Exp Med* (2020) 217(1):e20190295. doi: 10.1084/jem.20190295
77. Prokunina-Olsson L, Alphonse N, Dickenson RE, Durbin JE, Glenn JS, Hartmann R, et al. Covid-19 and Emerging Viral Infections: The Case for Interferon Lambda. *J Exp Med* (2020) 217(5):e20200653. doi: 10.1084/jem.20200653
78. Di Domizio J, Gulen MF, Saidoune F, Thacker VV, Yatim A, Sharma K, et al. The Cgas-Sting Pathway Drives Type I Ifn Immunopathology in Covid-19. *Nature* (2022) 603:145–51. doi: 10.1038/s41586-022-04421-w
79. Neufeldt CJ, Cerikan B, Cortese M, Frankish J, Lee J-Y, Plociennikowska A, et al. Sars-Cov-2 Infection Induces a Pro-Inflammatory Cytokine Response Through Cgas-Sting and Nf-Kb. *Commun Biol* (2022) 5:45. doi: 10.1038/s42003-021-02983-5
80. Andreakos E. Stinging Type I Ifn-Mediated Immunopathology in Covid-19. *Nat Immunol* (2022) 23:478–80. doi: 10.1038/s41590-022-01174-6
81. Berlin DA, Gulick RM, Martinez FJ. Severe Covid-19. *N Engl J Med* (2020) 383(25):2451–60. doi: 10.1056/NEJMcp2009575
82. Gandhi RT, Lynch JB, Del Rio C. Mild or Moderate Covid-19. *N Engl J Med* (2020) 383(18):1757–66. doi: 10.1056/NEJMcp2009249
83. Schroder K, Sweet MJ, Hume DA. Signal Integration Between Ifnγ and Tlr Signalling Pathways in Macrophages. *Immunobiology* (2006) 211(6-8):511–24. doi: 10.1016/j.imbio.2006.05.007
84. Hu X, Chen J, Wang L, Ivashkiv LB. Crosstalk Among Jak-Stat, Toll-Like Receptor, and Itam-Dependent Pathways in Macrophage Activation. *J Leukocyte Biol* (2007) 82(2):237–43. doi: 10.1189/jlb.1206763
85. Hu X, Chakravarty SD, Ivashkiv LB. Regulation of Interferon and Toll-Like Receptor Signaling During Macrophage Activation by Opposing Feedforward and Feedback Inhibition Mechanisms. *Immunol Rev* (2008) 226(1):41–56. doi: 10.1111/j.1600-065X.2008.00707.x
86. Hu X, Ivashkiv LB. Cross-Regulation of Signaling Pathways by Interferon-Γ: Implications for Immune Responses and Autoimmune Diseases. *Immunity* (2009) 31(4):539–50. doi: 10.1016/j.immuni.2009.09.002

87. Szelag M, Piaszyk-Borychowska A, Plens-Galaska M, Wesoly J, Bluyssen HA. Targeted Inhibition of Stats and Irfs as a Potential Treatment Strategy in Cardiovascular Disease. *Oncotarget* (2016) 7(30):48788. doi: 10.18632/oncotarget.9195
88. Piaszyk-Borychowska A, Széles L, Csermely A, Chiang H-C, Wesoły J, Lee C-K, et al. Signal Integration of Ifn-I and Ifn-Ii With Tlr4 Involves Sequential Recruitment of Stat1-Complexes and Nfκb to Enhance Pro-Inflammatory Transcription. *Front Immunol* (2019) 10:1253. doi: 10.3389/fimmu.2019.01253
89. Matsuyama T, Kubli SP, Yoshinaga SK, Pfeffer K, Mak TW. An Aberrant Stat Pathway Is Central to Covid-19. *Cell Death Differ* (2020) 27(12):3209–25. doi: 10.1038/s41418-020-00633-7
90. Boudewijns R, Thibaut HJ, Kaptein SJ, Li R, Vergote V, Seldeslachts L, et al. Stat2 Signaling Restricts Viral Dissemination But Drives Severe Pneumonia in Sars-Cov-2 Infected Hamsters. *Nat Commun* (2020) 11(1):1–10. doi: 10.1038/s41467-020-19684-y
91. Frieman MB, Chen J, Morrison TE, Whitmore A, Funkhouser W, Ward JM, et al. Sars-Cov Pathogenesis Is Regulated by a Stat1 Dependent But a Type I, Ii and Iii Interferon Receptor Independent Mechanism. *PloS Pathog* (2010) 6 (4):e1000849. doi: 10.1371/journal.ppat.1000849
92. Park C, Li S, Cha E, Schindler C. Immune Response in Stat2 Knockout Mice. *Immunity* (2000) 13(6):795–804. doi: 10.1016/S1074-7613(00)00077-7
93. Toth K, Lee SR, Ying B, Spencer JF, Tollefson AE, Sagartz JE, et al. Stat2 Knockout Syrian Hamsters Support Enhanced Replication and Pathogenicity of Human Adenovirus, Revealing an Important Role of Type I Interferon Response in Viral Control. *PloS Pathog* (2015) 11(8): e1005084. doi: 10.1371/journal.ppat.1005084
94. Gowen BB, Westover JB, Miao J, Van Wettere AJ, Rigas JD, Hickerson BT, et al. Modeling Severe Fever With Thrombocytopenia Syndrome Virus Infection in Golden Syrian Hamsters: Importance of Stat2 in Preventing Disease and Effective Treatment With Favipiravir. *J Virol* (2017) 91(3): e01942–16. doi: 10.1128/JVI.01942-16
95. Siddharthan V, Van Wettere AJ, Li R, Miao J, Wang Z, Morrey JD, et al. Zika Virus Infection of Adult and Fetal Stat2 Knock-Out Hamsters. *Virology* (2017) 507:89–95. doi: 10.1016/j.virol.2017.04.013
96. Zumla A, Hui DS, Azhar EI, Memish ZA, Maeurer M. Reducing Mortality From 2019-Ncov: Host-Directed Therapies Should Be an Option. *Lancet* (2020) 395(10224):e35–e6. doi: 10.1016/S0140-6736(20)30305-6
97. Liu Q, Zhou Y-h, Yang Z-q. The Cytokine Storm of Severe Influenza and Development of Immunomodulatory Therapy. *Cell Mol Immunol* (2016) 13 (1):3–10. doi: 10.1038/cmi.2015.74
98. Asokan I, Rabadia SV, Yang EH. The Covid-19 Pandemic and Its Impact on the Cardio-Oncology Population. *Curr Oncol Rep* (2020) 22(6):60. doi: 10.1007/s11912-020-00945-4
99. Kwenandar F, Japar KV, Damay V, Hariyanto TI, Tanaka M, Lugito NPH, et al. Coronavirus Disease 2019 and Cardiovascular System: A Narrative Review. *IJC Heart Vasculature* (2020) 29:100557. doi: 10.1016/j.ijcha.2020.100557
100. Guo J, Huang Z, Lin L, Lv J. Coronavirus Disease 2019 (Covid-19) and Cardiovascular Disease: A Viewpoint on the Potential Influence of Angiotensin-Converting Enzyme Inhibitors/Angiotensin Receptor Blockers on Onset and Severity of Severe Acute Respiratory Syndrome Coronavirus 2 Infection. *J Am Heart Assoc* (2020) 9(7):e016219. doi: 10.1161/JAHA.120.016219
101. Silhol F, Sarlon G, Deharo J-C, Vaïsse B. Downregulation of Ace2 Induces Overstimulation of the Renin–Angiotensin System in Covid-19: Should We Block the Renin–Angiotensin System? *Hypertension Res* (2020) 43(8):854–6. doi: 10.1038/s41440-020-0476-3
102. Lee SG, Fralick M, Sholzberg M. Coagulopathy Associated With Covid-19. *CMAJ* (2020) 192(21):E583–E. doi: 10.1503/cmaj.200685
103. Tang N, Li D, Wang X, Sun Z. Abnormal Coagulation Parameters Are Associated With Poor Prognosis in Patients With Novel Coronavirus Pneumonia. *J Thromb Haemostasis* (2020) 18(4):844–7. doi: 10.1111/jth.14768
104. Robba C, Battaglini D, Ball L, Valbusa A, Porto I, Della Bona R, et al. Coagulative Disorders in Critically Ill Covid-19 Patients With Acute Distress Respiratory Syndrome: A Critical Review. *J Clin Med* (2021) 10(1):140. doi: 10.3390/jcm10010140
105. Aldien AS, Ganesan GS, Wahbeh F, Al-Nassr N, Altarawneh H, Al Theyab L, et al. Systemic Inflammation May Induce Cardiac Injury in Covid-19 Patients Including Children and Adolescents Without Underlying Cardiovascular Diseases: A Systematic Review. *Cardiovasc Revasc Med* (2021) 35:169–78. doi: 10.1016/j.carrev.2021.04.007
106. Henry BM, De Oliveira MHS, Benoit S, Plebani M, Lippi G. Hematologic, Biochemical and Immune Biomarker Abnormalities Associated With Severe Illness and Mortality in Coronavirus Disease 2019 (Covid-19): A Meta-Analysis. *Clin Chem Lab Med (CCLM)* (2020) 58(7):1021–8. doi: 10.1515/cclm-2020-0369
107. Li D, Chen Y, Jia Y, Tong L, Tong J, Wang W, et al. Sars-Cov-2–Induced Immune Dysregulation and Myocardial Injury Risk in China: Insights From the Ers-Covid-19 Study. *Circ Res* (2020) 127(3):397–9. doi: 10.1161/CIRCRESAHA.120.317070
108. Guo T, Fan Y, Chen M, Wu X, Zhang L, He T, et al. Cardiovascular Implications of Fatal Outcomes of Patients With Coronavirus Disease 2019 (Covid-19). *JAMA Cardiol* (2020) 5(7):811–8. doi: 10.1001/jamacardio.2020.1017
109. Gabarre P, Dumas G, Dupont T, Darmon M, Azoulay E, Zafrani L. Acute Kidney Injury in Critically Ill Patients With Covid-19. *Intensive Care Med* (2020) 46(7):1339–48. doi: 10.1007/s00134-020-06153-9
110. Cheng Y, Luo R, Wang K, Zhang M, Wang Z, Dong L, et al. Kidney Disease Is Associated With in-Hospital Death of Patients With Covid-19. *Kidney Int* (2020) 97(5):829–38. doi: 10.1016/j.kint.2020.03.005
111. Frithiof R, Bergqvist A, Järhult JD, Lipcsey M, Hultström M. Presence of Sars-Cov-2 in Urine Is Rare and Not Associated With Acute Kidney Injury in Critically Ill Covid-19 Patients. *Crit Care* (2020) 24(1):1–3. doi: 10.1186/s13054-020-03302-w
112. Cohen JB, Hanff TC, Bress AP, South AM. Relationship Between Ace2 and Other Components of the Renin-Angiotensin System. *Curr Hypertension Rep* (2020) 22(7):1–5. doi: 10.1007/s11906-020-01048-y
113. Li Z, Wu M, Yao J, Guo J, Liao X, Song S, et al. Caution on Kidney Dysfunctions of Covid-19 Patients. (2020). doi: 10.1101/2020.02.08.20021212
114. Ekholm M, Kahan T. The Impact of the Renin-Angiotensin-Aldosterone System on Inflammation, Coagulation, and Atherothrombotic Complications, and to Aggravated Covid-19. *Front Pharmacol* (2021) 12:1534. doi: 10.3389/fphar.2021.640185
115. Vaduganathan M, Vardeny O, Michel T, McMurray JJ, Pfeffer MA, Solomon SD. Renin–Angiotensin–Aldosterone System Inhibitors in Patients With Covid-19. *N Engl J Med* (2020) 382(17):1653–9. doi: 10.1056/NEJMsr2005760
116. Fajgenbaum DC, June CH. Cytokine Storm. *N Engl J Med* (2020) 383 (23):2255–73. doi: 10.1056/NEJMra2026131
117. Legrand M, Bell S, Forni L, Joannidis M, Koyner JL, Liu K, et al. Pathophysiology of Covid-19-Associated Acute Kidney Injury. *Nat Rev Nephrol* (2021) 17(11):751–64. doi: 10.1038/s41581-021-00452-0
118. Migliorini A, Angelotti ML, Mulay SR, Kulkarni OO, Demleitner J, Dietrich A, et al. The Antiviral Cytokines Ifn-A and Ifn-B Modulate Parietal Epithelial Cells and Promote Podocyte Loss: Implications for Ifn Toxicity, Viral Glomerulonephritis, and Glomerular Regeneration. *Am J Pathol* (2013) 183(2):431–40. doi: 10.1016/j.ajpath.2013.04.017
119. Gurkan S, Cabinian A, Lopez V, Bhaumik M, Chang JM, Rabson AB, et al. Inhibition of Type I Interferon Signalling Prevents Tlr Ligand-Mediated Proteinuria. *J Pathol* (2013) 231(2):248–56. doi: 10.1002/path.4235
120. Castellano G, Franzin R, Sallustio F, Stasi A, Banelli B, Romani M, et al. Complement Component C5a Induces Aberrant Epigenetic Modifications in Renal Tubular Epithelial Cells Accelerating Senescence by Wnt4/Bcatenin Signaling After Ischemia/Reperfusion Injury. *Aging (Albany NY)* (2019) 11 (13):4382–406. doi: 10.18632/aging.102059
121. Yang AC, Kern F, Losada PM, Agam MR, Maat CA, Schmartz GP, et al. Dysregulation of Brain and Choroid Plexus Cell Types in Severe Covid-19. *Nature* (2021) 595(7868):565–71. doi: 10.1038/s41586-021-03710-0
122. Matschke J, Lütgehetmann M, Hagel C, Sperhake JP, Schröder AS, Edler C, et al. Neuropathology of Patients With Covid-19 in Germany: A Post-Mortem Case Series. *Lancet Neurol* (2020) 19(11):919–29. doi: 10.1016/S1474-4422(20)30308-2
123. Song E, Zhang C, Israelow B, Lu-Culligan A, Prado AV, Skriabine S, et al. Neuroinvasion of Sars-Cov-2 in Human and Mouse Brain. *J Exp Med* (2021) 218(3):e20202135. doi: 10.1084/jem.20202135

124. Brann DH, Tsukahara T, Weinreb C, Lipovsek M, Van den Berge K, Gong B, et al. Non-Neuronal Expression of Sars-Cov-2 Entry Genes in the Olfactory System Suggests Mechanisms Underlying Covid-19-Associated Anosmia. *Sci Adv* (2020) 6(31):eabc5801. doi: 10.1126/sciadv.abc5801
125. He L, Mäe MA, Muhl L, Sun Y, Pietilä R, Nahar K, et al. Pericyte-Specific Vascular Expression of Sars-Cov-2 Receptor Ace2–Implications for Microvascular Inflammation and Hypercoagulopathy in Covid-19. *medRxiv* (2020) 2020.05.11.088500. doi: 10.1101/2020.05.11.088500
126. Maiese A, Manetti AC, Bosetti C, Del Duca F, La Russa R, Frati P, et al. Sars-Cov-2 and the Brain: A Review of the Current Knowledge on Neuropathology in Covid-19. *Brain Pathol* (2021) 31(6):e13013. doi: 10.1111/bpa.13013
127. Boroujeni ME, Simani L, Bluyssen HA, Samadikhah HR, Zamanlui Benisi S, Hassani S, et al. Inflammatory Response Leads to Neuronal Death in Human Post-Mortem Cerebral Cortex in Patients With Covid-19. *ACS Chem Neurosci* (2021) 12(12):2143–50. doi: 10.1021/acschemneuro.1c00111
128. Kanberg N, Ashton NJ, Andersson L-M, Yilmaz A, Lindh M, Nilsson S, et al. Neurochemical Evidence of Astrocytic and Neuronal Injury Commonly Found in Covid-19. *Neurology* (2020) 95(12):e1754–e9. doi: 10.1212/WNL.0000000000010111
129. Diao B, Wang C, Tan Y, Chen X, Liu Y, Ning L, et al. Reduction and Functional Exhaustion of T Cells in Patients With Coronavirus Disease 2019 (Covid-19). *Front Immunol* (2020) 827. doi: 10.3389/fimmu.2020.00827
130. Deigendesch N, Sironi L, Kutza M, Wischnewski S, Fuchs V, Hench J, et al. Correlates of Critical Illness-Related Encephalopathy Predominate Postmortem Covid-19 Neuropathology. *Acta Neuropathol* (2020) 140 (4):583–6. doi: 10.1007/s00401-020-02213-y
131. Efe IE, Aydin OU, Alabulut A, Celik O, Aydin K. Covid-19– Associated Encephalitis Mimicking Glial Tumor. *World Neurosurg* (2020) 140:46–8. doi: 10.1016/j.wneu.2020.05.194
132. Gupta A, Madhavan MV, Sehgal K, Nair N, Mahajan S, Sehrawat TS, et al. Extrapulmonary Manifestations of Covid-19. *Nat Med* (2020) 26(7):1017–32. doi: 10.1038/s41591-020-0968-3
133. Li H, Chen C, Hu F, Wang J, Zhao Q, Gale RP, et al. Impact of Corticosteroid Therapy on Outcomes of Persons With Sars-Cov-2, Sars-Cov, or Mers-Cov Infection: A Systematic Review and Meta-Analysis. *Leukemia* (2020) 34 (6):1503–11. doi: 10.1038/s41375-020-0848-3
134. Robba C, Battaglini D, Ball L, Loconte M, Brunetti I, Vena A, et al. Distinct Phenotypes Require Distinct Respiratory Management Strategies in Severe Covid-19. *Respir Physiol Neurobiol* (2020) 279:103455. doi: 10.1016/j.resp.2020.103455
135. Seif F, Aazami H, Khoshmirsafa M, Kamali M, Mohsenzadegan M, Pornour M, et al. Jak Inhibition as a New Treatment Strategy for Patients With Covid-19. *Int Arch Allergy Immunol* (2020) 181(6):467–75. doi: 10.1159/000508247
136. Wu D, Yang XO. Th17 Responses in Cytokine Storm of Covid-19: An Emerging Target of Jak2 Inhibitor Fedratinib. *J Microbiol Immunol Infect* (2020) 53(3):368–70. doi: 10.1016/j.jmii.2020.03.005
137. Venugopal S, Bar-Natan M, Mascarenhas JO. Jaks to Stats: A Tantalizing Therapeutic Target in Acute Myeloid Leukemia. *Blood Rev* (2020) 40:100634. doi: 10.1016/j.blre.2019.100634
138. Wang A, Singh K, Ibrahim W, King B, Damsky W. Focus: Skin: The Promise of Jak Inhibitors for Treatment of Sarcoidosis and Other Inflammatory Disorders With Macrophage Activation: A Review of the Literature. *Yale J Biol Med* (2020) 93(1):187–95.
139. Bagca BG, Avci CB. The Potential of Jak/Stat Pathway Inhibition by Ruxolitinib in the Treatment of Covid-19. *Cytokine Growth Factor Rev* (2020) 54:51–61. doi: 10.1016/j.cytogfr.2020.06.013
140. Furqan M, Akinleye A, Mukhi N, Mittal V, Chen Y, Liu D. Stat Inhibitors for Cancer Therapy. *J Hematol Oncol* (2013) 6(1):1–11. doi: 10.1186/1756-8722-6-90
141. Miklossy G, Hilliard TS, Turkson J. Therapeutic Modulators of Stat Signalling for Human Diseases. *Nat Rev Drug Discov* (2013) 12(8):611–29. doi: 10.1038/nrd4088
142. Plens-Gałąska M, Woźniak T, Wesoły J, Bluyssen HA, Sinbad. Structural, Experimental and Clinical Characterization of Stat Inhibitors and Their Potential Applications. *Sci Data* (2022) 9:139. doi: 10.1038/s41597-022-01243-3
143. Song H, Wang R, Wang S, Lin J. A Low-Molecular-Weight Compound Discovered Through Virtual Database Screening Inhibits Stat3 Function in Breast Cancer Cells. *Proc Natl Acad Sci* (2005) 102(13):4700–5. doi: 10.1073/pnas.0409894102
144. Schust J, Sperl B, Hollis A, Mayer TU, Berg T. Stattic: A Small-Molecule Inhibitor of Stat3 Activation and Dimerization. *Chem Biol* (2006) 13 (11):1235–42. doi: 10.1016/j.chembiol.2006.09.018
145. Ashizawa T, Miyata H, Ishii H, Oshita C, Matsuno K, Masuda Y, et al. Antitumor Activity of a Novel Small Molecule Stat3 Inhibitor Against a Human Lymphoma Cell Line With High Stat3 Activation. *Int J Oncol* (2011) 38(5):1245–52. doi: 10.3892/ijo.2011.957
146. Czerwoniec A, Szelag M, Juszczak K, Wesoly J, Bluyssen HA. Cavs—Novel *In Silico* Selection Strategy of Specific Stat Inhibitory Compounds. *J Comput Sci* (2015) 10:186–94. doi: 10.1016/j.jocs.2015.03.001
147. Szelag M, Czerwoniec A, Wesoly J, Bluyssen HA. Identification of Stat1 and Stat3 Specific Inhibitors Using Comparative Virtual Screening and Docking Validation. *PloS One* (2015) 10(2):e0116688. doi: 10.1371/journal.pone.0116688
148. Plens-Galaska M, Szelag M, Collado A, Marques P, Vallejo S, Ramos-González M, et al. Genome-Wide Inhibition of Pro-Atherogenic Gene Expression by Multi-Stat Targeting Compounds as a Novel Treatment Strategy of Cvds. *Front Immunol* (2018) 9:2141. doi: 10.3389/fimmu.2018.02141
149. Toubiana J, Okada S, Hiller J, Oleastro M, Lagos Gomez M, Aldave Becerra JC, et al. Heterozygous Stat1 Gain-Of-Function Mutations Underlie an Unexpectedly Broad Clinical Phenotype. *Blood J Am Soc Hematol* (2016) 127(25):3154–64. doi: 10.1182/blood-2015-11-679902

Conflict of Interest: The authors declare that the research was conducted in the absence of any commercial or financial relationships that could be construed as a potential conflict of interest.

frontiers | Frontiers in Immunology

ORIGINAL RESEARCH
published: 25 May 2022
doi: 10.3389/fimmu.2022.892234

Staphylococcal Complement Evasion Protein Sbi Stabilises C3d Dimers by Inducing an N-Terminal Helix Swap

Rhys W. Dunphy[1], *Ayla A. Wahid*[1], *Catherine R. Back*[1], *Rebecca L. Martin*[2], *Andrew G. Watts*[2], *Charlotte A. Dodson*[2], *Susan J. Crennell*[1] *and Jean M. H. van den Elsen*[1,3]*

[1] Department of Biology and Biochemistry, University of Bath, Bath, United Kingdom, [2] Department of Pharmacy and Pharmacology, University of Bath, Bath, United Kingdom, [3] Centre for Therapeutic Innovation, University of Bath, Bath, United Kingdom

OPEN ACCESS

Edited by:
Uday Kishore, Brunel University London, United Kingdom

Reviewed by:
Peter Kraiczy, Goethe University Frankfurt, Germany
Brandon L. Garcia, East Carolina University, United States

***Correspondence:**
Jean M. H. van den Elsen
J.M.H.V.Elsen@bath.ac.uk

Specialty section:
This article was submitted to Molecular Innate Immunity, a section of the journal Frontiers in Immunology

Received: *08 March 2022*
Accepted: *25 April 2022*
Published: *25 May 2022*

Citation:
Dunphy RW, Wahid AA, Back CR, Martin RL, Watts AG, Dodson CA, Crennell SJ and van den Elsen JMH (2022) Staphylococcal Complement Evasion Protein Sbi Stabilises C3d Dimers by Inducing an N-Terminal Helix Swap. Front. Immunol. 13:892234. doi: 10.3389/fimmu.2022.892234

Staphylococcus aureus is an opportunistic pathogen that is able to thwart an effective host immune response by producing a range of immune evasion molecules, including *S. aureus* binder of IgG (Sbi) which interacts directly with the central complement component C3, its fragments and associated regulators. Recently we reported the first structure of a disulfide-linked human $C3d^{17C}$ dimer and highlighted its potential role in modulating B-cell activation. Here we present an X-ray crystal structure of a disulfide-linked human $C3d^{17C}$ dimer, which undergoes a structurally stabilising N-terminal 3D domain swap when in complex with Sbi. These structural studies, in combination with circular dichroism and fluorescence spectroscopic analyses, reveal the mechanism underpinning this unique helix swap event and could explain the origins of a previously discovered N-terminally truncated C3dg dimer isolated from rat serum. Overall, our study unveils a novel staphylococcal complement evasion mechanism which enables the pathogen to harness the ability of dimeric C3d to modulate B-cell activation.

Keywords: complement, structural biology, *Staphylococcus aureus*, C3d, 3D domain swapping

INTRODUCTION

The central complement component C3 is cleaved into its constituent fragments C3a and C3b by C3 convertase complexes generated by the classical/lectin (C4bC2a) or alternative (C3bBb) pathways, which subsequently trigger effective immune defence mechanisms against microbial pathogens (1). Upon activation of C3, opsonisation of microbial surfaces or cell debris in the surrounding environment by C3b enables clearance *via* opsonophagocytosis, whereas the C3a anaphylatoxin stimulates the inflammatory immune response (1). Our understanding of the mechanisms driving the cleavage of C3 have been advanced greatly by structural studies of native C3 and its fragments C3b and C3c (2, 3). Structures of C3b in complex with factor I (FI) and the short consensus repeat

(SCR) domains 1-4 of cofactor factor H have also helped us understand the processes by which C3b is proteolytically cleaved into the potent opsonin fragments iC3b and C3d(g) (4). Additionally, complexes of C3b with FH SCR domains 19 and 20 have been pivotal in explaining the regulatory measures, involving competitive binding to glycosaminoglycans and sialic acids on the host surface, that are in place to prevent the indiscriminate attachment of C3b and its fragments to self surfaces as opposed to non-self surfaces (5, 6).

Remarkably, during C3 activation only 10% of the C3b generated is deposited onto reactive surfaces, while the remaining 90% remains in the fluid phase where the highly reactive Cys-Gln thioester moiety within the thioester-containing C3d domain (TED) of C3 is exposed and undergoes hydrolysis resulting in the formation of C3(H_2O) (7). In this form, the cysteine free sulfhydryl is freely available and therefore capable of forming dimers of C3b, iC3b and C3d(g), which have been observed in several studies including in serum after 'aging' (8) or under non-reducing conditions such as the absence of *N*-ethylmaleimide (9, 10). Thioester linked C3b dimers have been reported to act as potent alternative pathway (AP) activators when complexed with IgG (11), enable the formation of AP C5 convertases by serving as a binding platform for factor B fragment Bb (12, 13), promote the release of histaminase from human polymorphonuclear leukocytes (8) and bind to complement receptor 1 (CR1) with a 25-fold higher affinity than monomeric C3b (9). More recently, we have reported on a crystal structure of a cysteine C17 disulfide-linked human C3d dimer and revealed that this dimeric C3d can bind to and crosslink CR2, enabling the modulation of B cell activation, which could potentially affect immunotolerance (14).

Staphylococcus aureus evasion proteins have been shown to effectively interfere with the process of complement activation. Along with elucidating their role in thwarting the immune system, structural and functional studies of these factors have been instrumental in furthering our understanding of the molecular mechanisms controlling C3 activation (15). Of the C3-interacting staphylococcal complement evasion proteins (16–21), Sbi is of particular interest as it is able to activate C3 through the alternative complement pathway and thereby cause fluid phase consumption of C3 (22–24). In addition to two N-terminal domains that bind the Fc region of IgG in a fashion similar to that of protein A (domains I and II) (25), we have previously shown that Sbi domains III and IV interact with complement proteins, whereby Sbi-IV binds to C3 fragments by interacting with the acidic residue-lined concave face of monomeric C3d (16), and in combination with Sbi domain III, activates the alternative complement pathway. We have recently shown that this property of Sbi can be harnessed as a vaccine adjuvant that promotes the opsonisation of antigens with a 'natural' coat of C3 breakdown products (26) *via* AP activation-mediated consumptive cleavage of C3 (22).

In this study we present the structure of a $C3d^{17C}$ dimer in complex with *S. aureus* immune evasion protein Sbi and show that through this interaction the dimer undergoes a unique N-terminal 3D domain swap. In combination with spectroscopic techniques such as circular dichroism and fluorescence spectroscopy we delineate the potential mechanism by which this structurally stabilising domain swap occurs. Our findings propose a potential new immune evasion mechanism enabling *S. aureus* to highjack the immunomodulatory properties of disulfide linked C3d dimers.

RESULTS

Sbi-IV Induces a Unique 3D Domain Swap in Dimeric C3d

Building on our recent structural and functional findings about the $C3d^{17C}$ dimer (14), we set out to determine the structure of a complex between dimeric $C3d^{17C}$ and Sbi-IV. The $C3d^{17C}$:Sbi-IV dimer complex (**Figure 1**, data collection and refinement statistics can be found in **Supplementary Tables S1, S2**) shows two molecules of Sbi-IV binding to the opposing concave binding surfaces on the $C3d^{17C}$ dimer (**Figure 1A**) *via* interactions identical to those observed in the previously reported $C3d^{17A}$:Sbi-IV structure (16). An additional binding mode observed in the $C3d^{17A}$:Sbi-IV structure, with Sbi-IV interacting with the convex surface of C3d close to the thioester region (**Supplementary Figure S2**), is absent in the $C3d^{17C}$:Sbi-IV dimer complex, prevented by the tight dimer interactions. Intriguingly, and in clear contrast to the unliganded $C3d^{17C}$ dimer, the Sbi-IV bound $C3d^{17C}$ dimer has undergone a 3D domain swap, whereby both the N-terminal α1 helices have been reciprocally exchanged between the $C3d^{17C}$ molecules within the dimer (**Figure 1A**). As detailed in **Figure 1B**, the helix α1 region M1 – G16 (residue numbering based on the crystal structure), located N-terminally from C17, has undergone a full polypeptide chain exchange in both $C3d^{17C}$ molecules, recreating identical interactions with the opposing C3d recipient without causing appreciable differences in relative orientation when compared to both monomers in the unliganded $C3d^{17C}$ dimer (PDB accession code 6RMT; main-chain RMSDs: 0.55 Å, residues 20-290 in Chain A; 0.15 Å, residues 20-290 in chain B). 2Fo-Fc electron density maps for the critical loop regions of the swapped α1 helices for each chain are shown in **Supplementary Figure S1**). This unique structural 3D domain swap phenomenon is highlighted in **Figure 1C**, showing a comparison between the unliganded $C3d^{17C}$ dimer and the $C3d^{17C}$:Sbi-IV dimer complex. Superpositioning of the A chains in the unliganded $C3d^{17C}$ dimer and the $C3d^{17C}$:Sbi-IV dimer complex reveals a slight but significant change in overall relative orientation of both monomers in the $C3d^{17C}$:Sbi-IV dimer and highlights the resulting change in conformation of the dimer disulfide bond as a result of the N-terminal helix swap (**Figure 1D**).

Helix Swapping Structurally Stabilises Dimeric C3d

In addition to stabilising the C17-C17 interchain disulfide, the helix α1 swap causes a substantial increase (640%) in joint buried

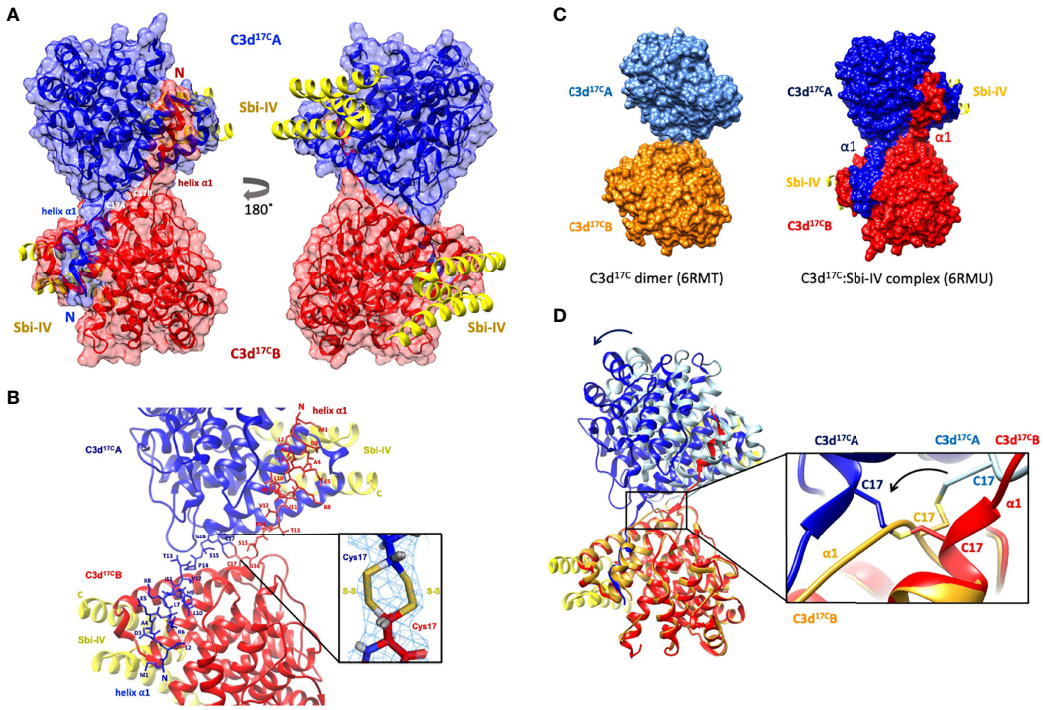

FIGURE 1 | Crystal structure of a human C3d^{17C} dimer in complex with Sbi-IV at 2.4 Å resolution. **(A)** Ribbon diagram of the C3d^{17C}:Sbi-IV dimer complex showing the cysteine C17 disulfide linked monomers in red and blue, respectively. A reciprocal 3D domain swap of both N-terminal α1 helices can be observed between the two C3d chains in the dimer, involving amino acids M1-G16. **(B)** Enlarged view of the C3d^{17C} dimer interface showing the side chains of helix α1 residues M1-C17. Inset: 2Fo-Fc electron density contoured at 1.0 σ of two possible interchain disulfide bonds (conformer A: 2.04 Å, conformer B: 2.06 Å) with a preference for the conformer B disulfide (occupancy: 0.66). The structure of C3d^{17C}:Sbi-IV dimer complex was submitted to the Protein Data Bank with PDB accession code: 6RMU. See **Supplementary Tables S1, S2** for data collection and refinement statistics. **(C)** Comparison of the unliganded C3d^{17C} dimer (PDB accession code 6RMT, with the molecular surface representations of the C3d monomers highlighted in gold and light blue) and the C3d^{17C}:Sbi-IV dimer complex (6RMU, with the C3d monomers shown in red and dark blue, and Sbi-IV in yellow), clearly showing the 3D domain swap of the N-terminal α1 helices in the latter dimer. **(D)** Superpositioning of the C3d A chains in both unliganded and Sbi-IV bound C3d dimer structures, highlighting the overall changes in relative orientation of the C3d B-chain within the unliganded C3d^{17C} and helix-swapped dimers upon superpositioning of A-chain (left), and the conformational differences in disulfide bond arrangement between both dimers (right). The images produced in this figure were generated using Chimera (27).

surface area from 698 Å^2 in the unliganded C3d^{17C} dimer to 4474 Å^2 in the Sbi-IV-bound helix-swapped C3d^{17C} dimer. This expansion in interface area is supported by 13 additional hydrogen bonds and 4 ionic interactions which are absent in the unliganded dimer (**Supplementary Figure S3**).

The Role of the Convex C3d Binding Mode of Sbi-IV in the Helix Swap

To further investigate the potential role of the interaction between Sbi-IV and helix α1 on the concave face of C3d (**Supplementary Figure S2**) we employed near-UV (320-250 nm) circular dichroism (CD) spectroscopic analyses of C3d^{17C} and C3d^{17A} collected as a function of temperature, where the absorption of aromatic side chains and disulfide bonds, absent in Sbi-IV, provides information about changes in C3d's tertiary structure (28) and binding energy of complex formation with Sbi-IV (**Figure 2**). After analysis of the sigmoidal fits of thermal denaturation curves, Sbi-IV was found to increase the melting temperature (ΔT_m) of C3d^{17C} by 7.4°C from 51.8 ± 0.1°C in the absence of Sbi-IV to 59.2 ± 1.5°C in the presence of Sbi-IV (**Figure 2A**; averaged ΔT_m at 280 and 296 nm), reflecting the binding energy of the complex. In comparison, the presence of Sbi-IV raises the ΔT_m of C3d^{17A} by 9°C, indicating a slightly stronger interaction energy for the binding between Sbi-IV and monomeric C3d^{17A} (**Figure 2B**; averaged DT_m at 280 and 296 nm).

Interestingly, whilst monomeric C3d^{17A} is thermally stable, it becomes unstable in the presence of wild-type Sbi-IV and unlike dimeric C3d^{17C} undergoes precipitation at temperatures above 65°C (**Figure 2C**). Intriguingly, the precipitation of C3d^{17A} does not occur in the presence of an N-terminally truncated Sbi-IV mutant (V198-D208del; residue numbering based on UniProt: Q2FVK5) lacking key residues that were previously shown to interact with helix α1 and its linker on the convex surface of C3d by crystal structure and NMR analyses of the C3d^{17A}:Sbi-IV complex (16) (**Supplementary Figure S2**). Whilst the ~7°C increase in T_m (**Figure 2D**) indicates that Sbi-IV$^{V198\text{-}D208del}$ is still able to bind C3d^{17A}, the lack of a temperature-induced precipitation in the presence of Sbi-IV$^{V198\text{-}D208del}$, suggests a

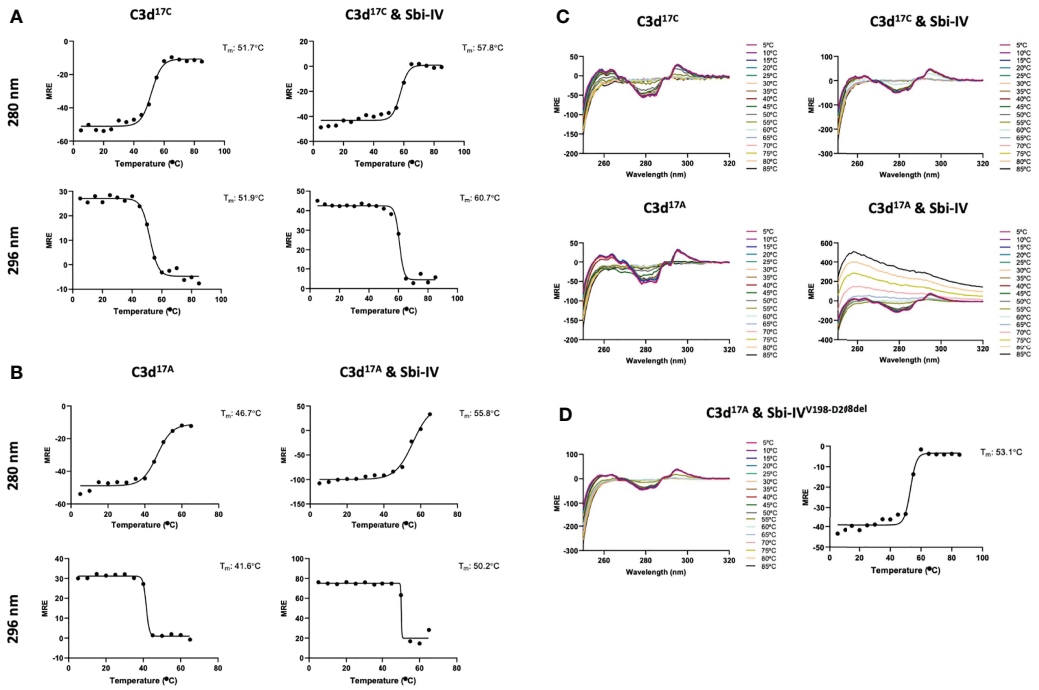

FIGURE 2 | Near-UV thermal melt circular dichroism spectroscopic studies of C3d^{17C} in the absence or presence of wild-type Sbi-IV. **(A)** Melting temperature (T_m) calculations for C3d^{17C} in the absence (Left) and presence (Right) of Sbi-IV, illustrated as Boltzmann sigmoidal fits of thermal denaturation curves at 280 nm (Top) and 296 nm (Bottom), showing an increase in T_m of 6°C and 9°C at 280 and 296 nm respectively when Sbi-IV is present. **(B)** Melting temperature (T_m) calculations for C3d^{17A} in the absence (Left) and presence (Right) of Sbi-IV, illustrated as Boltzmann sigmoidal fits of thermal denaturation curves at 280 and 296 nm, this shows an increase in T_m of ~9°C and at 280 and 296 nm respectively when Sbi-IV is present. MRE: mean residue ellipticity (deg cm^2 dmol^{-1} residue^{-1}). **(C)** CD spectra showing that C3d^{17A} in the presence of wild-type Sbi-IV undergoes aggregation and precipitation at high temperatures **(D)**. Precipitation of C3d^{17A} is not observed in the presence of a truncated Sbi-IV mutant (Sbi-IV$^{V198\text{-}D208del}$), lacking the N-terminal region of Sbi-IV helix α1, and Sbi-IV single mutant S199A. A T_m increase of 6.5° C indicates that the truncated Sbi-IV$^{V198\text{-}D208del}$ mutant hasn't lost its ability to bind C3d^{17A}.

potential role for the convex C3d binding mode of Sbi-IV in the displacement of the N-terminal α1 helix of C3d, whereby binding of Sbi-IV destabilises the helix, leading to aggregation and precipitation

We further explored the potential role of Sbi-IV's convex C3d binding mode in the helix swap observed in the C3d^{17C}:Sbi-IV dimer complex by examining single amino acid substitutions within Sbi-IV, which were chosen based on the Sbi-IV residues identified in the convex C3d binding mode of Sbi-IV, observed in the crystal structure of the C3d^{17A}:Sbi-IV complex and confirmed by subsequent NMR analyses (16) (**Supplementary Figure S2**). The Sbi-IV mutants were evaluated using near-UV CD analyses in the presence of monomeric C3d^{17A}. Similar to the N-terminally truncated Sbi-IV mutant (Sbi-IV$^{V198\text{-}D208del}$), alanine substitutions at positions S199, I204 and S219 in Sbi-IV exhibited no observable precipitation or aggregation (**Figures 3A-D**), suggesting that these residues could be important for Sbi-IV's convex C3d binding mode. E201A and K212A show a reduction of the levels of precipitation (**Figures 3E, F**), indicating that these residues are important for convex surface binding but likely enhance the binding stability once the protein is initially in position. In contrast, substitutions at D208A and D243A exhibited comparable levels of precipitation and aggregation to wild-type Sbi-IV (**Figures 3G, H**) and therefore presumably have less significant roles in the convex surface binding mode.

Both Sbi-IV and Sbi-III-IV Induce N-Terminal Helix Swapping in C3d

To investigate whether the helix swap observed in C3d^{17C} dimers is unique to Sbi-IV, we also included Sbi-III-IV in our analyses. Because the aromatic amino acids present in Sbi-III-IV make this construct unsuitable for the near-UV CD temperature melt analyses we used for Sbi-IV, we developed a bespoke tryptophan fluorescence spectroscopy method that exploits the fluorescence quenching effect on tryptophan brought about by histidine residues positioned in close proximity (29). Several C3d^{17C} mutants were generated to either substitute a natural tryptophan (W41, located on a loop between helices α2 and α3) with an alanine or introduce a histidine at position 4 close to W41. As detailed in the **Figure 4A** schematic, solutions of C3d^{A4H} or C3d^{W41A} are expected to form homodimers and show no change of tryptophan fluorescence in the event of an N-terminal helix swap, whilst mixed solutions of C3d^{A4H} with C3d^{W41A} can form heterodimers that should display an increase in tryptophan fluorescence as H4 no longer quenches W41 when

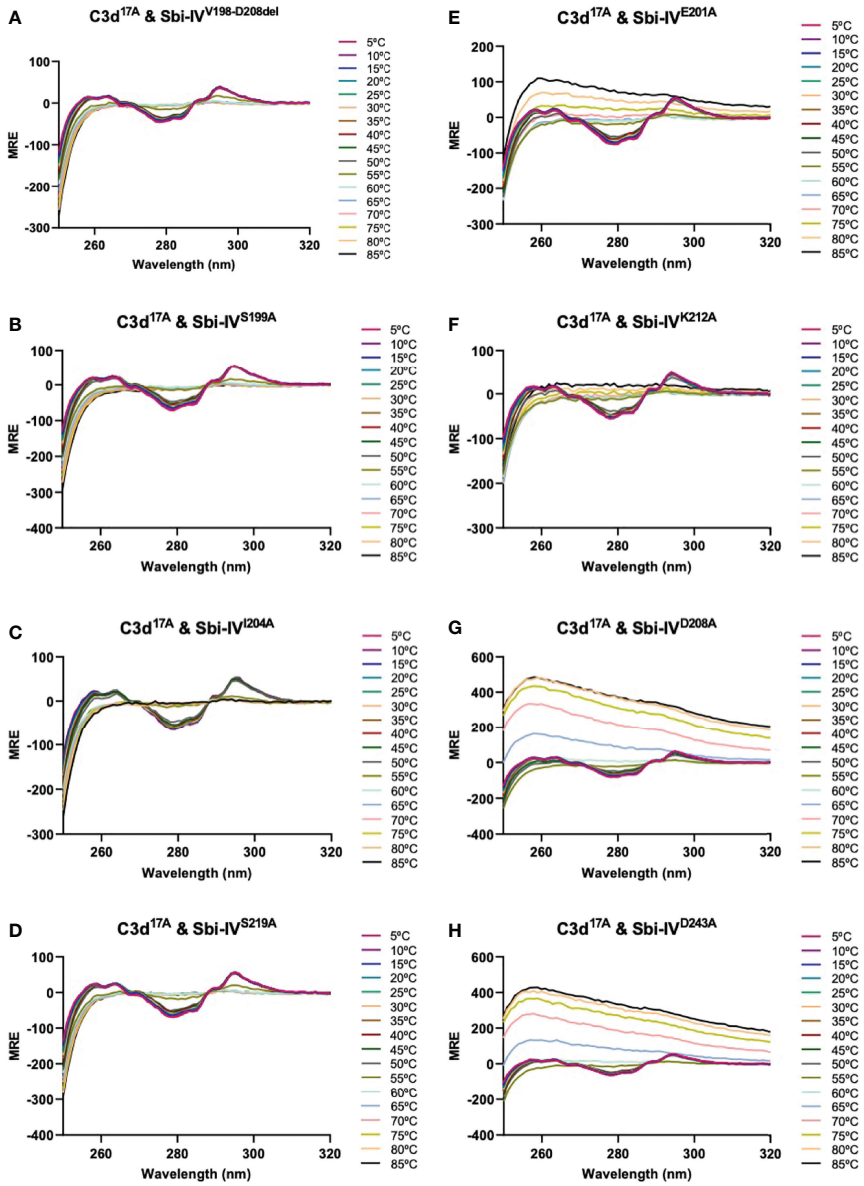

FIGURE 3 | Comparison of near-UV thermal melt circular dichroism spectroscopic studies of C3d^{17A} in the absence or presence of a truncated Sbi-IV mutant or Sbi-IV single mutants. **(A)** Whilst C3d^{17A} in the presence of wild-type Sbi-IV undergoes aggregation and precipitation at high temperatures (**Figure 2C**), this is not observed in the presence of truncated mutant Sbi-IV$^{V198\text{-}D208del}$, lacking the N-terminal region of Sbi-IV helix α1, and Sbi-IV single mutants S199A **(B)**, I204A **(C)** and S219 **(D)**. A reduced level of C3d^{17A} aggregation is observed in the presence of Sbi-IV single mutants E201A **(E)** and K212A **(F)**, whilst Sbi-IV single mutants D208A **(G)** and D243A **(H)** show aggregation levels comparable to those caused wild-type Sbi-IV.

the helix swap occurs. As expected, solutions of either C3d^{A4H} or C3d^{W41A} containing homodimers showed slight changes in fluorescence in the presence of Sbi-IV$^{V198\text{-}D208del}$, Sbi-IV or Sbi-III-IV (**Supplementary Figure S4**). However, adding these Sbi constructs to mixed solutions of C3d^{A4H} and C3d^{W41A}, expected to contain approximately 50% heterodimers of the two mutants, showed various changes in fluorescence. In the presence of Sbi-IV or Sbi-III-IV (**Figures 4B, C**) a clear increase in tryptophan fluorescence (27% and 17%, respectively) was observed when compared to their respective homodimers. These results indicate that W41 in C3d^{A4H} is no longer being quenched by its structural neighbour H4, which is suggestive of the occurrence of a Sbi-induced helix swap event. This is further supported by the reduced change in fluorescence intensity (2.5%) of the C3d^{A4H}-C3d^{W41A} heterodimer observed in the presence of Sbi$^{V198\text{-}D208del}$ (**Figures 4B, C**), emphasising that W41 remains quenched by H4 as the α1 helices cannot exchange when Sbi is unable to interact with the convex surface of C3d.

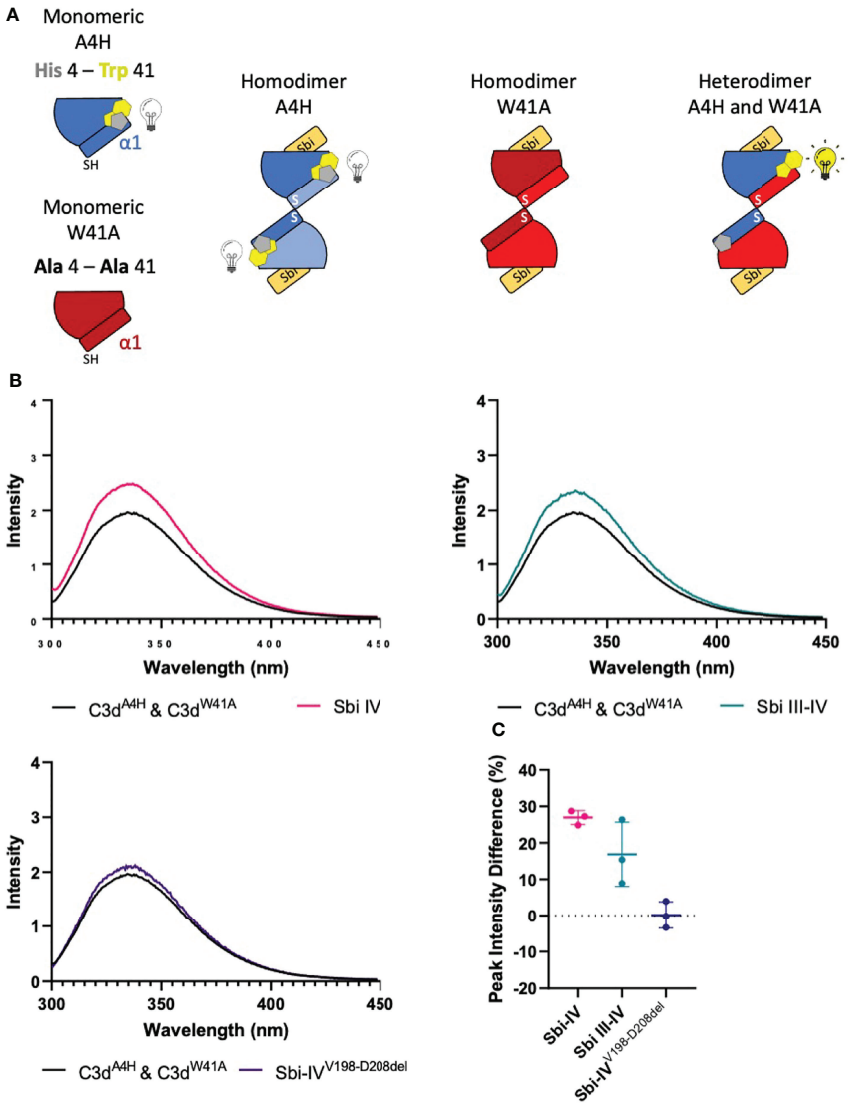

FIGURE 4 | Tryptophan fluorescence spectroscopic studies with C3d^{A4H} and C3d^{W41A} heterodimers in complex with wild-type Sbi-IV, a truncated Sbi-IV mutant and wild-type Sbi-III-IV. Shown is a schematic depicting the C3d^{17C} mutants C3d^{A4H} and C3d^{W41A} and highlighting the natural tryptophan W41 (yellow) and histidine H4 (grey) that was introduced to quench W41's fluorescence. Homodimers of C3d^{A4H}, C3d^{W41A} are expected to show no change of tryptophan fluorescence in the event of an N-terminal helix swap, whilst heterodimers of C3d^{A4H} with C3d^{W41A} should display an increase in tryptophan fluorescence as H4 no longer quenches W41 when the helix swap occurs **(A)**. Fluorescence spectra of C3d heterodimers in the absence and presence of wild-type Sbi-IV, wild-type Sbi-III-IV and truncated Sbi-IV$^{V198\text{-}D208del}$ mutant **(B)**. Scatter plot showing the tryptophan fluorescence intensity change with individual readings as well as the mean and SD values, with an average increase of 27%, 17% and 2.5% in the presence of Sbi-IV, Sbi III-IV and truncated Sbi-IV$^{V198\text{-}D208del}$ mutant respectively **(C)**.

DISCUSSION

We recently we presented the first crystal structure of dimeric human C3d^{17C} and uncovered its potential role in modulating B cell activation (14). In this paper we discover that in the presence of domain IV of the *S. aureus* immunomodulator Sbi, disulfide-linked C3d dimers undergo a rare N-terminal 3D domain swapping event, whereby the two C3d molecules in the dimer exchange their N-terminal α1 helices (**Figure 1**). 3D domain swapping has been reported to occur in a diverse range of proteins and is thought to be a mechanism for forming oligomeric states. Although in some cases, the formation of higher-order oligomers can lead to misfolding, aggregation, and disease, there is a subset of proteins whereby domain swapping leads to increased stability and regulates protein function (30). However, no examples of 3D domain swapping have been described in proteins involved in the complement system so far and this is also the first reported example of a ligand-induced domain swap.

The domain swap observed in the C3d^{17C}:Sbi-IV dimer complex structurally stabilises the dimer as evidenced by the

expansion in interaction surface and enhanced number of intermolecular interactions. In addition, the C3d^{17C} dimer in its Sbi-IV-bound state appears to have a more stable disulfide linkage, evidenced by well-defined electron density for two intact conformers of a C17-C17 interchain disulfide bond at the C3d dimer interface (**Figure 1B** inset). This in contrast to the unliganded C3d^{17C} dimer which only shows a partial disulfide bond (14). Although domain swapped proteins have been reported at acidic pH (3.5-4.0) (31), the helix swap detailed here occurred at neutral pH further supporting its physiological relevance.

Intriguingly, a secondary binding mode for Sbi-IV on the convex surface of C3d revealed previously through X-ray crystallographic, NMR chemical shift perturbation (16) and SAXS analyses (26), is located near the base or hinge region of the swapped C3d^{17C} α1 helix, close to cysteine C17. It is at this position, between helices α1 and α2, where Sbi-IV helix α1 forms interactions with the thioester cysteine C17/1010 and surrounding residues S15/1008 and Q20/1013 of C3d [(**Supplementary Figure S2** (17)]. Thus, this alternative binding mode of Sbi-IV to the hinge region of the N-terminal α1 helix of C3d, which is occluded in the C3d^{17C}:Sbi-IV dimer complex by tight dimer interactions, could play an important role in the Sbi-IV-mediated helix swap observed. Particularly, as helix α1 is prone to displacement, which has been shown to occur during the conversion of C3 to C3b (2). The binding of Sbi-IV could further increase the susceptibility of this specific helix in C3d to displacement such that when two C3d monomers bound by Sbi-IV on their convex surfaces are brought into close proximity, the helix α1-bound Sbi-IV molecules migrate to bind the concave face of the opposing C3d molecules, a favoured higher-affinity interaction, causing a reciprocal exchange of the C3d α1 helices followed by disulfide linkage of the thioester cysteine residues at position 17/1010 (**Figure 5**).

It is worth mentioning here that in a previously reported structure of a C3dg dimer, isolated from rat serum (32), the N-termini of both monomers have undergone severe proteolytic truncation. Intriguingly, both monomers lack the exact N-terminal region (M1/994 – G16/1009) (32) that we found to be involved in the helix swap in the C3d^{17C}:Sbi-IV dimer complex. The hydrophobic surfaces exposed by the removal of both α1 helices form the dimer-dimer interface in the rat C3dg dimer (**Supplementary Figure S5** and **Figure 5**). Although this dimer is not disulfide linked, its C17 cysteine residues are juxtaposed within ~8Å each other. This could suggest the truncated rat C3dg dimer is a relic of a helix swapped dimer, which became more susceptible to further degradation following the helix α1 swap, thereby leading to the formation of a more compact dimer (**Figure 5** and **Supplementary Figure S5**). In line with this, accessible surface area analysis shows that glycine G16, located N-terminally from the C17-C17 disulfide, is more solvent-exposed in C3d^{17C}:Sbi-IV dimer complex, when compared to the unliganded C3d^{17C} dimer, and may therefore be more prone to proteolytic cleavage.

Both the near-UV thermal melt CD analyses as well as the customised tryptophan fluorescence studies presented here (**Figures 2–4**), show that truncation of Sbi-IV helix α1 abolishes its ability to displace the N-terminal α1 helical region of C3d, providing support for the proposed role of Sbi-IV interactions with the convex binding site of C3d in the molecular mechanism underlying the observed helix swap (**Figure 5**). Our findings also indicate that this helix swap isn't caused exclusively by the Sbi-IV fragment, but also occurs in the presence of the larger Sbi-III-IV fragment (**Figure 4B**). In addition to establishing that Sbi binding to C3d's convex surface plays a likely role in the helix swap, we have also determined the significance of individual Sbi-IV residues involved in these interactions. Residues S199 and I204 appear to be important for interactions with the α1 helix hinge region of C3d, whilst the S219 residue located further down the α1 helix of Sbi-IV is likely involved in facilitating binding to the convex surface in the correct orientation and position (**Figure 3**). E201 and K212 residues appear to have a more supportive role in binding, suggesting that once in position they form stabilising interactions with the convex surface (**Figure 3**).

From a broader perspective, Sbi is known to hijack C3b or C3d components in complex with FHR-1 (24), enabling it to

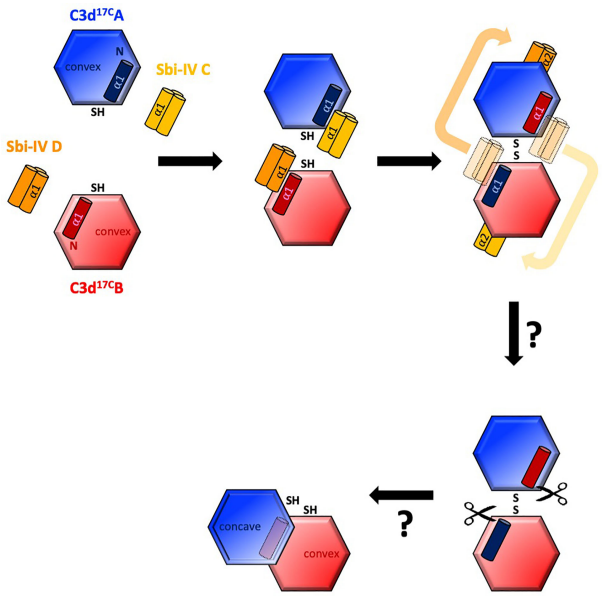

FIGURE 5 | Schematic model depicting the proposed mechanistic basis behind Sbi-IV-induced N-terminal helix swapping of dimeric C3d. Top left: In the fluid phase, Sbi-IV helix α1 binds to the N-terminal helix α1 and its adjoining loop on the convex thioester-containing face of C3d^{17C} monomer. Top middle and right: When two Sbi-IV-bound C3d^{17C} monomers come into close proximity, Sbi-IV helix α2 is attracted to and binds the concave face of C3d^{17C} (a more favourable higher affinity interaction), pulling C3d^{17C} helix α1 along with it, resulting in a reciprocal exchange of the N-terminal α1 helices of the two C3d^{17C} monomers. Bottom: The truncated rat C3dg dimer might be a relic of a helix swapped dimer, in which helix α1 has become more susceptibility to further proteolytic degradation following the 3D domain swap. This leads to the formation of a more compact dimer in which the hydrophobic surfaces exposed after proteolysis of both α1 helices face each other (see also **Supplementary Figure S5**).

upregulate complement activation in the local environment, thus hindering an effective response through depletion of local complement stores in the fluid phase away from the bacterial surface. It has also been shown that these complexes can form dimers *via* the N-terminal domains of FHR-1 (26). The possible incorporation of C3d dimers into these complexes could potentially lead to the formation of even larger multimeric complexes, creating an extensive platform for the upregulation of fluid phase complement. In addition to these complement evasion roles we reveal here that Sbi's immune-suppressive strategies may even be more intricate, involving the stabilisation of C3d dimers that, as we have shown previously, can crosslink CR2 and selectively modulate B cell activation, possibly to trigger tolerogenic pathways (14) and thereby increase the pathogen's survivability. Future investigations into hetero-dimerisation of complement components such as C3b or C4b and their potential roles in synergising co-stimulatory molecules *via* CR2-CR2 or CR2-CR3 crosslinking between immune cells, could provide even further insights into the complex links between various aspects of our immune system.

In summary, our novel discovery of Sbi domain IV's ability to induce a unique structurally stabilising domain swap in dimeric C3d reveals another dimension in the complex relationship between *S. aureus* and the immune system. Overall, our findings shed light on a fundamental aspect of complement and have the potential to inform the design of novel therapeutics for autoimmune diseases and vaccine design in the future.

MATERIALS AND METHODS

Expression and Purification of Recombinant Proteins

The DNA sequences of human C3d (residues 1-310) with a cysteine to alanine substitution at position 17 ($C3d^{17A}$) was previously cloned into the pET15b expression plasmid (33). To reproduce the wild-type sequence, the alanine at position 17 of the $C3d^{17A}$ construct was reverted to a cysteine ($C3d^{17C}$) using site-directed mutagenesis (14). Single amino acid mutants of $C3d^{17C}$ with an alanine to histidine substitution at position 4 (C3d)/997(pre-pro C3) ($C3d^{A4H}$) or with a tryptophan to alanine substitution at position 41(C3d)/1034(pre-pro C3) ($C3d^{W41A}$) were generated through site directed mutagenesis following the protocol detailed in the QuikChange II site-directed mutagenesis kit (Agilent) using Pfu polymerase (Promega) and the primers detailed in **Supplementary Table S3**.

All C3d constructs were expressed in the *Escherichia coli* Shuffle T7 cells (NEB) and purified using cation exchange chromatography (column: 1 mL HiTrap SP Sepharose HP [Cytivia], binding buffer: 50 mM MES, pH 5.5, elution buffer: 50 mM MES, 500 mM NaCl, pH 5.5) followed by size exclusion chromatography (column: HiLoad 16/600 Superdex 200 prep grade [GE Healthcare], buffer: 20 mM Tris, 150 mM NaCl, pH 7.4).

The DNA sequences of the Sbi constructs composed of domain IV (150-266 of full-length Sbi) and domains III and IV (198-266 of full-length Sbi), both bearing N-terminal 6x His-tags were previously cloned into the pQE-30 Xa plasmid [Sbi-IV (14); Sbi-III-IV (16)]. The DNA sequence of a truncated Sbi-IV construct lacking 11 residues located at the N-terminus of helix α1 (198-208 of full-length Sbi) ($Sbi\text{-}IV^{V198\text{-}D208del}$) was produced using PCR with designed primers (**Supplementary Table S3**) and cloned into the pET-28a plasmid. Various single amino acid mutants of Sbi-IV where residues at positions 199, 201, 204, 208, 212, 219 and 243 were substituted to alanines were produced through site-directed mutagenesis as described above for C3d using primers detailed in **Supplementary Table S3**.

All Sbi constructs were expressed in *E. coli* BL21(DE3) (Sigma Aldrich) cells and purified using nickel-affinity (column: 1mL HisTrap FF [Cytivia], binding buffer: 50 mM Tris, 15 mM NaCl, 20 mM Imidazole, pH 7.4, elution buffer: 50 mM Tris, 150 mM NaCl, 500 mM Imidazole, pH 7.4) and size exclusion chromatography (details as described above for C3d).

Crystallisation, Data Collection and Structure Determination

Crystallisation was performed at 18°C using the hanging drop vapour diffusion method. For the $C3d^{17C}$ dimer-Sbi-IV complex structure, needle-like co-crystals at a 1:1 molar (288 μM) ratio of Sbi-IV (2.66 mg ml^{-1}) and $C3d^{17C}$ (10 mg ml^{-1}) appeared in the condition containing 0.2 M Sodium citrate tribasic dihydrate, 20% PEG 3350 (PACT *premier* condition E11, Molecular Dimensions) (measured pH: 8.07).

Crystals were mounted on loops, flash-frozen in liquid nitrogen and X-ray diffraction data collected on the I04 beamline Dectris PILATUS 6M pixel detector at the Diamond Light Source synchrotron (Oxfordshire, UK) (See **Supplementary Table S1** for data collection statistics). Integration of diffraction images and data reduction were performed using Xia2-DIALS and AIMLESS respectively ($C3d^{17C}$ dimer-Sbi-IV complex structure: resolution: 2.4 Å, images 1601-3600 excluded). The automated BALBES pipeline and COOT were used for molecular replacement and model building. Refinement was carried out in REFMAC and Phenix (refinement statistics can be found in **Supplementary Table S2**) and UCSF Chimera was used for superpositioning and generation of images. Bond numbers and buried surface area were calculated with PDBePISA. The structure has been submitted to the Protein Data Bank with PDB submission code 6RMU ($C3d^{17C}$ dimer-Sbi-IV complex).

Circular Dichroism (CD) Spectroscopy

For tertiary structure thermal melt analyses, proteins were buffer exchanged into 10mM sodium phosphate pH 7.4 using Zeba™ Spin desalting columns (ThermoFisher) according to the manufacturer's instructions. Buffer-corrected CD measurements of 87.5 μM $C3d^{17C}$ or $C3d^{17A}$ alone or in the presence of an equimolar concentration of wild-type Sbi-IV, $Sbi\text{-}IV^{V198\text{-}D208del}$ and Sbi-IV mutants were acquired at wavelengths between 250 and 320 nm in 1 nm increments, and at temperatures ranging from 5°C to 85°C in 5°C increments followed by a final reading at

20°C. All measurements were obtained on a Chirascan spectrometer (Applied Photophysics) with a bandwidth of 2 nm and 2 second time per point. Millidegree values were converted to units of mean residue ellipticity, and deconvolution of secondary structural data was performed using DichroWeb. Melting temperature values were estimated using sigmoidal fits of thermal denaturation curves at different wavelengths performed using the Boltzmann function in GraphPad Prism (version 9.3.1). See **Figures 2A, B** respectively for $C3d^{17C}$ and $C3d^{17A}$ sigmoidal fits of thermal denaturation curves used for T_m calculations.

C3d Heterodimer Formation

The $C3d^{A4H}$ and $C3d^{W41A}$ proteins were initially buffer exchanged into 10 mM sodium phosphate pH 7.4 as detailed above. Prior to fluorometric analysis, the two mutant proteins at a concentration of 1 mg mL^{-1} were mixed together and treated with tris (2-carboxyethyl) phosphine (TCEP) (Merck) in TNE buffer (1 M Tris, 150 mM NaCl, 5 mM EDTA, pH 7.5) for 1 hour at 4°C, to partially reduce the proteins and cause any homodimers to dissociate. TCEP was subsequently removed allowing the formation of heterodimers by dialysis overnight at 4°C into 10 mM sodium phosphate pH 7.4 using Slide-A-Lyzer™ dialysis cassettes (ThermoFisher).

Fluorescence Spectroscopy

Following dialysis the $C3d^{A4H}/C3d^{W41A}$ protein solution was concentrated and used for fluorometry experiments. Samples containing, 100 µM of the $C3d^{A4H}/C3d^{W41A}$ solution alone or in the presence of an equimolar concentration of Sbi-IV, Sbi-III-IV and Sbi-$IV^{V198\text{-}D208del}$ were excited at the 295 nm wavelength and emissions between the 300 and 450 nm wavelengths were recorded. All measurements were obtained on an LS50B Luminescence Spectrometer (PerkinElmer) at room temperature using 6nm slits and a 250 ms scan speed. For analysis, the emission spectra were visualised in GraphPad Prism (version 9.3.1) as XY scatter representations. The Sbi construct intensity change was calculated for individual emission spectra by comparing the intensity reading for the $C3d^{A4H}/C3d^{W41A}$ peak alone with the Sbi intensity reading at the corresponding wavelength. These intensity changes were calculated as percentages and visualised as column representations that displayed the individual points, as well as the mean and standard deviation.

DATA AVAILABILITY STATEMENT

The original contributions presented in the study are included in the article/**Supplementary Material**. Further inquiries can be directed to the corresponding author/s.

AUTHOR CONTRIBUTIONS

JE, CD, AGW, AAW, and RD designed the experiments. CB performed preliminary structural studies and AAW performed the crystallisation. SC and AAW reprocessed the crystallography data and refined the structures. RD produced the truncated and mutated constructs. AAW and RD performed the circular dichroism experiments. RD performed the TCEP reduction, supported by RM. RD performed the tryptophan fluorescence spectroscopy experiments. JE and RD wrote the manuscript with valuable contributions from all the authors. All authors contributed to the article and approved the submitted version.

FUNDING

This research was supported by the Biotechnology and Biological Sciences Research Council Follow On Fund BB/N022165/1. AAW was sponsored by a PhD studentship granted by Raoul and Catherine Hughes and the University of Bath Alumni Fund. RD was supported by a Medical Research Council GW4 Doctoral Training Partnership (MR/N0137941/1).

ACKNOWLEDGMENTS

The authors would like to acknowledge the team at the Diamond Light Source synchrotron (Oxfordshire, UK) for access to the I04 beamline and Gyles Cozier for his help with data collection.

SUPPLEMENTARY MATERIAL

The Supplementary Material for this article can be found online at: https://www.frontiersin.org/articles/10.3389/fimmu.2022.892234/full#supplementary-material

REFERENCES

1. Sahu A, Lambris J. Structure and Biology of Complement Protein C3, a Connecting Link Between Innate and Acquired Immunity. *Immunol Rev* (2001) 180:1–35. doi: 10.1034/j.1600-065X.2001.1800103.x
2. Janssen B, Christodoulidou A, McCarthy A, Lambris J, Gros P. Structures of Complement Component C3 Provide Insights Into the Function and Evolution of Immunity. *Nature* (2005) 437:505–11. doi: 10.1038/nature04005
3. Janssen B, Christodoulidou A, McCarthy A, Lambris J, Gros P. Structure of C3b Reveals Conformational Changes That Underlie Complement Activity. *Nature* (2006) 444:213–6. doi: 10.1038/nature05172
4. Xue X, Wu J, Ricklin D, Forneris F, Di Crescenzio P, Schmidt C, et al. Regulator-Dependent Mechanisms of C3b Processing by Factor I Allow Differentiation of Immune Responses. *Nat Struct Mol Biol* (2017) 24:643–51. doi: 10.1038/nsmb.3427
5. Kajander T, Lehtinen M, Hyvarinen S, Bhattacharjee A, Leung E, Isenman D, et al. Dual Interaction of Factor H With C3d and Glycosaminoglycans in Host-Nonhost Discrimination by Complement. *Proc Natl Acad Sci USA* (2011) 108:2897–902. doi: 10.1073/pnas.1017087108
6. Morgan H, Schmidt C, Guariento M, Blaum B, Gillespie D, Herbert A, et al. Structural Basis for Engagement by Complement Factor H of C3b on a Self Surface. *Nat Struct Mol Biol* (2011) 18:463–70. doi: 10.1038/nsmb.2018

7. Law SKA, Dodds AW. The Internal Thioester and the Covalent Binding Properties of the Complement Proteins C3 and C4. *Protein Sci* (1997) 6:263–74. doi: 10.1002/pro.5560060201
8. Melamed J, Arnaout M, Colten H. Complement (C3b) Interaction With the Human Granulocyte Receptor - Correlation of Binding of Fluid-Phase Radiolabeled Ligand With Histaminase Release. *J Immunol* (1982) 128:2313–8.
9. Arnaout M, Melamed J, Tack B, Colten H. Characterization of the Human Complement (C3b) Receptor With a Fluid Phase C3b Dimer. *J Immunol* (1981) 127:1348–54.
10. Shigeoka A, Gobel R, Janatova J, Hill H. Neutrophil Mobilization Induced by Complement Fragments During Experimental Group-B Streptococcal (GBS) Infection. *Am J Pathol* (1988) 133:623–9.
11. Jelezarova E, Luginbuehl A, Lutz H. $C3b_2$-Igg Complexes Retain Dimeric C3 Fragments at All Levels of Inactivation. *J Biol Chem* (2003) 278:51806–12. doi: 10.1074/jbc.M304613200
12. Kinoshita T, Takata Y, Kozono H, Takeda J, Hong K, Inoue K. C5 Convertase of the Alternative Complement Pathway - Covalent Linkage Between 2 C3b Molecules Within the Trimolecular Complex Enzyme. *J Immunol* (1988) 141:3895–901.
13. Hong K, Kinoshita T, Pramoonjago P, Kim Y, Seya T, Inoue K. Reconstitution of C5 Convertase of the Alternative Complement Pathway With Isolated C3b Dimer and Factors B and D. *J Immunol* (1991) 146:1868–73.
14. Wahid AA, Dunphy RW, Macpherson A, Gibson BG, Kulik L, Whale K, et al. Insights Into the Structure-Function Relationships of Dimeric C3d Fragments. *Front Immunol* (2021) 12. doi: 10.3389/fimmu.2021.714055
15. Laarman A, Milder F, van Strijp J, Rooijakkers S. Complement Inhibition by Gram-Positive Pathogens: Molecular Mechanisms and Therapeutic Implications. *J Mol Med* (2010) 88:115–20. doi: 10.1007/S00109-009-0572-Y/FIGURES/3
16. Clark E, Crennell S, Upadhyay A, Zozulya A, Mackay J, Svergun D, et al. A Structural Basis for Staphylococcal Complement Subversion: X-Ray Structure of the Complement-Binding Domain of *Staphylococcus Aureus* Protein Sbi in Complex With Ligand C3d. *Mol Immunol* (2011) 48:452–62. doi: 10.1016/j.molimm.2010.09.017
17. Hammel M, Sfyroera G, Ricklin D, Magotti P, Lambris JD, Geisbrecht BV. A Structural Basis for Complement Inhibition by *Staphylococcus Aureus*. *Nat Immunol* (2007) 8:430–7. doi: 10.1038/ni1450
18. Ricklin D, Ricklin-Lichtsteiner SK, Markiewski MM, Geisbrecht BV, Lambris JD. Cutting Edge: Members of the *Staphylococcus Aureus* Extracellular Fibrinogen-Binding Protein Family Inhibit the Interaction of C3d With Complement Receptor 2. *J Immunol* (2008) 181:7463–7. doi: 10.4049/jimmunol.181.11.7463
19. Hammel M, Sfyroera G, Pyrpassopoulos S, Ricklin D, Ramyar KX, Pop M, et al. Characterization of Ehp, A Secreted Complement Inhibitory Protein From *Staphylococcus Aureus*. *J Biol Chem* (2007) 282:30051–61. doi: 10.1074/jbc.M704247200
20. Amdahl H, Jongerius I, Meri T, Pasanen T, Hyvarinen S, Haapasalo K, et al. Staphylococcal Ecb Protein and Host Complement Regulator Factor H Enhance Functions of Each Other in Bacterial Immune Evasion. *J Immunol* (2013) 191:1775–84. doi: 10.4049/jimmunol.1300638
21. Rooijakkers S, Wu J, Ruyken M, van Domselaar R, Planken K, Tzekou A, et al. Structural and Functional Implications of the Alternative Complement Pathway C3 Convertase Stabilized by a Staphylococcal Inhibitor. *Nat Immunol* (2009) 10(7):721–7. doi: 10.1038/ni.1756
22. Burman J, Leung E, Atkins K, O'Seaghdha M, Lango L, Bernado P, et al. Interaction of Human Complement With Sbi, a Staphylococcal Immunoglobulin-Binding Protein - Indications of a Novel Mechanism of Complement Evasion by Staphylococcus Aureus. *J Biol Chem* (2008) 283:17579–93. doi: 10.1074/jbc.M800265200
23. Smith E, Corrigan R, van der Sluis T, Grundling A, Speziale P, Geoghegan J, et al. The Immune Evasion Protein Sbi of Staphylococcus Aureus Occurs Both Extracellularly and Anchored to the Cell Envelope by Binding Lipoteichoic Acid. *Mol Microbiol* (2012) 83:789–804. doi: 10.1111/j.1365-2958.2011.07966.x
24. Haupt K, Reuter M, van den Elsen J, Burman J, Halbich S, Richter J, et al. The *Staphylococcus Aureus* Protein Sbi Acts as a Complement Inhibitor and Forms a Tripartite Complex With Host Complement Factor H and C3b. *PLoS Pathog* (2008) 4. doi: 10.1371/journal.ppat.1000250
25. Zhang L, Jacobsson K, Vasi J, Lindberg M, Frykberg L. A Second Igg-Binding Protein in Staphylococcus Aureus. *Microbiology* (1998) 144(4):985–91. doi: 10.1099/00221287-144-4-985
26. Yang Y, Back CR, Gräwert MA, Wahid AA, Denton H, Kildani R, et al. Utilization of Staphylococcal Immune Evasion Protein Sbi as a Novel Vaccine Adjuvant. *Front Immunol* (2019) 9:3139. doi: 10.3389/fimmu.2018.03139
27. Pettersen EF, Goddard TD, Huang CC, Couch GS, Greenblatt DM, Meng EC, et al. UCSF Chimera–A Visualization System for Exploratory Research and Analysis. *J Comput Chem* (2004) 25:1605–12. doi: 10.1002/JCC.20084
28. Kelly SM, Price NC. The Use of Circular Dichroism in the Investigation of Protein Structure and Function. *Curr Protein Pept Sc* (2000) 1:349–84. doi: 10.2174/1389203003381315
29. Sato S, Religa TL, Fersht AR. Φ-Analysis of the Folding of the B Domain of Protein a Using Multiple Optical Probes. *J Mol Biol* (2006) 360:850–64. doi: 10.1016/j.jmb.2006.05.051
30. Rousseau F, Schymkowitz J, Itzhaki LS. Implications of 3D Domain Swapping for Protein Folding, Misfolding and Function. *Adv Exp Med Biol* (2012) 747:137–52. doi: 10.1007/978-1-4614-3229-6_9
31. Liu Y, Eisenberg D. 3D Domain Swapping: As Domains Continue to Swap. *Protein Sci* (2002) 11:1285–99. doi: 10.1110/ps.0201402
32. Zanotti G, Bassetto A, Battistutta R, Folli C, Arcidiaco P, Stoppini M, et al. Structure at 1.44 Angstrom Resolution of an N-Terminally Truncated Form of the Rat Serum Complement C3d Fragment. *Biochim Biophys Acta Protein Struct Mol Enzym* (2000) 1478:232–8. doi: 10.1016/S0167-4838(00)00040-6
33. Nagar B, Jones R, Diefenbach R, Isenman D, Rini J. X-Ray Crystal Structure of C3d: A C3 Fragment and Ligand for Complement Receptor 2. *Science* (1998) 280:1277–81. doi: 10.1126/science.280.5367.1277

Conflict of Interest: The authors declare that the research was conducted in the absence of any commercial or financial relationships that could be construed as a potential conflict of interest.

frontiers | Frontiers in Immunology

ORIGINAL RESEARCH
published: 31 May 2022
doi: 10.3389/fimmu.2022.882298

Distinct Roles of Classical and Lectin Pathways of Complement in Preeclamptic Placentae

Beatrice Belmonte[1,2†], Alessandro Mangogna[3†], Alessandro Gulino[1], Valeria Cancila[1], Gaia Morello[1], Chiara Agostinis[3], Roberta Bulla[4], Giuseppe Ricci[3,5], Filippo Fraggetta[2], Marina Botto[6,7], Peter Garred[8,9] and Francesco Tedesco[10]*

[1] Tumor Immunology Unit, Department of Health Promotion, Mother and Child Care, Internal Medicine and Medical Specialties "G. D'Alessandro", University of Palermo, Palermo, Italy, [2] Pathology Unit, Azienda Sanitaria Provinciale (ASP) Catania, "Gravina" Hospital, Caltagirone, Italy, [3] Institute for Maternal and Child Health, IRCCS Burlo Garofolo, Trieste, Italy, [4] Department of Life Sciences, University of Trieste, Trieste, Italy, [5] Department of Medical, Surgical and Health Science, University of Trieste, Trieste, Italy, [6] Department of Immunology and Inflammation, Imperial College London, London, United Kingdom, [7] Imperial Lupus Centre, Imperial College Healthcare National Health Service (NHS) Trust, London, United Kingdom, [8] Laboratory of Molecular Medicine, Department of Clinical Immunology, Copenhagen University Hospital, Rigshospitalet, Copenhagen, Denmark, [9] Department of Clinical Medicine, University of Copenhagen, Copenhagen, Denmark, [10] Istituto Auxologico Italiano, Laboratory of Immuno-Rheumatology, IRCCS, Milan, Italy

OPEN ACCESS

Edited by:
Uday Kishore, Brunel University London, United Kingdom

Reviewed by:
Nandor Gabor Than, Hungarian Academy of Sciences (MTA), Hungary
Maciej Cedzynski, Institute for Medical Biology (PAN), Poland

***Correspondence:**
Francesco Tedesco
tedesco@units.it

†These authors have contributed equally to this work and share first authorship

Specialty section:
This article was submitted to Molecular Innate Immunity, a section of the journal Frontiers in Immunology

Received: *23 February 2022*
Accepted: *28 April 2022*
Published: *31 May 2022*

Citation:
Belmonte B, Mangogna A, Gulino A, Cancila V, Morello G, Agostinis C, Bulla R, Ricci G, Fraggetta F, Botto M, Garred P and Tedesco F (2022) Distinct Roles of Classical and Lectin Pathways of Complement in Preeclamptic Placentae. Front. Immunol. 13:882298. doi: 10.3389/fimmu.2022.882298

Pre-eclampsia is a pregnancy complication characterized by defective vascular remodeling in maternal decidua responsible for reduced blood flow leading to functional and structural alterations in the placenta. We have investigated the contribution of the complement system to decidual vascular changes and showed that trophoblasts surrounding unremodeled vessels prevalent in preeclamptic decidua fail to express C1q that are clearly detected in cells around remodeled vessels predominant in control placenta. The critical role of C1q is supported by the finding that decidual trophoblasts of female *C1qa*$^{-/-}$ pregnant mice mated to *C1qa*$^{+/+}$ male mice surrounding remodeled vessels express C1q of paternal origin. Unlike *C1qa*$^{-/-}$ pregnant mice, heterozygous *C1qa*$^{+/-}$ and wild type pregnant mice share a high percentage of remodeled vessels. C1q was also found in decidual vessels and stroma of normal placentae and the staining was stronger in preeclamptic placentae. Failure to detect placental deposition of C1r and C1s associated with C1q rules out complement activation through the classical pathway. Conversely, the intense staining of decidual endothelial cells and villous trophoblast for ficolin-3, MASP-1 and MASP-2 supports the activation of the lectin pathway that proceeds with the cleavage of C4 and C3 and the assembly of the terminal complex. These data extend to humans our previous findings of complement activation through the lectin pathway in an animal model of pre-eclampsia and provide evidence for an important contribution of C1q in decidual vascular remodeling.

Keywords: complement system, pre-eclampsia, vascular remodeling, C1q, ficolin-3

INTRODUCTION

Pre-eclampsia (PE) is a serious clinical condition that occurs in 3-5% of pregnant women in the second half of pregnancy after 20 weeks and more frequently after 34 weeks of gestation and is characterized by hypertension, proteinuria, liver and cerebral involvement (1). The disorder is responsible for maternal morbidity and mortality and adverse pregnancy outcomes, including preterm delivery, intrauterine growth retardation and fetal death (2). The diverse clinical presentations of PE argue for a multifactorial nature of this syndrome whose pathogenesis has not yet been clearly defined despite the efforts made over recent years to identify the possible causes.

As the clinical signs disappear with the termination of pregnancy after placental expulsion, the placenta has been recognized to play a major role in the development of PE. This newly formed organ at the feto-maternal interface undergoes structural and functional changes that start with defective remodeling of decidual spiral arteries, particularly evident in the early-onset PE (3, 4), and endothelial dysfunction (5, 6) resulting in high resistance vessels, reduced tissue perfusion and oxidative stress (7).

These changes stimulate an inflammatory response in the second stage of PE involving both cells and soluble molecules of the innate immune system (8, 9).

Complement (C) is a critical component of innate immunity and has been implicated in the development of PE. The system plays an important role in host defense and homeostasis following activation *via* the classical, the lectin and the alternative pathways, but it may also cause tissue damage under conditions of unrestricted activation (10–12). While the alternative pathway functions as an amplification loop for the classical and lectin pathways, the activation of latter two pathways requires the intervention of recognition molecules to initiate the triggering process. C1q serves this function for the classical pathway and acts in association with the serine proteases C1r and C1s. Conversely, the lectin pathway is triggered by a set of different recognition molecules belonging to the collectin family (mannose-binding lectin aka MBL, collectin-10 aka CL-10 and collectin-11 aka CL-11) and the ficolin family (ficolin-1, ficolin-2, and ficolin-3). All the recognition molecules of the lectin pathway are found associated with a set of serine proteases named MASPs (MASP-1, MASP-2 and MASP-3) and regulatory molecules named MAPs (MAP-1 and MAP-2) (13). Activation of the classical and lectin pathways leads to the enzymatic cleavage of C4, C3 and C5, and eventually results in the release of potent anaphylatoxins, C3a and C5a, and the assembly of the C5b-9 complex. Evidence has been collected over the years suggesting an involvement of C in placental alterations of PE (14, 15). Increased levels of C3a, C5a and the soluble sC5b-9 complex have been reported in the circulation of preeclamptic patients (16, 17) and in the urine of patients with severe eclampsia suggesting their contribution to C-mediated renal damage (18). The finding of high levels of Bb, a split product of the C factor B of the alternative pathway, in the early phase of gestation in women who later developed PE led Lynch and colleagues to propose Bb as an early biomarker for the development of PE (19). The observation, however, was not confirmed in a prospective study performed in Caucasian patients (16). These conflicting results may be due to racial differences in the patients studied since the levels of Bb were found to be significantly higher in African-American PE patients (20).

Immunohistochemical analysis of PE placenta revealed increased deposition of C components and C activation products in chorionic villi compared to control placentae (21–25). Diffuse C4 staining has been found to be associated with placental pathologic changes and fetal growth restriction, and has been proposed as biomarker for adverse pregnancy outcomes in PE patients (23, 25). However, the pathway of C activation and the mechanisms involved in C-mediated tissue damage have not been fully elucidated. More direct evidence for C involvement in PE has been obtained in an animal model where CBA/J female mice mated to DBA/2 males have high resorption rate and fetal growth retardation (26). The pregnant mice manifest features common to PE, including albuminuria, endotheliosis and increased sensitivity to angiotensin II that correlates with adverse pregnancy outcomes (27). The fetal loss in the CBA/J female mice can be prevented by administering either an inhibitor of the C3 convertase, Crry-Ig, or a neutralizing anti-C5 monoclonal antibody or a C5a receptor antagonist (28). The interesting observation by Singh *et al.* that pregnant C1q-deficient mice present the classical manifestations seen in PE patients, including hypertension, albuminuria, and increased levels of soluble VEGF receptor 1 (sFlt-1), suggests that C1q may exert a surprising protective role in pregnancy (29). In this respect, it is important to note that C1q is widely distributed in maternal decidua in normal pregnancy and is locally synthesized and secreted by macrophages as well as endothelial cells and extravillous trophoblasts (30, 31). Considering the controversial findings in the literature herein we aimed to investigate the contribution of C1q expressed by perivascular trophoblasts to the physiologic process of decidual vascular remodeling and to explore the impact that a defect in the local expression of C1q may have on the vascular changes. In addition, we sought to determine whether locally expressed C1q is involved in the activation of the classical pathway at placental site, and whether C activation may also be triggered *via* the lectin pathway as observed in an animal model of PE (32).

MATERIALS AND METHODS

Study Groups

Fifteen women with pregnancies complicated by early-onset PE that developed before 34 weeks of gestation and a control group of 15 healthy women with uncomplicated pregnancies were included in this investigation. Preeclampsia was defined as newly diagnosed high blood pressure (systolic blood pressure ≥140 mmHg or diastolic blood pressure ≥90 mmHg) with onset after 20 weeks of gestation and proteinuria (24-hour urine protein ≥300 mg or a dipstick ≥1+) measured on two or more occasions at 6-8 hour intervals (33). IUGR was observed in 7 out 15 (47%) PE patients.The clinical characteristics of the study groups are shown

in **Table 1**. Patients and control pregnant women were enrolled at the Institute for Maternal and Child Health, IRCCS Burlo Garofolo, Trieste, Italy. The study was reviewed and approved by the Regional Ethical Committee of FVG (CEUR), Udine, Italy (CEUR-2020-Os-156; Prot. 0022668/P/GEN/ARCS).

Human Placental Tissues

Three to four biopsy samples were taken from the central area of the maternal surface of placentae collected immediately after delivery and quickly washed in saline to remove residual blood. The specimens were fixed in 10% buffered formalin and paraffin-embedded. Informed consent was obtained from all participants in the study.

Mice

C57BL/6 mice were purchased from Harlan Laboratories. C1q deficient mice (*C1qa*$^{-/-}$) backcrossed on the C57BL/6 background were generated as previously described (34). Wild Type (WT) C57BL/6 males were mated with *C1qa*$^{-/-}$ females to generate heterozygous mice. Implantation sites were collected from pregnant mice on days 13-14, fixed in 10% buffered formalin and embedded in paraffin. All animals were handled in accordance with the institutional guidelines and in compliance with the European (86/609/EEC). The UK Home Office approved the procedure.

Histochemical, Immunohistochemical and Immunofluorescence Analysis

Four micrometers-thick serial sections were cut from deparaffinized and rehydrated human and mouse placental samples. Some sections were stained with hematoxylin-and-eosin and examined for the distribution of invasive extravillous trophoblast and the structure of decidual blood vessels.

Deposits of C components and C activation products were analyzed on adjacent sections immunostained after antigen retrieval using Novocastra Epitope Retrieval Solution at pH6, pH8 or pH 9 to unmask antigens in a thermostatic bath at 98°C for 30 min. Subsequently, the sections were brought to room temperature and washed in phosphate buffered saline (PBS). After neutralization of the endogenous peroxidases with 3% H_2O_2 and Fc-blocking by 0.4% casein in PBS (Novocastra), the sections were incubated with the primary antibodies listed in **Table 2**. Liver sections were used as positive controls for MBL, ficolin-2, C1r and C1s staining (**Supplemental Figure 1**).

For multiple-marker immunostaining, the sections were subjected to sequential rounds of single-marker immunostaining, and the binding of the primary antibodies was revealed using specific secondary antibodies conjugated with different enzymes or fluorophores.

Immunohistochemical staining was developed using the Novolink Polymer Detection Systems (Novocastra) or IgG (H&L)-specific secondary antibodies (Life Technologies, 1:500) and AEC (3-Amino-9-ethylcarbazole) or DAB (3,3'-diaminobenzidine) as substrate chromogens. Double immunohistochemistry (IHC) was performed by applying Signal Stain Boost IHC Detection (Cell Signaling) alkaline phosphatase-conjugated and Vulcan Fast Red as substrate chromogen.

The Opal Multiplex IHC kit (Akoya Biosciences) was used to stain the tissue sections with antibodies raised in the same species. After deparaffinization, antigen retrieval in pH9 buffer was brought to a boil at 100% power, followed by 20% power for 15 minutes using microwave technology. The sections were treated with blocking buffer for 10 minutes at room temperature before incubation with the primary antibody. The slides were then incubated with polymeric horseradish peroxidase-conjugated (HRP) secondary antibody for 10 minutes and the signal was visualized using Opal 520 fluorophore-conjugated tyramide signal amplification (TSA) at 1:100 dilution. The HRP catalyzes covalent deposition of fluorophores around the marker of interest. The slides were again processed with the microwave treatment to strip primary/secondary antibody complex and allow the next antigen-antibody staining. Another round of staining was performed with the second primary antibody incubation, followed by HRP secondary antibody and Opal 620 fluorophore-conjugated TSA at 1:100 dilution for signal visualization. Finally, the slides were again microwaved in antigen retrieval buffer and nuclei were subsequently visualized with DAPI (4',6-diamidin-2-fenilindolo). The slides were analyzed under a Zeiss Axioscope A1 microscope equipped with four fluorescence channels widefield IF. Microphotographs were collected using a Zeiss Axiocam 503 Color digital camera with the Zen 2.0 Software (Zeiss).

TABLE 1 | Clinical characteristics of women enrolled in the study.

Characteristics	Pre-eclampsia (n = 15)	Controls (n = 15)
Mean maternal age, y (SD)	35.1 (± 4)	33.5 (± 2)
Mean maternal BMI, kg/m^2 (SD)	25 (± 3)	19.5 (± 5)*
Nulliparity (%)	60%	40%
Highest diastole, mm Hg (SD)	89 (± 15)	66 (± 10)
Highest systole, mm Hg (SD)	141 (± 14)	109 (± 13)
Proteinuria, g/24 h (SD)	1996 (± 1202)	ND
Gestational age at delivery, weeks+ days (min-max in weeks)	29+3 (25–33)	39+4 (38–42)**
Birth weight, g (SD)	1040 (± 448)	3285 (± 276)**
Placenta weight, g (SD)	301 (± 78)	560 (± 58)*
Mode of delivery		
Cesarean section (%)	60%	20%

*SD, standard deviation. ND, not detectable by urine dipstick test. *p < 0.001; **p < 0.0001 (T-Student test).*

TABLE 2 | Antibody sources and dilutions.

Antigens	Reactivity	Dilution	Type	Code number	Source
C1q	human	1:500	rabbit pAb	A0136	Agilent, DK
C1r	human	1:100	rabbit pAb	HPA001551	Sigma Aldrich
C1s	human	1:250	goat pAb	A302	Quidel
Ficolin-1	human	1:50	mouse mAb	FCN166	(35)
Ficolin-2	human	1:500	mouse mAb	FCN219	(36)
Ficolin-3	human	1:1000	mouse mAb	FCN 309	(37)
MBL	human	1:1000	rabbit pAb	HPA002027	Sigma Aldrich
MASP-1	human	1:40	rabbit pAb	HPA001617	Sigma Aldrich
MASP-2	human	1:20	rabbit pAb	HPA029313	Sigma Aldrich
C3d	human	1:100	rabbit pAb	403A-76	Cell Marque
C4d	human	1:100	rabbit pAb	404A-16	Cell Marque
C9neo	human	1:50	mouse mAb	HM2264-IA	Hycult Biotech
CK-7	human	1:8000	rabbit mAb	Ab181598	Abcam
α-SMA	human	1:500	mouse mAb	SKU001	BioCare
C1q	mouse	1:400	rabbit pAb	NA	(38)
CK-7	mouse	1:8000	rabbit mAb	Ab181598	Abcam
CD31	mouse	1:50	rabbit pAb	Ab28364	Abcam

pAb, polyclonal antibody; mAb, monoclonal antibody; CK, cytokeratin; α-SMA, α- smooth muscle actin; NA, not available.

Statistical Analysis

Means and standard deviation were calculated for continuous variables, whereas frequencies and percentages were reported for categorical variables. Non-parametric data were assessed by Mann-Whitney U-tests. Patient data (**Table 1**) were analyzed by T-Student test. Data from *in vivo* mouse models were analyzed using two-way analysis of variance (ANOVA). Results were expressed as mean ± standard deviations. and P-values <0.05 were considered statistically significant. All statistical analyses were performed using GraphPad Prism software 9.0 (GraphPad Software Inc., La Jolla, CA, USA).

RESULTS

Analysis of Placental Deposition of Early C Components

To elucidate the mechanism of C activation in PE placentae, we searched for the presence and distribution of C components that may initiate C activation through the classical and/or the lectin pathway. C1q was detected in both control and PE placentae, though with different staining intensity. A detailed analysis of normal placentae showed that C1q was localized on vascular endothelium and stroma of decidua, while virtually undetectable in chorionic villi (**Figure 1**). The distribution pattern of C1q staining in PE placentae was similar to that of control placentae with the only difference that the staining was more intense in decidua and was also seen on syncytiotrophoblasts of some villi (**Figure 1**). We also examined the placentae for the presence of the initiators of the C lectin pathway and found that MBL was undetectable in both normal and pathological tissue samples (**Figure 1**) while clearly documented in the liver (**Supplemental Figure 1A**). Conversely, deposits of ficolin-3 were observed on decidual vascular endothelium and syncytiotrophoblasts of PE placentae. The staining was weak in 25% and more intense in 75% of PE placentae, while slightly detectable in the control samples (**Figure 1**). The anti-ficolin-1 antibody reacted almost exclusively with syncytiotrophoblasts of normal and PE samples with no significant difference in the staining intensity between the two groups of placentae (**Supplemental Figure 2**), while ficolin-2 was practically undetectable.

Placental Deposition of C4 Convertases

C activation was investigated by analyzing the presence of C4 convertases of the classical and lectin pathways. Despite the substantial deposits of C1q, we failed to reveal C1r and C1s in normal and PE placentae (**Figure 2**) using antibodies that were able to detect intracellular C1r and C1s in hepatocytes of paraffin-embedded liver tissue (**Supplemental Figures 1C, D**). Conversely, MASP-1 and MASP-2 exhibited a characteristic distribution pattern with a diffuse localization on decidual endothelial cells, syncytiotrophasts and villous microvessels of PE placentae but absent in normal controls (**Figure 3**). A substantial proportion of PE placentae were positive for MASP-1 (56%) and MASP-2 (87%) and the remaining placentae were weakly positive.

Deposition of C Activation Products in Placenta

As the presence of MASP-1 and MASP-2 deposition indicates that C activation may proceed through the lectin pathway, we stained the placental tissue for C4d and C3d that play a central role in the C cascade. Both C activation products were found in the decidual blood vessels and villous trophoblasts of 50% and 56% PE placentae respectively and were weakly positive in all the other pathologic placentae while hardly detectable in the control tissue samples (**Figure 4**). To further ascertain if the terminal pathway was also activated in PE placentae, the tissue samples were examined for the deposition of the terminal C complex C5b-9 using an antibody that detects a neoantigen of C9 (C9 neo) present in the assembled complex (39). Staining for C5b-9 complex was positive in 45% and weakly positive in 55% of PE placentae and was mainly observed in decidual vessels, but was absent in control placentae (**Figure 4**).

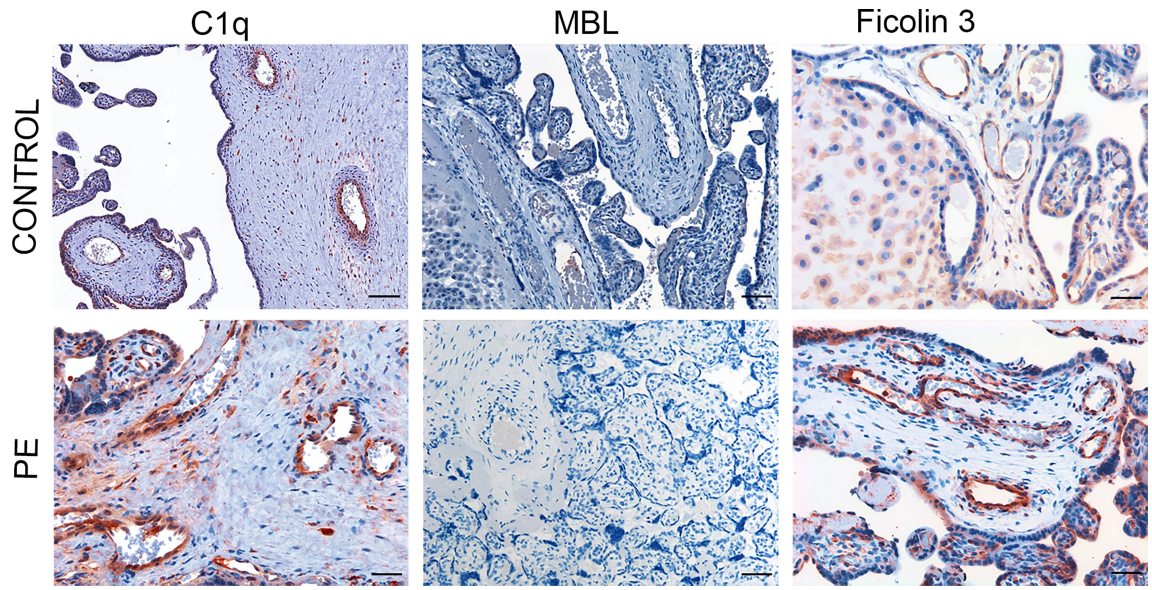

FIGURE 1 | Immunohistochemical analysis of initiators of the classical and lectin complement pathways in placental tissue. Sequential sections of pre-eclamptic (PE) and normal (CONTROL) placentae were stained for C1q, MBL and ficolin-3. The panel presents representative images from 15 early-onset PE patients and 15 controls showing localization of C1q in the decidual vessels of both control and early-onset PE placentae with more intense staining in the latter. Deposits of ficolin-3 were seen almost exclusively in decidual vessels of PE placenta while MBL was undetectable. Scale bars, 50 μm.

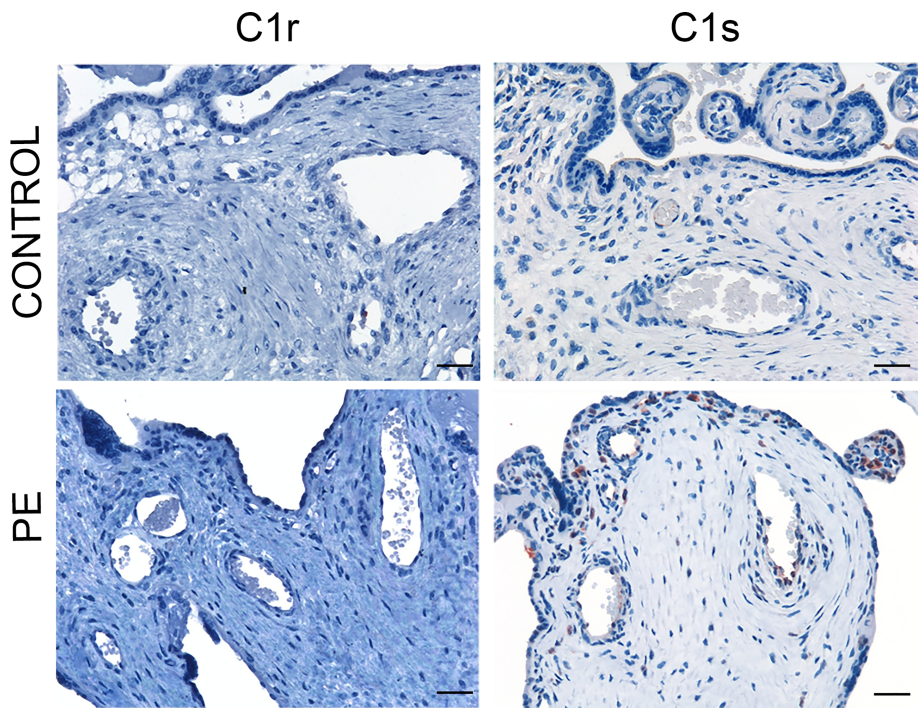

FIGURE 2 | Immunohistochemical analysis of C4 convertases of the classical complement pathway in placental tissue. Sections of pre-eclamptic (PE) and normal (CONTROL) placentae were stained for C1r and C1s. The panel shows representative images of PE and control placentae documenting complete absence of these C components in both groups of placentae. Scale bars, 50 μm.

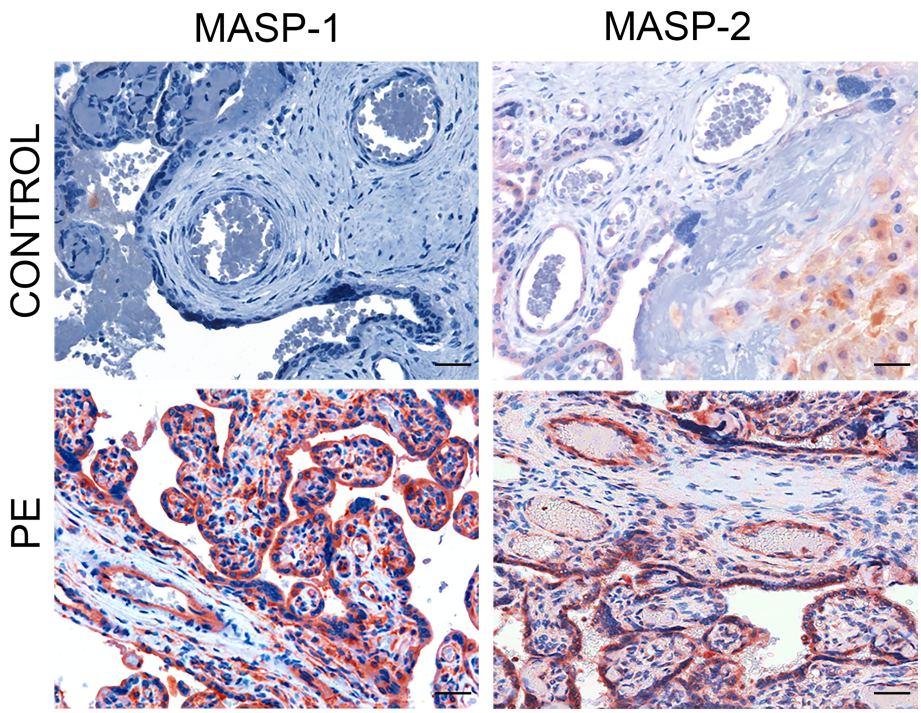

FIGURE 3 | Immunohistochemical analysis of C4 convertases of the lectin complement pathways in placental tissue. Sections of pre-eclamptic (PE) and normal (CONTROL) placentae were stained for MASP-1 and MASP-2. The panel shows representative images of MASP-1 and MASP-2 deposits on decidual vessels, syncytiotrophoblasts and villous microvessels of PE placentae that were not seen in control placentae. Scale bars, 50 µm.

C1q Expression in Perivascular Extravillous Trophoblasts

Following our previous observations that extravillous trophoblasts (EVT) acquire the ability to synthesize and secrete C1q used by these cells to invade the decidua (31), we sought to investigate the distribution of EVT expressing C1q in PE and control decidua and to determine their contribution to vascular remodeling. The extent of arterial changes was evaluated by examining the disruption of the muscle cells of tunica media in decidual vessels recognized by an antibody against α-smooth muscle actin (α-SMA). **Supplemental Figure 3** shows decidual vessels of a PE placenta with different degrees of vascular remodeling assessed by the decrease in the width of the muscle cell layer. Over 70% (72.86%) of decidual vessels in normal pregnancy undergo remodeling as opposed to 27% of unremodeled vessels, while this ratio is inverted in PE placentae with a prevalence of vessels that remain unremodeled (**Figure 5A**). PE placental sections were double-stained for C1q and cytokeratin 7 (CK7) to identify C1q-containing trophoblasts. Analysis of perivascular trophoblasts revealed the presence of C1q in cells surrounding remodeled vessels, in contrast to trophoblasts localized around unremodeled vessels that failed to express this C component (**Figure 5B**). The distribution pattern of trophoblasts with or without C1q around remodeled and unremodeled vessels, respectively, was similar in PE and control placentae. Interestingly, the absence of C1q was restricted to perivascular trophoblasts and did not involve interstitial trophoblasts migrating at some distance from spiral arteries that invariably contained C1q (**Supplemental Figure 4**).

Vascular Remodeling in Implantation Sites of *C1qa*$^{+/+}$, *C1qa*$^{+/-}$ and *C1qa*$^{-/-}$ Mice

We have previously reported reduced labyrinth development, decreased trophoblast invasion, and impaired vascular remodeling in the implantation site of pregnant *C1qa*$^{-/-}$ mice compared to WT animals of the same gestational age (31). To further investigate if trophoblasts synthesizing C1q are directly involved in the process of vascular remodeling, we examined the decidua of female *C1qa*$^{-/-}$ mice mated with either C1q sufficient or C1q deficient male mice and compared the results with those observed in the decidua of WT mice. As shown in **Figure 6A**, the percentage of decidual remodeled vessels in WT mice was significantly higher than that of unchanged vessels, whereas unremodeled vessels were prevalent in *C1qa*$^{-/-}$ mice. Interestingly, the percentages of changed and unchanged vessels in heterozygous *C1qa*$^{+/-}$ mice were essentially similar to those observed in WT mice (**Figure 6A**). Representative sections of placenta from WT, heterozygous and C1q deficient mice showing the distribution of remodeled and unremodeled vessels are presented in **Figure 6B**. Staining of placental sections from the three groups of mice revealed the presence of C1q in trophoblasts of both WT and heterozygous mice and the expected absence of C1q expression in C1q deficient mice (**Figure 6C**).

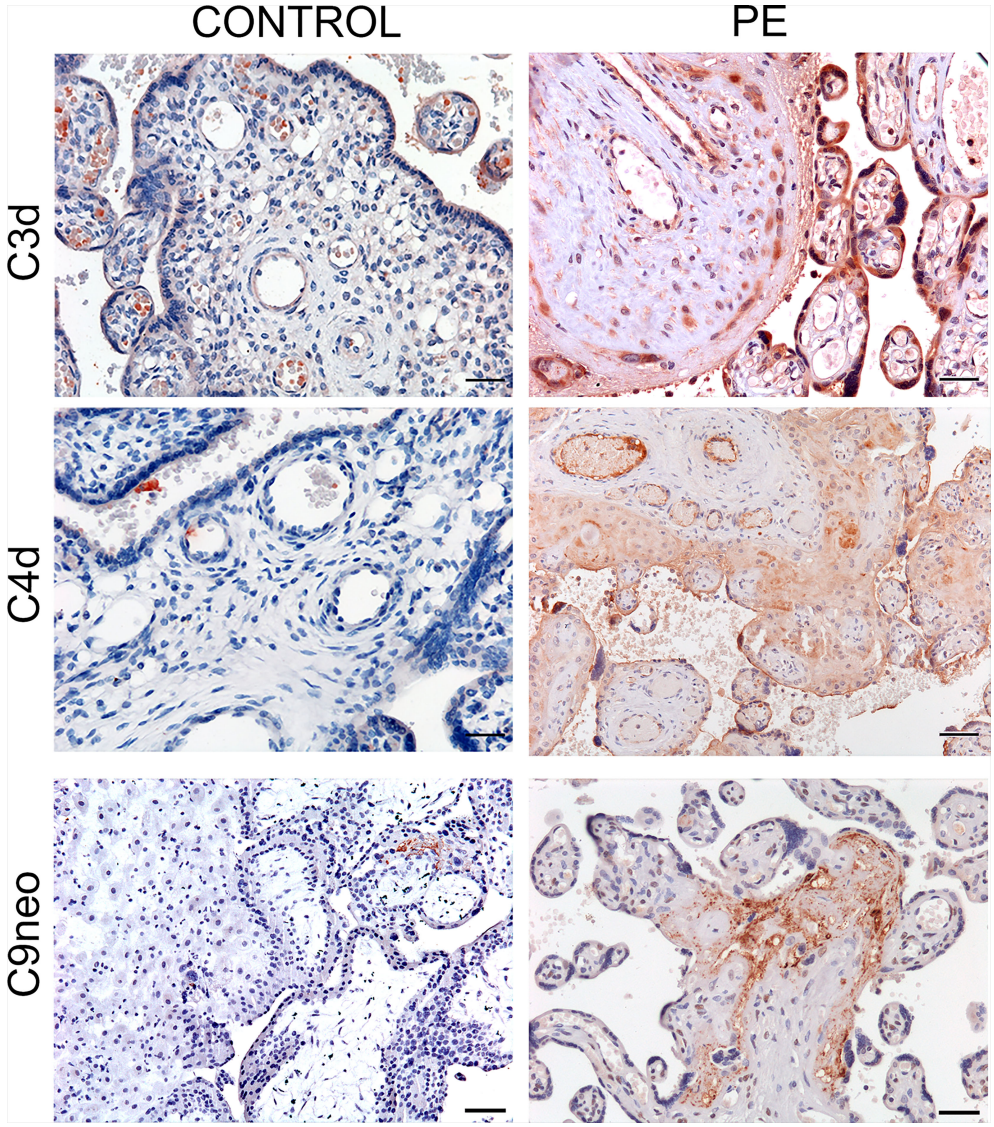

FIGURE 4 | Immunohistochemical analysis of C activation products in placental tissue. Sequential sections of pre-eclamptic (PE) and normal (CONTROL) placental tissue were stained for C4d, C3d and C9 neo. The panel shows representative images revealing localization of the C activation products in the decidual vessels and in some villi of PE placentae and their absence in the control tissue. Scale bars, 50 μm.

DISCUSSION

Previous studies have documented C deposits on chorionic villi and in particular on villous trophoblasts of PE placentae, suggesting the contribution of C to the development of placental alterations in PE (21–25). We have now extended the C analysis to the decidual tissue based on the understanding that the pathologic process starts in the decidua involving primarily the vessels and subsequently affects the villi. The data presented in this study show that C is activated in PE placenta through the lectin pathway and that the role of C1q is to promote vascular remodeling in decidua rather than to activate the C classical pathway.

Examination of the placentae from healthy controls revealed a negligible presence of C components, most likely due to an inflammatory-like process that develops in placental decidua as a result of tissue remodeling associated with embryo implantation (8, 9). The only exception to this general rule is the diffuse deposition of C1q on decidual vessels and stroma in all placental samples examined. This is consistent with our previous findings that C1q is synthesized and secreted by endothelial cells and extravillous trophoblasts in the decidua in normal pregnancy (30, 31). The increased expression of C1q observed in decidua and on the surface of villi in the PE patients may be attributed to the binding of C1q to endothelial cells and trophoblasts as a result of cellular changes that occur in PE.

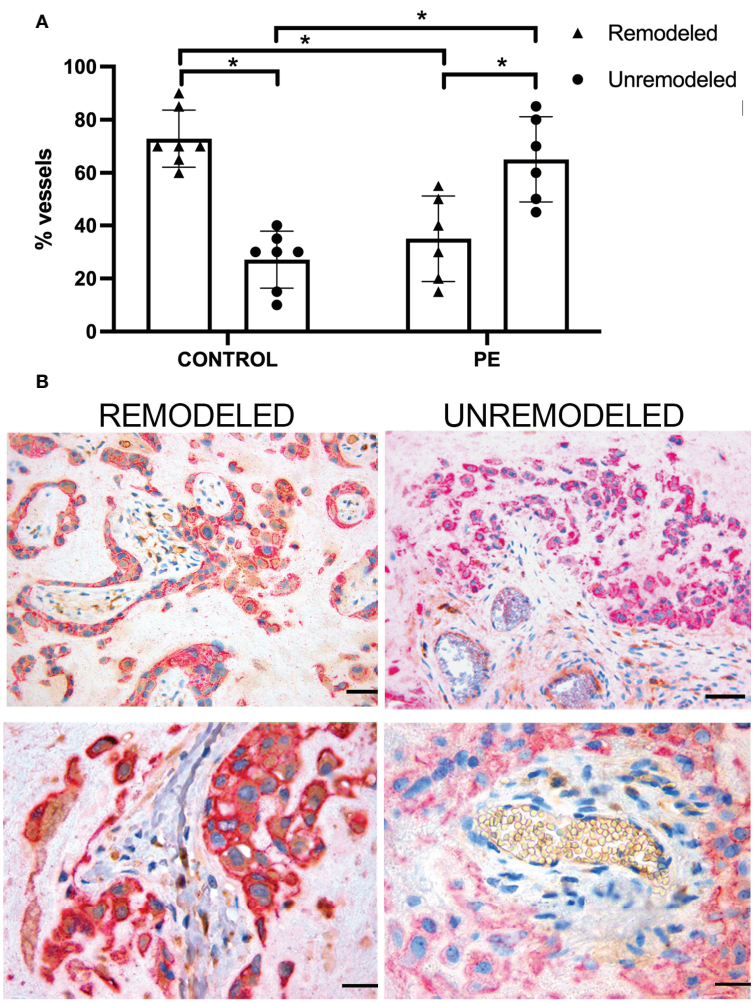

FIGURE 5 | Vascular remodeling in human placentae. Tissue sections were stained with hematoxylin and eosin and examined for the number of remodeled and unremodeled vessels in placental decidua. **(A)** The figure shows the percentage (± SD) of the two types of decidual vessels found in sections of normal (n = 7, CONTROL) and pre-eclamptic (n = 6, PE) placentae. After Mann-Whitney test add (*p < 0.001). **(B)** Representative images of placental sections double stained for C1q (brown) and cytokeratin 7 (red) expressed in trophoblasts. Note the presence of C1q in trophoblast surrounding remodeled vessels (upper and lower left panels) and its absence in trophoblasts surrounding unremodeled vessels (upper and lower right panels). Scale bars, 50 μm.

Different from C1q the other C components and the C activation products were focally distributed on decidual vessels and villous trophoblasts and were most likely deposited in areas of histopathologic alterations of the placental tissue. The localization of C4d and C3d in PE placenta is a clear indication of C activation that may reach completion with the deposition of terminal C complex revealed by a monoclonal antibody directed against a neoantigen of C9 expressed in C5b-9 complex (39). Linear deposits of C4d on syncytiotrophoblasts were reported to be associated with lower gestational age and fetal growth restriction in PE patients suggesting the contribution of C activation to the development of these clinical manifestations (23, 25). However, it is unclear whether C activation is a secondary event triggered by cells undergoing apoptosis or is directly responsible for trophoblast damage. It should be pointed out that syncytrophoblasts are relatively resistant to C-mediated killing, which requires the presence of cytotoxic antibodies and a marked decrease in the expression of the C regulators CD46 and CD59 (40). C dependent cytotoxic antibodies are infrequently found in PE patients except for those with antiphospholipid syndrome associated with PE (41). In addition, C regulators have been reported to be normally expressed both at molecular and protein levels in the placenta of PE patients (23, 24). However, we cannot exclude a sublytic effect of C on syncytiotrophoblasts resulting in the release of microparticles that circulate in maternal blood in normal pregnancy and at increased level in PE patients (42).

Most likely C activation plays a more critical role in decidua promoting inflammation and stimulating a hypercoagulable state that are both features of maternal abnormalities implicated in the second stage of PE pathogenesis (43). In this context C5a and C5b-9 have a significant impact on vascular endothelium by

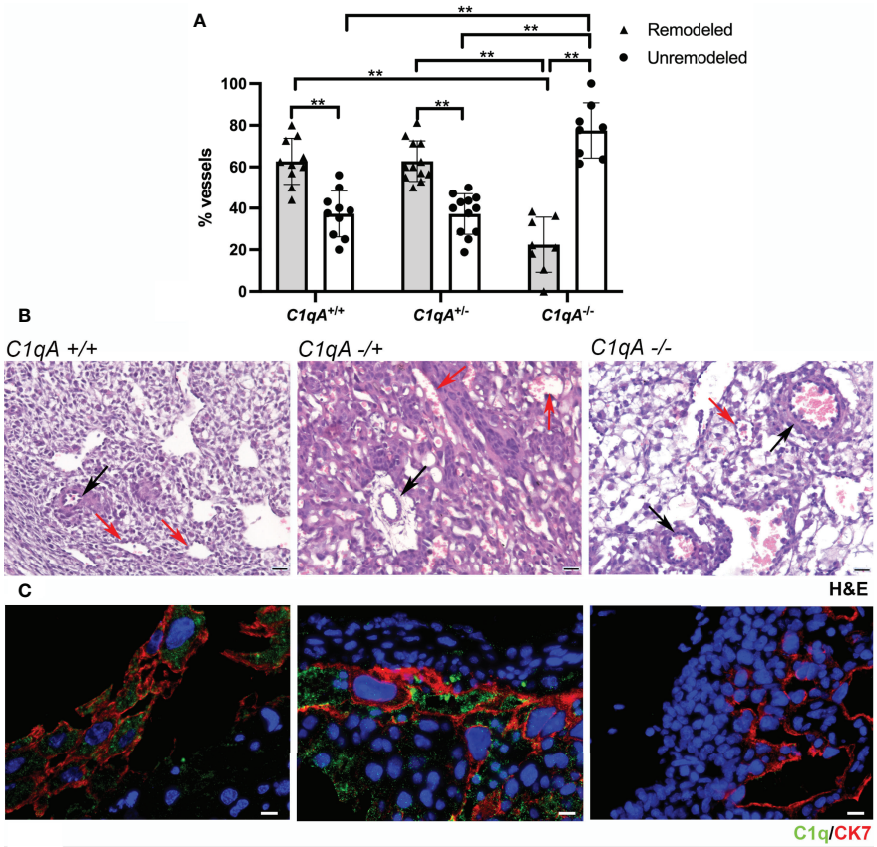

FIGURE 6 | Vascular remodeling in murine placentae. Tissue sections were stained with hematoxylin and eosin and examined for the number of remodeled and unremodeled vessels in placental decidua. **(A)** The upper panel shows the percentage (± SD) of the two types of decidual vessels found in embryo implantation sites from WT *C1qa*$^{+/+}$ (n = 10), heterozygous *C1qa*$^{+/-}$ (n = 12) and *C1qa*$^{-/-}$ (n = 8) mice. After (ANOVA) add (**p < 0.0001). **(B)** The middle panel shows representative sections of implantation sites from *C1qa*$^{+/+}$, *C1qa*$^{+/-}$ and *C1qa*$^{-/-}$ mice containing remodeled (red arrow) and unremodeled (black arrow) vessels. Scale bar, 50 µm. **(C)** The lower panel shows representative immunofluorescence images from sections of implantation sites from *C1qa*$^{+/+}$, *C1qa*$^{+/-}$ and *C1qa*$^{-/-}$ mice stained for C1q (green) and CK7 (red). Note the presence of C1q only in CK7 positive trophoblasts from *C1qa*$^{+/+}$ and *C1qa*$^{+/-}$ mice. Scale bars, 50 µm.

inducing release of proinflammatory cytokines, enhancing the expression of tissue factor and increasing vascular permeability (44). Whatever the mechanism involved in C-mediated placental damage in human preeclampsia, C activation has been shown to play an essential role in a mouse model of PE causing adverse pregnancy outcomes that can be prevented by the administration of C inhibitors (28, 32, 45).

The co-localization of C1q and C4 on syncytiotrophoblasts of PE placentae in the absence of MBL led Buurma and colleagues (23) to suggest that C is activated *via* the classical pathway possibly triggered by the binding of antibodies, although the association between C4d and immune complex deposits was not statistically significant. Our failure to detect C1r and C1s deposition at sites of C1q and C4d deposition in this study rules out the direct activation of the classical pathway and favors the activation of the lectin pathway. Consistent with this is our previous report that pregnancy loss in a mouse model of PE is mediated by MBL-dependent activation of the lectin pathway (32). However, we could not detect MBL in human PE placentae indicating that the results obtained in mice do not fully replicate the observations in PE patients as suggested by the different molecular organization of human and mouse MBL. Although mice and higher primates possess two *MBL* genes, *MBL1* and *MBL2*, only one *MBL* gene (*MBL2*) give rise to protein in man, while *MBL1* is expressed as pseudogene (*MBL1P1*) (46). By contrast, the two forms of MBL in mice are encoded by two distinct functional genes, known as *mbl-a* and *mbl-c*, and, consequently, the protein concentration of mouse MBL may be 10-fold higher than that of human MBL. Another important point to consider is that ficolin-3, the most abundant and most potent lectin pathway activator in man, is not present in mice, making a direct comparison of the lectin pathway activity between mice and humans difficult (47). Thus, the absence of MBL does not exclude activation of the lectin pathway by other initiators including ficolins and collectins as suggested by the strong staining of decidual vessels and villous syncytiotrophoblasts for ficolin-3, MASP-1, and MASP-2. The finding of ficolin-3 deposited on villous syncytiotrophoblasts of PE placentae is in

agreement with the observations by Wang and colleagues (48), who reported binding of ficolins to cells undergoing apoptosis and suggested that they may contribute to promote local inflammatory responses. While we are not excluding this possibility, our data showing deposition of MASPs and other C components on syncytiotrophoblasts indicate that ficolin-3 most probably acts as trigger of the lectin pathway. Ficolin-3-mediated C activation is likely to plays an important role in decidual vascular endothelium by contributing to endothelial activation and dysfunction as documented by the increased levels of endothelial-derived factors observed in PE patients, including inflammatory cytokines (6) and soluble adhesion molecules (49). Based on our results, we would speculate that the ficolin-3 gene, *FCN3*, may be turned on locally, particularly in the vascular bed, in response to different stimuli (50) and contributes to the pathophysiologic mechanisms causing PE in humans, a process that cannot be replicated in murine models (51). The subarachnoid hemorrhage in humans is another example of human pathologic condition associated with ficolin-3-dependent C activation (52).

We have previously provided evidence for an alternative role of C1q in normal pregnancy by showing impaired remodeling of the decidual vessel in C1q deficient pregnant mice (31), a recognized animal model of PE (27), and reduced levels of C1q mRNA transcripts in PE placental tissue (53). The finding that the unremodeled decidual vessels more frequently observed in PE patients are surrounded by trophoblasts that do not stain for C1q indicates that the vascular changes are associated with the expression of C1q in these cells. This is consistent with the observation that the defective remodeling of blood vessels in C1q deficient pregnant mice can be reversed by mating these animals with C1q sufficient mice, resulting in an increased number of remodeled vessels and the perivascular appearance of C1q-expressing trophoblasts. The EVT that invade the decidua in heterozygous and normal animals share the ability to synthesize C1q. The decreased and restricted expression of C1q to perivascular trophoblasts in decidual EVT from PE patients could be explained by the special microenvironment organized around the remodeled vessels that helps C1q-containing EVT to exert disruptive activity on the vascular wall (54). The mechanisms by which C1q modulates EVT effector functions remain to be defined.

In conclusion, we have shown that C components and C activation products are deposited on placental tissue obtained from PE patients but are absent in the control placentae except for C1q that is constitutively expressed at the placental level in physiological pregnancy. Our data support the notion that in human PE C is locally activated through the lectin pathway triggered by ficolin-3 whilst MBL does not appear to be involved. Equally, C1q is not implicated in the activation of the classical C pathway and should be considered a biomarker of EVTs that contribute to decidual vascular remodeling.

DATA AVAILABILITY STATEMENT

The original contributions presented in the study are included in the article/**Supplementary Material**. Further inquiries can be directed to the corresponding author.

ETHICS STATEMENT

The study was reviewed and approved by the Regional Ethical Committee of FVG (CEUR), Udine, Italy (CEUR-2020-Os-156; Prot. 0022668/P/GEN/ARCS). The patients/participants provided their written informed consent to participate in this study. The animal study was reviewed and approved by The UK Home Office.

AUTHOR CONTRIBUTIONS

FT, BB, and AM designed the study, analyzed the results, and wrote the manuscript. PG, MB, and RB provided resources, expertise and critically reviewed the manuscript. AG, VC, and GM performed the immunohistochemical staining. GR and FF organized patient recruitment. AM and CA prepared figures and tables and edited the manuscript. All authors contributed to the article and approved the submitted version.

FUNDING

This research was supported by grants from the Institute for Maternal and Child Health, IRCCS Burlo Garofolo, Trieste, Italy (RC20/16, RC23/18, 24/19 to G.R. and RC09/21 to CA).

ACKNOWLEDGMENTS

We thank Dr. Gabriella Zito and Dr. Livia Simoni for their help in patient enrollment.

SUPPLEMENTARY MATERIAL

The Supplementary Material for this article can be found online at: https://www.frontiersin.org/articles/10.3389/fimmu.2022.882298/full#supplementary-material

Supplementary Figure 1 | Immunohistochemical analysis of MBL, ficolin-2, C1r and C1s in liver tissue. Liver sections were stained for MBL **(A)**, ficolin-2 **(B)**, C1r **(C)** or C1s **(D)** as positive control for these C components that were undetectable in PE placentae. Scale bars, 50 μm.

Supplementary Figure 2 | Immunohistochemical analysis of ficolin-1 in placental tissue. Sections of pre-eclamptic (PE) and normal (CONTROL) placentae were stained for ficolin-1. The panel shows representative images of ficolin-1 deposits mainly localized on syncytiotrophoblasts of both PE and control placentae. Scale bars, 50 μm.

Supplementary Figure 3 | Analysis of vascular changes and trophoblast distribution in pre-eclamptic human placenta. The sections were stained anti-α-SMA antibody (brown) to reveal smooth muscle cells and CK7 (red) to document the presence of trophoblasts. A high proportion of vessels (arterioles) showed a preserved structure of the tunica media (upper and lower left panels). Along with preserved arterioles, vessels with various degrees of remodeling were also observed (upper and lower right panels). At sites of vascular remodeling trophoblast cells were detected in close proximity with the vessels. Scale bars, 50 μm.

Supplementary Figure 4 | C1q expression in interstitial trophoblast. Representative section of PE placenta double-stained for C1q (brown) and CK7 (red). The images show CK7 positive trophoblasts (red arrows) infiltrating the decidua at some distance from blood vessels and express C1q. Scale bars, 50 μm.

REFERENCES

1. Chaiworapongsa T, Chaemsaithong P, Yeo L, Romero R. Pre-Eclampsia Part 1: Current Understanding of its Pathophysiology. *Nat Rev Nephrol* (2014) 10 (8):466–80. doi: 10.1038/nrneph.2014.102
2. Burton GJ, Redman CW, Roberts JM, Moffett A. Pre-Eclampsia: Pathophysiology and Clinical Implications. *BMJ* (2019) 366:l2381. doi: 10.1136/bmj.l2381
3. Lyall F, Robson SC, Bulmer JN. Spiral Artery Remodeling and Trophoblast Invasion in Preeclampsia and Fetal Growth Restriction: Relationship to Clinical Outcome. *Hypertension* (2013) 62(6):1046–54. doi: 10.1161/HYPERTENSIONAHA.113.01892
4. Fisher SJ. Why is Placentation Abnormal in Preeclampsia? *Am J Obstet Gynecol* (2015) 213(4 Suppl):S115–22. doi: 10.1016/j.ajog.2015.08.042
5. Roberts JM, Taylor RN, Musci TJ, Rodgers GM, Hubel CA, McLaughlin MK. Preeclampsia: An Endothelial Cell Disorder. *Am J Obstet Gynecol* (1989) 161 (5):1200–4. doi: 10.1016/0002-9378(89)90665-0
6. Powe CE, Levine RJ, Karumanchi SA. Preeclampsia, a Disease of the Maternal Endothelium: The Role of Antiangiogenic Factors and Implications for Later Cardiovascular Disease. *Circulation* (2011) 123(24):2856–69. doi: 10.1161/CIRCULATIONAHA.109.853127
7. Rana S, Lemoine E, Granger J, Karumanchi SA. Preeclampsia. *Circ Res* (2019) 124(7):1094–112. doi: 10.1161/CIRCRESAHA.118.313276
8. Harmon AC, Cornelius DC, Amaral LM, Faulkner JL, Cunningham M, Wallace K, et al. The Role of Inflammation in the Pathology of Preeclampsia. *Clin Sci (Lond)* (2016) 130(6):409–19. doi: 10.1042/CS20150702
9. Redman CW, Sacks GP, Sargent IL. Preeclampsia: An Excessive Maternal Inflammatory Response to Pregnancy. *Am J Obstet Gynecol* (1999) 180(2 Pt 1):499–506. doi: 10.1016/s0002-9378(99)70239-5
10. Ricklin D, Hajishengallis G, Yang K, Lambris JD. Complement: A Key System for Immune Surveillance and Homeostasis. *Nat Immunol* (2010) 11(9):785–97. doi: 10.1038/ni.1923
11. Merle NS, Church SE, Fremeaux-Bacchi V, Roumenina LT. Complement System Part I - Molecular Mechanisms of Activation and Regulation. *Front Immunol* (2015) 6:262. doi: 10.3389/fimmu.2015.00262
12. Garred P, Tenner AJ, Mollnes TE. Therapeutic Targeting of the Complement System: From Rare Diseases to Pandemics. *Pharmacol Rev* (2021) 73(2):792–827. doi: 10.1124/pharmrev.120.000072
13. Garred P, Genster N, Pilely K, Bayarri-Olmos R, Rosbjerg A, Ma YJ, et al. A Journey Through the Lectin Pathway of Complement-MBL and Beyond. *Immunol Rev* (2016) 274(1):74–97. doi: 10.1111/imr.12468
14. Pierik E, Prins JR, van Goor H, Dekker GA, Daha MR, Seelen MAJ, et al. Dysregulation of Complement Activation and Placental Dysfunction: A Potential Target to Treat Preeclampsia? *Front Immunol* (2019) 10:3098. doi: 10.3389/fimmu.2019.03098
15. Burwick RM, Feinberg BB. Complement Activation and Regulation in Preeclampsia and Hemolysis, Elevated Liver Enzymes, and Low Platelet Count Syndrome. *Am J Obstet Gynecol* (2022) 226(2S):S1059–70. doi: 10.1016/j.ajog.2020.09.038
16. Derzsy Z, Prohaszka Z, Rigo JJr., Fust G, Molvarec A. Activation of the Complement System in Normal Pregnancy and Preeclampsia. *Mol Immunol* (2010) 47(7-8):1500–6. doi: 10.1016/j.molimm.2010.01.021
17. Denny KJ, Coulthard LG, Finnell RH, Callaway LK, Taylor SM, Woodruff TM. Elevated Complement Factor C5a in Maternal and Umbilical Cord Plasma in Preeclampsia. *J Reprod Immunol* (2013) 97(2):211–6. doi: 10.1016/j.jri.2012.11.006
18. Burwick RM, Fichorova RN, Dawood HY, Yamamoto HS, Feinberg BB. Urinary Excretion of C5b-9 in Severe Preeclampsia: Tipping the Balance of Complement Activation in Pregnancy. *Hypertension* (2013) 62(6):1040–5. doi: 10.1161/HYPERTENSIONAHA.113.01420
19. Lynch AM, Murphy JR, Byers T, Gibbs RS, Neville MC, Giclas PC, et al. Alternative Complement Pathway Activation Fragment Bb in Early Pregnancy as a Predictor of Preeclampsia. *Am J Obstet Gynecol* (2008) 198 (4):385.e1–9. doi: 10.1016/j.ajog.2007.10.793
20. Velickovic I, Dalloul M, Wong KA, Bakare O, Schweis F, Garala M, et al. Complement Factor B Activation in Patients With Preeclampsia. *J Reprod Immunol* (2015) 109:94–100. doi: 10.1016/j.jri.2014.12.002
21. Sinha D, Wells M, Faulk WP. Immunological Studies of Human Placentae: Complement Components in Pre-Eclamptic Chorionic Villi. *Clin Exp Immunol* (1984) 56(1):175–84.
22. Tedesco F, Radillo O, Candussi G, Nazzaro A, Mollnes TE, Pecorari D. Immunohistochemical Detection of Terminal Complement Complex and S Protein in Normal and Pre-Eclamptic Placentae. *Clin Exp Immunol* (1990) 80 (2):236–40. doi: 10.1111/j.1365-2249.1990.tb05240.x
23. Buurma A, Cohen D, Veraar K, Schonkeren D, Claas FH, Bruijn JA, et al. Preeclampsia is Characterized by Placental Complement Dysregulation. *hypertension* (2012) 60(5):1332–7. doi: 10.1161/HYPERTENSIONAHA.112.194324
24. Lokki AI, Heikkinen-Eloranta J, Jarva H, Saisto T, Lokki ML, Laivuori H, et al. Complement Activation and Regulation in Preeclamptic Placenta. *Front Immunol* (2014) 5:312. doi: 10.3389/fimmu.2014.00312
25. Kim EN, Yoon BH, Lee JY, Hwang D, Kim KC, Lee J, et al. Placental C4d Deposition is a Feature of Defective Placentation: Observations In Cases of Preeclampsia and Miscarriage. *Virchows Arch* (2015) 466(6):717–25. doi: 10.1016/j.jri.2014.12.002
26. Chaouat G, Kiger N, Wegmann TG. Vaccination Against Spontaneous Abortion in Mice. *J Reprod Immunol* (1983) 5(6):389–92. doi: 10.1016/0165-0378(83)90248-6
27. Ahmed A, Singh J, Khan Y, Seshan SV, Girardi G. A New Mouse Model to Explore Therapies for Preeclampsia. *PloS One* (2010) 5(10):e13663. doi: 10.1371/journal.pone.0013663
28. Girardi G, Yarilin D, Thurman JM, Holers VM, Salmon JE. Complement Activation Induces Dysregulation of Angiogenic Factors and Causes Fetal Rejection and Growth Restriction. *J Exp Med* (2006) 203(9):2165–75. doi: 10.1084/jem.20061022
29. Singh J, Ahmed A, Girardi G. Role of Complement Component C1q in the Onset of Preeclampsia in Mice. *Hypertension* (2011) 58(4):716–24. doi: 10.1161/HYPERTENSIONAHA.111.175919
30. Bulla R, Agostinis C, Bossi F, Rizzi L, Debeus A, Tripodo C, et al. Decidual Endothelial Cells Express Surface-Bound C1q as a Molecular Bridge Between Endovascular Trophoblast and Decidual Endothelium. *Mol Immunol* (2008) 45(9):2629–40. doi: 10.1016/j.molimm.2007.12.025
31. Agostinis C, Bulla R, Tripodo C, Gismondi A, Stabile H, Bossi F, et al. An Alternative Role of C1q in Cell Migration and Tissue Remodeling: Contribution to Trophoblast Invasion and Placental Development. *J Immunol* (2010) 185(7):4420–9. doi: 10.4049/jimmunol.0903215
32. Petitbarat M, Durigutto P, Macor P, Bulla R, Palmioli A, Bernardi A, et al. Critical Role and Therapeutic Control of the Lectin Pathway of Complement Activation in an Abortion-Prone Mouse Mating. *J Immunol* (2015) 195 (12):5602–7. doi: 10.4049/jimmunol.1501361
33. Hypertension in Pregnancy. Report of the American College of Obstetricians and Gynecologists' Task Force on Hypertension in Pregnancy. *Obstet Gynecol* (2013) 122(5):1122–31. doi: 10.1097/01.AOG.0000437382.03963.88
34. Botto M, Dell'Agnola C, Bygrave AE, Thompson EM, Cook HT, Petry F, et al. Homozygous C1q Deficiency Causes Glomerulonephritis Associated With Multiple Apoptotic Bodies. *Nat Genet* (1998) 19(1):56–9. doi: 10.1038/ng0598-56
35. Honore C, Rorvig S, Munthe-Fog L, Hummelshoj T, Madsen HO, Borregaard N, et al. The Innate Pattern Recognition Molecule Ficolin-1 is Secreted by Monocytes/Macrophages and is Circulating in Human Plasma. *Mol Immunol* (2008) 45(10):2782–9. doi: 10.1016/j.molimm.2008.02.005
36. Munthe-Fog L, Hummelshoj T, Hansen BE, Koch C, Madsen HO, Skjodt K, et al. The Impact of FCN2 Polymorphisms and Haplotypes on the Ficolin-2 Serum Levels. *Scand J Immunol* (2007) 65(4):383–92. doi: 10.1111/j.1365-3083.2007.01915.x

37. Munthe-Fog L, Hummelshoj T, Ma YJ, Hansen BE, Koch C, Madsen HO, et al. Characterization of a Polymorphism in the Coding Sequence of FCN3 Resulting in a Ficolin-3 (Hakata Antigen) Deficiency State. *Mol Immunol* (2008) 45(9):2660–6. doi: 10.1016/j.molimm.2007.12.012
38. Trouw LA, Seelen MA, Duijs JM, Benediktsson H, Van Kooten C, Daha MR. Glomerular Deposition of C1q and Anti-C1q Antibodies in Mice Following Injection of Antimouse C1q Antibodies. *Clin Exp Immunol* (2003) 132(1):32–9. doi: 10.1046/j.1365-2249.2003.02108.x
39. Wurzner R, Xu H, Franzke A, Schulze M, Peters JH, Gotze O. Blood Dendritic Cells Carry Terminal Complement Complexes on Their Cell Surface as Detected by Newly Developed Neoepitope-Specific Monoclonal Antibodies. *Immunology* (1991) 74(1):132–8.
40. Tedesco F, Narchi G, Radillo O, Meri S, Ferrone S, Betterle C. Susceptibility of Human Trophoblast to Killing by Human Complement and the Role of the Complement Regulatory Proteins. *J Immunol* (1993) 151(3):1562–70.
41. Tedesco F, Borghi MO, Gerosa M, Chighizola CB, Macor P, Lonati PA, et al. Pathogenic Role of Complement in Antiphospholipid Syndrome and Therapeutic Implications. *Front Immunol* (2018) 9:1388. doi: 10.3389/fimmu.2018.01388
42. Tannetta D, Masliukaite I, Vatish M, Redman C, Sargent I. Update of Syncytiotrophoblast Derived Extracellular Vesicles in Normal Pregnancy and Preeclampsia. *J Reprod Immunol* (2017) 119:98–106. doi: 10.1016/j.jri.2016.08.008
43. Sugimura M. Is Thrombin a "Toxin" in the Pathogenesis of Preeclampsia? *Hypertension Res Pregnancy* (2015) 3(1):13–8. doi: 10.14390/jsshp.3.13
44. Fischetti F, Tedesco F. Cross-Talk Between the Complement System and Endothelial Cells in Physiologic Conditions and in Vascular Diseases. *Autoimmunity* (2006) 39(5):417–28. doi: 10.1080/08916930600739712
45. Qing X, Redecha PB, Burmeister MA, Tomlinson S, D'Agati VD, Davisson RL, et al. Targeted Inhibition of Complement Activation Prevents Features of Preeclampsia in Mice. *Kidney Int* (2011) 79(3):331–9. doi: 10.1038/ki.2010.393
46. Garred P, Larsen F, Seyfarth J, Fujita R, Madsen HO. Mannose-Binding Lectin and its Genetic Variants. *Genes Immun* (2006) 7(2):85–94. doi: 10.1038/sj.gene.6364283
47. Garred P, Honore C, Ma YJ, Rorvig S, Cowland J, Borregaard N, et al. The Genetics of Ficolins. *J Innate Immun* (2010) 2(1):3–16. doi: 10.1159/000242419
48. Wang CC, Yim KW, Poon TC, Choy KW, Chu CY, Lui WT, et al. Innate Immune Response by Ficolin Binding in Apoptotic Placenta Is Associated With the Clinical Syndrome of Preeclampsia. *Clin Chem* (2007) 53(1):42–52. doi: 10.1373/clinchem.2007.074401
49. Krauss T, Kuhn W, Lakoma C, Augustin HG. Circulating Endothelial Cell Adhesion Molecules as Diagnostic Markers for the Early Identification of Pregnant Women at Risk for Development of Preeclampsia. *Am J Obstet Gynecol* (1997) 177(2):443–9. doi: 10.1016/s0002-9378(97)70213-8
50. Fernandez-Garcia CE, Burillo E, Lindholt JS, Martinez-Lopez D, Pilely K, Mazzeo C, et al. Association of Ficolin-3 With Abdominal Aortic Aneurysm Presence and Progression. *J Thromb Haemost* (2017) 15(3):575–85. doi: 10.1111/jth.13608
51. Garred P, Honore C, Ma YJ, Munthe-Fog L, Hummelshoj T. MBL2, FCN1, FCN2 and FCN3-The Genes Behind the Initiation of the Lectin Pathway of Complement. *Mol Immunol* (2009) 46(14):2737–44. doi: 10.1016/j.molimm.2009.05.005
52. Zanier ER, Zangari R, Munthe-Fog L, Hein E, Zoerle T, Conte V, et al. Ficolin-3-Mediated Lectin Complement Pathway Activation in Patients With Subarachnoid Hemorrhage. *Neurology* (2014) 82(2):126–34. doi: 10.1212/WNL.0000000000000020
53. Agostinis C, Tedesco F, Bulla R. Alternative Functions of the Complement Protein C1q at Embryo Implantation Site. *J Reprod Immunol* (2017) 119:74–80. doi: 10.1016/j.jri.2016.09.001
54. Harris LK, Smith SD, Keogh RJ, Jones RL, Baker PN, Knofler M, et al. Trophoblast- and Vascular Smooth Muscle Cell-Derived MMP-12 Mediates Elastolysis During Uterine Spiral Artery Remodeling. *Am J Pathol* (2010) 177(4):2103–15. doi: 10.2353/ajpath.2010.100182

Conflict of Interest: The authors declare that the research was conducted in the absence of any commercial or financial relationships that could be construed as a potential conflict of interest.

Publisher's Note: All claims expressed in this article are solely those of the authors and do not necessarily represent those of their affiliated organizations, or those of the publisher, the editors and the reviewers. Any product that may be evaluated in this article, or claim that may be made by its manufacturer, is not guaranteed or endorsed by the publisher.

frontiers | Frontiers in Immunology

REVIEW
published: 01 July 2022
doi: 10.3389/fimmu.2022.898298

Gasdermins: New Therapeutic Targets in Host Defense, Inflammatory Diseases, and Cancer

Laura Magnani, Mariasilvia Colantuoni and Alessandra Mortellaro *

San Raffaele Telethon Institute for Gene Therapy (SR-Tiget), IRCCS San Raffaele Scientific Institute, Milan, Italy

Gasdermins (GSDMs) are a class of pore-forming proteins related to pyroptosis, a programmed cell death pathway that is induced by a range of inflammatory stimuli. Small-scale GSDM activation and pore formation allow the passive release of cytokines, such as IL-1β and IL-18, and alarmins, but, whenever numerous GSDM pores are assembled, osmotic lysis and cell death occur. Such GSDM-mediated pyroptosis promotes pathogen clearance and can help restore homeostasis, but recent studies have revealed that dysregulated pyroptosis is at the root of many inflammation-mediated disease conditions. Moreover, new homeostatic functions for gasdermins are beginning to be revealed. Here, we review the newly discovered mechanisms of GSDM activation and their prominent roles in host defense and human diseases associated with chronic inflammation. We also highlight the potential of targeting GSDMs as a new therapeutic approach to combat chronic inflammatory diseases and cancer and how we might overcome the current obstacles to realize this potential.

Keywords: gasdermins, pyroptosis, inflammasome, host defense, cancer, therapeutics

OPEN ACCESS

Edited by:
Uday Kishore,
Brunel University London,
United Kingdom

Reviewed by:
Meredith O'Keeffe,
Monash University, Australia
Paras K. Anand,
Imperial College London,
United Kingdom

***Correspondence:**
Alessandra Mortellaro
mortellaro.alessandra@hsr.it

Specialty section:
This article was submitted to Molecular Innate Immunity, a section of the journal Frontiers in Immunology

Received: *17 March 2022*
Accepted: *06 June 2022*
Published: *01 July 2022*

Citation:
Magnani L, Colantuoni M and Mortellaro A (2022) Gasdermins: New Therapeutic Targets in Host Defense, Inflammatory Diseases, and Cancer. Front. Immunol. 13:898298. doi: 10.3389/fimmu.2022.898298

INTRODUCTION

Gasdermins (GSDMs) are a group of proteins whose discovery has occurred gradually over the past two decades, beginning with the identification of *Gsdma1* in mice and soon followed by the mapping of the orthologous human gene *GSDMA* (1–3). To date, six human (*GSDMA-E* and *PEJVAKIN*) and ten mouse GSDM genes (*GsdmA1-3, GsdmC1-4, GsdmD, GsdmE*, and *PJVK*) have been identified, with distinct patterns of expression that are highly conserved between the two species (**Table 1**). Early clues on the functions of GSDMs came from this pattern of expression throughout the barrier epithelia of the esophagus, stomach, colon, bladder, vagina, and prostate, with some also being expressed in leukocyte subsets (GSDMA), lymphocytes (GSDMB), and myeloid cells (GSDMD) (3–5, 18).

The most important advance in our understanding of GSDM biology came in 2015 when two seminal articles simultaneously identified GSDMD as the primary executor of a type of pro-

inflammatory programmed cell death known as pyroptosis (19, 20). Pyroptosis results from the formation of large numbers of GSDM pores that disrupt plasma membrane integrity, leading to cell death, and can be triggered by pathogen-derived or endogenous danger molecules (21). However, there is evidence of alternative outcomes of GSDM pore formation in which cells do not die, such as macrophage hyperactivation after nigericin stimulation or during *Salmonella typhimurium* infection in the presence of glycine (22), and a recent study illustrating a homeostatic role of GSDMD in mucus secretion in the gut (23). The factors that determine the extent of GSDM pore formation or its outcome are only just beginning to be understood. Nevertheless, it is clear that the balance between the two is central to the maintenance of health and in disease states.

Given the polarized outcomes of GSDM activation in cells, it is perhaps not surprising that there may be dire consequences when their function or regulation goes awry. While we now know that GSDMs are critical for protective responses to bacterial, fungal, and viral infections, recent research has also implicated these proteins in the pathogenesis of conditions as diverse as cancer (9, 24), alopecia (18), and asthma (6) (**Table 1**). This review highlights the most recent and important advances in the activation and innate immune functions of GSDMs and their roles in a range of pathologies. We will also examine the possibility of targeting this protein family therapeutically and reflect on the latest attempts to do so. Lastly, we will discuss the most pressing challenges and knowledge gaps that must be overcome to advance the field of GSDM research.

MOLECULAR INSIGHTS INTO GSDM ACTIVATION

Following the discovery that GSDMD is central to pyroptosis, most studies on GSDM activation have focused on this family member and its role in myeloid cells, such as macrophages. Exposing macrophages to pathogen-associated molecular patterns (PAMPs), environmental particulates or toxins, or endogenous danger-associated molecular patterns (DAMPs) such as high mobility group box 1 (HMGB1), adenosine triphosphate (ATP), or cholesterol crystals, triggers the formation of a multiprotein complex, known as the inflammasome (**Figure 1**) (21). This type of canonical inflammasome activation leads to the activating autoproteolytic cleavage of pro-caspase-1, with two important consequences: caspase-1 processes the precursors of the pro-inflammatory cytokines IL-1β and IL-18 into their biologically active forms, and it also processes full-length GSDMD. This processing allows the N-terminal domain of GSDMD to mediate its

TABLE 1 | Comparison of gasdermin protein expression, function, associated diseases and therapeutics in mice and humans.

Gasdermin genes		Protein expression pattern		Function		Disease association	Therapeutics targeting	
Human	**Mouse**	**Human**	**Mouse**	**Human**	**Mouse**	**Human**	**Drug**	**Indication**
GSDMA	GsdmA1 GsdmA2 GsdmA3	Epithelial cells [bladder (2), gastrointestinal tract (4), skin (5)]	Epithelial cells [bladder (2), gastrointestinal tract (4), skin (5)]	Cell death	Cell death	Asthma (6) Systemic sclerosis (7)	–	–
GSDMB	None	Epithelial cells [gastrointestinal tract, bladder, airways, bone marrow, lymphoid tissues (4, 5)]	–	Pyroptosis	–	Asthma (8) Pro-tumoral activity (9)	–	–
GSDMC	GsdmC1 GsdmC2 GsdmC3 GsdmC4	Epithelial cells (4, 5) (skin, bladder, gastrointestinal tract, female tissues)	Epithelial cells (4, 5) (skin, bladder, gastrointestinal tract, female tissues)	Unknown	Unknown	No clear association	–	–
GSDMD	GsdmD	Leukocytes, respiratory system, gastrointestinal tract, bone marrow, liver, gallbladder (4, 5)	Leukocytes, respiratory system, gastrointestinal tract, bone marrow, liver, gallbladder (4, 5)	Pyroptosis	Pyroptosis	Hyper-activation in autoinflammatory diseases (CAPS, FMF) (10)	Dimethyl-fumarate (11) Disulfiram (12) α-NETA (13)	Hyper-inflammation Cancer
GSDME	GsdmE	Gastrointestinal tract, muscle tissues, genital tissues, endocrine tissues (4, 5)	Gastrointestinal tract, muscle tissues, genital tissues, endocrine tissues (4, 5)	Pyroptosis Anti-tumor activity	Pyroptosis Anti-tumor activity	Deafness (14) Tubulo-interstitial fibrosis (15) Cancer (16)	Disulfiram (12) Z-DEVD-FMK (15) miRNA combined with cetuximab (breast cancer) (17)	Hyper-inflammation Tubulo-interstitial fibrosis Cancer
PJVK	Pvjk	Transcript mainly expressed in male tissues and brain (4, 5)	Kidney, testis (4, 5)	Mitochondrial homeostasis Pexophagy (hypothesized)	Mitochondrial homeostasis Pexophagy (14)	Deafness (14)	–	–

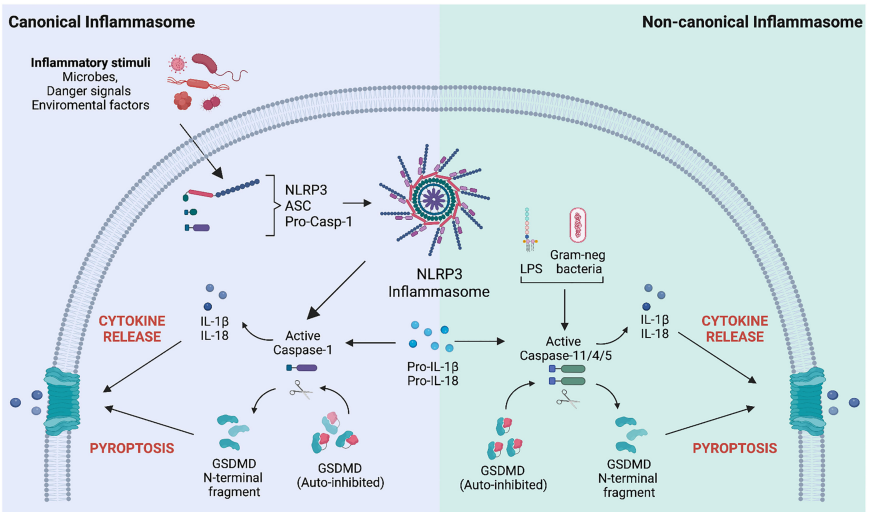

FIGURE 1 | Mechanisms of Gasdermin D activation following canonical and non-canonical inflammasome stimulation. *Left.* Canonical inflammasome activation is a well-structured process involving several steps. Upon sensing specific inflammatory stimuli (microbes, danger signals, and environmental factors), the inflammasome sensor (*i.e.*, NOD-like receptor protein 3, NLRP3) recruits the precursor of caspase-1 (pro-caspase-1) *via* the protein adaptor apoptosis-associated speck-like protein containing a CARD (ASC). Upon inflammasome complex formation, pro-caspase-1 is activated by autocatalytic processing and converts the pro-IL-1β and pro-IL-18 precursors into their bioactive forms. Matured caspase-1 also cleaves the pore-forming protein gasdermin D (GSDMD), generating the N-terminal domain of GSDMD (GSDMD-NT), which relocates to the plasma membrane and oligomerizes to form a pore. Pore formation allows the release of mature IL-1β and IL-18 and drives a type of inflammatory cell death known as pyroptosis. *Right.* The non-canonical inflammasome pathway is activated by intracellular sensing of Gram-negative bacteria or lipopolysaccharides (LPS). It involves the activation of human caspase 4/5 or caspase-11 in mice. Active caspases directly process the pro-IL-1β and pro-IL-18 precursors and GSDMD. Like the canonical inflammasome activation mode, GSDMD pores allow the passive release of IL-1β/IL-18 cytokines and pyroptosis.

oligomerization at the plasma membrane, thereby forming the pores that both allow IL-1β and IL-18 release while also – at least in some cases – leading to pyroptotic cell death (25, 26). Intracellular delivery of PAMPs, such as lipopolysaccharide (LPS), activates the non-canonical inflammasome, which also leads to IL-1β and IL-18 secretion and GSDMD processing, but, in this case, it is mediated by caspase-4 and -5 in humans, and caspase-11 in mice (**Figure 1**) (27). Nevertheless, there are exceptions to these rules. Inflammasome activation can selectively promote cytokine processing independently of pyroptosis as described in LPS-stimulated human monocytes (28) and *Salmonella*-infected mouse neutrophils (29) are resistant to pyroptosis while still being good producers of IL-1β. GSDMD pores serve as conduits for the passive release of IL-1β from hyperactivated but living macrophages in response to bacteria and DAMPs (30, 31). Cell vitality can be preserved by removing GSDMD pores *via* the transient recruitment of the endosomal sorting complexes required for transport (ESCRT) machinery at the plasma membrane (32). The ESCRT system is essential for many cellular processes, including membrane bending and fission reactions during the multivesicular body pathway, budding of enveloped viruses, membrane rupture phase in cytokinesis, and membrane repair. In particular, the ESCRT-III complex has been associated with all the ESCRT-mediated membrane patching functions (33). Ca^{2+} influx through GSDMD pores attracts the ESCRT-III complex at the damaged plasma membrane to remove GSDM pores and initiate the repair (32). Indeed, ESCRT-III protein inhibition enhanced IL-1β secretion and pyroptosis in human and mouse macrophages following inflammasome activation (32). These findings identify a fundamental role of the ESCRT complex in limiting GSDM-dependent pyroptosis cell death and cytokine release.

GSDM activation can also be achieved by proteases other than caspases under specific circumstances. For example, granzyme B, which is released in cytotoxic granules by $CD8^+$ T lymphocytes and passed into target cells *via* perforin pores, can process and activate GSDME, leading to the target cell pyroptosis (16) (**Figure 2**). Similarly, granzyme A released by cytotoxic NK and $CD8^+$ T cells into target cells can cause pyroptotic killing mediated by GSDMB (34). Furthermore, the neutrophil-specific serine protease elastase can produce a fully active GSDMD, resulting in NETosis, vital for effective pathogen clearance through neutrophil extracellular traps (NETs) formation (35, 36).

Alongside GSDM activation *via* the PAMP/DAMP-mediated inflammasome route or the alternative immune protease route, recent studies have uncovered links between the apoptotic program and GSDM-mediated pyroptosis. The extrinsic apoptotic pathway activates caspase-8, which can cleave GSDMD to elicit lytic cell death during infection of cells with *Yersinia spp* (37, 38). At the same time, other studies showed that GSDME is cleaved by the apoptotic caspase-3 in human cell lines *in vitro*, whose upstream activation can be triggered by etoposide

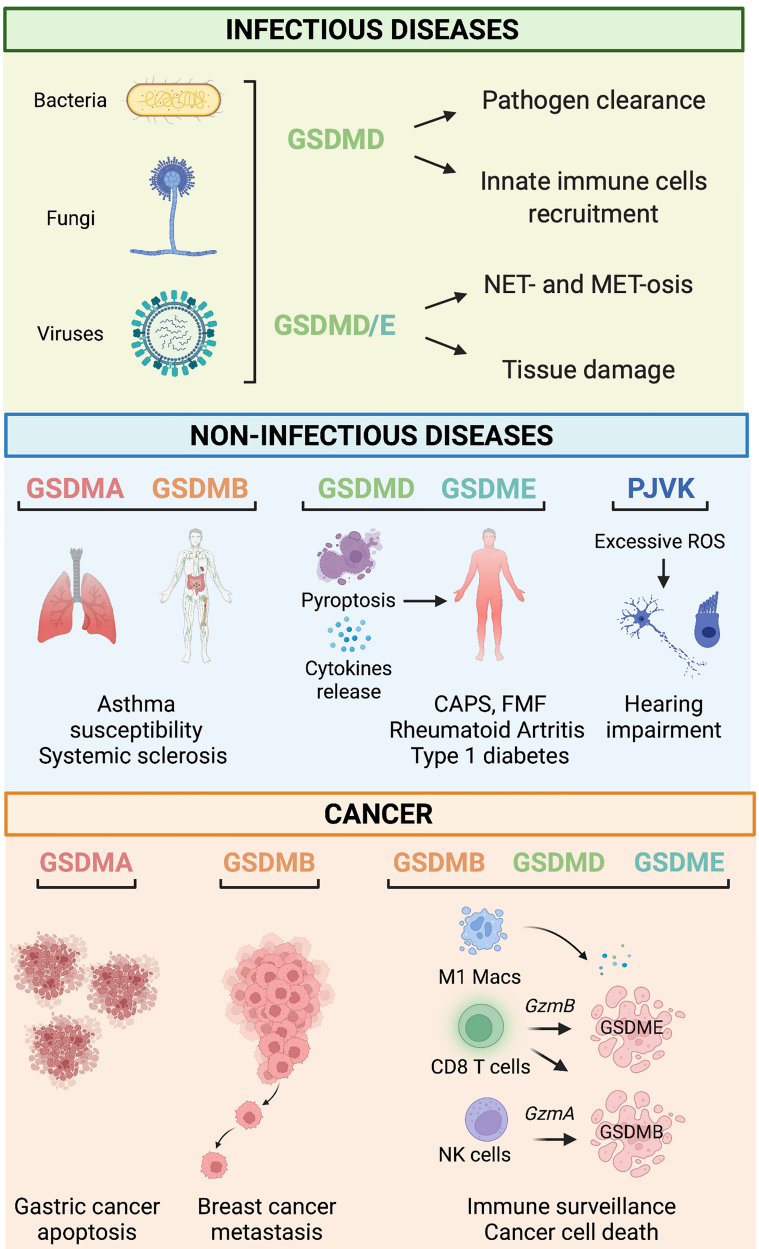

FIGURE 2 | Gasdermin-related functions in infectious and non-infectious diseases and cancer. *Infectious diseases.* During infections, GSDM-mediated pyroptosis is, in general, beneficial for the host because it leads to successful pathogens eradication by mediating innate immune cell recruitment, NET- and MET-osis. However, under some circumstances, detrimental pyroptosis occurs which causes unwarranted and permanent tissue damage. *Non-infectious diseases.* GSDMA and GSDMB polymorphisms are associated with asthma susceptibility, bronchial hyperresponsiveness, and increased risk of multiple sclerosis. GSDMD and GSDME mediate pyroptosis and cytokine release associated with many immune-mediated inflammatory diseases such as Cryopyrin-associated periodic syndrome (CAPS), Familial Mediterranean fever (FMF), rheumatoid arthritis, and type 1 diabetes. *PJVK*-deficiency triggers excessive generation of reactive oxygen species (ROS), which cause hearing impairment due to cell death of auditory cells and sensory neurons. *Cancer.* GSDMA reduces the growth of gastric cancer cells by promoting apoptosis. On the other hand, GSDMB overexpression has been linked to metastatic and invasive properties of breast cancer cells. Tumor-infiltrating immune cells (*i.e.*, M1 macrophages, $CD8^+$ T cells, and NK cells) promote cell death of cancer cells *via* a mechanism mediated by the granzyme-GSDMB/D/E pathway.

or vesicular stomatitis virus (VSV) infection (39). The broader physiological/pathological relevance of these findings is yet to be fully explored, but together these studies illuminate multiple pathways whose activation can converge on GSDM activation and downstream pore formation. It will be a topic of much interest to understand which pathways predominate in different situations and whether they result in different outcomes for pore-bearing cells.

NON-PYROPTOTIC EFFECTOR FUNCTIONS OF GSDMS

Some reports have also highlighted the non-pyroptotic functions of GSDMs in host defense against pathogens, which is an area of rapid development within the field. In bacterial infections, NET formation is a dominant mechanism of pathogen clearance, and Sollberger et al. recently revealed the role of GSDMD in promoting nuclear envelope permeabilization and extrusion of chromatin and other proteins to form NETs in both human and mouse neutrophils (36). A similar mechanism has now also been described in macrophages, where caspase-1-mediated GSDMD cleavage promotes membrane permeabilization, leading to "METosis," a type of macrophage cell death characterized by the release of NET-like chromatin webs that capture extracellular bacteria (40). The significance of this new role for GSDMD is yet to be assessed more widely, but these findings are intriguing nonetheless.

Alongside assisting in NET- and MET-osis, work by Zhang et al. has uncovered a novel role for GSDMD in mucus secretion in the murine digestive tract during both homeostasis and pathogenic bacterial infection, which was required for effective clearance of enteric pathogens in mice (23). It is not yet clear how/whether this observation translates to humans. Still, this study provides the first indication of a homeostatic role for GSDMD within the intestinal epithelium and further evidence of the importance of GSDMs that extends beyond pyroptosis and into steady-state functions relating to pore-mediated secretory pathways that are yet incompletely defined.

THE ROLE OF GSDMs IN THE INNATE IMMUNE RESPONSE TO INFECTION

GSDMs are critical innate immune factors that promote inflammation to fight bacterial, fungal, and viral infections, which they achieve by executing pyroptosis and allowing the release of IL-1β and IL-18 to the extracellular space (**Figure 2**). Recent studies have hinted at further roles around the intersection of innate and adaptive immunity and at specialized GSDM pathways within neutrophils and macrophages. This section will summarize the known pyroptosis and non-pyroptosis-related functions of the GSDM family members during infections.

Bacterial Infections

GSDM-mediated pyroptosis of infected cells releases numerous PAMPs and DAMPs, which actively promote phagocyte recruitment to the site of inflammation to mediate pathogen clearance. Human and mouse macrophages undergo pyroptosis upon infection with bacteria, as seen with *Yersinia* spp. (41), *Escherichia coli* (42), *Brucella* spp. (43), *Burkholderia thailandensis* (44), and *Salmonella enterica* spp. (45). During these infections, bacteria-derived molecules act as immunological "danger signals" and induce the inflammasome activation that drives GSDMs processing. Recent work identified *Staphylococcus aureus*-derived α-hemolysin (46) and lipoprotein 19 from *Brucella* bacteria as novel activators of the NLRP3 inflammasome and GSDMD processing. *Brucella* bacteria lipoprotein 16 leads to GSDME cleavage (43). However, in many cases, the precise pathogenic trigger is unknown.

Direct evidence of the importance of pyroptosis has been demonstrated recently by a study showing that non-canonical inflammasome activation through the caspase-11/GSDMD axis is critical for killing *Brucella abortus* inside the replicative niche (47). Indeed, *Gsdmd*- or *caspase-11*-deficient mice were more susceptible to *Brucella abortus* infection, probably due to defective recruitment of neutrophils, dendritic cells, and macrophages in spleens of infected mice (48). Other GSDM-mediated mechanisms have been shown to promote effective pathogen clearance by preventing bacterial replication. A cross-talk between GSDMD and autophagy has been proposed based on the observation that *Gsdmd*-deficient mice have an impaired autophagic process upon pulmonary infection with *Burkholderia cenopacia.* Indeed, less LC3-II conversion was observed in lung homogenates of infected *Gsdmd*-deficient mice (47). GSDMD-mediated direct killing of *Burkholderia thailandensis* was also demonstrated *in vitro* (44).

GSDMs can also alert tissue-resident cells surrounding the site of infection. *Yersinia* spp. infection triggered neutrophil and macrophage pyroptosis *via* a GSDMD/E-mediated pathway (38). Moreover, Chen et al. uncovered a crucial role of GSDME activation by the acetyltransferase YopJ of *Yersinia pseudotuberculosis* in the *in vivo* killing of infected neutrophils as a beneficial mechanism for the host (49). Moreover, neutrophils leverage NETs release to achieve successful pathogen clearance, and some evidence suggests that this occurs in a GSDM-dependent fashion (16, 33). For example, *Gsdmd*-deficient mice exhibited delayed neutrophil death and enhanced cytotoxic activity against *Escherichia coli* infection *in vivo*, further corroborating the GSDMD role for fine-tuning the immune response (33). As the involvement of GSDMs in METosis has only recently been described (49), it is not yet clear whether GSDM-driven over-activation of this process has relevance during infection, but this will be of great interest to study.

Pyroptosis is not always beneficial for the host. For example, the excessive inflammatory response caused by *Staphylococcus aureus*-induced pyroptosis is the leading cause of bovine mastitis, driving the damage of mammary tissue and epithelial cells (50). It has yet to be seen whether similar mechanisms operate in human mastitis, which is also predominantly caused by *Staphylococcus* spp. Craven et al. showed that α-hemolysin triggered the NLRP3 inflammasome in mouse and human monocytes, causing an enhanced IL-1β and LDH release (46). In human sepsis, Esquerdo et al. uncovered higher expression levels of inflammasome genes in patients who died of sepsis than those who survived (51), hinting at the possibility of GSDM involvement, but this has yet to be formally tested. However, in support of this notion, there is an earlier work showing that *Gsdmd*-deficient mice are protected from LPS-induced septic shock (20) and that administration of necrosulfonamide, which blocks GSDMD pore formation, lowers the level of systemic pro-inflammatory cytokines and prolongs survival in a murine model of lethal sepsis (52).

Fungal Infections

Inflammasome activation also operates during opportunistic fungal infections caused by *Aspergillus fumigatus* (53) and *Candida albicans* (54). Although inflammasome involvement during fungal infections was already established (55, 56), the role of GSDMs is still incompletely clarified. GSDMD-mediated pyroptosis is one of the leading cell death mechanisms occurring upon fungal infections. Upon *Aspergillus fumigatus* or *Candida albicans* infection, mouse and human macrophages activate inflammasome and undergo PANoptosis (pyroptosis, apoptosis, and necroptosis) *via* a mechanism that requires the innate immune sensor Z-DNA binding protein 1 (ZBP1) as an apical sensor of fungal infection (57). Yan et al. revealed a key role of GSDMD in eradicating *Aspergillus fumigatus*, showing that Toll-like receptor 2 was required for the expression of GSDMD, IL-1α, and IL-1β, thereby modulating the pyroptosis (53).

The role of GSDMD-induced pyroptosis has been recently elucidated in a mouse model of *Candida albicans* keratitis, a sight-threatening corneal infection. Expression levels of NLRP3, caspase-1, IL-1β, and GSDMD, and pyroptotic cell death were significantly increased in *Candida albicans*-infected corneas (54). shRNA-mediated NLRP3 knockdown in corneas reduced inflammation and clinical scores, indicating that NLRP3 inflammasome activation is involved in the progression of *Candida albicans* keratitis (54). Further investigations are needed to elucidate the exact activation mechanisms and effector actions of GSDMs throughout fungal infections.

Viral Infections

GSDMs are involved in the host response to viral infections, and there are examples showing the beneficial effects of GSDM-mediated pyroptosis in aborting viral replication in infected cells (58). *Gsdmd*-deficient mice were markedly more susceptible to rotavirus infection compared to wild-type, showing increased viral load and diarrhea (59). A recent paper highlighted that antibody-opsonized respiratory syndrome coronavirus 2 (SARS-CoV-2) virions triggered inflammation and pyroptosis in human blood monocytes of patients with COVID-19 *via* the NLRP3/AIM2 inflammasome pathway leading to caspase-1 and GSDMD processing. Lung macrophages also showed activated inflammasomes, suggesting that GSDMD-mediated inflammatory cell death restricts viral production but causes systemic inflammation that contributes to COVID-19 pathogenesis (60). In a lethal model of H5N1 influenza virus infection in non-human primates, histopathological sections of infected lungs showed significant pulmonary infiltration of neutrophils exhibiting upregulated expression of NETosis-related genes (61). Moreover, viral-activated macrophages and alveolar epithelial cells possibly contributed to the pathological outcomes through enhanced GSDMD-mediated pyroptosis and uncontrolled inflammasome activation (61).

The role of GSDMs in anti-viral cytokine release during viral infection is also beginning to be revealed. Type I interferons (IFNs) are well-characterized anti-viral agents, and new data showed that GSDMD mediates the non-canonical release of IFN-β and an enhanced response to IFN-stimulated genes during transmissible gastroenteritis virus and porcine delta coronavirus (pDCoV) infection *in vitro* (62). Alongside type I IFN, a recent study revealed a role for caspase-3-dependent cleavage of GSDME in the release of IL-1α from keratinocytes infected by VSV (63). This last study is the first to elucidate an anti-viral role for GSDME, calling for further investigation of this family member in the field of viral interactions.

Detrimental GSDMD activation was revealed in a STAT-1-deficient mouse model susceptible to norovirus (MNV) infection. MNV-infected macrophages and intestinal epithelial cells showed increased NLRP3 inflammasome activation, IL-1β maturation, and GSDMD-dependent pyroptosis, leading to gastrointestinal inflammation and increased lethality (64). Similarly, hepatitis C virus (HCV) caused hepatocyte pyroptosis soon after infection, but in the absence of GSDMD, HCV activated a caspase-3-mediated apoptotic program. On the other hand, caspase-3 knockout led to a reduced caspase-1 activation, suggesting that pyroptosis and apoptosis cooperate to enhance virus release from infected cells, thus contributing to liver pathogenesis (65). Concomitant apoptosis and pyroptosis also occurred in macrophages infected with the Zika virus, which may significantly impact viral pathogenesis in humans (66).

Viruses have evolved mechanisms to subvert the innate immune response, serving as the first line of defense. Accordingly, recent studies have uncovered multiple viral strategies to disable GSDM-mediated pore formation and pyroptosis. Influenza A virus avoids extensive pyroptosis by activating caspase-8-mediated processing of caspase-3, leading to the formation of the GSDMD p20 fragments, which are unable to form pores (67). In contrast, VSV infection activated GSDME in a caspase-3-dependent manner in keratinocytes. Mechanistically, VSV hijacked protein synthesis, which depletes host cells of anti-apoptotic proteins, such as BCL-2 family members, resulting in caspase-3-initiated GSDME-mediated pyroptosis (63). In addition, the viral protease pS273R of the African swine fever virus induced the processing of GSDMD into two pieces that cannot induce pyroptosis of the infected cells (68). The Nsp5 protease of porcine and human coronaviruses, including SARS-CoV-2, cleaved GSDMD into peptides unable to trigger pyroptotic cell death (69). Alternatively, SARS-CoV-2 nucleocapsid protein prevented GSDMD processing by binding to its linker region (70).

Together, these studies reveal a role for GSDMD-mediated pyroptosis in a wide range of infections and in several viral infections where immune evasion strategies are coming to the fore. This is a relatively new field of investigation. The examples listed here likely represent only a fraction of the actual number of infections in which pyroptosis is a key aspect of host defense. Further analysis of pathogen-mediated anti-GSDM/anti-pyroptosis strategies may reveal novel ways of interfering with this pathway therapeutically.

DYSREGULATED GSDM ACTIVATION IN NON-INFECTIOUS DISEASES

Given their critical and finely balanced roles in maintaining homeostasis and fighting infection, it is perhaps not surprising that aberrant GSDM activation can contribute to disease pathways (**Figure 2**). We have known for some time that single nucleotide polymorphisms in *GSDMA* and *GSMDB* are associated with asthma susceptibility, elevated IgE levels, and bronchial hyperresponsiveness in children with asthma; and that mice transgenic for the higher risk human *GSDMB* allele develop similar airway-hyperresponsiveness (8). More recently, a meta-analysis of genome-wide association studies in humans identified *GSDMA* and *GSDMB* variants associated with systemic sclerosis (7): macrophages from patients with systemic sclerosis who carried the risk variant rs3894194 showed GSDMA over-expression (71), but clear links between the functions of these less well-studied GSDMs and the pathophysiology of the disease remain to be elucidated.

As our understanding of the significance of GSDMs in inflammatory diseases grows, many studies are re-examining NLRP3-inflammasome-mediated conditions and asking whether GSDMs are involved. Cryopyrin-associated periodic syndromes (CAPS) result from gain-of-function mutations in the NLRP3 gene (10), and mouse models of CAPS exhibit excessive activation of GSDMD, which significantly contributes to the disease etiology (72). Another study showed that *Gsdmd* ablation in a mouse CAPS model rescued lethality, skin, spleen abnormalities, leukocytosis, and anemia (73). Similar results were seen in a mouse model of Familiar Mediterranean fever (FMF). The inflammasome-driven auto-inflammation that characterizes the condition was entirely ameliorated by the deletion of *Gsdmd* (74). However, there is some evidence from mice that, in the absence of GSDMD, GSDME can functionally compensate, maintaining high levels of IL-1β and IL-18 during constitutive NLRP3 inflammasome stimulation (12). The relevance of the GSDME pathways in conditions where inflammasome hyperactivation is implicated should be a priority research area.

Several GSDM family members have also been associated with other diseases characterized by immune dysregulation, including inflammatory bowel disease (IBD). GSDMA and *GSDMB* are susceptibility genes (75, 76) but with yet-undefined roles in the condition. However, in mice, there is evidence that GSDMD is required for microbiota-stimulated IL-18 release in the inflamed gut (77) and that it also mediates the non-lytic release of intestinal-epithelial-cell-derived inflammatory IL-1β-containing vesicles (78). In another auto-inflammatory disease, rheumatoid arthritis, there is a positive correlation between GSDME expression and TNF-induced pyroptosis mediated by the caspase-3/GSDME pathway in patients' monocytes. *Gsdme* deficiency decreases disease incidence and severity in a collagen-induced arthritis mouse model (79). Interestingly, the same caspase3-dependent GSDME-mediated pyroptotic pathway is seemingly involved in type 1 diabetes progression and diabetic nephropathy, a severe co-morbidity of diabetes (15). Future studies should reveal whether this route towards pyroptosis is more broadly activated in such conditions.

The GSDM family member PJVK is expressed in the sensory cells and neurons of the auditory part of the inner ear (4). Indeed, PJVK is a peroxisome-associated protein required for oxidative-stress-induced proliferation in sensory hair cells (80). Loss-of-function mutations in human and mouse *PJVK* are associated with hearing defects caused by impaired peroxisome degradation induced by excessive noise (14). Noise overexposure in *Pjvk*-deficient mice causes marked reactive oxygen species production, diminished antioxidant response, and inefficient autophagic degradation of peroxisomes (14). Gain-of-function *GSDME* variants are also related to hearing impairment by enhancing a detrimental cytotoxic activity of GSDME (81).

These studies reveal multiple roles of different GSDM family members in various auto-inflammatory and auto-immune conditions. However, in many cases, the picture is incomplete. Our ability to delve further into disease mechanisms is limited by our lack of knowledge of the upstream and downstream events of the less well-studied members of the GSDM family.

THE ROLE OF GSDMS IN CANCER

The ability of GSDMs to activate inflammatory pathways, leading to the recruitment of both innate and adaptive immune effector cells, and to execute cell death, has led to an increasing interest in their potential role in cancer (**Figure 2**). Multiple studies have reported the over/under-expression of GSDM proteins in various cancers. Still, a clear pattern has yet to emerge, and, again, a lack of basic knowledge limits our ability to interpret some of the data. For example, *GSDMA* is expressed at a lower level in human esophageal and gastric cancers than in normal tissue (82). Although this observation unveils a possible tumor suppressor role for GSDMA in gastric cancer, its biological significance is yet to be revealed. Epigenetic mechanisms such as methylation processes were at the basis of *GSDMA* silencing in the mucus-secreting pit cells of the gastric epithelium (83). Moreover, *GSDMA* expression was regulated by the transcription factor LIM domain only 1 induced by transforming growth factor-β (83, 84). On the other hand, GSDMB is overexpressed in gastric, head, and neck cancers (82). In the case of breast cancer, we understand a little more of the possible role of GSDMB: high GSDMB expression in tumor cells from patients with ERBB2-positive breast cancer correlates with poor prognosis, increased risk of metastasis and decreased survival (85), which may be linked to earlier *in vitro* observations of increased invasiveness and metastatic ability of GSDMB overexpressing immortalized MCF7 tumor cells (9). Hergueta-Redondo and colleagues suggested that the increased migration and invasion capacity of GSDMB-overexpressing cells could be associated with activation of Ras-related C3 botulinum toxin substrate 1 (Rac-1) and cell division cycle 42 (Cdc-42) GTPases (9).

A recent pan-cancer analysis more comprehensively examined patterns of GSDM expression and assessed their relationship with key immune parameters in tumors: the most

striking finding marked GSDMD overexpression in many cancer types, including gastric, colon adenocarcinoma, and breast cancers, which – in contrast to the negative correlations with GSDMB in breast cancer – was associated with increased numbers of potentially beneficial tumor-infiltrating $CD8^+$ T cells, M1 macrophages, and NK cells (82). In endometrial cancer, GSDMD expression is significantly higher in cancer cells than in healthy endometrial tissue, and its expression is linked with anti-tumor immune properties and a more favorable prognosis (86). Similarly, GSDME expression in patient-derived breast cancer cells correlates with increased survival of patients because of pyroptosis triggered by granzyme B released by cytotoxic T cells; accordingly, its absence is associated with reduced lifespan and a high risk of metastasis (16). There is emerging evidence that sub-optimal expression of GSDME, at least in some cancers, is due to hypermethylation of its promotor: Ibrahim et al. identified key sites of *GSDME* hypermethylation in colorectal cancer cells but not normal colorectal tissue (87), drawing fresh attention to an early study that showed demethylation by 5-aza-2'-deoxycytidine restored GSDME induction in a breast cancer cell line (88).

Together, these observations support the notion that GSDMD and GSDME act as tumor suppressors through programmed cell death and immune cell recruitment and propose them as prognostic markers for tumor progression and patient survival. It also seems likely that at least GSDMB plays a role in cancer progression. In this case, it appears to be detrimental, perhaps even acting against other GSDM family members within the same types of cancer (**Figure 2**). Further studies looking at all GSDM family members together will be required to understand better the complex interactions between tumor cells, pro- and anti-cancer GSDMs, the immune microenvironment, and their effect on patient outcomes.

THERAPEUTIC TARGETING OF GSDMS

It is now clear that dysregulated activation or expression of GSDMs can either drive or contribute to the pathology of unrestrained inflammation during infection, autoinflammation/autoimmunity, and cancer. This realization has led to a surge in interest in the possibility of targeting GSDM family members for therapeutic benefit and to some unexpected insights into the effects of already licensed drugs.

In the case of inflammatory disorders, the multiple sclerosis drug dimethyl-fumarate promotes anti-inflammatory immune responses, but until recently, much of its mechanism of action has been unclear. Studies in mice have now revealed that the drug blocks caspase-mediated GSDMD activation, thereby suppressing pyroptosis *in vitro* and ameliorating symptoms in murine models of multiple sclerosis and FMF (11). The same drug is undergoing trials to treat ischemic stroke, (89). An FDA-approved medication for alcoholism, tetraethyl thiuram disulfide (disulfiram), which produces an aversive physical response to alcohol ingestion by preventing its oxidation, has also recently been found to inhibit GSDMD activation. When administered to mouse CAPS models, this drug blocked IL-1β maturation and pyroptosis and prevented the autoinflammatory spectrum disorder associated with inflammasome hyperactivation in these mice (90). Possibilities for targeting the caspase-3/GSDME axis are on the horizon, with a recent pre-clinical study reporting the successful use of Z-DEVD-FMK to ameliorate tubulointerstitial fibrosis and declining renal function in diabetic mice (15). In summary, the idea of targeting GSDMs for the treatment of inflammatory disorders is in its infancy, but these studies represent a promising indication of future potential.

Pre-clinical GSDM-targeted therapies for cancer are also an emerging area of research. While apoptotic pathways are often disabled in cancer cells, the caspase-8-caspase-3-GSDME axis leading to pyroptosis may be operative (91): aiming to exploit this, Lu et al. showed that intratumoral delivery of adeno-associated virus expressing the N-terminal domain of GSDME induced pyroptosis in glioblastoma and breast cancer cells, leading to tumor regression and prolonged survival in preclinical cancer models (92), but this has yet to be tested in humans. Some conventional chemotherapeutic drugs, such as cisplatin and doxorubicin, also cause pyroptosis in cancer cell lines by activating the caspase-3-GSDME pathway (12, 93); while micro-RNA-mediated reactivation of GSMDE expression, in combination with cetuximab, effectively induced pyroptosis of tumor cells and reduced tumor volume in a mouse model of aggressive triple-negative breast cancer (17). GSDMD has also been investigated as a potential therapeutic target in cancer: treating endometrial or ovarian cancer cells with α-NETA, a reversible choline acetylcholine transferase inhibitor, induced pyroptosis *via* the GSDMD/caspase-4 pathway, and reduced tumor growth in mice (13). In addition, paclitaxel, a common chemotherapeutic drug, combined with ruthenium (II) polypyridyl complex, an anti-tumoral compound, led to extensive GSDMD-mediated pyroptotic cell death in a taxol-resistant cervical cancer cell line.

Whilst all the studies to date have focused on the pre-clinical properties of GSDM-targeting, the data are encouraging, and several clinical studies are planned for the coming years. In support of these studies, more basic data are needed to understand the roles of the different GSDM family members in cancer and how they interact in specific situations.

CURRENT CHALLENGES AND FUTURE DIRECTIONS

The discovery that GSDM family proteins regulate pyroptosis is one of the significant breakthroughs in the innate immune cell biology of the past decade. The concept that canonical and non-canonical inflammasome activation by microbial and endogenous signals regulates IL-1β/IL-18 maturation and release and the death of innate immune cells has been discussed for a long time: but the basis of the underlying mechanism was unknown. Through a series of careful molecular studies, we now know that GSDM proteins are the

main executioners of pyroptotic cell death *via* a process that requires their proteolytic cleavage by inflammatory caspases. Since these caspases are expressed in various cell types, including epithelial cells and keratinocytes, it is evident that GSDM-mediated pyroptosis also extends to non-immune cells. Increasing evidence shows that GSDMs are also involved in various physiological processes, including passive secretion of proteins and molecules that act as alarmins for the immune system, ROS production, MET/NETosis, and mucus layer formation in the gut. In recent years, a clear role of GSDM has emerged in numerous diseases; however, the exact mechanisms of how these proteins influence disease pathogenesis remain to be elucidated.

Among the questions that remain to be answered, some appear more pressing. For example, do the GSDMD features of auto-inhibition, activation, and pore formation also apply to the other members of the GSDM family? At present, the mechanisms of activation and the biological functions of GSDMA, GSDMB, and GSDMC are mainly unknown. Furthermore, it is paramount to uncover other upstream regulators of GSDM activation in immune and non-immune cells and to fully characterize the range of downstream consequences. The idea that GSDM pore formation is a terminal event leading to cell death is outdated, as GSDMD pores can also be exocytosed in the vesicles (32), and pore formation appears to be part of the normal mucin-granule release in the intestine (23). There may yet be other mechanisms of membrane recovery that we do not yet understand.

Several studies revealed the role of GSDMD in host defense against infections. GSDMs have also been associated with immune-mediated diseases, particularly those triggered by chronic inflammation. Mouse and human studies have pointed towards a role of GSDME in cancer tumorigenesis to such an extent that GSDM expression has been proposed as a biomarker for prognosis and response to treatment. Progress in the field has been rapid but – without exception – pre-clinical. Future studies must broaden our understanding of the triggers and functions of GSDM activation across homeostatic, pathogen-infected, and neoplastic tissues. Only then we will be able to manipulate GSDMs and realize the potential of therapeutics targeting their inflammatory or pyroptotic effects to treat human disease.

AUTHOR CONTRIBUTIONS

AM conceived the study and wrote the manuscript; LM collected the related manuscripts, wrote the manuscript, prepared the table, and revised the figures; MC prepared the figures and revised the manuscript. All authors approved the final manuscript.

FUNDING

This work was funded by a grant from Fondazione Telethon (TIGET22-AM Core Grant) and the Else Kröner Fresenius Prize for Medical Research 2020.

ACKNOWLEDGMENTS

The authors wish to thank Insight Editing London for the critical review of the manuscript. Figures were created with BioRender.com.

REFERENCES

1. Saeki N, Kuwahara Y, Sasaki H, Satoh H, Shiroishi T. Gasdermin (Gsdm) Localizing to Mouse Chromosome 11 is Predominantly Expressed in Upper Gastroiatestinal Tract But Significantly Suppressed in Human Gastric Cancer Cells. *Mamm Genome* (2000) 11(9):718–24. doi: 10.1007/s003350010138
2. Tamura M, Tanaka S, Fujii T, Aoki A, Komiyama H, Ezawa K, et al. Members of a Novel Gene Family, Gsdm, are Expressed Exclusively in the Epithelium of the Skin and Gastrointestinal Tract in a Highly Tissue-Specific Manner. *Genomics* (2007) 89(5):618–29. doi: 10.1016/j.ygeno.2007.01.003
3. Tanaka S, Mizushina Y, Kato Y, Tamura M, Shiroishi T. Functional Conservation of Gsdma Cluster Genes Specifically Duplicated in the Mouse Genome. *G3: Genes Genom Genet* (2013) 3(9):1843–50. doi: 10.1534/g3.113.007393
4. Fagerberg L, Hallstrom BM, Oksvold P, Kampf C, Djureinovic D, Odeberg J, et al. Analysis of the Human Tissue-Specific Expression by Genome-Wide Integration of Transcriptomics and Antibody-Based Proteomics. *Mol Cell Proteomics* (2014) 13(2):397–406. doi: 10.1074/mcp.m113.035600
5. Wu C, Orozco C, Boyer J, Leglise M, Goodale J, Batalov S, et al. BioGPS: An Extensible and Customizable Portal for Querying and Organizing Gene Annotation Resources. *Genome Biol* (2009) 10(11):R130. doi: 10.1186/gb-2009-10-11-r130
6. Lluis A, Schedel M, Liu J, Illi S, Depner M, von Mutius E, et al. Asthma-Associated Polymorphisms in 17q21 Influence Cord Blood ORMDL3 and GSDMA Gene Expression and IL-17 Secretion. *J Allergy Clin Immunol* (2011) 127(6):1587–94.e6. doi: 10.1016/j.jaci.2011.03.015
7. Terao C, Kawaguchi T, Dieude P, Varga J, Kuwana M, Hudson M, et al. Transethnic Meta-Analysis Identifies GSDMA and PRDM1 as Susceptibility Genes to Systemic Sclerosis. *Ann Rheum Dis* (2017) 76(6):1150–58. doi: 10.1136/annrheumdis-2016-210645
8. Das S, Miller M, Beppu AK, Mueller J, McGeough MD, Vuong C, et al. GSDMB Induces an Asthma Phenotype Characterized by Increased Airway Responsiveness and Remodeling Without Lung Inflammation. *Proc Natl Acad Sci U S A* (2016) 113(46):13132–37. doi: 10.1073/pnas.1610433113
9. Hergueta-Redondo M, Sarrio D, Molina-Crespo A, Megias D, Mota A, Rojo-Sebastian A, et al. Gasdermin-B Promotes Invasion and Metastasis in Breast Cancer Cells. *PLos One* (2014) 9(3):e90099. doi: 10.1371/journal.pone.0090099
10. Booshehri LM, Hoffman HM. CAPS and NLRP3. *J Clin Immunol* (2019) 39(3):277–86. doi: 10.1007/s10875-019-00638-z
11. Humphries F, Shmuel-Galia L, Ketelut-Carneiro N, Li S, Wang B, Nemmara VV, et al. Succination Inactivates Gasdermin D and Blocks Pyroptosis. *Science* (2020) 369(6511):1633–37. doi: 10.1126/science.abb9818
12. Wang C, Yang T, Xiao J, Xu C, Alippe Y, Sun K, et al. NLRP3 Inflammasome Activation Triggers Gasdermin D-Independent Inflammation. *Sci Immunol* (2021) 6(64):eabj3859. doi: 10.1126/sciimmunol.abj3859
13. Qiao L, Wu X, Zhang J, Liu L, Sui X, Zhang R, et al. α-NETA Induces Pyroptosis of Epithelial Ovarian Cancer Cells Through the GSDMD/caspase-4 Pathway. *FASEB J* (2019) 33(11):12760–67. doi: 10.1096/fj.201900483RR
14. Defourny J, Aghaie A, Perfettini I, Avan P, Delmaghani S, Petit C. Pejvakin-Mediated Pexophagy Protects Auditory Hair Cells Against Noise-Induced

Damage. *Proc Natl Acad Sci U S A* (2019) 116(16):8010–17. doi: 10.1073/pnas.1821844116
15. Li W, Sun J, Zhou X, Lu Y, Cui W, Miao L. Mini-Review: GSDME-Mediated Pyroptosis in Diabetic Nephropathy. *Front Pharmacol* (2021) 12:780790. doi: 10.3389/fphar.2021.780790
16. Zhang Z, Zhang Y, Xia S, Kong Q, Li S, Liu X, et al. Gasdermin E Suppresses Tumour Growth by Activating Anti-Tumour Immunity. *Nature* (2020) 579 (7799):415–20. doi: 10.1038/s41586-020-2071-9
17. Xu W, Song C, Wang X, Li Y, Bai X, Liang X, et al. Downregulation of miR-155-5p Enhances the Anti-Tumor Effect of Cetuximab on Triple-Negative Breast Cancer Cells *via* Inducing Cell Apoptosis and Pyroptosis. *Aging* (2021) 13(1):228–40. doi: 10.18632/aging.103669
18. Runkel F, Marquardt A, Stoeger C, Kochmann E, Simon D, Kohnke B, et al. The Dominant Alopecia Phenotypes Bareskin, Rex-Denuded, and Reduced Coat 2 are Caused by Mutations in Gasdermin 3. *Genomics* (2004) 84(5):824–35. doi: 10.1016/j.ygeno.2004.07.003
19. Shi J, Zhao Y, Wang K, Shi X, Wang Y, Huang H, et al. Cleavage of GSDMD by Inflammatory Caspases Determines Pyroptotic Cell Death. *Nature* (2015) 526(7575):660–65. doi: 10.1038/nature15514
20. Kayagaki N, Stowe IB, Lee BL, O'Rourke K, Anderson K, Warming S, et al. Caspase-11 Cleaves Gasdermin D for non-Canonical Inflammasome Signalling. *Nature* (2015) 526(7575):666–71. doi: 10.1038/nature15541
21. Zheng D, Liwinski T, Elinav E. Inflammasome Activation and Regulation: Toward a Better Understanding of Complex Mechanisms. *Cell Discov* (2020) 6:36. doi: 10.1038/s41421-020-0167-x
22. Heilig R, Dick MS, Sborgi L, Meunier E, Hiller S, Broz P. The Gasdermin-D Pore Acts as a Conduit for IL-1beta Secretion in Mice. *Eur J Immunol* (2018) 48(4):584–92. doi: 10.1002/eji.201747404
23. Zhang J, Yu Q, Jiang D, Yu K, Yu W, Chi Z, et al. Epithelial Gasdermin D Shapes the Host-Microbial Interface by Driving Mucus Layer Formation. *Sci Immunol* (2022) 7(68):eabk2092. doi: 10.1126/sciimmunol.abk2092
24. Carl-McGrath S, Schneider-Stock R, Ebert M, Rocken C. Differential Expression and Localisation of Gasdermin-Like (GSDML), a Novel Member of the Cancer-Associated GSDMDC Protein Family, in Neoplastic and non-Neoplastic Gastric, Hepatic, and Colon Tissues. *Pathology* (2008) 40 (1):13–24. doi: 10.1080/00313020701716250
25. Liu X, Zhang Z, Ruan J, Pan Y, Magupalli VG, Wu H, et al. Inflammasome-Activated Gasdermin D Causes Pyroptosis by Forming Membrane Pores. *Nature* (2016) 535(7610):153–58. doi: 10.1038/nature18629
26. Ding J, Wang K, Liu W, She Y, Sun Q, Shi J, et al. Pore-Forming Activity and Structural Autoinhibition of the Gasdermin Family. *Nature* (2016) 535 (7610):111–16. doi: 10.1038/nature18590
27. Ross C, Chan AH, von Pein JB, Maddugoda MP, Boucher D, Schroder K. Inflammatory Caspases: Toward a Unified Model for Caspase Activation by Inflammasomes. *Annu Rev Immunol* (2022) 40:249–69. doi: 10.1146/annurev-immunol-101220-030653
28. Vigano E, Diamond CE, Spreafico R, Balachander A, Sobota RM, Mortellaro A. Human Caspase-4 and Caspase-5 Regulate the One-Step non-Canonical Inflammasome Activation in Monocytes. *Nat Commun* (201) 6:8761. doi: 10.1038/ncomms9761
29. Chen KW, Gross CJ, Sotomayor FV, Stacey KJ, Tschopp J, Sweet MJ, et al. The Neutrophil NLRC4 Inflammasome Selectively Promotes IL-1beta Maturation Without Pyroptosis During Acute Salmonella Challenge. *Cell Rep* (2014) 8 (2):570–82. doi: 10.1016/j.celrep.2014.06.028
30. Evavold CL, Ruan J, Tan Y, Xia S, Wu H, Kagan JC. The Pore-Forming Protein Gasdermin D Regulates Interleukin-1 Secretion From Living Macrophages. *Immunity* (2018) 48(1):35–44 e6. doi: 10.1016/j.immuni.2017.11.013
31. Russo HM, Rathkey J, Boyd-Tressler A, Katsnelson MA, Abbott DW, Dubyak GR. Active Caspase-1 Induces Plasma Membrane Pores That Precede Pyroptotic Lysis and Are Blocked by Lanthanides. *J Immunol* (2016) 197 (4):1353–67. doi: 10.4049/jimmunol.1600699
32. Ruhl S, Shkarina K, Demarco B, Heilig R, Santos JC, Broz P. ESCRT-Dependent Membrane Repair Negatively Regulates Pyroptosis Downstream of GSDMD Activation. *Science* (2018) 362(6417):956–60. doi: 10.1126/science.aar7607
33. Jimenez AJ, Maiuri P, Lafaurie-Janvore J, Divoux S, Piel M, Perez F. ESCRT Machinery is Required for Plasma Membrane Repair. *Science* (2014) 343 (6174):1247136. doi: 10.1126/science.1247136
34. Zhou Z, He H, Wang K, Shi X, Wang Y, Su Y, et al. Granzyme A From Cytotoxic Lymphocytes Cleaves GSDMB to Trigger Pyroptosis in Target Cells. *Science* (2020) 368(6494):eaaz7548. doi 10.1126/science.aaz7548
35. Kambara H, Liu F, Zhang X, Liu P, Bajrami B, Teng Y, et al. Gasdermin D Exerts Anti-Inflammatory Effects by Promoting Neutrophil Death. *Cell Rep* (2018) 22(11):2924–36. doi: 10.1016/j.celrep.2018.02.067
36. Sollberger G, Choidas A, Burn GL, Habenberger P, Lucrezia RD, Kordes S, et al. Gasdermin D Plays a Vital Role in the Generation of Neutrophil Extracellular Traps. *Sci Immunol* (2018) 3(26):eaar6689. doi: 10.1126/sciimmunol.aar6689
37. Orning P, Weng D, Starheim K, Ratner D, Best Z, Lee B, et al. Pathogen Blockade of TAK1 Triggers Caspase-8-Dependent Cleavage of Gasdermin D and Cell Death. *Science* (2018) 362(6418):1064–69. doi: 10.1126/science.aau2818
38. Sarhan J, Liu BC, Muendlein HI, Li P, Nilson R, Tang AY, et al. Caspase-8 Induces Cleavage of Gasdermin D to Elicit Pyroptosis During Yersinia Infection. *Proc Natl Acad Sci U S A* (2018) 115(46):E10888–E97. doi: 10.1073/pnas.1809548115
39. Rogers C, Fernandes-Alnemri T, Mayes L, Alnemri D, Cingolani G, Alnemri ES. Cleavage of DFNA5 by Caspase-3 During Apoptosis Mediates Progression to Secondary Necrotic/Pyroptotic Cell Death. *Nat Commun* (2017) 8:1–14. doi: 10.1038/ncomms14128
40. Lee Y, Reilly B, Tan C, Wang P, Aziz M. Extracellular CIRP Induces Macrophage Extracellular Trap Formation *Via* Gasdermin D Activation. *Front Immunol* (2021) 12:780210(December). doi: 10.3389/fimmu.2021.780210
41. Bergsbaken T, Cookson BT. Macrophage Activation Redirects Yersinia-Infected Host Cell Death From Apoptosis to Caspase-1-Dependent Pyroptosis. *PLos Pathog* (2007) 3(11):1570–82. doi: 10.1371/journal.ppat.0030161
42. Goddard PJ, Sanchez-Garrido J, Slater SL, Kalyan M, Ruano-Gallego D, Marches O, et al. Enteropathogenic Escherichia Coli Stimulates Effector-Driven Rapid Caspase-4 Activation in Human Macrophages. *Cell Rep* (2019) 27(4):1008–17.e6. doi: 10.1016/j.celrep.2019.03.100
43. Ren H, Yang H, Yang X, Zhang G, Rong X, Huang J, et al. Brucella Outer Membrane Lipoproteins 19 and 16 Differentially Induce Interleukin-18 Response or Pyroptosis in Human Monocytic Cells. *J Infect Dis* (2021) 224 (12):2148–59. doi: 10.1093/infdis/jiab272
44. Wang J, Deobald K, Re F. Gasdermin D Protects From Melioidosis Through Pyroptosis and Direct Killing of Bacteria. *J Immunol* (2019) 202(12):3468–73. doi: 10.4049/jimmunol.1900045
45. Gram AM, Wright JA, Pickering RJ, Lam NL, Booty LM, Webster SJ, et al. Salmonella Flagellin Activates NAIP/NLRC4 and Canonical NLRP3 Inflammasomes in Human Macrophages. *J Immunol* (2021) 206 (3):631–40. doi: 10.4049/jimmunol.2000382
46. Craven RR, Gao X, Allen IC, Gris D, Bubeck Wardenburg J, McElvania-Tekippe E, et al. Staphylococcus Aureus Alpha-Hemolysin Activates the NLRP3-Inflammasome in Human and Mouse Monocytic Cells. *PLos One* (2009) 4(10):e7446. doi: 10.1371/journal.pone.0007446
47. Estfanous S, Krause K, Anne MNK, Eltobgy M, Caution K, Abu Khweek A, et al. Gasdermin D Restricts Burkholderia Cenocepacia Infection *In Vitro* and *In Vivo*. *Sci Rep* (2021) 11(1):1–20. doi: 10.1038/s41598-020-79201-5
48. Cerqueira DM, Gomes MTR, Silva ALN, Rungue M, Assis NRG, Guimaraes ES, et al. Guanylate-Binding Protein 5 Licenses Caspase-11 for Gasdermin-D Mediated Host Resistance to Brucella Abortus Infection. *PLos Pathog* (2018) 14(12):e1007519. doi: 10.1371/journal.ppat.1007519
49. Chen KW, Demarco B, Ramos S, Heilig R, Goris M, Grayczyk JP, et al. RIPK1 Activates Distinct Gasdermins in Macrophages and Neutrophils Upon Pathogen Blockade of Innate Immune Signaling. *Proc Natl Acad Sci U S A* (2021) 118(28):1–9. doi: 10.1073/pnas.2101189118
50. Wang X, Liu M, Geng N, Du Y, Li Z, Gao X, et al. Staphylococcus Aureus Mediates Pyroptosis in Bovine Mammary Epithelial Cell *via* Activation of

NLRP3 Inflammasome. *Vet Res* (2022) 53(1):10–0. doi: 10.1186/s13567-022-01027-y
51. Esquerdo KF, Sharma NK, Brunialti MKC, Baggio-Zappia GL, Assuncao M, Azevedo LCP, et al. Inflammasome Gene Profile is Modulated in Septic Patients, With a Greater Magnitude in non-Survivors. *Clin Exp Immunol* (2017) 189(2):232–40. doi: 10.1111/cei.12971
52. Rathkey JK, Zhao J, Liu Z, Chen Y, Yang J, Kondolf HC, et al. Chemical Disruption of the Pyroptotic Pore-Forming Protein Gasdermin D Inhibits Inflammatory Cell Death and Sepsis. *Sci Immunol* (2018) 3(26):eaat2738. doi: 10.1126/sciimmunol.aat2738
53. Yan W, Zhao YS, Xie K, Xing Y, Xu F. Aspergillus Fumigatus Influences Gasdermin-D-Dependent Pyroptosis of the Lung *via* Regulating Toll-Like Receptor 2-Mediated Regulatory T Cell Differentiation. *J Immunol Res* (2021) 2021:5538612. doi: 10.1155/2021/5538612
54. Lian H, Fang X, Li Q, Liu S, Wei Q, Hua X, et al. NLRP3 Inflammasome-Mediated Pyroptosis Pathway Contributes to the Pathogenesis of Candida Albicans Keratitis. *Front Med (Lausanne)* (2022) 9:845129. doi: 10.3389/fmed.2022.845129
55. Lamkanfi M, Malireddi RK, Kanneganti TD. Fungal Zymosan and Mannan Activate the Cryopyrin Inflammasome. *J Biol Chem* (2009) 284(31):20574–81. doi: 10.1074/jbc.M109.023689
56. Briard B, Karki R, Malireddi RKS, Bhattacharya A, Place DE, Mavuluri J, et al. Fungal Ligands Released by Innate Immune Effectors Promote Inflammasome Activation During Aspergillus Fumigatus Infection. *Nat Microbiol* (2019) 4 (2):316–27. doi: 10.1038/s41564-018-0298-0
57. Banoth B, Tuladhar S, Karki R, Sharma BR, Briard B, Kesavardhana S, et al. ZBP1 Promotes Fungi-Induced Inflammasome Activation and Pyroptosis, Apoptosis, and Necroptosis (PANoptosis). *J Biol Chem* (2020) 295(52):18276–83. doi: 10.1074/jbc.RA120.015924
58. Yogarajah T, Ong KC, Perera D, Wong KT. AIM2 Inflammasome-Mediated Pyroptosis in Enterovirus A71-Infected Neuronal Cells Restricts Viral Replication. *Sci Rep* (2017) 7(1):5845. doi: 10.1038/s41598-017-05589-2
59. Zhu S, Ding S, Wang P, Wei Z, Pan W, Palm NW, et al. Nlrp9b Inflammasome Restricts Rotavirus Infection in Intestinal Epithelial Cells. *Nature* (2017) 546(7660):667–70. doi: 10.1038/nature22967
60. Junqueira C, Crespo A, Ranjbar S, de Lacerda LB, Lewandrowski M, Ingber J, et al. FcgammaR-Mediated SARS-CoV-2 Infection of Monocytes Activates Inflammation. *Nature* (2022) 606(7914):576–84. doi: 10.1038/s41586-022-04702-4
61. Corry J, Kettenburg G, Upadhyay AA, Wallace M, Marti MM, Wonderlich ER, et al. Infiltration of Inflammatory Macrophages and Neutrophils and Widespread Pyroptosis in Lung Drive Influenza Lethality in Nonhuman Primates. *PLos Pathog* (2022) 18(3):e1010395. doi: 10.1371/journal.ppat.1010395
62. Zhao L, Li L, Xue M, Liu X, Jiang C, Wang W, et al. Gasdermin D Inhibits Coronavirus Infection by Promoting the Noncanonical Secretion of Beta Interferon. *mBio* (2022) 13(1):e03600-21. doi: 10.1128/mbio.03600-21
63. Orzalli MH, Prochera A, Payne L, Smith A, Garlick JA, Kagan JC. Virus-Mediated Inactivation of Anti-Apoptotic Bcl-2 Family Members Promotes Gasdermin-E-Dependent Pyroptosis in Barrier Epithelial Cells. *Immunity* (2021) 54(7):1447–62.e5. doi: 10.1016/j.immuni.2021.04.012
64. Dubois H, Sorgeloos F, Sarvestani ST, Martens L, Saeys Y, Mackenzie JM, et al. Nlrp3 Inflammasome Activation and Gasdermin D-Driven Pyroptosis are Immunopathogenic Upon Gastrointestinal Norovirus Infection. *PLos Pathog* (2019) 15(4):e1007709. doi: 10.1371/journal.ppat.1007709
65. Wallace HL, Wang L, Gardner CL, Corkum CP, Grant MD, Hirasawa K, et al. Crosstalk Between Pyroptosis and Apoptosis in Hepatitis C Virus-Induced Cell Death. *Front Immunol* (2022) 13:788138. doi: 10.3389/fimmu.2022.788138
66. Wen C, Yu Y, Gao C, Qi X, Cardona CJ, Xing Z. Concomitant Pyroptotic and Apoptotic Cell Death Triggered in Macrophages Infected by Zika Virus. *PLos One* (2022) 17(4):e0257408. doi: 10.1371/journal.pone.0257408
67. Wang Y, Karki R, Zheng M, Kancharana B, Lee S, Kesavardhana S, et al. Cutting Edge: Caspase-8 Is a Linchpin in Caspase-3 and Gasdermin D Activation to Control Cell Death, Cytokine Release, and Host Defense During Influenza A Virus Infection. *J Immunol* (2021) 207(10):2411–16. doi: 10.4049/jimmunol.2100757
68. Zhao G, Li T, Liu X, Zhang T, Zhang Z, Kang L, et al. African Swine Fever Virus Cysteine Protease Ps273r Inhibits Pyroptosis by Noncanonically Cleaving Gasdermin D. *J Biol Chem* (2022) 298(1):101480–80. doi: 10.1016/j.jbc.2021.101480
69. Shi F, Lv Q, Wang T, Xu J, Xu W, Shi Y, et al. Coronaviruses Nsp5 Antagonizes Porcine Gasdermin. *mBio*. (2022) 13(1):e0273921. doi: 10.1128/mbio.02739-21
70. Ma J, Zhu F, Zhao M, Shao F, Yu D, Ma J, et al. SARS-CoV-2 Nucleocapsid Suppresses Host Pyroptosis by Blocking Gasdermin D Cleavage. *EMBO J* (2021) 40(18):1–17. doi: 10.15252/embj.2021108249
71. Moreno-Moral A, Bagnati M, Koturan S, Ko JH, Fonseca C, Harmston N, et al. Changes in Macrophage Transcriptome Associate With Systemic Sclerosis and Mediate GSDMA Contribution to Disease Risk. *Ann Rheum Dis* (2018) 77(4):596–601. doi: 10.1136/annrheumdis-2017-212454
72. Zhen Y, Zhang H. NLRP3 Inflammasome and Inflammatory Bowel Disease. *Front Immunol* (2019) 10:276. doi: 10.3389/fimmu.2019.00276
73. Xiao J, Wang C, Yao JC, Alippe Y, Xu C, Kress D, et al. Gasdermin D Mediates the Pathogenesis of Neonatal-Onset Multisystem Inflammatory Disease in Mice. *PLos Biol* (2018) 16(11):e3000047. doi: 10.1371/journal.pbio.3000047
74. Kanneganti A, Malireddi RKS, Saavedra PHV, Vande Walle L, Van Gorp H, Kambara H, et al. GSDMD Is Critical for Autoinflammatory Pathology in a Mouse Model of Familial Mediterranean Fever. *J Exp Med* (2018) 215 (6):1519–29. doi: 10.1084/jem.20172060
75. Christodoulou K, Wiskin AE, Gibson J, Tapper W, Willis C, Afzal NA, et al. Next Generation Exome Sequencing of Paediatric Inflammatory Bowel Disease Patients Identifies Rare and Novel Variants in Candidate Genes. *Gut* (2013) 62(7):977–84. doi: 10.1136/gutjnl-2011-301833
76. Soderman J, Berglind L, Almer S. Gene Expression-Genotype Analysis Implicates GSDMA, GSDMB, and LRRC3C as Contributors to Inflammatory Bowel Disease Susceptibility. *BioMed Res Int* (2015) 2015:834805. doi: 10.1155/2015/834805
77. Gao H, Cao M, Yao Y, Hu W, Sun H, Zhang Y, et al. Dysregulated Microbiota-Driven Gasdermin D Activation Promotes Colitis Development by Mediating IL-18 Release. *Front Immunol* (2021) 12:750841. doi: 10.3389/fimmu.2021.750841
78. Bulek K, Zhao J, Liao Y, Rana N, Corridoni D, Antanaviciute A, et al. Epithelial-Derived Gasdermin D Mediates Nonlytic IL-1beta Release During Experimental Colitis. *J Clin Invest* (2020) 130(8):4218–34. doi: 10.1172/JCI138103
79. Zhai Z, Yang F, Xu W, Han J, Luo G, Li Y, et al. Attenuation of Rheumatoid Arthritis Through the Inhibition of Tumor Necrosis Factor-Induced Caspase 3/Gasdermin E-Mediated Pyroptosis. *Arthritis Rheumatol* (2022) 74(3):427–40. doi: 10.1002/art.41963
80. Delmaghani S, Defourny J, Aghaie A, Beurg M, Dulon D, Thelen N, et al. Hypervulnerability to Sound Exposure Through Impaired Adaptive Proliferation of Peroxisomes. *Cell* (2015) 163(4):894–906. doi: 10.1016/j.cell.2015.10.023
81. Park HJ, Cho HJ, Baek JI, Ben-Yosef T, Kwon TJ, Griffith AJ, et al. Evidence for a Founder Mutation Causing DFNA5 Hearing Loss in East Asians. *J Hum Genet* (2010) 55(1):59–62. doi: 10.1038/jhg.2009.114
82. Wang YY, Shi LY, Xu MH, Jing Y, Sun CC, Yang JH, et al. A Pan-Cancer Analysis of the Expression of Gasdermin Genes in Tumors and Their Relationship With the Immune Microenvironment. *Trans Cancer Res* (2021) 10(9):4125–47. doi: 10.21037/tcr-21-1635
83. Saeki N, Kim DH, Usui T, Aoyagi K, Tatsuta T, Aoki K, et al. GASDERMIN, Suppressed Frequently in Gastric Cancer, is a Target of LMO1 in TGF-Beta-Dependent Apoptotic Signalling. *Oncogene* (2007) 26(45):6488–98. doi: 10.1038/sj.onc.1210475
84. Wang M, Chen X, Zhang Y. Biological Functions of Gasdermins in Cancer: From Molecular Mechanisms to Therapeutic Potential. *Front Cell Dev Biol* (2021) 9:638710. doi: 10.3389/fcell.2021.638710
85. Hergueta-Redondo M, Sarrio D, Molina-Crespo Á, Vicario R, Bernadó-Morales C, Martínez L, et al. Gasdermin B Expression Predicts Poor Clinical Outcome in HER2-Positive Breast Cancer. *Oncotarget* (2016) 7 (35):56295–308. doi: 10.18632/oncotarget.10787
86. Zhang X, Yang Q. A Pyroptosis-Related Gene Panel in Prognosis Prediction and Immune Microenvironment of Human Endometrial Cancer. *Front Cell Dev Biol* (2021) 9:705828. doi: 10.3389/fcell.2021.705828

87. Ibrahim J, Op de Beeck K, Fransen E, Croes L, Beyens M, Suls A, et al. Methylation Analysis of Gasdermin E Shows Great Promise as a Biomarker for Colorectal Cancer. *Cancer Med* (2019) 8(5):2133–45. doi: 10.1002/cam4.2103
88. Fujikane T, Nishikawa N, Toyota M, Suzuki H, Nojima M, Maruyama R, et al. Genomic Screening for Genes Upregulated by Demethylation Revealed Novel Targets of Epigenetic Silencing in Breast Cancer. *Breast Cancer Res Treat* (2010) 122(3):699–710. doi: 10.1007/s10549-009-0600-1
89. Hou X, Xu H, Chen W, Zhang N, Zhao Z, Fang X, et al. Neuroprotective Effect of Dimethyl Fumarate on Cognitive Impairment Induced by Ischemic Stroke. *Ann Transl Med* (2020) 8(6):375. doi: 10.21037/atm.2020.02.10
90. Hu JJ, Liu X, Xia S, Zhang Z, Zhang Y, Zhao J, et al. FDA-Approved Disulfiram Inhibits Pyroptosis by Blocking Gasdermin D Pore Formation. *Nat Immunol* (2020) 21(7):736–45. doi: 10.1038/s41590-020-0669-6
91. Hanahan D, Weinberg RA. Hallmarks of Cancer: The Next Generation. *Cell* (2011) 144(5):646–74. doi: 10.1016/j.cell.2011.02.013
92. Lu Y, He W, Huang X, He Y, Gou X, Liu X, et al. Strategies to Package Recombinant Adeno-Associated Virus Expressing the N-Terminal Gasdermin Domain for Tumor Treatment. *Nat Commun* (2021) 2(1):7155. doi: 10.1038/s41467-021-27407-0
93. Wang Y, Gao W, Shi X, Ding J, Liu W, He H, et al. Chemotherapy Drugs Induce Pyroptosis Through Caspase-3 Cleavage of a Gasdermin. *Nature* (2017) 547(7661):99–103. doi: 10.1038/nature22393

Conflict of Interest: The authors declare that the research was conducted in the absence of any commercial or financial relationships that could be construed as a potential conflict of interest.

Publisher's Note: All claims expressed in this article are solely those of the authors and do not necessarily represent those of their affiliated organizations, or those of the publisher, the editors and the reviewers. Any product that may be evaluated in this article, or claim that may be made by its manufacturer, is not guaranteed or endorsed by the publisher.

Advantages of publishing in Frontiers

OPEN ACCESS
Articles are free to read for greatest visibility and readership

FAST PUBLICATION
Around 90 days from submission to decision

HIGH QUALITY PEER-REVIEW
Rigorous, collaborative, and constructive peer-review

TRANSPARENT PEER-REVIEW
Editors and reviewers acknowledged by name on published articles

Frontiers
Avenue du Tribunal-Fédéral 34
1005 Lausanne | Switzerland

Visit us: www.frontiersin.org
Contact us: frontiersin.org/about/contact

REPRODUCIBILITY OF RESEARCH
Support open data and methods to enhance research reproducibility

DIGITAL PUBLISHING
Articles designed for optimal readership across devices

FOLLOW US
@frontiersin

IMPACT METRICS
Advanced article metrics track visibility across digital media

EXTENSIVE PROMOTION
Marketing and promotion of impactful research

LOOP RESEARCH NETWORK
Our network increases your article's readership